Terms and Conditions of Use of Digitised Theses from Trinity College Library Dublin

Copyright statement

All material supplied by Trinity College Library is protected by copyright (under the Copyright and Related Rights Act, 2000 as amended) and other relevant Intellectual Property Rights. By accessing and using a Digitised Thesis from Trinity College Library you acknowledge that all Intellectual Property Rights in any Works supplied are the sole and exclusive property of the copyright and/or other IPR holder. Specific copyright holders may not be explicitly identified. Use of materials from other sources within a thesis should not be construed as a claim over them.

A non-exclusive, non-transferable licence is hereby granted to those using or reproducing, in whole or in part, the material for valid purposes, providing the copyright owners are acknowledged using the normal conventions. Where specific permission to use material is required, this is identified and such permission must be sought from the copyright holder or agency cited.

Liability statement

By using a Digitised Thesis, I accept that Trinity College Dublin bears no legal responsibility for the accuracy, legality or comprehensiveness of materials contained within the thesis, and that Trinity College Dublin accepts no liability for indirect, consequential, or incidental, damages or losses arising from use of the thesis for whatever reason. Information located in a thesis may be subject to specific use constraints, details of which may not be explicitly described. It is the responsibility of potential and actual users to be aware of such constraints and to abide by them. By making use of material from a digitised thesis, you accept these copyright and disclaimer provisions. Where it is brought to the attention of Trinity College Library that there may be a breach of copyright or other restraint, it is the policy to withdraw or take down access to a thesis while the issue is being resolved.

Access Agreement

By using a Digitised Thesis from Trinity College Library you are bound by the following Terms & Conditions. Please read them carefully.

I have read and I understand the following statement: All material supplied via a Digitised Thesis from Trinity College Library is protected by copyright and other intellectual property rights, and duplication or sale of all or part of any of a thesis is not permitted, except that material may be duplicated by you for your research use or for educational purposes in electronic or print form providing the copyright owners are acknowledged using the normal conventions. You must obtain permission for any other use. Electronic or print copies may not be offered, whether for sale or otherwise to anyone. This copy has been supplied on the understanding that it is copyright material and that no quotation from the thesis may be published without proper acknowledgement.

An investigation into the cellular and molecular signalling events which occur in β-amyloid-treated cultured cortical neurons

by

Marie Fogarty

Thesis submitted for the degree of Doctor of Philosophy
at the University of Dublin, Trinity College

Thesis submitted September 2003

Department of Physiology
Trinity College
Dublin 2

I Table of Contents

Chapter 2 Materials and Methods

II List of Figures

III List of Tables

IV Acknowledgements

I would like to acknowledge the help and support of many different people during the course of my project.

First and foremost, I would like to extend my sincere gratitude to Dr. Veronica Campbell for her constant support and ever-present enthusiasm and encouragement during the past three years. I could not have had a better mentor for the duration of the project. I wish her all the best for the future and hope we will meet again during the course of our respective scientific careers.

Sincere thanks to Prof. Chris Bell for allowing me to carry out my research in the Physiology department.

I would like to thank my lab co-workers, past and present, Dr Barry Boland, Eric Downer, Eric Farrell and Jaime O' Dwyer for making my time spent in the lab an enjoyable one. It has been a great pleasure to work with you.

I would also like to thank Prof. Marina Lynch for her advice, invaluable suggestions and the use of her laboratory equipment throughout the project.

Sincere thanks also to the members of the MAL lab (past and present) for providing support, advice and plenty of laughs. They are Dr. Yvonne Nolan, Dr. Aileen Lynch, Dr. Darren Martin, Dr. Áine Kelly, Frank Maher, Aedín Minogue, Claire Barry, Michelle Walsh, Peter Lonergan, Thady Kavanagh and Michelle Moore. Special thanks to Darren for ensuring I got my much needed morning caffeine-fix during the writing of this thesis.

I would also like to thank my fellow thesis writer and office companion Frank for his encouragement during the last three months, and I wish him all the best in the future.

I would like to thank the technical staff of the physiology department for their assistance and kindness: Kieran, Alice, Quentin, Siobhán, David, Leslie, Aidan Ann, Doreen and Bernard.

I acknowledge the Health Research Board, Enterprise Ireland and the Trinity Trust for financial support to carry out this study.

I would like to thank my parents without whom the educational opportunities I have has would not have been available.

A big thanks to my friends (soon to be doctors) Sinéad, Eileen and Janet, and also to Niamh, Louise and Aisling. I am lucky to have such great friends.

Finally I would like to dedicate this thesis with love to Fred, without whose commitment and constant support this thesis would not have been possible.

V Declaration

This thesis is submitted by the undersigned for the degree of Doctor in Philosophy at the University of Dublin, Trinity College and had not been submitted to any other university as an exercise for a degree. I declare that this thesis is entirely my own work and I give permission to the library to lend or copy this thesis upon request

Marie Fogarty

Marie Fogarty BSc.

VI Abstract

Deposition of β-amyloid around neurons is a neuropathological hallmark of Alzheimer's disease. The aim of this study was to investigate the cellular and molecular mechanisms underlying β-amyloid-mediated cell death in cultured cortical neurons. β-amyloid evoked a differential timeframe of activation of specific isoforms of the stress-activated protein kinases, c-jun-N-terminal kinase. To delineate the respective roles of c-jun-N-terminal kinase isoforms in β-amyloid-mediated cell death, antisense oligonucleotide technology was used. The results demonstrate that c-jun-N-terminal kinase 1 is the principal isoform involved in β-amyloid-mediated activation of caspase-3 and DNA fragmentation. c-jun-N-terminal kinase 1 also stabilised the tumour suppressor protein, p53, via phosphorylation at serine-15. The p53 inhibitor, pifithrin-α, reduced the β-amyloid-mediated increase in expression of pro-apoptotic Bax, activation of caspase-3, cleavage of the DNA repair enzyme, poly (ADP) ribose polymerase, and subsequent DNA fragmentation, indicating that β-amyloid, at least in part, arbitrates neuronal cell death in a p53-dependent manner. β-amyloid increased Bax and p53 expression at the mitochondria. The increased mitochondrial association of Bax and p53 coincided with release of mitochondrial cytochrome *c* to the cytosol suggesting that these proteins play a role in β-amyloid-mediated regulation of the mitochondrial membrane. A particularly exciting discovery was the observation that β-amyloid promoted the association of Bax and p53 with lysosomes. The association of these proteins with lysosomes coincided with an alteration in lysosomal integrity. Pifithrin-α attenuated the β-amyloid -mediated increase in cytosolic activity of the lysosomal protease, cathepsin-L, suggesting a novel mechanism whereby p53 may contribute to destabilisation of lysosomal membranes and promote leakage of lysosomal constituents.

An increase in intracellular calcium concentration was induced by β-amyloid and this influx of calcium was attenuated by treatment with the L-type voltage dependent calcium channel blocker, nicardipine. Nicardipine reduced the β-amyloid-mediated increases in c-jun-N-terminal kinase activity, p53 stabilisation, cathepsin-L activity,

caspase-3 activation, and DNA fragmentation. These results emphasise the importance of the L-type calcium channel in the β-amyloid-neurodegenerative cascade.

β-amyloid increased mRNA expression of the pro-inflammatory cytokine, tumour necrosis factor-α, and the associated transcription factor, nuclear factor-kappaB, demonstrating that β-amyloid elicits a local inflammatory response in cultured neurons. Analysis of the effects of the pro-inflammatory cytokine, interleukin-1β, on mRNA expression revealed an increase in mRNA expression of pro-apoptotic Bax and caspase-3, and anti-apoptotic Bcl-xl, demonstrating that pro-inflammatory signals in neuronal cells may favour the occurrence of apoptosis in these cells.

The data presented in this study demonstrates the diverse signalling pathways regulated by β-amyloid in cultured cortical neurons. Inhibition of various proteins involved in β-amyloid-mediated cell death resulted in a reduction in neurodegeneration and offers insight for potential targets which may aid prevention of the neuronal degeneration characteristic of Alzheimer's Disease.

VII List of Abbreviations

Ab	antibody
AD	Alzheimer's disease
AFC	7-amino-4-(trifluoromethyl) coumarin
ANOVA	analysis of variance
APAF	apoptosis activating factor
ApoE	apolipoprotein allelle type E
APP	amyloid precursor protein
APPs-$_{\alpha}$	soluble APP fragment cleaved by α-secretase
APPs-$_{\beta}$	soluble APP fragment cleaved by β-secretase
APS	ammonium persulphate
ARA-C	cytosine-arabino-furanoside
ASO	antisense oligonucleotides
ATF-2	activating transcription factor-2
ATP	adenosine 5'-triphosphate
$A\beta_{(25-35)}$	beta-amyloid fragment containing 25-35 amino acids
$A\beta_{(1-40)}$	beta-amyloid fragment containing 1-40 amino acids
$A\beta_{(1-42)}$	beta-amyloid fragment containing 1-42 amino acids
BACE	Beta site APP cleaving enzyme
βAPP	beta-amyloid precursor protein
BSA	bovine serum albumin
Ca^{2+}	calcium ion
$[Ca^{2+}]i$	intracellular calcium concentration
cDNA	copy deoxyribonucleic acid
CTF	Carboxy terminal fragment
CED	cell death domain
CNS	Central nervous system
-COOH	carboxy terminus
CPP32	cysteine protease of 32 kilo Daltons (caspase-3)

CREB	cAMP-responsive element binding protein
DAB	diaminobenzidine
DEPC	diethylpyrocarbonate
DEVD	aspartic-glutamic-valine-aspartic residue
DMSO	dimethyl sulphoxide
DNA	deoxyribonucleic acid
dNTP	deoxynucleotidetriphosphate
DNAse	deoxyribonucleic acid
DOPE	dioleoyl phosphatidylethenolamine
DOTMA	N[1-(2,3-dioleyloxy)propyl]-N,N,N-Trimethylammonium chloride
DTT	dithiothreitol
ECL	enhanced chemiluminescence
EDTA	ethylenediamine-tetraacetic acid
EGTA	ethylene glycol bis (β-amionethyether) N,N 'tetraacetic acid
ERK	extracellular response kinase
EtBr	ethidium bromide
EtOH	ethanol
FAD	familial alzheimer's disease
FDA	food and drug administration
FITC	flourescein isothiocyanate
GAPDH	glyceraldehyde-3-phosphate dehydrogenase
G-protein	GTP-binding protein
GTP	guanosine 5'-diphosphate
HEPES	(N-[2-Hydroxyethyl]piperazine-N'-[2-ethane-sulphonic acid])
H_20_2	hydrogen peroxide
HRP	horseradish peroxidase
hr	hour
HVA	high voltage activated

ICE	interleukin-1 converting enzyme
IgG	immunoglobulin G
IkB	inhibitor kappa B
IL-1	interleukin-1
IL-1ra	interleukin-1 receptor antagonist
IL-1β	interleukin-1β
IL-	Interleukin-
JIP	JNK interacting protein
JNK	c-jun-N-terminal kinases
KCl	potassium chloride
kDa	kilo Dalton
LAMP	lysosomal associated protein
LTP	long term potentiation
LVA	low voltage activated
mA	milliamp
MAPK	mitogen activated protein kinase
MAPKK	MAPK kinase
MAPKKK	MAPK kinase kinase
MAP-2	microtubule-associated protein 2
mg	milligram
$MgCl_2$	magnesium chloride
$MgSO_4$	magnesium sulphate
min	minute
mM	millimolar
Mn	manganese
mRNA	messenger ribonucleic acid
μM	micromolar
μm	micrometer
NBM	neurobasal medium
NF-κB	nuclear factor-kappa B
NFT	neurofibrillary tangles

ng	nanogram
nm	nanometer
$-NH_2$	amino terminal
NMDA	N-methyl-D-aspartate
Par-4	prostate apoptosis response-4
PAGE	polyacrylamide gel electrophoresis
PAR	poly (ADP) ribose
PARP	poly (ADP) ribose polymerase
PBS	phosphate-buffered saline
PC12	phaeochromocytoma cell line
PCR	polymerase chain reaction
PHF	paired helical fragments
PKA	protein kinase A
PMSF	phenylmethylsulphonyl fluoride
Pro	proline
PS	phosphatidylserine
PS1	presenilin-1
PS2	presenilin-2
RAGE	receptor for advanced glycation end products
RNA	ribonucleic acid
RNAse	ribonuclease
RNaseH	ribonuclease-H
RT	reverse transcription
ROS	reactive oxygen species
SAPK	stress-activated protein kinase
SDS	sodium dodecyl sulphate
SDS-PAGE	SDS-polyacrylamide gel electrophoresis
SEM	standard error of the mean
Se	serine
SK-N-SH	neuroblastoma cell line

TBE	tris borate edta
TBS	tris buffered saline
TBS-T	tbs-tween
TdT	terminal deoxynucleotidyl transferase
TEMED	N,N,N,-N-tetramethylenediamine
Thr	threonine
TNF	tumour necrosis factor
TUNEL	TdT-mediated-UTP-end nick labeling
Tyr	tyrosine
U	unit
UV	ultraviolet
VDCC	voltage dependent Ca^{2+} channel

Chapter 1

General introduction.

1.1 Alzheimer's Disease (AD): Clinical Characteristics

Alzheimer's disease (AD) is a progressive neurodegenerative disease clinically characterised by an irreversible loss of cognitive function, associated with impairment in activities of daily living, mental and physical deterioration with progressive behavioural disturbances, and ultimately by death. There are three main stages in the progression of Alzheimer's disease, with rate of disease progression varying from individual to individual. In the mild stage a person begins to lose short-term memory. The final stages of the disease are marked by severe cognitive decline with mental emptiness and loss of control of all bodily functions (Goldman and Coté, 1991). AD is the most common form of dementia accounting for over 60% of all dementia cases. Dementia denotes a progressive decline in mental function, memory, and in acquired intellectual skills (Goldman and Coté, 1991). Dementia can result from many causes, and is not by itself diagnostic of a specific disease. There are nearly 18 million people with dementia in the world, with over 700,000 people being affected in the UK and over 33,000 people suffering from dementia in Ireland (Alzheimer's Association of Ireland). It is estimated that 1 in 10 people over 65 and almost half of those over 85 have AD. AD is becoming more common in developed nations as average human life expectancy continues to increase.

1.2 Pathology of AD

The first case of AD was diagnosed by the Bavarian psychiatrist Alois Alzheimer in 1907 when he used the Bielschowsky silver staining technique to identify 'dense bundles' of neurofibrils and the 'deposition of a peculiar substance in the cerebral cortex and hippocampus' of the autopsy brain of a 51 year old woman. Today, the major histopathological hallmarks diagnostic of AD include synaptic dysfunction, nerve cell loss primarily in the cerebral cortex, the hippocampus, and the amygdala, and two kinds of deposits, senile plaques and neurofibrillary tangles (Selkoe, 1991). Senile plaques are roughly spherical complex extracellular deposits within the neuropil, composed of a central core containing beta-amyloid (Aβ) protein surrounded by activated microglia,

astrocytes, dystrophic neurites and cellular debris. Neurofibrillary tangles (NFT) consist of intraneuronal bundles of abnormal filaments composed of paired helical filaments (PHF), the major component of which is tau protein (Selkoe, 1995). Tau protein is normally associated with microtubules and functions in the stability of the neuronal cytoskeleton. However, abnormal phosphorylation of tau leads to a destabilisation in tau binding to tubulin, and promotes PHF and NFT formation due to aggregation of the abnormally phosphorylated tau (Hashiguchi *et al.*, 2000).

There has been much debate as to which of the hallmarks of AD, senile plaques or neurofibrillary tangles appear first in the disease. Some groups have proposed that hyper phosphorylation of tau precedes plaque formation in AD brain (Su *et al.*, 1994a; Pope *et al.*, 1994) and the appearance of neurofibrillary tangles has been demonstrated to correlate spatially and temporally with Alzheimer's disease severity (Braak and Braak, 1991). However, over the last 5-10 years the 'amyloid hypothesis' of AD had gained acceptance. According to the amyloid hypothesis, accumulation of Aβ in the brain is the primary influence driving AD pathogenesis. The formation of neurofibrillary tangles, containing tau protein is proposed to result from an imbalance between Aβ production and Aβ clearance (Hardy and Selkoe, 2002). Evidence that Aβ deposition precedes neurofibrillary tangle formation in AD is provided by the following observations. Mutations in the gene encoding tau protein cause frontotemporal dementia with parkinsoniam (Hutton *et al.*, 1998). This disease is characterized by severe deposition of tau in neurofibrillary tangles in the brain, but no deposition of amyloid. This demonstrates that profound neurofibrillary tangle formation leading to neurodegeneration is not sufficient to induce formation of the amyloid plaques characteristic of AD, providing evidence that the neurofibrillary tangles of wild-type tau seen in AD brains are likely to be deposited after changes in Aβ metabolism and plaque formation rather than before (Hardy *et al.*, 1998). In addition, transgenic mice overexpressing both mutant human APP and mutant human tau undergo increased formation of tangles as opposed to mice overexpressing tau alone, whereas the structure of amyloid plaques remained unaltered (Lewis *et al.*, 2001). This finding indicates that altered processing of APP protein precedes alterations in tau in the pathological cascade of AD. Development of amyloid deposits in the AD brain can be catergorised into three stages (A-C). Amyloid deposition initially develops in poorly myelinated areas of the basal neocortex (Stage A),

spreading to the adjoining areas of the hippocampus, neocortex archicortical areas and amygdala (Stage B), until finally populating the entire cortex (Braak and Braak, 1997; see Figure 1.1).

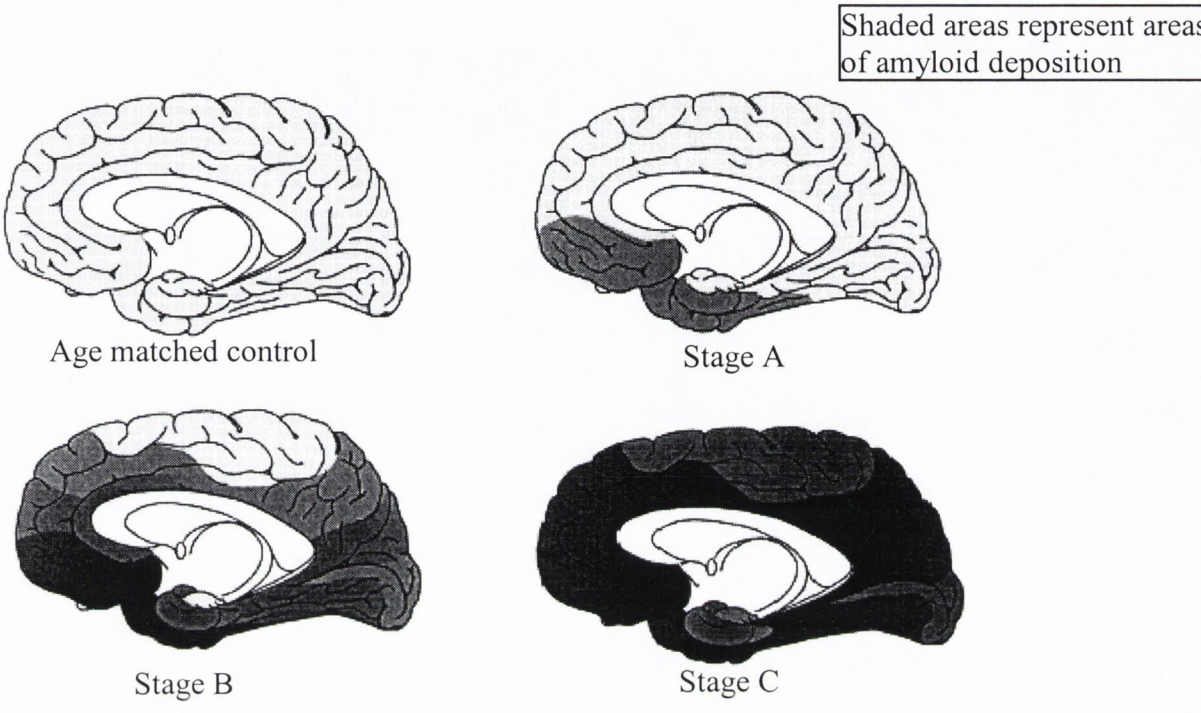

Figure 1.1 Stages of development of amyloid plaques in AD brain; Braak and Braak, 1997

1.3 Mutations in AD

AD can be divided into two subgroups, based on inheritance and mean onset age of the disease. The majority of AD cases are non-inherited and have a late mean age of onset, and are thereby classified as sporadic late-onset AD. The other form of AD is inherited and has an early mean age of onset, and is classified as familial early-onset AD (FAD). FAD is rare, being responsible for less then 10% of all cases of AD (Gandy *et al.*, 2000). FAD is associated with specific mutations of 3 particular genes (see Table 1.1). Initial attempts to understand the role of genetics in AD carried out in the 1980s demonstrated significant linkage of early onset FAD to chromosome 21. The gene encoding the

amyloid precursor protein (*APP*) is found on chromosome 21 and so this made *APP* a candidate gene for AD mutations. The first *APP* mutation was discovered in 1990 (Goate *et al.*, 1991). Since then, 11 different pathogenetic mutations have been identified in *APP*, all of which are missense mutations lying within or close to the domain encoding the Aβ peptide (Tanzi and Bertram, 2001). All *APP* mutations lead to increased production of either total Aβ or a specific Aβ isoform (Selkoe, 1994). In addition, *APP* mutations internal to the Aβ sequence heighten the self-aggregation of Aβ into amyloid fibrils (Wisniewski *et al.*, 1991). Down's Syndrome sufferers who inherit an extra copy of chromosome 21, and therefore an extra copy of the *APP* gene, develop AD pathology if they live past 40, providing further support for the role of *APP* in early development of AD (Armstrong, 1994). However, mutations in *APP* account for less than 0.1% of all AD cases (Tanzi, 1999).

Chromosome	**Gene defect**	**AD subtype**	**Effect on Aβ phenotype**	**Associated age of onset**
21	βAPP mutations	FAD	Production of total Aβ peptides or $A\beta_{1-42}$ peptides	50s
14	Presenilin1 mutations	FAD	Production of $A\beta_{1-42}$ peptides	40s and 50s
1	Presenilin 2 mutations	FAD	Production of $A\beta_{1-42}$ peptides	50s
19	ApoE4 polymorphism	Sporadic FAD	Density of Aβ plaques and vascular deposits	60s and older

Table 1.1 Genetic factors predisposing to Alzheimer's Disease (Selkoe, 2001)

The second and third AD genes identified were *presenilin1(PS1)* and *presenilin2(PS2)* found on chromosome 14 and 1, respectively (Selkoe, 2001). These genes encode for highly homologous, multitransmembrane proteins which are predominantly localised within the endoplasmic reticulum, and to a lesser extent in the Golgi compartment

(Walter *et al.*, 1996). The precise functions of presenilins within the cell is unknown but it has been suggested that PS1 and PS2 play a role in neurite outgrowth (Dowjat *et al.*, 1999). More than 90 missense mutations identified to date in PS1 and at least 6 in PS2 cause the most aggressive forms of familial AD yet recognised, with some PS1 mutations producing symptoms of dementia as early as in the twenties (Selkoe, 2002). All AD-causing PS mutations expressed to date in transgenic mice or cell culture models increase the production of the $A\beta_{1-42}$ form of Aβ (Selkoe, 2002). Together mutations in these two genes account for about 30 % of all FAD cases but only 2-3% of all AD cases.

The majority (>90%) of AD cases are late onset sporadic AD, not related to any single gene mutation. The etiology of sporadic AD is complex due to interactions between environmental conditions and genetic features of the individual. Individuals containing one or two E4 alleles of the *apoE* gene are predisposed to late onset Alzheimer's disease (Dekroom and Armati, 1994). ApoE is a major serum lipoprotein that is involved in regulation of cholesterol metabolism in the body by binding to lipoproteins and mediating transport of lipids to and from the bloodstream. In the brain, apoE is thought to be involved in membrane remodelling by mobilizing and redistributing cholesterol and phospholipids. It has been shown to be critical in deposition of Aβ peptide in transgenic mice overproducing APP (Raber *et al.*, 1998). Humans expressing apoE4 show no overall increase in Aβ production, it is therefore thought that the inheritance of apoE4 may leads to a rise in the steady-state levels of Aβ in the brain, by decreasing its clearance from the brain's extracellular space or by enhancing the fibrillogenic potential of Aβ (Schmechel *et al.*, 1993; Holtzman *et al.*, 2000). Despite its established association, the *apoE*4 allele is neither necessary nor sufficient to cause AD, but instead operates as a genetic risk modifier by decreasing the age of onset in a dose-dependent manner (Blacker *et al*, 1997; Meyer *et al.*, 1998).

Several other putative genetic risk factors for sporadic AD which lead to increased production of Aβ have been reported, including α2-macroglobulin encoded by two genes on chromosome 12 (Blacker *et al.*, 1998), and insulin degrading enzyme encoded by the IDE gene on chromosome 10 (Selkoe, 2001).

1.4 AD and Environmental factors

Several environmental risk factors have been implicated in development of late-onset AD including head injury, increased concentration of aluminium in drinking water, alcohol abuse, early or late parental age and vascular risk factors such as high cholesterol (Richard and Amouyel, 2001). Several protective factors have also been associated with a decreased risk for AD development including high education level, antioxidants such as vitamin C, E, and B12, hormone replacement therapy in women, polyunsaturated fatty acids, moderate wine consumption and use of anti-inflammatory drugs (Nourhashemi *et al.*, 2000, Richard and Amouyel, 2001). It is becoming increasingly clear that multiple environmental and genetic determinants interacting throughout life are likely to create susceptibility to sporadic late-onset Alzheimer's disease.

1.5 The Biogenesis of β-amyloid

Aβ, the 40-42 amino acid peptide which is the major constituent of the senile plaques associated with Alzheimer's disease (Selkoe *et al.*, 1991) is formed during constitutive proteolytic processing of its precursor protein, βAPP, that is encoded by a gene on human chromosome 21 (Kang *et al.*, 1987). Amyloid precursor proteins are a family of type 1 integral membrane proteins (Haass and Selkoe, 1993). It has been shown that in the brain a proportion of APP is present on the cell surface, and although the exact function of APP is still unknown it is proposed that this cell surface APP mediates the transduction of extracellular signals into the cell (Perez *et al.*, 1997). In addition, there is a considerable amount of evidence to indicate a role for APP in promoting neuronal survival. Exogenously added APP has been demonstrated to protect primary neuronal cultures and cell lines from a range of toxic insults including hypoglycemia, glutamate excitotoxicity or Aβ toxicity (Schubert and Behl, 1993; Mattson et al., 1993a; Goodman and Mattson, 1994). The protective effect of APP is thought to occur by lowering intracellular calcium ($[Ca^{2+}]_i$) levels (Mattson, 1993b). The amino-terminus of the Aβ peptide is located 99 residues proximal to the carboxy-terminus of APP (see Figure 1.2) and extends into the membrane-spanning domain (Howlett *et al.*, 2000). Thus, proteolytic

cleavage occurs at both the amino- and carboxy-termini of the Aβ domain within βAPP to yield the Aβ peptide.

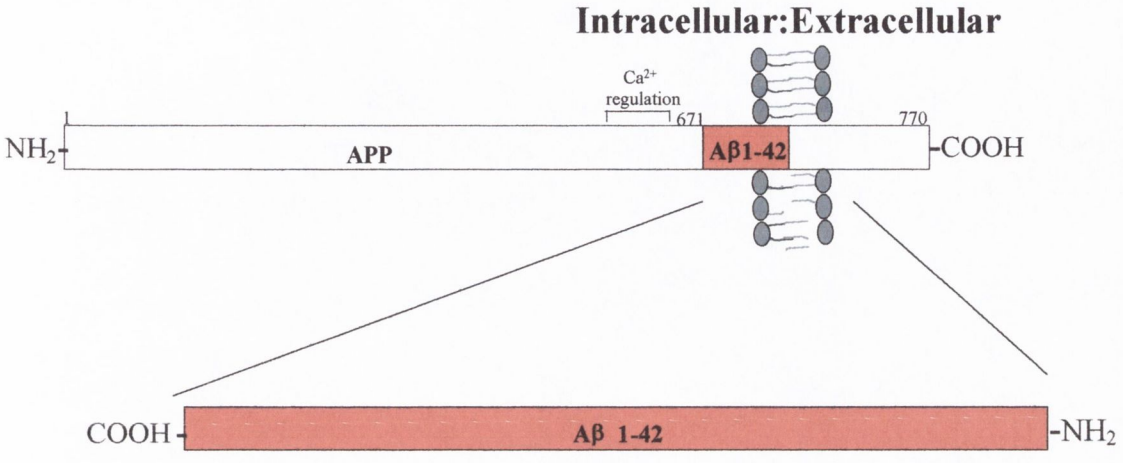

Figure 1.2 Structure of Amyloid Precursor Protein

The three key βAPP processing steps are mediated by enzymes referred to as α, β and γ-secretase (Tischer and Cordell, 1996). Figure 1.3 represents the pathways involved in normal and pathological processing of βAPP. βAPP is cleaved by α and β secretases, thereby shedding the large ectodomain and producing membrane anchored 83- and 99-amino acid carboxy terminal fragments (CTF83 and CTF99) with release of soluble derivatives of the protein termed α-APPs and β-APPs (Selkoe *et al.*, 1994). α-APPs are known to be neuroprotective and have been demonstrated to protect against ischemic brain injury (Smith-Swintosky *et al.*, 1994) and to protect hippocampal neurons from oxidative injury (Goodman and Mattson, 1994). The generated CTF83 and CTF99 fragments can serve as substrates for γ-secretase, which apparently cleaves within the transmembrane domain of the βAPP, to form the 40-42 amino acid Aβ peptide from CTF99 and an amino-terminal truncated non-pathological fragment of Aβ, p3, from CTF83 (Haass *et al.*, 1992). Aβ peptides are normal products of cellular matabolism with roughly 90% of Aβ being the 1-40 form of the peptide and 10% being the 1-42 variant.

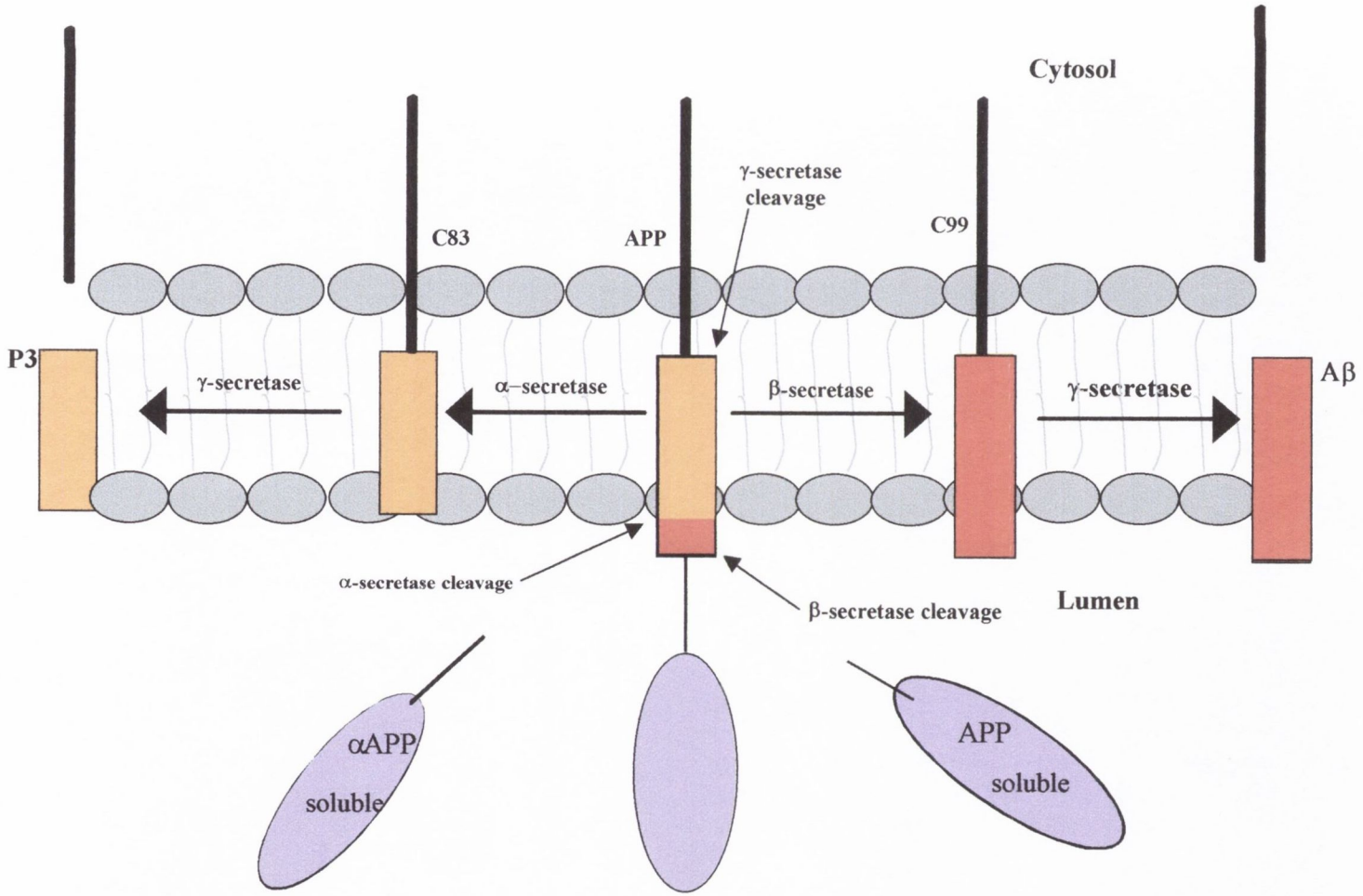

Figure 1.3 Cleavage of APP by α, β, and γ-secretase; adapted from Wolfe *et al.*, 1999

While $A\beta_{1-42}$ is less soluble and more amyloidogenic than $A\beta_{1-40}$ form of the peptide, neuritic plaques contain both forms of the peptide (Selkoe, 2001).

The disintegrin metalloproteinases ADAM 10 and ADAM 17 can serve as α-secretases for APP (Brown *et al.*, 2000; Buxbaum *et al.*, 1998). In 1999 an enzyme denoted Beta site APP cleaving enzyme 1 (BACE 1) was identified as β-secretase (Vassar *et al.*, 1999; Yan *et al.*, 1999). This enzyme is an aspartic protease, which cleaves APP 16 amino acids amino-terminal to the α-secretase site generating CTF99. The identity of the γ-secretase protease remains elusive, however it has been demonstrated to display some of the properties of an aspartyl protease (Wolfe *et al.*, 1999a). PS1 and PS2 have been established to be critical for γ-secretase action. For example, it has been reported that in primary fibroblast cultures from PS1 knockout mice, carboxy-terminal fragments that are normally processed by γ-secretase were increased and that subsequently Aβ production was dramatically reduced (De Strooper *et al.*, 1998). Two TM aspartases in PS1 have been identified that are critical for γ-secretase function (Wolfe *et al*, 1999b). Some reports suggest that the presenilins function as γ-secretases (Wolfe *et al.*, 1999a, Satoh *et al.*, 2001). However, this hypothesis remains controversial and further experimentation will need to be carried out in order to clarify the exact role of the presenilins in the genesis of the Aβ peptide.

1.6 Aβ and Neurotoxicity

According to the amyloid hypothesis of AD, Aβ generation, aggregation and deposition are decisive events in AD pathogenisis, resulting in severe neuronal degeneration and loss of synaptic density (Mcgeer and Mcgeer, 2001). The neurotoxic properties of Aβ are proposed to underlie AD. Early experiments *in vitro* in primary cultured cortical neurons (Yanker *et al.*, 1989) along with experiments *in vivo* in rat cerebral cortex (Kowall *et al.*, 1991) demonstrated the toxic nature of Aβ to neurons. The toxicity of Aβ has been demonstrated to reside on amino acids 25-35 of the Aβ fragment (Pike *et al.*, 1995). It was originally thought that it was necessary for Aβ to be aggregated into fibrils to display toxicity (Pike *et al.*, 1991). However, Aβ peptides can exert toxicity

before fibril formation and evidence from a number of recent reports has demonstrated that soluble oligomers of Aβ may be responsible for the synaptic dysfunction observed in the brains of patients with AD (Maclean *et al.*, 1999). A recent study has demonstrated that soluble oligomers of Aβ are neurotoxic and lead to inhibition of LTP in hippocampus (Walsh, 2002).

The mechanisms of Aβ toxicity have been a major focus of AD research for the past decade and are thought to involve a combination of three main causes – dysregulation of calcium (Ca^{2+}) homeostasis, generation of reactive oxygen species resulting in oxidative stress and neuroinflammation (Mattson *et al.*, 1993a; Storey and Cappai, 1999). Studies are ongoing to identify the downstream mechanisms arising from these three causes, which culminate in either neuronal apoptosis or necrosis and the main objective of this study is to further investigate the molecular and cellular events occurring as a result of neuronal exposure to Aβ. A brief summary outlining the known effects to date of Aβ on Ca^{2+} homeostasis, oxidative stress and inflammation is presented in the following sections.

1.6.1 Aβ and disruption of cellular Ca^{2+} homeostasis

Ca^{2+} is one of the most ubiquitous intracellular messengers transmitting cellular messages in a wide variety of cell types. An elaborate system maintains the intercytoplasmic concentration of Ca^{2+} at 50 – 200 nM despite an extracellular Ca^{2+} concentration of 1-2 mM. The resting intracellular calcium concentration ($[Ca^{2+}]_i$) is kept low by a combination of ATP-dependent Ca^{2+} pumps in the plasma membrane and in membranes of Ca^{2+} stores such as the mitochondria and endoplasmic reticulum, as well as by plasma membrane Na^{2+}-Ca^{2+} exchangers and cytosolic Ca^{2+} binding proteins (Mattson *et al.*, 1993b). Ca^{2+} enters the cell through either voltage-dependent Ca^{2+} channels or ligand-gated Ca^{2+} channels (Zamani and Allen, 2001).

Aβ toxicity involves a dysregulation of Ca^{2+} homeostasis resulting in increased $[Ca^{2+}]_i$ (Pascale and Etcheberrigaray, 1999). This alteration in regulation of Ca^{2+} homeostasis is proposed to be the underlying mechanism of Aβ-mediated neurotoxicity (Mattson *et al.*, 1993b). Neurons that are unable to keep intracellular Ca^{2+} concentrations

within a certain range are rendered vulnerable. Potential mechanisms for Aβ-induced dysregulation of $[Ca^{2+}]_i$ involve an Aβ-mediated increase in Ca^{2+} influx through voltage-gated Ca^{2+}channels (VDCCs; MacManus *et al.*, 2000), formation of a cation-selective ion channel after Aβ-peptide incorporation into the cellular membrane (Mirzabekov *et al.*, 1994) or triggering of intracellular store release of Ca^{2+} (He *et al.*, 2002). Intracellular Ca^{2+} stores and putative Aβ-formed Zn^{2+} dependent channels were recently reported to constitute 25.1 % and 13.9 % respectively of the contribution of Aβ to increased $[Ca^{2+}]_i$, while VDCCs were found to account for 61 % (He *at al.*, 2002).

One of the principal routes for Ca^{2+} entry into the cell is via the VDCCs. VDCCs are classified by the characteristic properties of the single channel activity as determined by electrophysiological patch clamp studies. They are a diverse group of multi subunit proteins containing 4-5 distinct subunits. They are composed of a pore-forming subunit (α_1) of about 190-250 kDa and several auxillary units including α_2 and δ subunits joined by a disulphide bridge (Figure 1.4; Takahashi *et al.*, 1982)

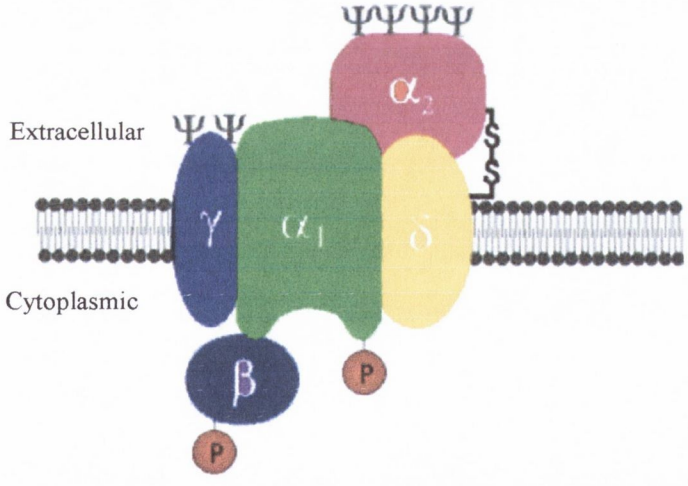

Figure 1.4 Substructure of VDCC. Ψ denotes areas of N-linked glycosylation; P denotes cAMP-dependent protein kinase phosphorylation sites.

In mammalian central nervous system (CNS) neurons, there is a clear distinction between low-conductance channels activated by moderate depolarisations of the plasma membrane (low voltage-activated, LVA) and high conductance channels activated by large depolarisations of the plasma membrane (high-voltage activated, HVA)

Name	Type	Channel α1-subunit	Single channel conductance (pS)	Localisation	Selective Blockers	Function
L	HVA	α_{1S}(Skeletal Muscle) α_{1C}(cardiac, brain) α_{1D}(neurosecretory α1F	34	Cell bodies Proximal dendrites	DHP antagonists	Regulation of transcription
N	HVA	α_{1B} (brain, PC12 cells)	13-20	Nerve terminals Dendrites	ωCTx-GVIA	Neurotransmitter release Dendritic Ca^{2+} transients
P	HVA	α_{1A} (brain, heart)	10-18	Nerve terminals Dendrites	ω-Agatoxin IVA	Neurotransmitter release Dendritic Ca^{2+} transients
Q	HVA	α_{1A} (brain)	?	Nerve terminals Dendrites	No specific blockers ω-Agatoxin IVA (>100nM) ω-CTx MVIIC (also blocks N, P)	Neurotransmitter release Dendritic Ca^{2+} transients
R	HVA/LVA	α_{1E} (brain)	?	Cell bodies Dendrites	None known	Neurotransmitter release
T	LVA	α_{1G} α_{1H}	8		No specific blockers Ni^{2+}, octanol, amiloride, carbamazepine, phenytoin.	Repetitive firing

Table 1.2 Properties of Ca^{2+} channels (adapted from Dolphin, 1995)

(Dolphin *et al.*, 1995). Members of the LVA Ca^{2+} channels include the T - and R- type channels. These channels generally have a low single-channel conductance of Ca^{2+}, of about 7-8 pS (Droogmans and Nilius, 1989). Members of the HVA Ca^{2+} channels include the L-, N-, P, and Q- type channels. The HVA Ca^{2+}channels typically have a high single channel conductance for Ca^{2+} ranging from 10-24 pS (Nilius *et al.*, 1985). Table 1.4 demonstrates the properties of different channel subtypes. The main factor which defines the different calcium currents is which α_1 subtype is included in the channel complex. In most neurons, L-type Ca^{2+} channels contain α_{1c} or α_{1d} subunits. Association with different β subunits also influences a channel gating substantially, allowing for diversity between Ca^{2+} channels in neurons (Caterwall, 1998). While the L-type Ca^{2+} channels are found in virtually all excitable tissues and in many non-excitable cells, the N-type and P-type channels are largely restricted to neurons. There are three major types of channel blockers – inorganic compounds, organic compounds including benzothiazepines and dihydropyridines (DHP) and peptides-venoms. Long closures of the L-type Ca^{2+} channel are brought about by DHP antagonists and they are thought to promote channel inactivation. In contrast, N type calcium channels are insensitive to DHP but are potently and irreversibly blocked by ω-conotoxins, in particular the ω-conotoxin GVIA, a toxin derived from the cone shell mollusc *Conus geographus* (Uchitel, 1997).

Previous work carried out in this laboratory demonstrated that the $A\beta_{1-40}$-mediated increase in influx of Ca^{2+} in rat cortical synaptosomes occurred via activation of the L- and N- type of VDCCs (MacManus *et al.*, 2000). Additionally, Aβ-mediated augmentation of the L-type VDCCs has been reported in a variety of cell types including PC12 cells and cultured neurons (Green and Peers, 2001; Ueda *et al.*, 1997). In this thesis, the role of the L-type VDCC in Aβ-mediated events was examined.

1.6.2 Aβ and oxidative stress

The first evidence that oxidative stress might be involved in Aβ toxicity was the observation that vitamin E and other lipophilic antioxidants rescue neuronal cell lines from Aβ-induced neurotoxicity (Behl *et al.*, 1992). A build up of reactive oxygen species is detectable in cells exposed to Aβ and this generation of free radicals results in lipid

peroxidation and protein oxidation rendering the cell more susceptible to death (Butterfield *et al.*, 1999). Under normal conditions, damage by oxygen radicals is kept in check by antioxidant systems, however oxidative damage occurs when the oxidative balance is disturbed such that reactive oxygen species exceeds the cellular antioxidant defenses. The brain is particularly vulnerable to oxidative stress, having low levels of catalase enzyme. This enzyme functions to break down hydrogen peroxide (H_20_2) into water (H_20) and oxygen (0_2) thus preventing the generation of free radicals (Davis *et al.*, 1996). Neurons in particular are vulnerable to attack by free radicals due to the fact that their glutathione content, an important natural antioxidant, is low and the fact that their membranes contain a high proportion of polyunsaturated fatty acids (Christen, 2000). The oxidative damage found in AD includes advanced glycation end products, nitration, and lipid peroxidation adduction products. Aβ has been demonstrated to contribute to oxidative damage in a number of ways. Iron, in a redox active state, is increased in amyloid deposits (Smith *et al.*, 1994). Iron catalyses the formation of hydroxl radicals ($^{\bullet}OH$) from H_2O_2 as well as producing damaging advanced glycation end products. Another method by which Aβ generates free radicals is through activation of microglia which are a source of NO and $O_2^{\bullet}$ (Meda *et al.*, 1995). In addition, Aβ can bind the receptor for advanced glycation end products (RAGE) to increase production of reactive oxygen (Yan *et al.*, 1996). *In vivo* findings that oxidative damage occurs in areas of the brain rich in senile plaques supports the pro-oxidant potential of Aβ (Smith *et al.*, 2002) .

1.6.3 Aβ and inflammation

Chronic long term neuroinflammation is a prominent feature in AD pathology (Giometto *et al.*, 1988). The general hypothesis of inflammation in AD is that Aβ leads to activation of glial cells, activated glial cells then lead to production of cytotoxic agents including pro-inflammatory cytokines such as interleukin-1β (IL-1β; McGeer and McGeer, 2002). IL-1β in turn, in combination with IFNγ, can positively influence the production of additional Aβ by supporting β-secretase cleavage of the immature APP molecule (Blasko *et al.*, 2000). In addition, activated microglia create more damage by contributing to formation of reactive oxygen species (Moore and O' Banion, 2002). This demonstrates the strong link that exists between the processes of inflammation and

oxidative stress in AD. Production of reactive oxygen species is also known to amplify microglial generation of the pro-inflammatory cytokine, interleukin-1β (IL-1β; Kasama *et al.*, 1989). Increased protein levels of the proinflammatory cytokines IL-1β, tumour necrosis factor-α (TNF-α) and interleukin-8 (IL-8) have been detected in the culture media of human microglia following exposure to Aβ (Lee *et al.*, 2002; Meda *et al.*, 1995). It is important to note that inflammation-related changes in AD brain may also be important in maintenance of function and repair of damage. Many cytokines have been shown to have protective roles, for example, the anti-inflammatory cytokine, IL-10, is thought to promote cell survival and also limit inflammation in the brain by reducing synthesis of proinflammatory cytokines, and suppressing cytokine receptor expression (Strle *et al.*, 2001). In addition, the anti-inflammatory cytokines IL-10, IL-4 and IL-13 have been demonstrated to suppress Aβ-induced production of pro-inflammatory cytokines TNF-α and IL-1β (Szczepanik *et al.*, 2001). Further investigation into the functions of such immune modulating cytokines in the brain may lead to a better understanding of the mechanisms by which a balance of pro-inflammatory and anti-inflammatory cytokines is achieved in the brain and lead to development of therapeutic strategies involving the stimulation of inhibitory cytokine pathways.

1.7 Aβ and apoptosis

Apoptosis is the genetically mediated mechanism by which individual cells orchestrate their own demise in normal and diseased tissues (Kerr *et al.*, 1972). It is an active process requiring gene transcription and synthesis of specific message RNA molecules (Staunton *et al.*, 1998). Necrosis, in contrast is a passive pathological event, which frequently arises from insult or trauma to cells (Behl, 2000). In necrosis no new gene transcription is required. Necrotic cells swell and burst, spilling their contents over neighbouring cells causing a damaging inflammatory response (Raff, 1998). Conversely, apoptosis is characterised by shrinkage of cell, membrane blebbing and chromatin condensation, leading to DNA fragmentation into apoptotic bodies (Behl, 2000). These apoptotic bodies are rapidly phagocytosed by neighbouring cells, before there is any leakage of their contents and thus avoiding an inflammatory response in apoptotic tissue (Williams and Smith, 1993). Apoptosis occurs in all cells as part of normal cellular turnover (Raff, 1998). It is crucial during development and afterwards for maintaining the balance between cell death and cell growth. Apoptosis can be triggered by internal or external stimuli (Blatt and Glick, 2001). External stimuli include binding of death signals such as Fas to death receptors, DNA damage due to chemotherapeutic drugs, generation of oxidative stress, and sustained increase in $[Ca^{2+}]_i$ (Raff, 1998).

Apoptosis can be divided into three main stages (Kreomer, 1997). In the first stage the cell receives an apoptotic stimuli. In the second stage of apoptosis, the cell integrates the various signals and may, or may not, commit to apoptosis (Blatt and Glick 2001). The final stages (known as the post-mortem phase) involve the activation of a common degradative signalling pathway which triggers the morphological features characteristic of apoptosis (Kreomer, 1997). Apoptosis is identified using biochemical methods which detect key events of apoptosis (Behl, 2000). One hallmark of apoptosis is cleavage of intranucleosomal DNA into 180 base pair fragments (bp) yielding the characteristic laddering pattern seen on agarose gels. This DNA fragmentation can also be detected using *in situ* labelling techniques such as TDT-mediated-UTP-end nick labelling (TUNEL) to identify the DNA breaks of apoptotic cells.

It was first proposed that apoptosis participates in the neuropathology of AD by Su *et al* (1994b) when evidence of DNA fragmentation and shrunken cell bodies in

neurons in AD brain was observed. Today the involvement of apoptosis in AD remains controversial with some reports suggesting the primary route to neuronal cell death in AD involves necrosis not apoptosis. In support of a role for apoptosis in AD pathology, increased expression of apoptosis-related proteins, including Bax and caspase-3, have been demonstrated to colocalise with DNA fragmentation in AD brain (Su *et al.*, 1997; Masliah *et al.*, 1998). Exposure to Aβ peptide has been demonstrated to directly induce apoptosis *in vitro* (Forloni *et al.*, 1993; Loo *et al.*, 1993). Furthermore, increased DNA damage and caspase activity, along with alterations in expression of apoptosis-related genes such as Bcl-2 family members, and DNA damage response genes, such as p53, have been found in neurons associated with amyloid deposits in the brains of AD patients (Su *et al.*, 1994; Masliah *et al.*, 1998; De la Monte *et al.*, 1997). Many signals can trigger apoptosis in neurons and the combined effects of increased Ca^{2+} influx, oxidative stress and production of an inflammatory response are thought to be among the factors leading to induction of Aβ-mediated apoptosis in AD (McGeer and McGgeer, 2003; Ekinci *et al.*, 2000). The main focus of this thesis is to characterise apoptotic mechanisms occurring downstream of these initiating events following treatment of cortical neurons with Aβ. The next section will describe the involvement of proteins which are integral to execution of apoptosis.

1.8 The apoptotic pathway

1.8.1 Cytochrome *c*

Mitochondria are suggested to be integrators of apoptotic stimuli; dysregulation of mitochondrial function causes the sequential reduction of transmembrane potential and generation of reactive oxygen species (Zamzami *et al.*, 1995). When the mitochondrial membrane is compromised cytochrome *c* is released. This protein normally resides in the space between the outer and inner membranes of the mitochondria, where it is responsible for electron-transport processes in the mitochondria (Reed, 1997). Once in the cytoplasm however this protein takes on a different function (Raff, 1998), where it binds to an adaptor molecule known as apoptosis protease activating factor 1 (apaf1), in

the presence of ATP, and thus activates the inactive precursor, procaspase-9, to its active form. This leads to initiation of a caspase cascade culminating in activation of pro-caspase-3 to its active form (Li *et al.*, 1997). This series of reactions is known as the mitochondrial pathway of caspase-3 activation. Cytochrome *c* release from the mitochondria has been shown to accompany apoptosis in every circumstance and cell line where it has been studied (Reed, 1997).

1.8.2 Bcl-2 proteins

The Bcl-2 (B-cell leukaemia/lymphoma 2-like proteins) family of proteins, of which 20 members have been identified to date includes members that inhibit apoptosis (Bcl-2, Bcl-xl, Mcl-1, A1, Bag1) and members that promote apoptosis (Bax, Bak, Bad, Bid, Bik, Bcl-xs; Korsmeyer S, 1999; Minn *et al.*, 1998). These cytosolic proteins are key regulators of cell apoptosis by virtue of their ability to regulate the integrity of the outer mitochondrial membrane (Korsmeyer, 1995). The members contain up to four conserved motifs known as Bcl-2 homology domains (BH1-4; Adams and Cory, 1998). The anti-apoptotic members contain all 4 domains, while the pro-apoptotic members possess between 1 and 3 domains. These proteins play a central role in controlling the mitochondrial pathway. They can localise or translocate to the mitochondrial membrane and modulate apoptosis by permeabilistion of the inner/outer membrane resulting in cytochrome-*c* release or stabilising barrier function (Herr and Debatin, 1998). Bcl-2 family members can form homo- and heterodimers through BH domain interaction and thus titrate each others function (Thornberry *et al.*, 1997). This suggests that the relative ratio of pro- and anti-apoptotic members determines whether a cell will live or die. Heterodimerisation is not a requirement for the function of these proteins.

Pro-apoptotic Bax is a cytosolic protein until stimulated by an apoptotic signal when a change in conformation of the protein allows it to translocate to the mitochondrial membrane (Ng and Shore, 1998). Bax is thought to facilitate release of cytochrome *c* by the formation of tetrameric channels in the mitochondrial membrane (Narita *et al.*, 1998) The anti-apoptotic proteins, Bcl-2 and Bcl-xl reside on the cytoplasmic face of the outer mitochondrial membrane (Blatt and Glick, 2001). Bcl-2 is also localised to the endoplasmic reticulum and nuclear membranes (Wolter et al., 1997). One method by

which Bcl-2 and Bcl-xl act to prevent apoptosis is to bind to and sequester Bax, preventing its translocation to the mitochondrial membrane (Mahajan *et al.*, 1998). Changes in levels of expression of the Bcl family of proteins have been reported in Aβ-mediated apoptosis (Tortosa *et al.*, 1998; Zhang *et al.*, 2002).

1.8.3 Caspase Cascade

The main executioners of apoptosis are a family of cysteine proteases called caspases (Thornberry and Lazebnik, 1998). These enzymes participate in a cascade in response to pro-apoptotic signals and bring about cleavage of certain proteins resulting in disassembly of the cell. Caspases were first identified as effectors of apoptosis when studies carried out on the nematode *Caenorhabditis elegans* (*C. elegans*) led to discovery of a gene required for cell death (ced-3; Raff, 1998). The human homolog of this gene is interleukin 1-β-converting enzyme (ICE/Caspase-1). Caspase-1 was the first identified member of this large family of proteases, of which 14 are known to date, whose members have distinct roles in inflammation and apoptosis. Members of the caspase family function as either effectors of apoptosis (cell disassembly) and initiators (initiation of this disassembly; Thornberry and Lazebnik, 1998). Oxidative stress, ultraviolet light, x-rays, and chemotheraputic drugs are known stimuli that activate early phase initiator caspases such as caspase-8, -9 and –10, which proceed to activate executioner caspases such as caspase-3, -6, and –7 (Hofmann, 1999). Caspases are synthesised as inactive pro-enzymes (pro-caspases) mainly in the cytosol. The protein is activated by cleavage at two aspartic acids. The pro-domain is discarded and the large and small subunits form the active enzyme (see Figure 1.5). Activated caspases consist of two large and two small subunits (Raff, 1998). Caspases are extremely specific proteases, cleaving only after an aspartate residue in the substrate.

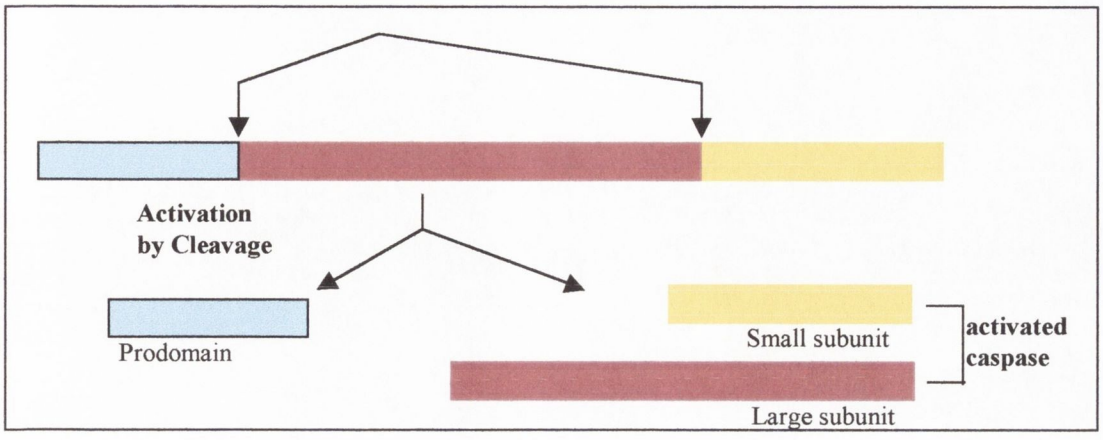

Figure 1.5 Activation of a caspase (adapted from Raff, 1998)

Caspases employ a number of mechanisms to execute apoptosis. One role of the caspases is to inactivate proteins that protect living cells from apoptosis. An example of this is cleavage of Bcl-2 proteins by caspases. Cleavage of Bcl-2 causes inactivation of the anti-apoptotic function of these proteins (Adams and Cory, 1998). Caspases also contribute to apoptosis by disassembling cell structures such as lamina and fodrin, or by cleavage of DNA repair enzymes such as poly (ADP)–ribose polymerase (PARP). Caspase proteins also contribute to apoptosis through reorganisation of the cell structure by cleaving proteins involved in regulation of the cytoskeleton (Kothakota *et al.*, 1997).

The effector caspase, caspase-3 is a key executioner of apoptosis in mammalian cells. Activation of caspase-3 involves cleavage of the 32-kDa inactive precursor protein to the hererodimeric form (17 kDa and 12 kDa; Slee *et al.*, 1999). Caspase-3 can be activated in a number of ways. As mentioned above the mitochondrial pathway of caspase-3 activation involves cleavage of pro-caspase-3 by a complex termed an apoptosome, consisting of caspase-9, Apaf-1, cytochrome *c* and dATP. In addition, caspase-3 is activated by the initiator caspase, caspase-8. Caspase-8 exists in an inactive form coupled to death receptors for TNF-α and Fas ligands. Activation of these death receptors leads to sequential activation of caspase-8 and caspase-3 (Schmitz *et al.*, 2000). Cleavage and thus activation of caspase-3 is also reported to occur by the lysosomal protease cathepsin-L (Ishisaka *et al.*, 1999). Expression levels of caspase-3 is increased in AD (Shimohama *et al.*, 1999; Stadelmann *et al.*, 1999) and several studies carried out *in*

vitro have demonstrated increased activity of caspase-3 in Aβ-treated neurons (Suzuki, 1997; Selznick *et al.*, 1999).

1.8.4 Poly (ADP)-Ribose Polymerase (PARP)

The DNA repair enzyme, poly (ADP)–ribose polymerase (PARP), is a vital substrate of caspase-3. PARP maintains cell survival by facilitating the opening of DNA strands and thus enabling DNA repair enzymes access to broken strands (Alvarez-Gonzalez *et al.*, 1994). The intact PARP enzyme has a molecular weight of 113 kDa, which is cleaved into fragments of 89 kDa and 24 kDa by apoptotic proteases, including caspase-3 (Tewari *et al.*, 1995) and lysosomal proteases (Gobeil *et al.*, 2001). Cleavage of PARP prevents repair of damaged DNA and consequently leads to cell death. PARP cleavage is widely accepted as a hallmark of apoptosis and had been implicated with the neuronal cell death observed in the AD brain (Love *et al.*, 1999).

1.9 Overview of Mitogen Activated Protein Kinases (MAPK)

The mitogen activated protein kinases (MAPK) comprise a family of proteins that are activated by phosphorylation on Serine (Ser) / Threonine (Thr) amino acid residues and in turn activate other kinases giving rise to a signalling cascade. The MAPK cascade is one of the principal intracellular signalling pathways linking activation of cell surface receptors to cytoplasmic and nuclear effectors. MAPK cascades have been strongly conserved through evolution demonstrating their importance in intracellular signalling (Sugden and Clerk, 1997). The three members which have been identified to date are the extracellular response kinases (ERKs), the c-jun-N-terminal Kinases (JNKs), and p38 MAPKs. Each MAPK member is preferentially recruited by distinct extracellular stimuli, therefore allowing the cell to respond in parallel to multiple divergent inputs (Herr and Debatin, 2001). The ERK cascade is involved in regulation of cell growth and differentiation, while JNK and p38 MAPKs are involved in cellular responses to environmental stress (Schaeffer and Weber, 1999).

The activation pathway of all MAPK members includes a linear sequence of activation events, (see Table 1.2), consisting of a three kinase cascade during which MAPK enzymes are activated by Thr and Tyrosine (Tyr) phosphorylation catalysed by a family of dual specificity kinases known as MAPK kinases (MEKs). MEKs in turn are regulated by Ser / Thr phosphorylation catalysed by several protein kinase families collectively referred to as MAPK-kinase-kinases (MAPKKKs; Schaeffer and Weber, 1999).

MAPKs are proline (pro)-directed kinases, that preferentially phosphorylate the consensus sequence Pro-Xaa-Ser/Thr-Pro or Ser/Thr-Pro in substrate proteins (Davis, 1993). Although the kinase cascade leading to activation of JNK is distinct from the kinase cascade leading to ERK, there is also potential for cross-talk between these cascades at each level of the signal transduction cascade, due to the fact that MAPK members share a common phosphorylation sequence. Consequently, the MAPK kinase, JNK kinase (JNKK) activates not only JNK, but also ERK (Minden and Karin, 1997).

Stimulus	Growth Factors	Inflammatory Cytokines Cellular Stresses
MAPKKK	Raf /Ras	MEKK MLK/DLK TAK ASK
MAPKK	MEK 1 / 2	MKK4/7 MKK3/6
MAPK	ERK 1 / 2	JNK P38
Responses	Proliferation,Differentiation Development	Inflammation, Apoptosis Development

Table 1.3 Activation sequence of the MAPK signalling cascade (Lee and MCubrey, 2002)

1.9.1 Extracellular Response Kinase (ERK)

The archetypical ERK signalling pathway was the first MAP kinase cascade to be characterized. The ERK family were originally identified as protein kinases which phosphorylated microtubule-associated protein 2 (MAP-2) and were initially referred to as MAPK. However, with further investigation it became clear that the MAPK cascade was a prototype for a family of signalling cascades and the term MAPK was used to describe the entire superfamily of signalling pathways consisting of ERK, JNK and p38 MAPK (Sweatt, 2001). There are 3 isoforms of ERK denoted ERK 1 (p44), ERK2 (p42) and ERK3 (p62) (Boulton *et al.*, 1990). ERK 1 and ERK2 are highly expressed in the brain (Miyasaka *et al.*, 1990), and have been shown to be essential for cellular growth and proliferation, acquisition and maintenance of a differentiated phenotype as well as apoptosis (Marshall, 1995; Schaeffer and Weber, 1999).

Activation of the ERK cascade is typically regulated through receptor tyrosine kinases and involves activation of the small G protein, Ras, leading to activation of the MAPKKK, Raf-1 (Schaeffer and Weber, 1999). Downstream activation by the dual

function kinases MEK1/MEK2 stimulates ERK. Upon activation ERK translocates to the nucleus where it acts to phosphorylate its nuclear substrates.

ERK1 and ERK2 have a wide range of substrates. Nuclear substrates include cAMP-responsive element binding protein (CREB), ELK-1 (Marais *et al.*, 1993) and RNA polymerase II (Dubois *et al.*, 1994). ERK1 and ERK2 also phosphorylate structural proteins such as MAP2 and tau while cytoplasmic substrates mainly include translation factors. A number of recent studies have implicated ERK activation in Aβ-induced cell death (Rapoport and Ferreira, 2000; Ekinci *et al.*, 1999a; Pyo *et al.*, 1998) This involvement of ERK is controversial with other studies disputing the role of ERK in this neurodegrative pathway (Abe and Saito, 2000). The effect of Aβ on ERK activation will be assessed in this thesis.

1.9.2 c-jun-N-terminal kinase (JNK)

JNK signalling has been implicated in a variety of cellular responses, including proliferation, differentiation, and cellular stress-induced apoptosis (Herr and Debatin, 2001). The effects of JNK on cellular responses appear to depend on cell type and the context of other signals received by the cells. JNK kinase proteins are encoded by three different genes - *jnk1, jnk2 and jnk3*. The *jnk1* and *jnk2* genes are ubiquitously expressed while *jnk3* gene is predominantly expressed in the brain, and to a lesser extent in the heart and testis (Gupta *et al.* 1996). The transcripts of all 3 genes can be alternatively spliced with 2 splicing variants of the 3′ end (Mielke and Herdegen, 2000). The spliced transcripts of *jnk1* and *jnk2* genes can encode proteins of 46kDa and 54kDa while the spliced transcripts of *jnk3* gene encodes larger protein isoforms of 48kDa and 57kDa. JNK is widely expressed in the nervous system (Mielke and Herdegen, 2000).

Studies of mice deficient in JNK1, JNK2, and JNK3 provide evidence for the functional diversity of isoforms, with mice deficient in JNK1 and JNK2 being embryonically lethal (Kuan *et al.*, 1999) and mice deficient in JNK3 displaying decreased susceptibility to kainic acid-induced hippocampal cell death (Yang *et al.*, 1997). There is growing evidence to suggest that JNK isoforms have differing specificities for downstream transcription factors (Gupta *et al.*, 1996, Yin *et al.*, 1997) suggesting distinct physiological roles of each JNK isoform.

JNK proteins are anchored and retained in the cytoplasm by proteins known as JNK interacting proteins (JIPs ; Dickens *et al.*, 1997). These proteins act as a scaffold and mediate signal transduction through upstream kinases leading to final activation of JNK (Whitmarsh *et al.*, 1998). Following dissociation from the retaining JIP anchor complex JNK can translocate to the nucleus where they associate with their substrates (Gupta *et al.*, 1995). JNK1 and JNK2 are activated by phosphorylation at their threonine and tyrosine residues in positions 183 and 185 (Mielke and Herdegen, 2000). Activated JNK molecules phosphorylate both nuclear and cytoplasmic substrates (Figure 1.6).

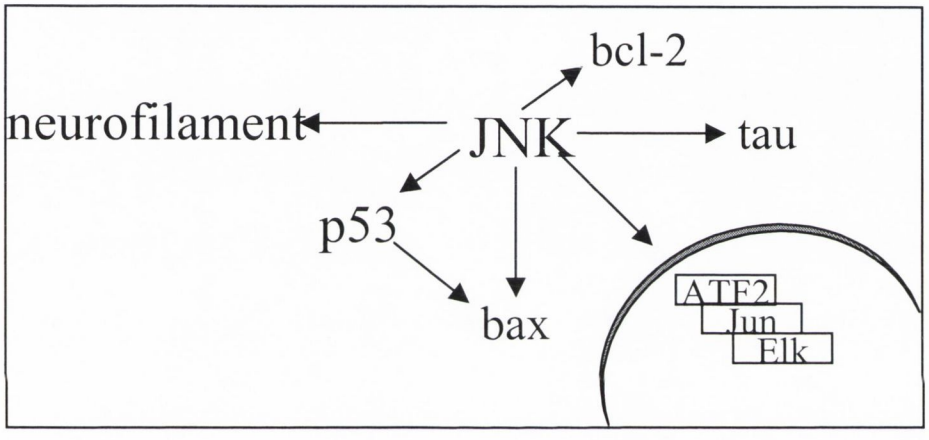

Figure 1.6 Cytoplasmic and Nuclear Substrates of JNK

Nuclear substrates of JNK include transcription factors c-jun (Herdegen *et al.*, 1997), activating transcription factor 2 (ATF-2; Gupta *et al.*, 1995) and ELK-1. So far the JNK family are the only kinases that phosphorylate c-jun at residues ser63 and ser73 and it was this property that led to their identification (Hibi *et al.*, 1993). Once phosphorylated these transcription factors act to regulate gene expression in response to cytokines, growth factors and other cellular stress stimuli. JNK also phosphorylates cytoplasmic substrates such as the tumour suppressor protein, p53 (Fuchs *et al.*, 1998), Bcl-2 (Park *et al.*, 1997), and cytoskeletal proteins such as tau. JNK can target p53 for ubiquitin-mediated degradation (Fuchs *et al.*, 1997) or can stabilise p53 by phosphorylation, thus inhibiting ubiquitin-mediated degradation (Fuchs *et al.*, 1998). These opposing effects of JNK on p53 expression are dependent on the p53 residue phosphoryhated by JNK. This demonstrates an important regulatory function of JNK.

JNK is also proposed to phosphorylate anti-apoptotic proteins Bcl-xl and Bcl-2 leading to inactivation of their cell protective functions (Park *et al.* 1997).

JNK can be linked to both neuroprotection and neurodegeneration (Herdegen *et al.*, 1997) with the final outcome, death or survival, depending on cellular context and the suitability of the surrounding environment, for example the availability of trophic molecules. There is increasing evidence that JNK proteins are potent effectors of apoptosis since JNK has been implicated as a mediator of cell death in response to a variety of stimuli including growth factor deprivation and oxidative stress (Eilers *et al.*, 2001; Yoshizumi *et al.*, 2002). One of the earliest studies implicating JNK in apoptosis demonstrated that sustained activation of JNK occurred in PC12 cells upon NGF withdrawal, and this was correlated with the resulting cell death which ensued (Xia *et al.*, 1995). A number of recent studies have proposed that Aβ mediates neuronal apoptosis through activation of JNK (Morishima *et al.*, 2001; Shoji *et al.*, 2001; Troy *et al.*, 2001). However, the identity of the JNK isoforms involved in Aβ-triggered cell death remain to be elucidated and will be addressed in this study.

1.10 p53

The tumour suppressor protein, p53, is critical in regulation of the cell cycle. It is a DNA-binding protein involved in regulating the expression of genes involved in cell cycle arrest and apoptosis (Levine, 1997). p53 can be referred to as the gate keeper of the cell; on mediation of cell cycle arrest it functions to integrate cellular responses promoting either cell repair or apoptosis depending on state of the cell and type of inducing stimulus (Levine, 1997). However, since most neuronal cells exist in a post-mitotic state, the cell cycle regulatory function of p53 is effectively redundant in these cells (Miller *et al.*, 2000). Therefore, in post-mitotic DNA damaged cells, p53 is associated with cell death mechanisms, rather than recovery (Enokido *et al.*, 1996). While the primary stimulus for activating p53 is DNA damage, it is also activated in response to other cell stresses such as heat shock, UV irradiation, oxidative stress and osmotic shock (Herr and Debatin, 2001). The induction of cell cycle arrest by p53 depends on its activity as a sequence-specific transcriptional activator and the $p21^{waf1}$ protein appears to be a major effector of p53 mediated G1 cell cycle arrest after DNA damage (Zörnig *et al.*,

2001). $p21^{waf1}$ damage exerts its effect by binding to and inhibiting cyclin-dependent kinases, thereby blocking cell proliferation. In contrast, p53-mediated apoptosis involves both transcriptional activation-dependent and independent pathways (Attardi *et al.*, 1996).

Normally p53 protein is kept at low concentrations within the cell due to its short half-life (20 minutes). Within the cell the oncoprotein, Mdm2, binds to p53 and negatively modulates its activity by targeting p53 for ubiquitin-mediated proteolysis and inhibiting the transcription factor function of p53 (Zörnig *et al.*, 2001). In response to DNA-damage or cellular stress, p53 becomes stabilised resulting in an increase in intracellular p53 concentration. It is suggested that in response to cellular stress p53 becomes phosphorylated on a critical serine residue in the Mdm2 binding domain of p53 thus disrupting Mdm2 / p53 binding and preventing p53 degradation (Evan and Littlewood, 1998). Interestingly Mdm2 is a p53-induced gene, and Mdm2 levels increase following p53 activation (Levine, 1997). Mdm2 in turn inactivates p53 thus forming a negative feedback loop. Phosphorylation of p53 is critical in the regulation of this pathway and a large number of kinases can phosphorylate p53, including ERK and JNK (Blatt and Glick, 2001).

A number of different mechanisms have been suggested by which p53 protein may signal to apoptotic machinery. At the gene level p53 has been shown to upregulate transcription of Bax and to repress Bcl-2 transcription in certain cell types, thus altering the Bcl-2/Bax ratio and favouring mitochondrial mediated apoptosis (Miyashita and Reed, 1995). Reactive Oxygen Species (ROS) may be produced by the p53-inducible gene, PIG3, resulting in apoptosis (Johnson *et al.*, 1996). Transcriptionally independent mechanisms of p53-mediated apoptosis include increased surface expression of CD95, thus sensitising cells to CD95-induced apoptosis (Bennet *et al.*, 1998) and direct signalling at the mitochondria (Marchenko *et al.*, 2000) resulting in cytochrome *c* release and apoptosis. Figure 1.7 demonstrates substrates of p53 involved in regulation of the cell cycle and apoptosis.

p53 accumulation has been linked to the neuronal apoptosis characteristically seen in Alzheimer's disease in a number of studies (de la Monte *et al.*, 1997; Laferla *et al.*, 1996; Culmsee *et al.*, 2001). The exact intracellular mechanism by which p53-mediated neurodegeneration may occur has yet to be fully investigated but increased expression of

the pro-apoptotic gene *bax* has been suggested as one possible mechanism (Culmsee *et al.*, 2001). In this thesis the role of p53 in Aβ-mediated apoptosis of cortical neurons will be examined and the mechanisms underlying p53 activation will be ascertained.

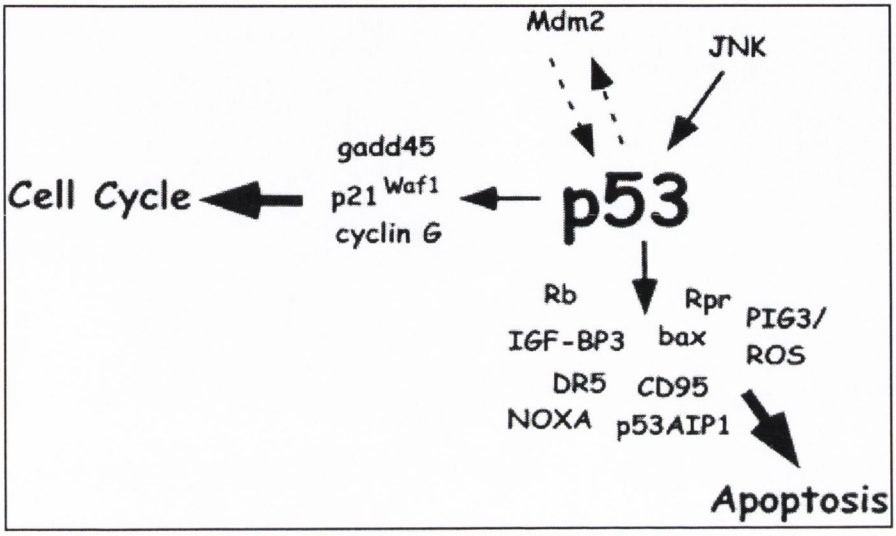

Figure 1.7 Substrates of p53 (Herr and Debatin, 2000)

1.11 Lysosomes and apoptosis

Lysosomes are membrane bound, acidified, cytoplasmic organelles centrally involved in the normal functioning of the neuronal cell (Nixon and Cataldo, 1995). Lysosomes are normally concerned with the digestion of cell nutrients, cell protein turnover, tissue remodelling, lysis of invaders, and autolysis of dead cells (Yamashima *et al.*, 1998). Lysosomes contain over 40 hydrolytic enzymes, which are mostly active only in acidic conditions (Ditaranto-Desmisome *et al.*, 2002). These hydrolytic enzymes function in break down of damaged macromolecules into smaller subunits that can be utilized by the cell for its own biosynthesis (Cataldo *et al.*, 1996). The acidic pH of lysosomes is preserved by the presence of H^+/ATPase pumps contained in the lysosomal membrane (Geisow, 1982). These pumps function via ATP-dependent active transport of H^+ ions through the concentration gradient from the cytosol to the lysosomal interior. In this way the physiological pH of the cytosol is also maintained. Lysosomes also function as intracellular Ca^{2+} regulators helping to maintain cellular calcium homeostasis (He *et al.*, 2002). The lysosomal membrane is composed of a phospholipid bilayer which allows passage of uncharged molecules. However, upon entry to the lysosomes these molecules become protonated and are prevented from passing through the hydrophobic layers and so become trapped.

Two types of lysosomes are present in the cell – primary lysosomes and secondary lysosomes. Primary lysosomes are homogenous in content containing acid hydrolases, but no digestible substrates. Secondary lysosomes are heterogenous in content and may contain pieces of enzymes, granules and parts of mitochondria inside. The ingestion of material into primary lysosomes sees its transition from a primary to a secondary lysosome. The lysosomal pH becomes more acidic leading to activation of the hydrolytic enzymes followed by digestion of the ingested material. There are two main methods by which lysosomes function, termed heterophagy and autophagy. Heterophagy is the digestion within a cell of an exogenous substance, such as a bacterium, phagocytosed from the cell's environment. Autophagy is used to recycle damaged or worn out organelles, such as mitochondria, within the cell. The lysosomal system can contribute to cell death in a number of ways, including excess autophagy, accumulation

of secondary lysosomes or residual bodies, rupture of the lysosomes or lysosome dysfunction (Yamashima *et al.*,1998).

The lysosomal membrane is known to be a physical barrier that protects the hydrolytic enzymes from digesting the cells own cytoplasmic components. Among the enzymes contained in the lysosomes are amylases (hydrolyse polysaccharides to starch or glucose), lipases (digest lipids to fatty acids and glycerol) and proteases (hydrolase proteins to amino acids; Adler, 1989). Lysosomal membrane disruption, with resultant leakage of lysosomal hydrolases to the cytosol, has a great potential for killing cells and lysosomal leakage has been implicated in apoptosis (Brunk *et al.*, 2001). Amongst the proteases found in lysosomes, the cathepsin family are the most prevalent. Cathepsins belong to a family of papain-like cysteine (cathepsin-B, -L, -S, -C, -K, -H, O, F, V, X) and aspartyl cleaving (cathepsin-D, E) hydrolytic enzymes (Turk *et al.*, 2000).

1.11.1 Cathepsin-L

Cathepsin-L is a broad-spectrum papain-like cysteine protease, potent in degrading extracellular proteins such as laminins and fibronectin, serum proteins, cytoplasmic proteins, such as caspase-3, and nuclear proteins (Barrett and Kirschke, 1981). Cathepsin-L is responsible for most of the intralysosomal breakdown of normal cells and is synthesised as an inactive proenzyme (31 kDa) preventing its premature activity. Conversion to the active enzyme (27 kDa) occurs intracellularly in the lysosomes at pH 3-3.5 by autocatalytic removal of the prosegment and extracellularly at pH 5.5-6.0 (Turk *et al.*, 1999; Mason and Massey, 1992). Cathepsin-L activity is normally localised to endosomes/lysosomes but can also be found in the nucleus (Keppler *et al.*, 1996).

There is increasing evidence to suggest the involvement of the lysosomal system in AD. In the brain, membrane stability of neuronal lysosomes is reduced as a result of aging (Nakamura *et al.*, 1989) and in AD (Bowen *et al.*, 1973). In addition, the endosomal-lysosomal system in AD brain is markedly altered (Cataldo *et al.*, 1996). One mechanism by which lysosomal function is thought to be compromised in AD is by increased uptake of Aβ peptide by endosomes / lysosomes, leading to oxidative stress and lysosomal leakage (Yang *et al.*, 1998). Another possible route to disruption of

lysosomes is due to increased $[Ca^{2+}]_i$ leading to release of lysosomal enzymes (Yamashima *et al.*, 1998). A recent report by Ji *et al* (2002) has demonstrated that $A\beta_{1-42}$ promotes lysosomal membrane instability and subsequent apoptosis in a neuronal cell line. In addition, Aβ has been demonstrated to increase cytosolic expression and activity of cathepsin-L in cultured neurons and the proclivity of Aβ to induce neurodegenerative changes, such as caspase-3 activation, and PARP cleavage, were prevented by inhibition of cathepsin-L (Boland and Campbell, 2003b). This study will investigate the impact of Aβ on the lysosomal system and will identify signalling molecules that couple Aβ to the regulation of the lysosomal branch of the apoptotic pathway.

1.12 Cytokines and Alzheimer's disease

Cytokines are multifunctional, pleiotropic proteins that play crucial roles in cell-communication and cellular activation. They comprise a large family of polypeptides including interleukins, chemokines, tumour necrosis factors, interferons, growth and cell stimulating factors and neurotrophins (Rothwell, 1999). Cytokines in the cental nervous system (CNS) have two possible origins: cytokines that originate from the peripheral immune system can access the CNS by crossing at leaky areas of the blood-brain barrier through the circumventricular organs (Watkins *et al.*, 1995), or cytokines can be produced endogenously by neuronal and glial cells within the CNS (Szelényi, 2000). Most cytokines are expressed at low or undetectable levels in the healthy adult brain, however they are rapidly induced in response to injury of infection (Hopkins and Rothwell, 1995). Cytokines have diverse actions in the brain, some of which may facilitate either neuroprotection or neurodegeneration. Cytokine classification can be split into pro-inflammatory and anti-inflammatory depending on the final balance of their effects in inflammation. Pro-inflammatory cytokines include interleukin-1 (IL-1), tumour necrosis factor-α (TNF-α), interleukin-6 (IL-6), interleukin-12 (IL-12), interleukin-18 (IL-18) and interferon-γ (IFN-γ; Watkins *et al.*, 1995). Anti-inflammatory cytokines include interleukin-4 (IL-4), interleukin-10 (IL-10) and interleukin-13 (IL-13). Cytokines exert their function in the CNS through engagement with their receptors (Farrar *et al.*, 1987; Sawada *et al.*, 1993) and through modulation of neurotransmitter function (Coogan and O' Connor, 1997). The shift of cytokine balance towards the side of pro-inflammatory cytokines like IL-1 and TNF-α is closely related to the process of neurodegeneration (Szelényi, 2000).

AD brain is characterised by neuroinflammatory changes, which are observed in both sporadic and familial AD (McGeer and McGeer, 2001). Although the role of neuroinflammation in the pathological process of AD is not yet fully understood, there is evidence for the involvement of inflammation at a number of stages in the disease. There is evidence to suggest that inflammatory mechanisms occur early in the pathological cascade, contributing to production and fibrillisation of Aβ; IL-1 and TNF-α have been demonstrated to regulate synthesis of APP and production of Aβ-peptides *in vitro*

(Rogers *et al.*, 1999; Blasko *et al.*, 1999). In addition, deposits of Aβ can induce a microglia-mediated inflammatory response resulting in further production of inflammatory cytokines, thus exacerbating the inflammatory response. Pro-inflammatory cytokines that are upregulated in AD brain include TNF-α, IL-1β, IL-1α and IL-6 (McGeer and McGeer, 2003). There is much debate as to whether activated microglia are beneficial or harmful in AD. While highly activated microglia produce neurotoxic substances such as the pro-inflammatory cytokines, they can also be beneficial because of their phagocytic potential to clear Aβ deposits (McGeer and McGeer, 2001). The harmful versus beneficial effects of microglial activation are likely to depend on the degree of activation. One of the most promising therapeutic avenues for AD treatment involves either active or passive immunisation with subunits of the Aβ peptide, leading to production of antibodies to Aβ which promote microglial clearance of Aβ (Bard *et al.*, 2000) or redistribution of the Aβ peptide from the brain (DeMattos *et al.*, 2001).

1.12.1 Interleukin-1β (IL-1β)

The interleukins are one of the most abundant cytokines in mammalian systems. There are, to date, 23 characterised interleukins which variously possess both anti- and pro-inflammatory cytokines (Rothwell, 1999). The interleukin (IL-1) family of interleukins are pro-inflammatory cytokines that orchestrate inflammatory and host defence responses (Mrak and Griffin, 2001). There are at least three known forms of IL-1 proteins that are the product of separate genes – IL-1α, IL-1β and IL-1γ. IL-1α and IL-1β are partially homologous isoforms that can induce signals by binding to their receptors (IL-1RI and IL-1RII). IL-1β represents the major secreted molecule and the predominant form of IL-1 found in the CNS (Dinarello, 1996). Synthesised as an inactive precursor of 32 kDa, pro-IL-1β requires cleavage by a specific IL-1β converting enzyme (ICE or caspase-1) to give the active form. Constitutive expression of IL-1β in the brain occurs in neurons, astrocytes, oligodendrocytes and endothelial cells.

IL-1β is usually expressed at low levels in healthy adult brain (Vitkovic *et al.*, 2000). In response to local brain injury or insult IL-1β is overexpressed by microglia. Increased expression of IL-1β has been linked with neurodegenerative disorders like

Down Syndrome and Alzheimer's disease (Griffin *et al.*, 1989) and IL-1β triggers cell death in mixed neuronal/glial cultures (Hu *et al.*, 1997). In addition, IL-1β has been proposed to contribute to increased synthesis of APP and deposition of Aβ in neurons (Forloni *et al.*, 1992; Rogers et al., 1999). Increased production of Aβ in turn activates microglia cells to release more IL-1β (Araujo and Cotman, 1992), thus exacerbating AD progression. It is now known that 78% of plaques containing aggregated Aβ peptide contain IL-1β immunoreactive microglia, demonstrating the importance of IL-1β in this disease. The effects of IL-1β, along with Aβ, on apoptosis-related genes will be examined in this thesis.

1.12.2. Tumour Necrosis Factor-α (TNF-α)

TNF- α is one of the main proinflammatory cytokines that plays a central role in initiating and regulating the cytokine cascade during an inflammatory response (Wallach *et al.*, 1999). It participates in local and systemic events involving inflammation. Along with interferon gamma (IFN-γ), TNF-α is a potent paracrine stimulator of other inflammatory cytokines, including IL-1, IL-6, and IL-8. Expression of TNF-α mRNA is present at low levels or absent in the normal brain (Vitkovic *et al.*, 2000), but is rapidly induced in response to injury. It had been detected in the hypothalamus, hippocampus, cortex, cerebellum and brainstem of normal rat brain. The biological effects of TNF-α are mediated by binding to its two main receptors, the p55 TNF receptor (TNFR1) and the p75 TNF receptor (TNFR2). TNF-α is produced by neurons, microglia, and astrocytes (Breder *et al.*, 1993). In a diseased state, TNF-α along with a variety of pro-inflammatory mediators and neurotoxic substances are produced by activated microglia. In astrocytes, TNF-α, along with other substances, is a strong inducer of pro-inflammatory IL-6 (Van Wagoner *et al.*, 1999). TNF-α also activates the transcription factor, NF-κB, which in turn stimulates the transcription of more TNF-α (Mattson and Camandola, 2001). TNF-α induces apoptosis in a number of cell types via the TNFR1 receptor (Wallach *et al.*, 1999). The TNFR2 receptor, which has a higher affinity for TNF-α can enhance TNFR1 mediated apoptosis. It is important to note that TNF-α does not cause cell death in normal rat brain, but can mediate cell death in damaged tissue (Szelenyi, 2000).

Expression of TNF-α is upregulated in AD brain (McGeer and McGeer, 2003). TNF-α had been reported to increase production of Aβ and inhibit production of neuroprotective soluble amyloid precursor proteins (sAPPs; Blasko *et al.*, 1999).

1.12.3 Nuclear Factor-kappaB (NF-κB)/ Inhibitor-kappaB (IκB)

The transcription factor, NF-κB, is implicated in the regulation of genes involved in immune and inflammatory responses, as well as in the control of genes involved in cell growth, differentiation and apoptosis (Denk *et al.*, 2000). The NF-κB transcription factor family consists of 5 members to date, Rel A, Rel B. c-Rel, p105/-50 ($NF\text{-}\kappa B_1$) and p100/p52 ($NF\text{-}\kappa B_2$) characterised by the presence of a Rel homology domain (RHD) which functions in DNA binding, dimerisation, and interactions with IκB forms. Active DNA-binding NF-κB consists of a hetero- or homodimer of two NF-κB subunits. The most intensively studied NF-κB dimer, referred to as classic NF-κB consists of a dimer containing RelA and p50 (Baldwin, 1996). A primary level of control for NF-κB is through interactions with the inhibitor protein, IκB. IκB is responsible for sequestering the NF-κB/IκB complex in the cytoplasm due to masking the nuclear translocation sequence of NF-κB. NF-κB is activated by cytokines including TNF-α and IL-1 (McGeer and McGeer, 2001). Activation of NF-κB by distinct inducers results in degradation of IκB, with subsequent translocation of NF-κB to the nucleus, where it activates transcription of its target genes including pro-inflammatory TNF-α and the transcription factor p53 (Baldwin, 1996). In the rat CNS a high level of constitutive NF-κB activity is detected in neurons and glia of the hippocampus and cerebral cortex (Denk *et al.*, 2000). In AD brain tissue, increased activity of NF-κB is detected in affected areas of the hippocampus and cerebral cortex (Terai *et al.*, 1996) and NF-κB activity is detected in the centre of primitive plaques and in neurons and astroglia surrounding these early plaque stages (Kaltscmidt *et al.*, 1997). Aβ has been demonstrated to activate NF-κB in neuroblastoma cells and primary cultures of cerebellar granule cells (Behl, 1994; Kaltscmidt *et al.*, 1997). While it remains to be resolved whether the role of NF-κB in AD is one of neuroprotection or neurodegeneration, the observation of a dramatic decrease in NF-κB activity from early

to late plaque stages in the cells surrounding plaques in AD brain in comparison to healthy controls suggests that loss of NF-κB activity may be important for the neurodegeneration observed in late plaque stages (Kaltschmidt *et al.*, 1999). The effect of Aβ on mRNA expression of NF-κB and IκB will be examined in this study.

1.13 Antisense Technology

The fundamental concept of Antisense Technology is to utilise precise nucleic acid sequences to down-regulate specific gene expression, in the cells of interest. Antisense is an important tool for studying the effects of individual proteins in normal and abnormal cellular states as well as having enormous therapeutic potential. It is useful in investigating the function of a particular protein when no inhibitors of this protein are available or when existing inhibitors do not distinguish between isoforms of a protein. Since there are no available inhibitors that distinguish between isoforms of the stress activated protein kinase, JNK, antisense oligonucleotides targeted to specific isoforms of JNK were employed in this thesis. During the normal process of protein expression a particular gene sequence is transcribed into mRNA in the nucleus. Newly synthesised mRNA then passes through the rough endoplasmic reticulum and carries the information to the protein building apparatus of the cell (the ribosome) where it is decoded and translated into protein. Antisense oligonucleotide (ASO) technology uses single stranded RNA or DNA to alter the intermediatory metabolism of specific mRNA, thereby modulating the transfer of information from gene to protein in a sequence-specific manner (Scanlon *et al.*, 1995). Antisense oligonucleotides are designed to hybridise to their specific target, causing a steric or conformational obstacle for protein translation. As a result the production of a specific protein is temporarily inhibited with out effecting the expression of other genes.

The specificity of antisense derives from the selectivity of Watson-Crick base pairing (adenine nucleic acid residues form complementary base pairs with thiamine (DNA) or uracil (RNA) via hydrogen bonding while guanine forms complementary base pairs with cytosine; Watson and Crick, 1953). The decrease in affinity/specificity associated with a mismatch base pair varies depending on position of the mismatch in the region of complementarity and the sequence surrounding the mismatch. A single base mismatch can result in a change in affinity of approximately 500 fold (Crook, 1996).

The most common type of interaction for designed antisense experiments involves the introduction of short (15-30 base pairs) DNA sequences which interact with the cells mRNA before translation. Administration techniques for efficient uptake of antisense oligonucleotides are similar to gene delivery techniques, including microinjection,

electroporation, endocytosis and liposome encapsulation. Electroporation subjects cells to a short electrical pulse which induces the formation of transient pores in the cell membrane, allowing the antisense oligonucleotides to enter the cell. Microinjection makes use of a fine pipette to inject antisense oligonucleotides directly into the cell. While this is a very efficient method of antisense delivery, it is a relatively slow process, with high precision being necessary to inject small cells such as neurons. The simplest method of introducing antisense oligonucleotides to the cell is via the natural process of receptor-mediated endocytosis. In a cell culture system the negatively charged antisense oligonucleotides are added to the supernatant medium and are taken up into the cells by active transport mechanisms. Uptake of antisense oligonucleotides can be enhanced by pre-incubation of the oligonucleotides with a cationic lipid formulation such as lipofectin transfection reagent. This cationic charge masks the anion charge of the ASO backbone, allowing the lipid/ASO complex to pass the cell membrane efficiently and quickly. Within the cells the oligonucleotides are first entrapped in the endosomes but are steadily released into the cytoplasm where they can bind specifically to target mRNA sequences.

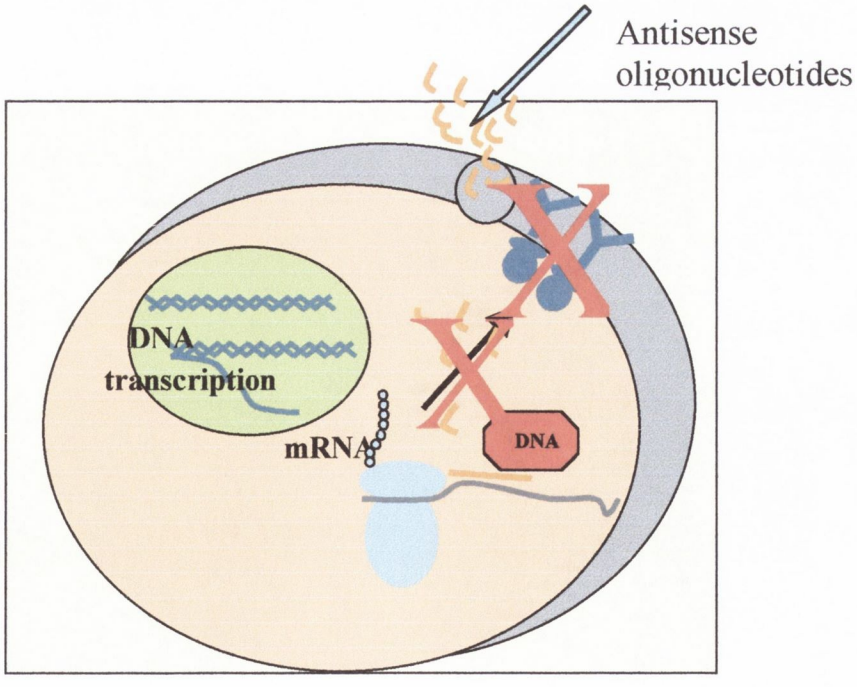

Figure 1.8 Antisense oligonucleotides bind to specific sequences of mRNA to prevent translation of that protein

There are three known mechanisms of inhibiting gene expression utilized by antisense technology – RNase H degradation, translational arrest and modulation of RNA processing. The primary mechanism for most antisense oligonucleotides is the specific enzymatic degradation of the target mRNA through activation of Rnase H after hybridisation to an antisense oligonucleotide. Rnase H comprises a family of ribonucleases that specifically cleave the RNA component of RNA-DNA duplexes (Walder and Walder, 1998). RNase H is found in both the nucleus and the cytoplasm of all cells, and its name is derived from the ability to cleave RNA that is found in an RNA:DNA hybrid. The RNA-DNA duplex resulting from the interaction of the antisense oligonucleotide with the mRNA provides an ideal substrate for RNase H (Minshull and Hunt, 1986). Post-cleavage, the antisense oligonucleotide is free to hybridise to another RNA transcript.

Translational arrest involves attachment of the oligonucleotide to the 5′ capping site of mRNA, thereby inhibiting the binding of translation initiation factors such as eif-4α and disrupting the capping reaction which is necessary for stabilisation of pre-mRNA (Baker *et al.*, 1992). This leads to disruption of the initial interaction between the mRNA and the ribosome 40S sub-unit. Splicing arrest occurs when antisense oligonucleotides bind to regions of the required pre-mRNA sequence, just after transcription, and prevent them from being spliced and processed into functional mRNA.

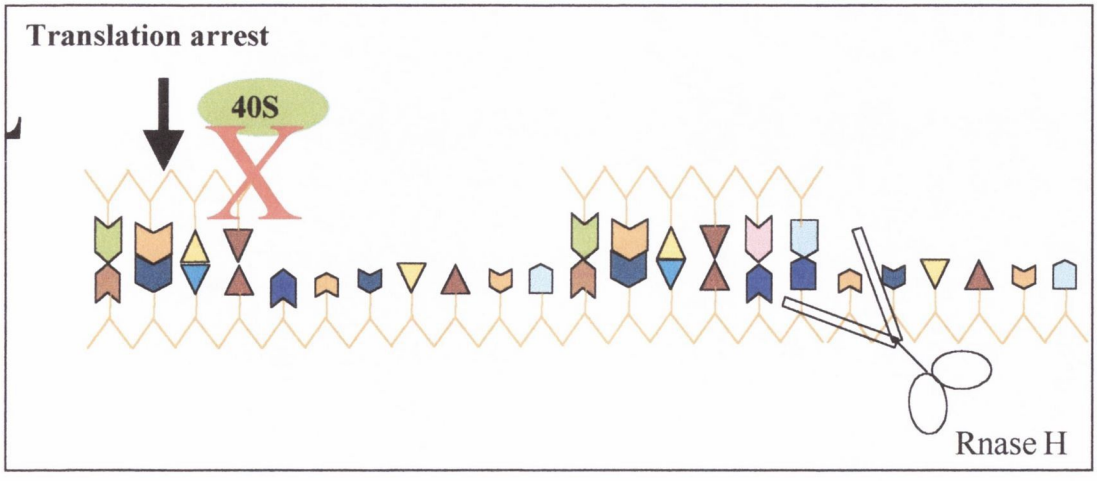

Figure 1.9 Mechansims of antisense-mediated inhibition of gene expression

Natural oligonucleotides consist of phosphodiester links. These phosphodiesters are extremely sensitive to nucleases present in serum and intracellularly with the half-life of unmodified natural oligonucleotides being about 30 minutes (Crook *et al.*, 1992). To try and increase oligonucleotide stability various chemical modifications have been introduced to the phosphate backbone of antisense oligonucleotides. Phosphorothioate oligonucleotides contain sulphur in place of one of the oxygen atoms in the DNA backbone. These phosphorothioates are highly resistant to exo- and endonucleases and are effective at low micromolar concentrations. They have a half-life of 48 hours in 10 % serum and are the only antisense drugs which have been approved by the FDA. In this study we have chosen a phosphorothioate oligodeoxynucleotide as a means to deplete JNK1 and JNK2 in rat cultured cortical neurons.

1.14 Aims

The aim of this project is to investigate the cellular and molecular mechanisms involved in $A\beta_{1-40}$-induced cell death in rat primary cultured cortical neurons.

- The effect of Aβ on phosphorylation of the mitogen activated protein kinase members, JNK and ERK, will be assessed by western immunoblotting using phospho-specific antibodies. To differentiate between isoforms of JNK, cells will be transfected with antisense oligonucleotides targeted to JNK1 and JNK2, and the role of JNK1 and JNK2 in the Aβ-mediated activation of the apoptotic cascade will be elucidated. Targets for investigation as markers of cell death include caspase-3 activation, PARP cleavage and DNA fragmentation.

- The effect of Aβ on the transcription factor, p53, a substrate for JNK, will also be ascertained. The effect of Aβ on the mRNA expression and phosphorylation status of p53 will be determined using RT-PCR and western immunoblotting. p53 will be inhibited using the selecive inhibitor, pifithrin-α, to determine the role of p53 in Aβ-mediated apoptosis. The effect of Aβ on mRNA and protein expression of pro-apoptotic Bax, a p53 substrate, will be investigated.

- In order to examine the effect of Aβ on subcellular distribution of p53 and Bax, intracellular localisation of these proteins will be carried out in conjunction with mitochondrial and lysosomal specific markers Also, the effect of Aβ on lysosomal membrane integrity will be assessed and the cytosolic activity of cathepsin-L will be quantified as an index of lysosomal destabilisation.

- The role of the L-type voltage dependent calcium channel (VDCC) in the Aβ-mediated activation of JNK, p53 and cathepsin-L activity will be examined. The role of the L-type VDCC in he later neurodegenerative changes (caspase-3 activity, DNA fragmentation) will also be ascertained.

- The mRNA expression of the pro-inflammatory cytokine, TNF-α, and the transcription factors NF-κB, and IκB, will be assessed as an indication of the inflammation-related changes which occur in Aβ-treated neurons. The effect of the pro-inflammatory cytokine, IL-1β, on mRNA expression of apoptosis-related genes *caspase-3*, *bax* and *bcl-xl* will be determined.

Overall this study will identify the signalling events which play a part in Aβ-induced neurodegeneration, with particular reference to the interaction between Ca^{2+} influx, activation of the JNK/p53 pathway, lysosomal destabilisation and late-stage apoptotic features, such as caspase-3 activation and DNA fragmentation.

Chapter 2

Materials and Methods

2.1 Cell Culture

2.1.1 Aseptic Technique

The use of sterile technique in cell cultivation is essential to prevent bacterial and fungal infection. The principle of aseptic technique is to keep sterile the internal areas of culture flasks, bottles and and any implements/plastics that cells may be exposed to. The following aseptic technique procedures were adhered to for all cell culture manipulations.

2.1.2 Sterilisation of glassware, plastics and dissection instruments.

All glassware, pipette tips, dissection instruments, deionised H_2O and microfuge tubes (Sarstedt, Leicester, England) were wrapped in aluminum foil and autoclave tape (Sigma-Aldrich, Dorset, England) and then autoclaved at 121°C for 20 min (Priorclave Ltd., Model #EH150, London, England) before being wiped down with 70 % ethanol (EtOH) and placed in the laminar flow hood. All equipment used in the dissection procedure was oven baked at 200 °C (Sanyo-Gallenkamp Hotbox Oven, Model #OHG050, Loughborough, England) for 1 hr prior to usage, ensuring sterility.

2.1.3 Sterility of Work Environment

All cell culture work was carried out in a laminar flow hood (Astec-Microflow laminar flow workstation, Florida, U.S.A). Air passes through HEPA (high efficiency particle air) filters at the top of the flowhood and flows downwards. The airflow creates a downward barrier in front of the open portion of the hood, the strength of this down draft of air prevents entry of external airborne contaminants into the laminar flow hood thus providing a sterile work area. Before using the laminar flow hood, the interior was sterilized by wiping down all accessible surfaces with 70% EtOH, followed by a 10 min exposure to ultraviolet (UV) light. Disposable latex gloves (sprayed with 70%

EtOH) were worn at all times when cell manipulations were being carried out in the hood. Gloves were changed regularly to avoid contamination.

2.1.4 Reagents and Medium formulation

Solutions such as phosphate buffered saline (PBS; 100 mM NaCl, 80 mM Na_2HPO_4, 20 mM NaH_2PO_4) were hand filtered through a 10 ml syringe (B.Braun Medical Ltd., Melsungen, Germany) with an attached 0.2 μm cellulose acetate membrane syringe filter (Pall Corporation, Michigan, USA) into autoclaved glass bottles or sterile 50 ml plastic tubes (BD Biosciences Pharmingen, San Diego, USA). Neurobasal medium (NBM; Invitrogen, Paisley, UK) supplemented with heat inactivated horse serum (10 %), penicillin (100 U/ml), streptomycin (100 U/ml) and glutamax (2 mM; Invitrogen, Paisley, UK) was filtered through a 0. 2μm cellulose acetate membrane (Millipore Ireland B.V, Cork, Ireland) in a Millipore Sterifil unit (Sigma-Aldrich, St. Louis, U.S.A.) connected to a vacuum pump. Care was taken to never let the side or tip of a pipette gain contact with anything except the sterile interiors of the containers one was working with. Pipettes were placed on sterile racks (Bell-Art Products, New Jersey, U.S.A.) between usage and were regularly wiped down with 70 % EtOH

2.1.5 Disposal

All used plastic ware was discarded in an autoclavable plastic bag (Bibby Sterilin Ltd., Staffordshire, England) with a biohazard symbol, for autoclaving.

2.2 Primary Culture of Cortical Neurons

The culturing of primary cortical neurons is an *in vitro* technique which involves dissection of the brain, removal of the cortex and dissociation of the cortical tissue so that a population of neurons is obtained. Primary neuronal cell cultures are superior to cell line models as they represent non-transformed unaltered phenotypes.

2.2.1 Preparation of sterile coverslips

To ensure sterility 13mm diameter glass coverslips (Chance Propper, West Midlands, England) were soaked in 70% EtOH, followed by an overnight exposure to UV light. Sterile coverslips were then coated with poly-l-lysine (60 μg/ml in sterile dH_20) in a final volume of 25 ml for 1 hr at 37 ^oC, so as to provide a suitable surface to which dissociated neurons would adhere. Coated coverslips were then air dried, placed in sterile 24-well plates (Greiner Bio One Gmbh, Kremsmuenster, Austria) and stored at 4 ^oC until required for use (maximum 2 week storage).

2.2.2 Animals

Postnatal one-day old wistar rats were born at the BioResources Unit of Trinity College Dublin. Animals were maintained under a 12 hr light/dark cycle and at an ambient temperature of 22-23 ^oC. On the day of birth, pups were removed from the litter cage and placed in a box with air holes and cotton wool for bedding. The pups were then taken back to the Physiology Department and brought into the cell culture room and killed by decapitation.

2.2.3 Dissection

Primary cortical neurons were established from postnatal one-day old wistar rats. Dissection of one rat brain yielded a preparation of 2 individual 24-well plates. Working in a laminar flow hood, rats were decapitated using a large pair of scissors. The skull was exposed by cutting skin with a pair of small scissors in a straight line from the neck to the top of the head. To remove the skull a sterile small scissors was used to cut around the skull, keeping the inside point of the scissors close to the inside of the skull. A large pair of forceps was used to lift back the skull and pull it away from the head, exposing the brain. The cerebral cortices were removed with the forceps and placed in a sterile petri dish (Greiner Bio One Gmbh, Kremsmuenster, Austria) containing sterile PBS. Any meninges were carefully removed using a fine forceps and cortices were chopped into 3 to 4 mm pieces with a sterile disposable scalpel (Schwann-Mann, Sheffield, England).

2.2.4 Dissociation Procedure

Tissue pieces were incubated in 5 ml of PBS containing trypsin (0.25 %, Sigma-Aldrich, Dorset, England) for 20 min at 37 ^{o}C. Trypsin digestion of connective tissue was followed by trituration (x5) of the dissociated neurons in PBS containing soyabean trypsin inhibitor (0. 1%, Sigma-Aldrich, Dorset, England), DNAse (0.2 mg/ml) and $MgSO_4$ (0.1 M). The suspension was then passed through a sterile 40 μm nylon mesh filter (Becton Dickinson Labware Europe, France) to remove tissue clumps. Following centrifugation (Sigma-Aldrich, Model #2K15C, St. Louis, USA), 2500 x *g* for 3min at 20^{o}C, the pellet was resuspended in neurobasal medium (NBM), supplemented with heat inactivated horse serum (10 %), penicillin (100 U/ml), streptomycin (100 U/ml), glutamax (2 mM) and the B27 (diluted 1:50 from a 50X solution). B27 was added to the NBM due to its neuroprotective antioxidant properties (Huang *et al.*, 2000). NBM and supplements were purchased from Invitrogen, Paisley, UK.

2.2.5 Plating of resuspended neurons

Resuspended neurons in NBM were placed on the centre of each coverslip at a density of 0.25 x 10^6 cells and allowed to adhere to the glass coverslip for 2 hr in a humidified incubator containing 5% CO_2: 95% air at 37°C (Model # 394-048, Jencons Scientific Ltd., Bedfordshire, England). Thereafter, 500 µl of pre-warmed neurobasal medium supplemented with heat inactivated horse serum (10 %), penicillin (100 U/ml), streptomycin (100 U/ml), glutamax (2 mM) and B27 (diluted 1:50 from a 50X solution) was added to each well and the cells were incubated for 3 days. On the 4th day *in vitro* the medium was replaced with supplemented NBM containing 5 ng/ml cytosine-arabino-furanoside (ARA-C; Sigma-Aldrich, Dorset, England). ARA-C was included in the culture medium to prevent proliferation of non-neuronal cells. ARA-C was removed from the media after 24hr and exchanged for 400 µl of supplemented neurobasal medium. Cells were grown in culture for up to 14 days and culture media was changed at least every 3 days, depending on treatment conditions. The cells were exposed to Aβ on day 7 *in vitro*. Cells were monitored by light microscopy (Nikon Labophot, Nikon Instech Co., Ltd, Kanagawa, Japan) on a daily basis to ensure that the cells appeared healthy and lacked fungal or bacterial infection. A sample photo of cultured cortical neurons at the initial stage of plating (i) and 4 days *in vitro* (ii) is depicted in Figure 2.1.

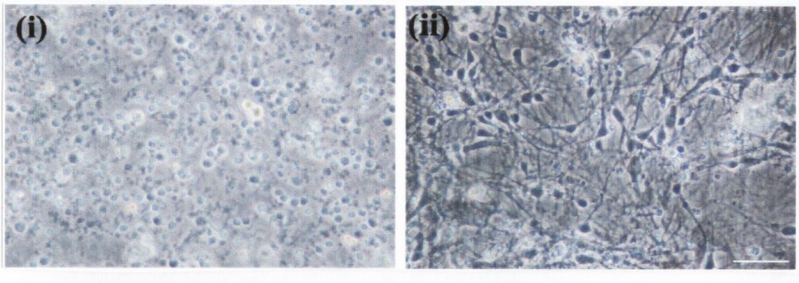

Figure 2.1 Time-dependent changes in cultured neuronal morphology. (i) Cells display rounded cell somas and an absence of neurites after initial plating. (ii) By day 4 in vitro, cells have developed pear-shaped bodies and an extensive neurite network, representative of a mature neuron. Scale bar is 100 µm.

2.3 CELL TREATMENTS

2.3.1 $A\beta_{1-40}$

$A\beta_{(1-40)}$ (BioSource International Inc, California, USA) lyophilised peptide was initially dissolved in sterile distilled H_2O (dH_2O) at 6 mg/ml then diluted to a 1 mg/ml stock solution with calcium-free sterile PBS. The peptide was supplied in a form that is not neurotoxic prior to an incubation step. The appearance of toxicity in response to treatment with Aβ has been shown to correlate to the extent of beta sheet structure (Wang *et al.*, 2001), therefore the peptide was allowed to aggregate for 48hr at 37 °C for this study. While the 1-42 fibrillar form of Aβ is the most abundant in the AD senile plaque, the less studied 1-40 peptide also has the proclivity to form fibrils and is present in mature senile plaque (Iwatsubo *et al.*, 1994). Thus, in this study the molecular and cellular signalling events induced by $A\beta_{(1-40)}$ were investigated. For treatment of cortical neurons, Aβ was diluted to a final concentration of 2 μM (10 ng/ml) in pre-warmed NBM.

2.3.2 p53 inhibitor

The p53 inhibitor pifithrin -α (Calbiochem International, Darmstadt, Germany) was made up as a stock solution of 1 mM in dimethyl sulfoxide (DMSO) and was used at a final concentration of either 50 nM or 100 nM. Cells were exposed to the p53 inhibitor for 60 min prior to Aβ treatment. This inhibitor is a cell permeable highly lipophilic molecule which efficiently inhibits p53-dependent transactivation of p53-responsive genes and reversibly blocks p53-mediated apoptosis (Culmsee *et al.*, 2001).

2.3.3. L-type voltage-dependent calcium channel blocker

The L-type voltage-dependent calcium channel blocker, nicardipine hydrochloride (Sigma-Aldrich, Dorset UK), was made up as a stock solution of 1 mM

in methanol and was used at a final concentration of either 1 μM or 5 μM. Cells were exposed to nicardipine for 20 min prior to Aβ treatment.

In all cases where a drug was dissolved in DMSO or methanol, control cells were treated with the same concentration of diluent to control for any non-specific effects.

2.3.4 IL-1β

IL-1β (kindly donated by Prof. Luke O'Neill, Trinity College Dublin) was made as a stock solution of 1 μg/ml in sterile distilled water and was used at a final concentration of 5 ng/ml.

2.3.5 Treatment with Antisense Oligonucleotides (ASOs)

To evoke a transient downregulation in expression of c-jun N-terminal kinase (JNK)1 or JNK2 an antisense approach was used. Phosphorothioate oligonucleotides complementary to the mRNA encoding JNK1 or JNK2, and corresponding scrambled control sequences, were synthesized by Biognostik (Gottingen, Germany). These oligonucleotides contain sulphur in the internucleotide phosphate linkages of the DNA backbone, which increases resistance to exo and endonucleases present in serum and intracellularly, respectively. The sequences used 5′-CTCATGATGGCAAGCAATTA-3′ (JNK1 antisense), 5′- ACTACTACACTAGACTAC-3′ (JNK1 scrambled control), 5′-GCTCAGTGGACATGGATGAG-3′ (JNK2 antisense) and 5`-GGACTACTACAC TAGACTAC-3` (JNK2 scrambled control) were in accordance with Hreniuk *et al.*, 2001. Antisense oligonucleotides were made up as a 100 μM stock solution in a provided antisense dilution buffer (Biognostik, Gottingen, Germany). Neurons were first incubated with 1.25 μM oligonucleotide in serum-free pre-warmed NBM (Invitrogen, Paisley, UK) containing N-[1-(2,3-dioleoyloxy)propyl]-N,N,N-trimethylammonium / dioleoylphosphatidylethanolamine (DOTMA/DOPE, 5 μg/ml; Life Technologies) to enhance oligonucleotide uptake. After 4 hours the medium was replaced with supplemented prewarmed NBM containing 2 μM oligonucleotide and the cells were incubated for a further 48 hours prior to further treatment with $A\beta_{(1-40)}$.

2.4 Protein Quantification

Calculation of protein concentration in cell samples was carried out according to the method of Bradford (1976). Standards were prepared from stock solution of 200 μg/ml Bovine Serum Albumin (BSA; Sigma-Aldrich, Dorset, U.K.) to a volume of 160 μl and ranged from 5 μg/ml to 200 μg/ml. Samples (10 μl) were diluted in 150 μl of distilled water. BioRad dye reagent (40 μl; Biorad Laboratories, Munich, Germany) was added to all preparations, which were then vortexed and incubated at room temperature for 5 min before being transferred to the wells of a 96-well plate (Sarstedt, Leicester, England). Absorbance readings were made at a wavelength of 630 nm using a 96 well plate reader (Labsystems Multiskan RC). A regression line was plotted (GraphPad Instat) and the concentration of protein was calculated and converted to mg protein/ml.

2.5 Sodium Dodecyl Sulphate-Polyacrylamide Gel Electrophoresis (SDS-PAGE)

2.5.1 Preparation of samples

(i) Preparation of total protein

Cells were harvested for SDS-PAGE analysis by two different protocols. The first protocol was designed to analyse total expression of protein and in this case cells were washed in Tris Buffered Saline (TBS; 20 mM Tris-HCl; 150 mM NaCl; pH 7.6) before harvesting by scraping coverslips using the rubber end of a 1 ml syringe piston (B.Braun Medical Ltd., Melsungen, Germany) into lysis buffer (composition: 25 mM HEPES, 5 mM $MgCl_2$, 5 mM EDTA, 5 mM DTT, 0.1 mM PMSF, 2 μg/ml leupeptin, 2 μg/ml aprotinin; pH 7.4). The sample was then homogenised (X 20 strokes) using a 1 ml glass homogeniser (Jencons, Bedfordshire, UK).

(ii) Preparation of cytosolic and mitochondrial fraction

The second protocol was designed to obtain cytosolic and mitochondrial protein fractions. In this case cells were washed in PBS before 100 µl of permeabilisation buffer (250 mM sucrose, 70 mM KCL, 137 mM NaCl, 4.5 mM Na_2HPO_4, 1.4 mM kH_2P0_4, 0.1 mM PMSF, 10 µg/ml leupeptin, 2 µg/ml aprotinin, 200 µg/ml digitonin; pH 7.2) was added to each well and left on ice for 5 min. The permeabilisation buffer was then removed and collected as the cytosolic fraction. 100 µl mitochondrial buffer (50 mM Tris Base, 150 mM NaCl, 2 mM EGTA, 0.2 % Triton-X-100, 0.3 % Igepal p-40, 0.1 mM PMSF, 10 µg/ml leupeptin, 2 µg/ml aprotinin; pH 7.2) was then added to each well before harvesting by scraping coverslips using the rubber end of a 1 ml syringe piston (B.Braun Medical Ltd., Melsungen, Germany). Cells were centrifuged (15000 x *g* for 20 min at 4 °C) and the supernatant containing the mitochondrial fraction was collected.

Total expression of protein (Protocol (i)) was assessed in all cases unless otherwise stated. All samples were prepared for SDS-polyacrylamide gel electrophoresis. Protein concentrations were assessed (see Section 2.4) and equalized with lysis buffer. An equal volume of sample buffer (0.5 M Tris-HCl pH 6.8; 10 % glycerol (v/v); 10 % SDS (w/v); 5 % β-mercaptoethanol (v/v); 0.05 % bromophenol blue (w/v)) to sample was added and samples boiled for 5 min. Samples were stored at -20 °C until required.

2.5.2 Gel electrophoresis

Polyacrylamide separation gels with a monomer concentration of either 7.5 %, 10 % or 12 % overlaid with 4 % stacking gel (See Appendix 1) were cast between 10 cm wide glass plates and mounted on an electrophoresis unit (Sigma Techware, Dorset, UK) using spring clamps. The upper and lower reservoirs of the unit were filled with electrode running buffer (25 mM Tris Base; 200 mM glycine; 17 mM SDS). Samples (10 µl) were loaded into the wells using a Hamilton Microliter syringe. Prestained

molecular weight standard (5 μl; Sigma-Aldrich, Dorset, UK) were also loaded to verify the molecular weight of protein bands. Proteins were separated by application of a 32 mA current to the gel apparatus and migration of the bromophenol blue was monitored. The current was switched off when the blue dye band reached the bottom of the gel (approximately 30 min).

2.6 Semi-dry electrophoresis blotting

The gel was removed from the gel apparatus and washed gently in ice cold (4 ^{o}C) transfer buffer (25 mM Tris-Base; 192 mM glycine; 20 % methanol (v/v); 0.05 % SDS (w/v)). The gel was placed on top of a sheet of nitrocellulose blotting paper (0.45 μm pore size; Sigma-Aldrich, Dorset, UK) wetted in transfer buffer, cut to the size of the gel. One piece of filter paper (Standard Grade No.3, Whatman, Kent, UK) was placed on top of the gel and one piece was placed beneath the nitrocellulose paper forming a sandwich. The sandwich was soaked in transfer buffer and placed on the platinum coated titanium electrode (anode) of a semi-dry blotter (Sigma-Aldrich, Dorset, UK). Air bubbles were removed from the sandwich by gently rolling a pasteur pipette over it. The lid of the blotter (stainless steel cathode) was placed down firmly on top of the sandwich. The uncovered portion of the cathode was shielded with a mylar cut-out (Sigma-Aldrich, Dorset, UK), ensuring all applied current passed directly through the sandwich. A constant current of 225 mA was applied for 90 min.

2.7 Western Immunoblotting

The nitrocellulose membrane was blocked for non-specific binding and probed with an antibody raised against the protein sought (for specific incubation protocols see sections 2.7.1-2.7.8). The membrane was washed and incubated with a horse-radish peroxidase (HRP)-linked secondary antibody. A chemiluminescence detection chemical (either SuperSignal Ultra (Pierce Biotechnology, Illinois, USA) or Enhanced Chemiluminescence (ECL) detection reagent (Amersham, Buckinghamshire, UK) was added and the membrane was exposed to 5 X 7 inch photographic film (Hyperfilm

ECL, Amersham, Buckinghamshire, UK) and developed using a Fuji Processor (Fuji X-Ray film processor, Model # RGII, FUJIFILM Medical systems, Stamford, USA).

2.7.1 JNK phosphorylation

In the case of JNK phosphorylation, non-specific binding was blocked by incubating nitrocellulose membranes for 2 hours at room temperature (RT) in TBS containing 2 % Bovine Serum Albumin (Sigma-Aldrich, Dorset, UK). The monoclonal primary antibody for p-JNK was added (10 ml; 1:200 dilution in TBS-Tween (TBS-T) containing 0.1 % BSA; Santa Cruz, California, USA, Catalogue no. SC-6254) and incubated overnight at 4 °C. The antibody was a mouse monoclonal IgG_1 raised against a peptide corresponding to a short amino-acid sequence of JNK1/JNK2 of human origin spanning the phosphorylated amino acids Thr-183 and Tyr-185. The nitrocellulose was washed for 15 min (3 times) in TBS-T. The secondary antibody was added (10 ml; 1:400 dilution; goat anti-mouse IgG-HRP in TBS-T containing 0.1% BSA; Sigma-Aldrich, Dorset, UK) and incubated for 60 min at room temperature. The membrane was washed for 15 min 5 times in TBS-T. ECL (Amersham, Buckinghamshire, UK) was added for 5 min and membranes were exposed to photographic film for 30 min in the dark after which time the film was developed.

2.7.2 Selective expression of JNK1 and JNK2

In order to assess JNK1 and JNK2 expression, non-specific binding was blocked by incubating the membrane in TBS containing 2 % BSA for 2 hr at RT. The antibodies used were mouse monoclonal antibodies recognising the epitope corresponding to amino acids 1-384 of JNK1, and the epitope corresponding to amino acids 1-424 of JNK2, of human origin, respectively (10 ml; 1:200 dilution in TBS-T containing 0.2 % BSA; Santa Cruz, California, USA, Catalogue no SC-4061; JNK1 and SC-4062; JNK2. Membranes were incubated overnight at 4 °C in the presence of the antibody and washed for 15 min, 3 times in TBS-T. The secondary antibody (10 ml; 1:400 dilution; goat-anti-mouse IgG-HRP in TBS-T containing 0.2 % BSA; Sigma-

Aldrich, Dorset, UK) was added and membranes were incubated for 60 min at RT. Membranes were washed for 15 min 5 times in TBS-T. ECL detection reagent (Amersham, Buckinghamshire, UK) was added to the membrane for 5 min and exposed to photographic film for 30 min in the dark before being developed.

2.7.3 Total JNK Expression

Following Western immunoblotting for JNK phosphorylation, blots were stripped with an antibody stripping solution (10ml; 1 in 10 dilution in dH_20; Reblot Plus Strong antibody stripping solution; Chemicon, California, USA) and reprobed for total JNK expression in order to confirm equal loading of protein. As before, non-specific binding was blocked by incubating the membrane in TBS containing 2 % BSA for 2 hours at RT. The primary antibody used was a rabbit IgG JNK polyclonal antibody recognising JNK1, JNK2 and JNK3 (10 ml; 1:1000 dilution in TBS-T containing 0.2 % BSA; Santa Cruz, California, USA, Catalogue no. SC-571) Membranes were incubated overnight at 4° C in the presence of the antibody and washed for 15 min, 3 times in TBS-T. The secondary antibody (10 ml; 1:1000 dilution; goat-anti-rabbit IgG-HRP in TBS-T containing 0.2% BSA; Amersham, Buckinghamshire, UK) was added and membranes were incubated for 1hr at RT. Membranes were washed for 15 min 5 times in TBS-T. ECL detection reagent (Amersham, Buckinghamshire, UK) was added to the membrane for 5 min and exposed to photographic film for 30min in the dark before being developed.

2.7.4 p53 expression

In order to assess p53 expression, non-specific binding was blocked by incubating the membrane in TBS containing 2 % BSA for 2 hr at RT. The primary antibody used was a polyclonal IgG antibody purified from goat serum which recognises an epitope mapping at the carboxy terminus of p53 of human origin (10 ml; 1:400 dilution in TBS-T containing 0.2 % BSA; Santa Cruz, California, USA, Catalogue no. SC-1311). Membranes were incubated overnight at 4° C in the presence

of the antibody and washed for 15 min 3 times in TBS-T. The secondary antibody (10 ml; 1:1500 dilution; donkey-anti-goat IgG-HRP in TBS-T containing 0.2 % BSA; Santa Cruz, California, USA) was added and membranes were incubated for 60 min at RT. Membranes were washed for 15 min 5 times in TBS-T. ECL detection reagent was added to membranes, incubated for 5 min and exposed to photographic film for 30 min at 4 °C in the dark before being developed.

2.7.5 Phosphorylated p53

In the case of phospho-p53 (serine (ser) 15), non-specific binding was blocked by incubating membranes in TBS containing 2 % BSA for 2 hr at RT. The primary antibody used was a rabbit phospho-p53 antibody recognising endogenous levels of p53 only when phosphorylated at residue ser 15 and does not recognize p53 phosphorylated at other sites (10 ml; 1:400 dilution in TBS-T containing 0.2 % BSA; Cell signalling technologies, Massachusetts, USA, Catalogue no. 9284S). Membranes were incubated overnight at 4 °C in the presence of antibody and washed for 15 min 3 times in TBS-T. Secondary antibody (10 ml; 1:1500 dilution; goat-anti-rabbit IgG-HRP in TBS-T containing 0.2 % BSA; Amersham, Buckinghamshire, UK) was added and incubation continued for 60 min at RT. Membranes were washed for 15 min 3 times in TBS-T. Supersignal (Pierce Biotechnology, Illinois, USA) was added for 5 min and membranes were exposed to photographic film for 10 sec in the dark before being developed.

In the case of phospho-p53 (ser 392) non-specific binding was blocked by incubating membranes in TBS containing 2 % BSA for 2 hours at RT. The primary antibody used was a rabbit polyclonal phospho-p53 antibody recognising p53 when phosphorylated at residue ser 392 (10 ml; 1:400 dilution in TBS-T containing 0.2 % BSA; Biosource International Inc, California, USA, Catalogue no. 44-640). Membranes were incubated overnight at 4 °C in the presence of antibody and washed for 15 min 3 times in TBS-T. Secondary antibody (10 ml; 1:1500 dilution; goat-anti-rabbit IgG-HRP in TBS-T containing 0.2% BSA; Amersham, Buckinghamshire, UK) was added and incubation continued for 60 min at RT. Membranes were washed for 15

min, 3 times in TBS-T. Supersignal (Pierce Biotechnology, Illinois, USA) was added for 5 min and membranes were exposed to photographic film for 10 sec in the dark before being developed.

2.7.6 Bax expression

In order to assess expression of Bax, two different cell-harvesting protocols were used (see section 2.5.1) in order to measure both total cellular expression of Bax and cytosolic/mitochondrial Bax expression. The primary antibody used was a mouse monoclonal IgG_{2b} antibody raised against amino acids 1-171 of Baxα of mouse origin (10 ml; 1:100 dilution in TBS-T containing 0.2 % BSA; Santa Cruz, California, USA, Catalogue no. SC-7480). Non-specific binding was blocked by incubating membranes in TBS containing 2 % BSA for 2 hours at RT and membranes were incubated overnight at 4° C in the presence of the antibody and washed for 15 min 3 times in TBS-T. The secondary antibody (10 ml; 1:400 dilution; goat-anti-mouse IgG-HRP in TBS-T containing 0.2 % BSA; Sigma-Aldrich, Dorset, UK) was added and membranes were incubated for 60 min at RT. Membranes were washed for 15 min 5 times in TBS-T. Supersignal (Pierce Biotechnology, Illinois, USA) was added for 5 min and membranes were exposed to photographic film for 10 sec in the dark before being developed.

2.7.7 Cytochrome *c* expression

Expression of cytochrome *c* was assessed in cytosolic fractions prepared as described in section 2.5.1. The primary antibody used was a rabbit polyclonal cytochrome *c* antibody raised against a recombinant protein corresponding to amino acids 1-104 representing full length cytochrome *c* of horse origin (10 ml; 1:250 dilution in TBS-T containing 2 % Marvel). Non-specific binding was blocked by incubating membranes in TBS containing 2 % BSA for 2 hours at RT and membranes were incubated overnight at 4° C in the presence of the antibody and washed for 15 min 3 times in TBS-T. The secondary antibody (10 ml; 1:1000 dilution; anti-rabbit IgG-HRP

in TBS-T containing 2 % Marvel; Sigma-Aldrich, Dorset, UK) was added and membranes were incubated for 60 min at RT. Membranes were washed for 15 min 5 times in TBS-T. Supersignal (Pierce Biotechnology, Illinois, USA) was added for 5 min and membranes were exposed to photographic film for 10 sec in the dark before being developed.

2.7.8 pERK

In order to assess levels of phosphorylated ERK non-specific binding was blocked by incubating membranes in TBS containing 1 % BSA for 2 hr at room temperature. The primary antibody used was a mouse monoclonal antibody raised against an epitope corresponding to a short amino acid sequence containing phosphorylated Tyr-204 of ERK 1 of human origin (identical to corresponding ERK2 sequence) (10 ml; 1:100 dilution in TBS-T containing 0.1 % BSA; Santa Cruz, California, USA, Catalogue no. SC-7383). Membranes were incubated overnight at 4 ^{o}C in the presence of antibody and washed for 15 min 3 times in TBS-T. Secondary antibody (10 ml; 1:1000 dilution; goat-anti-rabbit IgG-HRP in TBS-T containing 0.1% BSA; Amersham, Buckinghamshire, UK) was added and incubation continued for 60 min at RT. Membranes were washed for 15 min 3 times in TBS-T. ECL detection reagent (Amersham, Buckinghamshire, UK) was added to the membrane for 5 min and exposed to photographic film for 30 min in the dark before being developed.

2.7.9 Total actin Expression

Following Western immunoblotting for p53, phospho-p53, and Bax blots were stripped with an antibody stripping solution (2.7.3) and reprobed for analysis of total actin expression in order to confirm equal loading of protein. As before non-specific binding was blocked by incubating the membrane in TBS containing 2 % BSA for 2 hours at RT. The primary antibody used was a mouse monoclonal IgG_1 antibody corresponding to amino acid sequence mapping at the carboxy terminus of actin of human origin (10 ml; 1:200 dilution in TBS-T containing 0.2 % BSA; Santa Cruz,

California, USA, Catalogue no. SC-8432). Membranes were incubated overnight at 4°C in the presence of the antibody and washed for 15 min 3 times in TBS-T. The secondary antibody (10 ml; 1:500 dilution; goat anti-mouse IgG HRP in TBS-T containing 0.2 % BSA; Santa Cruz, California, USA) was added and membranes were incubated for 60 min at RT. Membranes were washed for 15 min 5 times in TBS-T. Supersignal (Pierce Biotechnology, Illinois, USA) was added for 5 min and membranes were exposed to photographic film for 10 sec in the dark before being developed.

Table 2.1 summarises the antibodies used for protein detection.

Protein Target	**Antibody Source**	**2° Antibody**	**Antibody Dilution % BSA in TBST**	**Protein Band Size**
Phosphorylated JNK1,2 and 3	Mouse	goat anti-mouse IgG	**1°** 1/200 0.1% BSA **2°** 1/400 0.1% BSA	JNK1 46 kDa JNK2 54 kDa JNK3 57 kDa
Expression of JNK1	Mouse	goat anti-mouse IgG	**1°** 1/200 0.2% BSA **2°** 1/400 0.2% BSA	46 kDa
Expression of JNK2	Mouse	goat anti-mouse IgG	**1°** 1/200 0.2% BSA **2°** 1/400 0.2% BSA	54 kDa
Expression of total JNK	Rabbit	goat-anti-rabbit IgG	**1°** 1/1000 0.2% BSA **2°** 1/1000 0.2% BSA	JNK1 46 kDa JNK2 54 kDa
Expression of p53	Goat	donkey-anti-goat IgG-	**1°** 1/400 0.1% BSA **2°** 1/1500 0.1% BSA	53 kDa
$p53^{ser15}$ phosphorylation	Rabbit	goat-anti-rabbit IgG	**1°** 1/400 0.2% BSA **2°** 1/1500 0.2% BSA	53 kDa
$p53^{ser392}$ phosphorylation	Rabbit	goat-anti-rabbit IgG	**1°** 1/400 0.2% BSA **2°** 1/1500 0.2% BSA	53 kDa
Bax	Mouse	goat anti-mouse IgG	**1°** 1/100 0.2% BSA **2°** 1/400 0.2% BSA	21 kDa
Cytochrone *c*	Rabbit	goat-anti-rabbit IgG	**1°** 1/250 0.2% BSA **2°** 1/1000 0.2% BSA	11.4 kDa
Phosphorylated ERK	Mouse	goat anti-mouse IgG	**1°** 1/100 0.2% BSA **2°** 1/1000 0.2% BSA	ERK1 44 kDa ERK2 42 kDa
Actin	Mouse	goat anti-mouse IgG	**1°** 1/200 0.2% BSA **2°** 1/500 0.2% BSA	46 kDa

Table 2.1 Antibodies used for Western Blotting

2.7.10 Densitometry

In all cases quantification of protein bands was achieved by densitometric analysis using the Zero-Dscan Image Analysis System (Scanalytics Inc., Fairfax, USA). Values are expressed as arbitrary units.

2.8 Immunocytochemistry

2.8.1 Activated Caspase-3 Immunocytochemistry

Cells were fixed in 4 % paraformaldehyde, permeabilised with 0.2 % (v/v) Triton X-100 and washed three times in PBS. Non-reactive sites were blocked in blocking buffer (5 % goat serum in PBS containing 0.2% Triton X-100) for 2 hours at RT. The cells were then incubated overnight with a polyclonal anti-active caspase-3 antibody (Promega Corporation, Madison, USA) diluted 1:250 in 10 % blocking buffer, overnight at 4 °C. This antibody was purified from rabbit serum and recognizes the 17 kDa cleaved and active fragment of caspase-3. Cells were washed three times in PBS and incubated with a biotinylated goat anti rabbit-IgG secondary antibody (100 ml; 1:50 dilution, 1 hour incubation, Vector Laboratories Inc., California, USA). Cells were washed 3 times in PBS before a 1:100 dilution of streptavidin conjugated to horseradish peroxidase (Amersham, Bedfordshire, UK) in PBS was added for 40 min at RT. Cells were washed 3 times in PBS before detection using the peroxidase substrate H_2O_2 and the stable chromogen diaminobenzidine (DAB, Dako Corporation, Carpinteria, U.S.A.) solution (2 ml; 1.81 ml DAB (1 mg/ml PBS), 80 µL of saturated Nikel Aluminum Sulphate ($(NH)_4SO_4NiSO_4.6H_2O$) and 11 µl of H_2O_2, Sigma-Aldrich, UK). Incubation proceeded until cells had taken on a stained appearance (approximately 10 min) The coverslips were washed in deionised water, dehydrated through graded alcohols and mounted on slides with DPX mounting medium (a mixture of distyrene (a polystyrene), tricresyl phosphate (plasticiser) and xylene with a refractive index of 1.5; BDH Laboratory Supplies, Dorset, England). Cells were then

viewed under light microscopy (Nikon Labophot, Nikon Instech Co., Ltd, Kanagawa, Japan) at x100 magnification where the active-caspase-3-positive cells stained dark purple. Cells displaying active caspase-3 immunoreactivity were counted and expressed as a percentage of the total number of cells examined (400-500 cells/coverslip).

2.8.2 Poly-(ADP-ribose)-polymerase (PARP) immunocytochemistry

Cells were fixed in 4 % paraformaldehyde for 30 min at room temperature, permeabilised with 0.2 % (v/v) Triton X-100, washed 3 times in PBS then blocked with 5 % bovine serum albumin in PBS for 1hr at room temperature. Cells were then incubated for 1 hour at RT with an anti-cleavage site specific PARP polyclonal antibody purified from goat serum (100 µl, 1:50 dilution in a 5 % solution of goat serum in PBS; Vector Laboratories Inc., California, USA) which specifically recognises the 85 kDa cleaved form of PARP. Immunoreactivity was detected with a biotinylated goat anti rabbit-IgG secondary antibody (100 µl; 1:50 dilution in PBS containing 5 % goat serum, BioSource International Inc, California, USA) applied for 1hr at RT, then washed 3 times in PBS. Streptavidin conjugated to horseradish peroxidase (100 µl; 1:100 dilution in PBS; Amersham, Buckinghamshire, UK) was then applied to the cells for 40 min at RT. Immunoreactive cells were visualised after incubation using a DAB solution (2 ml; Dako Corporation, Carpinteria, U.S.A.; 1.81 ml DAB 1 mg/ml PBS, 80 µl of saturated Nikel Aluminum Sulphate ($(NH)_4SO_4NiSO_4.6H_2O$) and 11 µl of H_2O_2) for 10 min, washed several times in deionised water and mounted onto microscope slides with DPX medium (BDH Laboratory Supplies, Dorset, England). Cells were then viewed under light microscopy at x 100 magnification (Nikon Labophot, Nikon Instech Co., Ltd, Kanagawa, Japan), where the nuclei of PARP cleavage positive cells stained dark purple. The number of cells displaying cleaved PARP immunoreactivity were counted and expressed as a percentage of the total number of cells examined (400-500 cells/coverslip).

2.9 Fluorescence Immunocytochemistry

2.9.1 JNK Fluorescence Immunocytochemistry

To evaluate the efficacy of the antisense oligonucleotides in downregulating JNK expression, immunolocalisation of non-phosphorylated JNK1 and JNK2 was assessed using anti-JNK1 or anti-JNK2 monoclonal antibodies purified from mouse serum antibody (Santa Cruz Biotechnology Inc, California). The antibodies used recognise the epitope corresponding to amino acids 1-384 representing full length JNK1, and the epitope corresponding to amino acids 1-424 representing full length JNK2 of human origin, respectively. Cells were fixed with 4 % paraformaldehyde, permeabilised with 0.1 % Triton X-100 and non-reactive sites were blocked with 5 % goat serum in phosphate buffered saline. Primary antibodies were applied (100 µl; 1: 400 dilution in 10 % blocking buffer) overnight at 4 °C. Coverslips were washed 3 times in PBS and secondary antibody was added (100 µl; 1:100 dilution; anti-mouse IgG conjugated to fluorescein isothiocyanate (FITC); Sigma-Aldrich, Dorset, England) for 1 hour at RT. Coverslips were washed several times in dH_20, before being mounted onto microscope slides using a mounting medium for fluorescence (Vector Laboratories Inc., California, USA) and the perimeter of each coverslip was sealed using nail varnish. Care was taken to minimise exposure of coverslips to light in order to prevent the fluorescent tag from bleaching. Mounted coverslips were viewed under x40 magnification by fluorescence microscopy (Leitz Orthoplan Microscope, Leica Microsystems AG, Wetzlar, Germany) using Improvision software (Improvision, Coventry, England). Cells were observed under excitation, 490 nm; emission, 520 nm for FITC labelled antibodies.

2.9.2 Phospho-JNK fluorescence Immunocytochemistry

Cells were fixed with 4 % paraformaldehyde, permeabilised with 0.1 % Triton X-100 and non-reactive sites were blocked with 5 % goat serum in phosphate buffered saline. To determine the intracellular distribution of active-JNK (phosphorylated JNK)

the cells were incubated overnight with an anti-active JNK antibody (100 µl; 1:400 dilution in 10 % blocking buffer; Santa Cruz Biotechnology Inc, California, USA) purified from mouse serum. This antibody was raised against a peptide corresponding to a short amino-acid sequence of JNK1/JNK2 of human origin containing phosphorylated Thr-183 and Tyr-185. Coverslips were washed 3 times in PBS and secondary antibody was added (100 µl; 1:100 dilution; anti-mouse IgG conjugated to FITC; Sigma-Aldrich, Dorset, UK) for 1 hour at RT. Coverslips were washed several times in dH_20, before being mounted onto microscope slides using a mounting medium for fluorescence (Vector Laboratories Inc., California, USA) and the perimeter of each coverslip was sealed using nail varnish. Care was taken to minimise exposure of coverslips to light in order to prevent the fluorescent tag from bleaching. Mounted coverslips were viewed under x40 magnification by fluorescence microscopy (Leitz Orthoplan Microscope, Leica Microsystems AG, Wetzlar, Germany) using Improvision software (Improvision, Coventry, England). Cells were observed under excitation, 490 nm; emission, 520 nm for FITC labelled antibodies.

2.10 Localisation of Intracellular Organelles using Fluorescence microscopy

2.10.1 Localisation of Mitochondria and Lysosomes

Fluorescent probes (MitoTracker Red, LysoTracker Red, Molecular Probes, Leiden, The Netherlands) were used to visualise neuronal mitochondria and lysosomes. After neurons had undergone the desired treatment protocol, the culture media was removed from the wells and pre-warmed neurobasal medium containing either MitoTracker (400 nM) or LysoTracker (700 nM) was added for 30 min, to incorporate the probe. Cells were then washed in PBS and fixed in 4 % paraformaldehyde/PBS for 30 min at 37 ^{o}C. Coverslips were mounted onto microscope slides as outlined in section 2.10.1. Mounted coverslips were viewed under x40 magnification by fluorescence microscopy (Leitz Orthoplan Microscope, Leica Microsystems AG, Wetzlar, Germany) using Improvision software (Improvision, Coventry, England). Cells were observed under excitation, 579 nm; emission, 599 nm.

2.10.2 Co-localisation Analysis

In order to assess the sub-cellular distribution of p53 and Bax, immunolocalisation of these proteins was carried out in cells which had been loaded with either Mitotracker (400 nM) or Lysotracker (700 nM) probes. Cells were permeabilised with 0.2 % Triton X-100 for 10 min and refixed in 4 % paraformaldehyde for 10 min. Cells were incubated in blocking buffer 5 % goat serum in PBS (p53 immunocytochemistry) and 5 % horse serum in PBS (Bax immunocytochemistry) for 2 hours at RT. Coverslips were washed three times in PBS and incubated with primary antibody (100 µl; 1:50 dilution in 10 % blocking buffer) overnight at 4 ^{o}C. The p53 primary antibody used was a rabbit phospho-p53 antibody recognising endogenous levels of p53 only when phosphorylated at residue ser 15 while the Bax primary antibody used was a mouse monoclonal IgG_{2b} antibody raised against amino acids 1-171 of Baxα of mouse origin. Immunoreactivity was detected with goat anti-rabbit IgG biotinylated secondary antibody (Vector Laboratories Inc., California, USA) for p53 immunocytochemistry and with horse anti-mouse IgG (Vector Laboratories Inc., California, USA) for Bax immunocytochemistry (100 µl; 1:50 dilution in PBS containing 10 % blocking buffer). Incubation proceeded for 1 hr at RT, coverslips were then washed 3 times in PBS. Cells were then incubated with extra-avidin-conjugated FITC (100 µl; 1:50 dilution; Sigma-Aldrich, Dorset, UK) for 40 min at RT, washed 8 times with dH_20 to remove any unbound FITC and mounted as outlined in section 2.10.1. Mounted coverslips were viewed under x40 magnification by fluorescence microscopy (Leitz Orthoplan Microscope, Leica Microsystems AG, Wetzlar, Germany) using Improvision software (Improvision, Coventry, England). Cells were observed under excitation, 579 nm; emmision, 599 nm for MitoTracker Red and Lysotracker Red, and excitation, 490 nm; emission, 520 nm for FITC labelled antibodies.

2.11 TdT-mediated-UTP-end nick labelling (TUNEL)

Following treatment of cultured cortical neurons, coverslips were washed in Tris Buffered Saline (TBS; Tris-HCl 20 mM, NaCl 150 mM, pH 7.4) and fixed in 4 % (w/v) paraformaldehyde for 30 minutes at RT. The paraformaldehyde was then removed and replaced with TBS and the cells were stored at 4 °C until required for analyses. Apoptotic cell death was assessed by monitoring DNA fragmentation, using the DeadEnd colorimetric apoptosis detection system (Promega Corporation, Madison, USA). Cells were prepared as described in section 2.4.1. Cells were then permeabilised with Triton X-100 (0.1 %, v/v), proteinase-K (1 μg /ml) in TBS and refixed in 4 % paraformaldehyde for 10 minutes. Cells were incubated in equilibration buffer (50 μl/coverslip; 200 mM potassium cacodylate (pH 6.6 at 25 °C), 25 mM Tris-HCl (pH 6.6 at 25 °C), 0.2 mM DTT, 0.25 mg/ml BSA, 2.5 mM cobalt chloride) for 10 minutes. A Reaction buffer (100 μL/coverslip; 1 μl biotinylated nucleotide mix (25 μM biotinylated nucleotide mix, 10 mM Tris-HCl, pH7.6, 1 mM EDTA), 1 μl Terminal deoxynucleotidyl Transferase (TdT) enzyme and 98 μL equilibration buffer, Promega Corporation, Madison, USA) was applied for 60 min at 37 °C in order to incorporate the biotinylated nucleotide to the 3'-OH DNA ends of fragmented DNA strands. Horseradish-peroxidase-labelled streptavidin was then bound to the biotinylated nucleotide (100 μl; 1:100 dilution in PBS for 1 hour at RT) and this was detected using a DAB solution. Incubation proceeded until cells had taken on a stained appearance (approximately 10 min) The coverslips were washed in deionised water, dehydrated through graded alcohols and mounted on slides with DPX mounting medium. Cells were then viewed under light microscopy (Nikon Labophot, Nikon Instech Co., Ltd, Kanagawa, Japan) at x100 magnification, where the nuclei of TUNEL positive cells stained dark purple. Apoptotic cells (TUNEL positive) were counted and expressed as a percentage of the total number of cells examined (400-500 cells/coverslip).

2.12 Measurement of cathepsin-L activity using Enzyme Activity Assay

Cleavage of the fluorogenic cathepsin-L substrate (Z-Phe-Arg-AFC; Alexis Biochemicals, Nottingham, England) to its fluorescent product was used to measure cathepsin-L activity. This peptide is a substrate for both cathepsin-B and cathepsin-L, however inactivation of cathepsin-B activity occurs by adding 4M urea and setting the pH of the incubation buffer to pH 5, making it specific for cathepsin-L activity (Kamboj et al., 1993). Cortical neurons were washed in PBS and harvested in a urea buffer (20 mM NaOAc, 4 mM EDTA, 8 mM DTT, 4 M Urea; pH 5) by scraping coverslips using the rubber end of a 1 ml syringe piston (B.Braun Medical Ltd., Melsungen, Germany). Cell were homogenised, subjected to 3 freeze-thaw cycles, and centrifuged at 10,000 x *g* for 10 min at 4 ^{o}C (Sigma-Aldrich, Model #2K15C, St. Louis, USA). Samples of supernatant containing the cytosolic fraction (90 µl) were incubated with the Z-Phe-Arg-AFC peptide (150 µM; 10 µl) for 1 hr at 37 ^{o}C in a 96 well microtest plate (Sarstedt, Leicester, UK). Fluorescence was assessed by spectrofluorometry (excitation, 400 nm; emission, 505 nm) using a Fluoroskan Ascent Florometer, (Labsystems, Vantaa, Finland). A standard curve was prepared from a 1 mM stock solution of 7-amino-4-(trifluoromethyl) coumarin (AFC; Sigma-Aldrich, Dorset, UK) and diluted in urea buffer into 1000 µM, 500 µM, 250 µM, 125 µM, 62.5 µM, 31.25 µM, 15.625 µM, 7.813 µM and 0 µM (urea buffer) standards. The enzyme activity in cell samples was calculated from the regression line plotted from the absorbance of the AFC standards and converted to pmoles AFC produced/mg/ml of protein/min (GraphPad Instat)

2.13 Lysosomal Integrity Assay – Acridine Orange uptake

Acridine Orange (AO) uptake was used as a method to investigate integrity of lysosomes. The degree of AO release from lysosomes to cytosol was monitored by fluorescence microscopy. Cells were exposed to an AO (Molecular probes, Leiden, The

Netherlands) solution (5 μg/ml in pre-warmed NBM) for 15 min to incorporate the AO probe. Cells were then rinsed in fresh pre-warmed NBM and incubated in the presence or absence of 2 μM Aβ for 6 hr. Following treatment for 6 hr, cells were washed in PBS and fixed in 4 % paraformaldehyde/PBS for 30 min at 37 °C. Coverslips were mounted onto microscope slides as outline in section 2.10.1. Mounted coverslips were viewed under x40 magnification by fluorescence microscopy (Leitz Orthoplan Microscope, Leica Microsystems AG, Wetzlar, Germany) using Improvision software (Improvision, Coventry, England). Cells were observed under excitation, 490 nm; emission, 520 nm.

2.14 ISOLATION OF RNA

2.14.1 Precautions

For RNA analysis certain precautions were taken since ubiquitous RNAse enzymes easily degrade RNA. RNase enzymes are resistant to autoclaving but can be inactivated by diethylpyrocarbonate (DEPC; 0.1 % (v/v) Sigma-Aldrich, Dorset, UK), thus all solutions used for RNA work were treated with DEPC. Solutions containing amines such as Tris cannot be DEPC-treated directly as DEPC is inactivated by these chemicals. These solutions were prepared in DEPC-treated water. Gloves and disposable sterile plastics were used at all times and any glassware used was baked overnight at 200 °C. Following the extraction procedure manipulations with RNA were carried out quickly and on ice to prevent degradation of RNA by endogenous RNAses.

2.14.2 RNA extraction from cultured cortical neurons

Total RNA was isolated from cells using TRI reagent (Sigma-Aldrich, Dorset, UK). This is a modified version of the single step method of acid guanidine thiocyanate-phenol-chloroform extraction (Chomczynski and Sacchi, 1987). Cultured neurons were rinsed with DEPC-treated PBS and lysed directly on 24 well culture plates by adding 50 μl reagent per well and scraping coverslips using the rubber end of

a 1 ml syringe piston (B.Braun Medical Ltd., Melsungen, Germany). Cells were incubated for 5 min at room temperature to permit the complete dissociation of nucleoprotein complexes. Phase separation was achieved by adding 0.2 ml of chloroform reagent (Sigma-Aldrich, Dorset, UK) per 1 ml of TRI reagent, samples were mixed by inversion and incubated at RT for 2-15 minutes. The resulting mixture was centrifuged at 12,000 x *g* for 15 min. Following centrifugation the mixture separates into a lower red, phenol-chloroform phase, an interphase, and the colour-less upper aqueous phase. RNA remains exclusively in the upper phase while DNA and proteins partition to the interphase and lower organic phase. The aqueous phase was transferred to a fresh tube. RNA was precipitated by adding 0.5 ml of isopropanol (Sigma-Aldrich, Dorset, UK) per 1 ml of reagent used. Samples were incubated at RT for 10 min then centrifuged at 12,000 x *g* for 20 min. RNA pellets were then washed once with 75 % ethanol (Sigma-Aldrich, Dorset, UK), allowed to air dry and dissolved in sterile DEPC treated water. RNA samples were stored at -80 ^{o}C until required for use.

2.14.3 Analysis of Isolated RNA by Gel Electrophoresis

To check that isolated RNA was intact and had not been degraded, samples were run on a 1 % (w/v) agarose gel (Figure 2.2). The gel was prepared by boiling the appropriate quantity of agarose (Promega Corporation, Madison, USA) in 100 ml of 1X tris borate EDTA (TBE) buffer (0.08 M Tris; 0.04 M boric acid; 1 mM EDTA; pH 8.3). Ethidium Bromide (EtBr; Sigma-Aldrich, Dorset, UK) was added to give a final concentration of 0.5 μg/ml and the gel cast into the horizontal gel system and allowed to set. RNA samples (1.5 μl) were prepared for electrophoresis by mixing with 3.5 μl of H_2O and 1 μl of 6X gel loading buffer (60 % (v/v) glycerol, 0.4 % (w/v) bromophenol blue). Samples (6 μl) were loaded into the wells and RNA was separated by application of a 90 V voltage to the gel apparatus. Migration of the bromophenol blue was monitored and the voltage was switched off when the blue dye band reached the bottom of the gel. The gel was visualized under UV light and photographed using a UV transluminator (Chromato-vue, model TL-33, UVP INC, California, USA).

2.14.4 DNAse 1 treatment of RNA

Contaminating DNA was removed from RNA preparations using Deoxyribonuclease 1 (DNAse 1; Invitrogen, Paisley, UK). DNAse 1 digests single and double-stranded DNA to oligonucleotides. 1.5 μg of RNA sample was incubated for 15 min at RT with 1.5 μl (1 U/ml) DNAse 1 and 1 μl 10x DNAse 1 reaction buffer. 1 μl of 25 mM EDTA solution was added to the reaction mixture in order to inactivate the DNAse and the tube contents incubated at 65 °C for 10 min.

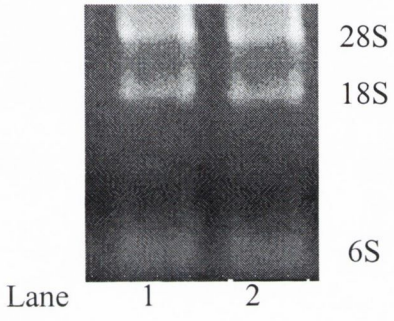

Figure 2.2 Sample Photo of 1 μg Total Rat RNA (in duplicate). An intact preparation of Total RNA exhibits distinct ribosomal RNA bands of 28S, 18S and 6S.

2.14.5 Quantitation of RNA

The quantity of RNA was determined spectrophotometrically by measuring the RNA at a wavelength of 260 nm. An absorbance value of 1 at this wavelength corresponds to 40 μg/ml of RNA.

2.15 Reverse Transcription-Polymerase Chain Reaction (RT-PCR)

Reverse-transcription polymerase chain reaction is a powerful technique which allows analysis of small quantities of specific messenger ribonucleic acid (mRNA). Total RNA is converted to complementary DNA (cDNA) using a reverse transcriptase enzyme. Specific cDNA's are then amplified by PCR using appropriate primer sequences. This PCR is semi-quantitative as a constitutively expressed gene (housekeeping gene), β-actin or glyceraldehyde-3-phosphate dehydrogenase (GAPDH) was amplified in parallel with each PCR reaction. This acted as an internal control and by calculating ratios of the target gene to β-actin/GAPDH relative amounts of the target gene could be determined.

2.15.1 Reverse Transcription

First strand cDNA synthesis of the mRNA was carried out using Superscript II RNASE H- Reverse-Transcriptase enzyme (Invitrogen, Paisley, UK). 1 μg of sample RNA was mixed with 1 μl of oligo dT Primer (Invitrogen, Paisley, UK) and 1 μl of dNTP mix (containing 10 mM each of dATP, dTTP, dCTP and dGTP; Promega Corporation, Madison, USA). This mixture was incubated at 65 ^{o}C for 5 min (to uncoil the RNA) then moved to ice. To this reaction mixture, 4 μl of 5X reaction buffer, 2 μl of 0.1 M dithiothreitol (DTT) and 1 μl of Ribonuclease (RNAse) Inhibitor (Promega Corporation, Madison, USA) were added and the reaction was preheated to 42 ^{o}C for 2 min before adding 1 μl (200 units) of Superscript Reverse-Transcription enzyme. The reaction was incubated at 42 °C for 50 min for cDNA synthesis and then at 75 °C for 10 min to inactivate the reverse transcriptase.

2.15.2 Polymerase Chain Reaction

A mastermix PCR reaction (final volume 25 µl) was made up containing 2.5 µl of 10x reaction buffer, 2.5-3 µl (2.5-3mM) magnesium chloride ($MgCl_2$), 1 µl dNTP mix (Promega Corporation, Madison, USA), 1 µl of each of the upstream and downstream primers (40 pmoles; MWG Biotech, Ebersberg, Germany), 12.5-13 µl sterile H_2O and 0.5 µl (5 units) Taq polymerase enzyme (Promega Corporation, Madison, USA). 2.5 µl of sample cDNA was added to this mastermix. The reaction contents were then overlayed with mineral oil (to prevent evaporation of the reaction contents) and placed in the thermocycler (Biometra GmbH, Gottingen, Germany). The PCR was run with an initial denaturing step of 95 °C followed by 25-35 cycles consisting of a denaturing step of 95 °C for 1 min, an annealing step of 50-55 °C (see table 2.1 for optimal annealing temp) for 1 min and an extension step of 72 °C for 1 min 30 seconds. A final extension step of 72 °C for 10 min was carried out to ensure complete extension of the PCR products. The PCR products (5 µl) were loaded into the wells and separated on a 1.5 % (w/v) agarose gel containing ETBR (0.5 µg/ml) and visualized under UV) light using a UV transilluminator. In all cases a DNA 100bp ladder was also loaded to determine the size of DNA bands.

2.15.3 Densitometry

In all cases quantification of PCR bands was achieved by densitometric analysis using the Zero-Dscan Image Analysis System (Scanalytics Inc., Fairfax, USA). Values are expressed as arbitrary units.

Target Gene	Primer Sequence	Annealing Temperature (^{o}C)	Fragment Size (base-Pairs)
p53	Fw: 5′ GGCCATCTACAAGAAGTCAC 3′ Rv: 5′ CCAGAAGATTCCCACTGGAG 3′	53	317 bp
β-actin*	Fw: 5′ GAAATCGTGCGTGACATTAAAGAGAAGCT 3′ Rv: 5′ TCAGGAGGAGCAATGATCTTGA 3′	52	360 bp
Caspase-3	Biosource international rat apoptosis signalling quantitative PCR detection kit Catalogue number #QRM0050	58	318 bp
bcl-xl	Biosource international rat apoptosis signalling quantitative PCR detection kit Catalogue number #QRM0050	58	398 bp
GAPDH	Biosource international rat apoptosis signalling quantitative PCR detection kit Catalogue number #QRM0050	58	532 bp
Bax **	Fw: 5′ GCAGAGAGGATGGCTGGGGAGA 3′ Rv: 5′ TCCAGACAAGCAGCCGCTCACG 3′	52	352 bp
NF-κB	Biosource international rat TNF signalling quantitative PCR detection kit Catalogue number #QRM0051	58	396 bp
IκB	Biosource international rat TNF signalling quantitative PCR detection kit Catalogue number #QRM0051	58	167 bp
TNF-α	Biosource international rat TNF signalling quantitative PCR detection kit Catalogue number #QRM0051	58	270 bp

Table 2.1 Primer pairs used for PCR

* Primers from Nakajimaiijima et al., 1985

** Primers from Ray et al., 2000

2.16 Analysis of Intracellular calcium levels $[Ca^{2+}]_i$

Free cytosolic calcium concentration was quantified in freshly dissociated neuronal suspensions by fluorescence imaging using the Ca^{2+} indicator dye Fura-2AM (Molecular Probes, Leiden, The Netherlands). Fura-2AM is a cell permeable dye which binds reversibly to calcium. Upon calcium binding, the maximum fluorescent excitation of the indicator dye undergoes a blue shift from 363 nm (Ca^{2+}-free) to 335 nm (Ca^{2+}-saturated), while the fluorescence emission maximum is relatively unchanged at 510 nm. The indicator is typically excited at 340 nm and 380 nm respectively and the ratio of the fluorescent intensities corresponding to the two excitations is used in calculating the intracellular concentrations of calcium. Measurement of $[Ca^{2+}]_i$ using this ratiometric method allows efficient measurement of calcium levels while cancelling out variability due to instrument efficiency and uneven dye distribution (Grynkiewicz *et al.*, 1985).

2.16.1 Preparation of Samples

Suspensions of neurons were prepared as described in section 2.2.3-2.2.4. However, in this experiment neurons were not resuspended in NBM but in filter-sterilised Hank's Balanced Salt Solution (HBSS; Sigma-Aldrich, Dorset, UK) containing HEPES 30 mM, $MgSO_4$ 1 mM, $CaCl_2$ 2 mM, 1 ml Pen/Strep pH 7.4. Cells were not allowed to adhere to coverslips, but instead were maintained in suspension in 1.5 ml sterile tubes (Sarstedt, Leicester, UK) at a concentration of 2.7 x 10^4 cells/ml. Suspensions were pre-treated with nicardipine (500 nM; 20 min; Sigma-Aldrich, Dorset, UK) at 37 ^{o}C in a $C0_2$ incubator. Cell suspensions were then treated with Aβ (2 μM) for a 1 hr or 6 hr incubation period. Following Aβ incubation, suspensions were loaded with Fura2-AM (5 μM) for 30 min (37 ^{o}C, 5 % CO_2). Cell suspensions were transferred to 15 ml tubes (Sarstedt, Leicester, UK), centrifuged at 3500 x g for 3 min and suspension pellets were resuspended in 1 ml HBSS (NaCl 145 mM, KCl 5 mM, $MgCl_2$ 1 mM, $CaCl_2$ 2 mM, Mg_2SO_4 1 mM, KH_2PO_4, 1 mM, Glucose 10 mM HEPES 30 mM; pH 7.4). To remove any unloaded Fura-2AM, the cells were again centrifuged

at 3500 x *g* for 3 min and resuspended in 1.5 ml HBSS. Suspensions were incubated for a further 10 min (37 °C, 5 % CO_2) to ensure sufficient intracellular hydrolysis of Fura-2AM to Fura-2.

2.16.2 Recording of $[Ca^{2+}]_i$ measurements

1.5 ml aliquots of Fura-2 loaded cell suspension cultures were placed in the cuvette holder of a Cairn spectrophotometer (Cairn, Faversham, UK). This apparatus consisted of a sealed chamber with channels in the side walls to allow light to pass through the cuvette. Excitation light from a xenon arc lamp passed through a filter wheel (32 revs/sec) containing alternating 340 nm and 380 nm filters into the cuvette chamber. The ratio of the 340/380 fluorescence signal emitted from the Fura-2 containing cells (R) was transmitted through a 510 nm filter, amplified through a photomultiplier tube, digitised and stored on hard disk for later analyis (Maclab Chart; see Figure 2.2) The maximum fluorescence ratio (R_{max}) was achieved by addition of Triton (2 %) until the saturated ratio value was attained. The minimum fluorescence ratio (R_{min}) was achieved by addition of the Ca^{2+} chelating agent EGTA (200 mM), until the minimum ratio plateau was reached.

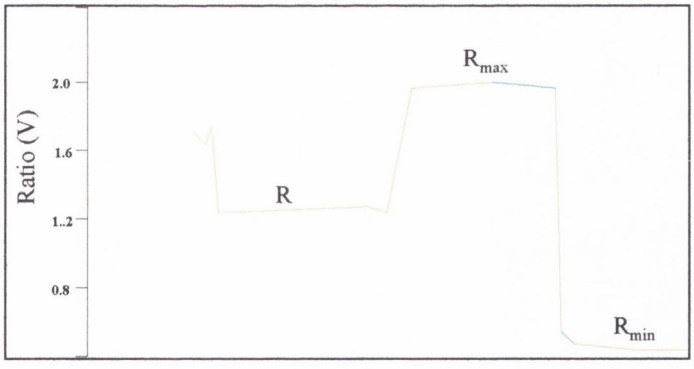

Figure 2.3 Sample trace of ratio (340/380 nm) for a given cortical suspension

2.16.3 Calculation of $[Ca^{2+}]_i$

The ratio of the fluorescence emission at the two different excitation wavelengths was used to determine $[Ca^{2+}]_i$ according to the formula

$$[Ca^{2+}]_i \text{ (nM)} = Kd.\beta \frac{R-R_{min}}{R_{max}-R}$$ Grynkiewicz *et al.*, 1985

where R = the ratio for each treatment, Kd = the dissociation constant for Fura-2 (197 nM under the experimental conditions described) and $\beta = [F_{380}$ at R_{min}/ F_{380} at $R_{max}]$ i.e. the ratio of fluorescence intensity evoked by excitation at 380nm at minimum and saturated calcium concentration.

2.17 Statistical Analysis

Data are expressed as means ± standard error of the means (SEM). Statistical Analysis was carried out by use of a one-way analysis of variance, followed by a post hoc Student Newman-Keuls test when significance was indicated. When comparisons were being made between two treatments, a paired Student's t-test was performed to determine whether significant differences existed between the conditions. In all cases the alpha level was set at 0.05. All statistical analysis was carried out using Graphpad Prism software.

Chapter 3

The role of c-jun-N-terminal kinase in Aβ-mediated neuronal apoptosis

3.1 Introduction

The MAPK cascade represents a prototypic signal transduction system, linking extracellular stimuli to intracellular responses. MAPK cascades are evolutionarily conserved in all eukaryotes demonstrating their importance in intracellular signalling. The three principal members ERK, JNK and p38 comprise 3 distinct, but similarly organised, signalling pathways. JNK kinases share sequence homology with ERK kinases and both JNK and ERK can be activated simultaneously by phosphorylation via their respective parallel cascades in response to the same stimuli, for example, the endotoxin lipopolysacharide (LPS) activates both ERK and JNK in macrophages (Pyo *et al.*, 1998).

Generally activation of ERK is associated with regulation of growth and differentiation, while JNK signalling functions in stress responses, such as DNA damage and apoptosis. However, this is not always the case, since cells are simultaneously exposed to multiple extracellular stimuli, each cell must integrate these signals and choose an appropriate response. Consequently, the biological context of a signal plays an important role in how the cell will respond to MAPK activation. For example, JNK signalling can lead to opposing cellular responses such as proliferation or apoptosis depending on the cell type and the context of other signals received by the cell (Herr and Debatin, 2001). Moreover, ERK activation can lead to contrasting physiological responses in the same cellular type, with transient stimulation of the ERK cascade leading to proliferation in PC12 cells, whereas sustained stimulation leads to differentiation (Marshall, 1995). Thus, the cellular response to ERK and JNK signalling may be specific to cell type as well as depending on the nature of the stimulus received by the cell and the physiological environment surrounding the cell.

There is increasing evidence that JNK proteins are potent effectors of neurodegeneration, since JNK has been implicated as a mediator of cell death in response to a variety of stimuli including growth factor deprivation, oxidative stress and exposure to ionizing radiation (Eilers *et al.*, 2001; Yoshizumi *et al.*, 2002; Mielke and Herdegen, 2000). Activation of JNK induces apoptosis in cultured neuronal cells (Virdee *et al.*, 1997), as well as in peripheral neurons in vivo (Chen *et al.*, 1996). Several features of the JNK signalling cascade suggest that it may be a target for Aβ modulation. JNK activation can occur in response to oxidative stress (Maroney *et al.*, 1999) and since Aβ can induce

oxidative stress (Behl *et al.*, 1994), this raises the possibility that Aβ may induce activation of JNK. A number of recent studies have suggested that JNK may play a role in Aβ-mediated effects. In sympathetic neurons, PC12 cells and cultured cortical neurons, the 1-42 fragment of Aβ activates JNK and the synthethic JNK inhibitor, CEP-1347, blocks Aβ-mediated neurotoxicity (Troy *et al.*, 2001; Bozyczko-Coyne *et al.*, 2001). In addition, JNK activation was demonstrated to associate with intracellular Aβ accumulation in cerebral neurons of PS1-linked AD patients (Shoji *et al.*, 2001). JNKs are encoded by three separate genes *jnk1*, *jnk2* and *jnk3*. *jnk1* and *jnk2* are ubiquitously expressed. In contrast, *jnk3* is predominantly expressed in the brain (Herr and Debatin, 2000). Studies of mice deficient in JNK1, JNK2 or JNK3 provide evidence for the functional diversity of isoforms, with mice lacking JNK1 and JNK2 being embryonic lethal, showing increased apoptotic death in the fore brain and reduced apoptotic death in the hind brain (Kuan *et al.*, 1999). Mice lacking JNK3 display decreased susceptibility to kainic acid-induced hippocampal cell death (Yang *et al.*, 1997). This provides evidence that different JNK isoforms have diverse effects in the central nervous system and that these effects may depend on cellular context. Substrates of JNK include transcription factors c-jun and activating transcription factor 2 (ATF-2) as well as cytoplasmic substrates p53 and bcl-2 (Mielke and Herdegen, 2000). The discovery that various JNK isoforms differ in their specificity for downstream transcription factors (Gupta *et al.*, 1996) as well as in stress-induced activation (Yin *et al.*, 1997) suggest that JNK isoforms have differing physiological roles. Aβ has the potential to couple with JNK1, JNK2 or JNK3. However, the JNK inhibitor applied in previous studies (Troy *et al.*, 2001) is unable to distinguish between JNK isoforms. In this study I applied antisense technology to determine the roles of the specific JNK isoforms in Aβ-mediated degeneration of cultured cortical neurons.

In addition to inducing activation of JNK, Aβ has been reported to increase ERK activity in a number of studies (Pyo *et al.*, 1998; Rapoport and Ferreira, 2000) and there is evidence of ERK activation in the Alzheimer's disease brain (Perry *et al.*, 1999). Studies from this laboratory (MacManus *et al.*, 2000) and others (Ueda *et al.*, 1997) have demonstrated that Aβ induces calcium influx in cultured cortical neurons via activation of the L- and N- type voltage calcium channels. A recent study provides evidence that Aβ activates calcium channels via ERK-dependent phosphorylation, resulting in sustained

accumulation of calcium, reactive oxygen species (ROS) and apoptosis (Ekinci *et al.*, 1999a). In contrast, other reports dispute this, finding no link between Aβ-mediated neurotoxicity and the ERK cascade (Abe and Saito, 2000). ERK is generally proposed to have an anti-apoptotic role in neurons, with reports that ERK activation can protect certain populations of neurons against specific insults (Hetman and Xia, 2000; Anderson and Tolkovsky, 1999). Thus, the role of ERK signalling in Aβ-mediated events has yet to be elucidated.

The experimental work carried out in this chapter uses extracellular application of Aβ in order to investigate the roles of the MAPKs, JNK and ERK, in Aβ-induced neurotoxicity. The initial aim of this study was to establish whether MAPK family members, ERK and JNK, are activated following exposure to Aβ. I then sought to determine the cellular consequences, and ultimate fate, of cultured cortical neurons subsequent to activation of these signalling kinases. Expression of JNK1 and JNK2 were transiently downregulated using selective antisense oligonucleotide sequences, so that the role of each JNK isoform could be determined. Proteolytic cleavage of the inactive precursor of caspase-3 to its active form is a key event in determining whether cells will undergo apoptosis (Thornberry and Lazebnik, 1998). DNA fragmentation occurs downstream of caspase-3 activation and is a signature of apoptosis (Johnson *et al.*, 1996). It marks the end-point of the apoptotic signalling cascade, culminating in cell death. The role of the specific JNK isoforms in the proclivity of Aβ to activate these apoptotic parameters, namely caspase-3 activity and DNA fragmentation, was assessed in cortical neurons which had been depleted of JNK1 or JNK2 proteins using santisense technology.

3.2 Results

3.2.1 Aβ mediates increased phospho-JNK expression throughout neuronal cells

Activation of JNK occurs when JNK becomes phosphorylated at threonine and tyrosine residues. Expression and localisation of phospho-JNK was investigated using immunofluorescence microscopy. Phospho-JNK immunofluorescence was visualised by probing neurons with an anti-active JNK antibody, which recognises both JNK1 and JNK2 phosphorylated on amino acid residues Thr-183 and Tyr-185, and a fluorescein-conjugated secondary antibody. Cells were then examined under a fluorescence microscope at an excitation wavelength of 490 nm. Figure 3.1 depicts the changes in phospho-JNK expression, evoked by Aβ at 1 hr and 24 hr. In control cells, phospho-JNK immunoreactivity was detected in some cells (Figure 3.1 (i) and (iii)), reflecting a basal level of JNK activation. However, in cells treated with Aβ (2 μM) for 1 hr or 24 hr (Figure 3.1 (ii) and (iv)), a higher intensity of phospho-JNK immunoreactivity was observed in the nucleus and within discrete areas of cytoplasm. This result demonstrated that Aβ1-40 activates JNK in cultured cortical neurons and the distribution of phospho-JNK immunostaining indicates that activated JNK has both cytosolic and nuclear targets.

3.2.2 Time course of Aβ-mediated activation of JNK1 and JNK2

In order to characterise the time course for Aβ-mediated JNK activation, and to determine the nature of the JNK isoforms activated by Aβ, cortical neurons were exposed to Aβ (2 μM) over a range of time-points from 5 min to 48 hr. Expression of phospho-JNK was analysed by western immunoblot using an anti-active JNK antibody, which recognises JNK1 and JNK2, phosphorylated on amino acid residues Thr-183 and Tyr-185. Expression of total JNK was analysed by western immunoblot with a polyclonal antibody which recognises JNK1 and JNK2. Analysis of mean densitometric data (Figure 3.2A) demonstrates that Aβ evoked a rapid increase in JNK1 activation, as assessed by phosph-JNK1 expression, at 5 min from a control

value of 0.89 ± 0.07 (mean band width ± SEM; arbitrary units) to 1.08 ± 0.07 in Aβ-treated cells ($p<0.05$, students paired t-test, n=6). Similarly, a significant increase in JNK1 activity was observed following Aβ-treatment for 1 hour and 6 hours. For the 1 hour time-point, JNK1 activity in control cells was 0.98 ± 0.23 and this was significantly increased to 1.18 ± 0.068 by Aβ ($p < 0.01$, students paired t-test, n=6). At the 6 hr time-point, JNK1 activity in control cells was 0.9 ± 0.029 and this was significantly increased to 1.045 ± 0.04 ($p < 0.05$, student's paired t-test, n=6). In contrast, cells treated with Aβ for 18 hr, 24 hr and 48 hr showed no observable increase in JNK1 activation. Thus, JNK1 activity was 0.81 ± 0.11 in control and 0.76 ± 0.13 in Aβ-treated cells at 18 hr, 0.84 ± 0.05 in control and 0.8 ± 0.05 in Aβ-treated cells at 24 hr and 0.81 ± 0.022 in control and 0.78 ± 0.044 in Aβ-treated cells at 48 hr. Figure 3.2C demonstrates that levels of total JNK1 expression were unaffected by Aβ at all time-points examined.

A different pattern of activation was observed for JNK2. Figure 3.2B demonstrates that Aβ had no effect on JNK2 activity at the earlier time-points of 5 min -18 hr. Thus, JNK2 activity, as assessed by phospho-JNK2 expression, was 0.892 ± 0.01 in control and 0.98 ± 0.06 in Aβ-treated cells at 5 min, 1.008 ± 0.01 in control and 1.058 ± 0.009 in Aβ-treated cells at 1 hr, 0.93 ± 0.021 in control and 1.0 ± 0.063 in Aβ-treated cells at 6 hr and 0.94 ± 0.01 in control and 1.025 ± 0.14 in Aβ-treated cells at 18 hr. However, JNK2 activity was significantly increased by Aβ at the later time-points of 24 hr and 48 hr. Thus, at 24 hr JNK2 activity in control cells was 0.919 ± 0.005 (mean band width ± SEM; arbitrary units) and this was significantly increased to 1.119 ± 0.06 by Aβ ($p < 0.05$ students paired t-test, n=4). At the 48 hour time-point JNK2 activity was significantly increased from a control value of 0.95 ± 0.017 to 1.111 ± 0.05 in Aβ-treated cells ($p < 0.05$ students paired t-test, n=4). Figure 3C demonstrates that levels of total JNK2 protein expression were unaffected by Aβ at all time-points examined.

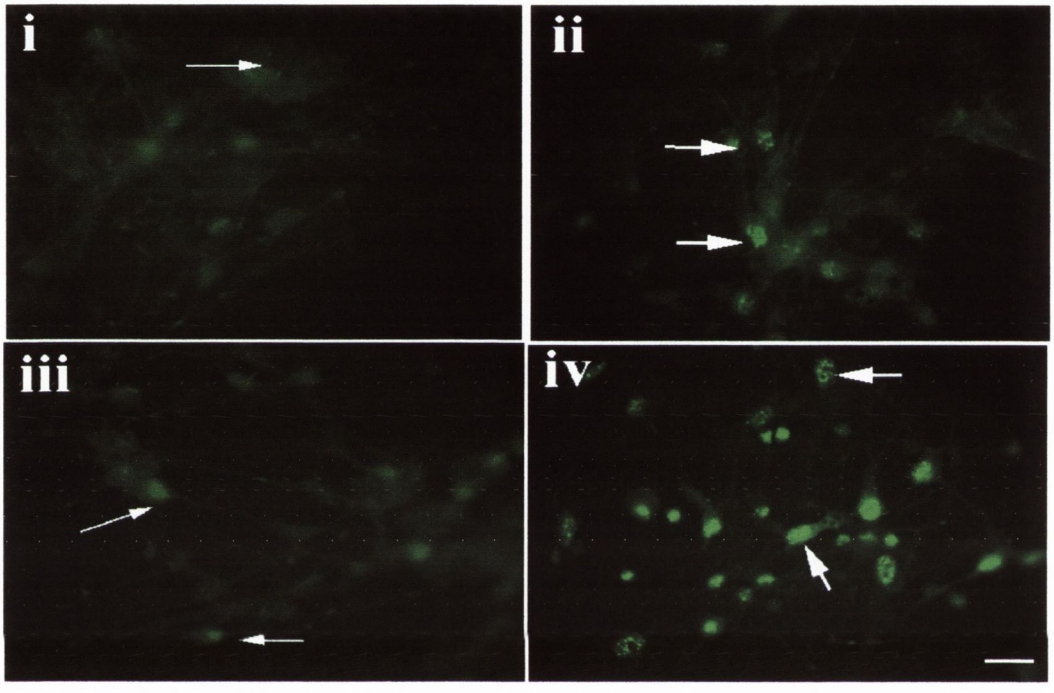

Figure 3.1 Aβ-treated cortical neurons display increased JNK activation

Cortical neurons were exposed to Aβ (2 μM) and JNK immunoreactivity was examined using fluorescence immunocytochemistry with the phospho-specific JNK antibody in (i) control (1 hr) (ii) Aβ-treated (1 hr) (iii) control (24hr) and (iv) Aβ-treated (24 hr). Arrows indicate cells displaying phospho-JNK immunoreactivity. Scale bar is 20 μm

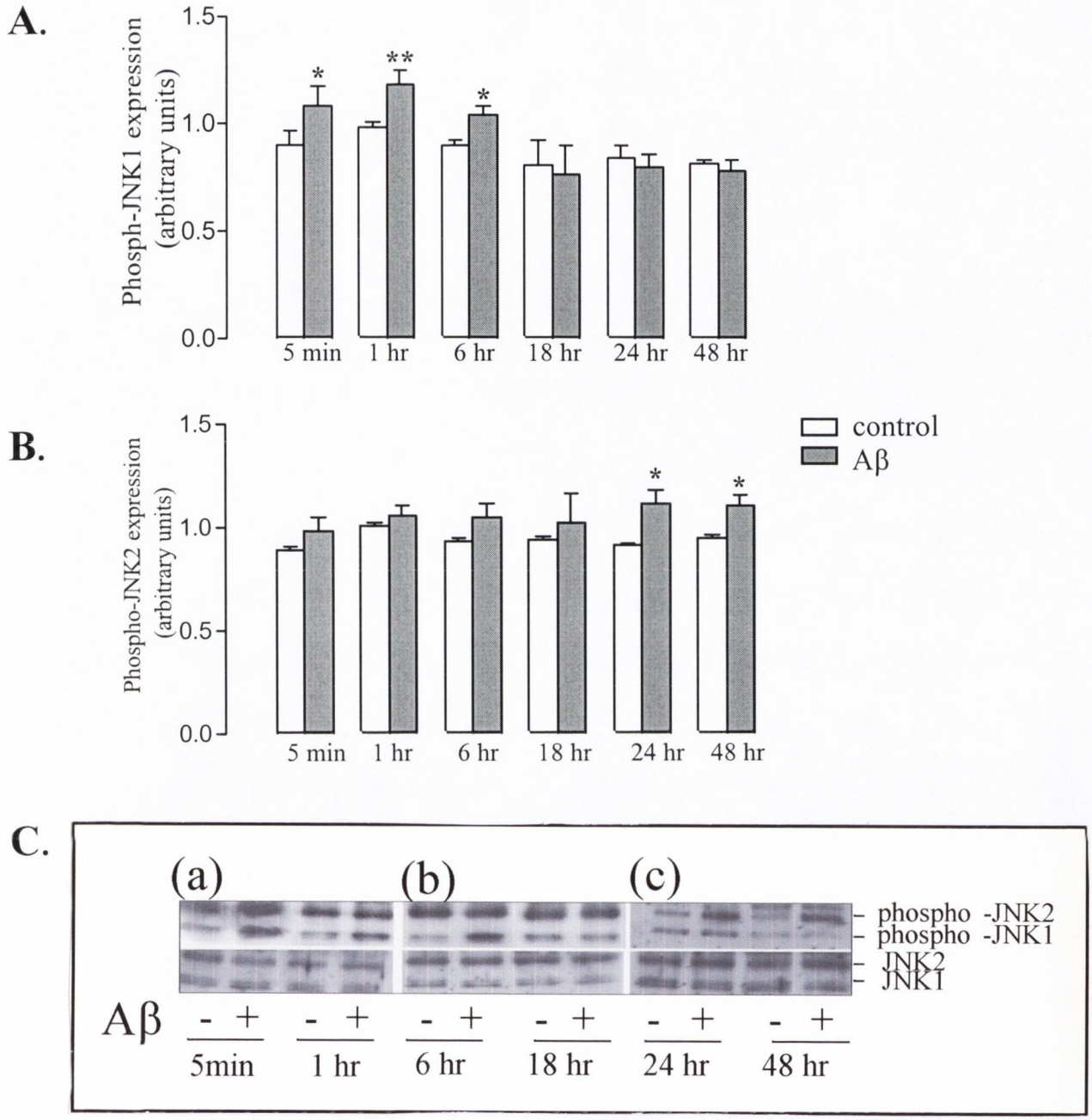

Figure 3.2 Aβ-mediated JNK activation is time dependent

A. Cortical neurons were treated with Aβ (2 μM) over a range of time-points (5 min - 48 hr). Expression of phospho-JNK1 was examined by western immunoblot. Aβ significantly increased phospho-JNK1 expression at 5 min, 1hr and 6 hr. Results are expressed as mean ± SEM for 6 observations, *$p<0.05$, ** $p<0.01$.

B. Expression of phoshpo JNK2 was measured by western immunoblot. Aβ significantly increased phospho-JNK2 expression at 24 hr and 48 hr. Results are expressed as mean ± SEM for 6 observations, *$p<0.05$.

C. Sample western blot showing JNK1 and JNK2 (phospho and total) expression. Cells were treated with Aβ over a range of time points - 5 min, 1 hr (panel a), 6 hr, 18 hr, (panel b), 24 hr and 48 hr (panel c).

A sample immunoblot illustrating the time-dependent activation of JNK1 and JNK2 by Aβ is shown in Figure 3.2C. Also shown is an immunoblot demonstrating that total JNK1 and JNK2 protein expression is unaffected by Aβ.

3.2.3 Aβ does not mediate activation of JNK3 in cultured cortical neurons

While JNK1 and JNK2 are ubiquitously expressed, expression of JNK3 is predominantly restricted to the brain, where it is expressed in neurons (Mielke and Herdegen, 2000). This indicates that JNK3 may play an important role in modulating the neuronal response to stress. Consequently, activation of JNK3 in response to Aβ-treatment was investigated. Expression of phospho-JNK3 was analysed by western immunoblot using an anti-active JNK antibody, which recognises JNK3 phosphorylated on amino acid residues Thr-183 and Tyr-185. Low levels of expression of phospho-JNK3 were found in cortical neurons when compared with expression of the phospho-JNK1 and phospho-JNK2 isoforms (Figure 3.3(A-D) n=6) therefore it was not possible to measure phosphorylation of JNK3 using densitometry. Aβ did not alter the phosphorylation status of JNK3 at any of the examined time-points. It was therefore concluded that Aβ does not regulate JNK3 phosphorylation in this system.

3.2.4 Aβ does not mediate activation of ERK in cultured cortical neurons

ERK is activated via phosphorylation at threonine and tyrosine residues. In order to analyse the proclivity of Aβ to mediate activation of ERK, cortical neurons were exposed to Aβ (2 μM) for incubation periods of 5 min – 48 hr and analysed for ERK phosphorylation by western immunoblot using an antibody which recognises the dually phosphorylated active forms of ERK1 and ERK2. Phospho-ERK1 was not expressed at sufficiently high levels for densitometric analysis and so the densitometric data presented is for expression of phospho-ERK2 (Figure 3.4). No observable change in ERK2 phosphorylation was detected at any of the examined time-points (n=6). Thus, ERK2 activity was 2.359 ± 0.12 in control, and 2.492 ± 0.44 in Aβ treated cells at 5 min; 2.449 ± 0.14 in control, and 2.339 ± 0.21 in Aβ treated cells at 1 hr; 2.481 ± 0.38

in control, and 2.498 ± 0.18 in Aβ treated cells at 6 hr; 2.05 ± 0.236 in control, and 2.077 ± 0.236 in Aβ treated cells at 18 hr; 2.335 ± 0.15 in control, and 2.203 ± 0.07 in Aβ treated cells at 24 hr; and 2.536 ± 0.471 in control and 2.59 ± 0.74 in Aβ treated cells at 48 hr. This result indicates that ERK is not modulated by Aβ in this system. A sample immunoblot demonstrating that ERK phosphorylation is unaffected by Aβ is shown in Figure 3.4B. Also shown is a sample ERK immunoblot stripped and reprobed for actin expression to confirm equal loading of protein. Similar actin expression was observed in control and Aβ-treated neurons.

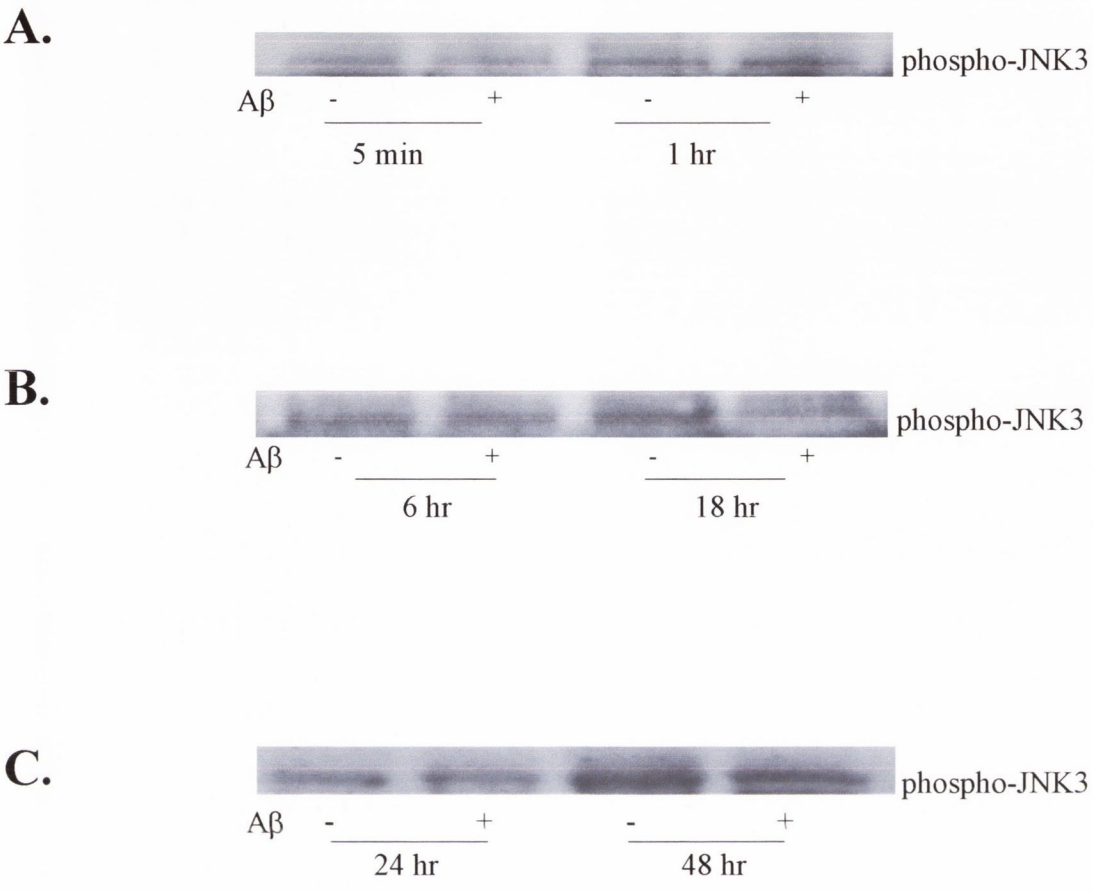

Figure 3.3 JNK3 activity in not modulated by Aβ

Cortical neurons were treated with Aβ (2 μM) over a range of time points (5-48 hr). Expression of phospho-JNK3 expression was measured by western immunoblot.

A. Sample western blot demonstrating JNK3 activity at 5 min and 1 hr post Aβ-treatment

B. Sample western blot demonstrating JNK3 activity at 6 hr and 18 hr post Aβ-treatment

C. Sample western blot demonstrating JNK3 activity at 24 hr and 48 hr post Aβ-treatment. Aβ had no effect on JNK3 activity at any of the examined time-points.

A.

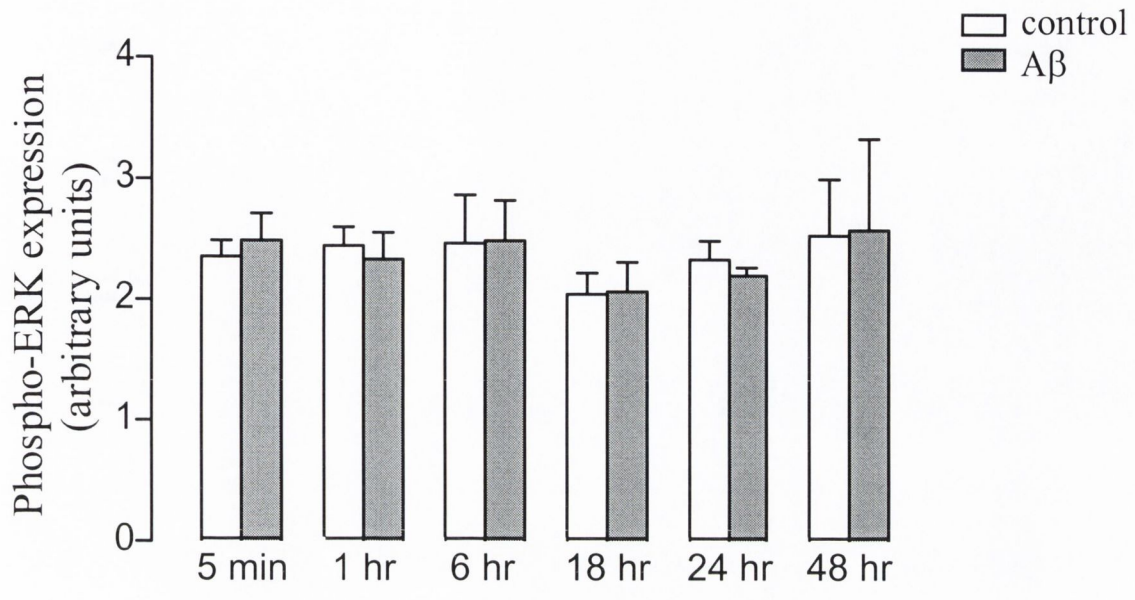

B.

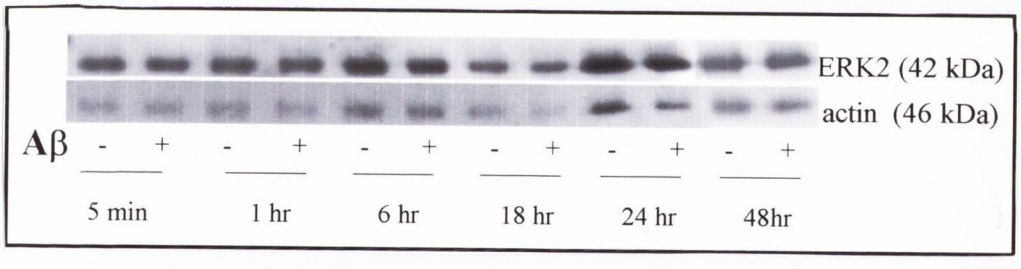

Figure 3.4 Aβ does not induce activation of ERK

A. Cortical neurons were treated with Aβ (2 μM) over a range of time-points (5-48 hr). Expression of phospho-ERK was examined by western immunoblot. Aβ had no effect on ERK activity at any of the time points examined.

B. Sample western blot showing ERK2 phospho-expression. Also present is a sample immunoblot showing actin expression to confirm equal loading of protein.

3.2.5 Antisense oligonucleotides are efficiently incorporated into cultured cortical neurons

There is currently no available JNK inhibitor, which can distinguish between JNK isoforms. Therefore, in this study antisense technology was employed to selectively deplete cell of JNK1 and JNK2. Phosphorothioate antisense oligonucleotides, complementary to the mRNA encoding JNK1 or JNK2 were incorporated into the culture medium to evoke a transient downregulation in expression of JNK1 or JNK2. To ensure that this treatment protocol enabled the oligonucleotides to enter neuronal cells, the efficient uptake of antisense oligonucleotides by neurons was first assessed by analysing the fluorescence of cells incubated with a FITC labelled control oligonucleotide for a range of time-points (1 – 24 hr). Figure 3.5 demonstrates the rapid and efficient incorporation of antisense oligonucleotides into neurons within 1 hr of their inclusion into neurobasal medium. Immunofluorescence was localised throughout cells indicating both cytosolic and nuclear presence of oligonucleotides. Oligonucleotides which gain cytoplasmic or nuclear locations are able to interact with target mRNA and thus induce antisense-mediated depletion. Since sufficient uptake of the control oligonucleotide was seen as early as 1 hr, it was therefore accepted that following treatment of cortical neurons with target antisense oligonucleotide, an adequate uptake of oligonucleotide occurred.

3.2.6 Time course of JNK depletion in JNK antisense treated cells

In order to identify the time-point at which JNK expression was maximally depleted in JNK antisense-treated cells, neuronal cultures were incubated with JNK antisense oligonucleotides over a range of time-points from 1 hr – 48 hr and JNK expression was evaluated by western immunblot using antibodies which recognise the epitopes corresponding to full length JNK1 or JNK2. Figure 3.6(A,B) demonstrates that maximal JNK1 and JNK2 depletion occurred following exposure to the respective antisense oligonucleotide for 48 hr. No observable decrease in JNK1 and JNK2 expression was observed at the earlier time-points of 1 hr, 6 hr, 12 hr and 24 hr,

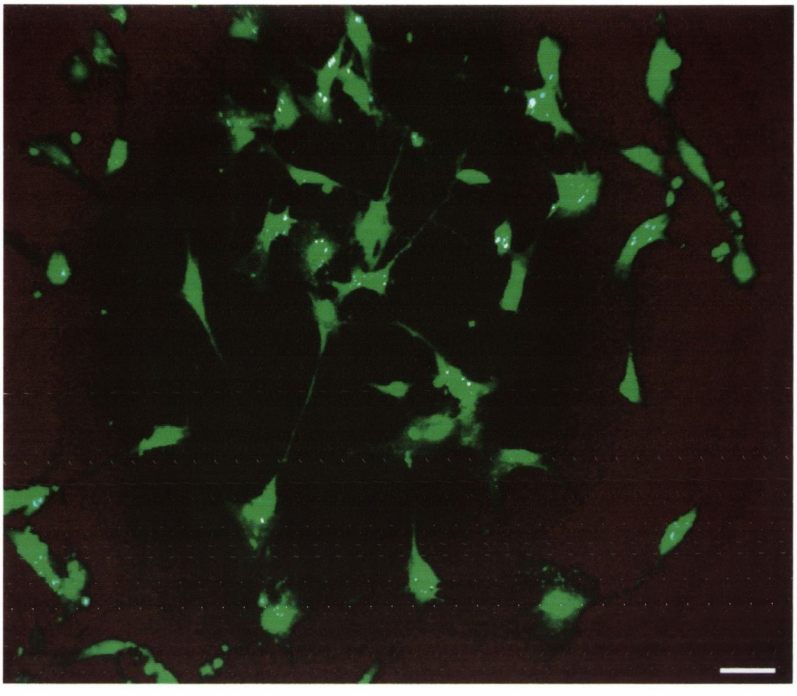

Figure 3.5 Uptake of FITC-labelled oligonucleotide in cultured cortical neurons at 1 hr

Cortical neurons were treated with 2 μM FITC-labelled antisense oligionucleotides over a range of time points (1-24 hr) and viewed by fluorescence microscopy (excitation, 490 nm; emission, 520 nm). Scale bar is 25 μm

A.

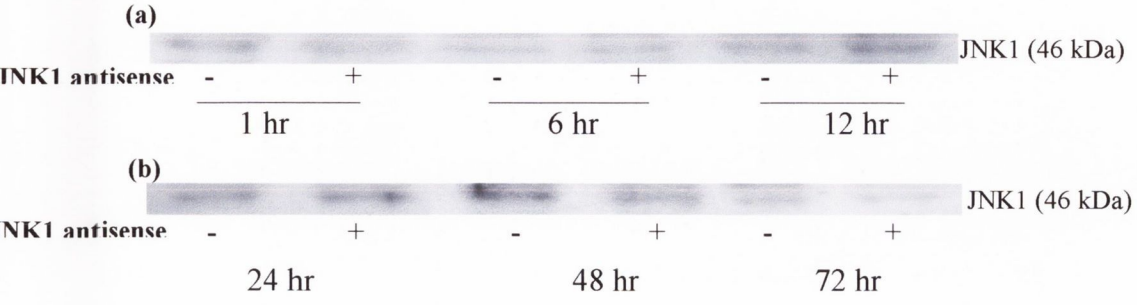

B.

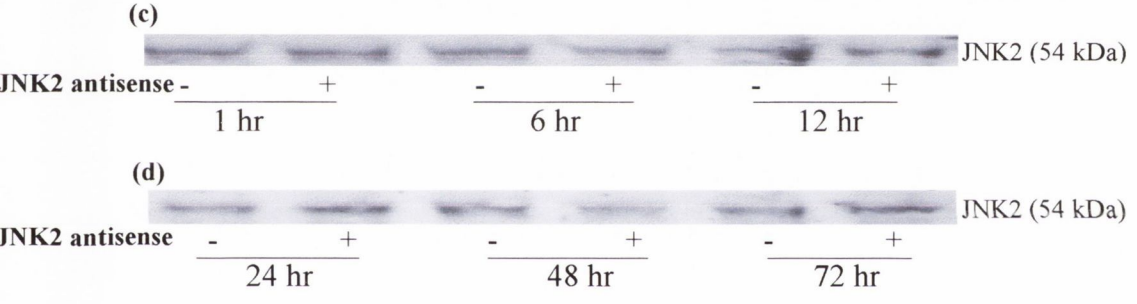

Figure 3.6 Time course of JNK depletion in antisense treated cells.

A. Cultured neurons were treated with JNK1 and JNK2 antisense oligonucleotides (2 μM) over a range of time points (1 hr-72 hr). JNK1 or JNK2 expression was assessed by western immunoblot. Sample immunoblot demonstrating JNK1 activity in control and JNK1-antisense treated neurons at 1 hr, 6 hr 12 hr (panel a) and 24 hr, 48 hr and 72 hr (panel b).

B. Sample immunoblot demonstrating JNK2 activity in control and JNK2-antisense treated neurons at 1 hr, 6 hr 12 hr (panel c) and 24 hr, 48 hr and 72 hr (panel d). Expression of JNK1 and JNK2 were efficiently downregulated following incubation for 48 hr with the relevant antisense sequence.

indicating that cells needed to be incubated with the oligonucleotides for 48 hr in order to obtain efficient JNK depletion.

3.2.7 Effect of JNK1 antisense oligonucleotides on JNK1 expression

To visualise the intracellular reduction of JNK1 protein, following treatment with JNK1 antisense oligonucleotides for 48 hr, fluorescence immunostaining was carried out using a specific JNK1 monoclonal antibody, recognising the epitope corresponding to full length JNK1 protein. The intracellular JNK1 immunoreactivity observed in control cells (Figure 3.7i) was markedly downregulated in cells transfected with the JNK1 antisense sequence (Figure 3.7ii).

3.2.8 JNK1 antisense oligonucleotides selectively deplete expression of JNK1 protein

The extent of JNK1 protein depletion following incubation with JNK antisense oligonucleotides for 48 hr was quantified by western immunoblot using the JNK1 monoclonal antibody and densitometric analysis. Figure 3.8A demonstrates that there was no difference in JNK1 expression in untreated cells (1.6 ± 0.01; mean band width ± SEM) compared to cells treated with the scrambled JNK1 control oligonucleotide (1.8 ± 0.6, n=4). However, in cells treated with the antisense JNK1 oligonucleotide for 48 hr, JNK1 expression was significantly reduced by 80% to 0.38 ± 0.15 ($p<0.05$, one-way ANOVA, n=4). The sample immunoblot shown in Figure 3.8B demonstrates the efficacy of JNK1 antisense oligonucleotides in downregulating JNK1 protein.

In order to confirm the selective downregulation of JNK1 protein by JNK1 antisense, cell cultures which had been incubated with JNK2 antisense oligonucleotides (2 μM) and JNK2 scrambled oligonucleotides (2 μM) were assessed for JNK1 expression by western immunoblot. Figure 3.8C demonstrates that JNK2 antisense had no effect on expression of JNK1. Thus, JNK1 protein expression was 0.9 ± 0.087 (n=4) in control, 0.83 ± 0.02 (n=4) in cells treated with JNK2 scrambled oligonucleotide and 0.83 ± 0.01 (n=4) in cells treated with JNK2 antisense oligonucleotide.

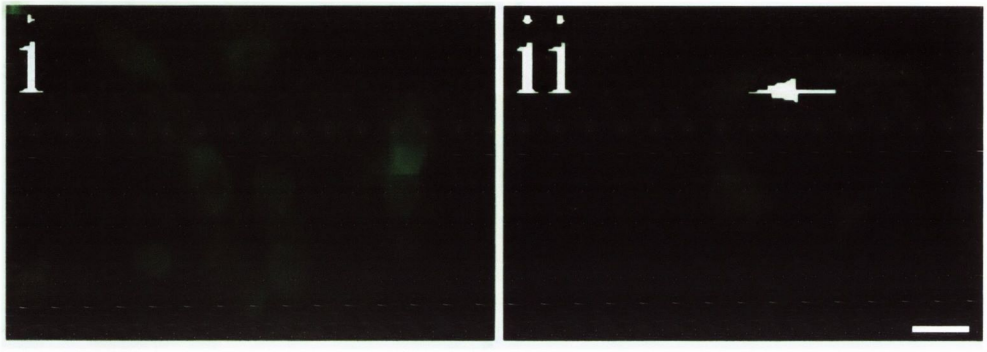

Figure 3.7 Effect of JNK1 antisense oligonucleotides on JNK1 expression at 48 hr.

Cortical neurons were exposed to antisense oligonucleotides (2 μM) targeted to JNK1 for 48 hr and JNK1 expression was monitored by immunofluorescence (excitation, 490 nm; emission, 520 nm).

(i) In non treated cells, JNK1 expression was localised throughout the cytoplasm with a high level of immunoreactivity at the inner plasma membrane

(ii) JNK1 immunostaining was markedly reduced in JNK1 antisense-treated cells. Scale bar is 10 μM

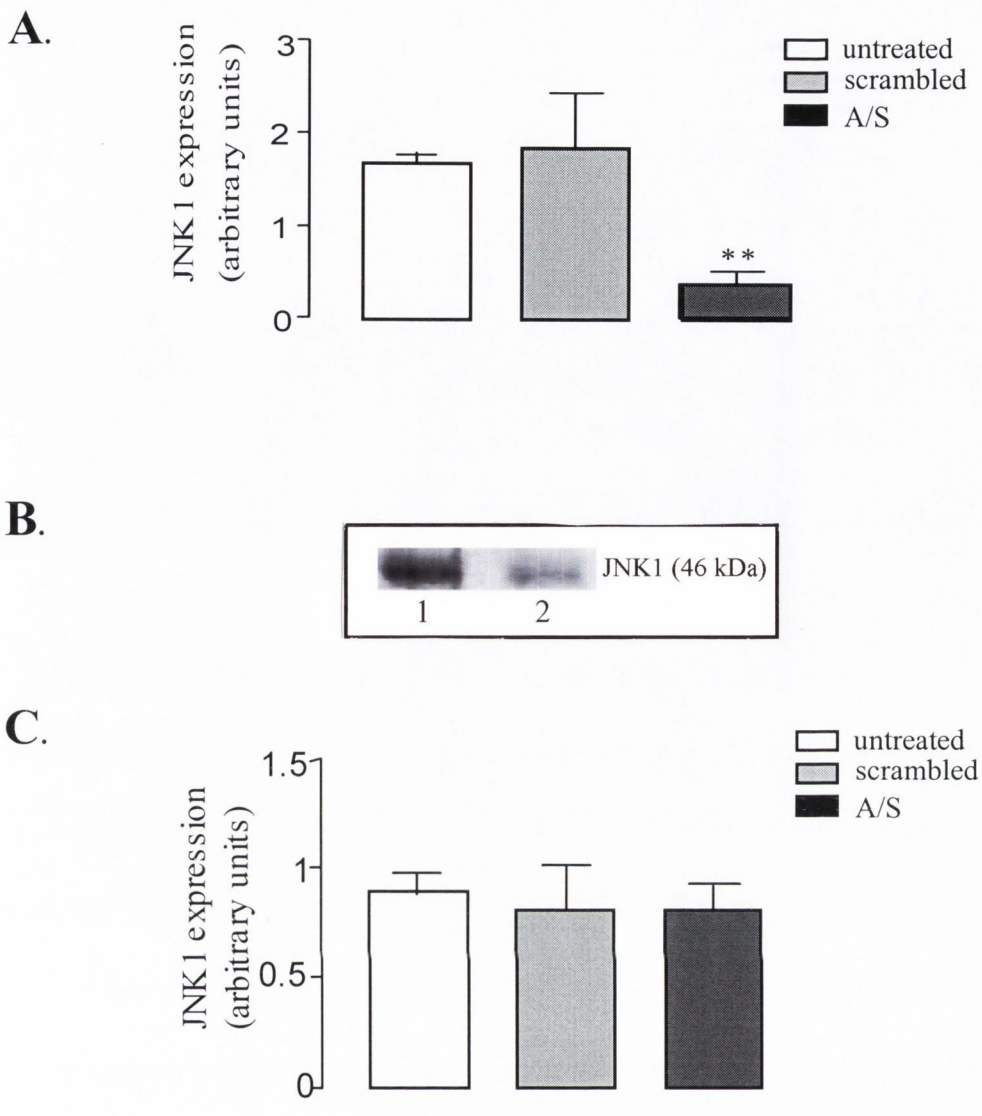

Figure 3.8 JNK1 antisense selectively downregulates JNK1 expression at 48 hr

A. Cortical neurons were treated with JNK1 antisense (A/S) or JNK1 scrambled oligonucleotide (2 μM) for 48 hr and JNK1 total expression was examined by western immunoblot. JNK1 A/S significantly depleted total JNK1 expression at 48 hr. Results are expressed as mean band width ± SEM, for 4 independent observations, ** $p<0.05$.

B. Sample western blot demonstrating levels of JNK1 protein expression in control (lane 1) and JNK1-antisense treated cells (lane 2)

C. Cortical neurons were exposed to JNK2 A/S or JNK2 scrambled control (2 μM) for 48 hr and JNK1 total expression was examined by western immunoblot. JNK2 A/S had no effect on expression of JNK1 protein. Results are expressed as mean band width ± SEM, for 4 independent observations, ** $p<0.05$

3.2.9 Depletion of total JNK1 abolishes the Aβ-mediated increase in phospho-JNK1 expression

Maximal phosphorylation of JNK1 occurred following a 1 hr treatment with Aβ (see Figure 3.2A), therefore, the effect of JNK1 depletion on JNK1 phosphorylation was examined at this time-point. Figure 3.9A demonstrates that in cells treated with the JNK1 scrambled oligonucleotide, activated phospho-JNK1 was significantly increased from 0.609 ± 0.046 (mean band width ± SEM, arbitrary units) to 0.729 ± 0.09 ($p < 0.05$, one-way ANOVA, n=6) following treatment with 2 μM Aβ. However, in JNK1 antisense oligonucleotide-treated cells the basal expression of activated phospho-JNK1 was 0.613 ± 0.039 (n=6) in control cells, and 0.503 ± 0.057(n=6) following incubation with Aβ. This result demonstrates that the JNK1 antisense was effective in reducing the Aβ-mediated stimulation of JNK1 phosphorylation. A sample immunoblot demonstrating that Aβ-mediated JNK1 phosphorylation is significantly reduced in JNK1 antisense-treated cells is shown in (Figure 3.9A).

3.2.10 Effect of JNK2 antisense oligonucleotides on JNK2 expression

To visualise the intracellular reduction of JNK2, following treatment with JNK2 antisense oligonucleotides for 48 hr, fluorescence immunostaining was carried out using a specific JNK2 monoclonal antibody, recognising the epitope corresponding to full length JNK2 protein. The intracellular JNK2 immunoreactivity observed in control cells (Figure 3.10i) was markedly downregulated in cells transfected with the JNK2 antisense sequence (Figure 3.10ii).

A.

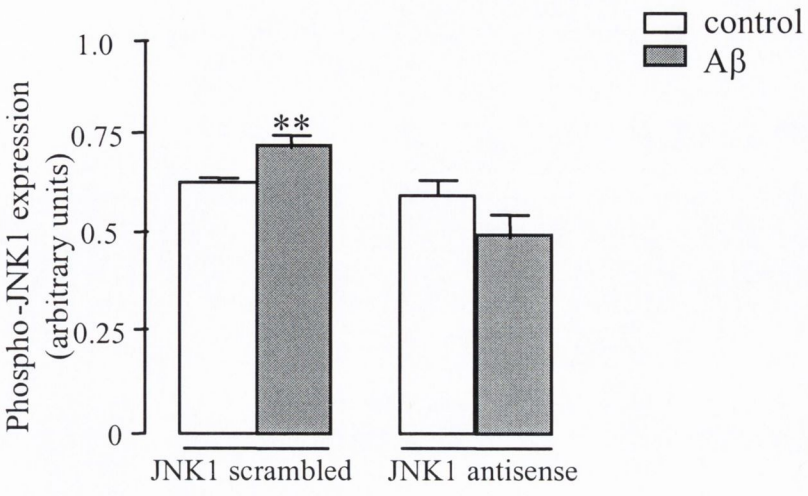

B.

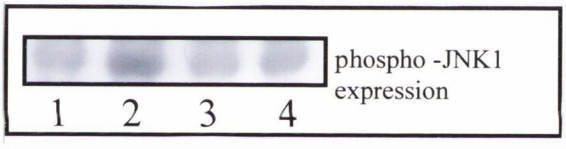

Figure 3.9 Effect of JNK1 depletion on phospho-JNK1 expression

A. Cortical neurons were pre-treated with JNK1 antisense and scrambled oligonucleotides (2 μM) for 48 hours before treatment with Aβ (2 μM) Phospho-JNK1 expression was examined by western immunoblot. Aβ significantly increased phospho-JNK1 expression after 1 hr. The Aβ-mediated increase in JNK1 phospho-expression was significantly reduced in JNK1 antisense treated cells. Results are expressed as mean band width ± SEM, for 6 independent observations, ** $p<0.05$.

B. Sample western blot showing phospho-JNK1 expression in (1) control (2) Aβ-treated cells (3) JNK1 antisense treated cells (4) Aβ + JNK1 antisense treated cells.

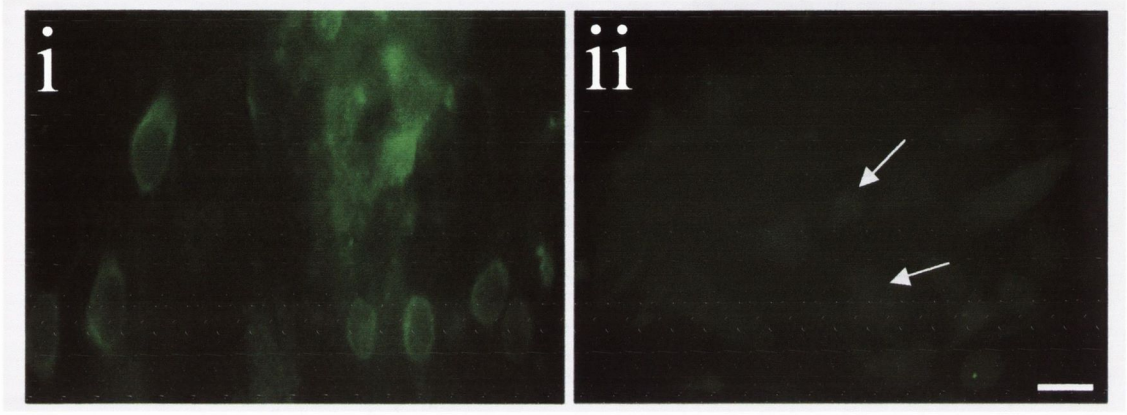

Figure 3.10 Effect of JNK2 antisense oligonucleotides on JNK2 expression at 48 hr.

Cortical neurons were exposed to antisense oligonucleotides (2 μM) targeted to JNK2 for 48 hr and JNK2 expression was monitored by immunofluorescence (excitation, 490 nm; emission, 520 nm).

(i) In non treated cells, JNK2 expression was localised throughout the cytoplasm with a high level of immunoreactivity at the inner plasma membrane

(ii) JNK2 immunostaining was markedly reduced in JNK2 antisense-treated cells. Scale bar 10μm

3.2.11 JNK2 antisense oligonucleotides selectively deplete expression of JNK2 protein

The extent of JNK2 protein depletion following incubation with JNK2 antisense oligonucleotides for 48 hr was quantified by western immunoblot using a JNK2 monoclonal antibody and densitometric analysis. Figure 3.9A demonstrates that there was no difference in JNK2 expression in untreated cells (2.8 ± 0.04; mean band width ± SEM) compared to cells treated with the scrambled JNK2 control oligonucleotide (3.6 ± 0.37, n=4). However, in cells treated with the antisense JNK2 oligonucleotide for 48 hr, JNK2 expression was significantly reduced by 65% to 0.98 ± 0.36 ($p<0.05$, one-way ANOVA, n=4). A sample immunoblot demonstrating the efficacy of JNK2 antisense oligonucleotides in downregulating JNK2 protein is shown in Figure 3.11B

In order to confirm the selective downregulation of JNK2 protein by JNK2 antisense, cell cultures which had been incubated with JNK1 antisense oligonucleotides (2 μM) and JNK1 scrambled oligonucleotides (2 μM), were assessed for JNK2 expression by western immunoblot. Figure 3.11C confirms that JNK1 antisense had no effect on expression of JNK2. Thus, JNK2 protein expression was 0.55 ± 0.01 (n=4) in control cells, 0.59 ± 0.03 (n=4) in cells treated with JNK1 scrambled oligonucleotide and 0.57 ± 0.008 (n=4) in cells treated with JNK1 antisense oligonucleotide

3.2.12 Depletion of JNK2 abolishes the Aβ-mediated increase in phospho-JNK2 expression

Maximal activation of JNK2 occurred following a 24 hr treatment with Aβ (see Figure 3.2B), therefore the effect of JNK2 depletion on JNK2 activation was examined at this time-point. Figure 3.12A demonstrates that in cells treated with the JNK2 scrambled oligonucleotide expression of phospho-JNK2 was significantly increased from 1.92 ± 0.08 (mean band width ± SEM, arbitrary units) to 2.3 ± 0.1 by Aβ (2 μM) ($p<0.05$, one-way ANOVA, n=6). In JNK2 antisense oligonucleotide-treated cells the expression of activated phospho-JNK2 was unaffected by treatment with 2 μM Aβ (1.9

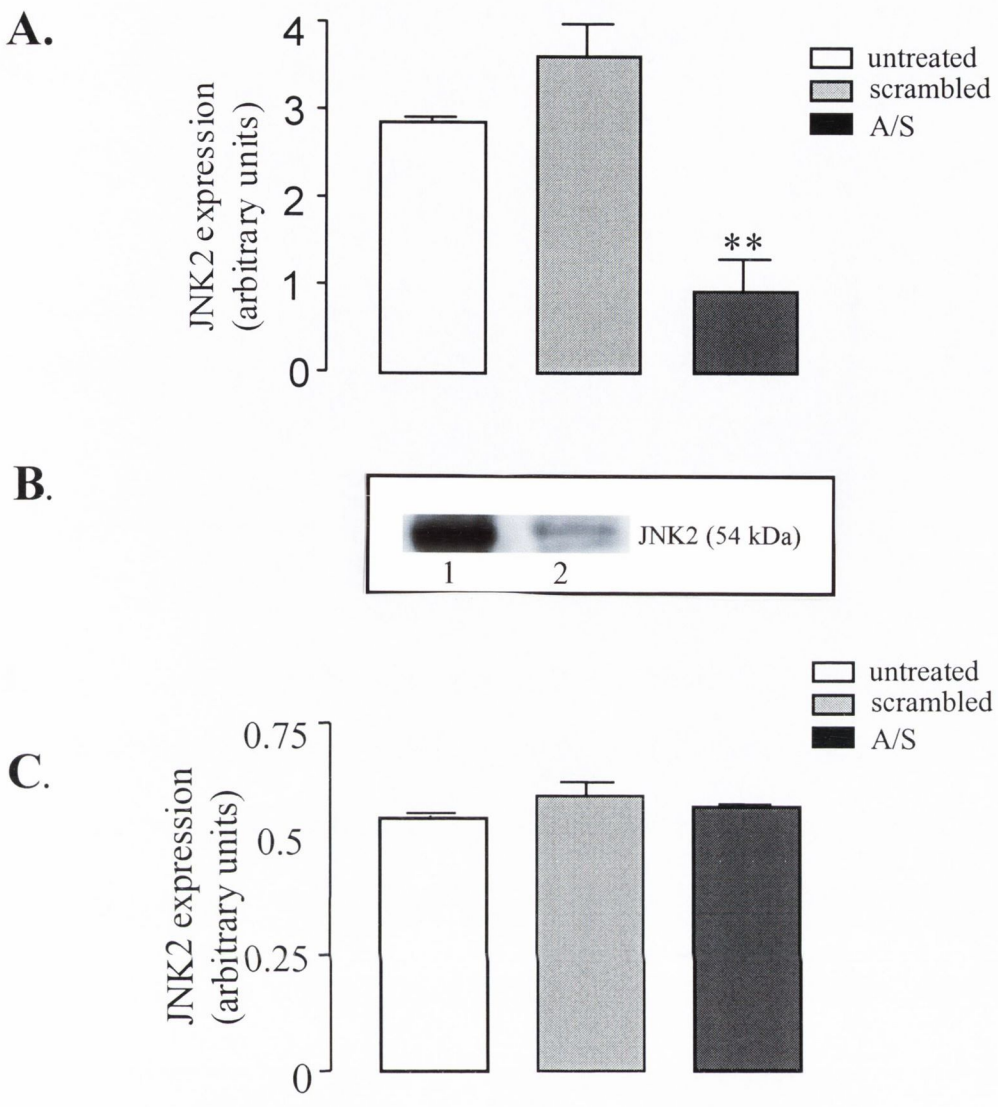

Figure 3.11 JNK2 antisense selectively downregulates JNK2 expression at 48 hr

A. Cortical neurons were treated with JNK2 antisense (A/S) or JNK2 scrambled control (2 μM) for 48 hr and total JNK2 expression was examined by western immunoblot. JNK2 A/S significantly depleted total JNK2 expression at 48 hr. Results are expressed as mean band width ± SEM, for 4 independent observations, ** $p<0.05$.

B. Sample western blot demonstrating levels of JNK2 protein expression in control (lane 1) and JNK2-antisense treated cells (lane 2).

C. Cortical neurons were exposed to JNK1 A/S or JNK1 scrambled control oligonucleotides (2 μM) for 48 hr and JNK2 total expression was examined by western immunoblot. JNK1 A/S had no effect on expression of JNK2 protein. Results are expressed as mean band width ± SEM, for 4 independent observations, ** $p<0.05$.

A.

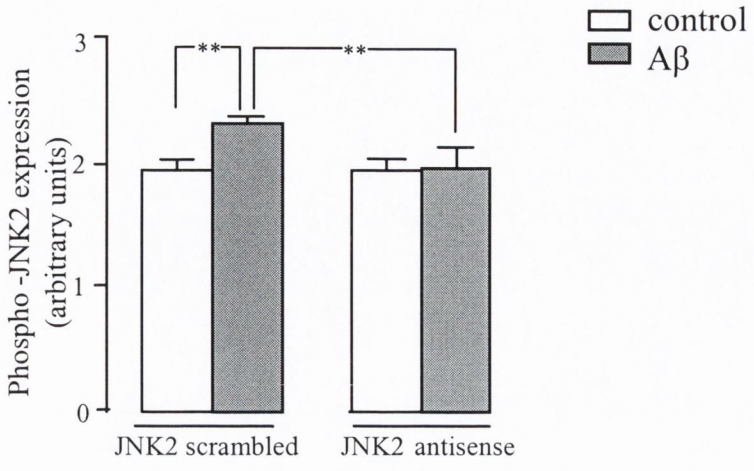

B.

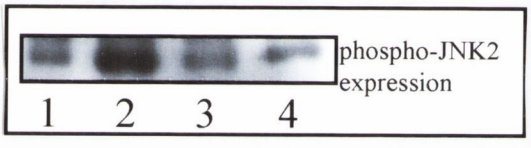

Figure 3.12 Effect of JNK2 depletion on expression of phospho-JNK2

A. Cortical neurons were pre-treated with JNK2 antisense and scrambled oligonucleotides (2 μM) for 48 hours before treatment with Aβ (2 μM). Expression of phospho-JNK2 was measured by western immunoblot. Aβ significantly increased phospho-JNK2 expression after 24 hr Aβ treatment. The Aβ-mediated increase in JNK2 phospho-expression was significantly reduced in JNK2 antisense treated cells. Results are expressed as mean band width ± SEM, for 6 independent observations, ** $p<0.05$.

B. Sample western blot showing phospho-JNK2 expression in (1) control (2) Aβ-treated cells (3) JNK2 antisense treated cells (4) Aβ + JNK2 antisense treated cells.

± 0.16, n=6) In contrast, the JNK2 antisense oligonucleotide significantly reduced that Aβ-mediated phosphorylation of JNK2 to 1.94 ± 0.15 ($p < 0.05$, one-way ANOVA, n = 6). This result demonstrates that the JNK2 antisense efficiently reduces the Aβ-mediated increase in expression of phospho-JNK2. A sample immunoblot demonstrating that Aβ-mediated JNK2 phosphorylation is significantly reduced in JNK2 antisense-treated cells is shown in Figure 3.12B.

3.2.13 Effect of JNK depletion on Aβ-mediated activation of caspase-3 at 24 hr

A downstream consequence of JNK activation is a commitment to the cell death pathway (Mielke and Herdegen, 2000). Since Aβ activates both JNK1 and JNK2 in cortical neurons, the respective roles of JNK1 and JNK2 in coupling Aβ to activation of the apoptotic cascade was assessed following downregulation of JNK1 or JNK2 using the antisense approach. Caspase-3 is a key executioner of apoptosis and is cleaved following treatment with 2 μM Aβ for 24 hours (Boland and Campbell, 2003a). The effect of JNK depletion on activation of caspase-3 was assessed by immunocytochemistry using an anti-active caspase-3 antibody. Cells were pre-treated with JNK1 or JNK2 antisense, or scrambled oligonucleotides, for 48 hr and then exposed to Aβ (2 μM) for a further 24 hr. Figure 3.13 demonstrates that in untreated cells the percentage of cells displaying active-caspase-3 immunoreactivity was 18 ± 2% (mean ± SEM) and this was significantly increased to 44 ± 4% by Aβ ($p<0.05$, ANOVA, n=6 observations). In cells incubated with JNK1 scrambled control oligonucleotide the Aβ-mediated stimulation of caspase-3 was retained. Thus, the percentage of cells staining positive for active caspase-3 was 21 ± 3 % in JNK 1 scrambled control-treated cells and 41 ± 1 % in Aβ + JNK1 scrambled control-treated cells ($p<0.05$, ANOVA, n=6 observations). In contrast, the JNK1 antisense oligonucleotide significantly reduced the Aβ-mediated stimulation of caspase-3 activity to 22 ± 4% (n=6 observations). This result demonstrates that JNK1 is pertinent in the Aβ-mediated activation of caspase-3 in cultured cortical neurons.

In contrast, depletion of JNK2 had no effect on Aβ-mediated activation of caspase-3. Cells pre-treated with JNK2 scrambled oligonucleotides prior to Aβ

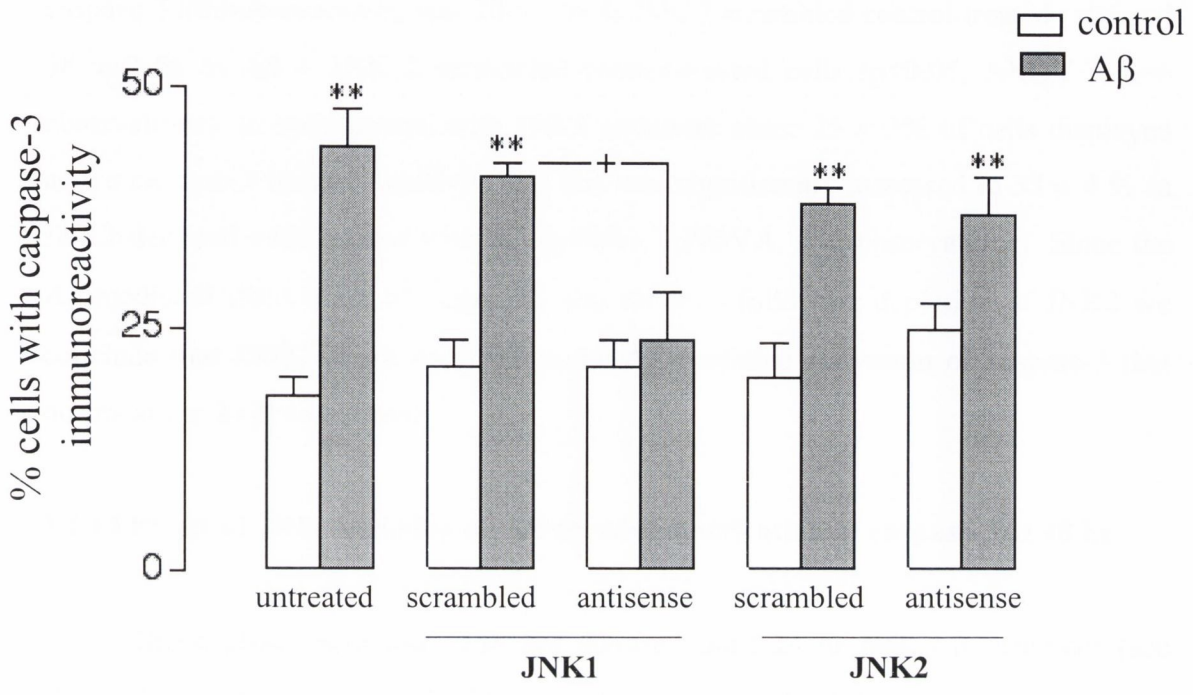

Figure 3.13 Effect of JNK1 and JNK2 depletion on Aβ-induced activation of caspase-3 activity at 24 hr

Cortical neurons were treated with JNK antisense oligonucleotides or JNK scrambled oligionucleotides (2 μM) in the presence or absence of Aβ (2 μM) for 24 hr. Caspase-3 activity was examined by immunocytochemistry using an anti-active caspase-3 antibody. Aβ significantly increased the percentage cells with active caspase-3 immunoreactivity at 24 hr. For JNK1 scrambled oligonucleotide, Aβ also evoked a significant increase in active caspase-3 immunoreactivity, however this effect was abrogated in JNK1 antisense-treated cells. In contrast, neither the JNK2 scrambled nor the JNK2 antisense oligonucleotide had any effect on the proclivity of Aβ to evoke the increase in active caspase-3 immunoreactivity. Results are expressed as the mean ± SEM for 6 independent observations,** $P<0.05$; $^{+}P<0.05$.

exposure displayed similar levels of caspase-3 activation to cells that had not been exposed to oligonucleotides. Thus, the percentage of cells staining positive for active caspase-3 immunoreactivity was 20 ± 3 % in JNK 2 scrambled control-treated cells and 38 ± 2 % in Aβ + JNK 2 scrambled control-treated cells ($p<0.05$, ANOVA, n=6 observations). In cells treated with JNK2 antisense alone 25 ± 3% of cells displayed active-caspase-3 immunoreactivity and this was significantly increased to 38 ± 4 % in JNK2-depleted cells treated with Aβ ($p<0.05$, ANOVA, n=6 observations). Since the Aβ-mediated stimulation of caspase-3 was retained following depletion of JNK2 we conclude that JNK2 is not involved in the Aβ-mediated activation of caspase-3 that occurs at the 24 hr time-point.

3.2.14 Effect of JNK depletion on Aβ-mediated activation of caspase-3 at 48 hr

Since JNK2 activation was not detected until 24 hr post Aβ-treatment (see Figure 3.2), our finding that JNK2 was not involved in the Aβ-mediated activation of caspase-3 at 24 hr is not surprising. To determine whether JNK2 was involved in caspase-3 activation at later time-points the experiment was repeated by monitoring the effect of JNK1 and JNK2 antisense on Aβ-mediated activation of caspase-3 at 48 hours, a time-point that would be expected to be downstream of JNK2 activation. Figure 3.14 demonstrates that in untreated cells the percentage of cells displaying active-caspase-3 immunoreactivity was 13 ± 3% (mean ± SEM) and this was significantly increased to 45 ± 8% following treatment with Aβ for 48 hours ($p<0.05$, ANOVA, n=6 observations). Following transfection with the JNK1 scrambled oligonucleotide the Aβ-mediated stimulation of caspase-3 was retained. Thus, the percentage of cells staining positive for active caspase-3 was 24 ± 5 % in JNK1 scrambled control-treated cells and 55 ± 6 % in Aβ + JNK1 scrambled control-treated cells ($p<0.05$, ANOVA, n=6 observations). In contrast, the JNK1 antisense oligonucleotide significantly reduced the Aβ-mediated stimulation of caspase-3 activity ($p<0.05$, ANOVA; compared to cells treated with Aβ + JNK1 scrambled oligonuclotide, n=6 observations). Thus, in cells transfected with JNK1 antisense alone the percentage of cells with active-caspase-3 immunostaining was 19 ± 4% and in cells

A.

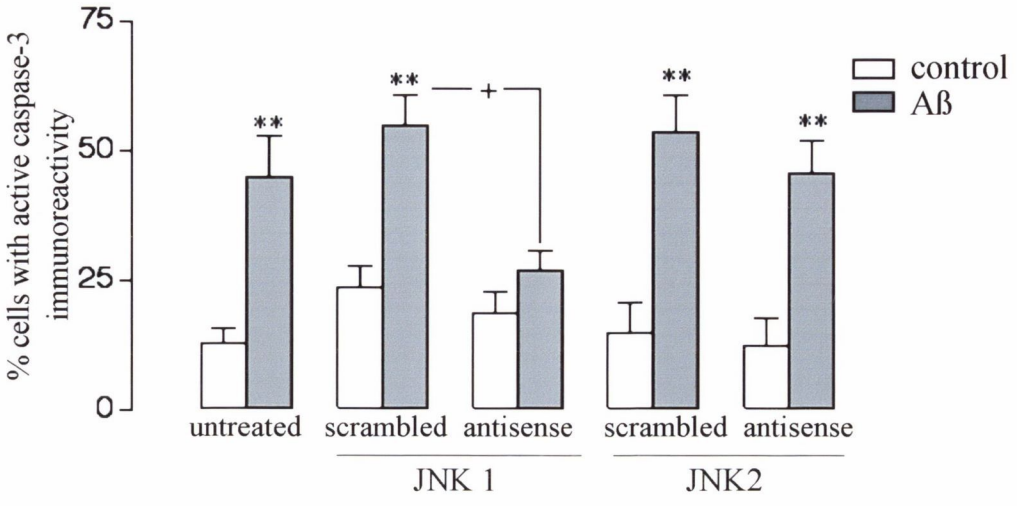

B.

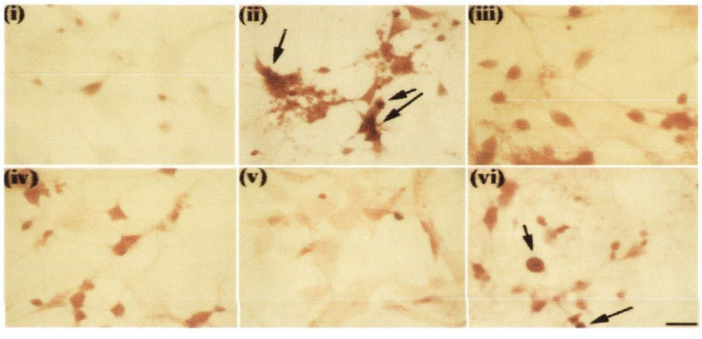

Figure 3.14 Effect of JNK1 and JNK2 depletion on Aβ-induced activation of caspase-3 activity at 48 hr

A. Cortical neurons were treated with JNK antisense oligonucleotides or JNK scrambled oligonucleotides (2 μM) in the presence or absence of Aβ (2 μM) for 48 hr and caspase-3 activity was examined by immunocytochemistry. Aβ significantly increased the percentage of cells with active caspase-3 immunoreactivity at 48 hr. For JNK1 scrambled oligonucleotide, Aβ also evoked a significant increase in the percentage cells with active caspase-3 immunoreactivity, however this effect was abrogated in JNK1 antisense-treated cells. In contrast, neither the JNK2 scrambled nor the JNK2 antisense oligonucleotide had any effect on the proclivity of Aβ to evoke the increase in active caspase-3 immunoreactivity. Results are expresses as the mean ± SEM for 6 independent observations,** $P<0.05$; $^{+}P<0.05$.

B. Representative image of cortical neurons stained for activated caspase-3 immunoreactivity. Arrows indicate cells with active-caspase-3 immunoreactivity in (i) control (ii) Aβ (iii) JNK1 antisense (iv) Aβ + JNK1 antisense (v) JNK2 antisense (iv) Aβ + JNK2 antisense treated cells. Scale bar is 25 μm

treated with Aβ in the presence of JNK1 antisense oligonucleotide 25 ± 4% of cells displayed active-caspase-3 immunoreactivity (n=6 observations). This result demonstrates that JNK1 is pertinent in the Aβ-mediated activation of caspase-3 in cultured cortical neurones at 48 hours.

In contrast, depletion of JNK2 had no effect on Aβ-mediated activation of caspase-3 at 48 hours. Following transfection with the JNK2 scrambled oligonucleotide the Aβ-mediated stimulation of caspase-3 was retained. Thus, the percentage of cells staining positive for active caspase-3 immunoreactivity was 15 ± 6 % in JNK2 scrambled control-treated cells and 54 ± 7 % in Aβ + JNK2 scrambled control-treated cells ($p<0.05$, ANOVA, n=6 observations). Similarly, following transfection with the JNK2 antisense oligonucleotide the Aβ-mediated stimulation of caspase-3 was retained. Thus, in cells treated with JNK2 antisense alone, 13 ± 6 % of cells displayed active-caspase-3 immunoreactivity and this was significantly increased to 46 ± 6 % in JNK2-depleted cells treated with Aβ for 48h ($p<0.05$, ANOVA, n=6 observations). These results demonstrate that JNK1, and not JNK2, is involved in the coupling of Aβ to caspase-3 activation at the 48 hr time-point

3.2.15 Role of JNK depletion on Aβ-mediated DNA fragmentation at 72 hr

One of the biochemical events occurring in the later stages of apoptosis is the fragmentation of nuclear DNA. Aβ causes maximal increase in DNA fragmentation 72 hr post-treatment (Boland and Campbell, 2003a), therefore this time-point was used to examine the roles of JNK1 and JNK2 in Aβ-mediated DNA fragmentation. TUNEL analysis was used to assess levels of DNA fragmentation following antisense-mediated depletion of the JNK1 and JNK2 isoforms (Figure 3.15). In untreated cortical neurons the percentage of cells with fragmented DNA (TUNEL positive cells) was 21 ± 2 % (mean ± SEM) and this was significantly increased to 52 ± 8 % by Aβ (2 μM; $p < 0.05$, one-way ANOVA, n=6 observations). Following transfection with the JNK1 scrambled control oligonucleotide the Aβ-induced DNA fragmentation was retained (53.2 ± 4.9 %, n=6). In contrast, the JNK1 antisense oligonucleotide significantly reduced the Aβ-mediated stimulation in DNA fragmentation by 80 % to 33 ± 3 % ($p<0.05$, ANOVA,

compared to cells treated with Aβ in the presence of JNK1 scrambled oligonucleotide, n=6 observations). This result demonstrates that JNK1 is pertinent in the induction of DNA fragmentation by Aβ.

To determine the role of JNK2 in Aβ-mediated DNA fragmentation the cells were transfected with the JNK2 antisense oligonucleotide. Depletion of JNK2 had no effect on Aβ-mediated DNA fragmentation at 72 hr. Following transfection with the JNK2 scrambled oligonucleotide the Aβ-induced increase in DNA fragmentation was retained. Thus, the percentage of TUNEL positive cells was 22 ± 3 % in JNK2 scrambled control-treated cells and 52 ± 5 % in Aβ + JNK2 scrambled control-treated cells ($p<0.05$, ANOVA, n=6 observations). Similarly, following transfection with the JNK2 antisense oligonucleotide the Aβ-mediated increase in DNA fragmentation was retained. Thus, in cells treated with JNK2 antisense alone, 20 ± 2 % of cells displayed active-caspase-3 immunoreactivity and this was significantly increased to 39 ± 4 % in JNK2-depleted cells ($p < 0.05$, one-way ANOVA, n = 6). This result demonstrates that JNK2 does not play a role in coupling Aβ to induction of DNA fragmentation. The data from this series of experiments indicate JNK1 as the principal JNK isoform involved in the Aβ-mediated increase in DNA fragmentation in cortical neurons.

A.

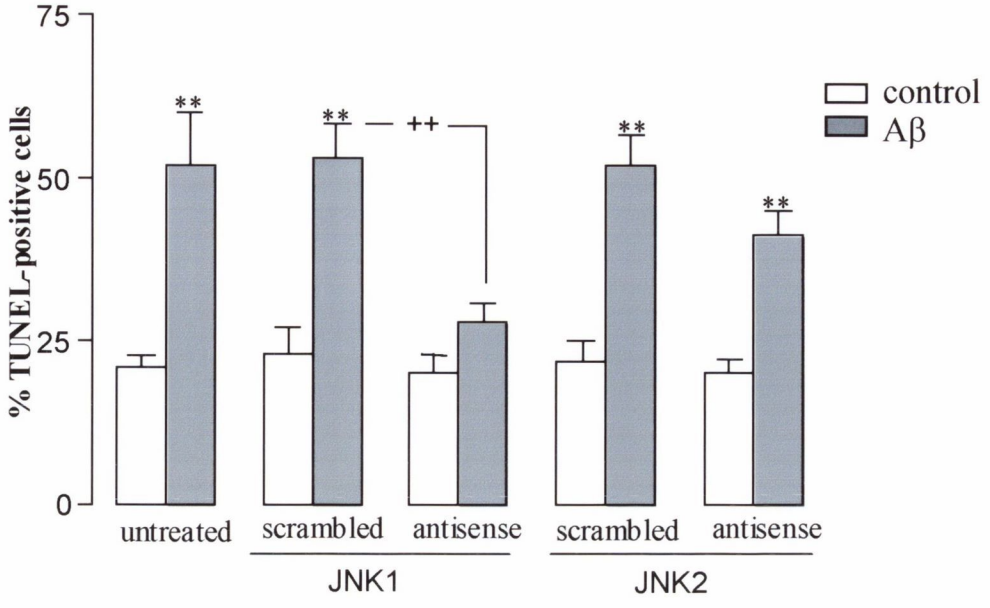

B.

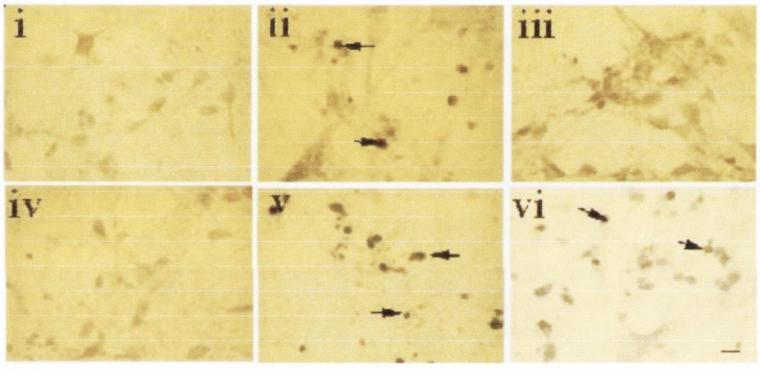

Figure 3.15 Effect of JNK1 and JNK2 depletion on Aβ-induced DNA fragmentation

A. Cortical neurons were treated with JNK antisense oligonucleotides or JNK scrambled oliginucleotides (2 μM) in the presence or absence of Aβ (2 μM) for 72 hr, and DNA fragmentation was examined by TUNEL analysis. Aβ significantly increased DNA fragmentation at 72 hr. For JNK1 scrambled oligonucleotide, Aβ also evoked a significant increase in DNA fragmentation, however this effect was abrogated in JNK1 antisense-treated cells. In contrast, neither the JNK2 scrambled nor the JNK2 antisense oligonucleotide had any effect on the proclivity of Aβ to evoke the increase in active DNA fragmentation. Results are expressed as the mean ± SEM for 6 coverslips,** $P<0.05$; $^{++}P<0.05$.

B. Representative image of cortical neurons stained for DNA fragmentation.. Arrows indicate TUNEL positive cells in (i) JNK1 scrambled oligonucleotide (ii) Aβ + JNK1 scrambled oligonucleotide (iii) Aβ + JNK1 antisense (iv) JNK2 scrambled oligonucleotide (v) Aβ + JNK2 scrambled oligonucleotide (vi) Aβ + JNK2 antisense. Scale bar is 20 μm.

3.3 Discussion

The aim of this study was to investigate whether MAPK family members, JNK and ERK, are activated following $A\beta_{(1-40)}$ treatment of cultured cortical neurons and to elucidate the role of activation of these kinases in Aβ-mediated effects. The results demonstrate that ERK is not activated by Aβ at any of the examined time-points. Conversely, Aβ mediates a differential time frame of activation of JNK1 and JNK2 in cultured cortical neurons. JNK1 is activated within minutes of Aβ-treatment, whereas JNK2 activation was delayed until 24 hr post Aβ-treatment. In the absence of a suitable pharmacological inhibitor to distinguish between JNK1 and JNK2-mediated effects, antisense technology was employed to selectively downregulate JNK1 and JNK2 expression in order to examine their respective roles in the apoptotic pathway. Analysis of caspase-3 cleavage and nuclear DNA fragmentation revealed that Aβ-mediated caspase-3 activation and induction of DNA fragmentation was JNK1 dependent in cortical neurons. In contrast, depletion of JNK2 was found to have no effect on Aβ-mediated activation of the apoptotic cascade.

The concentration of Aβ that was selected for the experimental work carried out in this thesis was 2 μM. This is a relatively low concentration of Aβ in comparison with other studies on cultured neurons with concentrations of up to 50 μM being used to induce neurotoxicity in some studies (McDonald *et al.*, 1998). However, Aβ has been demonstrated to induce neurotoxicity at concentrations as low as 0.5 μM (Pillot *et al.*, 1999). For this study a concentration of 2 μM was chosen as the concentration of Aβ that activated intracellular changes that could be monitored over a longer time-frame than that seen at higher micromolar concentrations. This also allowed identification of rapid signalling events which occur following Aβ-treatment which might have been overlooked if higher concentrations of peptide had been used. Previous results have established that Aβ used at this concentration is sufficient to induce significant levels of neuronal apoptosis within 72 hours of treatment (Boland and Campbell, 2003a).

Treatment with Aβ increased phospho-JNK expression in cortical neurons, with activated JNK immunoreactivity being localised to discrete regions within the nucleus and cytosol. This pattern of distribution is consistent with the distribution of phospho-JNK in response to other stress stimuli, where nuclear staining may reflect the ability of JNK to regulate transcription of stress-induced genes (Pena *et al.*, 2000). The punctate distribution of phospho-JNK detected in the cytosol following exposure to Aβ may represent mitochondrial targeting of JNK (Ito *et al.*, 2001) or association of JNK with cytosolic substrates such as p53 and bcl-2 (Fuchs *et al.*, 1998; Park *et al.*, 1997). Two time-points were initially chosen to assess JNK immunoreactivity, following exposure of neurons to Aβ. Increased phospho-JNK immunofluorescene, indicative of active JNK, was observed at both examined time-points, 1 hour and 24 hours.

To further clarify the time frame for Aβ-mediated JNK activation, western immunoblotting was employed over a range of time-points from 5 minutes to 48 hours. The results revealed a differential temporal activation of JNK1 and JNK2. JNK1 was activated rapidly at 5 minutes post Aβ treatment. This activation was sustained for several hours, peaking within 1 hour and returning to basal levels by 18 hours. This rapid activation of JNK1 is not atypical, with previous studies showing rapid JNK activation within 1-15 minutes of treatment (Pyo *et al.*, 1998, Yin *et al.*, 1997). Such a transient activation of JNK1 represents the temporal effectiveness of the signalling cascade. In contrast, Aβ failed to induce an early activation of JNK2 but activity of JNK2 was increased at the later timepoints of 24 and 48 hours. A high basal level of active JNK2 was observed in untreated cells, this is in accordance with the literature, with substantial expression and activity of JNK being detected in untreated rat brain (Herdegen *et al.*, 1997) and JNK activity being constitutively high in neurons compared with other cell types (Morishima *et al.*, 2001), thus providing evidence for a physiological role for active JNK in neurons.

Our finding that $A\beta_{1-40}$ increased phospho-JNK expression in cortical neurons agrees closely with the effects of other Aβ fragments in neuronal systems. $A\beta_{1-42}$ and $A\beta_{25-35}$ have been reported to increase JNK activity in cortical neurons (Bozcyzko-Coyne *et al.*, 2001) and $A\beta_{1-42}$ increases JNK phosphorylation in sympathetic neurons

and PC12 cells (Troy *et al.*, 2001). While there are similarities between the ability of different Aβ peptides to impact on the JNK pathway, it is of note that the time frame for JNK activation varies considerably between different Aβ peptide species. In this study we have demonstrated that JNK1 is activated within 5 minutes of exposure to $A\beta_{1-40}$ while the Aβ-mediated activation of JNK2 is not apparent until 24 hours. In contrast, $A\beta_{25-35}$ increases JNK1 activity at 4 hours, but not at earlier time-points (Bozcyzko-Coyne *et al.*, 2001) and $A\beta_{1-42}$ causes peak activation of both JNK1 and JNK2 within 2-6 hours in PC12 cells (Troy *et al.*, 2001). It is therefore likely that temporal variations in JNK activation may depend on the nature of the Aβ fragment and cell type.

JNK3 expression is predominantly restricted to the brain, implying a significant role for the JNK3 isoform in the brain. In addition, JNK3 has been shown to be required for neuronal death in the hippocampus, following excitotoxic injury (Yang *et al.*, 1997). I investigated whether JNK3 was phosphorylated following exposure of cultured cortical neurons to 2 μM Aβ and found no alteration in phosphorylation of JNK3. This result is in direct contrast with the study carried out by Morishima *et al.* (2001), which reports modulation of JNK3 activity in cortical neurons by Aβ. However, a number of important differences exist between the two studies. Firstly, in the study by Morishima *et al* (2001) cortical neurons were prepared from embryonic rats, while the cultures employed in my study were prepared from 1-day postnatal rat pups. There is evidence that JNK activity varies depending on the developmental stage of the brain. Carboni *et al* (1998) reported that mRNA levels of JNK isoforms differ in postnatal development of the rat brain, so the contradicting results for the involvement of JNK3 in Aβ-mediated neuronal apoptosis may be explained by the different development stages of the culture preparations, with the embryonic cultures representing developmental neurons and the rat pup cultures demonstrating a more mature neuron. Another difference between the two studies is the concentration of Aβ used. In the study carried out by Morishima *et al* (2001) 25 μM Aβ was used for all experiments. It is possible that the lower dose of 2 μM used in my study does not induce JNK3 phosphorylation while at higher concentrations, with the cell being

exposed to higher levels of stress, JNK3 phosphorylation may occur. At this stage of the study it was concluded that JNK3 phoshorylation was not regulated by $A\beta_{1-40}$ (2 μM) in this preparation.

Previous reports have demonstrated concurrent activation of parallel MAPK cascades in response to the same stimuli (Westwick. *et al.*, 1994; Pyo *et al.*, 1998). To establish whether the JNK and ERK signalling cascades were simultaneously activated by Aβ treatment, levels of ERK phosphorylation were examined over the same time frame at which JNK phosphorylation had been assessed, ranging from 5 minutes to 48 hours. No alteration in ERK activity was established at the examined time-points indicating that $A\beta_{1-40}$ does not induce parallel activation of JNK and ERK in this system. A number of previous studies have implicated ERK in Aβ-induced neuronal cell death. However, the results remain conflicted on the exact mechanism by which ERK may act to induce neurotoxicity. Rapoport and Ferreira (2000) report an $A\beta_{1-40}$-induced sustained phosphorylation of ERK in cultured neurons, showing maximal induction at 24 hr. In contrast, Ekinci *et al* (1999a) report no change in ERK phosphorylation following $A\beta_{1-40}$ treatment of cultured neurons. However, in a parallel study, Abe and Saito (2000) found a significant increase in ERK phosphorylation in preparations of mixed neuron-glia cultures. Interestingly, in the study carried out by Rapoport and Ferreira, neurons were grown in glia conditioned medium for biochemical experiments, creating the possibility that the Aβ-mediated ERK phosphorylation observed may have been as a result of non-neuronal cells present in the cultures. In support of this idea, several studies have demonstrated Aβ-mediated phosphorylation of ERK in microglial and astrocyte cultures (Pyo *et al.*, 1998, Mcdonald *et al.*, 1998, Abe and Saito, 2000). It is possible that Aβ induces ERK phosphorylation in neurons that are in contact with astrocytes, however our finding in pure (>95%) neuronal cultures provides evidence that $A\beta_{1-40}$ does not mediate activation of ERK in neuronal cells alone. A further study, which reports no alteration in ERK phosphorylation following Aβ-treatment (Ekinci *et al.*, 1999), demonstrates instead a relocation of ERK activity from cytosol to membrane.

Since JNK, but not ERK, was found to be activated by $A\beta_{1-40}$ in our cellular system, we sought to determine the role of individual JNK isoforms in coupling Aβ to the stress-response pathway. A number of recent studies have reported that the various JNK isoforms i.e JNK1, JNK2 and JNK3 differ in their specificity for downstream substrates. Gupta *et al.* (1996) demonstrated differing affinities of JNK isoforms for transcription factors ATF2, Elk1 and c-jun *in vitro*. Preferential activation of specific JNK isoforms in specfic tissue types and in response to particular stress stimuli have also been established. Yin *et al* (1997) observed no activation of JNK in heart and kidney following ischemia, however in response to ischemia/reperfusion the 55 kDa isoform of JNK only, was activated in the heart with both the 46 and 55 kDa isofoms of JNK being activated in the kidney. Further evidence of differing roles for JNK isofoms in apoptosis is offered by a recent study by Hochedlinger *et al* (2002) reporting that JNK1 deficient primary embryonic fibroblasts were more resistant to UV-induced cell death, while fibroblasts lacking JNK2 were more sensitive to UV-induced cell death. The aim of this study was to determine the specific roles of JNK1 and JNK2 in Aβ-treated cortical neurons. The currently available JNK inhibitors CEP-1347 (Cephalon, USA), D-JNKI1 and SP600125 (Alexis Biochemicals, UK) inhibit JNK1, JNK2 and JNK3 isoforms. Since there are no available JNK inhibitors that can differentiate between specific JNK isoforms, an antisense approach was designed in order to deplete cells of JNK1 or JNK2 protein. The respective roles of these proteins in the Aβ cascade could then be resolved.

The antisense oligonucleotides applied to cells consisted of phosphorothioate-DNA oligonucleotides. This type of antisense oligonucleotide contains sulphur in place of one of the oxygen atoms of the DNA backbone. This modification increases the half-life of the antisense oligonucleotides to greater than 48 hours as compared to a half-life of 30 minutes in natural unmodified oligonucleotides (Crooke, 1992). Oligonucleotides are taken up into the cell by the natural process of receptor-mediated endocytosis, however this delivery method can prove inefficient, requiring long amounts of time for sufficient accumulation. To enhance cellular uptake oligonucleotides were pre-incubated with DOTMA/DOPE lipofectin reagent (Roche products Ltd, UK). Lipofectin is a synthetic cationic lipid polymer that can fuse with

the cell membrane and allows antisense to enter the cell efficiently and rapidly. Another efficient method of antisense administration is the use of microinjection. This method makes use of a fine pipette to inject antisense oligonucleotides directly into the cell. While this is a very efficient method of antisense delivery, it is a relatively slow process, with high precision being necessary to inject small cells such as neurons. Given the high quantity of protein required for efficient analysis of antisense-mediated protein depletion, for example western immunoblot analysis, lipofectin-mediated administration of antisense oligonucleotides was chosen as the most efficient method for rapidly depleting JNK protein in large quantities of cells.

In order to confirm the efficient uptake of antisense oligonucleotides by neuronal cells, FITC-labelled antisense oligonucleotides were incorporated into cells. Flouresence microscopy confirmed the presence of the FITC oligonucleotides in the cell 1 hour after incubation. However, immunoblot analysis of JNK expression in cells treated with antisense over a time-course of 1 hour – 72 hours revealed antisense-mediated depletion of JNK did not occur until 48 hour. Therefore, for all experiments a 48 hour incubation of cells with antisense was carried out to ensure sufficient depletion of JNK protein. Florescence immunocytochemistry revealed a marked downregulation of JNK1 and JNK2 expression in cells treated with antisense for 48 hours. The ability of Aβ to induce phosphorylation of JNK1 and JNK2 was also selectively abolished in antisense-treated cells. A basal amount of JNK phosphorylation was still detectable in JNK depleted cells. This may reflect endogenous activity of the residual JNK that remained following antisense treatment or may be due to an enhanced stability of the phosphorylated form of JNK.

It is well characterised that JNK is activated in response to cellular stress (Herr and Debatin, 2001). JNK activation has been linked to apoptosis, in response to cellular stress including DNA damage, gamma irradiation and pro-inflammatory cytokines (Mielke and Herdegen, 2000). However, JNK has also been proposed to have an anti-apoptotic role, inducing caspase-3 activity in double-knock out of JNK1 and JNK2 in embryonic brain (Kuan *et al.*, 1999) and protecting against UV-mediated toxicity in cultured fibroblasts. The final outcome of whether JNK will lead to death or survival is determined by a number of factors, including the nature of the stimulus and the effects

of other signalling pathways acting simultaneously. To clarify whether JNK plays a role in cell survival or cell death in Aβ-treated cortical neurons and to delineate the specific role of JNK isoforms in this pathway, the effect of antisense-mediated JNK1 and JNK2 depletion on caspase-3 activation and DNA fragmentation, two markers of apoptosis, was assessed. Aβ mediated a significant increase in caspase-3 activation at 24 hours and 48 hours, and a significant increase in levels of DNA fragmentation at 72 hours. This time-scale of Aβ-mediated increase in caspase-3 cleavage and DNA fragmentation has previously been reported (Boland and Campbell, 2003a). Following depletion of JNK1 the proclivity of Aβ to activate caspase-3 and induce DNA fragmentation was significantly attenuated. Conversely, JNK2 depletion had no effect on the Aβ-mediated activation of caspase-3 or increase in DNA fragmentation, and this suggests that JNK1 is the principal JNK isoform involved in Aβ-mediated activation of the apoptotic cascade. JNK1 has previously been reported to play a preferential role in ischemia / reoxygenation induced apoptosis (Hreniuk *et al.*, 2001). It is of note that while both JNK1 and JNK2 are activated by Aβ, JNK2 does not seem to play a role in Aβ-induced neuronal apoptosis. This poses the question as to what the role of Aβ-induced activation of JNK2 may be. JNK1 activation is an early event in this system, becoming activated as early as five minutes. It is possible that early activation of JNK1 leads to subsequent induction of JNK substrates and the apoptotic cascade, and that by 24 hours when JNK2 has become activated the cell is already commited to undergoing cell death. Evidence for this is provided by the observation of significant activation of caspase-3, a major effector of apoptosis, at 24 hours following Aβ-treatment. Activation of JNK2 at this stage may be a reaction to the stressful environment in which the cell is placed, but may not actually play a specific role in induction of the apoptotic cascade. A recent study by Hochedlinger *et al* (2002) reports a negative regulation of JNK1 activity by JNK2. This may explain the finding that JNK1 phosphorylation has returned to basal levels following 24 hours Aβ treatment, at which time JNK2 has become significantly phosphorylated.

While Aβ induced caspase-3 cleavage in this system, it is important to note that the role of caspase-3 in Aβ-mediated neurodegeneration remains a matter of debate. In cortical neurons a caspase-3 inhibitor has been found to protect neurons against some

aspects of Aβ-mediated cell death (Harada *et al.*, 1999), while caspase-3 has been found to have no role in Aβ-mediated hippocampal cell death (Troy *et al.*, 2000). The role of caspase-3 in Aβ-neurodegeneration has therefore been proposed to be brain-region specific (Selznick *et al.*, 1999). We have demonstrated that Aβ-mediated activation of caspase-3 in cultured cortical neurons is JNK dependent and that in JNK1 depleted cells caspase-3 activation is attenuated with subsequent rescue from cell death. This is in strong agreement with the study by Bozyczko-Coyne *et al.* (2001), which suggests that in cortical neurons caspase-3 activation is integral to neurodegeneration. The finding that JNK1 and JNK2 have distinct activation profiles and different roles in the Aβ-mediated induction of the apoptotic cascade highlights the complexity of JNK signalling. Furthermore, although the use of *jnk3* knockout mice has identified a role for JNK3 in Aβ-mediated neurotoxicity (Morishma *et al.*, 2001) in the present study no evidence of JNK3 activation by $A\beta_{1\text{-}40}$ was found and the results suggest a prominent role for JNK1 in Aβ-mediated DNA fragmentation in this system. This lends further support for the idea that the patterns of JNK signalling utilised by Aβ are diverse and may be subject to developmental factors, cell type and animal species. This study provides evidence for the 1-40 fragment of Aβ coupling to JNK1 upstream of cell death in the cortex and this is relevant since $A\beta_{1\text{-}40}$ is detected in the mature senile plaque (Iwatsubo *et al.*, 1994).

The results from this study demonstrate that Aβ induces phosphorylation of JNK1 and JNK2 in cortical neurons with a distinct temporal pattern. While JNK1 is pertinent in the Aβ-mediated activation of caspase-3 and induction of DNA fragmentation, JNK2 is not involved in coupling Aβ to these apoptotic events. An increase in phospho-JNK expression in the AD brain has been reported (Zhu *et al.*, 2001) and our study indicates that JNK1 may contribute to the pathology of the disease by activating the apoptotic cascade. Early activation of JNK, before initiation of apoptotic events, places the JNK pathway at a proximal point in the death pathway, suggesting it as a plausible target for intervention. An ability to inhibit a specific pathological JNK isoform using antisense technology, while retaining JNK activity for

physiological roles, might inhibit apoptosis and the associated brain damage which occurs in AD brain.

Chapter 4

The role p53 in Aβ-mediated neuronal apoptosis

4.1 Introduction

The tumour suppressor protein, p53, is a nuclear phospho-protein, which plays a key role in apoptosis, cell cycle and DNA damage repair, through binding DNA and activating transcription (Levine, 1997). However, in the case of neuronal cells, the role of p53 is somewhat altered, with the cell cycle regulatory function of p53 being effectively redundant. This is due to the fact that most neuronal cells exist in a post-mitotic state (Miller *et al.*, 2000). A functional neuron must therefore survive and maintain its genome for long periods, throughout the lifetime of the organism to which it belongs. In post-mitotic neurons with damaged DNA, p53 induction is associated with mechanisms underlying cell death rather than recovery (Enokido *et al.*, 1996; Jordan *et al.*, 1997). A potential role for p53 in the apoptosis of post-mitotic neurons was originally suggested based on the observation of increased p53 expression following neuronal injury (Morrison *et al.*, 1996; Napieralski *et al.*, 1999), and the finding that p53 was sufficient to induce apoptosis in post-mitotic cortical and hippocampal neurons (Jordan *et al.*, 1997, Xiang *et al.*, 1996). Accumulating evidence now suggests that p53 may be necessary for neuronal apoptosis. For example, cerebellar granule cells cultured from p53 null mice are resistant to treatments with DNA damaging agents such as ara-c (Enokido *et al.*, 1996). In addition, other *in vivo* studies have shown that knocking out the p53 gene protects hippocampal neurons from seizure-induced cell death (Morrison *et al.*, 1996) Furthermore, adenovirus-mediated transfection of the p53 gene results in apoptotic cell death of hippocampal and cortical neurons (Xiang *et al.*, 1996; Jordan *et al.*, 1997). p53 expression is increased in the temporal and frontal lobes of brains from AD patients and is expressed in neurons associated with plaques in AD brains (De la Monte e*t al.*, 1997). In addition, Aβ accumulation is associated with activation of p53 and DNA fragmentation in transgenic mice that overexpress Aβ (LaFerla *et al.*, 1996). Two recent studies have demonstrated that the $A\beta_{1-42}$ peptide mediates neuronal apoptotic cell death through p53-dependent pathways (Culmsee *et al.*, 2001; Zhang *et al.*, 2002a). However, the exact mechanism by which Aβ arbitrates p53-dependent apoptosis remains to be clarified.

p53 can be post-translationally modified by phosphorylation and acetylation on at least 18 sites, located on both the amino-terminal and carboxy terminal domain of the

protein (Apella and Anderson, 2000). In unstressed cells, p53 is kept at low levels due to targeted degradation of the protein (Zörnig *et al.,* 2001). However, in response to cellular stress, p53 can become stabilised, via phosphorylation at critical residues (Ashcroft *et al,* 2000). Several kinases that can detect genotoxic stresses and initiate signalling pathways through p53 phosphorylation have been identified, including the stress activated protein kinases, JNK and p38 (Adler *et al.*, 1997; Zhu *et al.*, 2002), as well as double stranded DNA-activated kinase (DNA-PK) and casein kinase (Lees-Miller *et al.*, 1990; Milne *et al.*, 1992). While phosphorylation of p53 occurs at differing residues, depending on the phosphorylating kinase and the stress stimuli received, phosphorylation of p53 at serine-15 is thought to be one of the critical signals through which the p53 response to stress is regulated (Appella and Anderson 2001). Phosphorylation at another critical residue, serine 392, has been shown to enhance p53-dependent transcription in response to DNA damage (Lu *et al.*, 1998).

Once activated, p53 promotes apoptosis by modulating the expression of select target genes. Pro-apoptotic genes regulated by p53 include the Bcl_2 family member, Bax, and the p53 inducibile genes (PIGs; Herr and Debatin, 2000). p53 has been demonstrated to increase transcription of Bax in several studies (Karpinich *et al.*, 2002; Culmsee *et al.*, 2002) and it is generally assumed that Bax is essential for p53-dependent cell death in neurons. Bax is a cytosolic protein, however cell damage can promote translocation of Bax from cytosol to mitochondria (Morrison and Kinoshita, 2000). Relocation of Bax to the mitochondria has been associated with a reduction in mitochondrial membrane potential, mitochondrial release of cytochrome *c* and activation of caspases (Xiang *et al.*, 1996; Karpinich *et al.*, 2002). Evidence for the essential role of Bax in p53-mediated cell death is provided by the findings that Bax-deficient neurons are protected from cell death induced by DNA damaging agents, as well as adenovirus-mediated p53 over-expression (Xiang *et al.*, 1998). In addition, increased Bax immunoreactivity has been observed in neuritic plaques of AD brain (Tortosa *et al.*, 1998) indicating that Bax may play an important role in neuronal apoptosis associated with AD.

The experimental work carried out in this chapter aimed to establish a role for p53 and Bax in Aβ induced apoptosis in cortical neurons. The rationale behind this approach was based on the hypothesis that oxidative stress plays an essential role in Aβ-mediated neurotoxicity (Behl *et al.*, 1994) and that p53 is activated in response to diverse cellular

stress, including oxidative stress (Zörnig *et al.*, 2000). Expression of p53 and Bax were assessed at both the mRNA and protein level, in order to determine the mechanism by which Aβ-mediated alterations in p53 expression and Bax expression may occur. Given that p53 is a target substrate for regulation by JNK (Adler *et al.*, 1997), and that the results from the previous chapter demonstrate a role for JNK1 in Aβ-mediated neuronal apoptosis, I considered whether the Aβ-mediated alterations in p53 stability occurred in a JNK1-dependent manner. To investigate this, p53 expression was examined in the presence or absence of Aβ, in cells which had first been depleted of JNK1, using selective JNK1 antisense oligonucleotides. To investigate the events which occur downstream of p53 in Aβ-treated neurons, the synthetic p53 inhibitor, pifithrin-α, was applied to cells. This inhibitor acts by inhibiting p53 DNA binding activity, and so inhibits transcription of p53-responsive genes such as *bax* (Culmsee *et al.*, 2001). The role of p53 in Aβ-mediated induction of the apoptotic cascade, namely Bax expression, caspase-3 activity, DNA repair enzyme PARP cleavage and DNA fragmentation, was assessed in pifithrin-α-treated cells

4.2 Results

4.2.1 Aβ induces increased expression of p53 protein.

To determine whether Aβ impacts on the cell cycle regulatory protein, p53, expression of total cellular p53 protein was monitored, following exposure of cultured neurons to Aβ over a range of time points. Cells were incubated with Aβ (2 μM) for 5 min, 1 hr, 6 hr and 18 hr, and p53 protein expression was assessed by western immunoblot using an antibody which recognises an epitope mapping the carboxy terminus of p53. Figure 4.1 demonstrates that Aβ did not significantly modulate p53 expression at 5 min post Aβ-treatment. Thus, p53 expression was 0.99 ± 0.06 (mean band width ± SEM; arbitrary units) in control and 0.95 ± 0.05 in Aβ-treated cells at 5 min (n=4). Conversely, following Aβ treatment for 1 hr, a significant 30 % increase in protein expression was observed in Aβ-treated cells, with p53 expression increasing from 0.9 ± 0.078 to 1.14 ± 0.088 ($p<0.05$, students paired t-test, n=8). Following exposure of neurons to Aβ for 6 hours, expression of p53 was increased from 0.977 ± 0.03 to 1.1 ± 0.027 but was considered not quite significant ($p<0.073$, student's paired t-test, n = 5). In contrast cells treated with Aβ for 18 hr showed no increase in p53 expression. Thus p53 expression was 0.93 ± 0.038 in control and 0.91 ± 0.059 in Aβ-treated cells (n =4). A sample immunoblot illustrating the temporal increase in p53 protein expression, mediated by Aβ is shown in Figure 4.1B.

4.2.2 Effect of Aβ on p53 mRNA expression.

To establish whether the Aβ-mediated increase in expression of p53 protein was due to increased transcription of the p53 gene, cortical neurons were incubated with Aβ over a range of time points from 5 - 18 hr. Levels of p53 mRNA expression were examined by RT-PCR, with gene-specific primers for p53 and β-actin (Figure 4.2). Analysis of densitometric data demonstrates that Aβ had no significant modulatory effect on p53 mRNA at any of the examined time points (control: 1.067 ±

A.

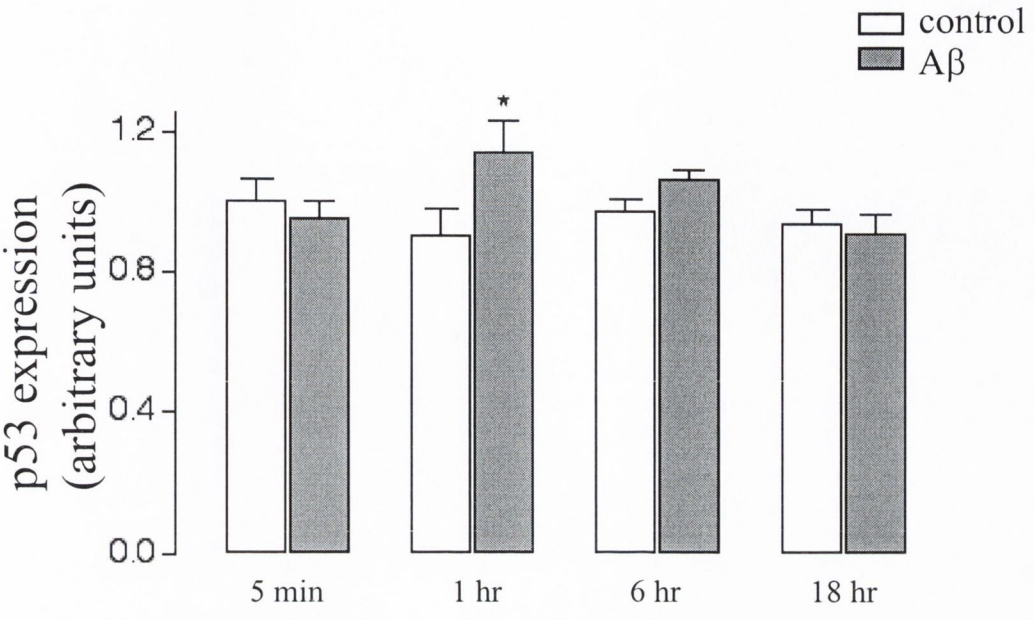

B.

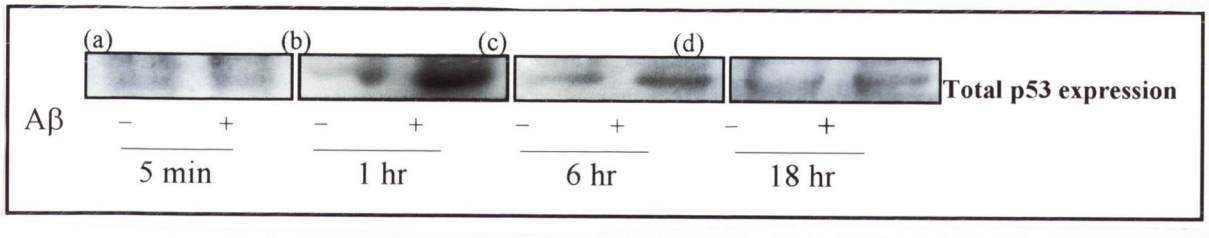

Figure 4.1 Aβ increases expression of p53 protein

A. Cortical neurons were treated with Aβ (2 μM) over a range of time points (5 min –18 hr). Expression of p53 was examined by western immunoblot. Aβ significantly increased p53 expression at 1hr. Results are expressed as mean ± SEM for 6 observations, * $p<0.05$

B. Sample western blot showing p53 expression. Cells were treated with Aβ (2 μM) over a range of time points, 5 min (panel a), 1 hr (panel b), 6 hr (panel c), 18 hr (panel d).

A.

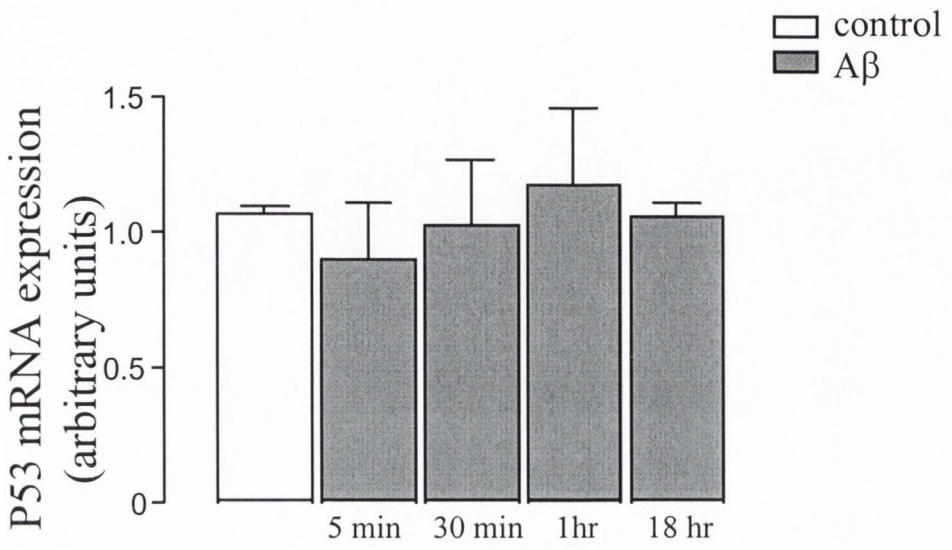

B.

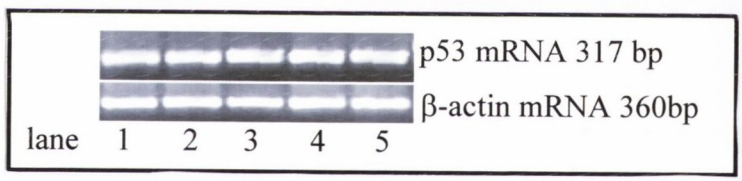

Figure 4.2 Aβ does not modulate transcription of p53 mRNA

A. Cells were exposed to Aβ (2 μM) over a range of time points (5 min –18 hr) and p53 mRNA was assessed using RT-PCR. Aβ had no effect on expression of p53 mRNA. Results are expressed as mean ± SEM for 6 observations.

B. Representative image of agarose gel demonstrating levels of p53 and β-actin mRNA expression in control cells (lane1) and in cells treated with Aβ(2 μM) for 5 min (lane 2), 30 min (lane 3), 1 hour (lane 4) and 18 hr (lane 5).

0.02; Aβ-treated neurons: 0.895 ± 0.212 (5 min); 1.021 ± 0.243 (1 hr); 1.173 ± 0.28(6 hr); 1.053 ± 0.055(18 hr); mean band width ± SEM, n=6). The mRNA expression of p53 was normalised to that of the housekeeping gene β-actin. A sample agarose gel demonstrating that p53 mRNA expression is unaffected by Aβ is shown in Figure 4.2B.

4.2.3 Aβ leads to phosphorylation of p53 at residue serine-15

Since the Aβ-mediated increase in p53 protein expression was not due to increased transcription of p53, we investigated whether the increase in p53 expression was due to a posttranslational modification event. Phosphorylation of p53 at specific residues has been demonstrated to stabilise p53 by preventing ubiquitin-mediated degradation (Pena *et al.*, 2000). Therefore, I examined whether the increase in p53 expression was due to increased phosphorylation of the protein. Phosphorylation of p53 at residue serine-15, a key target site for p53 stabilisation (Appella and Anderson, 2001), was assessed following treatment of cells with Aβ (Figure 4.3). Cells were treated with Aβ for 5 min and 1 hr, and p53 phosphorylation at residue serine-15 was assessed by western immunoblot using an antibody which specifically recognises p53 phosphorylated at residue serine-15. Aβ significantly increased phospho-p53^{ser15} expression from 0.58 ± 0.055 (mean band width ± SEM; arbitrary units) to 1.03 ± 0.116 ($p<0.01$, student's paired t-test, n=8) at 5 min and from 0.837 ± 0.02 to 1.265 ± 0.118 ($p<0.05$, student's paired t-test, n=8) at 1 hr. This result suggests that Aβ increases p53 protein expression by stabilisation of the protein via phosphorylation at serine-15. Figure 4.3B demonstrates the Aβ-mediated increase in p53 phosphorylation at residue serine-15.

A.

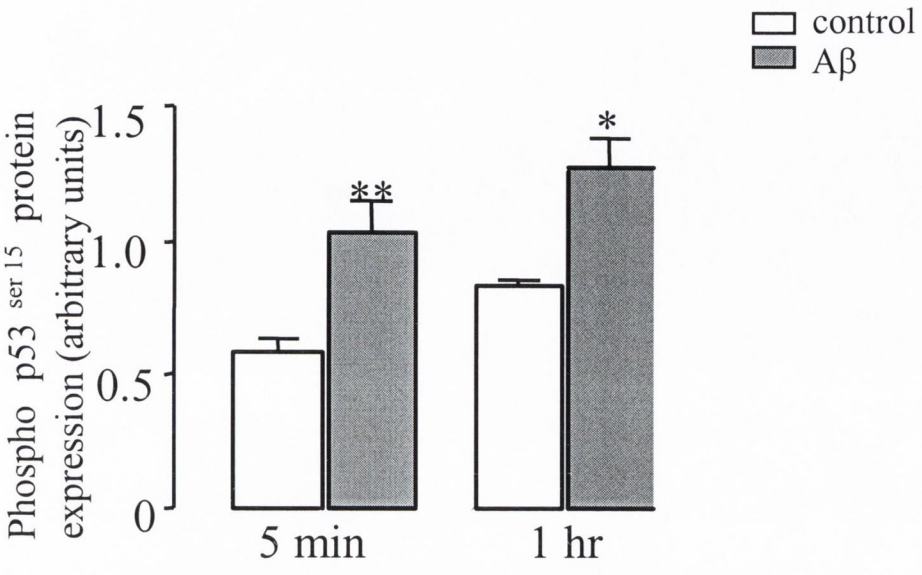

B.

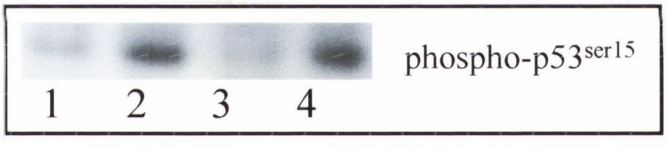

Figure 4.3 Aβ mediates phosphorylation of p53 at residue serine-15.

A. Cortical neurons were treated with Aβ (2 μM) for 5 min and 1 hr. p53 phosphorylation at residue serine-15 was examined by western immunoblot. Aβ significantly increased p53 phosphorylation at 5 min and 1 hr. Results are expressed as mean ± SEM for 8 observations, *$p<0.05$ ** $p<0.01$.

B. Sample western immunoblot demonstrating levels of phosphorylated p53 in control (lane 1) and Aβ-treated cells (lane2; 5 min) and control (lane 3) and Aβ-treated cells (lane 4; 1hour).

4.2.4 Effect of Aβ on phosphorylation of p53 at residue serine-392.

In order to investigate whether Aβ phosphorylated p53 at another critical residue for stabilisation, serine-392, cells were exposed to Aβ for a range of time points (5 min-18 hr) and phosphorylation at residue serine-392 was assessed by western immunoblot using an antibody which specifically recognises p53 phosphorylated at residue serine-392. Figure 4.4 demonstrates that Aβ failed to induce phosphorylation of p53 at residue serine-392 at 5 min, 1 hour and 6 hr post Aβ treatment. Thus, phospho-$p53^{ser392}$ expression was 0.092 ± 0.054 (mean band width ± SEM, arbitrary units) in control, and 0.91 ± 0.12 in Aβ-treated cells at 5 min (n = 4); 0.97 ± 0.13 in control, and 0.94 ± 0.12 in Aβ-treated cells at 1 hr (n=6); 1.0 ± 0.056 in control, and 1.129 ± 0.052 in Aβ-treated cells at 6 hr (n=4). In contrast, at 18 hr Aβ induced a significant increase in phospho-$p53^{ser392}$ expression from a control value of 1.17 ± 0.026 to 1.35 ± 0.041 in Aβ -treated cells ($p < 0.05$, student's t-test, n =3) indicating that phosphorylation of p53 at serine 392 occurs later than phosphorylation at residue serine-15. This result suggests that phosphorylation at serine-392 does not contribute to the observed stabilisation of the p53 protein at 1 hour post Aβ–treatment. The sample immunoblot in Figure 4.4B demonstrates the effect of Aβ on p53 phosphorylation at residue serine-392.

4.2.5 Phosphorylation of p53 at residue serine-15 is JNK1 dependent

p53 is a target substrate for JNK (Alder *et al.*, 1997). Since the observed Aβ-mediated activation of JNK1 was an early event that could potentially be upstream of p53 phosphorylation, the Aβ-mediated phosphorylation of p53 at residue serine-15 was assessed in JNK1 depleted cells. Cells were treated with JNK scrambled and antisense oligonucleotides (2 μM) for 48hr, prior to treatment with Aβ for 1hr, and phosphorylation of p53 at residue serine-15 was analysed by western immunoblot. Figure 4.5A demonstrates that in cells treated with the JNK1 scrambled oligonucleotide, phospho-$p53^{ser15}$ was significantly increased from a control value of 0.84 ± 0.01 (mean band width ± SEM, arbitrary units) to 1.09 ± 0.08 following

treatment with Aβ ($p<0.05$, one way ANOVA, n=7). JNK1 antisense alone had no effect on p53 phosphorylation. However, it abolished the stimulatory effect of Aβ on p53 phosphorylation (JNK1 antisense: 0.83 ± 0.071; Aβ + JNK1 antisense: 0.83 ± 0.064, $p<0.05$, one way ANOVA, n=7). A sample immunoblot illustrating the effect of JNK1 depletion on phospo-p53^{ser15} expression is shown in Figure 4.5B. This result demonstrates that JNK1 plays a role in phosphorylation of p53 at serine-15 in this system.

A.

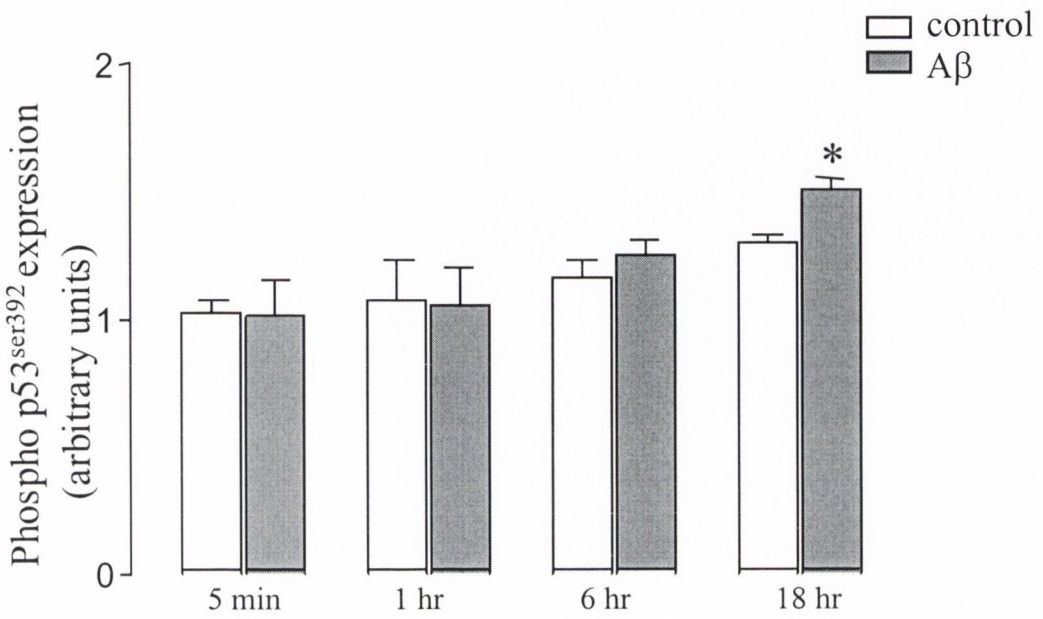

B.

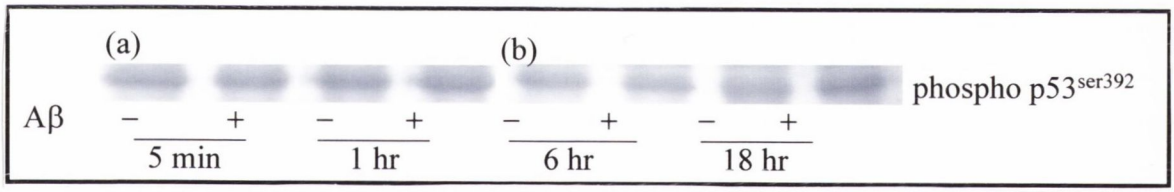

Figure 4.4 Aβ mediates phosphorylation of p53 at residue serine-392.

A. Cortical neurons were treated with Aβ (2 μM) over a range of time points (5 min –18 hr). p53 phosphorylation at residue serine-392 was examined by western immunoblot. Aβ significantly increased p53 phosphorylation at serine-392 at 18 hr. Results are expressed as mean ± SEM for 3-4 observations, * $p<0.05$.

B. Sample western blot showing phosho-p53^{ser392} expression. Cells were treated with Aβ (2 μM) over a range of time points - 5 min, 1 hr (panel a), 6 hr and 18 hr (panel b)

4.2.6 Effect of Aβ on Bax protein expression

Since pro-apoptotic Bax is a target for modulation by p53, the effects of Aβ on total cellular Bax protein expression was investigated. Neurons were incubated with Aβ over a range of time points from 1 hr –12 hr and Bax expression was assessed by western immunoblot using an antibody which recognises the full form of Bax. Figure 4.6 demonstrates that Aβ increased expression of Bax from 0.99 ± 0.017 (mean band width ± SEM; arbitrary units) to 1.18 ± 0.066 (n=6) at 1 hr, but this value did not reach statistical significance. However, by 6 hr expression of Bax had significantly increased to 1.34 ± 0.09 ($p<0.01$, one-way ANOVA, n=6). This Bax expression was further increased to a value of 1.6 ± 0.22 following 12hr incubation with Aβ ($p<0.001$ one-way ANOVA, n=5). This demonstrates that Aβ-mediated regulation of Bax expression is regulated in a temporal manner. Figure 4.6B demonstrates the Aβ-mediated temporal increase in total Bax expression.

4.2.7 Aβ increases expression of Bax mRNA

To determine whether the increase in Bax protein expression was a result of increased transcription of the *bax* gene, mRNA expression of Bax was assessed by RT-PCR, using gene specific-primers for Bax and β-actin (Figure 4.7). Since Aβ significantly increased protein expression of Bax at 6 hr, this time point was selected to assess Bax mRNA expression. Aβ (2 μM) significantly increased expression of Bax mRNA from 0.99 ± 0.03 (mean band width ± SEM; arbitrary units) to 1.3 ± 0.09 ($p<0.05$, student's t test, n= 9) in Aβ-treated cells. This indicates that the Aβ-mediated increase in expression of Bax protein is as a direct result of increased transcription of the *bax* gene. The mRNA expression of Bax was normalised to that of the housekeeping gene β-actin. A sample agarose gel demonstrating the effect of Aβ on Bax mRNA expression is depicted in Figure 4.7B.

A.

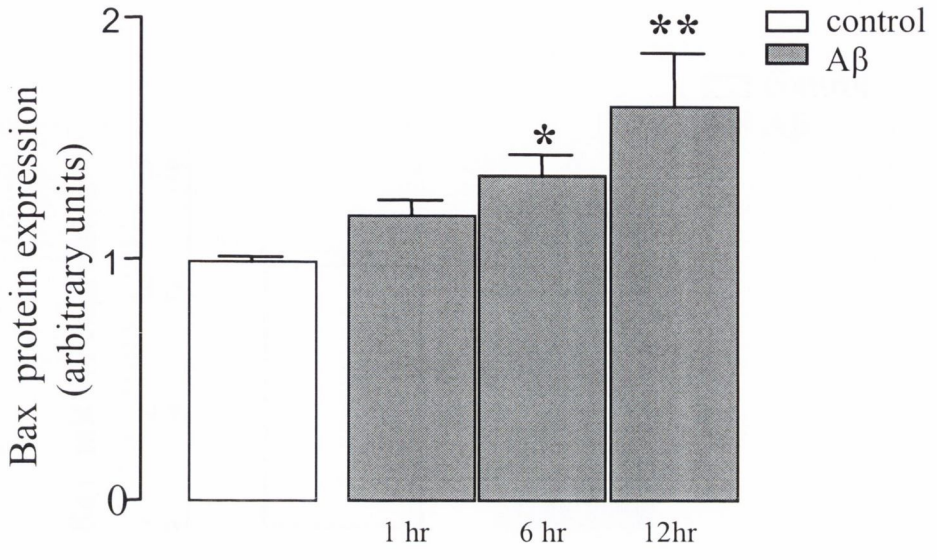

B.

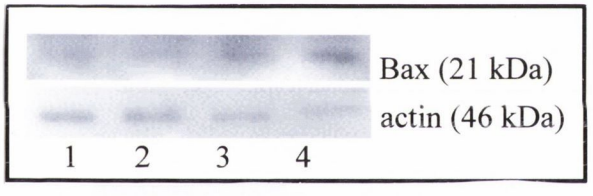

Figure 4.6 Aβ-mediates a temporal increase in Bax protein expression

A. Cortical neurons were treated with Aβ (2 μM) over a range of time points (5 min –12 hr). Bax protein expression was examined by western immunoblot. Aβ significantly increased Bax expression at 6 hr and 12 hr. Results are expressed as mean ± SEM for 6 observations, *$p<0.01$ ** $p<0.001$.

B. Sample western immunoblot demonstrating levels of Bax and actin expression in control (lane 1) and Aβ-treated cells at 1 hr (lane 2), 6 hr (lane 3) and 12 hr (lane 4).

A.

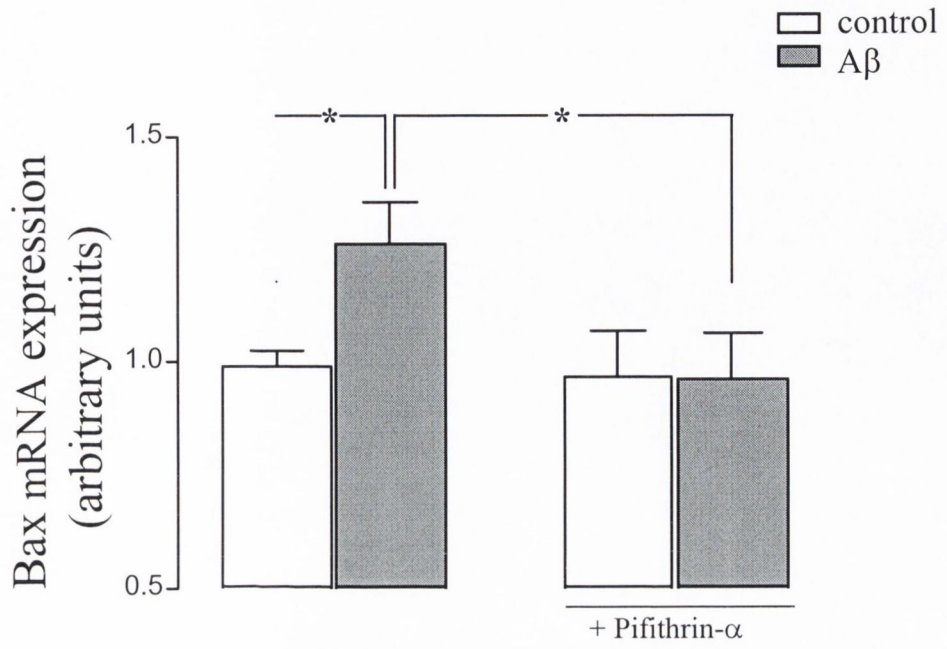

B.

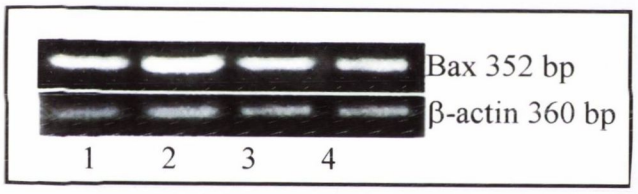

Figure 4.8 Aβ-mediated increase in Bax mRNA expression is p53 dependent

A. Cortical neurons were treated with pifithrin-α (100 nM) in the presence or absence of Aβ (2 μM) for 6 hr and Bax mRNA expression was assessed using RT-PCR. Aβ significantly increased Bax mRNA expression at 6 hr. In the presence of pifithrin-α the Aβ-mediated increase in Bax mRNA expression was significantly reduced. Results are expressed as mean ± SEM for 6 observations, * $p<0.05$.

B. Representative image of agarose gel demonstrating levels of Bax and β-actin mRNA expression in control (lane1); Aβ-treated cells (lane 2); pifithrin-α-treated cells (lane 3) and Aβ + pifithrin-α-treated cells (lane 4)

A.

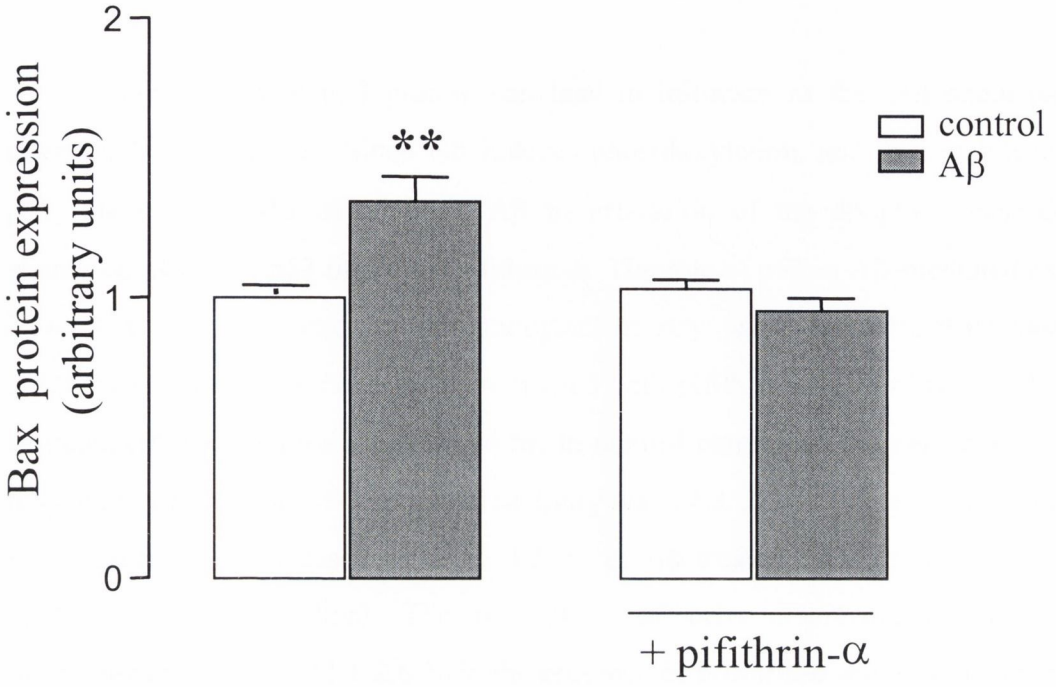

B.

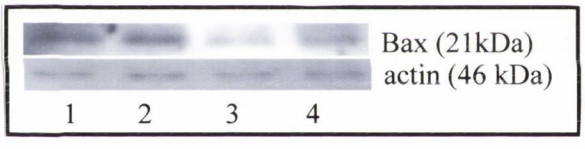

Figure 4.9 Aβ-mediated increase in Bax protein expression is p53 dependent

A. Cortical neurons were treated with pifithrin-α inhibitor (100 nM) in the presence or absence of Aβ (2 μM) for 6 hr and Bax protein expression was assessed using western immunoblot. Aβ significantly increased Bax protein expression at 6 hr. In the presence of pifithrin-α the Aβ-mediated increase in Bax expression was reduced. Results are expressed as mean ± SEM for 6 observations, $p<0.01$.

B. Sample western immunoblot demonstrating levels of Bax and actin protein expression in control (lane1); Aβ-treated cells (lane 2); pifithrin-α-treated cells (lane 3) and Aβ + pifithrin-α-treated cells (lane 4).

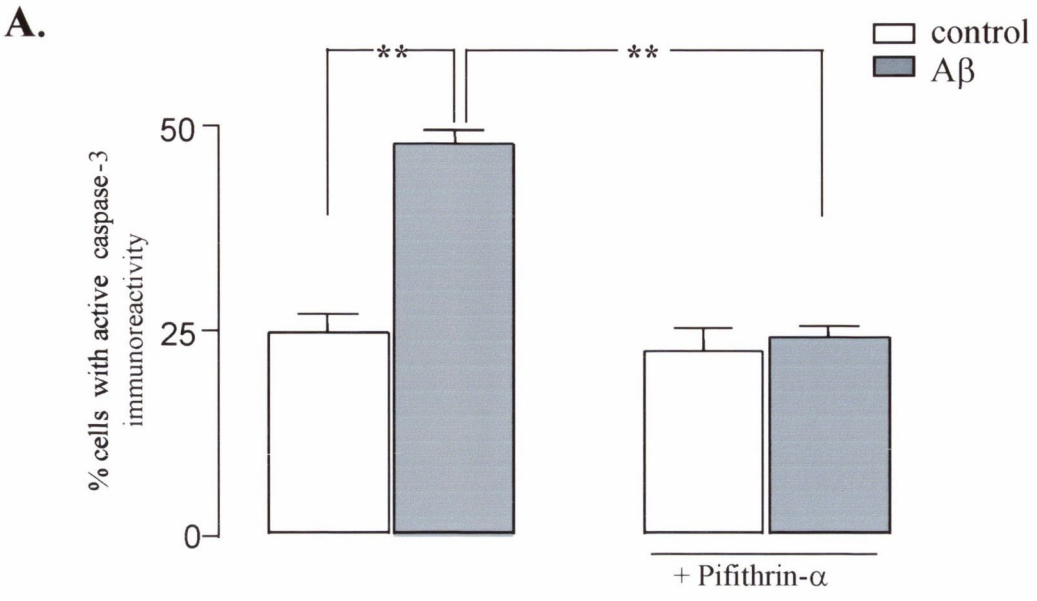

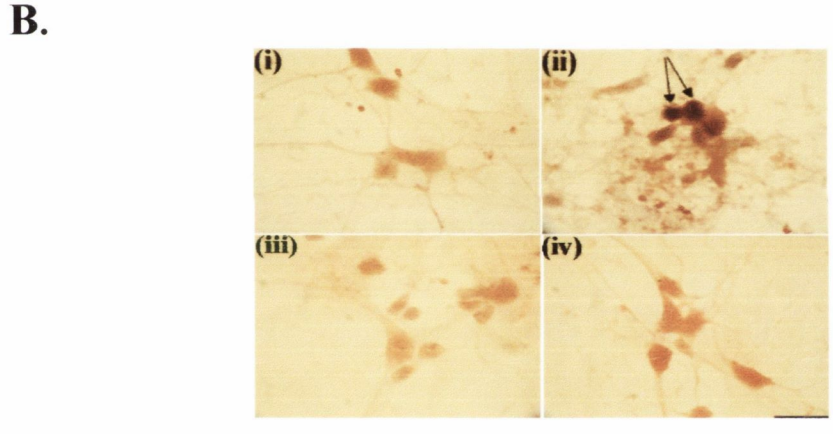

Figure 4.10 Aβ-mediated caspase-3 cleavage is p53 dependent.

A. Cortical neurons were treated with pifithrin-α inhibitor (100 nM) in the presence or absence of Aβ (2 μM) for 24 hr and caspase-3 activity was examined by immunocytochemistry. Aβ significantly increased the percentage of cells displaying active caspase-3 immunoreactivity at 24 hr. In the presence of pifithrin- α, the Aβ–induced increase in caspase-3 activity was abolished. Results are expressed as the mean ± SEM for 6 independent observations,** $P<0.01$.

B. Representative image of cortical neurons stained for activated caspase-3 immunoreactivity. Arrows indicate active caspase-3 in cells treated with (i) vehicle control (ii) Aβ (iii) pifithrin-α (iv) Aβ + pifithrin-α. Arrows indicate cells displaying representative caspase-3 immunostaining. Scale bar is 25 μm.

A.

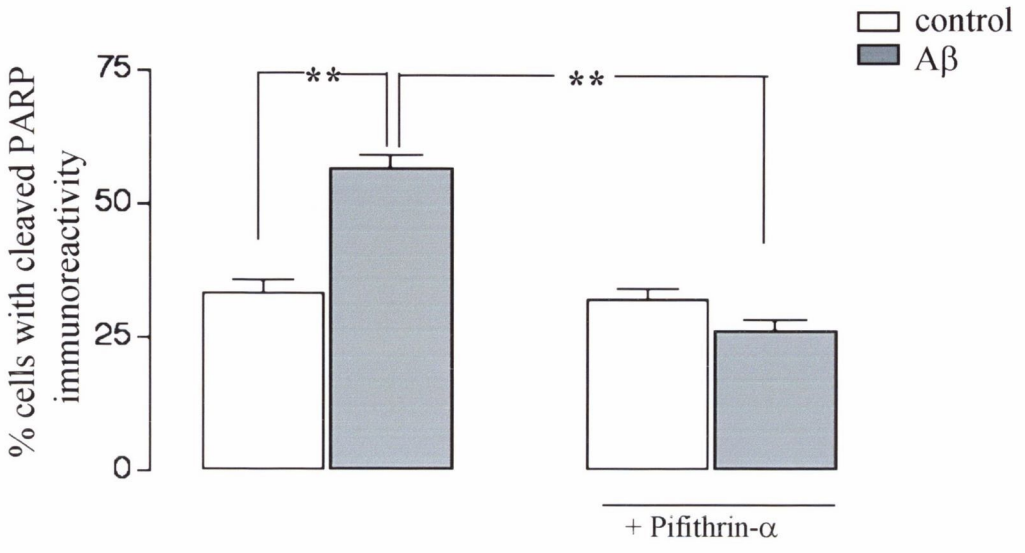

B.

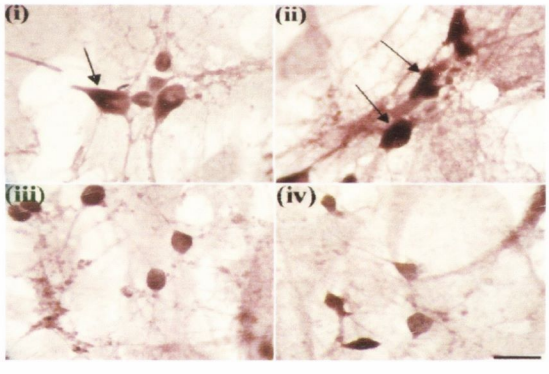

Figure 4.11 Aβ-mediated PARP cleavage is p53 dependent.

A. Cortical neurons were treated with pifithrin-α inhibitor (100 nM) in the presence or absence of Aβ (2 μM) for 72 hr and PARP cleavage was examined by immunocytochemistry. Aβ significantly increased cleavage of PARP at 72 hr. In the presence of pifithrin- α the Aβ mediated increase in PARP cleavage was abolished. Results are expressed as the mean ± SEM for 6 independent observations,** $P<0.01$

B. Representative image of cortical neurons displaying cleaved PARP immunoreactivity in cells treated with (i) vehicle control (ii) Aβ (iii) pifithrin-α (iv) Aβ + pifithrin- α. Arrows indicate cells displaying representative cleaved PARP immunostaining. Scale bar is 25 μm.

immunoreactivity for the cleaved form of PARP from 38 ± 3 % (mean ± SEM) to 67 ± 3 % ($p < 0.01$, one-way ANOVA, n=6 coverslips). The percentage of cells displaying immunoreactivity for the cleaved form of PARP was 37 ± 2 % in the presence of the pifithrin-α alone (n=6 coverslips). The Aβ-mediated increase in cells displaying immunoreactivity for the cleaved form of PARP was significantly reduced to 30 ± 2.6 % in cells co-treated with Aβ + pifithrin-α ($p<0.05$, one way ANOVA, n=6), indicating that the Aβ-induced increase in PARP cleavage is p53 dependent. A sample photo of cells stained for the cleaved fragment of PARP is shown in Figure 4.11B.

4.2.12 Effect of pifithrin-α on Aβ-induced DNA fragmentation

To further demonstrate the role of p53 in Aβ-mediated neuronal apoptosis, levels of DNA fragmentation were assessed in cells which were treated with the p53 inhibitor pifithrin-α (100 nM) for 1 hr, prior to treatment with Aβ for 72 hr (Figure 4.12). TUNEL analysis was carried out to measure the percentage of cells displaying fragmented DNA. Exposure to Aβ (2μM; 72hr) significantly increased the percentage of TUNEL positive cells from 24 ± 2.3 % (mean ± SEM) to 47 ± 2.4 ($p < 0.01$, one-way ANOVA, n=6 coverslips). The percentage of TUNEL positive cells was 27 ± 2 % in the presence of the pifithrin-α alone (n=6 coverslips). The Aβ-mediated increase in the percentage of TUNEL positive cells was significantly reduced to 21 ± 1.4% in cells co-treated with Aβ + pifithrin-α $p<0.05$, one way ANOVA, n=6). This result demonstrates the involvement of p53 in the Aβ-mediated induction of DNA fragmentation in cortical neurons. A sample photo of TUNEL stained cells is shown in Figure 4.12B.

A.

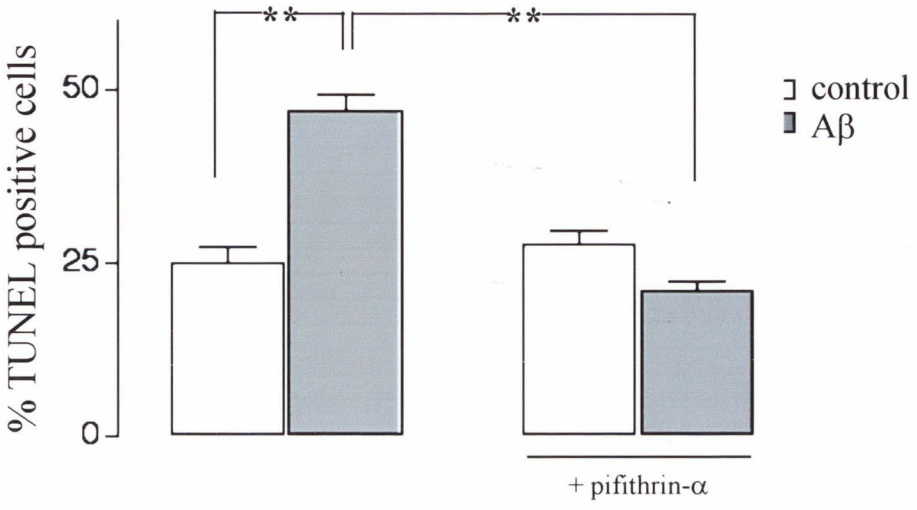

B.

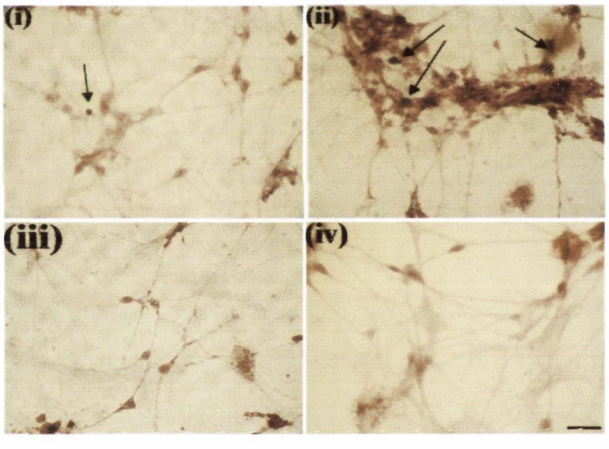

Figure 4.12 Aβ-mediated DNA fragmentation is p53 dependent.

A. Cortical neurons were treated with pifithrin-α inhibitor (100 nM) in the presence or absence of Aβ (2 μM) for 72 hr and DNA fragmentation was assessed using TUNEL analysis. Aβ significantly increased DNA fragmentation at 72 hr. In the presence of pifithrin- α, the Aβ–induced increase in DNA fragmentation was abolished. Results are expressed as the mean ± SEM for 6 independent observations,** $P<0.01$

B. Representative image of cortical neurons stained for DNA fragmentation. Arrows indicate TUNEL positive cells following exposure to (i) vehicle control (ii) Aβ (iii) pifithrin-α (iv) Aβ + pifithrin- α. Scale bar is 25 μm.

4.3 Discussion

The aim of this study was to establish the role of the transcription factor, p53, in Aβ-mediated neurotoxicity of cultured cortical neurons. The results demonstrate that Aβ increases p53 expression in a temporal manner. The increase in p53 expression was found to be independent of transcription. Increased p53 expression occurred as a result of increased stabilisation of p53 protein via phosphorylation at residue serine-15 of the protein. A candidate kinase which can phosphorylate and thus stabilize p53 is JNK (Adler *et al.*, 1997). Using an antisense approach to selectively deplete cells of specific JNK isoforms, I established that phosphorylation of p53 in response to Aβ-treatment occurs in a JNK1-dependent manner. Expression of pro-apoptotic Bax, a p53-responsive gene, was significantly increased following Aβ-treatment. To determine the signalling events which occur downstream of p53 in Aβ-mediated neuronal cell death, the p53 inhibitor, pifithrin-α, was applied to cells. The Aβ-mediated increase in Bax expression was reversed in pifithrin-α treated cells. Furthermore analysis of caspase-3 activity, PARP cleavage and nuclear DNA fragmentation demonstrated that p53 signalling plays an integral role in the Aβ-mediated induction of the apoptotic cascade.

The previous chapter demonstrated that 2 μM Aβ was sufficient to induce JNK activation, and induction of the apoptotic cascade in cultured cortical neurons. Therefore, this concentration was again employed, to further examine signalling events associated with Aβ neurotoxicity. Aβ increased expression of p53 in a time dependent manner. At 5 min exposure, Aβ had no effect on p53 protein expression. However, by 1 hr, Aβ had significantly increased p53 protein expression by 30 %. This increased p53 expression was short-lived and by 6 hr p53 expression remained elevated by 12 %, but not significantly so. At 18 hours, Aβ no longer had any effect on p53 expression. It was concluded from this experiment that the Aβ-induced increase in p53 expression was an early signalling event, potentially leading to an alteration in associated downstream signalling events.

Evidence of alterations in neuronal p53 expression, in response to cellular stress is provided by many studies. For example, increased expression of p53 occurs in damaged

neurons in acute models of injury such as ischemia (Miller *et al.*, 2000), and in brain tissue samples, derived from animal models, and patients with chronic neurodegenerative diseases (LaFerla et al., 1996; De la Monte *et al.*, 1997). Increased p53 expression can occur as a result of increased transcription of the p53 gene, or due to stabilisation of the protein by post-translational modification (Zörnig *et al.*, 2001). In non-stressed neurons, p53 has a short half-life, being exported from the nucleus by the associated regulatory protein, Mdm2, and targeted for ubiquitin-mediated degradation in the cytosol. However, modification of p53 by phosphorylation or acetylation at its amino-terminal domain can change the confirmation of p53, thus abolishing the interaction between p53 and the negative regulator Mdm2 (Ashcroft *et al.*, 2000). As a result, p53 is not shuttled to the cytoplasm for degradation, but instead accumulates in the nucleus and is trans-activated in its capacity as a transcription factor to activate transcription of its target genes. To clarify the mechanism leading to the Aβ-mediated increase in expression of p53 protein, by Aβ, RT-PCR was carried out to determine whether increased expression of p53 was due to increased transcription of the p53 gene. A previous study has observed increase transcription of p53 following treatment with $A\beta_{1-35}$ in cultured cortical neurons (Yan *et al.*, 2000). However, my results demonstrated that $A\beta_{1-40}$ did not modulate transcription of p53 at the time points examined. This indicated that the increased expression of p53, following Aβ treatment, might be due to a stabilisation event. In response to cellular stress, p53 can be stabilised via phosphorylation at critical residues (Ashcroft *et al.*, 2000). Phosphorylation at one such residue, serine-15, has been shown to be critical in mediating the p53 response to stress (Siliciano *et al.*, 1997) and serine-15 has been shown to be phosphorylated in response to the DNA damaging agents, cisplatin, camptothecin and etoposide (Appella *et al.*, 2001). Phosphorylation at this residue is associated with the apoptotic effect of p53 (Unger *et al.*, 1999). We investigated whether Aβ might mediate stabilisation of p53 by phosphorylation at serine-15. Since the increased p53 protein expression observed, occurred at 1 hr, it seemed likely that any stabilisation event would occur at, or before, this time. Accordingly, phosphorylation of p53 at serine-15 was monitored at the 1 hr time point and at the earlier time point of 5 min. Following treatment with Aβ, p53 phosphorylation at serine-15 was increased by 44 % at 5 min and 34 % at 1 hr. The Aβ-mediated phosphorylation of p53 strongly correlates with the temporal pattern of increased p53 protein expression, indicating that increased

phosphorylation of p53 at serine-15 is responsible for the increased p53 protein expression observed. In support for this idea, phosphorylation of p53 at serine-15 has previously been shown to correlate with increased p53 protein expression in lymphoblast cell lines, following UV irradiation (Siliciano *et al.*, 1997). Post-translational modifications also occur at the carboxy-terminus of p53, and phosphorylation at residue serine-392 within the carboxy- terminus domain, occurs in response to DNA damage (Lu *et al.*, 1998). Following treatment with Aβ over a range of times from 5 min – 18 hr, increased phosphorylation of p53 at residue serine-392 was found to occur at 18 hr, but not at earlier time points. This result suggests that phosphorylation of p53 at serine-392 does not play a role in the increased protein expression of p53, observed at 1 hr. At 18 hr post Aβ treatment, it is likely that some DNA damage has occurred, although maximal DNA fragmentation is not observed until 72 hr (Boland and Campbell, 2003a). Therefore, the Aβ-mediated phosphorylation at serine-392 found to occur at 18 hr may be a consequence of possibly a cellular response to DNA damage within the cell.

The evidence from this study and others (Laferla *et al*, 1996, Culmsee *et al.*, 2001) supports an interaction between p53 and Aβ. However, the mechanism of Aβ-induced stabilisation of p53 remains to be elucidated. Several candidate kinases have been proposed as stabilisers of p53, including DNA-PK and JNK (Lees-Miller *et al.*, 1990; Adler *et al.*, 1997). In the previous chapter, I demonstrated that JNK1 and JNK2 were activated by Aβ, so in order to determine the relationship between Aβ-mediated JNK activation and p53 stabilisation, cells were depleted of JNK using antisense oligonucleotides. Since Aβ-mediated activation of JNK2 did not occur until 24 hrs, it seemed unlikely that JNK2 was involved in p53 phosphorylation at residue serine-15, which occurred 1 hr post Aβ-treatment. Activation of JNK1 was an earlier event, which could potentially be upstream of p53 phosphorylation. Consequently, cells were depleted of JNK1, with selective JNK1 antisense oligonucleotides, to establish the role of JNK1 in the Aβ-mediated phosphorylation of p53. p53 phosphorylation at serine-15 was abolished in JNK1 depleted cells, placing JNK1 upstream of p53. In non-neuronal cells, JNK signalling has previously been reported to stabilise and activate p53, by phosphorylation at Threonine-81 (Fuchs *et al.*, 1998; Buschmann *et al.*, 2001). Furthermore, JNK1 has been demonstrated to bind p53 and mediate phosphorylation at serine-34 and serine-15 following UV irradiation and oxidative stress respectively (Milne *et al.*, 1995, Cheng *et*

al., 2003). An interaction between JNK1 activation and p53 phosphorylation at serine-15, has not previously been reported in neurons. Conversely, non-active JNK has been demonstrated to negatively regulate p53 expression and target p53 for ubiquitin-mediated degradation in an Mdm2-independent manner (Fuchs *et al.*, 1997). A further degree of complexity is added to the interrelationship between JNK and p53 signalling, by the fact that following DNA damage activation of p53 can occur upstream of JNK activation. Aditionally, p53 can regulate activity of JNK1 and JNK2 in tumour cell lines (Zhang *et al.*, 2002b). Interactions between JNK and p53 are therefore likely to be dependent on cell type and stimulus type received by the cell. JNK2 and JNK3 can also serve as p53 N-terminal serine 34 kinases in response to cellular stress (Hu *et al.*, 1997). However, since depletion of JNK1 completely abrogated the Aβ-mediated phosphorylation of p53 and Aβ-mediated activation of JNK2 was only detected at the later time points of 24hr and 48 hr, which was much later than the time required to stabilise p53, it was concluded that JNK2 was not pertinent in the Aβ-mediated activation of p53.

The pro-apoptotic protein Bax is a p53-responsive gene, which plays an important role in apoptosis. Increased Bax immunoreactivity has been observed in AD brain (Tortosa *et al.*, 1998). Since my study demonstrates an increase in p53 phosphorylation in Aβ-treated neurons, I investigated whether expression of the p53 substrate, Bax, was altered following treatment with Aβ. Neurons were exposed to Aβ over a range of time points and expression of Bax mRNA and Bax protein were monitored. Bax protein expression was significantly increased by 25 % following exposure to Aβ for 6 hr and by 38 % following a 12 hr exposure to Aβ. This was mirrored by a 24 % Aβ-induced increase in Bax mRNA at 6 hr post Aβ-treatment. Upregulation of Bax mRNA has previously been reported to occur within 1 hr of exposure to $A\beta_{31-35}$ (Yan *et al.*, 2000). That study used a higher concentration of Aβ (25 μM), which may account for the earlier increase in Bax mRNA observed. In addition, two recent studies have reported increased Bax protein expression in the CA1 region of the hippocampus, and in the differentiated SK-N-BE neuroblastoma cell line, following administration of $A\beta_{1-40}$, thus providing further evidence for the involvement of Bax in Aβ-mediated neurotoxicity (Minogue *et al.*, 2003; Tamagno *et al.*, 2003).

Downstream consequences of p53-mediated induction of Bax include release of mitochondrial cytochrome *c* and activation of caspase-3 (Karpinich *et al.*, 2001). This process is regulated by members of the Bcl family of proteins. While translocation of pro-apoptotic Bax to the mitochondrial membrane facilitates release of cytochrome *c* through formation of a pore in the outer mitochondrial membrane, Bcl-2 is anti-apoptotic by virtue of its ability to inhibit cytochrome *c* release (Zörnig *et al.*, 2001). The ratio of bcl-2:bax expression represents a mechanism which dictates whether cells will survive or undergo apoptosis in response to particular stimuli (Rosse *et al.*, 1998). Alternatively, p53 can target directly to the mitochondria to induce a transcription-independent apoptotic signal (Marchenko *et al.*, 2000). To further delineate the relationship between Aβ, p53, and induction of the apoptotic cascade, the p53 inhibitor pifithrin-α was applied to cells. This inhibitor acts to interfere with the DNA-binding ability of p53 and thus, inhibits the transcriptional activity of p53 (Culmsee *et al.*, 2001). The Aβ-mediated increase in Bax mRNA, and subsequent Bax protein expression, was abolished in pifithrin-α treated cells, thus indicating that the Aβ-mediated increase in Bax expression occurred as a direct result of p53 signalling. In accordance with this result, pifithrin-α has previously been reported to selectively inhibit $A\beta_{1-42}$ mediated induction of Bax in hippocampal neurons (Culmsee *et al.*, 2001). In contrast, a study by Giovanni *et al.* (2001) described Aβ-induced apoptosis in cultured embryonic neurons obtained from p53 knock out mice as being p53-independent. This highlights the complexity of ascertaining the involvement of a given signalling pathway in neuronal cells. It is probable that multiple signalling pathways interact to determine the fate of a given neuronal cell, following a stressful stimulus, and it is likely that compensatory signalling occurs in the absence of expression of certain regulatory genes. Thus, in a model whereby expression of an important transcription factor such as p53 is knocked out, it is possible that multiple signalling pathways converge to achieve the desired outcome.

To further clarify the role of p53 in Aβ-mediated neurotoxicity, the effect of pifithrin-α on aspects of the Aβ induced apoptotic cascade were examined. The proclivity of Aβ to activate caspase-3 was significantly attenuated in pifithrin-α treated cells. Moreover, Aβ failed to promote significant cleavage of the DNA repair enzyme PARP, and to induce increased levels of fragmented DNA, consequent to pre-treatment with

pifithrin-α. Taken together, these results provide strong indication that p53 plays an important role in Aβ-mediated neuronal apoptosis. p53 mediates its effects at a pre-mitochondrial stage, placing it at a proximal point for intervention in the apoptotic cascade. Since neuronal cells are, for the most part, post-mitotic and can not regenerate, the prospect of temporarily inactivating p53 protein and potentially preventing further brain damage is an attractive one. Administration of pifithrin-α offers a potential drug therapy in the treatment of chronic neurodegenerative diseases such as AD. It penetrates the blood brain barrier and has been demonstrated to offer protection against kainate-induced excitotoxicity in the hippocampus *in vivo*. My finding along with others (Culmsee *et al.*, 2001; Tamagno *et al.*, 2003), demonstrates that pifithrin-α offers protection against Aβ induced neurtoxicity, making it a worthy candidate for more research.

In conclusion, the results presented in this chapter demonstrate that Aβ increases expression of p53 protein. This increase in p53 protein expression was not attributable to increased transcription of the p53 gene, as no associated increase in p53 mRNA was observed. Instead the observed increase in protein expression occurred by stabilisation of the p53 protein through phosphorylation of p53 on its amino-terminal domain, at residue serine-15. Treatment with JNK1 antisense reversed the Aβ-mediated increase in p53 phosphorylation, placing p53 stabilisation via phosphorylation downstream of JNK1 in the Aβ signalling cascade. Aβ also induced increased expression of the p53-responsive gene, Bax. Application of pifithrin-α, an inhibitor of p53-induced transcriptional activation, attenuated the Aβ-mediated increase in Bax expression. This suggests that Aβ-induced Bax expression occurs downstream of JNK-mediated stabilisation of p53. In addition, exposure to pifithrin-α significantly reduced Aβ-mediated induction of the apoptotic events, caspase-3 cleavage, PARP cleavage and DNA fragmentation. These results demonstrate the importance of p53 signalling in Aβ-mediated neuronal cell death.

Chapter 5

Subcellular localisation of p53 and Bax in cultured cortical neurons

5.1 Introduction

Disruption of intracellular organelles is a common event in apoptosis. The involvement of the mitochondria is often considered an initiating and basic event in apoptosis (Zörnig *et al.*, 2001). Mitochondria control apoptosis by sequestering pro-apoptotic proteins, such as cytochrome *c* and apoptosis inducing factor (AIF), in the mitochondrial intermembrane space (Blatt and Glick, 2001). However, in response to apoptotic stimuli these proteins are released from the intermembrane space and can directly activate cell death programmes within the cell. Once in the cytosol cytochrome-*c* binds the caspase adaptor, apaf-1, in the presence of ATP, and thus activates the inactive precursor, procaspase-9, to its active form. This leads to initiation of a caspase cascade culminating in activation of the effector caspase, caspase-3, and induction of DNA fragmentation and apoptosis (Raff, 1998). Release of cytochrome *c* from the mitochondria can occur in association with loss of mitochondrial membrane potential and rupture of the outer mitochondrial membrane or can occur independent of collapse of mitochondrial membrane potential due to a transient opening if the permeability transition pore (Blatt and Glick, 2001).

As well as mitochondria being involved in apoptosis, there is an increasing body of evidence to suggest a role for the lysosomes in the apoptotic process (Li *et al.*, 2000; Brunk *et al.*, 2001). However, the role of lysosomes in apoptosis is less well defined. Lysosomes are membrane bound, cytoplasmic organelles containing over 40 hydrolytic enzymes, which are mostly active only in acidic conditions (Ditaranto-Desimone *et al.*, 2003). Lysosomes are normally concerned with cellular housekeeping, removing damaged macromolecules from the cellular environment and converting them into reusable products, thus replenishing pools of amino acids and glucose for new protein synthesis (Cataldo *et al.*, 1996). Christian de Duve, who first identified lysosomes, coined the term 'suicide bags' to describe their potential for orchestrating cellular destruction (De Duve, 1969). De Duve proposed that an uncontrolled leakage of lysosomal enzymes to the cytosol might be dangerous, or even lethal, for cells. Nevertheless, for some time lysosomes have been considered stable organelles that lose integrity only in the later stages of death. This is due to the observation of seemingly intact lysosomes even in the later stages of apoptosis (Li *et*

al., 2000). However, lysosomes may look ultrastructurally intact, even after the leakage of a substantial amount of lysosomal enzyme into the cytosol (Brunk and Ericsson, 1972). More recent studies have shown that moderate release of lysosomal enzymes leads to apoptosis, while more pronounced release is associated with necrotic cell death (Brunk *et al.*, 2001; Salvesen, 2000). It is suggested that leakage of lysosomal proteases can promote apoptosis directly by activation of procaspases, or indirectly by attacking the mitochondria leading to release of pro-apoptotic factors such as cytochrome *c*. (Li *et al.*, 2000). Evidence for the role of lysosomes in apoptosis is provided by the finding that cathepsin-B has the capacity to activate several cytosolic caspases (Ishisaka *et al.*, 1999) and that cathepsin-L leads to activation of caspase-3 in the cytosol, with subsequent apoptosis (Hishita *et al.*, 2001; Boland and Campbell, 2003b). In addition, cathepsin-D is proposed to mediate translocation of cytochrome *c* from the mitochondria to the cytosol (Roberg *et al.*, 2002).

Abnormalities in both mitochondria and lysosomes occur in AD. Reduced rate of brain metabolism, due to compromised mitochondrial function, is one of the best-documented abnormalities in AD (Blass, 2001). Also, the endosomal-lysosomal system in AD brain is markedly altered. This alteration is an early event in the disease, with almost all pyramidal neurons in vulnerable prefrontal and hippocampal areas exhibiting abnormally high densities of endosomes/lysosomes (Cataldo *et al.*, 1996). This accumulation of lysosomes is associated with an upregulation of the lysosomal system by means of increased expression of lysosomal hydrolases (Cataldo *et al.*, 1995) and increased trafficking of cathepsins from their site of translation in the trans-golgi network to their entry into the lysosomes (Cataldo *et al.*, 1996). While the role of mitochondria in Aβ-mediated apoptosis is widely reported (Fu *et al.*, 1998; Butterfield *et al.*, 1999; Culmsee *et al.*, 2001), there is an increasing body of evidence to suggest that lysosomes are also involved in Aβ-mediated neuronal apoptosis. In a neuronal cell line, $A\beta_{1-42}$ has been shown to promote lysosomal membrane instability and subsequent apoptosis (Ji *et al.*, 2002). In addition, recent work from this laboratory has shown that $A\beta_{1-40}$ promotes release of lysosomal proteases into the cytosol (Boland and Campbell, 2003b) as an early event in the neurodegenerative cascade. The exact mechanisms by which Aβ leads to deregulation of mitochondria and lysosomes remain to be fully elucidated.

The previous chapter demonstrated an increase in expression of the tumour suppressor protein, p53, through increased phosphorylation of p53 at serine-15, and an associated increase in expression of pro-apoptotic Bax. Therefore, in this aspect of the study, I sought to determine the mechanistic role of these proteins in orchestrating Aβ-mediated neuronal apoptosis. Previous studies from this laboratory have demonstrated that Aβ mediates release of cytochrome *c* from mitochondria (Boland and Campbell, unpublished observation) and cathepsin-L from lysosomes (Boland and Campbell, 2003b), possibly due to $A\beta_{1\text{-}40}$ altering the membrane integrity of these organelles. Consequently, the aim of this aspect of the study was to examine whether p53 and Bax impact on the mitochondria and lysosomes. Irrespective of the initiating stimulus, all apoptotic pathways generally converge to a common execution phase of apoptosis that requires activation of caspase-3 (Stoka *et al.*, 2001). Since activation of caspase-3 can occur in response to release of apoptotic factors such as cytochrome *c* from mitochondria (Blatt and Glick, 2001) and also following release of proteases such as cathepsin-L from the lysosomes (Hishita *et al.*, 2001), I hypothesised that the mechanism by which these apoptotic factors are released, might be similar for both organelles. Pro-apoptotic Bax is critical in the control of mitochondrial-mediated apoptosis and can associate with the mitochondrial membrane and thus regulate the release of cytochrome *c* (Blatt and Glick, 2001). p53 has also been shown to directly interact with the mitochondrial membrane and form complexes with the anti-apoptotic Bcl-2 proteins resulting in the release of cytochrome *c* (Mihara *et al.*, 2003). While the role of p53 and Bax in regulating the lysosomal branch of the apoptotic pathway is less clear, lysosomal destabilisation has been reported to occur in p53-induced apoptosis (Yuan *et al.*, 2002) and overexpression of bcl-2 has been shown to inhibit lysosomal-dependant apoptosis by stabilising the lysosome (Zhao *et al.*, 2000).

The experimental work carried out in this chapter therefore aimed to determine a role for p53 and Bax in Aβ-mediated alterations of mitochondrial and lysosomal membrane integrity. Expression of Bax was assessed in cytosolic and mitochondrial fractions, in order to determine if the increased expression of Bax demonstrated in the previous chapter was accompanied by a redistribution of Bax from the cytosol to specific intracellular organelles in order to serve its pro-apoptotic function. The association of Bax and phospho-$p53^{ser15}$ with mitochondrial and lysosomal membranes

was investigated by immunocytochemistry in conjunction with the specific mitochondrial dye, Mitotracker Red, and the specific lysosomal dye, Lysotracker Red (Molecular Probes, The Netherlands), respectively. Lysosomal integrity was assessed using the acridine orange (AO) relocation technique. Finally to determine the role of p53 in the previously reported Aβ-mediated increased cytosolic activity of cathepsin-L (Boland and Campbell, 2003b), cathepsin-L activity was assessed in cells which had been treated with the p53 inhibitor, pifithrin-α.

5.2 Results

5.2.1 Aβ reduces expression of Bax in the cytosol

To establish whether cellular relocation of Bax occurs following Aβ treatment, cells were incubated in the presence or absence of Aβ for 6 hr and cytosolic and mitochondrial fractions were prepared as described in Section 2.5.1(ii). Cytosolic expression of Bax was assessed by western immunoblot using a monoclonal antibody that recognises the full form of Bax. Figure 5.1 demonstrates that Aβ (2 μM) leads to a significant reduction in cytosolic Bax expression at 6 hr from 1.05 ± 0.05 (mean band width ± SEM) to 0.95 ± 0.09 ($p<0.05$, student's t-test, $n=6$). This indicates that Aβ may mediate translocation of Bax from the cytosol to target organelles within the cell. A sample immunoblot demonstrating the Aβ-mediated reduction in cytosolic Bax expression at 6 hr is shown in Figure 5.1B.

5.2.2 Effect of Aβ on Bax expression at mitochondria.

Since the mitochondria is one target organelle at which Bax can mediate its pro-apoptotic effects (Blatt and Glick, 2001), the effect of Aβ on Bax expression at the mitochondria was examined. Cells were incubated in the presence or absence of Aβ for 6 hr and mitochondrial expression of Bax was assessed by western immunoblot. Figure 5.2 demonstrates that Aβ increases expression of Bax at the mitochondria, but not significantly so. Thus, Bax expression was 0.42 ± 0.01 in control (mean band width ± SEM) and 0.47 ± 0.03 in Aβ-treated cells ($p<0.076$, student's t-test, $n=6$). Although Aβ significantly reduced Bax expression in the cytosol (Figure 5.1) this did not correlate with a significant increase in Bax expression within the mitochondrial fraction as assessed by western immunoblot.

A.

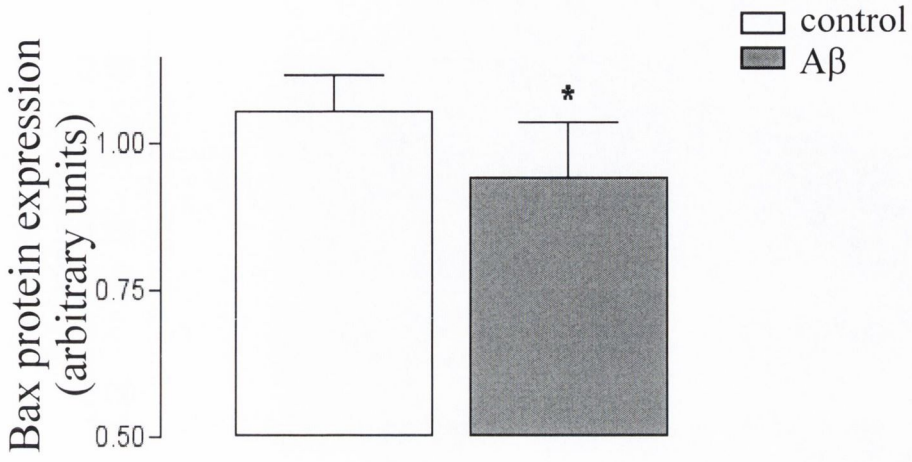

B.

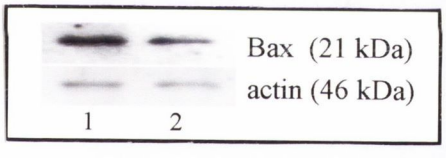

Figure 5.1 Aβ reduces cytosolic expression of Bax protein

A. Cortical neurons were treated with Aβ (2 μM) for 6 hr and expression of Bax protein was assessed in cytosolic fractions using western immunoblot. Aβ significantly reduced expression of Bax in the cytosol at 6 hr. Results are expressed as mean ± SEM for 6 observations, * $p<0.05$.

B. Sample western immunoblot demonstrating levels of Bax and actin protein expression in control (lane1) and Aβ-treated cells (lane 2).

A.

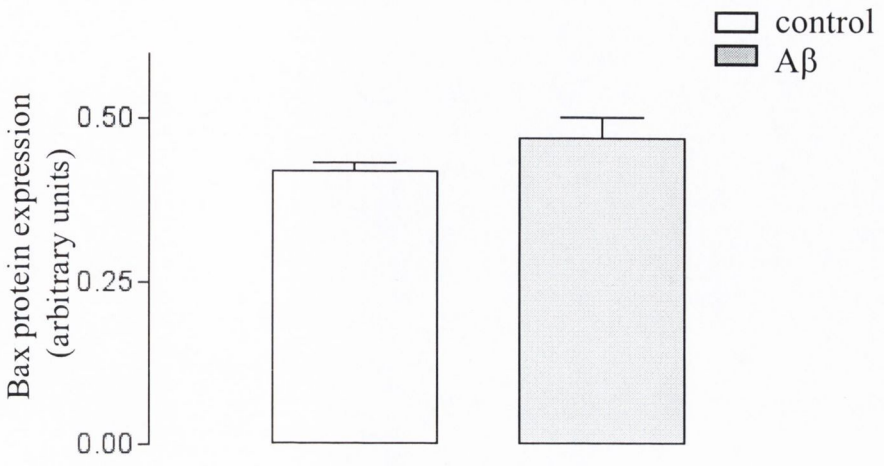

B.

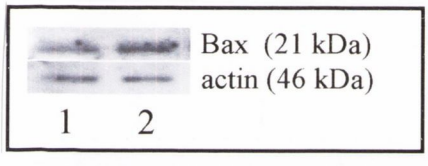

Figure 5.2 Effect of Aβ on mitochondrial expression of Bax

A. Cortical neurons were treated with Aβ (2 μM) for 6 hr and mitochondrial expression of Bax protein was assessed by western immunoblot. Aβ increased expression of mitochondrial Bax at 6 hr, but not significantly so. Results are expressed as mean ± SEM for 6 observations, $p<0.076$.

B. Sample western immunoblot demonstrating levels of mitochondrial Bax and actin protein expression in control (lane1) and Aβ-treated cells (lane 2).

5.2.3 Bax expression co-localises with mitochondria in Aβ-treated cells

To further examine the effect of Aβ on redistribution of Bax from the cytosol to mitochondria, expression of Bax was assessed in association with the specific mitochondrial marker, Mitotracker Red. Cells were incubated in the presence or absence of Aβ (2 μM) for 6 hr, prior to incubation with Mitotracker Red (400 nM) for 30 min. Bax expression was detected by immunocytochemistry using a monoclonal Bax-specific antibody and cells were visualised by fluorescence microscopy. Figure 5.3(i) and (ii) demonstrates the location of mitochondria in control and Aβ-treated cells, respectively, following loading with Mitotracker Red. Figure 5.3(iii) represents Bax immunostaining in control cells and this Bax immunofluorescence was increased in Aβ-treated cells (Figure 5.3(iv)). Furthermore, in Aβ-treated cells increased co-localisation of Bax expression with mitochondria was observed (Figure 5.3(vi)). This result indicates that the Aβ-mediated increase in Bax expression is associated with increased association of Bax at the mitochondria. However, regions remained within the cell where Bax expression did not co-localise with mitochondria, indicating alternative intracellular sites for Bax. A negative control image is displayed in Figure 5.3(vii); cells were stained with a secondary FITC-labelled antibody only. No primary antibody was employed. The resulting staining is diffuse, representative of non-specific staining.

5.2.4 Phospho-p53^{ser15} expression co-localises with mitochondria in Aβ-treated cells at 1 hr and 6 hr.

p53 has previously been reported to interact directly at the mitochondria to promote apoptosis (Marchenko *et al.,* 2000). To determine whether p53 interacts with mitochondria in Aβ-treated neurons, co-localisation of p53 expression and mitochondria was assessed. Since the previous chapter demonstrates that Aβ induced an increase in p53 expression at 1 hr, via phosphorylation of p53 at residue serine-15, expression of phospho-p53^{ser15} was assessed. Cells were incubated in the presence or absence of Aβ (2 μM) for 1 hr and 6 hr, prior to a 30 min incubation with Mitotracker

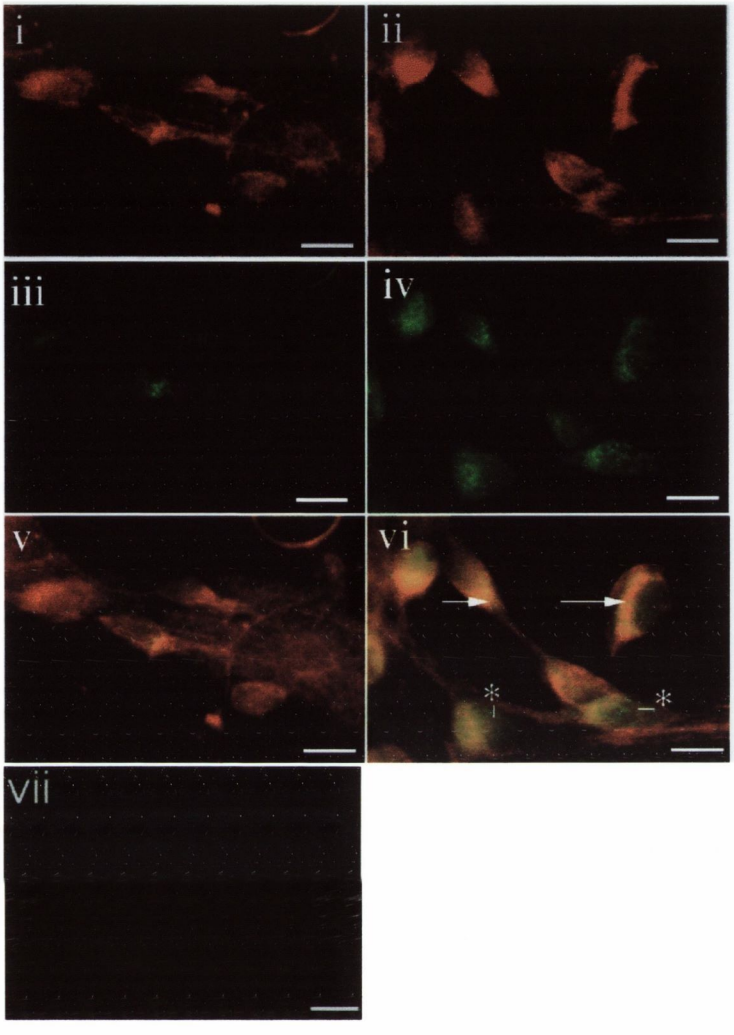

Figure 5.3 Aβ increases expression of Bax at the mitochondria

Fluorescence microscopy was used to visualise the distribution of Bax within cortical neurons following treatment with Aβ (2 μM, 6 hr). Cells were double labelled with the mitochondrial-specific marker, Mitotracker Red, and a FITC-labelled Bax antibody.

Mitotracker Red staining represents the distribution of mitochondria in (i) control (ii) and Aβ-treated cells (excitation 579 nm; emission, 599 nm). Analysis of Bax immunostaining in (iii) control and (iv) Aβ-treated cells demonstrated increased expression of Bax in Aβ-treated cells (excitation, 490 nm; emission, 520 nm). Co-localisation analysis of Bax and mitochondria in (v) control and (vi) Aβ-treated cells (v, vi) revealed increased localisation of Bax at the mitochondria in Aβ-treated cells. Arrows indicate regions of co-localisation, Stars indicate regions where co-localisation does not occur. The image displayed in (vii) is a negative control. Scale bar is 10 μm.

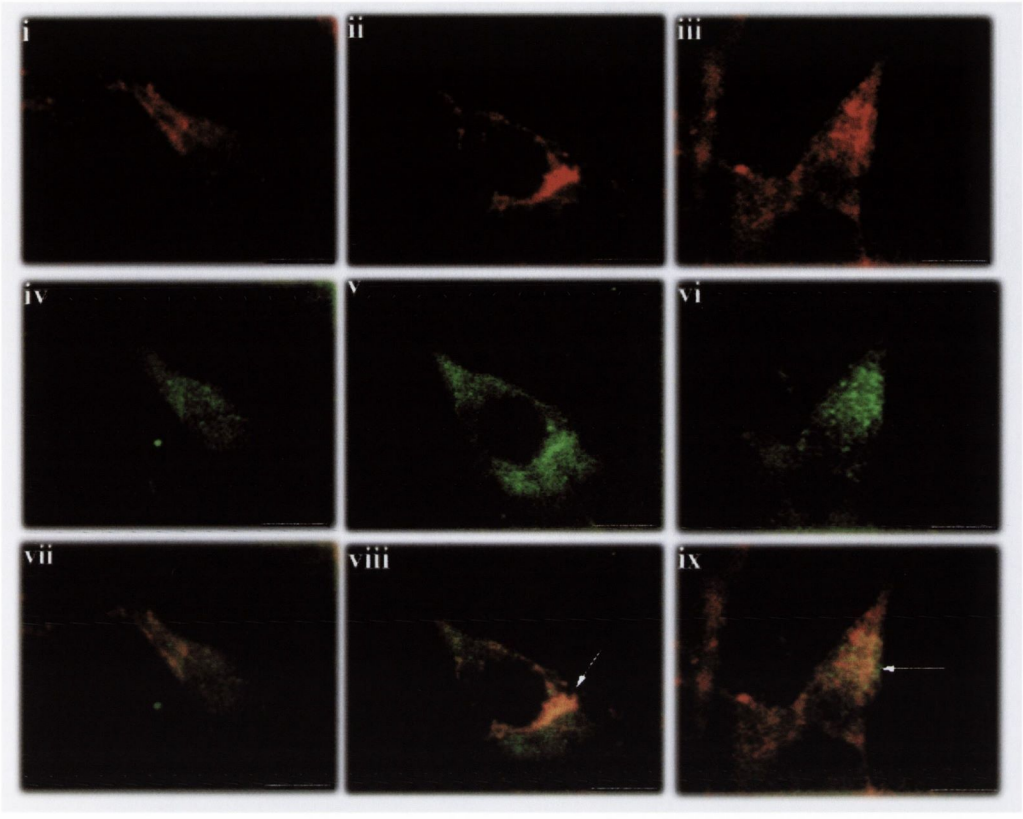

Figure 5.4 Effect of Aβ on phospho-p53^{ser15} expression at the mitochondria at 1 hr

Fluorescence microscopy was used to visualise the distribution of phospho-p53^{ser15} within cortical neurons following treatment with Aβ (2 μM, 1 hr). Cells were double labelled with the mitochondrial-specific marker, Mitotracker Red, and a FITC-labelled phospho-p53^{ser15} antibody.

Mitotracker Red staining represents the distribution of mitochondria in (i) control and (ii, iii) Aβ-treated cells (excitation 579 nm; emission, 599 nm).
Analysis of phospho-p53^{ser15} expression in (iv) control and (v,vi) Aβ-treated cells demonstrated increased expression of phospho-p53^{ser15} in Aβ-treated cells (excitation, 490 nm; emission, 520 nm).
Co-localisation analysis of phospho-p53^{ser15} and mitochondria in (vii) control and (viii,ix) Aβ-treated cells revealed increased localisation of phospho-p53^{ser15} at the mitochondria in Aβ-treated cells. Arrows indicate areas of co-localisation. Scale bar is 10 μm.

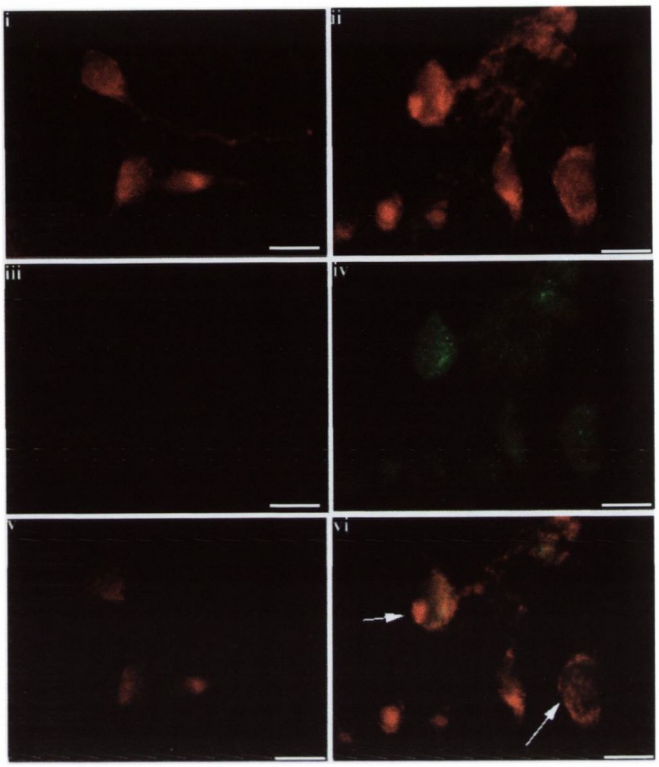

Figure 5.5 Effect of Aβ on phospho-p53^{ser15} expression at the mitochondria at 6 hr

Fluorescence microscopy was used to visualise the distribution of phospho-p53^{ser15} within cortical neurons following treatment with Aβ (2 μM, 6 hr). Cells were double labelled with the mitochondrial-specific marker, Mitotracker Red, and a FITC-labelled phospho-p53^{ser15} antibody.

Mitotracker Red staining represents the distribution of mitochondria in (i) control and (ii) Aβ-treated cells (excitation 579 nm; emission, 599 nm).
Analysis of phospho-p53^{ser15} expression in (iii) control and (iv) Aβ-treated cells demonstrated increased expression of phospho-p53^{ser15} in Aβ-treated cells (excitation, 490 nm; emission, 520 nm).
Co-localisation analysis of phospho-p53^{ser15} and mitochondria in (v) control and (vi) Aβ-treated cells revealed increased localisation of phospho-p53^{ser15} at the mitochondria in Aβ-treated cells. Arrows indicate areas of co-localisation. Scale bar is 10 μm.

Red (400 nM). Phospho-p53^{ser15} expression was detected by immunochemistry using an antibody which specifically recognises p53 phosphorylated at serine-15 and cells were visualised using fluorescence microscopy. Figure 5.4(i) and (ii,iii) demonstrates the location of mitochondria in control and Aβ-treated cells at 1 hr, respectively, following loading with Mitotracker Red. Figure 5.4(iv) represents p53 immunostaining in control cells and this p53 immunofluorescence was increased in Aβ-treated cells at 1 hr (Figure 5.4(v,vi)). Furthermore, in Aβ-treated cells increased co-localisation of phospho-p53^{ser15} expression with mitochondria was observed at 1 hr (Figure 5.4(vii,ix)).

Figure 5.5(i) and (ii) demonstrates the location of mitochondria in control and Aβ-treated cells at 6 hr, following loading with Mitotracker Red. Figure 5.5(iii) represents p53 immunostaining in control cells and this p53 immunofluorescence was increased in Aβ-treated cells at 6 hr (Figure 5.5(v)). Furthermore, in Aβ-treated cells increased co-localisation of phospho-p53^{ser15} expression with mitochondria was observed at 6 hr (Figure 5.5(vi). This result indicates that the Aβ-mediated increase in phospho-p53^{ser15} expression is coupled with increased association of phospho-p53^{ser15} at the mitochondria. Regions remained within the cell where phospho-p53^{ser15} expression did not co-localise with mitochondria, indicative of alternative intracellular sites for phospho-p53^{ser15} within the cell.

5.2.5 Aβ increases cytosolic cytochrome *c* expression

A potential consequence of disruption of mitochondrial membrane stability is translocation of mitochondrial cytochrome *c* into the cytosol. To determine whether Aβ mediated translocation of cytochrome *c* to the mitochondria, cells were treated in the presence or absence of Aβ for 6 hr and cytosolic fractions were prepared as described in Section 2.5.1(ii). Cytosolic expression of cytochrome *c* was assessed by western immunoblot using a polyclonal antibody that recognises free cytosolic cytochrome *c* at 11.4 kDa (Pettigrew and Seilman, 1982). Figure 5.6 represents a sample immunoblot

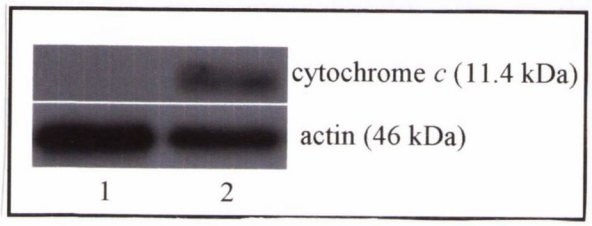

Figure 5.6 Aβ increases cytosolic cytochrome *c* expression

Cortical neurons were treated with Aβ (2 μM) for 6 hr and expression of cytochrome *c* was assessed in cytosolic fractions using western immunoblot. Sample immunoblot demonstrating cytochrome *c* and actin expression in control (lane 1) and Aβ-treated cells (lane 2). Aβ increased expression of cytochrome *c* in the cytosol at 6 hr.

demonstrating that Aβ leads to an increase in cytosolic cytochrome c expression at 6 hr.

5.2.6 Bax expression co-localises with Lysosomes in Aβ-treated cells

In order to determine whether Bax impacts on the lysosomal system, expression of Bax was assessed in association with the lysosomal specific dye, Lysotracker Red. Cells were incubated in the presence or absence of Aβ (2 μM) for 6 hr, prior to incubation with Lysotracker Red (700 nM) for 30 min. Bax expression was detected by immunocytochemistry using a monoclonal Bax-specific antibody and cells were visualised using fluorescence microscopy. Figure 5.7 (i) and (ii) demonstrates the location of lysosomes in control and Aβ-treated cells, respectively, following loading with Lysotracker Red. Figure 5.7(iii) represents Bax immunostaining in control cells and this Bax immunofluorescence was increased in Aβ-treated cells (Figure 5.7(iv)). Figure 5.7(v) and 5.7(vi) demonstrates co-localisation of Bax expression with lysosomes in control and Aβ-treated cells. Bax immunofluorescence at the lysosome was increased following Aβ treatment. This result suggests a role for Bax at the lysosome during Aβ signalling. Regions remained within the cell where Bax expression did not co-localise with lysosomes and these areas are likely to represent Bax expression at mitochondrial membranes, as demonstrated in Figure 5.3.

5.2.7 Phospho-p53^{ser15} expression co-localises with lysosomes in Aβ-treated cells at 1 hr and 6 hr

In order to determine whether p53 impacts at the lysosomal membrane, expression of phospho-p53^{ser15} was assessed by immunocytochemistry. Cells were incubated in the presence or absence of Aβ (2 μM) for 1 hr or 6 hr, prior to a 30 min incubation with the lysosomal marker, Lysotracker Red (700 nM). Phospho-p53^{ser15} expression was detected by immunocytochemistry using an antibody which specifically recognises p53 phosphorylated at serine-15 and cells were visualised by fluorescence microscopy. Figure 5.8(i) and (ii) demonstrates the location of lysosomes in control

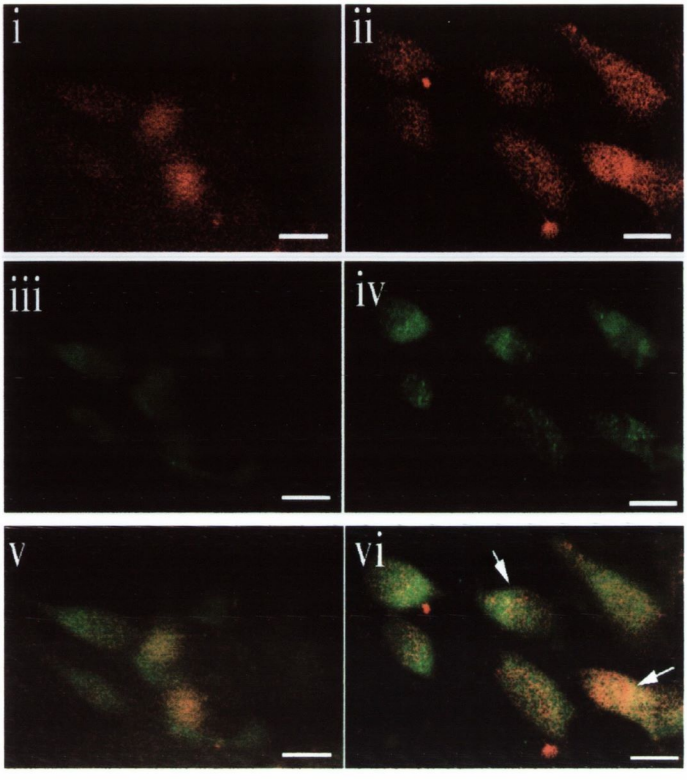

Figure 5.7 Aβ increases expression of Bax at the lysosome at 6 hr

Fluorescence microscopy was used to visualise the distribution of Bax within cortical neurons following treatment with Aβ (2 μM, 6 hr). Cells were double labelled with the lysosomal-specific marker, Lysotracker Red, and a FITC-labelled Bax antibody.

Lysotracker Red staining represents the distribution of lysosomes in (i) control and (ii) Aβ-treated cells (excitation 579 nm; emission, 599 nm).
Analysis of Bax expression in (iii) control and (iv) Aβ-treated cells (excitation, 490 nm; emission, 520 nm) demonstrated increased expression of Bax in Aβ-treated cells.
Co-localisation analysis of Bax and lysosomes in (v) control and (vi) Aβ-treated cells revealed increased localisation of Bax at the lysosomes in Aβ-treated cells. Arrows indicate regions of co-localisation. Scale bar is 10 μm.

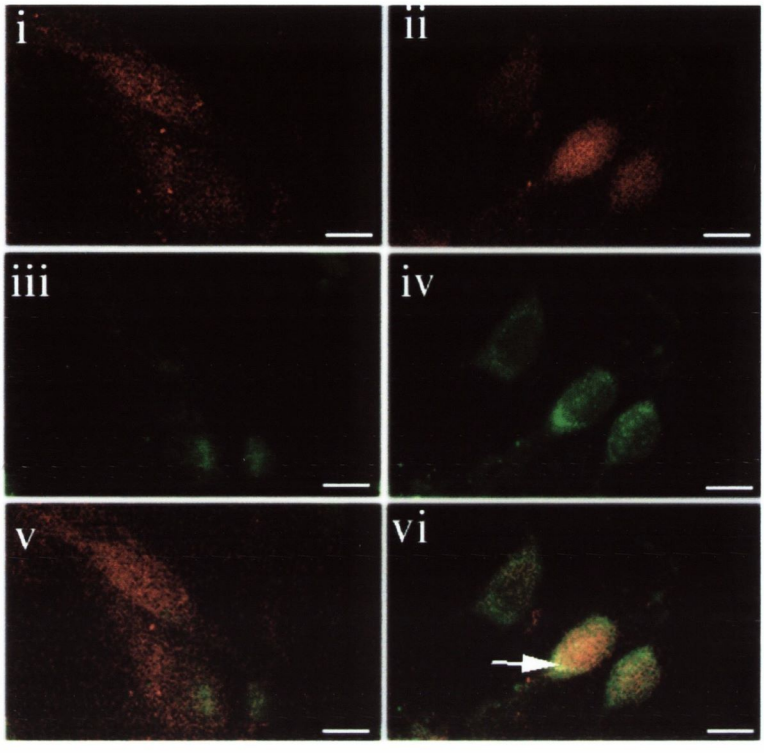

Figure 5.8 Effect of Aβ on phospho-p53^{ser15} expression at the lysosomes at 1 hr

Fluorescence microscopy was used to visualise the distribution of phospho-p53^{ser15} within cortical neurons following treatment with Aβ (2 μM, 1 hr). Cells were double labelled with the lysosomal specific agent, Lysotracker Red, and a FITC-labelled phospho-p53^{ser15} antibody.

Distribution of lysosomes was visualised in (i) control and (ii) Aβ-treated cells (excitation 579 nm; emission, 599 nm).
Analysis of phospho-p53^{ser15} expression in (iii) control and (iv) Aβ-treated cells (excitation, 490 nm; emission, 520 nm) demonstrated increased expression of phospho-p53^{ser15} in Aβ-treated cells.
Co-localisation analysis of phospho-p53^{ser15} and lysosomes in (v) control and (vi) Aβ-treated cells revealed increased localisation of phospho-p53^{ser15} at the lysosomes in Aβ-treated cells. Scale bar is 10 μm.

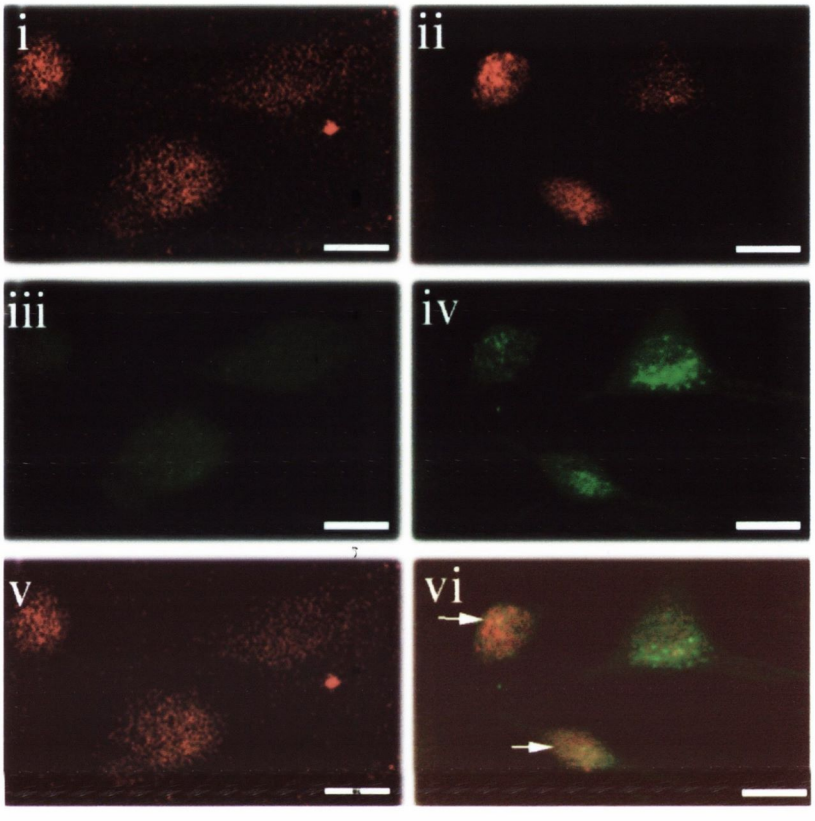

Figure 5.9 Effect of Aβ on phospho-p53^{ser15} expression at the lysosomes at 6 hr

Fluorescence microscopy was used to visualise the distribution of phospho-p53^{ser15} within cortical neurons following treatment with Aβ (2 μM, 6 hr). Cells were double labelled with the lysosomal specific marker, Lysotracker Red, and a FITC-labelled phospho-p53^{ser15} antibody.

Lysosomal Red staining represents the distribution of lysosomes (i) control and (ii) Aβ-treated cells (excitation 579 nm; emission, 599 nm). Analysis of phospho-p53^{ser15} expression in (iii) control and (iv) Aβ-treated cells (excitation, 490 nm; emission, 520 nm) demonstrated increased expression of phospho-p53^{ser15} in Aβ-treated cells.
Co-localisation analysis of phospho-p53^{ser15} and lysosomes in (v) control and (vi) Aβ-treated cells revealed increased localisation of phospho-p53^{ser15} at the lysosomes in Aβ-treated cells. Scale bar is 10 μm.

and Aβ-treated cells at 1 hr, following loading with Lysotracker Red. Figure 5.8(iii) represents p53 immunostaining in control cells and this p53 immunofluorescence was increased in Aβ-treated cells at 1 hr (Figure 5.8(iv)). Furthermore, in Aβ-treated cells increased co-localisation of phospho-p53^{ser15} expression with lysosomes was observed at 1 hr (Figure 5.8(vi)).

Figure 5.9(i) and (ii) demonstrates the location of lysosomes in control and Aβ-treated cells at 6 hr, following loading with Lysotracker Red. Figure 5.9(iii) represents p53 immunostaining in control cells and this p53 immunofluorescence was increased in Aβ-treated cells at 6 hr (Figure 5.9(iv)). Furthermore, in Aβ-treated cells increased co-localisation of phospho-p53^{ser15} expression with mitochondria was observed at 6 hr (Figure 5.9(vi)). This result indicates that the Aβ-mediated increase in phospho-p53^{ser15} expression is coupled with increased association of phospho-p53^{ser15} at the lysosome. Regions remained within the cell where p53 expression did not co-localise with lysosomes and these areas are likely to represent p53 expression at mitochondrial membranes, as demonstrated in Figure 5.4 and Figure 5.5.

5.2.8 Aβ leads to alterations in lysosomal membrane integrity.

Lysosomal rupture can result in apoptosis of the cell (Li *et al.*, 2000). To assess the effect of Aβ on integrity of lysosomal membranes, cellular location of acridine orange (AO) was assessed. Relocation of AO from lysosomes to the cytosol is indicative of lysosomal disruption (Brunk *et al.*, 1997). Neurons were incubated with AO (5 μg/ml) for 15 min, prior incubation with Aβ (2 μM) for 6 hr and lysosomal integrity was visualised by fluorescence microscopy (Figure 5.10). In control cells, AO can be seen in discrete regions of the cell, representative of localised AO within intact lysosomes. However, in Aβ-treated cells, the distribution of AO is mainly cytosolic, with a diffuse pattern of staining, indicating lysosomal leakage. This result suggests that Aβ may disrupt the integrity of lysosomes leading to release of AO from lysosomes.

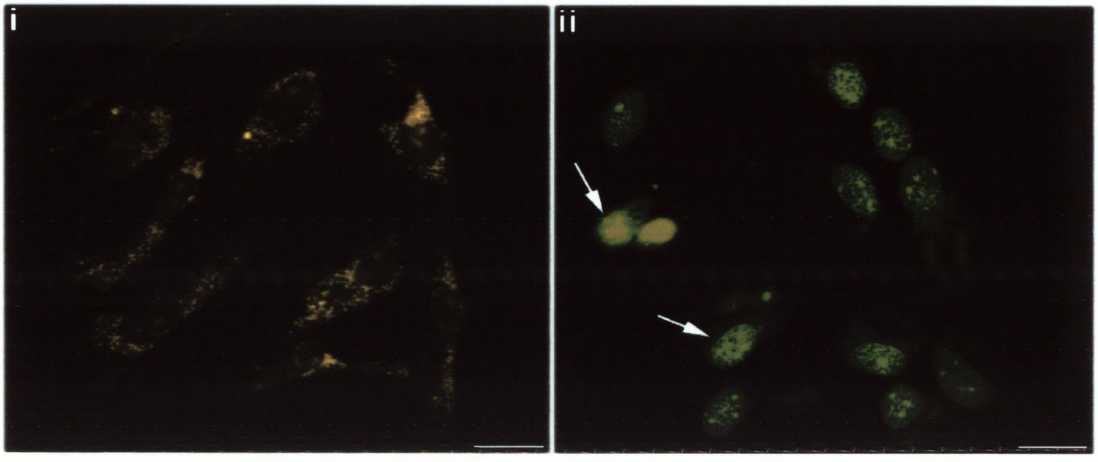

Figure 5.10 Effect of Aβ on lysosomal membrane integrity

Neurons were exposed to acridine orange (AO; 5 μg/ml) for 15 min prior to incubation with Aβ for 6 hr. Relocation of AO from the lysosomes to cytosol was assessed.
i. In control cells AO displayed an orange fluorescence and was localised in discrete punctate compartments within the cell reflecting lysosomal distribution of AO.
ii. Exposure to Aβ for 6 hr resulted in the disappearance of AO orange fluorescence and an increase in diffuse cytosolic fluorescence. Scale bar is 10 μm.

5.2.9 Aβ-mediated increase in cathepsin-L activity is p53 dependent

To further clarify the role of p53 in Aβ-mediated lysosomal disruption, activity of the lysosomal protease, cathepsin-L, was assessed in cells treated with the p53-inhibitor, pifithrin-α. Previous studies from this laboratory have shown that Aβ significantly increases cathepsin-L activity within 6 hr of treatment (Boland and Campbell, 2003b). Cells were treated with pifithrin-α for 1 hr, prior to treatment with Aβ for 6 hr and activity of cathepsin-L was assessed by measuring cleavage of a fluorogenic cathepsin-L substrate. Figure 5.11 demonstrates that Aβ significantly increased activity of cytosolic cathepsin-L from 29.2 ± 2.1 pmole AFC produced/mg protein/min (mean ± SEM) to 40 ± 3.6 pmole AFC produced/mg protein/min ($p<0.05$, ANOVA, n=10). Pifithrin-α alone had no effect on cathepsin-L activity (25.3 ± 4.9 pmole AFC produced/mg protein/min, n=6), but it abolished the Aβ-mediated increase in cathepsin-L activity, where cathepsin-L activity was 20.77 ± 3.9 (n=6) in cells which were co-incubated with Aβ + pifithrin-α. This result provides further evidence that p53 impacts on the lysosomes, in Aβ-treated cells.

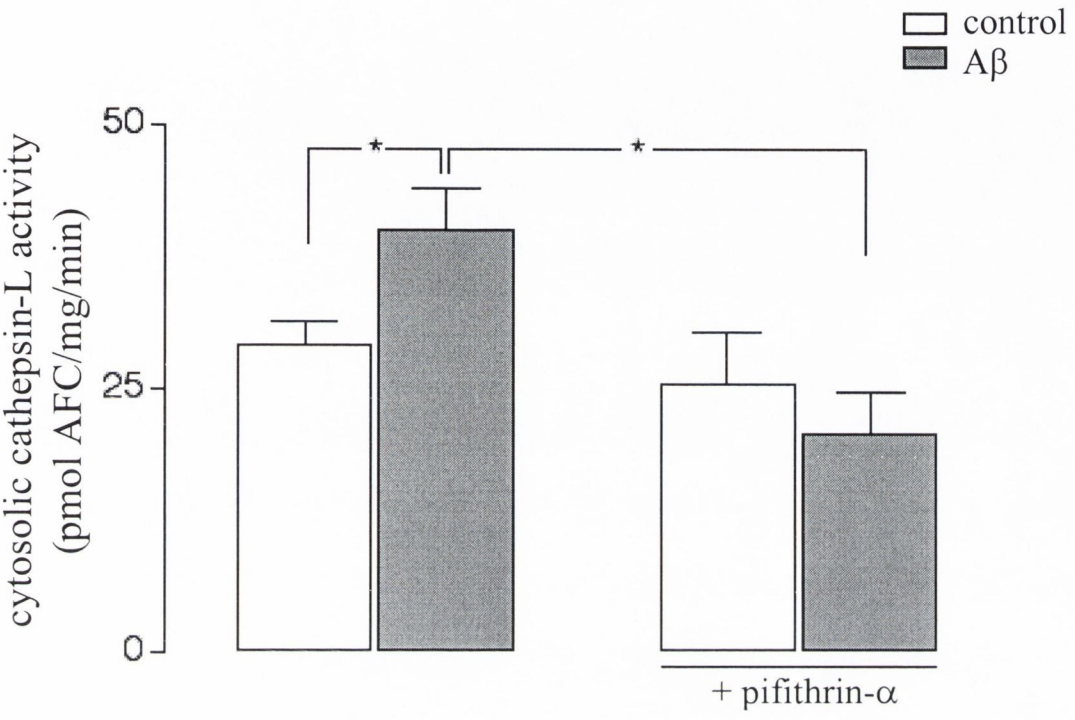

Figure 5.11 Aβ-mediated increase in cathepsin-L activity is p53-dependent

Cortical neurons were treated with pifithrin-α inhibitor (100 nM) in the presence or absence of Aβ (2 μM) for 6 hr and cathepsin-L activity was measured using the fluorogenic substrate Arg-Phe-AFC. Aβ significantly increased cathepsin-L activity at 6 hr. In the presence of pifithrin-α, the Aβ-mediated increase in cathepsin-L activity was significantly reduced. Results are expressed as mean ± SEM for 6 observations, * $p<0.05$.

5.3 Discussion

Experimental work carried out in this chapter investigated the effect of Aβ on the subcellular distribution of the cell cycle regulatory protein, p53, and the pro-apoptotic protein, Bax. The data provide evidence for Aβ promoting Bax translocation to lysosomal membranes, in addition to mitochondrial membranes. Analysis of cellular location of phospho-p53^{ser15} protein expression revealed increased expression of phospho-p53^{ser15} at both mitochondrial and lysosomal membranes. The time-course for phospho-p53^{ser15} and Bax association with lysosomal membranes coincided with the Aβ-mediated reduction in integrity of the lysosomal membrane and increase in cytosolic activity of the lysosomal protease, cathepsin-L. The proclivity of Aβ to increase activity of cathepsin-L was abolished by the p53 inhibitor, pifithrin-α, demonstrating that the Aβ-mediated increase in cathepsin-L activity was p53-dependent. These results indicate that p53 and Bax can associate with lysosomes, as well as with mitochondria, in cultured cortical neurons, suggesting that Bax and p53 may play an important role in the regulation of release of lysosomal and mitochondrial constituents during the neurodegenerative process. The observation that the Aβ-mediated increase in activity of cathepsin-L within the cytosol was p53 dependent suggests an interplay between p53 and the release of lysosomal proteases. Thus, p53 may have an important role in the lysosomal branch of the apoptotic pathway.

Bax is a member of the Bcl-2 family of proteins that can induce (Bax, Bid) or inhibit (Bcl-2, Bcl-xl), apoptosis by virtue of their ability to associate with the mitochondrial membrane and induce or block cytochrome-*c* release, respectively. In its inactive state, Bax normally resides in the cytosol of the cell. Upon activation Bax translocates to the mitochondria, where it can facilitate release of cytochrome *c* through formation of pores in the outer mitochondrial membrane (Gao and Dou, 2000). $A\beta_{1-40}$ has recently been reported to increase mitochondrial expression of Bax in the CA1 region of the hippocampus (Minogue *et al.*, 2003). In order to determine whether Aβ leads to translocation of Bax from the cytosol to mitochondria in Aβ-treated cultured cortical neurons, expression of Bax protein was assessed in cytosolic and

mitochondrial fractions by western immunoblot. A significant decrease in cytosolic Bax expression was observed at 6 hour post Aβ-treatment. This was coupled with an increase in Bax expression in mitochondrial fractions. However, the Aβ-mediated increase in mitochondrial expression of Bax failed to reach statistical significance. To further examine the relocalisation of Bax following treatment with Aβ, immunofluorescence microscopy was employed. This technique represents a more sensitive approach with which to monitor protein expression in a cell monolayer. Expression of Bax was monitored in association with the fluorescent mitochondrial marker, Mitotracker Red. Increased expression of Bax occurred at the mitochondria in Aβ-treated cells. The observation that regions remained within the cell where Bax expression did not co-localise with mitochondria, coupled with the demonstrated increase in total expression of Bax in Aβ-treated cells, suggested that Aβ may evoke translocation of Bax to other intracellular organelles.

The previous chapter demonstrated an increased expression of p53 protein in Aβ-treated cortical neurons at 1 hour post Aβ-treatment. The increased p53 expression occurred as a result of stabilisation of p53 at residue serine-15. In this part of the study, the cellular location of phospho-p53^{ser15} in Aβ-treated cells was investigated. Phospho-p53 ^{ser15} expression was found to associate with the mitochondrial membrane at 1 hour and 6 hour following Aβ-treatment. This provides evidence that along with mediating transcriptional induction of Bax (see chapter 4), phospho-p53^{ser15} may play a direct role in regulation of mitochondrial membrane stability in Aβ-treated neuronal cells. In support for this, p53 has previously been demonstrated to traffic to mitochondria following DNA damage (Marchenko *et al.*, 2000). As observed in co-localisation analysis of Bax expression with mitochondria, regions remained within the cell where phospho-p53^{ser15} expression did not co-localise with mitochondria and this reflects the association of phospho-p53 with other subcellular compartments.

A key event in the apoptotic cascade is the translocation of mitochondrial cytochrome *c* into the cytosol. The present study demonstrates an Aβ-mediated increase in cytosolic cytochrome *c* expression at 6 hr. The release of cytochrome *c* to the cytosol is normally regulated by members of the Bcl family of proteins (Zörnig *et*

al., 2001). The present study demonstrates that $A\beta_{1-40}$ promotes the association of Bax with mitochondria, it is therefore likely that this contributes to the Aβ-mediated release of cytochrome *c* observed within a similar time frame. In addition, an association of p53 with the mitochondrial membrane has previously been demonstrated to precede cytochrome *c* release and caspase-3 activation following DNA damage (Marchenko *et al.*, 2000). This represents an alternative mechanism whereby mitochondrial membrane stability may be altered as a consequence of p53 association with the mitochondrial membrane, resulting in release of mitochondrial cytochrome *c* to the cytosol.

There is increasing evidence to suggest that lysosomes are involved in the cell death cascade (Zhao *et al.*, 2001; Wang, 2000). Therefore, in this aspect of the study the cellular location of pro-apoptotic Bax in relation to the lysosomes was investigated. To this end the lysosomal specific marker, Lysotracker Red, was employed. Lysotracker probes are fluorescent acidotropic probes for labelling and tracing acidic organelles in live and fixed cells. They are freely permeant to cell membranes and typically have high selectivity for acidic organelles such as lysosomes and therefore concentrate in these organelles. Following a 6 hour Aβ-treatment, expression of Bax was found to associate with lysosomes. Previous results from this laboratory have demonstrated that $A\beta_{1-40}$ promotes release of cathepsin-L from the lysosome (Boland and Campbell, 2003b). It is therefore possible that lysosomal-associated Bax plays a role in destabilising the lysosomal membrane to promote cathepsin release, in a similar fashion to the role of Bax in inducing cytochrome *c* release from the mitochondria, however this remains to be established. In support for this idea an increase in Bax expression correlates with deficits in lysosomal integrity during glioblastoma apoptosis (Chen *et al.*, 2001). In addition, there is an increasing body of evidence to suggest a functional interaction between the Bcl family of proteins and lysosomes. Phosphorylation of Bcl-2 has been demonstrated to block oxidative stress-induced apoptosis by stabilising lysosomes (Zhao *et al.*, 2001) and cleavage of bcl-2 by the calcium-dependent protease, calpain, is thought to be another likely mechanism for disruption of lysosomal membrane integrity (Wang, 2000) Thus, Bcl proteins may be intricately linked with lysosomal stability and the results from this study demonstrating

that Aβ increases Bax association with lysosomes suggests that Bax may play a key role in Aβ-mediated alterations in lysosomal membrane integrity.

Downstream of lysosomal membrane disruption, cathepsins have been shown to interact with the Bcl family of proteins to promote apoptosis. In a cell free system, the pro-apoptotic Bcl family member, Bid, was found to be cleaved in the presence of lysosomal proteases (Stoka *et al.*, 2001). Cleaved Bid then went on to induce cytochrome *c* release from the mitochondria. In addition, cathepsin D has been demonstrated to trigger Bax activation in human T lymphocytes, with resulting apoptosis (Bidere *et al.*, 2003). These findings highlight the complexity of the relationship between lysosomes and the Bcl family of proteins. In some systems the Bcl family acts to regulate lysosomal stability (Zhao *et al.*, 2001; Chen *et al.*, 2001) while in other systems following disruption of lysosomal membrane integrity, lysosomal proteases regulate the Bcl proteins in the cytosol (Stoka *et al.*, 2001; Bidere *et al.*, 2003). The role of Bcl proteins in lysosomal-mediated apoptosis is therefore likely to be cell type specific as well as being dependent on the nature of the apoptotic stimulus. The association of Bax with lysosomal membranes in Aβ-treated cortical neurons is a novel finding which warrants further investigation in order to clarify the exact nature of the interactions between Bcl proteins and lysosomal membranes in Aβ-mediated neuronal apoptosis.

p53 has previously been reported to play a role in initiation of lysosomal destabilisation (Yuan *et al.*, 2002) with ensuing apoptosis. Therefore it was appropriate to investigate whether phospho-p53^{ser15} might be redirected to the lysosome following treatment with Aβ. Increased expression of phospho-p53^{ser15} with lysosomes was evident at 1 hour and 6 hour post Aβ-treatment. An important question arising from the increased expression of p53 and Bax with lysosomes is: what are the downstream consequences of association of these proteins with the lysosomes? In an effort to address this question the integrity of lysosomal membranes was assessed.

Lysosomal rupture has been observed to be an early event preceding apoptosis caused by a variety of agents including oxidative stress and photo-oxidative damage (Brunk and Svenson, 1999; Li *et al.*, 2000). Furthermore, lysosomal proteases have been shown to activate cytosolic caspases including caspase-8 and caspase-3 (Ishisaka

et al., 1999) indicating that lysosomal proteases are released into the cytosol in response to apoptotic stimuli. For the present study the AO relocation technique was used in order to examine the integrity of lysosomal membranes. AO is a lysomotropic weak base that can diffuse across cellular membranes and become protonated in acidic environments. Once protonated it is prevented from passing through the hydrophobic layers of membranes and therefore becomes trapped and accumulates in acidic organelles such as lysosomes and thus labels them. It is generally accepted that leakage of AO from lysosomes to the cytosol is representative of decreased lysosomal membrane integrity (Li *et al.*, 2000; Yuan *et al.*, 2002). The results of the present study demonstrated that in the control situation AO fluorescence exhibited a punctate distribution, reflective of a lysosomal distribution of AO. In contrast, a diffuse pattern of AO fluorescence was observed in Aβ-treated cells, reflecting leakage of the dye from the lysosomal compartment.

Previous work carried out in this laboratory has demonstrated that $A\beta_{1\text{-}40}$ promotes a time- and dose-dependent release of the lysosomal protease, cathepsin-L, into the cytosol, with increased cytosolic activity of cathepsin-L being induced 6 hour post Aβ-treatment (Boland and Campbell, 2003b). It was also demonstrated in that study that Aβ-mediated neurodegenerative changes were cathepsin-L-dependent. The time-scale of increased cathepsin-L activity was consistent with the time frame for phospho-$p53^{ser15}$ association with the lysosomal membrane observed in the present study, therefore the involvement of p53 in the Aβ-mediated increase in cathepsin-L activity was investigated. In the previous chapter the p53 inhibitor, pifithrin-α, was demonstrated to abrogate the Aβ-induced increase in Bax expression. There is also evidence that pifithrin-α can inhibit phosphorylation of p53 at serine-15 (Lin *et al.*, 2002) but whether pifithrin-α abolished Aβ-induced phosphorylation of p53 at serine-15 was not confirmed for this study. The Aβ-mediated increase in cathepsin-L activity at 6 hour was abolished in pifithrin-α treated cells, indicating that the Aβ-mediated increase in cathepsin-L activity is p53-dependent. This result supports the hypothesis that p53 impacts on the lysosomal system and is responsible for mediating an upregulation in activity of the lysosomal protease, cathepsin-L.

Whether p53 and Bax act in a synergistic manner or have a separate function in regulation of lysosomal membrane integrity remains to be clarified and further experiments will need to be carried out to resolve the exact mechanism by which these proteins control lysosomal membrane integrity. It is possible that Bax may mediate release of cathepsins from the lysosomes by formation of pores in the lysosomal membrane, in a similar fashion to which Bax facilitates release of cytochrome *c* from the mitochondria (Zörnig *et al.*, 2001). The effect of Aβ on the pore forming ability of Bax was not addressed in the present study but it merits consideration for future experimentation. In addition, given that Aβ alters the integrity of lysosomal membranes, the effect of p53 and Bax on lysosomal membrane proteins such as LAMP1 and LAMP2 (lysosomal associated membrane proteins) warrants investigation. These proteins are extensively glycosylated to protect them from intracellular proteolysis (Kundra and Kornfeld, 1999). The loss of these proteins in a double knock out transgenic model has been reported to lead to embryonic lethality (Andrejewski *et al.*, 1999), demonstrating the importance of these proteins in lysosomal stability. A p53 or Bax mediated alteration in integrity of LAMP may serve as a trigger for lysosomal cathepsin release.

There is a good deal of evidence in the literature indicating that cross talk occurs between lysosomes and mitochondria during apoptosis. Several reports have suggested that lysosomal membrane disruption precedes mitochondrial membrane disruption in apoptosis (Boya *et al.*, 2003; Yuan *et al.*, 2002). However, the extent of mitochondrial input in lysosomal-mediated cell death is subject to debate. While Neuzil *et al* (1999) report that α-tocopheryl-mediated apoptosis in Jurkat T cells requires both lysosomal and mitochondrial destabilisation, Li *et al* (2000) report that lysosomal mediated cell death in a macrophage cell line, which was exposed to the lysosomtrophic agent O-methyl-serine dodecylamide hydrochloride (MSDH), can occur either indirectly via mitochondrial attack by lysosomal proteases or can occur directly by lysosomal protease activation of caspase-3. In contrast, Hishita *et al* (2001) report that lysosomal dependent death in a myelomonocytoid cell line does not involve mitochondria. It is therefore likely that the involvement of mitochondria in lysosomal mediated apoptosis is cell type specific. The observations from the present study, that

Aβ-mediated release of cytochrome *c* from the mitochondria, and release of cathepsin-L from lysosomes at 6 hour post Aβ-treatment is concomitant with the association of phospho-p53 and Bax with the mitochondria and the lysosomes indicates that there is at least some degree of cross-talk occurring in this system. Further experiments will need to be carried out to clarify the importance of cross talk between mitochondria and lysosomes in Aβ-treated cells and to determine whether disruption of lysosomal membrane integrity occurs upstream of mitochondria membrane permeabilisation.

An alteration in neuronal endosomal-lysosomal systems is an early event in AD (Cataldo *et al.*, 1995). Furthermore, lysosomal leakage is thought to be the earliest detectable event during apoptosis induced by lysomotrophic agents. This corroborates the work presented in this thesis demonstrating an early association of the apoptotic effectors p53 and Bax with the lysosomes following Aβ-treatment. Consistent with the idea that $A\beta_{1-40}$-mediated neuronal cell death may involve lysosomes, a number of studies have demonstrated that $A\beta_{1-42}$ promotes lysosomal leakage and subsequent apoptosis *in vitro* (Yang *et al.*, 1998; Ji *et al.*, 2002). Therefore, the cellular mechanisms underlying the role of lysosomal components in Aβ-mediated cell death warrant further investigation, as intervention at an early stage would have important implications for disease progression of AD. It is important to note that AD is not the only neurodegenerative disease featuring lysosomal instability. For example, lysosomal dysfunction has been shown to accompany alpha-synuclein aggregation in a mouse model of Parkinson's Disease (Meredith *et al.*, 2001). In Huntington's disease, abnormal protein deposition has also been linked to lysosomal dysfunction (Bahr and Bendiske, 2002. Therefore a greater understanding of the signalling pathways involved in lysosomal dysfunction will be of benefit to a variety of neurodegenerative conditions.

In conclusion, the results presented in this chapter demonstrate that Aβ leads to tranlocation of Bax from the cytosol in cultured cortical neurons. The reduction in cytosolic Bax expression correlated with an association of Bax with both the mitochondrial and lysosomal membrane. The observation that Bax associates with the lysosome is a novel discovery which has not been previously documented in neuronal cells. Phospho-$p53^{ser15}$ was also found to associate with both mitochondrial and

lysosomal membranes in Aβ-treated cells. The association of phospho-p53 with lysosomal membranes correlated with Aβ-mediated alterations in lysosomal membrane integrity. In addition, application of pifithrin-α, an inhibitor of p53-induced transcriptional activation, attenuated the Aβ-mediated increase in cathepsin-L activity, providing further evidence that p53 is involved in regulation of lysosomes. These results indicate a possible mechanism whereby p53 and Bax contribute to a lysosomal and mitochondrial branch of the apoptotic pathway in Aβ-treated cultured cortical neurons.

Chapter 6

Effect of Aβ on the L-type Ca2+ channel in cultured cortical neurons

6.1 Introduction

Disruption of intracellular neuronal calcium (Ca^{2+}) homeostasis is thought to be an underlying mechanism contributing to AD pathology (Mattson *et al*, 1992; Mattson *et al* 1993a). Ca^{2+} is an important intracellular messenger in the brain, being essential for neuronal development and synaptic transmission and plasticity (Mattson *et al*, 1993b). Intracellular free calcium levels, $[Ca^{2+}]_i$, are usually maintained at approximately 100 nM and neurons which cannot maintain the intracellular Ca^{2+} levels within certain limits are rendered vulnerable to excitotoxicity and cell death (Mattson *et al.*, 1993a). Persuasive evidence indicates that aggregated Aβ mediates its neurotoxic effects by dysregulation of Ca^{2+} homeostasis. Mattson *et al.*, (1992) and Ueda *et al* (1997) demonstrated that exposure of human cortical cell cultures to $A\beta_{1-42}$ and $A\beta_{25-35}$ destabilises Ca^{2+} homeostasis. Chronic exposure to Aβ results in an elevation of resting $[Ca^{2+}]_i$ which is directly related to the aggregation state of the peptide (Mattson *et al.*, 1992). In addition, previous studies carried out in this laboratory have demonstrated that acute application of $A\beta_{1-40}$ increases $^{45}Ca^{2+}$ influx resulting in increased $[Ca^{2+}]_i$ in rat cortical synaptosomes and cultured cortical neurons (MacManus *et al.*, 2000).

Aβ can destabilise intracellular Ca^{2+} balance via two pathways, either by enhancing extracellular Ca^{2+} influx, or by triggering intracellular store release of Ca^{2+} from organelles such as the mitochondria, endoplasmic reticulum, or lysosome (He *et al.*, 2002). Enhanced extracellular Ca^{2+} influx is postulated to occur due to the Aβ-mediated formation of Ca^{2+} permeable channels on the cell membrane (Arispe *et al.*, 1994; Sanderson *et al.*, 1997) or by Aβ-mediated modulation of voltage-dependent Ca^{2+} channels (VDCCs; Ueda *et al.*, 1997; MacManus *et al.*, 2000) or ligand-gated Ca^{2+} channels (Zamani and Allen, 2001). A previous report from this laboratory has demonstrated that the $A\beta_{1-40}$ -mediated increase in $^{45}Ca^{2+}$ influx in rat cortical synaptosomes occurred via activation of the L- and N-type of VDCC (MacManus *et al.*, 2000). In addition, $A\beta_{1-40}$ and $A\beta_{25-35}$ have both been demonstrated to augment L-type VDCCs in PC12 cells (Green and Peers, 2001). Similarly, $A\beta_{25-35}$-mediated neurotoxicity was found to be attenuated in cultured neurons by application of the L-type Ca^{2+} channel blocker, nimodipine, and in that study the N-type Ca^{2+} channel was

demonstrated not to be involved (Ueda *et al.*, 1997). The variation in reports seems to be due to differences in cell type and drug concentration used, therefore more studies need to be carried out to clarify the extent of the involvement of Aβ in the regulation of VDCCs.

Intracellular free Ca^{2+} serves as a second messenger and regulates a wide variety of cellular processes including cell cycle control and signal transduction (Bedridge *et al.*, 2003). The MAPKs, which play crucial roles in signal transduction from the cell surface to the nuclear and cytoplasmic effectors, have been demonstrated to be regulated by Ca^{2+} (Nozaki *et al.*, 2001). Ca^{2+} has been demonstrated to mediate activation of the stress-activated protein kinase, JNK, in mouse cortical cell cultures (Ko *et al.*, 1998) as well as in rat fibroblasts (Mitchell *et al.*, 1995). It is therefore reasonable to propose that one method by which Aβ might exert its effects is through Ca^{2+}-mediated activation of JNK. In addition, disruption of Ca^{2+} homeostasis has been proposed to be a critical event in apoptosis and has been demonstrated as a mechanism for Aβ-mediated neuronal cell death in a variety of studies (Mattson *et al.*, 1992; Ekinci *et al.*, 2000 Yagami *et al.*, 2002). The discovery that the Bcl-2 family of proteins can modulate Ca^{2+} compartmentalisation within the cell has provided further support for the link between Ca^{2+} and apoptosis (Orrenius *et al.*, 2003).

The experimental work carried out in this chapter aimed to clarify the role of the L-type VDCC in Aβ-mediated neuronal apoptosis. To this end the selective L-type Ca^{2+} channel blocker, nicardipine, was employed. Intracellular Ca^{2+} concentration was assessed in Aβ-treated cortical neurons by spectrophotometry using the Ca^{2+} indicator dye, Fura-2AM. The involvement of the L-type Ca^{2+} channel in Aβ-mediated activation of JNK, p53, and cathepsin-L was investigated. In addition the role of the L-type Ca^{2+} channel in the Aβ-mediated regulation of components of the apoptotic cascade, namely caspase-3 activation and DNA fragmentation, was examined.

6.2 Results

6.2.1 Aβ increases $[Ca^{2+}]_i$ in dissociated suspension cells and this increase in $[Ca^{2+}]_i$ is attenuated by the L-type $[Ca^{2+}]_i$ blocker, nicardipine.

Since Aβ has been shown to alter Ca^{2+} homeostasis (MacManus *et al.*, 2000) the effect of Aβ on intracellular Ca^{2+} concentration, $[Ca^{2+}]_i$, was determined in suspensions of dissociated neuronal cells. Cells were treated with Aβ (2 μM) for 1 hr and 6 hr. Cells were then loaded with Fura-2AM and $[Ca^{2+}]_i$ was recorded on a Cairn spectrophotometer (Figure 6.1). Following a 1 hr incubation with Aβ, $[Ca^{2+}]_i$ was increased from 440 ± 82 nM (mean ± SEM) to 687 ± 99 nM (n=8), but not significantly so. However, following a 6 hr exposure to Aβ, $[Ca^{2+}]_i$ was significantly increased from 449 ± 88 nM to 883 ± 166 nM ($p<0.05$, student's t-test, n=8). The role of the L-type Ca^{2+} channel in the Aβ-mediated increase in $[Ca^{2+}]_i$ was investigated using the L-type Ca^{2+} channel blocker, nicardipine. In cells treated with nicardipine (0.5 μM) for 30 min, prior to treatment with Aβ, Aβ failed to increase $[Ca^{2+}]_i$ concentration; where $[Ca^{2+}]_i$ was 402 ± 64 nM at 1 hr and 545 ± 89 nM at 6 hr, in cells which were co-incubated with Aβ + nicardipine ($p<0.05$, one way ANOVA, n=10). This result indicates a role for the L-type Ca^{2+} channel in the Aβ-mediated increase in $[Ca^{2+}]_i$.

6.2.2 Aβ mediated increase in phospho-JNK1 is attenuated in cells treated with the L-type Ca^{2+}-channel blocker, nicardipine

To establish whether the L-type Ca^{2+} channel plays a role in the Aβ-mediated activation of JNK1 observed at 1 hr (see Figure 3.2), cells were treated with the L-type Ca^{2+} channel blocker, nicardipine (5 μM) for 30 min, prior to treatment with Aβ (2 μM) for 1 hr. Expression of phospho-JNK1 was assessed by western immunoblot using an anti-active JNK antibody. Figure 6.2 demonstrates that Aβ induced a significant increase in phospho-JNK1 expression at 1 hr. Thus, phospho-JNK1 expression in control cells was 1.064 ± 0.019 (mean band width ± SEM;

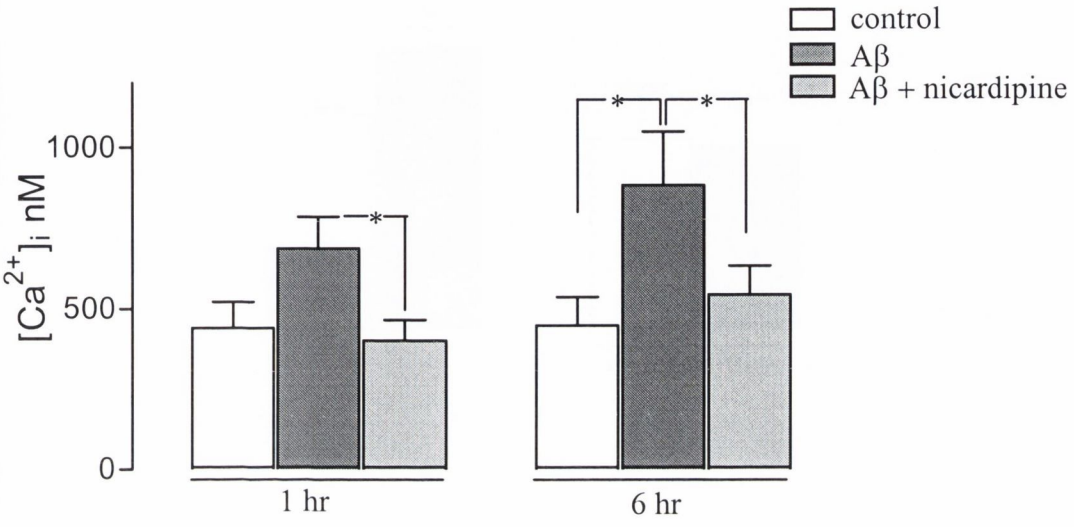

Figure 6.1 Effect of the L-type Ca $^{2+}$ channel antagonist, nicardipine, on the Aβ-mediated increase in $[Ca^{2+}]_i$

Cortical neurons were treated with the L-type Ca^{2+} channel blocker, nicardipine (0.5 μM) in the presence or absence of Aβ (2 μM) for 1 hr or 6 hr. $[Ca^{2+}]_i$ was measured in Fura-2AM (2 μM) loaded cells and recorded on a Cairn spectrophotometer.

Aβ increased mean basal $[Ca^{2+}]_i$ at 1 hr but not significantly so. The Aβ-mediated increase in mean basal $[Ca^{2+}]_i$ at 1 hr was significantly reduced in nicardipine treated cells. Results are expressed as mean SEM for 8 observation, * $p<0.05$.

Aβ significantly increased mean basal $[Ca^{2+}]_i$ at 6 hr. The Aβ-mediated increase in mean basal $[Ca^{2+}]_i$ at 6 hr was significantly reduced in nicardipine-treated cells. Results are expressed as mean SEM for 8 observations, * $p<0.05$.

arbitrary units) and this was increased to 1.236 ± 0.056 by Aβ ($p<0.05$, one-way ANOVA, n=12). Nicardipine alone had no effect on phospho-JNK1 expression (1.000 ± 0.169, n=7), but it abolished the Aβ-mediated increase in phospho-JNK1 expression; where expression of phospho-JNK1 was 0.979 ± 0.126 (n=7) in cells which were co-treated with Aβ + nicardipine. This result is suggestive of a role for the L-type Ca^{2+} channel in Aβ-induced increase in phospho-JNK1 expression. A sample immunoblot illustrating the effect of nicardipine on the Aβ-mediated increase in expression of phospho-JNK1 is shown in Figure 6.2B.

6.2.3 Aβ mediated increase in phospho-$p53^{ser15}$ is attenuated in cells treated with the L-type Ca^{2+}-channel blocker, nicardipine

Since the Aβ-mediated increase in phospho-$p53^{ser15}$ expression at 1 hr was found to be JNK1 dependent (see Figure 4.5), the role of the L-type Ca^{2+} channel in this component of the signalling pathway was investigated. Cells were treated with the L-type Ca^{2+} channel blocker, nicardipine (0.05 μM), for 30 min prior to treatment with Aβ (2 μM) for 1 hr, and expression of phospho- $p53^{ser15}$ was assessed by western immunoblot using an antibody which recognises p53 phosphorylated at this residue. Figure 6.3 demonstrates that Aβ induced a significant increase in phospho-$p53^{ser15}$ expression at 1 hr. Thus, phospho- $p53^{ser15}$ expression in control cells was 1.017 ± 0.010 (mean band width ± SEM; arbitrary units) and this was increased to 1.306 ± 0.1 by Aβ ($p<0.05$, one-way ANOVA, n=7). Nicardipine alone had no effect on phospho-JNK1 expression (1.011 ± 0.058, n=7), but it abolished the Aβ-mediated increase in phospho-JNK1 expression; where expression of phospho-JNK1 was 0.988 ± 0.08 (n=7) in cells which were co-treated with Aβ + nicardipine. This result indicates that the L-type Ca^{2+} channel plays a role in the Aβ-induced increase in phospho-$p53^{ser15}$ expression. A sample immunoblot illustrating the effect of nicardipine on the Aβ-mediated increase in expression of phospho-$p53^{ser15}$ is shown in Figure 6.3B.

A.

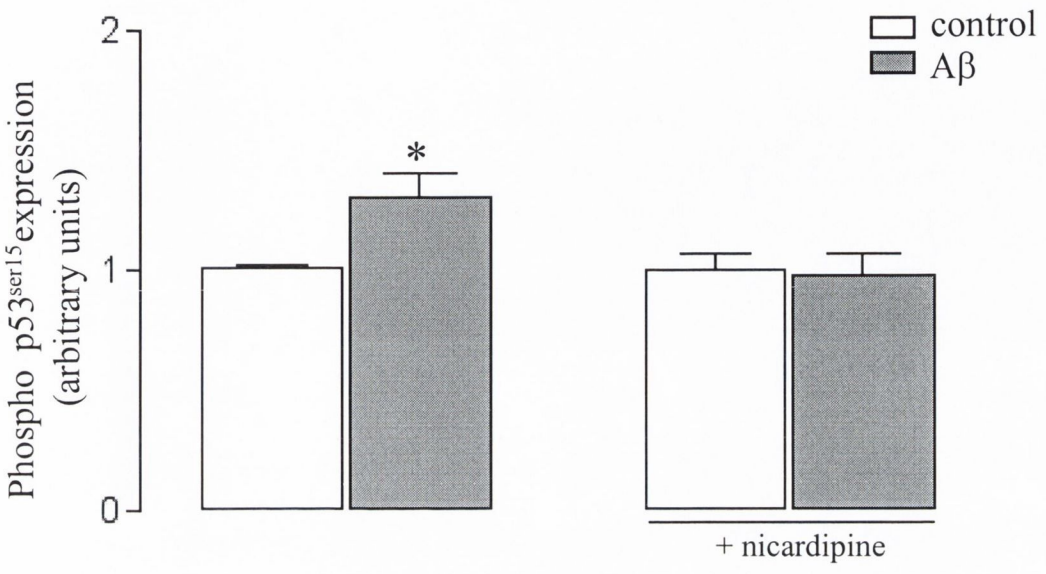

B.

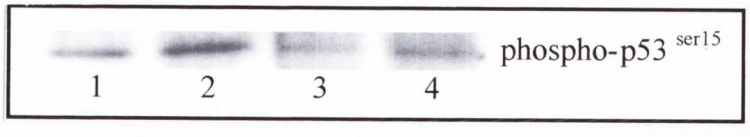

Figure 6.3 The Aβ induced increase in phospho-p53^{ser15} expression is reduced by the L-type Ca^{2+} channel antagonist, nicardipine

A. Cortical neurons were treated with the L-type Ca^{2+} channel blocker nicardipine (0.5 μM) in the presence or absence of Aβ (2 μM) for 1 hr. p53 phosphorylation at residue serine-15 was examined by western immunoblot. Aβ significantly increased phospho-p53^{ser15} protein expression at 1 hr. In the presence of nicardipine the Aβ-mediated increase in phospho-p53^{ser15} expression was reduced. Results are expressed as mean ± SEM for 7 observations, *$p<0.05$.

B. Sample western immunoblot demonstrating levels of phospho-p53 protein expression in control (lane1); Aβ-treated cell (lane2); nicardipine-treated cells (lane 3) and Aβ + nicardipine-treated cells (lane 4).

6.2.4 Aβ-induced increase in cathepsin-L activity is blocked by the L-type Ca^{2+}-channel blocker, nicardipine

Aβ was found to increase cytosolic activity of the lysosomal protease cathepsin-L (Figure 5.11) and since Ca^{2+} is known to play a role in disruption of the lysosomal membrane (Gardella *et al.*, 2001), the role of the L-type Ca^{2+} channel in the Aβ-mediated increase in cathepsin-L activity was assessed. Cells were treated with the L-type Ca^{2+} channel blocker, nicardipine (0.5 μM), for 30 min prior to treatment with Aβ (2 μM) for 6 hr, and activity of cathepsin-L was assessed by measuring cleavage of a fluorogenic cathepsin-L substrate. Figure 6.4 demonstrates that Aβ significantly increased mean basal activity of cathepsin-L at 6 hr from 28.49 ± 1.46 pmol AFC produced/mg protein/min (mean ± SEM) to 39.32 ± 5.46 pmol AFC/mg/min ($p<0.05$; one way ANOVA, n=12). Nicardipine alone had no effect on cathepsin-L activity (31.78 ± 3.24 pmol AFC/mg/min, n=7), but it abolished the Aβ-mediated increase in cathepsin-L activity; where cathepsin-L activity was 33.2 ± 4.08 pmol AFC/mg/min (n=7) in cells which were co-treated with Aβ + nicardipine. This result suggests that Aβ-mediated activation of cathepsin-L involves upstream activation of the L-type Ca^{2+} channel.

6.2.5 Aβ-induced cleavage of caspase-3 is abrogated by the L-type Ca^{2+}-channel blocker, nicardipine

To examine the role of the L-type Ca^{2+} channel in Aβ-mediated induction of the apoptotic cascade, caspase-3 activity was evaluated. Cells were treated with the L-type Ca^{2+} channel blocker, nicardipine (5 μM), for 30 min prior to treatment with Aβ (2 μM) for a further 24 hr, and caspase-3 activity was assessed by immunocytochemistry using an anti-active caspase-3 antibody (Figure 6.5). In control conditions the percentage of cells displaying active caspase-3 immunoreactivity was 19.5 ± 2.41 % (mean ± SEM) and this was significantly increased to 38.7 ± 6.43% in Aβ-treated cells ($p < 0.01$, one-way ANOVA, n=6 coverslips). The percentage of cells

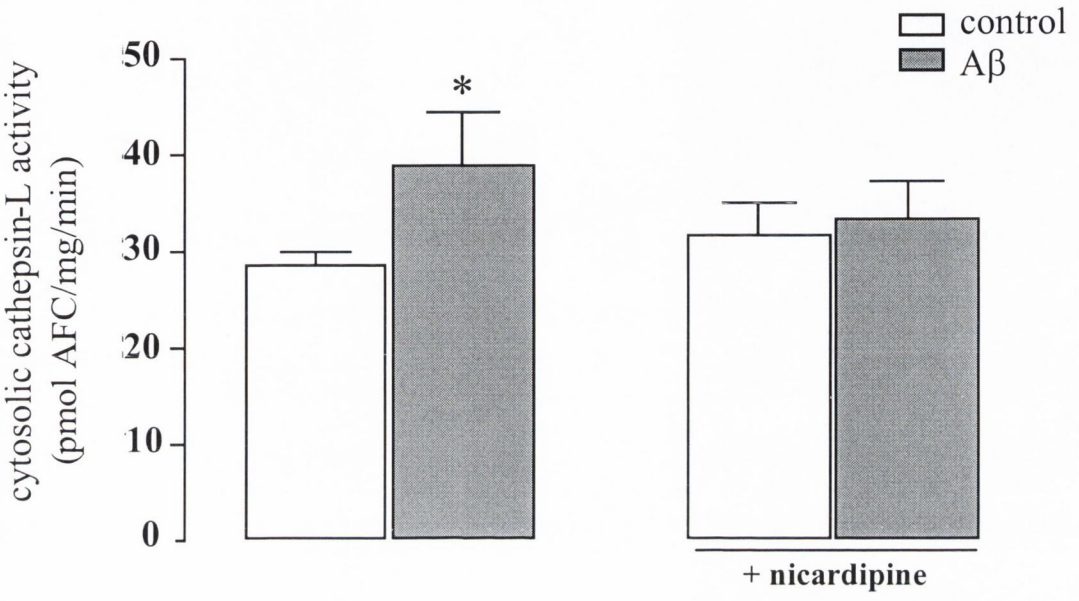

Figure 6.4 Aβ-mediated increase in cathepsin-L activity is blocked by by the L-type Ca^{2+} channel antagonist, nicardipine

Cortical neurons were treated with the L-type Ca^{2+} channel blocker nicardipine (0.5 μM) in the presence or absence of Aβ (2 μM) for 6 hr and cathepsin-L activity was measured using the fluorogenic substrate Arg-Phe-AFC. Aβ significantly increased cathepsin-L activity at 6 hr. In the presence of nicardipine, the Aβ-mediated increase in cathepsin-L activity was abolished. Results are expressed as mean ± SEM for 6 observations, * $p < 0.05$.

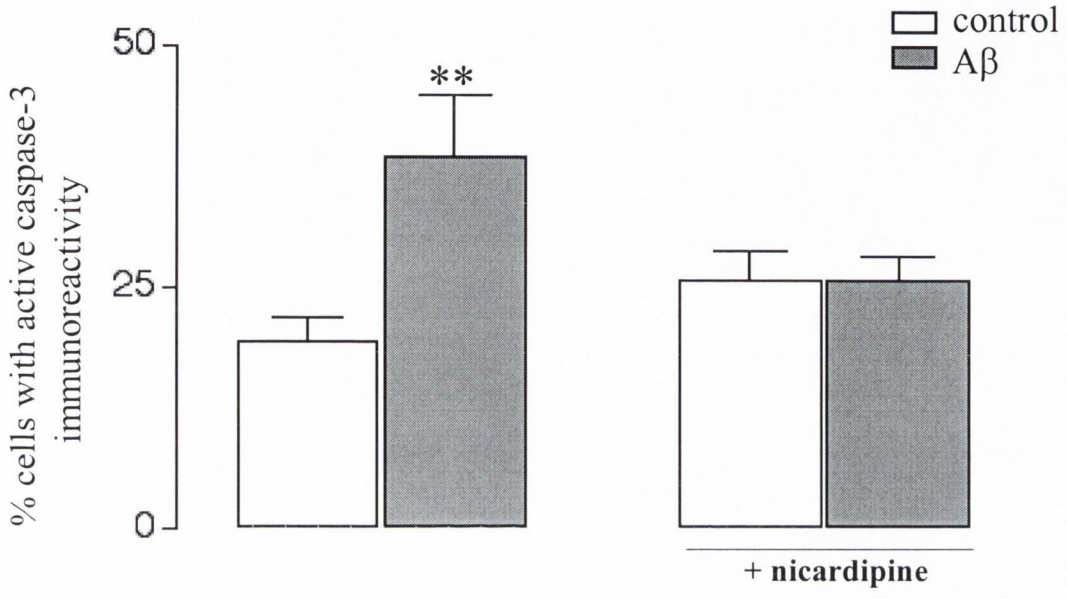

Figure 6.5 Aβ-mediated caspase-3 cleavage is attenuated by the L-type Ca^{2+} channel antagonist, nicardipine

A. Cortical neurons were treated with the L-type Ca^{2+} channel blocker nicardipine (5 μM) in the presence or absence of Aβ (2 μM) for 24 hr and caspase-3 activity was examined by immunocytochemistry. Aβ significantly increased the percentage of cells displaying active caspase-3 immunoreactivity at 24 hr. In the presence of nicardipine, the Aβ-induced increase in caspase-3 activity was abolished. Results are expressed as the mean ± SEM for 6 independent observations,** $P<0.01$.

displaying active-caspase-3 immunoreactivity was 25.75 ± 3.18 % in the presence of nicardipine alone (n=6 coverslips) and 25.75 ± 2.51 % (n=6 coverslips) in cells treated with Aβ + nicardipine. This result indicates that the Aβ-induced activation of caspase-3 is dependent on signalling via the L-type Ca^{2+} channel.

6.2.6 Aβ-induced DNA fragmentation is abrogated by the L-type Ca^{2+}- channel blocker, nicardipine

To further demonstrate the role of the L-type Ca^{2+} channel in Aβ-mediated neuronal apoptosis, levels of DNA fragmentation were assessed in cells treated with the L-type Ca^{2+} channel blocker, nicardipine (2 μM), for 30 min prior to treatment with Aβ for 72 hr (Figure 6.6). TUNEL analysis was carried out to measure the percentage of cells displaying fragmented DNA. Exposure to Aβ (2μM; 72hr) significantly increased the percentage of TUNEL positive cells from 16.92 ± 2.44 % (mean ± SEM) to 36.69 ± 7.22 ($p < 0.01$, one-way ANOVA, n=6 coverslips). The percentage of TUNEL positive cells was 17.55 ± 2.43 % in the presence of the nicardipine alone and 15.32 ± 1.76 % in cells co-treated with Aβ + nicardipine. Thus, nicardipine prevented the Aβ-mediated increase in DNA fragmentation and this result demonstrates the involvement of the L-type Ca^{2+} calcium channel in the Aβ-mediated induction of DNA fragmentation in cortical neurons.

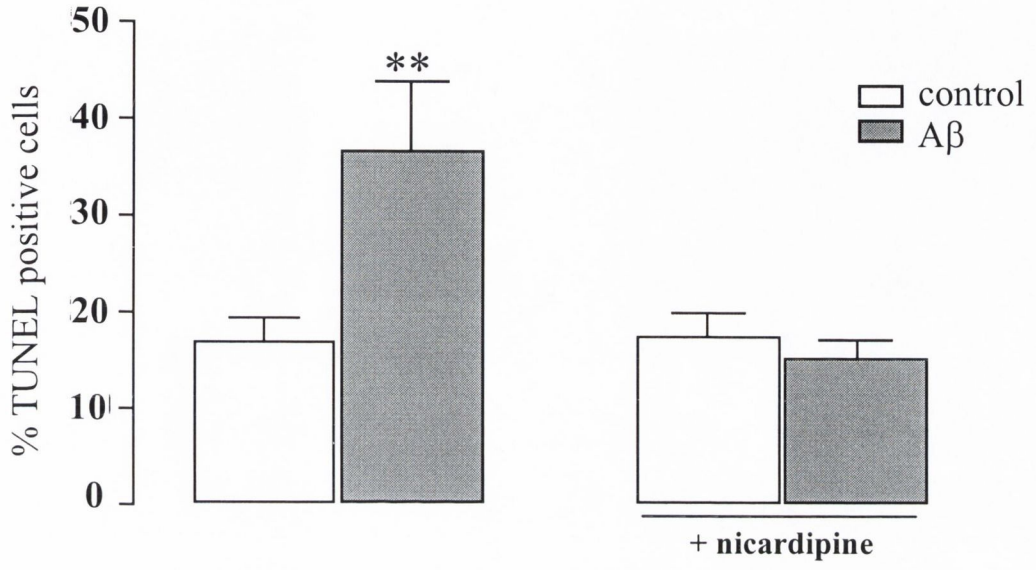

Figure 6.6 Aβ-mediated DNA fragmentation is attenuated by the L-type Ca^{2+} antagonist, nicardipine

Cortical neurons were treated with the L-type Ca^{2+} channel blocker nicardipine (5 μM) in the presence or absence of Aβ (2 μM) for 72 hr and DNA fragmentation was assessed using TUNEL analysis. Aβ significantly increased DNA fragmentation at 72 hr. In the presence of nicardipine the Aβ-induced increase in DNA fragmentation was abolished. Results are the mean ± SEM for 6 independent observations,** $P<0.01$.

6.3 Discussion

The aim of this aspect of the study was to determine the role of the L-type voltage dependent calcium channel (VDCC) in Aβ signalling and induction of neuronal apoptosis. The results obtained demonstrate an increase in $[Ca^{2+}]_i$ in Aβ-treated cells. The observed increase in $[Ca^{2+}]_i$ was attenuated in cells which had been treated with the L-type Ca^{2+} channel blocker, nicardipine. To determine the signalling events which occur downstream of Aβ-mediated Ca^{2+} influx, nicardipine was applied to cells prior to Aβ treatment. Aβ-mediated phosphorylation of JNK1 and p53 was blocked in nicardipine treated cells. Similarly, the Aβ-mediated increase in cytosolic cathepsin-L activity was blocked by nicardipine. This result suggests a link between dysregulation of $[Ca^{2+}]_i$ and disruption of lysosomal membrane stability in Aβ-treated cells. Temporal downstream Aβ-induced events such as cleavage of caspase-3 and DNA fragmentation, were also blocked by nicardipine providing further evidence that disruption of neuronal $[Ca^{2+}]_i$ is integral to Aβ-mediated apoptosis. The L-type Ca^{2+} channel is a key protein involved in the early Aβ effects that ultimately lead to the demise of the cell.

Since disruption of calcium homeostasis is thought to be fundamental in induction of apoptosis (Orrenius *et al.*, 2003), it was of interest in the present study to determine the effect of Aβ on $[Ca^{2+}]_i$ levels in cultured cortical neurons. $[Ca^{2+}]_i$ was quantified by the Ca^{2+} indicator dye Fura2-AM. In dissociated cortical neurons treated with Aβ, $[Ca^{2+}]_i$ was elevated by 35 % at 1 hour and 50 % at 6 hour, although the increase observed at 1 hour failed to reach statistical significance. Treatment with the L-type calcium channel blocker, nicardipine, reduced the Aβ-mediated increase in $[Ca^{2+}]_i$. This result indicates that the Aβ-mediated increase in $[Ca^{2+}]_i$ occurs via the L-type Ca^{2+} channel. While this result is in agreement with other studies (Ueda *et al.*, 1997; Green and Peers, 2001), it disagrees with a previous study from this laboratory which reports that in primary cultured cortical neurons $A\beta_{1-40}$ led to an increase in amplitude of the N- and P-type calcium channels but had little effect on amplitude of the L-type calcium channel (Macmanus *et al.*, 2000). It is important to note that for the present study the quantification of $[Ca^{2+}]_i$ was carried out on freshly dissociated

cortical neurons in suspension. This type of cell preparation is possibly more vulnerable to calcium influx, as neuronal cells in culture normally require adherence to a negatively charged surface for stability. Also, in the previous study carried out by MacManus et al (2000) a lower concentration of 1 μM Aβ was applied to cells; it is possible that the higher concentration of 2 μM Aβ employed in this study leads to activation of the L-type VDCC.

Since it was demonstrated in an earlier chapter (Chapter 3) that Aβ-mediates phosphorylation of JNK1, the role of the L-type VDCC in Aβ-mediated JNK activation was assessed. The Aβ-mediated phosphorylation of JNK1 was attenuated in nicardipine treated cells, suggesting a role for the L-type Ca^{2+} channel in this signalling event. The role of Ca^{2+} in the activation of JNK remains to be fully established. It has been demonstrated that increased Ca^{2+} influx leads to increased production of reactive oxygen species within the cell (Kruman and Mattson, 1999; Ekinci *et al.*, 2000). Mitochondria are the primary site of reactive oxygen species (ROS) generation within the cell (Brunk and Terman, 2002). In addition, mitochondria also play important roles in regulating cellular Ca^{2+} homeostasis. They can remove large quantities of Ca^{2+} from the cytoplasm via the activity of a uniporter located on the inner mitochondrial membrane. Excessive uptake of Ca^{2+} by the mitochondria has been demonstrated to result in increased ROS production and subsequent apoptosis (Kruman and Mattson, 1999). JNK is activated by ROS (Mielke and Herdegen, 2000) and so ROS-mediated activation of JNK represents one mechanism whereby increased $[Ca^{2+}]_i$ may indirectly lead to activation of JNK1. However, it has previously been reported that extracellular Ca^{2+} is necessary and sufficient for rapid JNK1 activation in NMDA treated cortical neurons, indicating that the activation of JNK1 can occur as a direct result of increased Ca^{2+} influx to the cell (Ko *et al.*, 1998). In line with this, the Ca^{2+}-sensitive kinase, Pyk2, and the calcium/calmodulin-dependent kinase IV, have been demonstrated to be involved in upstream signalling pathways involved in JNK1 activation (Enslen *et al.*, 1996; Yu *et al.*, 1996). Activation of another member of the MAPK family, ERK, has previously been shown to be prevented by blocking the L-type Ca^{2+} channel in neuronal cells (Ekinci *et al.*, 1999a), thus providing further evidence that voltage-dependent Ca^{2+} channels can impact on kinase cascades.

Since phosphorylation of p53 at serine-15 was established to be downstream of JNK1 activation in Aβ-treated neurons (see Figure 4.5), at this stage of the study it was appropriate to investigate whether phosphorylation of p53 by Aβ also occurred via the L-type Ca^{2+} channel. The result demonstrated that nicardipine prevented the Aβ-mediated phosphorylation of p53. This result strengthens the case of a role for the L-type Ca^{2+} channel as an upstream regulator in the Aβ-mediated phosphorylation of JNK1 and p53 and demonstrates that the proclivity of Aβ to modulate Ca^{2+} homeostasis underlies the Aβ-mediated impact on the JNK / p53 pathway.

Previous studies from this laboratory have demonstrated a Aβ-induced increase in cytosolic activity of cathepsin-L (Boland and Campbell, 2003b). In addition, in the previous chapter it was demonstrated that Aβ leads to alterations in lysosomal membrane integrity possibly via a mechanism involving association of p53 at the lysosome. Therefore, the involvement of the L-type Ca^{2+} channel in the Aβ-mediated increase in cytosolic cathepsin-L activity was examined. The stimulatory effect of Aβ on cathepsin-L activity was abrogated in nicardipine treated cells, providing evidence of a link between the L-type VDCC and the Aβ-mediated increase in cytosolic cathepsin-L activity. The effect of nicardipine on the Aβ-mediated increase in cathepsin-L activity may be due to a number of sources. Given that Aβ promotes association of phospho-p53 with the lysosomes, and since nicardipine prevents p53 phosphorylation, the impact of nicardipine on the Aβ-mediated increase in cathepsin-L activity may be due to the prevention of p53 activation. p53 has previously been reported to induce lysosomal destabilisation (Yuan *et al.*, 2002), and it was demonstrated in the previous chapter that treatment with the p53 transcriptional inhibitor, pifithrin-α, attenuated the Aβ induced increase in cathepsin-L activity. Therefore an interaction between Ca^{2+} and p53 may represent a possible mechanism for cathepsin-L release from the lysosome.

There is evidence that Ca^{2+} may control lysosomes function in exocytosis by inducing fusion of lysosomes with the plasma membrane (Rodriguez *et al.*, 1997). In addition, in dendritic cells Ca^{2+}-mediated lysosomal exocytosis is followed by release of cathepsins (Gardella *et al.*, 2001). Interestingly, the Ca^{2+} binding protein, calpain,

has been demonstrated to be activated at the lysosomal membrane and to cause release of cathepsins from the lysosomes via proteolysis of the lysosomal membrane (Yamashima *et al.*, 1998). Calpain requires an increase in $[Ca^{2+}]_i$ to induce its activation (Ishiura *et al.*, 1978). Further evidence for the involvement of calpain in the Aβ-mediated increase in cathepsin-L activity is supplied by a previous finding in this laboratory of a Aβ-mediated increase in calpain activity (Boland and Campbell, 2003a). In addition, the increase in cytosolic expression of cathepsin-L induced by Aβ was not observed in cells treated with the calpain inhibitor, MDL28170 (Boland and Campbell; unpublished observation). My finding that the Aβ-mediated increase in cathepsin-L activity involves the L-type VDCC suggests that Ca^{2+} influx through this channel may impact on calpain, as well as JNK1 and p53, leading to cathepsin-L release.

The results of the previous chapters demonstrate that $A\beta_{1\text{-}40}$-mediated induction of apoptotic events including caspase-3 activation and DNA fragmentation occur downstream of the Aβ-mediated increase in activity of JNK, $p53^{ser15}$ and cytosolic cathepsin-L To further clarify the role of the L-type VDCC in Aβ-mediated neuronal apoptosis, nicardipine was applied to cells to block this subtype of Ca^{2+} channel. The proclivity of Aβ to activate caspase-3 was significantly attenuated consequent to nicardipine treatment. Aβ also failed to increase DNA fragmentation in nicardipine treated cells. These results are consistent with the idea that Aβ-mediated neuronal apoptosis involves the L-type Ca^{2+} channel. Although, more experimental work will need to be carried out to clarify the exact mechanism of L-type Ca^{2+} channel coupling to the apoptotic pathway, it is likely that the neuroprotective effect of nicardipine is due to the upstream inhibitory effects of nicardipine on the Aβ-mediated increase in JNK and p53 phosphorylation and cathepsin-L activity.

In summary, the data presented in this chapter provide strong evidence that dysregulation of Ca^{2+} homeostasis plays a role in Aβ-mediated neurodegeneration. The observed Aβ-mediated increase in $[Ca^{2+}]_i$ can be attributed, at least in part, to Ca^{2+} influx through the L-type Ca^{2+} channel. Treatment with the L-type Ca^{2+} channel blocker, nicardipine, reversed the Aβ-mediated increase in JNK1 placing increased

Ca^{2+} influx upstream of these phosphorylation events and indicating that increased activation of the L-type Ca^{2+} channel is an early event in the Aβ-signalling cascade. Treatment with nicardipine also prevented the Aβ induced increase in cathepsin-L activity, providing evidence that increased Ca^{2+} influx impacts on the integrity of lysosomal membranes. In addition, exposure to nicardipine significantly reduced Aβ-mediated induction of the apoptotic events, caspase-3 cleavage and DNA fragmentation. Taken together, these results provide ample evidence of a role for the L-type Ca^{2+} channel in Aβ-mediated neurodegeneration.

Chapter 7

Aβ and IL-1β regulate mRNA expression of pro- and anti-apoptotic genes

7.1 Introduction

Neuroinflammation involves an innate immune reaction of sufficient intensity that self-attack on neurons occurs. Along with neuritic plaques and neurofibrillary tangles, neuroinflammation is considered a hallmark feature of AD (McGeer and McGeer, 2001). Although it has not yet been fully established whether neuroinflammation occurs as a cause or consequence of AD pathology, there is increasing evidence to suggest that inflammation plays an integral part in development of AD (Moore and O' Banion, 2002). A long list of inflammatory proteins, such as complement factors, acute-phase proteins, and pro-inflammatory cytokines, have been identified in AD brains (Akiyama *et al.*, 2000). In addition, findings that amyloid plaques in AD brains are characterised by the presence of activated complement factors, as well as clusters of activated microglia (Eikelenbloom *et al.*, 2002), indicates that some form of inflammatory process is taking place. Since there is no apparent influx of leukocytes from the blood in AD brain it is assumed that Aβ deposits in AD brains are associated with a locally induced, non-immune-mediated, chronic inflammatory-type response (Eikelenbloom *et al.*, 2002). Inflammation can be triggered by the accumulation of proteins with abnormal conformations, such as amyloid fragments, or by molecules released from injured neurons, such as inflammatory cytokines. (Wyss-Coray and Mucke, 2002).

Microglia, the smallest of the glia cells are macrophage-like cells present in the central nervous system. Microglia function as immune cells for the brain, playing a critical surveillance and protective role, similar to immune cells in the peripheral nervous system (McGeer and McGeer, 2001). However, in response to neuronal injury or stress, microglia become rapidly activated and can lead to degeneration of the very neurons they were intended to protect. One way in which they do this is by initiating a cytokine response, releasing a number of factors such as pro-inflammatory cytokines which can exacerbate the inflammatory response and result in neurodegeneration. Pro-inflammatory cytokines which are found to be upregulated in AD brain include TNF-α, IL-1β, IL-1α and IL-6 (McGeer and McGeer, 2003). Activated astrocytes in the AD brain have also been shown to secrete a wide range of cytotoxic substances including

pro-inflammatory cytokines and reactive oxygen species (Grammas and Ovase, 2001). Aβ is a strong candidate for the triggering of neuroinflammation in AD (Moore and O'Banion, 2002). Evidence for this comes from *in vitro* studies which have demonstrated that Aβ and APP can activate glia in a dose- and time-dependent manner as measured by expression of the potent pro-inflammatory cytokines interleukin-1β (IL-1β) and tumour necrosis factor-α (TNFα; Akama *et al.*, 1998; Hu *et al.*, 1999). In addition, reactive glial cells are consistently located with Aβ deposits in AD brain (MacKenzie *et al.*, 1995).

Of particular interest in our laboratory are the changes in expression in cytokines associated with the AD brain. TNF-α is a well-characterised mediator of apoptosis, which sets up a delicate life/death balance within the cell (Smith, 1994). It can induce apoptotic changes in cells via activation of caspase-3 (Guicciardi *et al.*, 2000). TNF-α has been reported to increase production of Aβ and inhibit the secretion of soluble APPs (Blasko *et al.*, 1999). TNF-α also activates the key transcription factor NF-κB which has a role in regulation of neuronal survival. Analysis of AD patients has revealed strong NF-κB activity in the centre of primitive plaques and in neurons and astrocytes surrounding these plaques (Kaltscmidt *et al.*, 1997). There is a great amount of evidence in the literature to suggest that the NF-κB family of transcription factors regulate cell survival by suppression of apoptosis (Barkett *et al.*, 1999). However, a pro-apoptotic role for NF-κB has also been suggested. Neuronal cell death was shown to correlate with NF-κB activation and was blocked by salicylates, which interfere with activation of NF-κB (Grilli *et al.*, 1996). This signalling cascade is even more complicated by the fact that NF-κB can in turn induce gene production of pro-inflammatory TNF-α (Mattson and Camandola, 2001). There is also evidence to suggest that TNF- α may have a neuroprotective role through increased expression of anti-apoptotic Bcl-2 (Tarkowski *et al.*, 2003).

Overexpression of the pro-inflammatory cytokine, IL-1β, in AD brain was first shown by Griffin *et al*, (1989) and it is now known that 78% of plaques containing aggregated Aβ peptide contain IL-1β immunoreactive microglia (Griffin *et al.*, 1995). Excessive expression of IL-1β in the AD brain has been proposed to contribute to

additional processing of Aβ in neurons (Forloni *et al*, 1992). Furthermore, a common polymorphism in the IL-1β gene is associated with a 4-fold increase in production of IL-1β and an associated increased risk of AD (Mrak and Griffin, 2001). Previous results from this laboratory have demonstrated an IL-1β dependent increase in calcium concentration in rat cortical synaptosomes (Campbell *et al.*, 1998). In addition, IL-1β has been reported to increase activation of JNK *in vitro* and *in vivo* (Vereker *et al.*, 2000) and recent work by Minogue *et al* (2003) shows an increased concentration of IL-1β in Aβ-treated cortical neurons. This provides evidence that IL-1β may play a role in neurodegeneration and demonstrates IL-1β as a worthy candidate for further investigation.

Although there is evidence that neurons, as well as glial cells, express pro-inflammatory cytokines such as TNF-α (Perry *et al.*, 2001) and IL-1β (Lechan *et al.*, 1990), little experimental work has been carried out to examine the role of neuronal cytokine expression in neurodegeneration. The objective of this study was to determine whether Aβ lead to an alteration in mRNA expression of the apoptosis-related genes caspase-3, Bcl-xl, TNF-α and NF-κB in cultured cortical neurons. Expression of the endogenous NF-κB inhibitor, IκB, was also assessed. In addition, since the pro-inflammatory cytokine IL-1β is also implicated in neuronal apoptosis, we chose to assess the effect of IL-1β on mRNA expression of the apoptotic effector caspase-3 and the apoptosis associated Bcl-family members, Bax and Bcl-xl.

7.2 Results

7.2.1 Aβ increases caspase-3 mRNA expression

Since caspase-3 is a key executioner of apoptosis, the effects of Aβ on caspase-3 mRNA expression were examined. Cells were treated with Aβ (2 μM) for 18 hr and caspase-3 mRNA expression was assessed by RT-PCR with gene-specific primers for caspase-3 and GAPDH. Figure 7.1 demonstrates that Aβ evoked a significant increase in caspase-3 mRNA from 1.0 ± 0.025 (mean band width ± SEM; arbitrary units) to 1.107 ± 0.03 ($p<0.05$, student's t-test, n=9). The mRNA expression of caspase-3 was normalised to that of the housekeeping gene GAPDH. A sample agarose gel demonstrating the effect of Aβ on caspase-3 mRNA expression is depicted in Figure 7.1B.

7.2.2 Effect of Aβ on mRNA expression of Bcl-xl

The effect of Aβ on mRNA expression of anti-apoptotic Bcl-xl was assessed. Cells were treated with Aβ (2 μM) for 18 hr and Bcl-xl mRNA expression was assessed by RT-PCR with gene-specific primers for Bcl-xl and GAPDH. Figure 7.2 demonstrates that Aβ had no effect on Bcl-xl mRNA expression. Thus Bcl-xl mRNA expression was 0.95 ± 0.082 (mean band width ± SEM; arbitrary units) in control cells and 1.0 ± 0.077 (n=9) in Aβ-treated cells. The mRNA expression of Bcl-xl was normalised to that of the housekeeping gene GAPDH. A sample agarose gel demonstrating the effect of Aβ on Bcl-xl mRNA expression is depicted in Figure 7.2B.

7.2.3 Aβ increases expression of cytokine TNF-α

Since altered expression of cytokines such as TNF-α have been observed in AD brain (McGeer and McGeer, 2003) and have been reported to potentiate the neurotoxic action of Aβ (Pollock *et al.*, 2002) levels of expression of the mRNA species encoding

A.

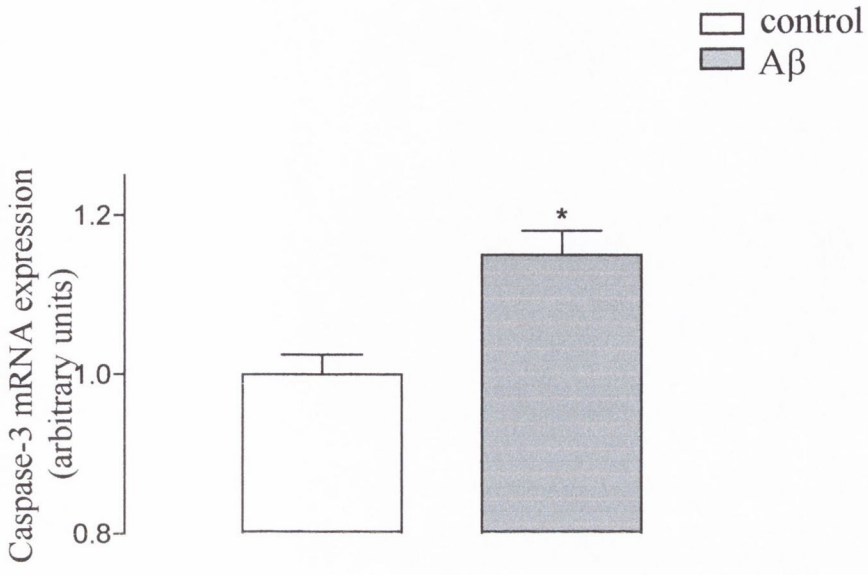

B.

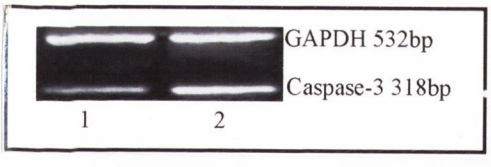

Figure 7.1 Aβ increases expression of caspase-3 mRNA in cultured cortical neurons

A. Cortical neurons were treated with Aβ (2 μM) for 18 hr and caspase-3 mRNA expression was assessed using RT-PCR. Aβ significantly increased mRNA expression of caspase-3. Results are expressed as mean ± SEM for 8 independent observations * $p<0.05$

B. Representative image of agarose gel demonstrating levels of caspase-3 and GAPDH mRNA expression in control (lane1) and Aβ-treated cells (lane 2).

A.

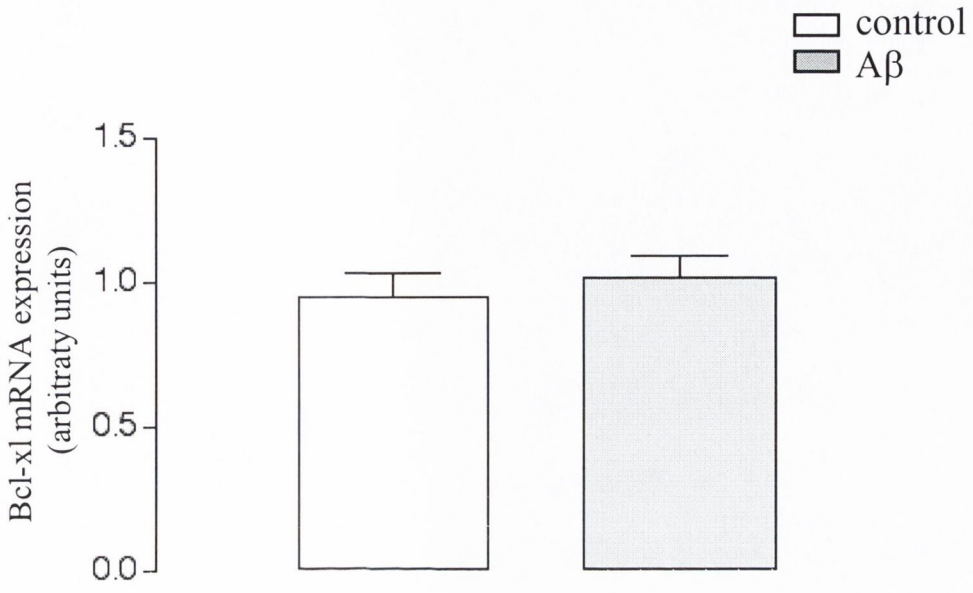

B.

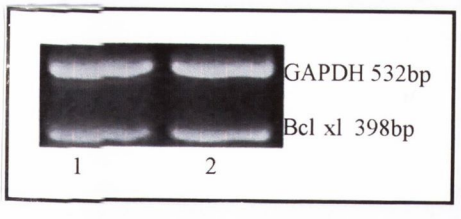

Figure 7.2 Aβ does not alter expression of Bcl-xl mRNA in cultured cortical neurons

A. Cortical neurons were treated with Aβ (2 μM) for 18 hr and Bcl-xl mRNA expression was assessed using RT-PCR. There was no change in mRNA expression of Bcl-xl following treatment with Aβ. Results are expressed as mean ± SEM for 6 independent observations.

B. Representative image of agarose gel demonstrating levels of Bcl-xl and GAPDH mRNA expression in control (lane1) and Aβ-treated cells (lane 2).

A.

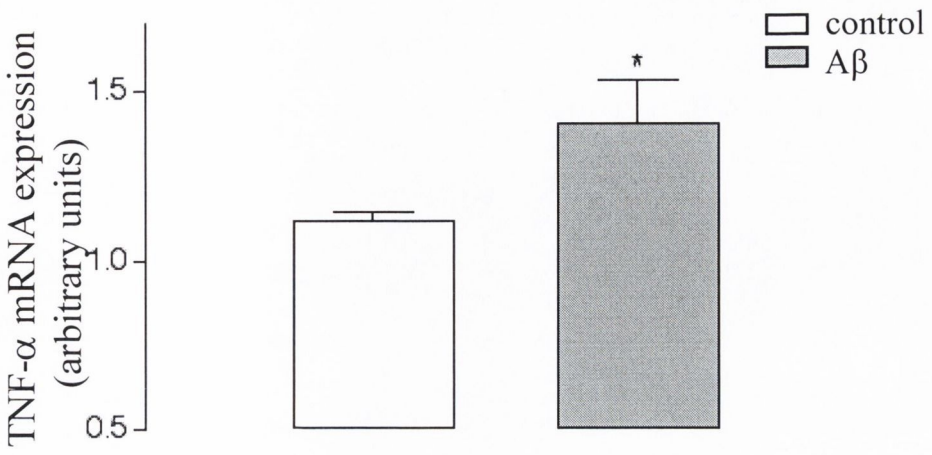

B.

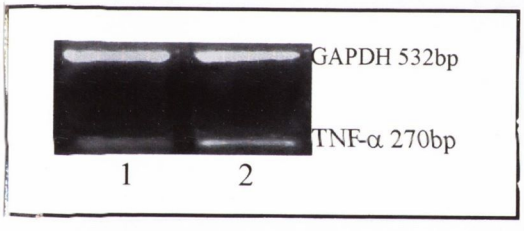

Figure 7.3 Aβ increases expression of TNF-α mRNA in cultured cortical neurons

A. Cortical neurons were treated with Aβ (2 μM) for 18 hr and TNF-α mRNA expression was assessed using RT-PCR. Aβ significantly increased mRNA expression of TNF-α. Results are expressed as mean ± SEM for 8 independent observations * $p<0.05$

B. Representative image of agarose gel demonstrating levels of TNF-α and GAPDH mRNA expression in control (lane1) and Aβ-treated cells (lane 2).

the cytokine TNF-α was examined in Aβ-treated cultured neurons. Cells were treated with Aβ (2 μM) for 18 hr and TNF-α mRNA expression was assessed by RT-PCR with gene-specific primers for TNF-α and GAPDH. Figure 7.3 demonstrates that Aβ evoked a significant 22 % increase in TNF-α mRNA expression from a control value of 1.12 ± 0.03 (mean band width ± SEM; arbitrary units) to 1.4 ± 0.12 ($p<0.05$, student's t-test, n=9). The mRNA expression of TNF-α was normalised to that of the housekeeping gene GAPDH. Figure 7.3B is a sample agarose gel demonstrating the Aβ-mediated increase in TNF-α mRNA.

7.2.4 Aβ increases expression of the transcription factor NF-κB but not IκB

The effect of Aβ on mRNA expression of the cytokine-associated transcription factors NF-κB and IκB was assessed. Cells were treated with Aβ (2 μM) for 18 hr and mRNA expression of NF-κB and IκB were assessed by RT-PCR with gene-specific primers for NF-κB, IκB and GAPDH. Figure 7.4 demonstrates that Aβ evoked a significant increase in levels of the dual-functioning transcription factor NF-κB from 1.12 ± 0.11 (mean band width ± SEM; arbitrary units) to 1.272 ± 0.069 ($p<0.05$, student's t-test, n=6). In contrast, Aβ had no modulatory effect on mRNA expression of IκB (Figure 7.5). Thus mRNA expression of IκB was 0.99 ± 0.01 in control and 1.073 ± 0.09 in Aβ-treated cells. The mRNA expression of both NF-κB and IκB were normalised to that of the housekeeping gene GAPDH. Figure 7.4B and 7.5B are sample agarose gels demonstrating the effect of Aβ on NF-κB and IκB mRNA expression.

A.

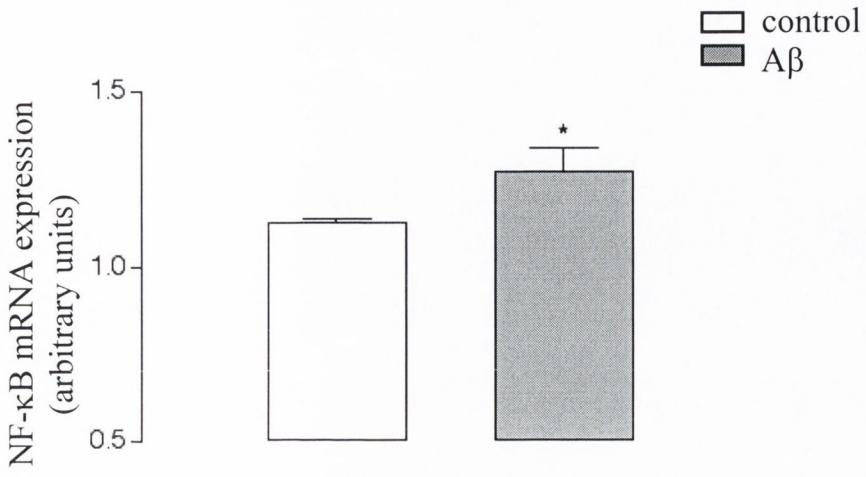

B.

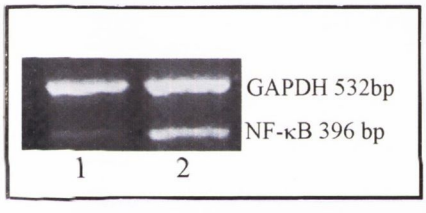

Figure 7.4 Aβ increases expression of NF-κB mRNA in cultured cortical neurons

A. Cortical neurons were treated with Aβ (2 μM) for 18 hr and NF-κB mRNA expression was assessed using RT-PCR. Aβ significantly increased mRNA expression of NF-κB. Results are expressed as mean ± SEM for 6 independent observations, * $p<0.05$.

B. Representative image of agarose gel demonstrating levels of NF-κB and GAPDH mRNA expression in control (lane1) and Aβ-treated cells (lane 2).

A.

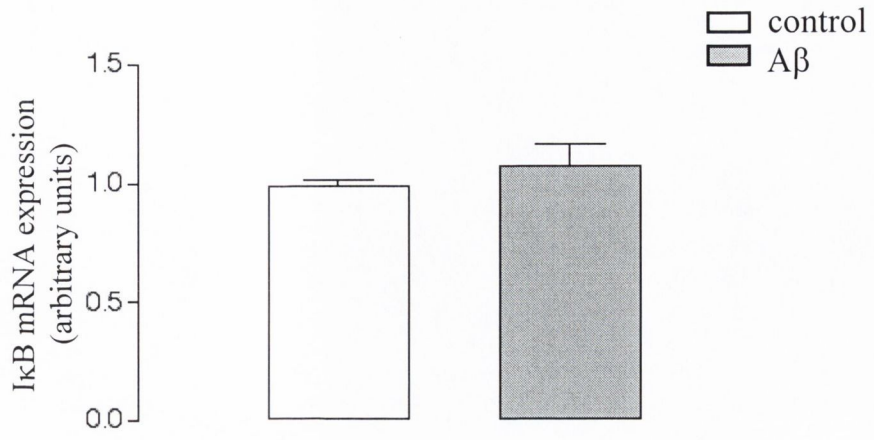

B.

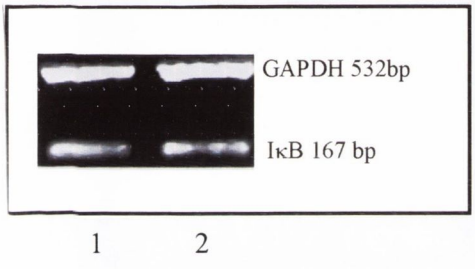

Figure 7.5 Aβ has no effect on expression of IκB mRNA in cultured cortical neurons

A. Cortical neurons were treated with Aβ (2 μM) for 18 hr and IκB mRNA expression was assessed using RT-PCR. Aβ did not effect mRNA expression of IκB. Results are expressed as mean ± SEM for 6 independent observations.

B. Representative image of agarose gel demonstrating levels of IκB and GAPDH mRNA expression in control (lane1) and Aβ-treated cells (lane 2).

7.2.5 IL-1β increases caspase-3 mRNA expression

In order to assess the effect of IL-1β on caspase-3 mRNA expression, cells were treated with IL-1β (5 ng/ml) for 18 hr and RT-PCR was carried out with gene specific primers for caspase-3 and GAPDH. Figure 7.6 demonstrates that IL-1β significantly increased caspase-3 mRNA expression from a control value of 1.02 ± 0.17 (mean band width ± SEM; arbitrary units) to 1.368 ± 0.04 ($p<0.05$, student's t-test, n=6). The mRNA expression of caspase-3 was normalised to that of the housekeeping gene GAPDH. A sample agarose gel demonstrating the effect of IL-1β on caspase-3 mRNA expression is depicted in Figure 7.6B.

7.2.6 IL-1β increases mRNA expression of pro-apoptotic Bax

The effect of IL-1β on mRNA expression of Bax was assessed. Cells were treated with 5 ng/ml IL-1β for 18 hr and RT-PCR was carried out using gene specific primers for Bax and GAPDH. Figure 7.7 demonstrates that IL-1β significantly increased Bax mRNA expression from a control value of 1.023 ± 0.01 (mean band width ± SEM; arbitrary units) to 1.23 ± 0.07 ($p<0.05$, student's t-test, n=6). The mRNA expression of Bax was normalised to that of the housekeeping gene GAPDH. A sample agarose gel demonstrating the effect of IL-1β on Bax mRNA expression is depicted in Figure 7.7B.

7.2.7 IL-1β leads to an increase in mRNA expression of anti-apoptotic Bcl-xl.

Expression of the bcl-2 family member, Bcl-xl, was assessed following exposure of cells to IL-1β for 18 hr. RT-PCR was carried out with gene specific primers for Bcl-xl and GAPDH (Figure 7.8). IL-1β (5ng/ml) lead to a significant 25 % increase in expression of Bcl-xl from a control value of 1.017 ± 0.01 (mean band width ± SEM; arbitrary units) to 1.23 ± 0.092 ($p<0.05$, student's t-test, n=6). The mRNA expression of Bcl-xl was normalised to that of the housekeeping gene GAPDH. A

sample agarose gel demonstrating the effect of IL-1β on Bcl-xl mRNA expression is depicted in Figure 7.8B.

A.

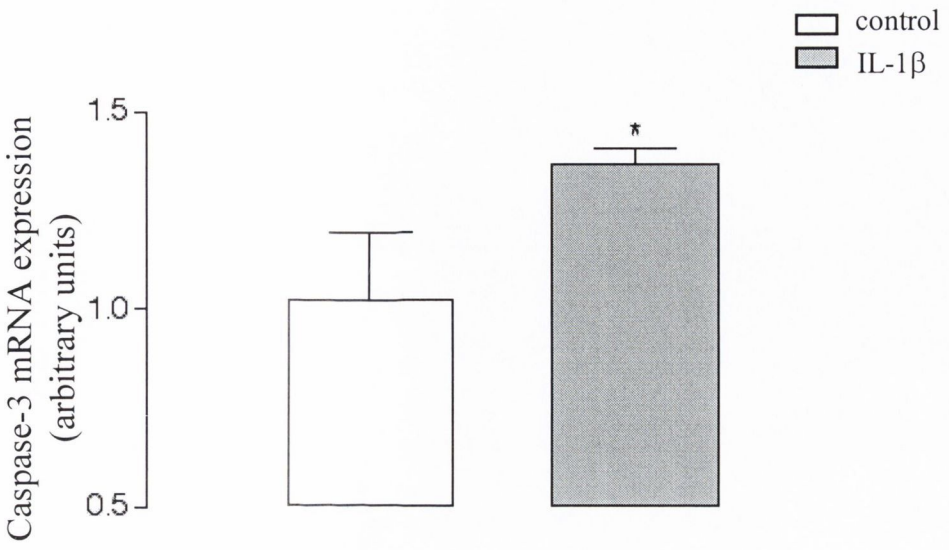

B.

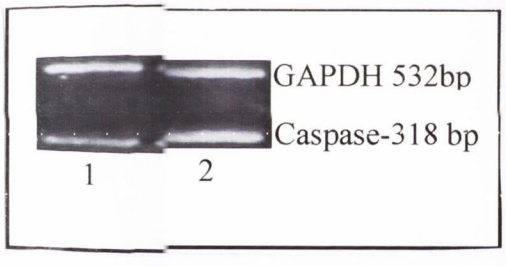

Figure 7.6 IL-1β increases expression of caspase-3 mRNA in cultured cortical neurons

A. Cortical neurons were treated with IL-1β (5 ng/ml) for 18 hr and caspase-3 mRNA expression was assessed using RT-PCR. IL-1β significantly increased mRNA expression of caspase-3. Results are expressed as mean ± SEM for 6 independent observations * $p<0.05$.

B. Representative image of agarose gel demonstrating levels of caspase-3 and GAPDH mRNA expression in control (lane1) and IL-1β-treated cells (lane 2).

A.

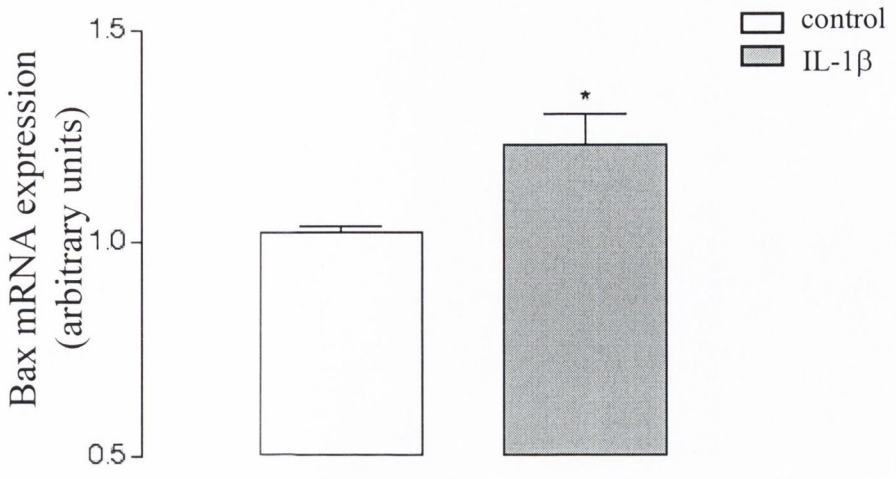

B.

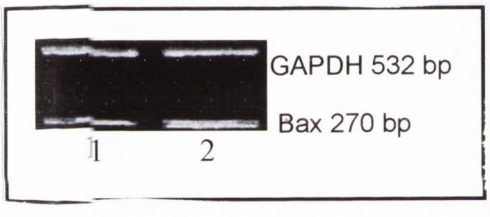

Figure 7.7 IL-1β increases expression of Bax mRNA in cultured cortical neurons

A. Cortical neurons were treated with IL-1β (5 ng/ml) for 18 hr and Bax mRNA expression was assessed using RT-PCR. IL-1β significantly increased mRNA expression of Bax. Results are expressed as mean ± SEM for 6 independent observations * $p<0.05$

B. Representative image of agarose gel demonstrating levels of Bax and GAPDH mRNA expression in control (lane1) and IL-1β-treated cells (lane 2).

A.

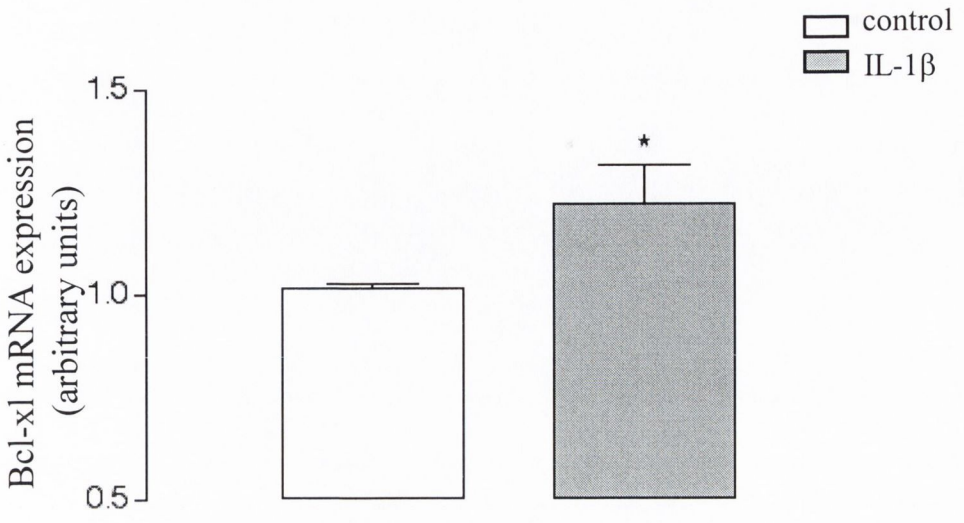

B.

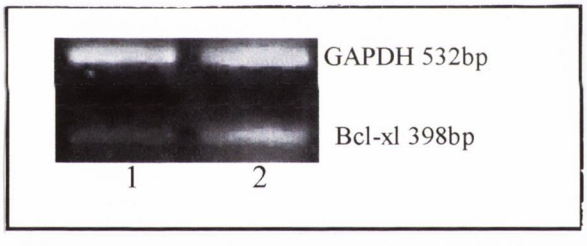

Figure 7.8 IL-1β increases expression of Bcl-xl mRNA in cultured cortical neurons

A. Cortical neurons were treated with IL-1β (5 ng/ml) for 18 hr and Bcl-xl mRNA expression was assessed using RT-PCR. IL-1β significantly increased mRNA expression of Bcl-xl. Results are expressed as mean ± SEM for 6 independent observations * $p<0.05$.

B. Representative image of agarose gel demonstrating levels of Bcl-xl and GAPDH mRNA expression in control (lane1) and IL-1β-treated cells (lane 2).

7.3 Discussion

The aim of this study was to identify the nature of the pro-and anti-apoptotic mRNA species regulated by Aβ and the proinflammatory cytokine, IL-1β, in cultured cortical neurons. The results demonstrate that Aβ evokes a significant increase in mRNA expression of pro-apoptotic caspase-3, but no change in expression of anti-apoptotic Bcl-xl. In addition, Aβ increased mRNA expression of the pro-inflammatory cytokine, TNF-α, and the associated transcription factor, NF-κB. No alteration in mRNA expression of the endogenous NF-κB inhibitor, IκB, occurred following Aβ-treatment. Analysis of the effects of IL-1β on mRNA expression in cultured cortical neurons demonstrated a significant increase in mRNA expression of pro-apoptotic Bax and caspase-3, and anti-apoptotic Bcl-xl. These results indicate that neurons, as well as glial cells, can produce cytokines such as TNF-α in response to stressful stimuli and that exposure to stressors such as Aβ or IL-1β leads to an alteration in neuronal mRNA expression of apoptosis-related genes.

Altered levels of gene expression is a central event in apoptosis and this study employed RT-PCR to characterize the molecular events that occur in response to treatment of cortical neurons with $A\beta_{1-40}$ and IL-1β. Having previously demonstrated that Aβ mediates an increase in expression of pro-apoptotic Bax protein but does not alter mRNA expression of p53, the effect of Aβ on mRNA expression of the apoptosis-related genes caspase-3 and Bcl-xl was examined. Increased activity of caspase-3 in response to Aβ treatment has been reported in numerous studies (Bozyczko-Coyne *et al.*, 2001; Marin *et al.*, 2000; Allen *et al.*, 2001). In our system, increased activity of caspase-3 has been demonstrated to occur following 24 hrs $A\beta_{1-40}$ treatment (Boland and Campbell, 2003a), therefore a time point upstream of this was chosen at which to assess caspase-3 mRNA expression. An 18 hr incubation period was chosen and this incubation period was used for all subsequent experiments carried out in this chapter. Aβ evoked a significant increase in transcription of caspase-3 mRNA at 18 hr. Although an Aβ-induced increase in caspase-3 message has not previously been reported, the present finding is in accordance with other studies of neuronal apoptosis

where an increase in caspase-3 mRNA was observed in injured brain (Yang *et al.*, 2002; Eldadeh *et al.*, 1997; Ginham *et al.*, 2001). Yang *et al* (2002) found transcription of caspase-3 mRNA to precede an increase in caspase-3 protein activity and our laboratory has previously reported that caspase-3 activity is increased in Aβ-treated cortical neurons after 24 hours (Boland and Campbell, 2003a). Since our results demonstrate an Aβ-mediated increase in caspase-3 mRNA expression at 18 hours, it is therefore probable that Aβ leads to an increase in transcription of the *caspase-3* gene, which is likely followed by increased translation of the protein and an upregulation of enzymatic activity.

The Bcl family member, Bcl-xl, is the closest mammalian relative of Bcl-2 and similarly to Bcl-2 it acts as a cell death repressor. Bcl-xl is expressed in the human nervous system and expression is found to be particularly high in the brain (Zörnig *et al.*, 2001). Significant Bcl-xl expression has been demonstrated in reactive microglia of patients with AD, and Bcl-xl-positive microglia have been found to colocalise with Aβ plaques in AD, suggesting a general role for Bcl-xl in areas of pathology (Drache *et al.*, 1997). In this study Aβ was found to have no effect on mRNA expression of Bcl-xl. This is in contrast to the findings of a number of other studies. Luetjens *et al* (2001) found increased expression of Bcl-xl mRNA and protein following treatment of PC12 cells with $A\beta_{1-40}$ and Kim *et al* (1998) report a decrease in the ratio of Bcl-xl / Bcl-xs following treatment with $A\beta_{25-35}$. In a further study, exposure of cultured neurons to Aβ was associated with a transient, non-persistent increase in Bcl-xl mRNA expression (Iwasaki *et al.*, 1996). While the study carried out by Luetjens's group examined expression of Bcl-xl following a 6 hour exposure to Aβ, the present study examined gene expression following 18 hours Aβ-treatment. It is possible that increased trarscription of Bcl-xl may have occurred at an earlier time point in an attempt to increase resistance of neurons to Aβ-neurotoxicity and that by 18 hour levels of Bcl-xl mRNA have returned to basal levels. However, further experiments will need to be carried out to determine whether this is the case.

Overexpression of cytokines in the brain is an important factor in the pathogenesis of neurodegenerative disorders and altered expression of cytokines is

observed in the brain of Alzheimer's disease patients (Bauer *et al.*, 1991). Neurodegeneration is closely related to the shift of cytokine balance towards the side of pro-inflammatory cytokines like TNF-α. Expression of TNF- α is rapidly induced by microglia and astrocytes in injury brain and leads to apoptosis in a number of cell types (Wallach *et al.*, 1999). The experiments carried out in this study demonstrated increased expression of TNF- α in cultured neurons following treatment with Aβ, indicating that neurons as well as glial cells produce cytokines in a stressful environment. However, the *in vitro* situation is not always reflective of the events occurring in the brain and it can not be ruled out that, in the presence of glia, the production of cytokines by neurons may prove to be negligible. TNF-α-induced apoptosis is mediated by the TNF-receptor-1 (TNFR-1) and results in initiation of the caspase cascade by activation of caspase-8 (Zörnig *et al.*, 2001). Caspase-8 in turn leads to cleavage and activation of caspase-3. Work carried out in our laboratory has demonstrated that $A\beta_{1\text{-}40}$ leads to increased activity of caspase-3 in cultured cortical neurons (Boland and Campbell, 2003a) Therefore, increased expression of TNF-α in Aβ-treated cultured neurons may represent a mechanism whereby increased activity of caspase-3 may occur. In addition, TNF-α can lead to activation of JNK (Barbin *et al.* 2001; Mielke and Herdegen, 2002). Given that JNK activation was demonstrated to be integral to Aβ-mediated apoptosis in an earlier chapter, TNF-α -mediated activation of JNK may be an upstream event in Aβ signalling in cultured cortical neurons. Interestingly, TNF-α also activates the dual functioning transcription factor NF-κB. NF-κB has been demonstrated to act as a powerful suppressor of apoptosis in many systems (Mattson and Cammandola, 2001). In this way TNF- α can act as a regulatory molecule within the cell leading to activation of anti-apoptotic factors such as NF-κB, in addition to pro-apoptotic factors such as caspase-3.

Aβ lead to a significant increase in mRNA expression of NF-κB, with no concomitant increase in transcription of its endogenous inhibitor, IκB. NF-κB normally resides in a complex with IκB and is sequestered in the cytosol in an inactive form. On activation by an inducing stimulus, NF-κB is released and can migrate to the nucleus and activate transcription of its target genes (Denk *et al.*, 2000). The increased

expression of NF-κB is possibly reflective of a compensatory effort by neurons to counteract the numerous pro-apoptotic events occurring such as activation of JNK and caspase-3. However, since a pro-apoptotic role for NF-κB has also been suggested (Grilli *et al.*, 1996, Wang *et al.*, 1996) the significance of increased NF-κB expression by Aβ in the neurodegenerative cascade remains to be established.

Several reports have provided evidence of a role for IL-1β in the etiology of AD (Griffin *et al.*, 1989; Mrak and Griffin, 2001). A link between Aβ and IL-1β has also been described in several studies; for example Aβ has been shown to stimulate production of IL-1β in a microglial cell line (Szczepanik *et al.*, 2001). IL-1β in turn, in combination with IFNγ, can positively influence the production of additional Aβ by supporting β-secretase cleavage of the immature APP molecule (Blasko *et al.*, 2000). The present study demonstrates an IL-1β-mediated increase in expression of caspase-3 mRNA. This is consistent with other reports in which increased caspase-3 activity has been linked with expression of IL-1β (Lynch and Lynch, 2002; Martin *et al.*, 2002). The finding that IL-1β, as well as Aβ, leads to increased caspase-3 mRNA expression suggests the possibility that some of the actions of Aβ may be mediated through IL-1β. In support for this idea recent work carried out in this laboratory, in collaboration with Professor Marina Lynch, has demonstrated that Aβ-induced increases in activation of JNK and caspase-3 and in TUNEL staining were inhibited by the caspase-1 inhibitor, Ac-YVAD-CMK (Minogue *et al.*, 2003). The initial proteolytic cleavage of inactive pro-IL-1β to active IL-1β is carried out by the protease, caspase-1, so the finding that a caspase-1 inhibitor prevents these Aβ-mediated effects suggests a role for IL-1β in mediating some of the actions of Aβ.

The present study demonstrates that IL-1β lead to an increase in mRNA expression of Bax. In an earlier chapter of this thesis (Chapter 4), it was demonstrated that Aβ also leads to increased mRNA expression of Bax, strengthening the possibility of the involvement of IL-1β in Aβ-mediated events. However, while IL-1β evoked a significant increase in mRNA expression of Bcl-xl, Aβ did not alter Bcl-xl mRNA expression. This result demonstrates that while IL-1β may be responsible for mediating some of the effects of Aβ, it also plays a separate role in modulating the cells response

to stressful stimuli. Further experiments would aim to clarify the exact nature of the link between Aβ and IL-1β in Aβ-mediated neurotoxicity.

In conclusion, the results presented in this chapter demonstrate that Aβ leads to increased mRNA expression of pro-apoptotic caspase-3. In addition, Aβ modulates neuronal transcription of the cytokine TNF-α, and its associated transcription factor, NF-κB. These results suggest that neurons, as well as glial cells, can produce an inflammatory-type response following exposure to Aβ. Analysis of the effects of IL-1β on neuronal cells demonstrates that IL-1β mirrors some of the effects of Aβ, leading to increased mRNA expression of caspase-3 and Bax. This suggests the possibility that some of the apoptotic effects of Aβ in cultured cortical neurons may be mediated through IL-1β signalling.

Chapter 8

Final Discussion

8.1 General Discussion

Alzheimer's Disease (AD) is the most common neurodegenerative disorder and the most prevalent cause of dementia with aging. Although a number of pharmacological treatments for AD have been demonstrated to have some beneficial effects on cognitive, functional, and behavioural symptoms of AD, there is still no effective treatment for prevention or cure of this dehabilitating disease. The pharmacological treatments employed over the last decade largely involve the use of acetylcholinesterase inhibitors to compensate for cholinergic deficits which occur in AD (Hirai, 2000). These inhibitors prevent the break down of acetylcholine and prolong cholinergic transmission at synapses. One of the major pathological hallmarks of AD is the presence of amyloid plaques throughout the cerebral cortex and hippocampus of the brain, the main constituent of these plaques is an aggregated form of Aβ peptide. Evidence gathered from studies carried out on the inherited form of AD has demonstrated a central role for this Aβ peptide in the pathogenesis of AD since all AD causing mutations identified to date increase the production of Aβ (Selkoe, 2001).

New therapeutic approaches are targeted more closely to the pathogenesis of the disease and are based on Aβ biology. Pharmacological inhibition of β and γ secretase is one approach which is currently under investigation. Inhibition of β-secretase is thought to be an ideal therapeutic target as it catalyses the first step of Aβ production (Scarpini *et al.*, 2003). β-secretase knockout mice have no clinical phenotype except for low Aβ concentration (Luo *et al.*, 2001). However, little is known about the function of Beta site APP cleaving enzyme 2 (BACE2), the second β-secretase enzyme identified (Saunders *et al.*, 1999) and it will be important to elucidate its physiological role. In the case of γ-secretase, potent membrane-permeable inhibitors have been designed that reduce Aβ (Hardy and Selkoe, 2002). However, there is concern that these inhibitors may also effect Notch signalling, a pathway which is important for cell fate decisions during embryogenesis, hematopoiesis, and neuronal stem cell differentiation (Haas and Stooper, 1999). A second approach, which has received much press, is to prevent fibrilisation of Aβ or to enhance its clearance from the brain. This approach, termed immunotherapy, involves active or passive Aβ

immunisation, in which antibodies to Aβ decrease cerebral levels of the peptide, by promoting microglial clearance (Bard, 2000), or by redistributing peptide from the brain (DeMattos *et al.*, 2001). However, the first clinical trials using an $A\beta_{42}$ peptide, coupled with an immune adjuvant, were halted when 17 out of 360 patients developed signs of brain inflammation (Shenk, 2002). Since then studies are ongoing to develop modified forms of the vaccine which will not elicit an inflammatory response. Studies on a new form of the vaccine containing just residues 4-10 of the Aβ peptide have been demonstrated to recognise Aβ plaques in animals without causing inflammation (Check, 2003). A third approach is to prevent the neurodegenerative effects triggered by Aβ accumulation. This approach includes potential intervention using small anti-apoptotic molecules to prevent Aβ-mediated apoptosis (Waldmeier, 2003).

The mechanisms of Aβ toxicity have been a major focus of AD research for the past decade and are likely to involve dysregulation of Ca^{2+} homeostasis, generation of reactive oxygen species resulting in oxidative stress and neuroinflammation (Mattson *et al.*, 1993a; Storey and Cappai, 1999). Indeed, previous findings from this laboratory have demonstrated the proclivity of Aβ to lead to disruption of intracellular Ca^{2+} homeostasis in cultured neurons (MacManus *et al.*, 2000).

The primary objective of this study was to investigate the downstream cellular and molecular signalling events associated with the neurodegeneration observed in $A\beta_{1-40}$-treated cultured cortical neurons, with particular emphasis on the role of the MAPK superfamily of kinases. The application of Aβ directly to cultured cells represents an *in vitro* model for extracellular Aβ deposition in the cerebral cortex of the brain. Several observations lead to the establishment of this project. Firstly, previous experiments carried out in this system, applying the aggregated form of $A\beta_{1-40}$ to cultured cortical neurons, had established that Aβ induces degenerative hallmarks including caspase-3 activity and DNA fragmentation (Boland and Campbell, 2003a). In addition, the finding that $A\beta_{1-40}$ leads to cleavage of the DNA repair enzyme, PARP, suggests that the observed $A\beta_{1-40}$ -dependent neurodegeneration is as a result of apoptotic cell death. Secondly, the MAPK family, which are the principal intracellular signalling kinases linking activation of cell surface receptors to cytoplasmic and nuclear effectors, have been demonstrated to play important roles in the regulation of

neurodegeneration in numerous studies. Specifically, the stress activated protein kinase, JNK, has been demonstrated as a potent effector of neurodegeneration in response to a variety of stimuli including oxidative stress and Ca^{2+} signalling (Mielke and Herdegen 2000; Ko *et al.*, 1998). Furthermore, several JNK substrates including p53 and Bax have been demonstrated to be upregulated in AD brain (De la Monte *et al.*, 1998; Tortosa *et al.*, 1998). It was therefore appropriate to examine the role of MAPK family members and downstream substrates, as potential effectors in the Aβ-mediated neurodegenerative cascade.

The results presented in this study provide a strong case for the involvement of JNK in Aβ-mediated neurodegeneration. My finding that JNK activity is increased following exposure to $A\beta_{1-40}$ in cortical neurons concurs with the effects of other Aβ fragments in neuronal systems (Bozcyzko-Coyne *et al.*, 2001; Troy *et al.*, 2001). However, it is of note that the time frame for JNK activation varies considerably between the different JNK isoforms. Maximal activation of JNK1 was found to occur at 1 hr, while maximal activation of JNK2 did not occur until 24 hours following treatment with $A\beta_{1-40}$. However, $A\beta_{1-40}$ failed to have any effect on the brain-specific JNK isoform, JNK3. These results demonstrate the functional diversity that exists between JNK isoforms. Since, the commercially available inhibitors of JNK do not differentiate between specific JNK isoforms, an antisense approach was employed in order to resolve the respective roles of JNK1 and JNK2 in the Aβ cascade. The results obtained demonstrate that JNK1 is the principal JNK isoform involved in Aβ-mediated neuronal cell death and place JNK1 upstream of caspase-3 activation and DNA fragmentation in Aβ-treated cortical neurons. In contrast, JNK2 was not found to be involved in Aβ-mediated regulation of these cell-death events. These results may have important implications in the search for therapeutic approaches to prevent Aβ-associated neurodegeneration. JNK can be linked to neuroprotection, as well as neurodegeneration and plays a role in regulating the final cellular outcome depending on cellular context and the effects of other signalling pathways acting simultaneously (Herdegen *et al.*, 2000). Therefore, complete inhibition of JNK may result in a loss of this regulatory function and result in preserving dysfunctional cells. The results presented herein suggest that JNK1 is the principal JNK isoform involved in carrying out the

neurodegenerative effects of Aβ. Therefore, a therapeutic strategy targeted specifically to depletion, or inactivation, of JNK1 may offer an efficient method of preventing apoptosis of functional cells while retaining activity of the other JNK isoforms involved in the physiological removal of dysfunctional cells. Antisense technology is ideally suited to the purpose of selectively blocking the biosynthesis of harmful proteins in the brain. However, technical limitations which need to be overcome include sufficient penetration of the blood-brain barrier, which is only permeable to lipophilic molecules of less than 600 kDa (Boado *et al.*, 1998), and the prevention of antisense oligonucleotide catabolism *in vivo*. Some progress has been made in enhancing stability of oligonucleotides through the introduction of phosphorothioate oligonucleotides to the phosphate backbone of antisense oligonucleotides (Estibeiro and Godfray, 2001). However, if antisense oligonucleotides are to be effective therapeutics for brain *in vivo*, it is necessary to conjugate antisense oligonucleotides to specialised delivery systems. Antisense delivery to the brain has been demonstrated to be enhanced by conjugation to peptides that facilitate transport across the blood–brain barrier and into cells, for example, conjugation of antisense to a monoclonal antibody to the rat transferrin receptor (Boado *et al.*, 1998).

In order to determine whether the JNK and ERK signalling cascades were simultaneously activated, phosphorylation of ERK was assessed over the same time frame at which JNK phosphorylation had been assessed. No alteration in ERK activity was observed at any of the examined time points. This result is in agreement with a study by Ekinci *et al* (1999) where it was demonstrated that no change in ERK activity occurs following $A\beta_{1\text{-}40}$-treatment, instead the authors observe an Aβ-dependent relocation of ERK activity from cytosol to membrane. In addition, that study reports that the enhanced activity of ERK at the membrane leads to activation of the L-type Ca^{2+} channel in neurons, proposing a mechanism whereby Aβ leads to Ca^{2+} dysregulation in neurons through redirection of ERK from cytosolic to membrane proteins. While the cellular distribution of ERK was not assessed as part of this study, the possibility that ERK activity may modulate the previously reported dysregulation of Ca^{2+} homeostasis observed in this system following Aβ-treatment (Macmanus *et al.*, 2000) is an appealing prospect which will warrant future experimentation.

Analysis of p53 expression in Aβ-treated cells revealed an Aβ-mediated stabilisation of p53 protein via phosphorylation at residue serine-15 of the protein. This stabilisation of p53 occurred in a transcription-independent manner and was evident within 5 minutes and 1 hr of Aβ-treatment. The evidence of an interaction between Aβ and p53 is supported by other studies (Laferla *et al.*, 1996; Culmsee *et al.*, 2001). Targeted depletion of JNK1 using specific antisense oligonucleotides demonstrated that phosphorylation of p53 was JNK1 dependent and therefore provides evidence that p53 is downstream of JNK1 in Aβ-mediated signalling events. Analysis of the effects of Aβ on the pro-apoptotic Bcl-2 family member, Bax, indicated that $A\beta_{1-40}$ increases mRNA and protein expression of Bax in a time-dependent manner, with significantly increased Bax expression of mRNA and protein being observed at 6 hours post-treatment. Application of the p53 inhibitor, pifithrin-α, revealed that the Aβ-mediated increase in Bax expression was mediated through p53, placing Bax downstream of JNK1 and p53 in the Aβ cascade. These findings are consistent with the time frame at which Aβ-mediated effects are observed, with JNK1 and p53 being phosphorylated within 5 minutes and 1 hour of Aβ-treatment and increased expression of Bax being observed at the later time point of 6 hours. Furthermore, the proclivity of Aβ to impact on markers of the apoptotic cascade – namely caspase-3 activity, PARP cleavage and DNA fragmentation was significantly attenuated in pifithrin-α-treated cells placing p53 upstream of these apoptotic events. The emerging paradigm from these results is of an Aβ pathway involving early activation of JNK and p53 and a later increased expression of Bax (see proposed scheme). The consequences of these Aβ-mediated alterations in signalling events include increased caspase-3 activity, PARP cleavage and DNA fragmentation (see proposed scheme). Pifithrin-α has enormous potential as a drug therapy for preventing nerve cell death. Its ability to cross the blood-brain barrier, coupled with the fact that p53-mediated its effects at a pre-mitochondrial stage of the cell death pathway, makes it a prime candidate for therapeutic intervention. The findings of this study, along with other studies investigating the effects of $A\beta_{1-42}$ fragments (Culmsee *et al.*, 2001; Tamagno *et al.*, 2003), demonstrate that pifithrin-α offers protection against Aβ-mediated neurotoxicity. The prospect of using

antiapoptotic compounds in the treatment of chronic neurodegenerative diseases, such as Alzheimer's disease, while attractive, also may lead to problems such as the preservation of dysfunctional cells or a shift from apoptosis to necrosis, which could worsen the target pathology by eliciting inflammatory responses. The potential of preserving dysfunctional cells or shifting from apoptosis to necrosis is likely to be greater, the further downstream in the apoptotic cascade this occurs. For this reason, the results of this study demonstrating an early activation of JNK and p53 in $A\beta_{1\text{-}40}$ treated cells places them at a proximal point for intervention in the apoptotic cascade.

Having established a role for p53 and Bax in Aβ-mediated signalling events, the next series of experiments aimed to assess the subcellular distribution of p53 and Bax following treatment with Aβ. Bax normally resides in the cytosol of the cell. Upon activation, Bax translocates to the mitochondria, where it can facilitate release of cytochrome *c* through formation of pores in the outer mitochondrial membrane (Gao and Dou, 2000). Analysis of Bax expression in cytosolic and mitochondrial fractions demonstrated an Aβ-mediated reduction in Bax expression in cytosolic fractions. This coincided with an increase in Bax expression in mitochondrial fractions. However, the increase in Bax expression in mitochondrial fractions did not reach significance. Closer inspection of cellular expression of Bax in association with the fluorescent mitochondrial marker, Mitotracker Red, revealed increased association of Bax with mitochondria in Aβ-treated cells. In addition, increased expression of phospho-$p53^{ser15}$ was also found to be associated with the mitochondria. The time frame of Bax and p53 association with mitochondria at 6 hours coincides with relocation of the apoptotic-mediator cytochrome *c* from the inner mitochondrial space to the cytosol. Translocation of cytochrome *c* to the cytosol is a defining characteristic of the cells commitment to apoptotic cell death (Yang *et al.*, 1997) which is often regulated by members of the Bcl-2 family, including Bax (Zörnig *et al.*, 2001). Additionally, association of p53 with the mitochondrial membranes has been demonstrated to precede cytochrome *c* release and caspase activation (Marchenko *et al.*, 2001). These results provide evidence that p53, as well as Bax, may be involved in regulation of mitochondrial membrane stability. The co-localisation analysis of Bax and p53 expression with mitochondria demonstrated that regions remained within the cell where expression of Bax and p53 did not co-localise with mitochondria. These results

suggest that Aβ may evoke translocation of these proteins to other intracellular organelles.

There is increasing evidence to suggest that lysosomes are involved in the cell death cascade (Zhao *et al.*, 2001; Wang, 2000). Previous work carried out in this laboratory has demonstrated an increase in cytosolic activity of the lysosomal protease, cathepsin-L (Boland and Campbell, 2003b), suggestive of an Aβ-mediated translocation of cathepsin-L from the lysosome to the cytosol. In addition, inhibition of cathepsin-L prevented the Aβ-mediated increase in caspase-3 activity, PARP cleavage and DNA fragmentation. These findings led to the investigation of the cellular location of Bax and p53 in the present study. Expression of Bax and p53 was assessed in association with the fluorescent lysosomal marker, Lysotracker Red. At 6 hr post Aβ-treatment, increased expression of Bax was observed at the lysosome. Since Bax is integral in inducing cytochrome *c* release from the mitochondria in the apoptotic process (Zörnig *et al.*, 2001), the observation of increased association of Bax with lysosomes suggests that Bax may play a similar role at the lysosome, destabilising the lysosomal membrane to promote cathepsin protease release.

Increased expression of phospho-p53^{ser15} at the lysosomes was also evident at 6 hrs post Aβ-treatment. Since p53 has previously been reported to play a role in initiation of lysosomal destabilisation (Yuan *et al.*, 2002), the effect of Aβ on lysosomal integrity was assessed using the Acridine Orange (AO) technique. A diffuse pattern of AO staining was observed in Aβ-treated cells reflective of a compromised lysosomal membrane. Application of pifithrin-α abolished the Aβ-mediated increase in cytosolic cathepsin-L indicating that the Aβ-mediated increase in cathepsin-L activity is p53-dependent. These findings indicate a possible mechanism whereby p53 and Bax contribute to a lysosomal and mitochondrial branch of the apoptotic pathway in Aβ-treated cultured cortical neurons. Since an alteration in neuronal endosomal-lysosomal systems is an early event in AD and lysosomal leakage is thought to be one of the earliest detectable event during apoptosis (Cataldo *et al.*, 1996), the finding that p53 is involved in destabilisation of the lysosomal membrane offers a target for therapeutic intervention at an early stage.

Previous reports from this laboratory have demonstrated an $A\beta_{1-40}$ mediated increase in $[Ca^{2+}]_i$ in rat cortical synaptosomes via activation of the L- and N-type of voltage-dependent Ca^{2+} channels (VDCC; MacManus *et al.*, 2000). Having established some of the downstream events involved in Aβ-mediated neurotoxicity, I sought to identify the potential upstream mechanisms leading to initiation of these degenerative events. To this end, the role of the L-type VDCC in Aβ-mediated signalling and induction of neuronal apoptosis were investigated. The results demonstrate that Aβ-promotes as increase in $[Ca^{2+}]_i$ in dissociated cortical neurons; an effect that is reversed by the L-type VDCC blocker, nicardipine. Furthermore, the Aβ-mediated increases in JNK1 phosphorylation, p53 stabilisation, cytosolic cathepsin-L activity, caspase-3 activity and DNA fragmentation were attenuated in nicardipine-treated cells. Previously published data from this laboratory indicate that the Ca^{2+}-activated protease, calpain, is likely to be involved in this signalling cascade stemming from Aβ-mediated dysregulation of Ca^{2+} (Boland and Campbell, 2003a). The results presented here implicate the L-type Ca^{2+} channel as a key player involved in the early effects of Aβ that ultimately lead to the demise of the cell.

The final set of experiments carried out were aimed at establishing the role of neuroinflammation in Aβ-mediated events. In addition, the nature of the pro-and anti-apoptotic mRNA species regulated by Aβ and the proinflammatory cytokine, IL-1β were assessed. Aβ increased mRNA expression of the pro-apoptotic effector, caspase-3. This result provides evidence that the Aβ-mediated increase in caspase-3 activity may be attributed to the Aβ-mediated increase in caspase-3 mRNA. Aβ also increased mRNA expression of the pro-inflammatory cytokine, TNF-α and its associated transcription factor, NF-κB. These results demonstrate that neurons, as well as glial cells, can produce cytokines such as TNF-α in response to stressful stimuli. TNF-α–mediated apoptosis involves activation of the caspase cascade including activation of caspase-3 and has also been demonstrated to lead to JNK activation (Zörnig *et al.*, 2001, Barbin *et al.*, 2001). Therefore, TNF-α -mediated activation of JNK may be a further upstream event in Aβ signalling in cultured cortical neurons. The proinflammatory cytokine, IL-1β, increased mRNA expression of pro-apoptotic Bax

and caspase-3, and anti-apoptotic, Bcl-xl. Since a link between Aβ and IL-1β has been demonstrated in several studies (Szczepanik *et al.*, 2001; Minogue *et al.*, 2003) the finding that IL-1β, as well as Aβ, leads to increased mRNA expression of caspase-3 and Bax supports the notion that some of the actions of Aβ may be mediated through IL-1β.

In summary, this study characterised cellular and molecular mechanisms leading to cell death in Aβ-treated cultured cortical neurons. Previous results from this laboratory described the proclivity of Aβ to disrupt Ca^{2+} homeostasis and the present study provides evidence that at least some of the effects of Aβ leading to neuronal apoptosis stem from Ca^{2+} influx through the L-type Ca^{2+} VDCC (see proposed scheme). These include JNK activation, p53 stabilisation, cathepsin-L activity, caspase-3 activation and DNA fragmentation. Increased activity of the stress activated protein kinase, JNK, occurred following Aβ-treatment. Antisense-mediated depletion of specific JNK isoforms demonstrated that JNK1 was the principal JNK isoform involved in Aβ-induced cell death, mediating caspase-3 activation and DNA fragmentation. Increased stability of p53, mediated by Aβ, was found to be JNK1 dependent. Aβ provoked increased expression of Bax mRNA and protein and this was abolished by the p53 inhibitor, pifithrin-α, placing it downstream of p53 in this pathway. Furthermore, caspase-3 activity, PARP cleavage, and DNA fragmentation were found to be mediated by p53. On further investigation of the cellular location of p53 and Bax, it was found that p53 and Bax associate with the mitochondria in Aβ-treated cells and that this association coincided with release of cytochrome *c* from the mitochondria. One of the most interesting findings of this study is the Aβ-mediated association of p53 and Bax with the lysosomes. Inhibition of p53 attenuated the Aβ-mediated increase in cytosolic cathepsin-L, supporting a role for p53 in regulating lysosomal membrane integrity. Evidence is also provided that Aβ provokes a local inflammatory response leading to increased mRNA expression of the pro-inflammatory cytokine TNF-α and it's associated transcription factor NF-κB. The pro-inflammatory cytokine, IL-1β, was found to increase mRNA expression of caspase-3, Bax and Bcl-xl, suggesting that some of the effects of Aβ may be mediated by IL-1β.

This study revealed some of the molecular mechanisms involved in the multi-faceted nature of the cell-death response mediated by Aβ. It is important to note that it is likely that several pathways and interactions between these pathways are involved in Aβ-mediated signalling and that the final outcome of whether apoptosis will occur depends on multiple signalling events. Inhibition of the L-type calcium channel, the stress activated protein kinase, JNK1, and the transcription factor, p53, protected neurons from Aβ-mediated cell death. An understanding of the multiple signalling pathways involved in Aβ-induced cell death will allow design of compounds which will interfere with the cell death process, in a specific manner and will prove to be beneficial in slowing or preventing the progression of AD.

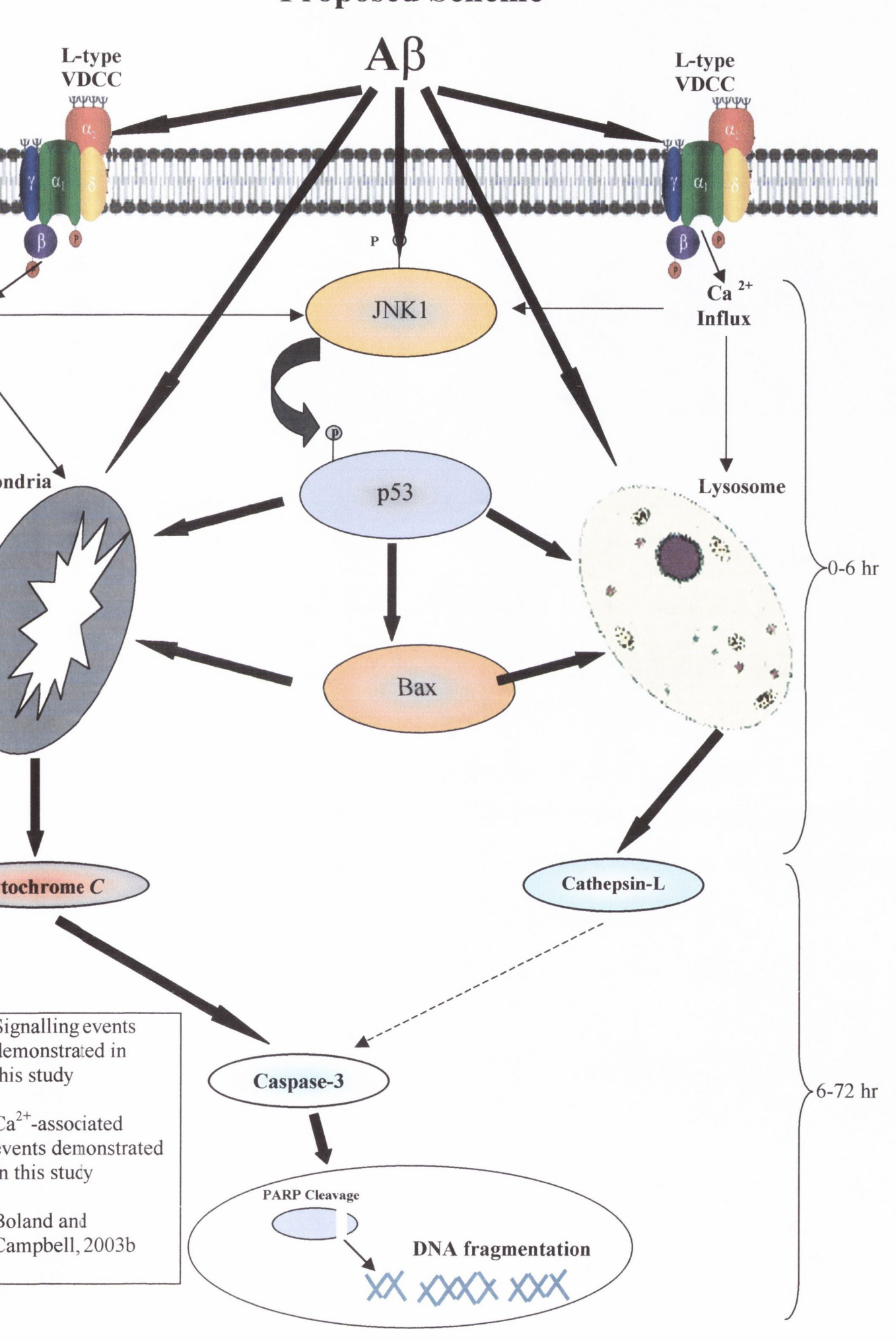
Proposed Scheme
Aβ
L-type VDCC
L-type VDCC
P
JNK1
Ca 2+ Influx
ondria
p53
Lysosome
0-6 hr
Bax
tochrome C
Cathepsin-L
Caspase-3
6-72 hr
PARP Cleavage
DNA fragmentation
Signalling events demonstrated in this study
Ca2+-associated events demonstrated in this study
Boland and Campbell, 2003b

8.2 Future Work

Several important questions arise from the data presented in this study. Inhibition of JNK1 prevented Aβ-induced p53 stabilisation, caspase-3 activity, and DNA fragmentation. Inhibition of p53 prevented the Aβ-mediated increase in Bax expression, cathepsin-L activity, as well as the preventing the later stage markers of apoptosis, PARP cleavage and DNA fragmentation. Since inhibition of JNK1 prevented the Aβ-mediated stabilisation of p53, it will be important to assess whether JNK1 inhibition is capable of preventing the events occurring downstream of p53, namely increased expression of Bax, and increased activity of cytosolic cathepsin-L activity. This will establish whether the Aβ-signalling pathway diverges at the stage of p53 or at the level of Bax or whether the Aβ-mediated signalling events stem from increased activation of JNK1. Although JNK2 was activated within 24 hours of Aβ-treatment, JNK2 did not participate Aβ-mediated apoptosis. The function of activated JNK2 in the Aβ cascade therefore remains to be clarified.

Analysing the effect of p53 inhibition on cytochrome *c* release will determine whether the observed association of p53 with mitochondria has a direct role in release of cytochrome *c* from the mitochondria. Also, assessment of Bax expression in association with the mitochondria in p53 inhibited cells will determine whether p53-mediated inhibition of Bax will prevent the Aβ-mediated increase in Bax expression at the mitochondria.

One of the most important questions arising from the data presented in this study is the mechanism by which Aβ-mediated lysosomal destabilisation occurs, possibly resulting in release of cathepsin-L to the cytosol. Some clues are provided from the observation of increased expression of p53 and Bax at the lysosomes. Analysis of lysosomal membrane stability in p53-inhibited cells using the AO relocation technique will be beneficial in determining the exact involvement of p53 in lysosomal destabilisation. Isolation of lysosomal fractions from cultured cells will aim to clarify the quantity of increased p53 and Bax expression at these organelles. In addition, it will be important to determine whether p53 and Bax play a role in regulating lysosomal membrane proteins. Target proteins for investigation include the

lysosomal associated membrane proteins (LAMP) proteins, which have been demonstrated to play an important role in maintaining lysosomal membrane stability (Andrejewski *et al.*, 1999). To clarify whether the role of Bax at the lysosome is similar to the documented role of Bax in regulating mitochondrial stability (Zörnig et *al.*, 2001), experiments investigating the pore forming ability of Bax at the lysosome will be necessary. The effects of targeted Bax inhibition on lysosomal stability will also be useful in determining the role of Bax in Aβ-mediated destabilisation of the lysosomes.

The present study demonstrated a role for the L-type VDCC in Aβ-mediated neurodegeneration. Studies aimed at determining the mechanism of activation of this channel will provide an insight into the early events which occur in the Aβ cascade. It will be interesting to determine whether ERK plays a role in activation of these channels since previous work has demonstrated the ability of ERK to relocate from the cytosol to the membrane and to phosphorylate membrane proteins such as the L-type VDCC (Ekinci *et al.*, 1999).

VIII Bibliography

Abe, K. and Saito, H. (2000) Amyloid beta neurotoxicity not mediated by the mitogen-activated protein kinase cascade in cultured rat hippocampal and cortical neurons. *Neuroscience Letters,* **292,** 2921-2924.

Adams, J. M. and Cory, S. (1998) The Bcl-2 protein family: Arbiters of cell survival. *Science,* **281,** 1322-1326.

Adler, A. J. (1989) Selective presence of acid hydrolases in the interphotoreceptor matrix. *Experimental Eye research,* **49,** 1067-1077.

Adler, V., Pincus, M. R., Minamato, T., Fuchs, S. Y., Bluth, M. J., Brandt-Rauf, P. W., Friedman, F. K., Robinson, R. C., Chen, J. M., Wang, X. W., Harris, C. C. and Ronai, Z. (1997) Conformation-dependent phosphorylation of p53. *Proceedings of the National Academy of Sciences of the United States of America,* **94,** 1686-1691.

Akama, K. T., Albanese, C., Pestell, R. G. and Van Eldik, L. J. (1998) Amyloid beta-peptide stimulates nitric oxide production in astrocytes through an NFkappaB-dependent mechanism. *Proceedings of the National Acadamey of Sciences of the United States of America,* **95,** 5795-5800.

Akiyama, H., Arai, T., Kondo, H., Tanno, E., Haga, C. and Ikeda, K. (2000) Cell mediators of inflammation in the Alzheimer disease brain. *Alzheimer Disease and Associated Disorders,* **14,** S47-S53.

Allen, J. W., Eldadah, B. A., Huang, X., Knoblach, S. M. and Faden, A. I. (2001) Multiple caspases are involved in beta-amyloid-induced neuronal apoptosis. *Journal of Neuroscience Research,* **65,** 45-53.

Alvarez-Gonzalez, R., Pacheco-Rodriguez, G. and Mendoza-Alvarez, H. (1994) Enzymology of ADP-ribose polymer synthesis. *Molecular and Cellular Biochemistry,* **138,** 33-37.

Alzheimer, A. (1907) Über eine eigenartige Erkrankung der Hirnrinde. *Allgemeine Zietschrift fur Psychiatrie und Psychisch-gerichtliche Medizin,* **64,** 146-148.

Anderson, C. N. and Tolkovsky, A. M. (1999) A role for MAPK/ERK in sympathetic neuron survival: protection against a p53-dependent, JNK-independent induction of apoptosis by cytosine arabinoside. *Journal of Neuroscience,* **19,** 664-673.

Andrejewski, N., Punnonen, E. L., Guhde, G., Tanaka, Y., Lullmann-Rauch, R., Hartmann, D., von Figura, K. and Saftig, P. (1999) Normal lysosomal morphology and function in LAMP-1-deficient mice. *Journal of Biological Chemistry,* **274,** 12692-12701.

Appella, E. and Anderson, C. W. (2001) Post-translational modifications and activation of p53 by genotoxic stresses. *European Journal of Biochemistry,* **268,** 2764-2772.

Araujo, D. M. and Cotman, C. W. (1995) Differential effects of interleukin-1 beta and interleukin-2 on glia and hippocampal neurons in culture. *International journal of Development Neuroscience,* **13,** 201-212.

Arispe, N., Pollard, H. B. and Rojas, E. (1994) The ability of amyloid beta-protein [A beta P (1-40)] to form Ca2+ channels provides a mechanism for neuronal death in Alzheimer's disease. *Annals of the New York Academy of Sciences,* **747,** 256-266.

Armstrong, R. A. (1994) Differences in beta-amyloid (beta/A4) deposition in human patients with Down's syndrome and sporadic Alzheimer's disease. *Neuroscience Letters,* **169,** 133-136.

Ashcroft, M., Taya, Y. and Vousden, K. H. (2000) Stress signals utilize multiple pathways to stabilize p53. *Molecular and Cellular Biology,* **20,** 3224-3233.

Attardi, L. D., Lowe, S. W., Brugarolas, J. and Jacks, T. (1996) Transcriptional activation by p53, but not induction of the p21 gene, is essential for oncogene-mediated apoptosis. *European Molecular Biology Organization Journal,* **15,** 3693-3701.

Bahr, B. A. and Bendiske, J. (2002) The neuropathogenic contributions of lysosomal dysfunction. *Journal of Neurochemistry,* **83,** 481-489.

Baker, B. F., Miraglia, L. and Hagedorn, C. H. (1992) Modulation of eucaryotic initiation factor-4E binding to 5'-capped oligoribonucleotides by modified anti-sense oligonucleotides. *Journal of Biological Chemistry,* **267,** 11495-11499.

Baldwin, A. S. J. (1996) The NF-kappa B and I kappa B proteins: new discoveries and insights. *Annual Review in Immunology,* **14,** 649-683.

Barbin, G., Roisin, M. P. and Zalc, B. (2001) Tumor necrosis factor alpha activates the phosphorylation of ERK, SAPK/JNK, and P38 kinase in primary cultures of neurons. *Neurochemical Research,* **26,** 107-112.

Bard, F., Cannon, C., Barbour, R., Burke, R. L., Games, D., Grajeda, H., Guido, T., Hu, K., Huang, J., Johnson-Wood, K., Khan, K., Kholodenko, D., Lee, M., Lieberburg, I., Motter, R., Nguyen, M., Soriano, F., Vasquez, N., Weiss, K., Welch, B., Seubert, P., Schenk, D. and Yednock, T. (2000) Peripherally administered antibodies against amyloid beta-peptide enter the central nervous system and reduce pathology in a mouse model of Alzheimer disease. *Nature Medicine,* **6,** 916-919.

Barkett, M. and Gilmore, T. D. (1999) Control of apoptosis by Rel/NF-kappaB transcription factors. *Oncogene,* **18,** 6910-6924.

Barrett, A. J. and Kirschke, H. (1981) Cathepsin B, Cathepsin H, and cathepsin L. *Methods in Enzymology,* **80,** 535-561.

Bauer, J., Strauss, S., Volk, B. and Berger, M. (1991) IL-6-mediated events in Alzheimer's diseasepathology. *Immunology Today,* **12,** 217-219.

Bedridge, M. J., Bootman, M. D. and Llewelyn Roderick, H. (2003) Calcium signalling: Dynamics, Homeostasis and remodelling. *Nature Reviews Molecular Cell Biology,* **4,** 517-529.

Behl, C. (2000) Apoptosis and Alzheimer's disease. *Journal of Neural Transmission,* **107,** 1325-1344.

Behl, C., Davis, J., Cole, G. M. and Schubert, D. (1992) Vitamin E protects nerve cells from amyloid beta protein toxicity. *Biochemical and Biophysical Research Communications,* **186,** 944-950.

Behl, C., Davis, J. B., Lesley, R. and Schubert, D. (1994) Hydrogen peroxide mediated amyloid protein toxicity. *Cell,* **77,** 817-827.

Bennet, M., Macdonald, K., Chan, S. W., Luzio, J. P., Simari, P. and Weissberg, P. (1998) Cell surface trafficking of Fas: a rapid mechanism of p53-mediated apoptosis. *Science,* **282,** 290-293.

Bidere, N., Lorenzo, H. K., Carmona, S., Laforge, M., Harper, F., Dumont, C. and Senik, A. (2003) Cathepsin D Triggers Bax Activation, Resulting in Selective Apoptosis-inducing Factor (AIF) Relocation in T Lymphocytes Entering the Early Commitment Phase to Apoptosis. *Journal of Biological Chemistry,* **278,** 31401-31411.

Blacker, D. and Haines JL, R. L., Terwedow H, Go RC, Harrell LE, Perry RT, Bassett SS, Chase G, Meyers D, Albert MS, Tanzi R. (1997) ApoE-4 and age at onset of Alzheimer's disease: the NIMH genetics initiative. *Neurology,* **48,**

Blacker, D., Wilcox, M. A., Laird, N. M., Rodes, L., Horvath, S. M., Go, R., Perry, R., Watson, B. J., Bassett, S. S., McInnis, M. G., Albert, M. S., Hyman, B. T. and Tanzi,

R. E. (1998) Alpha-2 macroglobulin is genetically associated with Alzheimer disease. *Nature Genetics,* **19,** 357-360.

Blasko, I., Veerhuis, R., Stampfer-Kountchev, M., Saurwein-Teissl, M., Eikelenboom, P., Grubeck-Loebenstein, B. and Haass, C. (2000) Costimulatory effects of interferon-gamma and interleukin-1beta or tumor necrosis factor alpha on the synthesis of Abeta1-40 and Abeta1-42 by human astrocytes. *Neurobiology of Disease,* **7,** 682-689.

Blass, J. P. (2001) Brain metabolism and brain disease: is metabolic deficiency the proximate cause of Alzheimer dementia? *Journal of Neuroscience Research,* **66,** 851-856.

Blatt, N. B. and Glick, G. D. (2001) Signaling pathways and effector mechanisms pre-programmed cell death. *Bioorganic and Medicinal Chemistry,* **9,** 1371-1384.

Boado, R. J., Tsukamoto, H. and Pardridge, W. M. (1998) Drug delivery of antisense molecules to the brain for treatment of Alzheimer's disease and cerebral AIDS. *Journal of Pharmacological Sciences,* **87,** 1308-1315.

Boland, B. and Campbell, V.A. (2003a) -amyloid (1-40)-induced apoptosis of cultured cortical neurons involves calpain-mediated cleavage of poly-ADP-ribose polymerase. *Neurobiology of aging,* **24,** 179-186.

Boland, B. and Campbell, V. A.(2003b) Ab-mediated activation of the apoptotic cascade in cultured neurones: a role for cathepsin-L. *Neurobiology of aging*,in press

Boulton, T. G., Gregory, J. S. and Cobb, M. H. (1991) Purification and properties of extracellular signal-regulated kinase 1, an insulin-stimulated microtubule-associated protein 2 kinase. *Biochemistry,* **30,** 278-289.

Bowen, D. M. and Smith, C. B. (1973) Molecular changes in senile dementia. *Brain,* **96,** 849-856.

Boya, P., Andreau, K., Poncet, D., Zamzami, N., Perfettini, J. L., Metivier, D., Ojcius, D. M., Jaattela, M. and Kroemer, G. (2003) Lysosomal membrane permeabilization induces cell death in a mitochondrion-dependent fashion. *Journal of Experimental medicine,* **197,** 1323-1334.

Bozyczko-Coyne, D., O'Kane, T. M., Wu, Z. L., Dobrzanski, P., Murthy, S., Vaught, J. L. and Scott, R. W. (2001) CEP-1347/KT-7515, an inhibitor of SAPK/JNK pathway activation, promotes survival and blocks multiple events. *Journal of Neurochemistry,* **77,** 849-863.

Braak, H. and Braak, E. (1991) Neuropathological stageing of Alzheimer-related changes. *Acta Neuropathology,* **82,** 239-259.

Braak, H. and Braak, E. (1997) Frequency of Stages of Alzheimer-Related Lesions in Different Age Categories. *Neurobiology of aging,* **18,** 351-357.

Bradford, M. (1976) A Rapid and Sensitive Method for the quantification of Microgram Quantities of Protein Utilizing the Principle pf Protein-Dye Binding. *Analytical Biochemistry,* **72,** 248-254.

Breder, C. D., Tsujimoto, M., Terano, Y., Scott, D. W. and Saper, C. B. (1993) Distribution and characterization of tumor necrosis factor-like immunoreactivity in the murine central nervous system. *The Journal Of Comparative Neurology,* **337,** 543-567.

Brown, M. S., Ye, J., Rawson, R. B. and Goldstein, J. L. (2000) Regulated intramembrane proteolysis: a control mechanism conserved from bacteria to humans. *Cell,* **100,** 391-398.

Brunk, U. T., Dalen, H., Roberg, K. and Hellquist, H. B. (1997) Photo-oxidative disruption of lysosomal membranes causes apoptosis of cultured human fibroblasts. *Free Radical Biology and Medicine,* **23,** 616-626.

Brunk, U. T. and Ericsson, J. L. (1972) Cytochemical evidence for the leakage of acid phosphatase through ultrastructurally intact lysosomal membranes. *Histochemical Journal,* **4,** 479-491.

Brunk, U. T., Neuzil, J. and Eaton, J. W. (2001) Lysosomal involvement in apoptosis. *Redox Report,* **6,** 91-97.

Brunk, U. T. and Svensson, I. (1999) Oxidative stress, growth factor starvation and Fas activation may all cause apoptosis through lysosomal leak. *Redox Report,* **4,** 3-11.

Brunk, U. T. and Terman, A. (2002) The mitochondrial-lysosomal axis theory of aging: accumulation of damaged mitochondria as a result of imperfect autophagocytosis. *European Journal of Biochemistry,* **269,** 1996-2002.

Buschmann, T., Potapova, O., Bar-Shira, A., Ivanov, V., N. , Fuchs, S. Y., Henderson, S., Fried, V. A., Minamoto, T., Alarcon-Vargas, D., Pincus, M. R., Gaarde, W. A., Holbrook, N. J., Shiloh, Y. and Ronai, Z. (2001) Jun NH2-terminal kinase phosphorylation of p53 on Thr-81 is important for p53 stabilization and transcriptional activities in response to stress. *Molecular and Cellular Biology,* **21,** 2743-2754.

Butterfield, D. A., Yatin, S. M., Varadarajan, S. and Koppal, T. (1999) Amyloid beta-peptide-associated free radical oxidative stress, neurotoxicity, and Alzheimer's disease. *Methods in Enzymology,* **309,** 746-768.

Buxbaum, J. D., Liu, K. N., Luo, Y., Slack, J. L., Stocking, K. L., Peschon, J. J., Johnson, R. S., Castner, B. J., Cerretti, D. P. and Black, R. A. (1998) Evidence that tumor necrosis factor alpha converting enzyme is involved in regulated alpha-secretase

cleavage of the Alzheimer amyloid protein precursor. *Journal of Biological Chemistry,* **273,** 27765-27767.

Cadwallader, K., Beltman, J., McCormick, F. and Cook, S. (1997) Differential regulation of extracellular signal-regulated protein kinase 1 and Jun N-terminal kinase 1 by Ca2+ and protein kinase C in endothelin-stimulated Rat-1 cells. *Biochemical Journal,* **321,** 795-804.

Campbell, V. A., Segurado, R. and Lynch, M. A. (1998) Regulation of intracellular Ca2+ concentration by interleukin-1beta in rat cortical synaptosomes: an age-related study. *Neurobiology of aging,* **19,** 575-579.

Carboni, L., Carletti, R., Tacconi, S., Corrado, C. and Ferraguti, F. (1998) Differential expression of SAPK isoforms in the rat brain. An in situ hybridisation study in the adult rat brain and during post-natal development. *Molecular Brain Research,* **60,** 57-68.

Cataldo.A.M., Barnett, J. L., Berman, S. A. s., Li, J., Quarless, S., Bursztajn, S., Lippa, C. F. and Nixon, R. A. (1995) Gene expression and cellular content of cathepsin D in Alzheimer's disease brain: evidence for early up-regulation of the endosomal-lysosomal system. *Neuron,* **14,** 671-680.

Cataldo.A.M., Hamilton, D. J., Barnett, J. L., Paskevich, P. A. and Nixon, R. A. (1996) Properties of the endosomal-lysosomal system in the human central nervous system: disturbances mark most neurons in populations at risk to degenerate in Alzheimer's disease. *Jounal of Neuroscience,* **16,** 186-199.

Catterall, W. A. (1998) Structure and function of neuronal Ca2+ channels and their role in neurotransmitter release. *Cell Calcium,* **24,** 307-323.

Check, E. (2003) Battle of the mind. *Nature,* **422,** 370-372.

Chen, J. W., Madamanchi, N., Madamanchi, N. R., Trier, T. T. and Keherly, M. J. (2001) Lamp-1 is upregulated in human glioblastoma cell lines induced to undergo apoptosis. *Journal of Biomedical Science,* **8,** 365-374.

Chen, Y. R., Meyer, C. F. and Tan, T. H. (1996) Persistent activation of c-Jun N-terminal kinase 1 (JNK1) in gamma radiation-induced apoptosis. *Journal of Biological Chemistry,* **271,** 631-634.

Cheng, W. H., Zheng, X., Quimby, F. R., Roneker, C. A. and Lei, X. G. (2001) Low levels of glutathione peroxidase 1 activity in selenium-deficient mouse liver affect c-Jun N-terminal kinase activation and p53 phosphorylation on Ser-15 in pro-oxidant-induced aponecrosis. *Biochemical Journal,* **370,** 927-934.

Chomczynski. P. and Sacchi, N. (1987) Single-step method of RNA isolation by acid guanidinium thiocyanate-phenol-chloroform extraction. *Analytical Biochemistry.,* **162,** 156-159.

Christen, Y. (2000) Oxidative stress and Alzheimer disease. *American Journal of Clinical Nutrition,* **71,** 621S-629S.

Coogan, A. and O'Connor, J. J. (1997) Inhibition of NMDA receptor-mediated synaptic transmission in the rat dentate gyrus in vitro by IL-1 beta. *Neuroreport,* **8,** 2107-2110.

Crooke, S. T. (1992) Therapeutic applications of oligonucleotides. *Annual Review of Pharmacology and Toxicology,* **32,** 329-376.

Crooke, S. T. (1996) Progress in antisense therapeutics Medical Research Review. *Cell,* **77,** 841-852.

Culmsee, C., Zhu, X., Yu, Q. S., Chan, S. L., Camandola, S., Guo, Z., Greig, N. H. and Mattson, M. (2001) A synthetic inhibitor of p53 protects neurons against death induced

by ischemic and excitotoxic insults, and amyloid beta-peptide. *Journal of Neurochemistry,* **77,** 220-228.

Davis, J. B. (1996) Oxidative mechanisms in beta-amyloid cytotoxicity. *Neurodegeneration,* **5,** 441-444.

De Duve, C. (1969) Evolution of the peroxisome. *Annals of the New York Academy of Sciences,* **168,** 369-381.

De la Monte, S. M., Sohn, Y. K. and Wands J, R. (1997) Correlates of p53- and Fas (CD95)-mediated apoptosis in Alzheimer's disease. *Journal of the Neurological Sciences,* **152,** 73-83.

De Strooper, B., Saftig, P., Craessaerts, K., Vanderstichele, H., Guhde, G., Annaert, W., Von Figura, K. and Van Leuven, F. (1998) Deficiency of presenilin-1 inhibits the normal cleavage of amyloid precursor protein. *Nature,* **391,** 387-390.

Dekroom, R. M. and Armati, P. J. (2001) Synthesis and processing of apoE in human brain cultures. *Glia,* **33,** 298-305.

DeMattos, R. B., Bales, K. R., Cummins, D. J., Dodart, J. C., Paul, S. M. and Holtzman, D. M. (2001) Peripheral anti-A beta antibody alters CNS and plasma A beta clearance and decreases brain A beta burden in a mouse model of Alzheimer's disease. *Proceedings of the National Acadamey of Sciences of the United States of America,* **98,** 8850-8855.

Denk, A., Wirth, T. and Baumann, B. (2000) NF-kappaB transcription factors: critical regulators of hematopoiesis and neuronal survival. *Cytokine Growth Factor Review,* **11,** 303-320.

Dickens, M., Rogers, J. S., Cavanagh, J., Raitano, A., Xia, Z., Halpern, J. R., Greenberg, M. E., Sawyers, C. L. and Davis, R. J. (1997) A cytoplasmic inhibitor of the JNK signal transduction pathway. *Science,* **277,** 693-696.

Dinarello, C. A. (1996) Biologic basis for interleukin-1 in disease. *Blood,* **87,** 2095-2147.

Ditaranto-Desimone, K., Saito, M., Tekirian, T. L., Saito, M., Berg, M., Dubowchik, G. M., Soreghan, B., Thomas, S., Marks, N. and Yang, A. J. (2003) Neuronal endosomal/lysosomal membrane destabilization activates caspases and induces abnormal accumulation of the lipid secondary messenger ceramide. *Brain Research Bulletin,* **59,** 523-531.

Dolphin, A. C. (1995) The G.L. Brown Prize Lecture. Voltage-dependent calcium channels and their modulation by neurotransmitters and G proteins. *Experimental Physiology,* **80,** 1-36.

Dowjat, W. K., Wisniewski, T., Efthimiopoulos, S. and Wisniewski, H. M. (1999) Inhibition of neurite outgrowth by familial Alzheimer's disease-linked presenilin-1 mutations. *Neuroscience Letters,* **267,** 141-144.

Drache, B., Diehl, G. E., Beyreuther, K., Perlmutter, L. S. and Konig, G. (1997) Bcl-xl-specific antibody labels activated microglia associated with Alzheimer's disease and other pathological states. *Journal of Neuroscience Research,* **47,** 98-108.

Droogmans, G. and Nilius, B. (1989) Kinetic properties of the cardiac T-type calcium channel in the guinea-pig. *Journal of Physiology,* **419,** 627-650.

Eikelenboom, P., Bate, C., Van Gool, W. A., Hoozemans, J. J., Rozemuller, J. M., Veerhuis, R. and Williams, A. (2002) Neuroinflammation in Alzheimer's disease and prion disease. *Glia,* **40,** 232-239.

Eilers, A., Whitfield, J., Shah, B., Spadoni, C., Desmond, H. and Ham, J. (2001) Direct inhibition of c-Jun N-terminal kinase in sympathetic neurones prevents c-jun promoter activation and NGF withdrawal-induced death. *Journal of Neurochemistry,* **76,** 1439-1454.

Ekinci, F. J., Linsley, M. D. and Shea, T. B. (2000) Beta-amyloid-induced calcium influx induces apoptosis in culture by oxidative stress rather than tau phosphorylation. *Brain Research Molecular Brain Research,* **76,** 389-395.

Ekinci, F. J., Malik, K. U. and Shea, T. B. (1999) Activation of the L voltage-sensitive calcium channel by mitogen-activated protein (MAP) kinase following exposure of neuronal cells to beta-amyloid. MAP kinase mediates beta-amyloid-induced neurodegeneration. *Journal of Biological Chemistry,* **274,** 30322-30327.

Eldadah, B. A., Yakovlev, A. G. and Faden, A. I. (1997) The role of CED-3-related cysteine proteases in apoptosis of cerebellar granule cells. *Journal of Neuroscience,* **17,** 6105-6113.

Ellis, R. E., Yuan, J. Y. and Horvitz, H. R. (1991) Mechanisms and functions of cell death. *Annual Review of Cell and Developmental Biology,* **7,** 663-698.

Enokido, Y., Araki, T., Tanaka, K., Aizawa, S. and Hatanaka, H. (1996) Involvement of p53 in DNA strand break-induced apoptosis in postmitotic CNS neurons. *European Journal of Neuroscience,* **8,** 1812-1821.

Enslen, H., Tokumitsu, H., Stork, P. J., Davis, R. J. and Soderling, T. R. (1996) Regulation of mitogen-activated protein kinases by a calcium/calmodulin-dependent protein kinase cascade. *Proceedings of the National Acadamey of Sciences of the United States of America,* 10803-10808.

Estibeiro, P. and Godfray, J. (2001) Antisense as a neuroscience tool and therapeutic agent. *Trends in Neurosciences,* **24,** S56-S62.

Evan, G. and Littlewood, T. (1998) A matter of life and cell death. *Science,* **281,** 1317-1322.

Farrar, W. L., Kilian, P. L., Ruff, M. R., Hill, J. M. and Pert, C. B. (1987) Visualization and characterization of interleukin 1 receptors in brain. *Journal of Neuroimmunology,* **139,** 459-463.

Forloni, G., Demicheli, F., Giorgi, S., Bendotti, C. and Angeretti, N. (1992) Expression of amyloid precursor protein mRNAs in endothelial, neuronal and glial cells: modulation by interleukin-1. *Brain Research Molecular Brain Research,* **16,** 128-134.

Forloni, G., Mangiarotti, F., Angeretti, N., Lucca, E. and De Simoni, M. G. (1997) Beta-amyloid fragment potentiates IL-6 and TNF-alpha secretion by LPS in astrocytes but not in microglia. *Cytokine Growth Factor Review,* **9,** 759-762.

Fu, W., Luo, H., Parthasarathy, S. and Mattson, M. P. (1998) Catecholamines potentiate amyloid beta-peptide neurotoxicity: involvement of oxidative stress, mitochondrial dysfunction, and perturbed calcium homeostasis. *Neurobiology of Disease,* **5,** 229-243.

Fuchs, S. Y., Adler, V., M.R., P. and Z., R. (1998) MEKK1/JNK signaling stabilizes and activates p53. *Proceedings of the National Acadamey of Sciences of the United States of America,* **95,** 10541-10546.

Fuchs, S. Y., Xie, B., Adler, V., Fried, V. A., Davis, R. J. and Z., R. (1997) c-Jun NH2-terminal kinases target the ubiquitination of their associated transcription factors. *Journal of Biological Chemistry,* **272,** 32163-32168.

Fuduka, M., Gotoh, Y. and Nishida, E. (1997) Interaction of MAP kinase with MAP kinase kinase: its possible role in the control of nucleocytoplsmic transport of MAP kinase. *European Molecular Biology Organization Journal,* **16,** 1901-1908.

Gandy, S. and Petanceska, S. (2000) Regulation of Alzheimer -amyloid precursor trafficking and metabolism. *Biochimica et Biophysica Acta,* **1502,** 44-52.

Gao, G. and Dou, Q. P. (2000) N-terminal cleavage of bax by calpain generates a potent proapoptotic 18-kDa fragment that promotes bcl-2-independent cytochrome C release and apoptotic cell death. *Journal of Cellular Biochemistry,* **80,** 53-72.

Gardella, S., Andrei, C., Lotti, L. V., Poggi, A., Torrisi, M. R., Zocchi, M. R. and Rubartelli, A. (2001) CD8(+) T lymphocytes induce polarized exocytosis of secretory lysosomes by dendritic cells with release of interleukin-1beta and cathepsin D. *Blood,* **98,** 2152-2159.

Geisow, M. (1982) Lysosome proton pump identified. *Nature,* **298,** 515-516.

Ginham, R., Harrison, D. C., Facci, L., Skaper, S. and Philpott, K. L. (2001) Upregulation of death pathway molecules in rat cerebellar granule neurons undergoing apoptosis. *Neuroscience Letters,* **302,** 113-116.

Giometto, B., Argentiero, V., Sanson, F., Ongaro, G. and Tavolato, B. (1988) Acute-phase proteins in Alzheimer's disease. *European Neurology,* **28,** 30-33.

Giovanni, A., Keramaris, E., Morris, E. J., Hou, S. T., O'Hare, M., Dyson, N., Robertson, G. S., Slack, R. S. and Park, D. S. (2000) E2F1 mediates death of B-amyloid-treated cortical neurons in a manner independent of p53 and dependent on Bax and caspase 3. *Journal of Biological Chemistry,* **275,** 11553-11560.

Glading, A., Uberall, F., Keyse, S. M., Lauffenburger, D. A. and Wells, A. (2001) Membrane proximal ERK signaling is required for M-calpain activation downstream of epidermal growth factor receptor signaling. *Journal of Biological Chemistry,* **276,** 23341-23348.

Goate, A., Chartier-Harlin, M. C., Mullan, M., Brown, J., Crawford, F., Fidani, L., Giuffra, L., Haynes, A., Irving, N. and James, L. (1991) Segregation of a missense mutation in the amyloid precursor protein gene with familial Alzheimer's disease. *Nature,* **349,** 704-706.

Gobeil S, B. C., Nadeau D, Poirier GG. (2001) Characterization of the necrotic cleavage of poly(ADP-ribose) polymerase (PARP-1): implication of lysosomal proteases. *Cell Death Differention,* **8,** 588-594.

Goldman, J. and Cote, L. 1991. Aging of the brain:Dementia of the Alzheimer's type. Kandel, E.R., Schwartz, J.Z. and Jessel, T.M. *Principles of Neural Science*, **3rd edition**, 974-983. Apppelton & Lange Nowralk, Connecticut, USA.

Goodman, Y. and Mattson, M. P. (1994) Secreted forms of beta-amyloid precursor protein protect hippocampal neurons against amyloid beta-peptide-induced oxidative injury. *Experimental Neurology,* **128,** 1-12.

Grammas, P. and Ovase, R. (2001) Inflammatory factors are elevated in brain microvessels in Alzheimer's disease. *Neurobiology of aging,* **22,** 837-842.
Green, D. R. and Reed, J. C. (1998) Mitochondria and apoptosis. *Science,* **281,** 1309-1312.

Green, K. N. and Peers, C. (2001) Amyloid beta peptides mediate hypoxic augmentation of Ca(2+) channels. *Journal of Neurochemistry,* **77,** 953-956.

Griffin, W. S., Sheng, J. G., Roberts, G. W. and Mrak, R. E. (1995) Interleukin-1 expression in different plaque types in Alzheimer's disease: significance in plaque evolution. *Journal of Neuropathological and Experimental Neurology,* **54,** 276-281.

Griffin, W. S. T., Stanley, L. C., Ling, C., White, L., Macleod, V., Perrot, L. J., White, C. L. I. and Araoz, C. (1989) Brain interleukin 1 and S-100 immunoreactivity are

elevated in Down syndrome and Alzheimer's disease. *Proceedingsa of the National Acadamey of Sciences of the United States of America,* **86,** 7611-7615.

Grilli, M., Pizzi, M., Memo, M. and Spano, P. (1996) Neuroprotection by aspirin and sodium salicylate through blockade of NF-kappaB activation. *Science,* **274,** 1383-1385.

Grynkiewicz, G., Poenie, M. and Tsíen, R. Y. (1985) A new generation of Ca2+ indicators with greatly improved fluorescence properties. *Journal of Biological Chemistry,* **260,** 3440-3450.

Guicciardi, M. E., Deussing, J., Miyoshi, H., Bronk, S. F., Svingen, P. A., Peters, C., Kaufmann, S. H. and Gores, G. J. (2000) Cathepsin B contributes to TNF-alpha-mediated hepatocyte apoptosis by promoting mitochondrial release of cytochrome c. *Journal of Clinical Investigation,* **106,** 1127-1137.

Guo, Q., Fu, W., Xie, J., Luo, H., Sells, S. F., Geddes, J. W., Bondada, W., V.M, R. and Mattson, M. P. (1998) Par-4 is a mediator of neuronal degeneration associated with the pathogenesis of Alzheimers disease. *Nature,* **4,** 957-962.

Gupta, S., Barrett, T., Whitmarsh, A. J., Cavanagh, J., Sluss, H. K., Derijard, B. and Davis, R. J. (1996) Selective interaction of JNK protein kinase isoforms and transcription factors. *European Molecular Biology Organization Journal,* **15,** 2760-2770.

Gupta, S., Campbell, D., Derijard, B. and Davis, R. (1995) Transcription factor ATF2 regulation by the JNK signal transduction pathway. *Science 267, 389-393.,* **267,** 389-393.

Haass, C. and De Strooper, B. (1999) The Presenilins in Alzheimer's Disease--Proteolysis Holds the Key. *Science,* **286,** 916-919.

Haass, C., Schlossmacher, M. G., Hung, A. Y., Vigo-Pelfrey, C., Mellon, A., Ostaszewski, B. L., Lieberburg, I., Koo, E. H. and Schenk, D. T. D. e. a. (1992) Amyloid beta-peptide is produced by cultured cells during normal metabolism. *Nature,* **359,** 322-325.

Haass, C. and Selkoe, D. J. (1993) Cellular processing of -amyloid precursor protein and the genesis of Amyloid -peptide. *Cell,* **75,** 1039-1042.

Harada, J. and Sugimoto, M. (1999) Activation of caspase-3 in beta-amyloid-induced apoptosis of cultured rat cortical neurons. *Brain Research,* **842,** 311-323.

Hardy, J., Duff, K., Hardy, K. G., Perez-Tur, J. and Hutton, M. (1998) Genetic dissection of Alzheimer's disease and related dementias: amyloid and its relationship to tau. *Nature Neuroscience,* **1,** 355-358.

Hardy, J. and Selkoe, D. J. (2002) The amyloid hypothesis of Alzheimer's disease: progress and problems on the road to therapeutics. *Science,* **297,** 353-356.

Hashiguchi, M., Sobue, K. and Paudel, H. K. (2000) 14-3-3 Is an Effector of Tau Protein Phosphorylation. *Journal of Biological Chemistry,* **275,** 25247-25254.

He, L. M., Chen, L. Y., Lou, X. L., Qu, A. L., Zhou, Z. and Xu, T. (2002) Evaluation of -amyloid peptide 25–35 on calcium homeostasis in cultured rat dorsal root ganglion neurons. *Brain Research,* **939,** 65-75.

Herdegen, T., Skene, P. and Bähr, M. (1997) The c-Jun transcription factor-bipotential mediator of neuronal cell death, survival and regeneration. *Trends in Neurosciences,* **20,** 227-231.

Herr, I. and Debatin, K. M. (2001) Cellular stress response and apoptosis in cancer therapy. *Blood,* **98,** 2603-2614.

Hetman, M. and Xia, Z. (2000) Signaling pathways mediating anti-apoptotic action of neurotrophins. *Acta Neurobiologiae experimentalis,* **60,** 531-545.

Hibi, M., Lin, A., Smeal, T., Minden, A. and Karin, M. (1993) Identification of an oncoprotein- and UV-responsive protein kinase that binds and potentiates the c-Jun activation domain. *Genes & Development,* **7,** 2135-2148.

Hirai, S. (2000) Alzheimer disease: current therapy and future therapeutic strategies. *Alzheimer Disease and Associated Disorders,* **14,** S11-S17.

Hishita, T., Tada-Oikawa, S., Tohyama, K., Miura, Y., Nishihara, T., Tohyama, Y., Yoshida, Y., Uchiyama, T. and Kawanishi, S. (2001) Caspase-3 activation by lysosomal enzymes in cytochrome c-independent apoptosis in myelodysplastic syndrome-derived cell line P39. *Cancer research,* **61,** 2878-2884.

Hochedlinger, K., Wagner, E. F. and Sabapathy, K. (2002) Differential effects of JNK1 and JNK2 on signal specific induction of apoptosis. *Oncogene,* **21,** 2441-2445.

Holtzman, D. M., Bales, K. R., Tenkova, T., Fagan, A. M., Parsadanian, M., Sartorius, L. J., Mackey, B., Olney, J., McKeel, D., Wozniak, D. and Paul, S. M. (2000) Apolipoprotein E isoform-dependent amyloid deposition and neuritic degeneration in a mouse model of Alzheimer's disease. *Proceedings of the National Acadamey of Sciences for the United States of America,* **97,** 2892-2897.

Hopkins, S. J. and Rothwell, N. J. (1995) Cytokines and the nervous system. I: Expression and recognition. *Trends in Neurosciences,* **18,** 83-88.

Howlett, D. R., Simmons, D. L., Dingwall, C. and Christie, G. (2000) In search of an enzyme: the -secretase of Alzheimers's disease is an aspartic proteinase. *Trends in neurosciences,* **23,** 565-572.

Hreniuk, D., Garay, M., Gaarde, W., Monia, B., McKay, R. and Cioffi, C. L. (2001) Inhibition of c-Jun N-terminal kinase 1, but not c-Jun N-terminal kinase 2, suppresses

apoptosis induced by ischemia/reoxygenation in rat cardiac myocytes. *Molecular Pharmacology,* **59,** 867-874.

Hu, J. and Van Eldik, L. J. (1999) Glial-derived proteins activate cultured astrocytes and enhance beta amyloid-induced glial activation. *Brain Research,* **842,** 46-54.

Hu, S., Peterson, P. K. and Chao, C. C. (1997) Cytokine-mediated neuronal apoptosis. *Neurochemistry International,* **30,** 427-431.

Huang, H.M., Ou, H.C. and Hsieh, S.J. (2000) Antioxidants prevent amyloid peptide-induced apoptosis and alteration of calcium homeostasis in cultured cortical neurons. *Life Sciences*, **66**, 1879-1892.

Hutton, M., Lendon, C. L., Rizzu, P., Baker, M., Froelich, S., Houlden, H., Pickering-Brown, S., Chakraverty, S., Isaacs, A., Grover, A., Hackett, J., Adamson, J., Lincoln, S., Dickson, D., Davies, P., Petersen, R. C., Stevens, M., de Graaff, E., Wauters, E., van Baren, J., Hillebrand, M., Joosse, M., Kwon, J. M., Nowotny, P. and Heutink, P. (1998) Association of missense and 5'-splice-site mutations in tau with the inherited dementia FTDP-17. *Nature,* **18,** 702-705.

Imafuku, I., Masaki, T., Waragai, M., Takeuchi, S., Kawabata, M., Hirai, S., Ohno, S., Nee, L. E., Lippa, C. F., Kanazawa, I., Imagawa, M. and Okazawa, H. (1999) Presenilin 1 suppresses the function of c-Jun homodimers via interaction with QM/Jif-1. *Journal of Cell Biology,* **147,** 121-134.

Ishisaka, R., Utsumi, T., Kanno, T., Arita, K., Katunuma, N., Akiyama, J. and Utsumi, K. (1999) Participation of a cathepsin L-type protease in the activation of caspase-3. *Cell Structure and Function,* **24,** 465-470.

Ishiura, S., Murofushi, H., K., S. and K., I. (1978) Studies of a calcium-activated neutral protease from chicken skeletal muscle. I. Purification and characterization. *Journal of Biochemistry,* **84,** 225-230.

Ito, Y., Mishra, N. C., Yoshida, K., Kharbanda, S., Saxena, S. and D., K. (2001) Mitochondrial targeting of JNK/SAPK in the phorbol ester response of myeloid leukemia cells. *Cell Death and Differentiation,* **8,** 794-800.

Iwasaki, K., Sunderland, T., Kusiak, J. W. and Wolozin, B. (1996) Changes in gene transcription during A-mediated cell death. Molec. Psychiatry 1 (1996), pp. 65–71. Abstract-MEDLINE. *Molecular Psychiatry,* **1,** 65-71.

Iwatsubo, T., Odaka, A., Suzuki, N., Mizusawa, H., Nukina, N. and Ihara, Y. (1994) Visualization of A beta 42(43) and A beta 40 in senile plaques with end-specific A beta monoclonals: evidence that an initially deposited species is A beta 42(43). *Neuron,* **13,** 45-53.

Ji, Z. S., Miranda, R. D., Newhouse, Y. M., Weisgraber, K. H., Huang, Y. and Mahley, R. W. (2002) Apolipoprotein E4 potentiates amyloid beta peptide-induced lysosomal leakage and apoptosis in neuronal cells. *Journal of Biological Chemistry,* **277,** 21821-21828.

Johnson, T. M., Yu, Z. X., Ferrans, V. J., Lownstein, R. A. and Finkel, T. (1996) Reaction oxgen species are downstream mediators of p53-dependent apoptosis. *Proceedings of the National Acadamey of Sciences of the United States of America,* **93,** 11848-11852.

Jordan, J., Galindo, M. F., Prehn, J. H., Weichselbaum, R. R., Beckett, M., Ghadge, G. D., Roos, R. P., Leiden, J. M. and Miller, R. J. (1997) p53 expression induces apoptosis in hippocampal pyramidal neuron cultures. *Journal of Neuroscience,* **17,** 1397-1405.

Kaltschmidt, B., Uherek, M., Volk, B., Baeuerle, P. A. and Kaltschmidt, C. (1997) Transcription factor NF-kappaB is activated in primary neurons by amyloid beta peptides and in neurons surrounding early plaques from patients with Alzheimer

disease. *Proceedings of the National Acadamey of Sciences of the United States of America,* **94,** 2642-2647.

Kaltschmidt, B., Uherek, M., Wellmann, H., Volk, B. and Kaltschmidt, C. (1999) Inhibition of NF-kappaB potentiates amyloid beta-mediated neuronal apoptosis. *Proceedings of the National Acadamey of Sciences of the United States of America,* 9409-9414.

Kang, J., Lemaire, H. G., Unterbeck, A., Salbaum, J., Masters, C., Grzeschik, K., Multhaup, G., Beyreuther, K. and Müller-Hill, B. (1987) The precursor of Alzheimer's disease resembles a cell surface receptor. *Nature,* **325,** 733-736.

Karpinich, N. O., Tafani, M., Rothman, R. J., Russo, M. A. and Farber, J. L. (2002) The course of etoposide-induced apoptosis from damage to DNA and p53 activation to mitochondrial release of cytochrome c. *Journal of Biological Chemistry,* **277,** 16547-16552.

Kasama, T., Kobayashi, K., Fukushima, T., Tabata, M., Ohno, I., Negishi, M., Ide, H., Takahashi, T. and Niwa, Y. (1989) Production of interleukin 1-like factor from human peripheral blood monocytes and polymorphonuclear leukocytes by superoxide anion: the role of interleukin 1 and reactive oxygen species in inflamed sites. *Clinical Immunology and Immunopathology,* **53,** 439-448.

Keppler, D., Sameni, M., Moin, K., Mikkelsen, T., Diglio, C. A. and Sloane, B. F. (1996) Tumor progression and angiogenesis: cathepsin B & Co. *Biochemistry and Cell Biology,* **74,** 799-810.

Kerr, J., Wyllie, A. H. and Currie, A. R. (1972) Apoptosis: a basic biological phenomenon with wide-ranging implications in tissue kinetics. *British Journal of Cancer,* **26,** 239-257.

Kim, E. S., Kim, R. S., Ren, R. F., Hawver, D. B. and Flanders, K. C. (1998) Transforming growth factor-beta inhibits apoptosis induced by beta-amyloid peptide fragment 25-35 in cultured neuronal cells. *Brain Research Molecular Brain Research,* **62,** 122-130.

Kitamura, Y., Shimohama, S., Kamoshima, W., Matsuoka, Y., Nomura, Y. and Taniguchi, T. (1997) Changes of p53 in the brains of patients with Alzheimer's disease. *Biochem Biophys Res Commun.,* **232,** 418-421.

Ko, H. W., Park, K. Y., Kim, H., Han, P. L., Kim, Y. U., Gwag, B. J. and Choi, E. J. (1998) Ca2+-mediated activation of c-Jun N-terminal kinase and nuclear factor kappa B by NMDA in cortical cell cultures. *Journal of Neurochemistry,* **71,** 1390-1395.

Kobayashi, T. and Mori, Y. (1998) Ca2+ channel antagonists and neuroprotection from cerebral ischemia. *European Journal of Pharmacology,* **363,** 1-15.

Korsmeyer , S. (1999) BCL-2 gene family and the regulation of programmed cell death. *Journal of Cancer Research,* **59,** 1693-1700.

Korsmeyer, S. J. (1995) Regulators of cell death. *Trends in Genetics,* **11,** 101-105.

Kothakota, S., Azuma, T., Reinhard, C., Klippel, A., Tang, J., Chu, K., McGarry, T. J., Kirschner, M. W., Koths, K., Kwiatkowski, D. J. and Williams, L. T. (1997) Caspase-3-generated fragment of gelsolin:effector of morphological change in apoptosis. *Science,* **278,** 294-298.

Kowall, N. W., Beal, M. F., Busciglio, J., Duffy, L. K. and Yankner, B. A. (1991) An in vivo model for the neurodegenerative effects of beta amyloid and protection by substance P. *Proceedings of the National Acadamey of Sciences of the United States of America,* **88,** 7247-7251.

Kroemer, G., Zamzami, N. and Susin, S. (1997) Mitochondrial conrol of apoptosis. *Immunology today,* **18,** 44-51.

Kruman, I. I. and Mattson, M. P. (1999) Pivotal role of mitochondrial calcium uptake in neural cell apoptosis and necrosis. *Journal of Neurochemistry,* **72,** 529-540.

Kuan, C. Y., Yang, D. D., Samanta Roy, D. R., Davis, R. J., Rakic, P. and Flavell, R. A. (1999) The Jnk1 and Jnk2 protein kinases are required for regional specific apoptosis during early brain development. *Neuron,* **22,** 667-676.

Kuida, K., Zheng, T. S., Na, S., Kuan, C., Yang, D., Karasuyama, H., Rakic, P. and Flavell, R. A. (1996) Decreased apoptosis in the brain and premature lethality in CPP32-deficient mice. *Nature,* **384,** 368-372.

Kundra, R. and Kornfeld, S. (1999) Asparagine-linked oligosaccharides protect Lamp-1 and Lamp-2 from intracellular proteolysis. *Journal of Biological Chemistry,* **274,** 31039-31046.

LaFerla, F. M., Hall, C. K., Ngo, L. and Jay, G. (1996) Extracellular deposition of beta-amyloid upon p53-dependent neuronal cell death in transgenic mice. *Journal of Clinical Investigation,* **98,** 1626-1232.

Lechan, R. M., Toni, R., Clark, B. D., Cannon, J. G., Shaw, A. R., Dinarello, C. A. and Reichlin, S. (1990) Immunoreactive interleukin-1 beta localization in the rat forebrain. *Brain Research,* **514,** 135-114-130.

Lee, F. S., Hagler, J., Chen, Z. J. and Maniatis, T. (1997) Activation of the IkB kinase complex by MEKK1, a kinase of the JNK pathway. *Cell,* **88,** 213-222.

Lee, J. T. J. and McCubrey, J. A. (2002) The Raf/MEK/ERK signal transduction cascade as a target for chemotherapeutic intervention in leukemia. *Leukemia,* **16,** 486-507.

Lee, Y. B., Nagai, A. and Kim, S. U. (2002) Cytokines, chemokines, and cytokine receptors in human microglia. *Journal of Neuroscience Research,* **69,** 94-103.

Lees-Miller, S. P., Chen, Y. R. and Anderson, C. W. (1990) Human cells contain a DNA-activated protein kinase that phosphorylates simian virus 40 T antigen, mouse p53, and the human Ku autoantigen. *Molecular and Cellular Biology,* **10,** 6472-6481.

Levine, A. (1997) p53 the Cellular Gatekeeper for Growth and Division. *Cell,* **88,** 323-331.

Lewis, J., Dickson, D. W., Lin, W. L., Chisholm, L., Corral, A., Jones, G., Yen, S. H., Sahara, N., Skipper, L., Yager, D., Eckman, C., Hardy, J., Hutton, M. and McGowan, E. (2001) Enhanced neurofibrillary degeneration in transgenic mice expressing mutant tau and APP. *Science,* **293,** 1487-1491.

Li, P., Nijhawan, D., Budihardjo, I., Srinivasula, S. M., Ahmad, M., Alnemri, E. S. and Wang, X. (1997) Cytochrome c and dATP-dependent formation of Apaf-1/caspase-9 complex initiates an apoptotic protease cascade. *Cell,* **91,** 479-489.

Li, W., Yuan, X. M., Nordgren, G., Dalen, H., Dubowchik, G. M., Firestone, R. A. and Brunk, U. T. (2000) Induction of cell death by the lysosomotropic detergent MSDH. *FEBS Letters,* 35-39.

Lin, H. Y., Shih, A., Davis, F. B., Tang, H. Y., Martino, L. J., Bennett, J. A. and Davis, P. J. (2002b) Resveratrol induced serine phosphorylation of p53 causes apoptosis in a mutant p53 prostate cancer cell line. *Journal of Urology,* **168,** 748-755.

Loo, D. T., Copani, A. P., Pike, C. J., Whittemore, E. R., Walencewicz, A., J., and Cotman, C. W. (1993) Apoptosis is induced by beta-amyloid in cultured central nervous system neurons. *Proceedings of the National Acadamey of Sciences of the United States of America,* **90,** 7951-7955.

Love, S., Barber, R. and Wilcock, G. K. (1999) Increased poly(ADP-ribosyl)ation of nuclear proteins in Alzheimer's disease. *Brain,* **122,** 247-254.

Lu, H., Taya, Y., Ikeda, M. and Levine, A. J. (1998) Ultraviolet radiation, but not gamma radiation or etoposide-induced DNA damage, results in the phosphorylation of the murine p53 protein at serine-389. *Proceedings of the National Acadamey of Sciences of the United States of America,* **95,** 6399-6404.

Luetjens, C. M., Lankiewicz, S., Bui, N. T., Krohn, A. J., Poppe, M. and Prehn, J. H. M. (2001) Up-regulation of Bcl-xL in response to subtoxic -amyloid: role in neuronal resistance against apoptotic and oxidative injury. *Neuroscience,* **102,** 139-150.

Luo, C., Zhu, C., Jiang, J., Lu, Y., Zhang, G., Yuan, G., Cai, R. and Ye, T. (1999) Alterations of bcl-2, bcl-x and bax protein expressions in area CA-3 of rat hippocampus following fluid percussion brain injury. *Chin J Traumatol,,* **2,** 101-104.

Lynch, A. M. and Lynch, M. A. (2002) The age-related increase in IL-1 type I receptor in rat hippocampus is coupled with an increase in caspase-3 activation. *European Journal of Neuroscience,* **15,** 1779-1788.

Mackenzie, I. R., Hao, C. and Munoz, D. G. (1995) Role of microglia in senile plaque formation. *Neurobiology of aging,* **16,** 797-804.

MacManus, A., Ramsden, M., Murray, M., Henderson, Z., Pearson, H. A. and Campbell, V. A. (2000) Enhancement of (45)Ca(2+) influx and voltage-dependent Ca(2+) channel activity by beta-amyloid-(1-40) in rat cortical synaptosomes and cultured cortical neurons. Modulation by the proinflammatory cytokine interleukin-1beta. *Journal of Biological Chemistry,* **275,** 4713-4718.

Mahajan, N. P., Linder, K., Berry, G., Gordon, G. W., Heim, R. and Herman, B. (1998) Bcl-2 and Bax interactions in mitochondria probed with green fluorescent protein and fluorescence resonance energy transfer. *Nature Biotechnology,* **16,** 547-552.

Marais, R. W. J. and Treisman, R. (1993) The SRF Accessory Protein Elk-1 Contains a Growth Factor-regulated Transcriptional Activation Domain. *Cell,* **73,** 381-393.

Marchenko, N., Zaika, A. and Moll, U. M. (2000) Death signal-induced localization of p53 protein to mitochondria. A potential role in apoptotic signaling. *Journal of Biological Chemistry,* **275,** 16202-16212.

Marin, N., Romero, B., Bosch-Morell, F., Llansola, M., Felipo, V., Roma, J. and Romero, F. J. (2000) Beta-amyloid-induced activation of caspase-3 in primary cultures of rat neurons. *Mechanisms of Ageing and Development,* **119,** 63-67.

Maroney, A. C., Finn, J. P., Bozyczko-Coyne, D., O'Kane, T. M., Neff, N. T., Tolkovsky, A. M., Park, D. S., Yan, C. Y., Troy, C. M. and Greene, L. A. (1999) CEP-1347 (KT7515), an inhibitor of JNK activation, rescues sympathetic neurons and neuronally differentiated PC12 cells from death evoked by three distinct insults. *Journal of Neurochemistry,* **73,** 1901-1912.

Marshall, C. J. (1995) Specificity of receptor tyrosine kinase signaling: transient versus sustained extracellular signal-regulated kinase activation. *Cell,* **80,** 179-185.

Martin, D. S., Lonergan, P. E., Boland, B., Fogarty, M. P., Brady, M., Horrobin, D. F., Campbell, V. A. and M.A., L. (2002) Apoptotic Changes in the Aged Brain Are Triggered by Interleukin-1beta -induced Activation of p38 and Reversed by Treatment with Eicosapentaenoic Acid. *Journal of Biological Chemistry,* **277,** 34239-34246.

Masliah, E., Mallory, M., Alford, M., Tanaka, S. and Hansen, L. A. (1998) Caspase dependent DNA fragmentation might be associated with excitotoxicity in Alzheimer disease. *Journal of Neuropathology and Experimental Neurology,* **57,** 1041-1052.

Mason, R. W. and Massey, S. D. (1992) Surface activation of pro-cathepsin L. *Biochemical and Biophysical Research Communications,* **189,** 1659-1666.

Mattson, M. and Camandola, S. (2001) NF-kB in neuronal plasticity and neurodegenerative disorders. *Clinical Investigation,* **107,** 247-254.

Mattson, M. P., Barger, S. W., Cheng, B., Lieberburg, I., Smith-Swintosky, V. L. and Rydel, R. E. (1993b) beta-Amyloid precursor protein metabolites and loss of neuronal Ca2+ homeostasis in Alzheimer's disease. *Trends in Neurosciences,* **16,** 409-414.

Mattson, M. P., Cheng, B., Culwell, A. R., Esch, F. S., Lieberburg, I. and Rydel, R. E. (1993a) Evidence for excitoprotective and intraneuronal calcium-regulating roles for secreted forms of the beta-amyloid precursor protein. *Neuron,* **10,** 243-254.

Mattson, M. P., Cheng, B., Davis, D., Bryant, K., Lieberburg, I. and Rydel, R. E. (1992) beta-Amyloid peptides destabilize calcium homeostasis and render human cortical neurons vulnerable to excitotoxicity. *Journal of Neuroscience,* **12,** 376-389.

McDonald, D. R., Bamberger, M. E., Combs, C. K. and Landreth, G. E. (1998) beta-Amyloid fibrils activate parallel mitogen-activated protein kinase pathways in microglia and THP1 monocytes. *Journal of Neuroscience,* **18,** 4451-4460.

McGeer, E. G. and McGeer, P. L. (2003) Inflammatory processes in Alzheimer's disease. *Progress in Neuro-Psychopharmacology and Biological Psychiatry,* **27,** 741-749.

McGeer, P. L. and McGeer, E. G. (2001) Inflammation, autotoxicity and Alzheimer disease. *Neurobiology of aging,* **22,** 799-809.

McLean, C. A., Cherny, R. A., Fraser, F. W., Fuller, S. J., Smith, M. J., Beyreuther, K., Bush, A. I. and Masters, C. L. (1999) Soluble pool of Abeta amyloid as a determinant

of severity of neurodegeneration in Alzheimer's disease. *Annals of Neurology,* **46,** 860-866.

Meda L, Cassatella MA, Szendrei GI, Otvos L Jr, Baron P, Villalba M, Ferrari D and F., R. (1995) Activation of microglial cells by beta-amyloid protein and interferon-gamma. *Nature,* **374,** 647-650.

Meredith, G. E., Totterdell, S., Petroske, E., Santa Cruz, K., Callison, R. C. J. and Lau, Y. S. (2002) Lysosomal malfunction accompanies alpha-synuclein aggregation in a progressive mouse model of Parkinson's disease. *Brain Research,* **956,** 156-165.

Meyer, M. R., Tschanz, J. T., Norton, M. C., Welsh-Bohmer, K. A., Steffens, D. C., Wyse, B. W. and Breitner, J. C. (1998) APOE genotype predicts when--not whether--one is predisposed to develop Alzheimer disease. *Nature Genetics,* **19,** 321-322.

Mielke, K. and Herdegen, T. (2000) JNK and p38 stress kinases-degenerative effectors of signal-transduction-cascades in the nervous system. *Progress in Neurobiology,* **61,** 45-60.

Mielke, K. and Herdegen, T. (2002) Fatal shift of signal transduction is an integral part of neuronal differentiation: JNKs realize TNFalpha-mediated apoptosis in neuronlike, but not naive, PC12 cells. *Molecular and Cellular Neuroscience,* **20,** 211-224.

Mihara, M., Erster, S., Zaika, A., Petrenko, O., Chittenden, T., Pancoska, P. and Moll, U. M. (2003) p53 has a direct apoptogenic role at the mitochondria. *Molecular Cell,* **11,** 577-590.

Miller, F. D., Pozniak, C. D. and Walsh, G. S. (2000) Neuronal life and death: an essential role for the p53 family. *Cell Death Differentiation,* **7,** 880-888.

Milne, D. M., Campbell, L. E., Campbell, D. G. and Meek, D. W. (1995) p53 is phosphorylated in vitro and in vivo by an ultraviolet radiation-induced protein kinase

characteristic of the c-Jun kinase, JNK1. *Journal of Biological Chemistry,* **10,** 5511-5518.

Milne, D. M., Palmer, R. H., Campbell, D. G. and Meek, D. W. (1992) Phosphorylation of the p53 tumour-suppressor protein at three N-terminal sites by a novel casein kinase I-like enzyme. *Oncogene.,* **7,** 136-139.

Minden, A. and Karin, M. (1997) Regulation and function of the JNK subgroup of MAP kinases. *Biochemica et Biophysica Acta,* **1333,** 85-104.

Minn, A. J., Swain, R. E., Ma, A. and Thompson, C. B. (1998) Recent progress on the regulation of apoptosis by Bcl-2 family members. *Advances in Immunology,* **70,** 245-279.

Minogue, A. M., Schmid, A. W., Fogarty, M. P., Moore, A. C., Campbell, V. A., Herron, C. E. and Lynch, M. A. (2003) Activation of the c-Jun N-terminal Kinase Signaling Cascade Mediates the Effect of Amyloid-{beta} on Long Term Potentiation and Cell Death in Hippocampus: A ROLE FOR INTERLEUKIN-1 ? *Journal of Biological Chemistry,* **278,** 27971-27980.

Minshull, J. and Hunt, T. (1986) The use of single-stranded DNA and RNase H to promote quantitative 'hybrid arrest of translation' of mRNA/DNA hybrids in reticulocyte lysate cell-free translations. *Nucleic Acids Research,* **14,** 6433-6451.

Mirzabekov, T., Lin, M. C., Yuan, W. L., Marshall, P. J., Carman, M., Tomaselli, K., Lieberburg, I. and Kagan, B. L. (1994) Channel formation in planar lipid bilayers by a neurotoxic fragment of the beta-amyloid peptide. *Biochemical and Biophysical Research Communications,* **202,** 1142-1148.

Mitchell, F. M., Russell, M. and Johnson, G. L. (1995) Differential calcium dependence in the activation of c-Jun kinase and mitogen-activated protein kinase by muscarinic acetylcholine receptors in rat 1a cells. *Biochemical Journal,* **309,** 381-384.

Miyasaka, T., Miyasaka, J. and Saltiek, A.R. (1990) Okadaic acid stimulates the activity of microtubule associated protein kinase in PC-12 pheochromocytoma cells. *Biochemical and Biophysical Research Communications,* **168**, 1237-1243.

Moore, A. H. and O'Banion, M. K. (2002) Neuroinflammation and anti-inflammatory therapy for Alzheimer's disease. *Advanced Drug Delivery Reviews,* **54,** 1627-1656.

Morishma, Y., Gotoh, Y., Zieg, J., Barrett, T., Takano, H., Flavell, R., Davis, R. J., Shiraski, Y. and Greenberg, M. E. (2001) -amyloid induced neuronal apoptosis via a mechanism that involves the c-jun N-terminal kinase pathway and the induction of Fas Ligand. *Jounal of Neuroscience,* **21,** 7551-7560.

Morrison, R. S., Wenzel, H. J., Kinoshita, Y., C.A., R., Donehower, L. A. and Schwartzkroin, P. A. (1996) Loss of the p53 tumor suppressor gene protects neurons from kainate-induced cell death. *Journal of Neuroscience,* **16,** 1337-1345.

Mrak, R. E. and Griffin, W. S. (2001) Interleukin-1, neuroinflammation, and Alzheimer's disease. *Neurobiology of Aging,* **22,** 903-908.

Nakajima-Iijima S, Hamada H, Reddy P, Kakunaga T. (1985) Molecular structure of the human cytoplasmic beta-actin gene: interspecies homology of sequences in the introns. *Proceedings of the National Acadamey of Sciences for the United States of America,* **82,** 6133-7.

Nakamura, Y., Takeda, M., Suzuki, H., Morita, H., Tada, K., Hariguchi, S. and Nishimura, T. (1989) Age-dependent change in activities of lysosomal enzymes in rat brain. *Mechanisms of Ageing and Development,* **50,** 215-225.

Napieralski, J. A., Raghupathi, R. and McIntosh, T. K. (1999) The tumor-suppressor gene, p53, is induced in injured brain regions following experimental traumatic brain injury. *Brain Research Molecular Brain Research,* **71,** 78-86.

Narita, M., Shimizu, S., Ito, T., Chittenden, T., Lutz, R. J., Matsuda, H. and Tsujimoto, Y. (1998) Bax interacts with the permeability transition pore to induce permeability transition and cytochrome c release in isolated mitochondria. *Proceedings of the National Acadamey of Sciences of the United States of America,* **95,** 14681-14686.

Narita, M., Shimizu, S., Ito, T., Chittenden, T., Lutz, R. J., Matsuda, H. and Tsujimoto, Y. (1998) Bax interacts with the permeability transition pore to induce permeability transition and cytochrome c release in isolated mitochondria. *Proceedings of the National Acadamey of Sciences of the United States of America,* **95,** 14681-14686.

Neuzil, J., Svensson, I., Weber, T., Weber, C. and Brunk, U. T. (1999) alpha-tocopheryl succinate-induced apoptosis in Jurkat T cells involves caspase-3 activation, and both lysosomal and mitochondrial destabilisation. *FEBS Letters,* **445,** 295-300.

Ng, F. W. and Shore, G. C. (1998) Bcl-XL cooperatively associates with the Bap31 complex in the endoplasmic reticulum, dependent on procaspase-8 and Ced-4 adaptor. *Journal of Biological Chemisty,* **273,** 3140-3143.

Nilius, B., Hess, P., Lansman, J. B. and Tsien, R. W. (1985) A novel type of cardiac calcium channel in ventricular cells. *Nature,* **316,** 443-446.

Nixon, R. A. and Cataldo, A. M. (1995) The endosomal-lysosomal system of neurons: new roles. *Trends in Neurosciences,* **18,** 489-496.

Nourhashemi, F., Gillette-Guyonnet, S., Andrieu, S., Ghisolfi, A., Ousset, P. J., Grandjean, H., Grand, A. and Pous, J. (2000) Alzheimer disease: protective factors. *American Journal of Clinical Nutrition,* **71,** 643S-649S.

Nozaki, K., Nishimura, M. and Hashimoto, N. (2001) Mitogen-activated protein kinases and cerebral ischemia. *Molecular Neurobiology,* **23,** 1-19.

Orrenius, S., Zhivotovsky, B. and Nicotera, P. (2003) Regulation of cell death: the calcium-apoptosis link. *Nature Reviews Molecular Cell Biology,* **4,** 552-565.

Park, J., Kim, I. O. Y., Lee, K., Han, P. L. and Choi, E. J. (1997) Activation of c-Jun N-terminal kinase antagonizes an anti-apoptotic action of Bcl-2. *Journal of Biological Chemistry,* **272,** 16725-16728.

Pascale, A. and Etcheberrigaray, R. (1999) Calcium alterations in Alzheimer's disease: pathophysiology, models and therapeutic opportunities. *Pharmacological Research,* **39,** 81-88.

Pena, E., Berciano, M. T., Fernandez, R., Crespo, P. and Lafarga, M. (2000) Stress-induced activation of c-Jun N-terminal kinase in sensory ganglion neurons: accumulation in nuclear domains enriched in splicing factors and distribution in perichromatin fibrils. *Experimental Cell Research,* **256,** 179-191.

Perez, R. G., Zheng, H., Van der Ploeg, L. H. T. and Koo, E. H. (1997) The -amyloid precursor protein of Alzheimer's disease enhances neuron viability and modulates neuronal polarity. *Journal of Neuroscience,* **17,** 9407-9414.

Perry, G., Roder, H., Nunomura, A., Takeda, A., Friedlich, A. L., Zhu, X., Raina, A. K., Holbrook, N. S. S. L., Harris, P. L. and M.A., S. (1999) Activation of neuronal extracellular receptor kinase (ERK) in Alzheimer disease links oxidative stress to abnormal phosphorylation. *Neuroreport,* **10,** 2411-2415.

Perry, R. T., Collins, J. S., Wiener, H., Acton, R. and Go, R. C. (2001) The role of TNF and its receptors in Alzheimer's disease. *Neurobiology of Aging,* 873-883.

Pettigrew, G. W. and Seilman, S. (1982) Purification and properties of a cross-linked complex between cytochrome c and cytochrome c peroxidase. *Biochemical Journal,* **201,** 9-18.

Pike, C. J., Walencewicz, A. J., Glabe, C. G. and Cotman, C. W. (1991) Aggregation-related toxicity of synthetic beta-amyloid protein in hippocampal cultures. *European Journal of Biochemistry,* **207,** 367-368.

Pike, C. J., Walencewicz-Wasserman, A. J., Kosmoski, J., Cribbs, D. H., Glabe, C. G. and Cotman, C. W. (1995) Structure-activity analyses of beta-amyloid peptides: contributions of the beta 25-35 region to aggregation and neurotoxicity. *Journal of Neurochemistry,* **64,** 253-265.

Pillot, T., B., D., Queille, S., Labeur, C., Vandekerchkhove, J., Rosseneu, M., Pincon-Raymond, M. and Chambaz, J. (1999) The nonfibrillar amyloid beta-peptide induces apoptotic neuronal cell death: involvement of its C-terminal fusogenic domain. *Journal of Neurochemistry,* **73,** 1626-1634.

Pope, W. B., Lambert, M. P., Leypold, B., Seupaul, R., Sletten, L., Krafft, G. and Klein, W. L. (1994) Microtubule-associated protein tau is hyperphosphorylated during mitosis in the human neuroblastoma cell line SH-SY5Y. *Experimental Neurology,* **126,** 185-194.

Price, D. L. and Sisodia, S. S. (1998) Mutant genes in familial Alzheimer's disease and trasgenic models. *Annual Review of Neuroscience,* **21,** 479-505.

Pyo, H., Jou, I., Jung, S., Hong, S. and Joe, E. (1998) Mitogen-activated protein kinases activated by lipopolysaccharide and -amyloid in cultured rat microglia. *Neuroreport,* **9,** 871-874.

Raber, J., Wong, D., Buttini, M., Orth, M., Bellosta, S., Pitas, R. E., Mahley, R. W. and Mucke, L. (1998) Isoform-specific effects of human apolipoprotein E on brain function

revealed in ApoE knockout mice: Increased susceptibility of females. *Proceedings of the National Acadamey of Sciences for the United States of America,* **92,** 9480-9484.

Raff, M. (1998) Cell suicide for beginners. *Nature,* **396,** 119-122.

Rapoport, M. and Ferreira, A. (2000) PD98059 prevents neurite degeneration induced by fibrillar beta-amyloid in mature hippocampal neurons. *Journal of Neurochemistry,* **74,** 125-133.

Ray, S. K., Fidan, M., Nowak, M. W., Wilfor, G. G., Hogan, E. L. and Banik, N. L. (2000) Oxidative stress and Ca2+ influx upregulate calpain and induce apoptosis in PC12 cells. *Brain Research,* **852,** 326-334.

Reed, J. C. (1997) Cytochrome c: can't live with it--can't live without it. *Cell,* **91,** 559-562.

Richard, F. and Amouyel, P. (2001) Genetic susceptibility factors for Alzheimer's disease. *European Journal Pharmacology,* **412,** 1-12.

Roberg, K., Kagedal, K. and Ollinger, K. (2002) Microinjection of cathepsin d induces caspase-dependent apoptosis in fibroblasts. *American Journal of Pathology,* **161,** 89-96.

Rogers, J. T., Leiter, L. M., McPhee, J., Cahill, C. M., Zhan, S. S., Potter, H. and Nilsson, L. N. (1999) Translation of the alzheimer amyloid precursor protein mRNA is up-regulated by interleukin-1 through 5'-untranslated region sequences. *Journal of Biological Chemistry,* **274,** 6421-6431.

Rosenbaum, D. M., Michaelson, M., Batter, D. K., Doshi, P. and Kessler, J. A. (1994) Evidence for hypoxia-induced, programmed cell death of cultured neurons. *Annals of Neurology,* **36,** 864-870.

Rosse, T., Olivier, R., Monney, L., Rager, M., Conus, S., Fellay, I., Jansen, B. and Borner, C. (1998) Bcl-2 prolongs cell survival after Bax-induced release of cytochrome c. *Nature,* **391,** 441-442.

Rothwell, N. J. (1999) Annual review prize lecture cytokines - killers in the brain? *Journal of Physiology,* **514,** 3-17.

Sakaguchi, K., Sakamoto, H., Lewis, M. S., Anderson, C. W., Erickson, J. W., Appella, E. and Xie, D. (1997) Phosphorylation of serine 392 stabilizes the tetramer formation of tumor suppressor protein p53. *Biochemistry,* **36,** 10117-10124.

Salvesen, G. S. (2000) A lysosomal protease enters the death scene. *Journal of Clinical Investigation,* **107,** 21-22.

Sanderson, K. L., Butler, L. and Ingram, V. M. (1997) Aggregates of a beta-amyloid peptide are required to induce calcium currents in neuron-like human teratocarcinoma cells: relation to Alzheimer's disease. *Brain Research,* **744,** 7-14.

Satoh, J. and Kuroda, Y. (2001) Nicastrin, a key regulator of presenilin function, is expressed constitutively in human neural cell lines. *Neuropathology.,* **21,** 115-122.

Saunders, A. J., Kim, T.-W. and Tanzi, R. E. (1999) *BACE* Maps to Chromosome 11 and a *BACE* Homolog, *BACE2*, Reside in the Obligate Down Syndrome Region of Chromosome 21. *Science,* **286,** 1255a.

Sawada, M., Suzumura, A., Itoh, Y. and Marunouchi, T. (1993) Production of interleukin-5 by mouse astrocytes and microglia in culture. *Neuroscience Letters,* **155,** 175-178.

Scanlon, K. J., Ohta, Y., Ishida, H., Kijima, H., Ohkawa, T., Kaminski, A., Tsai, J., Horng, G. and Kashani-Sabet, M. (1995) Oligonucleotide-mediated modulation of mammalian gene expression. *FASEB Journal,* **9,** 1288-1296.

Scarpini, E., Scheltens, P. and Feldman, H. (2003) Treatment of Alzheimer's disease: current status and new perspectives. *The Lancet Neurology,* **2,** 539-547.

Schaeffer, H. J. and Weber, M. J. (1999) Mitogen-activated protein kinases: specific messages from ubiquitous messengers. *Molecular and Cellular Biology,* **19,** 2435-2444.

Schenk, D. (2002) Amyloid-beta immunotherapy for Alzheimer's disease: the end of the beginning. *Nature Reviews Neuroscience,* **3,** 824-828.

Schmechel, D. E., Saunders, A. M., Strittmatter, W. J., Crain, B. J., Hulette, C. M., Joo, S. H., Pericak-Vance, M. A., Goldgaber, D. and Roses, A. D. (1993) Increased amyloid beta-peptide deposition in cerebral cortex as a consequence of apolipoprotein E genotype in late-onset Alzheimer disease. *Proceedings of the National Acadamey of Sciences of the United States of America,* **90,** 9649-9653.

Schmitz, I., Kirchhoff, S. and Krammer, P. H. (2000) Regulation of death receptor-mediated apoptosis pathways. *International Journal of Biochemistry and Cell Biology,* **32,** 1123-1136.

Schubert, D. and Behl, C. (1993) The expression of amyloid beta protein precursor protects nerve cells from beta-amyloid and glutamate toxicity and alters their interaction with the extracellular matrix. *Brain Research,* **629,** 275-282.

Selkoe, D. J. (1991) The molecular pathology of Alzheimer's disease. *Neuron,* **6,** 487-498.

Selkoe, D. J. (1994) Amyloid beta-protein precursor: new clues to the genesis of Alzheimer's disease. *Current Opinion in Neurobiology,* **4,** 708-716.

Selkoe, D. J. (1995) Missense in the membrane. *Nature,* **375,** 734-735.

Selkoe, D. J. (2001) Alzheimer's disease: genes, proteins, and therapy. *Physiology Review,* **81,** 741-766.

Selkoe, D. J. (2002) Deciphering the genesis and fate of amyloid-b-protein yields novel therapies for Alzheimer disease. *Journal of Clinical Investigation,* **110,** 1375-1381.

Selznick, L. A., Holtzman, D. M., Han, B. H., Gokden, M., Srinivasan, A. N., Johnson, E. M. J. and Roth, K. A. (1999) In situ immunodetection of neuronal caspase-3 activation in Alzheimer disease. *Journal of Neuropathology and Experimental Neurology,* **58,** 1020-1026.

Shimohama, S., Tanino, H. and Fujimoto, S. (1999) Changes in caspase expression in Alzheimer's disease: comparison with development and aging. *Biochemical and Biophysical Research Communications,* **256,** 381-384.

Shoji, M., Iwakami, N., Takeuchi, S., Waragai, M., Suzuki, M., Kanazawa, I., Lippa, C. F., Ono, S. and Okazawa, K. (2001) JNK activation is associated with intracellular -amyloid accumulation. *Molecular Brain Research,* **85,** 221-233.

Siliciano, J. D., Canman, C. E., Taya, Y., Sakaguchi, K., Appella, E. and Kastan, M. B. (1997) DNA damage induces phosphorylation of the amino terminus of p53. *Genes Development,* **11,** 3471-3481.

Slee, E. A., Harte, M. T., Kluck, R. M., Wolf, B. B., Casiano, C. A., Newmeyer, D. D., Wang, H. G., Reed, J. C., Nicholson, D. W., Alnemri, E. S., Green, D. R. and Martin, S. J. (1999) Ordering the cytochrome c-initiated caspase cascade: hierarchical activation of caspases-2, -3, -6, -7, -8, and -10 in a caspase-9-dependent manner. *Journal of Cell Biology,* **144,** 281-292.

Smith, C. A., Farrah, T. and Goodwin, R. G. (1994) The TNF receptor superfamily of cellular and viral proteins: activation, costimulation, and death. *Cell,* **76,** 959-962.

Smith, M. A., Richey, P. L., Taneda, S., Kutty, R. K., Sayre, L. M., Monnier, V. M. and Perry, G. (1994) Advanced Maillard reaction end products, free radicals, and protein oxidation in Alzheimer's disease. *Annals of the New York Academy of Sciences,* **738,** 447-454.

Smith, M. A., Rottkamp, C. A., Nunomura, A., Raina, A. K. and Perry, G. (2000) Oxidative stress in Alzheimer's disease. . *Biochim. et Biophys. Acta,* **1502,** 139-144.

Smith-Swintosky, V. L., Pettigrew, L. C., Craddock, S. D., Culwell, A. R., Rydel, R. E. and Mattson, M. P. (1994) Secreted forms of beta-amyloid precursor protein protect against ischemic brain injury. *Journal of Neurochemistry,* **63,** 781-784.

Stadelmann, C., Deckwerth, T. L., Srinivasan, A., Bancher, C., Bruck, W., Jellinger, K. and Lassmann, H. (1999) Activation of caspase-3 in single neurons and autophagic granules of granulovacuolar degeneration in Alzheimer's disease. Evidence for apoptotic cell death. *American Journal of Pathology,* **155,** 1459-1466.

Staunton, M. J. and E.F., G. (1998) Apoptosis:Basic concepts and poetential significance in human cancer. *Arch Pathol Lab Med,* **122,** 310-319.

Stoka, V. s., Turk, B., Schendel, S. L., Kim, T. H., Cirman, T., Snipas, S. J., Ellerby, L. M., Bredesen, D., Freeze, H., Abrahamson, M., Bromme, D., Krajewski, S., Reed, J. C., Yin, X. M., Turk, V. and Salvesen, G. S. (2001) Lysosomal protease pathways to apoptosis. Cleavage of bid, not pro-caspases, is the most likely route. *Journal of Biological Chemistry,,* **276,** 3149-3157.

Storey, E. and Cappai, R. (1999) The amyloid precursor protein of Alzheimer's disease and the Abeta peptide. *Neuropathology and Applied Neurobiology,* **25,** 81-97.

Strle, K., Zhou, J. H., Shen, W. H., Broussard, S. R., Johnson, R. W., Freund, G. G., Dantzer, R. and Kelley, K. W. (2001) Interleukin-10 in the brain. *Critical Reviews in Immunology,* **21,** 427-449.

Su, J. H., Anderson, A. J., Cummings, B. J. and Cotman, C. W. (1994b) Immunohistochemical evidence for DNA fragmentation in neurons in the AD brain. *NeuroReport,* **5,** 2529-2533.

Su, J. H., Cummings, B. J. and Cotman, C. W. (1994a) Early phosphorylation of tau in Alzheimer's disease occurs at Ser-202 and is preferentially located within neurites. *Neuroreport,* **5,** 2358-2362.

Su, J. H., Deng, G. and Cotman, C. W. (1997) Bax protein expression is increased in Alzheimer's brain: correlations with DNA damage, Bcl-2 expression, and brain pathology. *Journal of Neuropathological and Experimental Neurology,* **56,** 86-93.

Sugden, P. H. and Clerk, A. (1997) Regulation of the ERK Subgroup of MAP Kinase Cascades Through G Protein-Coupled Receptors. *Cell Signalling,* **9,** 337-351.

Suzuki, A. (1997) Amyloid -beta protein Induces Necrotic Cell Death Mediated by ICE Cascade in PC12 Cells. *Experimental Cell Research,* **234,** 507-511.

Sweatt, J. D. (2001) The neuronal MAP kinase cascade: a biochemical signal integration system subserving synaptic plasticity and memory. *Journal of Neurochemistry,* **76,** 1-10.

Szczepanik, A. M., Funes, S., Petko, W. and Ringheim, G. E. (2001) IL-4, IL-10 and IL-13 modulate A beta(1--42)-induced cytokine and chemokine production in primary murine microglia and a human monocyte cell line. *Journal of Neuroimmunology,* **113,** 49-62.

Szelenyi, J. (2000) Cytokines and the central nervous system. *Brain Research Bulletin,* **54,** 329-338.

Takahashi, M., Seagar, M. J., Jones, J. F., Reber, B. F. and Catterall, W. A. (1982) Subunit structure of dihydropyridine-sensitive calcium channels from skeletal muscle. *Proceedings of the National Acadamey of Sciences of the United States of America,* **84,** 5478-5482.

Tamagno, E., Parola, M., Guglielmotto, M., Santoro, G., Bardini, P., Marra, L., Tabaton, M. and Danni, O. (2003) Multiple signaling events in amyloid beta-induced, oxidative stress-dependent neuronal apoptosis. *Free Radical Biology and Medicine,* **35,** 45-58.

Tanzi, R. E. (1999) A genetic dichotomy model for the inheritance of Alzheimer's disease and common age-related disorders. *Journal of Clinical Investigation,* **104,** 1175-1179.

Tanzi, R. E. and Bertram, L. (2001) New Frontiers in Alzheimer's Disease Genetics. *Neuron,* **32,** 181-184.

Tarkowski, E., Liljeroth, A.-M., Minthon, L., Tarkowski, A., Anders Wallin, A. and Blennow, K. (2003) Cerebral pattern of pro- and anti-inflammatory cytokines in dementias. *Brain Research Bulletin,* **61,** 225-260.

Terai, K., Matsuo, A. and McGeer, P. L. (1996) Enhancement of immunoreactivity for NF-kappa B in the hippocampal formation and cerebral cortex of Alzheimer's disease. *Brain Research,* **735,** 159-168.

Tewari M, Q. L., O'Rourke K, Desnoyers S, Zeng Z, Beidler DR, Poirier GG, Salvesen GS, Dixit V.M. (1995) Yama/CPP32 beta, a mammalian homolog of CED-3, is a CrmA-inhibitable protease that cleaves the death substrate poly(ADP-ribose) polymerase. *Cell,* **81,** 801-809.

Thornberry, N. A. and Lazebnik, Y. (1998) Caspases: Enemies within. *Science,* **281,** 1312-1316.

Thornberry, N. A., Rano, T. A., Peterson, E. P., Rasper, D. M., Timkey, T., Garcia-Calvo, M., Houtzager, V. M., Nordstrom, P. A., Roy, S., Vaillancourt, J. P., Chapman, K. T. and Nicholson, D. W. (1997) A combinatorial approach defines specificities of members of the caspase family and granzyme B. Functional relationships published for key mediators of apoptosis. *Journal of Biological Chemistry,* **272,** 17907-17911.

Tischer and Cordell, B. (1996) -amyloid precursor protein: Location of transmembrane domain and specificity of -secretase cleavage. *Journal of Biological Chemistry,* **271,** 21914-21919.

Tortosa, A., Lopez, E. and Ferrer, I. (1998) Bcl-2 and Bax protein expression in Alzheimer's disease. *Acta Neuropathologica,* **95,** 407-412.

Troy, C. M., Rabacchi, S. A., Friedman, W. J., Frappier, T. F., Brown, K. and Shelanski, M. L. (2000) Caspase-2 mediates neuronal cell death induced by beta-amyloid. *Journal of Neuroscience,* **20,** 1386-1392.

Troy, C. M., Rabacchi, S. A., Xu, Z., Maroney, A. C., Connors, T. J., Shelanski, M. L. and Greene, L. A. (2001) -amyloid-induced neuronal apoptosis requires c-Jun N-terminal kinase activation. *Journal of Neurochemistry,* **77,** 157-164.

Turk, B., Dolenc, I., Lenarcic, B., Krizaj, I., Turk, V., Bieth, J. G. and Bjork, I. (1999) Acidic pH as a physiological regulator of human cathepsin L activity. *European Journal of Biochemistry,* **259,** 926-932.

Ueda, K., Shinohara, S., Yagami, T., Asakura, K. and Kawasaki, K. (1997) Amyloid beta protein potentiates Ca2+ influx through L-type voltage-sensitive Ca2+ channels: a possible involvement of free radicals. *Journal of Neurochemistry,* **68,** 265-271.

Unger, T., Sionov, R. V., Moallem, E., Yee, C. L., Howley, P. M., Oren, M. and Haupt, Y. (1999) Mutations in serines 15 and 20 of human p53 impair its apoptotic activity. *Oncogene,* **18,** 3205-3212.

Van Wagoner, N. J., Oh, J. W., Repovic, P. and Benveniste, E. N. (1999) IL-6 (IL-6) production by astrocytes: autocrine regulation by IL-6, and the soluble IL-6 receptor. *Journal of Neuroscience,* **19,** 5236-5244.

Vassar, R., Bennett, B. D., Babu-Khan, S., Kahn, S., Mendiaz, E. A., Denis, P., Teplow, D. B., Ross, S., Amarante, P., Loeloff, R., Luo, Y., Fisher, S., Fuller, J., Edenson, S., Lile, J., Jarosinski, M. A., Biere, A. L., Curran, E., Burgess, T., Louis, J. C., Collins, F., Treanor, J., Rogers, G. and Citron, M. (1999) Beta-secretase cleavage of Alzheimer's amyloid precursor protein by the transmembrane aspartic protease BACE. *Science,* **286,** 735-741.

Vereker, E., O'Donnell, E. and Lynch, M. A. (2000) The inhibitory effect of interleukin-1beta on long-term potentiation is coupled with increased activity of stress-activated protein kinases. *Journal of Neuroscience,* **20,** 6811-6819.

Virdee, K., Bannister, A. J., Hunt, S. P. and Tolkovsky, A. M. (1997) Comparison between the timing of JNK activation, c-Jun phosphorylation, and onset of death commitment in sympathetic neurones. *Journal of Neurochemistry,* **69,** 550-561.

Vitkovic, L., Bockaert, J. and Jacque, C. (2000) "Inflammatory" cytokines: neuromodulators in normal brain? *Journal of Neurochemistry,,* **74,** 457-471.

Walder, R. Y. and Walder, J. (1988) Role of RNase H in hybrid-arrested translation by antisense oligonucleotides. *Proceedings of the National Acadamey of Sciences of the United States of America,* **85,** 5011-5015.

Waldmeier, P. C. (2003) Prospects for antiapoptotic drug therapy of neurodegenerative diseases. *Progress in Neuro-Psychopharmacology and Biological Psychiatry,* **27,** 303-321.

Wallach, D., Varfolomeev, E. E., Malinin, N. L., Goltsev, Y. V., Kovalenko, A. V. and Boldin, M. P. (1999) Tumor necrosis factor receptor and Fas signalling mechanisms. *Annual Review Immunology,* **17,** 331-367.

Walsh, D. M., Klyubin, I., Fadeeva, J. V., Cullen, W. K., Anwyl, R., Wolfe, M. S., Rowan, M. J. and Selkoe, D. J. (2002) Naturally secreted oligomers of amyloid beta protein potently inhibit hippocampal long-term potentiation in vivo. *Nature,* **416,** 535-539.

Walter, J., Capell, A., Grunberg, J., Pesold, B., Schindzielorz, A., Prior, R., Podlisny, M. B., Fraser, P., Hyslop, P. S., Selkoe, D. J. and Haass, C. (1996) The Alzheimer's disease-associated presenilins are differentially phosphorylated proteins located predominantly within the endoplasmic reticulum. *Molecular Medicine,* **2,** 673-691.

Wang, C. Y., Mayo, M. W. and Baldwin, A. S. J. (1996) TNF- and cancer therapy-induced apoptosis: potentiation by inhibition of NF-kappaB. *Science,* **274,** 784-787.

Wang, K. K. W. (2000) Calpain and Caspase: Can you tell the difference. *Trends in Neurosciencess,* **23,** 20-26.

Wang, Y. and Eckhart, W. (1992) Phosphorylation sites in the amino-terminal region of mouse p53. *Proceedings of the National Acadamey of Sciences of the United States of America,* **89,** 4231-4235.

Watkins, L. R., Maier, S. F. and Goehler, L. E. (1995) Cytokine-to-brain communication: a review & analysis of alternative mechanisms. *Life Sciences,* **57,** 1011-1026.

Watson, J. D. and Crick, F. H. (1953) Molecular structure of nucleic acids. *Nature,* **171,** 737-738.

Westwick, J. K., Cox, A. D., Der, C. J., Cobb, M. H., Hibi, M., Karin, M. and Brenner, D. A. (1994) Oncogenic Ras activates c-Jun via a separate pathway from the activation of extracellular signal-regulated kinases. *Proceedings of the National Acadamey of Sciences of the United States of America,* **91,** 6030-6034.

Whitmarsh, A. J., Shore, P., Sharrock, A. D. and Davis, R. J. (1995) Integration of MAP kinase signal transduction pathways at the serum response element. *Science,* **269,** 403-407.

Williams, G. T. and Smith, C. A. (1993) Molecular regulation of apoptosis:genetic controls on cell death. *Cell,* **74,** 777-779.

Wisniewski, T., Ghiso, J. and Frangione, B. (1991) Peptides homologous to the amyloid protein of Alzheimer's disease containing a glutamine for glutamic acid substitution have accelerated amyloid fibril formation. *Biochemical and Biophysical Research Communications,* **180,** 1528.

Wolfe, M. S., De Los Angeles, J., Miller, D. D., Xia, W. and Selkoe, D. J. (1999a) Are presenilins intramembrane-cleaving proteases? Implications for the molecular mechanism of Alzheimer's disease. *Biochemistry,* **38,** 11223-11230.

Wolfe, M. S., Xia, W., Ostaszewski, B. L., Diehl, T. S., Kimberly, W. T. and Selkoe, D. J. (1999b) Two transmembrane aspartates in presenilin-1 required for presenilin endoproteolysis and gamma-secretase activity. *Nature,* **398,** 513-517.

Wolter, K. G. and , Y.-T. H., * Carolyn L. Smith, Amotz Nechushtan,* Xu-Guang Xi,* and Richard J. Youle. (1997) Movement of Bax from the Cytosol to Mitochondria during Apoptosis. *Journal of Cell Biology,* **139,** 1281-1292.

Wyss-Coray, T. and Mucke, L. (2002) Inflammation in Neurodegenerative Disease—A Double-Edged Sword. *Neuron,* **35,** 419-432.

Xia, Z., Dickens, M., Raingeaud, J., Davis, R. J. and Greenberg, M. E. (1995) Opposing effects of ERK and JNK-p38 MAP kinases on apoptosis. *Science,* **270,** 1326-1333.

Xiang, H., Hochman, D. W., Saya, H., Fujiwara, T., Schwartzkroin, P. A. and Morrison, R. S. (1996) Evidence for p53-mediated modulation of neuronal viability. *Journal of Neuroscience,* **16,** 6753-6765.

Yagami, T., Ueda, K., Asakura, K., Sakaeda, T., Nakazato, H., Kuroda, T., Hata, S., Sakaguchi, G., Itoh, N., Nakano, T., Kambayashi, Y. and Tsuzuki, H. (2002) Gas6 rescues cortical neurons from amyloid beta protein-induced apoptosis. *Neuropharmacology,* **43,** 1289-1296.

Yamashima, T., Kohda, Y., Tsuchiya, K., Ueno, T., Yamashita, J., Yoshioka, T. and Kominami, E. (1998) Inhibition of ischaemic hippocampal neuronal death in primates with cathepsin B inhibitor CA-074: a novel strategy for neuroprotection based on 'calpain-cathepsin hypothesis'. *European Journal of Neuroscience,* **10,** 1723-1733.

Yan, R., Bienkowski, M. J., Shuck, M. E., Miao, H., Tory, M. C., Pauley, A. M., Brashier, J. R., Stratman, N. C., M.W.R., Buhl, A. E., Carter, D. B., Tomasselli, A. G., Parodi, L. A., Heinrikson, R. L. and M.E., G. (1999) Membrane anchores aspartyl protease with Alzheimer's disease beta-secretase activity. *Nature,* **402,** 533-537.

Yan, S. D., Chen, X. L., Fu, J., Chen, M., Zhu, H., Roher, A., Slattery, T., Zhao, L., Nagashima, M., Morser, J., Migheli, A., Nawroth, P., Stern, D. and Schmidt, A. M. (1996) RAGE and amyloid-beta peptide neurotoxicity in Alzheimer's disease. *Nature,* **382,** 685-691.

Yan, X., Xiao, R., Dou, Y., Wang, S., Qiao, Z. and Qiao, J. (2000) Carbachol blocks beta-amyloid fragment 31-35-induced apoptosis in cultured cortical neurons. *Brain Research Bulletin,* **51,** 465-470.

Yang, A. J., D., C., Margol, L. and Glabe, C. G. (1998) Loss of endosomal/lysosomal membrane impermeability is an early event in amyloid Abeta1-42 pathogenesis. *Journal of Neuroscience Research,* **52,** 691-698.

Yang, D. D., Kuan, C. Y., Whitmarsh, A. J., Rincon, M., Zheng, T. S., Davis, R. J., Rakic, P. and Flavell, R. A. (1997) Absence of excitotoxicity-induced apoptosis in the hippocampus of mice lacking the Jnk3 gene. *Nature,* **389,** 865-870.

Yang, X., Yang, S., Zhang, J., Xue, L. and Hu, Z. (2002) Role of Caspase 3 in neuronal apoptosis after acute brain injury. *Chin J Traumatol,* **5,** 250-253.

Yankner, B. A., Dawes, L. R., Fisher, S., Villa-Komaroff, L., Oster-Granite, M. L. and Neve, R. L. (1989) Neurotoxicity of a fragment of the amyloid precursor associated with Alzheimer's disease. *Science,* **245,** 417-420.

Yin, T., Sandhu, G., Wolfgang, C. D., Burrier, A., Webb, R. L., Rigel, D. F., Hai, T. and Whelan, J. (1997) Tissue-specific pattern of stress kinase activation in ischemic/reperfused heart and kidney. *Journal of Biological Chemistry,* **272,** 19943-19950.

Yoshizumi, M., Kogame, T., Suzaki, Y., Fujita, Y., Kyaw, M., Kirima, K., Ishizawa, K., Tsuchiya, K., Kagami, S. and Tamaki, T. (2002) Ebselen attenuates oxidative stress-induced apoptosis via the inhibition of the c-Jun N-terminal kinase and activator protein-1 signalling pathway in PC12 cells. *British Journal of Pharmacology,* **136,** 1023-1032.

Yu, H., Li, X., Marchetto, G. S., Dy, R., Hunter, D., Calvo, B., Dawson, T. L., Wilm, M., Anderegg, R. J., Graves, L. M. and Earp, H. S. (1996) Activation of a novel

calcium-dependent protein-tyrosine kinase. Correlation with c-Jun N-terminal kinase but not mitogen-activated protein kinase activation. *Journal of Biological Chemistry,* **271,** 29993-29998.

Yuan, X. M., Li, W., Dalen, H., Lotem, J., Kama, R., Sachs, L. and Brunk, U. T. (2002) Lysosomal destabilization in p53-induced apoptosis. *Proceedings of the National Acadamey of Sciences of the United States of America,* **99,** 6286-6291.

Zamani, M. R. and Allen, Y. S. (2001) Nicotine and its interaction with beta-amyloid protein: a short review. *Biological Psychiatry,* **49,** 221-232.

Zamzami, N., Marchetti, P., Castedo, M., Decaudin, D., Macho, A., Hirsch, T., Susin, S. A., Petit, P. X., Mignotte, B. and Kroemer, G. (1995) Sequential reduction of mitochondrial transmembrane potential and generation of reactive oxygen species in early programmed cell death. *Journal of Experimental Medicine,* **182,** 367-377.

Zhang, Y., McLaughlin, R., Goodyer, C. and LeBlanc, A. (2002a) Selective cytotoxicity of intracellular amyloid beta peptide1-42 through p53 and Bax in cultured primary
human neurons. *Journal of Cell Biology,* **56,** 519-529.

Zhao, M., Eaton, J. W. and Brunk, U. T. (2000) Protection against oxidant-mediated lysosomal rupture: a new anti-apoptotic activity of Bcl-2? *Febs letters,* **485,** 104-108.

Zhao, M., Eaton, J. W. and Brunk, U. T. (2001) Bcl-2 phosphorylation is required for inhibition of oxidative stress-induced lysosomal leak and ensuing apoptosis. *FEBS Letters,* **509,** 405-412.

Zhu, X., Raina, A. K., Rottkamp, C. A., Aliev, G., Perry, G., Boux, H. and Smith, M. A. (2001) Activation and redistribution of c-jun N-terminal kinase/stress activated protein kinase in degenerating neurons in Alzheimer's disease. *Journal of Neurochemistry,* **76,** 435-441.

Zhu, Y., Mao, X. O., Sun, Y., Xia, Z. and Greenberg, D. A. (2002) p38 Mitogen-activated protein kinase mediates hypoxic regulation of Mdm2 and p53 in neurons. *Journal of Biological Chemistry,* **277,** 22909-22914.

Zörnig, M., Hueber, A., Baum, W. and Evan, G. (2001) Apoptosis regulators and their role in tumorigenesis. *Biochimica et Biophysica Acta,* **1551,** F1-37.

IX Appendix 1 - Solutions

Cell Culture Solutions

70% Ethanol, 100mL

70mL, EtOH; 30mL, H_2O.

PBS (cell culture)

10mL Dulbecco's Modified Phosphate Buffered Saline (DM-PBS, Na_2HPO_4 (80mM), NaH_2PO_4 (20mM), NaCl, (100mM)/ 100mL H_2O.

Trypsin Solution (cell culture)

0.3mg trypsin/mL PBS.

Trypsin Inhibitor Solution (cell culture)

Soyabean trypsin inhibitor (SBTI; 0.2mg/mL), DNase (0.2mg/mL), $MgSO_4$ (0.1M) /mL PBS.

Supplemented Neurobasal Medium (day 1)

Heat inactivated horse serum (10%, 10mL); Penicillin/Streptomycin (100U/mL; 1mL); Glutamax; (2mM ; 1ml); B27 (1%, 1mL) / 100mL Neurobasal Medium.

Antimitotic Neurobasal Medium (day 4)

Heat inactivated horse serum (10mL); Penicillin/Streptomycin, 100U/mL (1mL); Glutamax; 2mM (1ml); ARA-C (5ng/mL) / 100mL Neurobasal Medium.

Replacement Neurobasal Medium (day 5)

Heat inactivated horse serum (10mL); Penicillin/Streptomycin, 100U/mL (1mL); Glutamax; 2mM (1ml)/ 100mL Neurobasal Medium.

Cell Harvesting Solutions

Lysis Buffer, pH 7.4 (Harvesting total protein)

HEPES (20mM), KCl (10mM), EGTA (1mM), $MgCl_2$ (1.5mM), EDTA, (1mM), DTT, (1mM), PMSF, (0.1mM), Leupeptin, (2μg/ml), Aprotinin, (2μg/ml), Sucrose, (200mM).

Permeabilisation Buffer pH 7.2 (Harvesting cytosolic extracts)

Sucrose (250mM), KCl (70mM), NaCl (137mM), Na_2HPO_4 (4.5mM), KH_2PO_4 (1.4mM), PMSF (100μM), leupeptin (10μg/mL), aprotinin (2μg/mL), digitonin (200μg/mL).

Mitochondrial Lysis Buffer pH 7.4 (Harvesting mitochondrial extracts)

Tris Base (50mM), NaCl (150mM), EGTA (2mM), Triton-X (0.2%), Igepal P-40 (0.3%), PMSF (100μM), leupeptin (10μg/mL), aprotinin (2μg/mL).

SDS-PAGE Solutions

Phosphate buffered saline-Tween 20 (PBS-Tween), pH 7.4

Na_2HPO_4 (80mM), NaH_2PO_4 (20mM), NaCl, (100mM), Tween 20 (0.1%).

Tris buffered saline-Tween 20 (TBS-Tween), pH 7.4

Tris-HCl, (20mM), NaCl, (150mM), Tween 20 (0.1%).

Sample buffer (pH 6.8)

Tris-HCl (0.05M), Glycerol 20% (v/v), SDS 2% (w/v), β-Mercaptoethanol 5% (v/v), bromophenol blue 0.05% (w/v).

Stacking gel (4%, pH 6.8)

Acrylamide/bis-acrylamide (30% stock, 13% (v/v), dH_2O 60% (v/v), Tris-HCl (0.05M, pH 6.8, 25% (v/v)), SDS (10% w/v stock, 1% (v/v)), APS (10% w/v stock, 0.5% (v/v)), TEMED, 0.5% (v/v).

Separating gel (10%, pH 8.8)

Acrylamide/bis-acrylamide (30% stock, 33% (v/v)), dH_2O, 40% (v/v), Tris-HCl, (0.05M, pH 6.8, 25% (v/v)), SDS (10% w/v stock, 1% (v/v), APS (10% w/v stock, 0.5% (v/v)), TEMED, 0.05% (v/v).

Separating gel (12%, pH 8.8)

Acrylamide/bis-acrylamide (30% stock, 40% (v/v)), dH_2O, 33% (v/v), Tris-HCl, (0.05M, pH 6.8, 25% (v/v), SDS (10% w/v stock), 1% (v/v), APS (10% w/v stock),, 0.5% (v/v), TEMED, 0.05% (v/v).

Electrode running buffer

Tris base (25mM), Glycine (192mM), SDS (0.1% (w/v)).

Transfer buffer (pH 8.3)

Tris base (25mM), Glycine (192mM), MeOH (20% (v/v)), SDS (0.05% (w/v)).

Polymerase Chain Reaction Gel Electrophoresis solutions

Tris Borate EDTA (TBE) Buffer, pH 8.3

Tris base (0.08M), Boric Acid (0.04 M), EDTA (1 mM).

RNA seperating agarose gel (1 %, pH8.3)

Agarose 1% (w/v), 100 ml TBE Buffer.

PCR products seperating agarose gel (1.5 %, pH8.3)

Agarose 1.5% (w/v), 100 ml TBE Buffer.

Fluorogenic Assay Solutions

Lysis Buffer (Cathepsin-L assay, pH 5)

NaOAc(20mM), EDTA (4mM), DTT (8mM), Urea (4M)

Incubation Buffer (Cathepsin-L assay, pH 7.4)

Hepes (100mM) DTT (5mM)

X Appendix II – Suppliers addresses

ALEXIS Corporation LTD., P.O. Box 6757, Bingham, Nottingham, NG13 8LS, England.

Alomone Labs, Shatner Center 3, P.O. Box 4287, Jerusalem, Isreal.

Amersham plc, Amersham Place, Little Chalfont, Buckinghamshire, HP79NA, England.

Astec-Microflow Systems, 2180 Andrea Lane, Fort Myers, FL33912, U.S.A.

B.Braun Melsungen AG, Carl-Braun Srtaβe 1, D-34212 Melsungen, Germany.

Bachem Ltd., PO Box 260, 17 Westside Industrial Estate, Jackson Street, St. Helens, Meyerside WA9 3AJ, England.

BD Biosciences Pharmingen, 10975 Torreyana Road, San Diego, CA 921121, U.S.A.

BDH Laboratory Supplies, Poole, Dorset, BH151TD, England.

Becton Dickinson Labware Europe, Becton Dickinson France S.A., 1 rue Aristide Berges, BP4, 38800 Le Pont De Claix, France.

Bel-Art Products Inc., 6 Industrial Road, Pequannock, New Jersey 07440, U.S.A.

Bibby Sterilin Ltd., Tilling Drive, Staffordshire, ST15OSA, England.

Biognostik GmbH., Gerhard-Gerdes-Str.19, 37079 Göttingen, Germany.

Biometra GmbH, Rudolph-Wissell Straβe 30, D-37079 Gottingen, Germany.

Bio-Rad Laboratories GmbH., Heidemannstrasse 164, D-80939 Munich, Germany.

Biosource International, 542 Flynn Road, Camarillo, California USA 93012, U.S.A.

Calbiochem International, Merck KGaA, Frankfurter Str. 250, D-64293 Darmstadt, Germany.

Cell Signalling Technology, INC, 166B Cummings Center, Beverly, MA 01915

Chance Propper Ltd, P O Box 53, Spon Lane South, Smethwick, West Midlands, B66 1NZ, England.

Chivers Ireland Ltd., Coolock, Dublin 5, Ireland.

Dako Corporation, 6392 Via Road, Carpinteria, CA93013, U.S.A.

DiaChem International Ltd, Unit 5, Gardiners Place,West Gillibrands, Skelmersdale, Lancashire, WN8 9SP. England.

FUJIFILM Medical Systems USA, Inc. Headquarters: 419 West Avenue Stamford, CT 06902, U.S.A.

Greiner Bio-One GmbH, Bad Haller Strasse 32, 4550 Kremsmuenster, Austria.

Improvision Software, Viscount Centre II, University of Warwick Science Park, Millburn Hill Road, Coventry , CV4 7HS, England.

InVitrogen Ltd., Inchinnan Business Park, 3 Fountain Drive, Paisley PA49RF, Scotland.

Jencons Scientific Ltd., Cherrycourt Way Industrial Estate, Stanbridge Road, Lancashire, WN8 9SP. England.

Leica Microsystems AG, Ernst-Leitz-Strasse 17-37, Wetzlar, 35578, Germany.

Millipore Ireland B.V. Tullagreen Carrigtwohill, Co.Cork, Ireland.

Molecular Probes Europe BV, PoortGebouw, Rijnsburgerweg 10, 2333 AA Leiden, The Netherlands.

Nikon Instech Co., Ltd. Parale Mitsui Bldg., 8, Higashida-cho, Kawasaki-ku, Kawasaki, Kanagawa 210-0005, Japan.

Pall Corporation, 600 South Wagner Road, Ann Arbour, MI48103-9019 U.S.A.

Perkin Elmer Ltd., 710 Bridgeport Avenue Shelton, Connecticut 06484-4794, U.S.A.

Pierce Biotechnology, 3747 N.Meridian Rd, P.O. Box 117, Rockford, IL61105, U.S.A.

Priorclave Ltd., 129-131 Nathan Way, Thamesmead, London, SE28OAB, England.

Promega Sciences, 2800 Woods Hollow Road Madison WI 5371, U.S.A.

Roche Diagnostics Ltd., Bell Lane, Lewes, East Sussex, BN7 1LG, England.

Rocol Ltd, Rocol House, Wakefield Road, Swillington, Leeds, LS268BS, England.

Sanyo-Gallenkamp Ltd., Monarch Way, Loughborough, LE115XG, England.

Sarstedt Ltd., 68 Boston Road, Beumount Leys, Leicester, LE41AW, England,

Sartorius AG Ltd., 94-108 Weender Landstraβe, D-37075 Goettingen, Germany.

Scanalytics Inc. 8550 Lee Highway, Suite 400, Fairfax, VA 22031, USA.

Sigma-Aldrich Company Ltd., The Old Brickyard, New Road, Gillingham, Dorset, SP84XT, England.

Swann-Morton Limited, Owlerton Green, Sheffield, S62BJ, England.

Thermo Labsystems, Thermo Labsystems Oy, Ratastie 2, P.O.Box 100, Vantaa, 01620, Finland.

Vector Laboratories Inc., Burlingame, CA94010, U.S.A.

Whatman International Ltd., Whatman House, St. Leonard's Road, 20/20 Maidstone, Kent, ME16OLS, England.

XI Publications

Fogarty, M.P., Downer, E.J. and Campbell, V.A. (2003) Characterisation of the role of JNK isoforms in β-amyloid-mediated p53 activation and apoptosis. *Biochemical Journal* 371, 789-798

Minogue, A.M., Schmid, A.W., **Fogarty, M.P.,** Moore,C.A., Campbell,V.A, Herron,C.A. and Lynch, M.A. (2003) Activation of the JNK signalling cascade mediates the effect of Aβ on LTP and cell death in hippocampus: A role for IL-1β. *Journal of Biological Chemistry* 278, 27971-27980

Downer, E.J., **Fogarty, M.P.** and Campbell, V.A. Tetrahydrocannabinol-induced neurotoxicity depends on CB1 receptor mediated c-Jun N-Terminal Kinase activation in cultured cortical neurons. *British Journal of Pharmacology* **140,** 547-557

Martin, D.S., Lonergan, P.E., Boland, B., **Fogarty, M.P.,** Brady, M., Horrobin, D.F., Campbell, V.A. and Lynch M.A. (2002) Apoptotic Changes in the Aged Brain Are Triggered by Interleukin-1beta -induced Activation of p38 and Reversed by Treatment with Eicosapentaenoic Acid. *Journal of Biological Chemistry* 277, 34239-34246

Downer, E., Boland, B., **Fogarty, M**. and Campbell V.A.. (2001) Δ^9-Tetrahydrocannabinol induces the apoptotic pathway in cultured cortical neurons via activation of the CB1 receptor. *Neuroreport.* 12,3973-3978.

Fogarty, M.P. and Campbell, V. A. (2003) β-amyloid couples to $p53^{ser15}$ in cultured cortical neurons. Proceedings of the Physiological Society - Abstracts 551P: C70.

Fogarty, M.P., Downer E.J. and Campbell, V. (2002) Aβ mediated neurotoxicity through the stress activated protein kinase JNK. American Society for Neuroscience Abstracts 688:W2.

Fogarty, M.P. and Campbell, V. (2001) A role for ERK in β-amyloid-mediated toxicity in cultured cortical neurons. American Society for Neuroscience Abstracts.322:XX33

A role for c-Jun N-terminal kinase 1 (JNK1), but not JNK2, in the β-amyloid-mediated stabilization of protein p53 and induction of the apoptotic cascade in cultured cortical neurons

Marie P. FOGARTY, Eric J. DOWNER and Veronica CAMPBELL[1]
Department of Physiology, Trinity College Institute of Neuroscience, Trinity College, Dublin 2, Ireland

β-Amyloid (Aβ) peptide has been shown to induce neuronal apoptosis; however, the mechanisms underlying Aβ-induced neuronal cell death remain to be fully elucidated. The stress-activated protein kinase, c-Jun N-terminal kinase (JNK), is activated in response to cellular stress and has been identified as a proximal mediator of cell death. In the present study, expression of active JNK was increased in the nucleus and cytoplasm of Aβ-treated cells. Evaluation of the nature of the JNK isoforms activated by Aβ revealed a transient increase in JNK1 activity that reached its peak at 1 h and a later activation (at 24 h) of JNK2. The tumour suppressor protein, p53, is a substrate for JNK and can serve as a signalling molecule in apoptosis. In cultured cortical neurons, we found that Aβ increased p53 protein expression and phosphorylation of p53 at Ser^{15}. Thus it appears that Aβ increases p53 expression via phosphorylation-mediated stabilization of the protein. Given the lack of availability of a JNK inhibitor that can distinguish between JNK1- and JNK2-mediated effects, we employed antisense technology to deplete cells of JNK1 or JNK2 selectively. Using this strategy, the respective roles of JNK1 and JNK2 on the Aβ-mediated activation of the apoptotic cascade (i.e. p53 stabilization, caspase 3 activation and DNA fragmentation) were examined. The results obtained demonstrate a role for JNK1 in the Aβ-induced stabilization of p53, activation of caspase 3 and DNA fragmentation. In contrast, depletion of JNK2 had no effect on the proclivity of Aβ to activate capase 3 or induce DNA fragmentation. These results demonstrate a significant role for JNK1 in Aβ-mediated induction of the apoptotic cascade in cultured cortical neurons.

Key words: antisense, apoptosis, β-amyloid, c-Jun N-terminal kinase, p53, caspase-3.

INTRODUCTION

Deposition of β-amyloid (Aβ) protein around neurons is a feature of Alzheimer's disease (AD) [1]. Although the 1–42 fibrillar form of Aβ is the most abundant in the AD senile plaque, the 1–40 peptide also has the proclivity to form fibrils and is present in the senile plaque, but to a lesser extent than the 1–42 species [2]. In AD brains, neuropathological hallmarks of apoptosis such as DNA fragmentation have been detected [3] and Aβ is assumed to contribute directly to this pathology by inducing neuronal apoptosis [4]. In support of the hypothesis that Aβ deposition drives the neurodegenerative process, both $Aβ_{1-40}$ and $Aβ_{1-42}$ have been shown to induce neuronal apoptosis *in vitro* [5,6]. There has been a significant interest in identifying the pathways that underlie neuronal responses to Aβ in an attempt to develop novel neuroprotective therapeutic strategies. To date, many signalling pathways have been proposed as mediators of Aβ-induced neuronal apoptosis and these include reactive oxygen species [7], Ca^{2+}-sensitive proteases [8] and cysteine proteases [9]. The stress-activated protein kinase, c-Jun N-terminal kinase (JNK), has been proposed as a mediator of cell death in response to a variety of stimuli such as growth factor deprivation [10], excitotoxicity [11] and oxidative stress [12]. Recent studies [13–15] have also suggested that JNK plays a role in Aβ-mediated effects. In sympathetic neurons and PC12 cells, the 1–42 fragment of Aβ activates JNK and the synthetic JNK inhibitor, CEP-1347, blocks Aβ-mediated neurotoxicity [14]. Three JNK isoforms have been identified, JNK1, JNK2 and JNK3, and these are encoded by independent genes. Since each of these isoforms is expressed in the brain [16], Aβ has the potential to couple with JNK1, JNK2 or JNK3. Thus although the study of Troy et al. [14] provides compelling evidence of a role for JNK in Aβ-mediated neurodegeneration, the synthetic JNK inhibitor used in their study is unable to distinguish between the different JNK isoforms. In the present study, we used antisense technology to determine the respective roles of the JNK isoforms in $Aβ_{1-40}$-mediated neurodegeneration of cultured cortical neurons.

The multifunctional tumour suppressor protein, p53, has been suggested to play a role in the cell death pathway as well as having a role in the regulation of the cell cycle and DNA repair [17]. An increase in p53 expression has been reported in the brain of patients with AD [18] and in transgenic mice that overexpress Aβ [19]. cDNA expression of a dominant-negative p53 mutant [20] and application of a chemical inhibitor of p53 [21] offer protection against Aβ-mediated toxicity. Taken together, these studies provide compelling evidence of a role for p53 in Aβ-mediated neurodegeneration. However, the mechanisms that underlie Aβ-mediated activation of p53 remain to be elucidated. p53 has the proclivity to regulate a variety of functions and this diversity in function arises from the presence of several phosphorylation sites on p53 [22]. Thus phosphorylation on Ser^{15} is associated with the apoptotic effect of p53 [23], whereas phosphorylation at Ser^{392} promotes formation of the p53 tetramer that activates transcription from several cell-cycle-regulating genes in response to DNA damage [24]. The stress-activated protein kinase, p38, has been shown to phosphorylate p53 at Ser^{15} during hypoxic cell

Abbreviations used: Aβ, β-amyloid; AD, Alzheimer's disease; JNK, c-Jun N-terminal kinase; TUNEL, terminal transferase deoxytidyl uridine end-labelling.

[1] To whom correspondence should be addressed (e-mail vacmpbll@tcd.ie).

death [25] and chemical stress-induced apoptosis [26]. p53 is also a substrate for JNK [27] and there is evidence for a role for JNK signalling in the regulation of p53 stability and apoptotic capacity [28]. Given that Aβ can couple with the JNK pathway [13,15], the aim of the present study was to evaluate the role of the JNK isoforms, JNK1 and JNK2, in the Aβ-mediated activation of p53 and induction of the apoptotic cascade.

The results from the present study demonstrate a differential time frame of JNK1 and JNK2 activation by Aβ in this system with JNK1 being activated rapidly by Aβ (within minutes), whereas JNK2 activation was delayed by 24 h. Aβ caused an increase in p53 protein expression and phosphorylation of p53 at Ser^{15}. Use of JNK antisense demonstrated that the regulation of p53 by $A\beta_{1-40}$ was mediated via JNK1 as was the Aβ-mediated activation of caspase 3 and DNA fragmentation. These results demonstrate that Aβ has a differential pattern of signalling via the JNK pathway and provide evidence for an interaction between JNK1 and p53 in this system.

EXPERIMENTAL

Culture of cortical neurons

Primary cortical neurons were established from postnatal 1-day-old Wistar rats and maintained in neurobasal medium (Gibco BRL, Paisley, Renfrewshire, Scotland, U.K.). Rats were decapitated and cerebral cortices removed. The dissected cortices were incubated in PBS containing trypsin (0.25 %) for 20 min at 37 °C. The tissue was then triturated (5×) in PBS containing soyabean trypsin inhibitor (0.1 %) and DNase (0.2 mg/ml) and gently filtered through a sterile mesh filter. After centrifugation (2000 ***g*** for 3 min at 20 °C), the pellet was resuspended in neurobasal medium, supplemented with heat-inactivated horse serum (10 %, v/v), penicillin (100 units/ml), streptomycin (100 units/ml) and glutamax (2 mM). Suspended cells were plated out at a density of 0.25×10^6 cells on circular 10 mm diameter coverslips, coated with 60 μg/ml of poly(L-lysine) and incubated in a humidified atmosphere containing 5 % CO_2/95 % air at 37 °C. After 48 h, 5 ng/ml of cytosine arabinofuranoside was included in the culture medium to prevent proliferation of non-neuronal cells. Culture media were exchanged every 3 days and cells were grown in culture for 12 days before Aβ treatment.

Drug treatment

$A\beta_{1-40}$ (BioSource International, U.K.) was made up as a 1 mM stock solution in PBS and allowed to aggregate for 48 h at 30 °C. For treatment of cortical neurons, Aβ was diluted to a final concentration of 2 μM in prewarmed neurobasal medium. This concentration has been previously used to induce activation of the apoptotic cascade in these cells [8].

Antisense-mediated depletion of JNK1 and JNK2

20-mer phosphorothioate oligonucleotides were purchased from Biognostik (Gottingen, Germany), and the sequences used were complementary with the mRNA encoding rat JNK1 and JNK2 proteins [26]. The sequences used were: JNK1 antisense oligonucleotide, 5′-CTCATGATGGCAAGCAATTA-3′; JNK1 scrambled oligonucleotide, 5′-ACTACTACACTAGACTAC-3′; JNK2 antisense oligonucleotide, 5′-GCTCAGTGGACATGGATGAG-3′; and JNK2 scrambled oligonucleotide, 5′-GGACTACTAC-ACTAGACTAC-3′. Neurons were incubated with 1.2 μM oligonucleotide in serum-free prewarmed neurobasal medium containing 5 μg/ml of *N*-[1-(2,3-dioleoyloxy)propyl]-*N*,*N*,*N*-trimethylammonium/dioleoyl phosphatidylethanolamine (Life Technologies, Paisley, Renfrewshire, Scotland, U.K.). After 4 h, the medium was replaced with supplemented prewarmed neurobasal medium containing 1.2 μM oligonucleotide. The cells were incubated for a further 48 h before treatment with Aβ.

Western-immunoblot analysis of phospho-JNK and phospho-p53 expression

After incubation with Aβ, cortical neurons were harvested in lysis buffer (20 mM Hepes, 10 mM KCl, 1.5 mM $MgCl_2$, 1 mM EGTA, 1 mM EDTA, 1 mM dithiothreitol, 0.1 mM PMSF, 5 μg/ml pepstatin A, 2 μg/ml leupeptin and 2 μg/ml aprotinin; pH 7.4) and left on ice for 20 min. The cells were centrifuged (15000 ***g*** for 20 min at 4 °C) and the supernatant was diluted to 50 μg of protein/ml with sample buffer [150 mM Tris/HCl (pH 6.8), 10 % (v/v) glycerol, 4 % (w/v) SDS, 5 % (v/v) 2-mercaptoethanol and 0.002 % (w/v) Bromophenol Blue]. Samples were then heated to 100 °C for 3 min. Proteins (1 μg/lane) were separated by electrophoresis on a 10 % (v/v) polyacrylamide minigel, transferred on to a nitrocellulose membrane and immunoblotted with an anti-active JNK monoclonal antibody (1 : 1000; Santa Cruz Biotechnology, CA, U.S.A.) purified from mouse serum, which recognizes the active forms of JNK1 (p46), JNK2 (p54) and JNK3 (p57) after phosphorylation on Thr^{183} and Tyr^{185}. To monitor expression of non-phosphorylated JNK, the blots were stripped and re-probed with an anti-JNK polyclonal antibody purified from rabbit serum (1 : 1000; Santa Cruz Biotechnology), which recognizes JNK1, JNK2 and JNK3. To monitor p53 phosphorylation, the anti-[phosphoSer^{15}]p53 (1 : 1000; Cell Signaling Technology, Beverly, MA, U.S.A.) and anti-[phosphoSer^{392}]p53 (Biosource International, Nivelles, Belgium) polyclonal antibodies purified from rabbit serum, which recognize p53 phosphorylated on Ser^{15} and Ser^{392} respectively, were used. Expression of the non-phosphorylated form of p53 was established using an anti-p53 polyclonal antibody purified from rabbit serum (Santa Cruz Biotechnology). Immunoreactive bands were detected using the horseradish peroxidase-conjugated anti-mouse IgG (for active JNK) or anti-rabbit IgG (for non-phosphorylated JNK, active p53 and non-phosphorylated p53) and enhanced chemiluminescence. Bandwidths were quantified by densitometry (D-Scan PC software).

p53 mRNA expression

Total RNA was extracted from cortical neurons using TRI Reagent (Sigma–Aldrich). cDNA synthesis was performed on 1 μg of total RNA using oligo(dT) primer according to the manufacturer's instructions (Life Technologies). The RNA was treated with RNase-free DNase I (Life Technologies) at 1 unit/μg of RNA for 15 min at 37 °C. Equal amounts of cDNA were used for PCR amplification for a total of 28 cycles. The cycling conditions were 95 °C for 5 min, followed by cycles of 95 °C for 1 min 15 s, 52 °C for 1 min 15 s and 72 °C for 1 min 30 s. A final extension step was performed at 70 °C for 10 min. Primers were pretested through an increasing number of amplification cycles to obtain reverse transcriptase–PCR products in the exponential range. The PCR products were analysed by electrophoresis on 1.5 % (w/v) agarose gels, visualized by ethidium bromide staining, photographed and quantified using densitometry. Primers used were as follows: rat p53 sense, 5′-GGCCATCTACAAGAAGTCAC-3′ and antisense, 5′-CCAGAAGATTCCCACTGGAG-3′; rat β-actin

sense, 5′-GAAATCGTGCGTGACATTAAAGAGAAGCT-3′ and antisense, 5′-TCAGGAGGAGCAATGATCTTGA-3′ [30]. The primers generated a p53 PCR product of 317 bp and a β-actin PCR product of 360 bp. To control for any residual genomic DNA contamination, β-actin primers were chosen to span an intron. This meant that any amplification of genomic, rather than cDNA, would result in larger products than those expected. This semi-quantitative technique facilitated estimation of p53 mRNA expression using β-actin as a reference gene. No observable change in β-actin mRNA was observed in any of the treatment conditions.

Terminal transferase deoxytidyl uridine end-labelling (TUNEL)

Apoptotic cell death was assessed using the DeadEnd colorimetric apoptosis detection system (Promega, Madison, WI, U.S.A.). Cells were treated with Aβ for 72 h to evoke maximal DNA fragmentation [8]. Cells were then fixed with paraformaldehyde (4 %, w/v), permeabilized with Triton X-100 (0.1 %) and biotinylated nucleotide was incorporated at 3′-OH DNA ends using the enzyme terminal deoxynucleotidyl transferase. Horseradish peroxidase-labelled streptavidin then bound to the biotinylated nucleotide and this was detected using the peroxidase substrate H_2O_2 and the chromogen diaminobenzidine. Cells were then viewed under light microscopy at ×40 magnification, where the nuclei of TUNEL-positive cells stained brown. Apoptotic cells (TUNEL-positive) were counted and expressed as a percentage of the total number of cells examined. To exclude the possibility that the number of living cells present on the coverslip had an effect on the TUNEL-positive ratio, the same number of cells (approx. 400) was counted for each treatment.

Measurement of caspase 3 activity

Caspase 3 activity was assessed by immunocytochemistry using an anti-active caspase 3 antibody (Promega). Briefly, cells were treated with Aβ for 24 h, fixed with 4 % paraformaldehyde, blocked with 5 % (v/v) goat serum in PBS, incubated with anti-active caspase 3 antibody (1 : 200 dilution, overnight incubation at 4 °C). Immunoreactivity was detected using a biotinylated anti-rabbit IgG antibody and streptavidin conjugated to horseradish peroxidase. Immunoreactive cells were visualized with the chromogen diaminobenzidine, and the number of immunoreactive cells was counted and expressed as a percentage of the total number of cells examined (400–500 cells/coverslip).

Fluorescence immunocytochemistry

Cells were fixed with 4 % paraformaldehyde, permeabilized with 0.1 % Triton X-100 and non-reactive sites were blocked with 5 % goat serum in PBS. To determine the intracellular distribution of active JNK, the cells were incubated overnight with an anti-active JNK antibody (Santa Cruz Biotechnology) purified from mouse serum. To evaluate the efficacy of the antisense oligonucleotides in down-regulating JNK expression, immunolocalization of non-phosphorylated JNK1 and JNK2 was assessed using anti-JNK1 or anti-JNK2 monoclonal antibodies purified from mouse serum antibody (Santa Cruz Biotechnology). Cells were then incubated with anti-mouse IgG conjugated to FITC (Sigma-Aldrich) and viewed by fluorescence microscopy at an excitation of 510 nm.

Statistics

Statistical analysis was performed using ANOVA followed by the *post hoc* Student–Newman–Keuls test and the significance (at the 0.05 level) was indicated. When comparisons were being made between two treatments, a paired Student's t test was performed and $P < 0.05$ or $P < 0.01$ were considered significant.

RESULTS

Aβ activates JNK in cortical neurons

Cortical neurons were exposed to Aβ (2 μM) for 1 and 24 h and JNK activity was examined by fluorescence immunocytochemistry using an antibody that recognizes phosphorylated JNK (Figure 1A). In control conditions phospho-JNK immunoreactivity was detected in some cells, demonstrating a basal level of JNK activation. However, in cells treated with Aβ, a higher intensity of phospho-JNK immunoreactivity was observed in the cytoplasm and nucleus, a distribution which indicates that activated JNK has both cytosolic and nuclear substrates. Potential nuclear substrates of JNK include the transcription factor, c-Jun [16], which has been shown to be responsible for regulating gene expression in response to cellular insults such as Aβ accumulation [15]. The finding that activated JNK also localized in the cytosol may reflect the association of phospho-JNK with cytosolic substrates such as p53 [28].

Time course of Aβ-mediated activation of JNK1 and JNK2

Western-immunoblot analysis was employed to characterize the time course of Aβ-mediated JNK activation and to determine the nature of the JNK isoforms activated by Aβ in lysates prepared from cortical neurons. Aβ evoked a rapid increase in JNK1 activation, as assessed by expression of phosphorylated JNK1 (Figure 1B). Thus at 5 min, the expression of active JNK1 in control cells was 449 ± 36 (mean bandwidth ± S.E.M.; arbitrary units) and this was significantly increased to 541 ± 45 in Aβ-treated cells ($P < 0.05$, Student's paired t test, $n = 6$). Similarly, a significant increase in JNK1 activity was observed after Aβ treatment for 1 and 6 h. At the 1 h time point, JNK1 activity in control cells was 491 ± 12 and this was significantly increased to 593 ± 45 by Aβ ($P < 0.01$, Student's paired t test, $n = 6$). At the 6 h time point, JNK1 activity in control cells was 450 ± 15 and this was significantly increased to 522 ± 20 by Aβ ($P < 0.05$, Student's paired t test, $n = 6$). In contrast, cells treated with Aβ for 18, 24 and 48 h had no observable increase in JNK1 activation. This result demonstrates the temporal nature of the Aβ-mediated activation of JNK1. Although JNK1 activation in response to Aβ occurs rapidly and is sustained for several hours, the activation is decreased by 18 h. A sample immunoblot illustrating the time-dependent activation of JNK1 by Aβ is shown in Figure 1(D). Also shown is an immunoblot demonstrating that total JNK1 protein expression is unaffected by Aβ.

In contrast, a different pattern of JNK2 activation by Aβ was observed. Aβ had no effect on JNK2 activity at the earlier time points of 5 min–18 h; however, JNK2 activity was significantly increased by Aβ at the later time points of 24 and 48 h ($P < 0.05$, Student's t test, $n = 6$; Figure 1C). A sample immunoblot illustrating the time-dependent activation of JNK2 by Aβ is shown in Figure 1(D). Also shown is an immunoblot demonstrating that total JNK2 protein expression is unaffected by Aβ. It is to be noted that significant basal activity of JNK2 is observed in untreated cells; this is consistent with our immunocytochemical results,

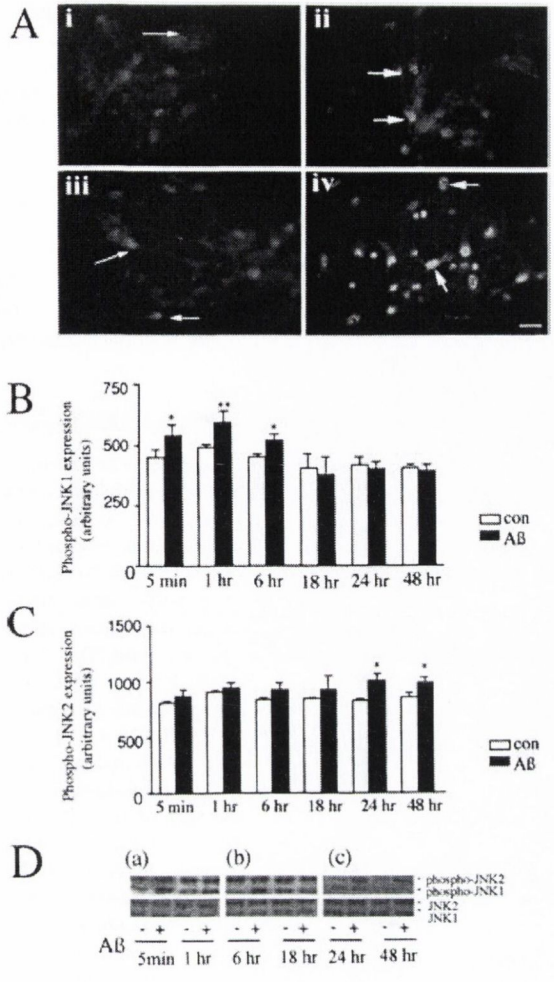

Figure 1 Aβ activates JNK1 and JNK2 within different time frames

(**A**) Cortical neurons were exposed to Aβ (2 μM) for 1 and 24 h and expression of phospho-JNK was monitored by immunofluorescence. In untreated cells (**i**, **iii**) active JNK immunoreactivity is apparent in a subpopulation of cells. In cells exposed to Aβ for 1 h (**ii**) or 24 h (**iv**) more intense phospho-JNK immunostaining is observed in the nucleus and in discrete areas within the cytosol. Arrows indicate cells displaying phospho-JNK immunoreactivity. Scale bar = 20 μm. (**B**) Cells were exposed to Aβ over a range of time points (5 min to 48 h) and phospho-JNK1 expression was monitored by Western-immunoblot analysis. Aβ caused a significant increase in phospho-JNK1 expression at 5 min, 1 and 6 h, but not at subsequent time points. Results are means ± S.E.M. from six independent observations. $^*P < 0.05$, $^{**}P < 0.01$. Statistical analysis was performed using Student's paired *t* test. (**C**) Cells were incubated with Aβ over a range of time points (5 min to 48 h) and phospho-JNK2 expression was monitored by Western-immunoblot analysis. Aβ caused a significant increase in phospho-JNK2 expression at 24 and 48 h, but not at earlier time points. Results are means ± S.E.M. from six independent observations. $^*P < 0.05$. Student's paired *t* test was used for statistical analysis. (**D**) Sample immunoblot demonstrating the Aβ-mediated increase in phospho-JNK1 expression with no concomitant change in expression of phospho-JNK2 or non-phosphorylated forms of JNK1 or JNK2 at (a) 5 min, 1 h, (b) 6 h and (c) 24 and 48 h.

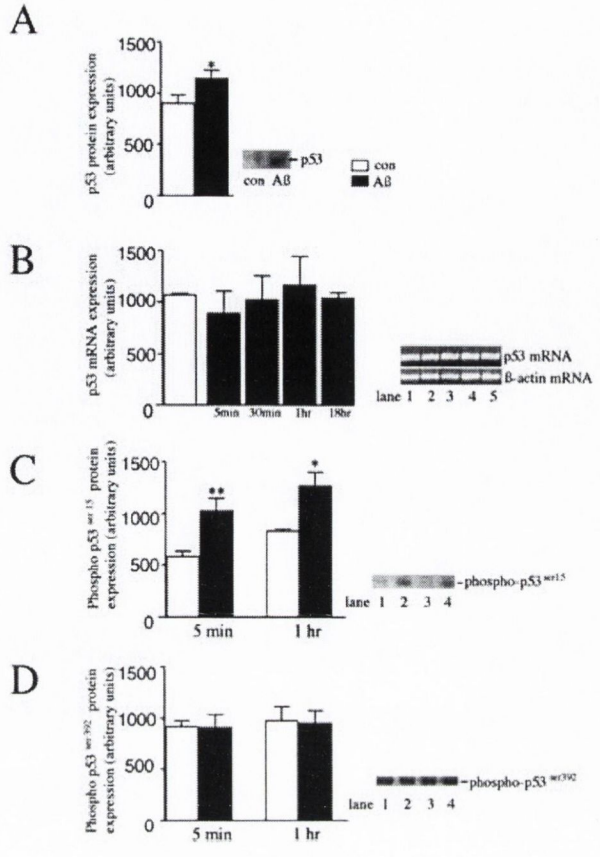

Figure 2 Aβ increases p53 expression and phosphorylation at Ser^{15}

(**A**) Cells were exposed to Aβ (2 μM) for 1 h and p53 expression was assessed by Western-immunoblot analysis. Aβ evoked a significant increase in p53 expression. A sample immunoblot demonstrating the Aβ-mediated increase in p53 expression is shown as an inset. Results are means ± S.E.M. from six independent observations. $^*P < 0.05$. Statistical analysis was performed using Student's paired *t* test. (**B**) Cells were treated with Aβ for a range of time points (5 min to 18 h), total RNA was extracted and expression of p53 mRNA was examined by PCR. A representative image of the ethidium bromide-stained gel is shown as an inset. No change in basal (lane 1) p53 mRNA expression was observed after treatment with Aβ for 5 min (lane 2), 30 min (lane 3), 1 h (lane 4) or 18 h (lane 5). Results are means ± S.E.M. from six independent observations. (**C**) After incubation of the cells with Aβ, the expression of p53 phosphorylated on Ser^{15} was examined by Western-immunoblot analysis. Aβ caused a significant increase in phosphorylation of p53 at Ser^{15} at 5 min and 1 h. A sample immunoblot demonstrating the Aβ-mediated increase in [phosphoSer^{15}]p53 is shown as an inset. At 5 min, basal expression of [phosphoSer^{15}]p53 (lane 1) is increased by Aβ (lane 2). Similarly, at 1 h, basal expression of [phosphoSer^{15}]p53 (lane 3) is increased by Aβ (lane 4). Results are means ± S.E.M. from eight independent observations. $^*P < 0.05$, $^{**}P < 0.01$. Statistical analysis was performed using Student's paired *t* test. (**D**) The effect of Aβ on phosphorylation of p53 at Ser^{392} was assessed by Western-immunoblot analysis. Aβ had no effect on the expression of p53 phosphorylated at Ser^{392} at 5 min or 1 h. A sample immunoblot demonstrating the lack of effect of Aβ on phosphorylation of p53 at Ser^{392} is shown as an inset. At 5 min, basal expression of [phosphoSer^{392}]p53 ('phospho-p53^{ser392}') (lane 1) is unaffected by Aβ (lane 2). Similarly, at 1 h basal expression of [phosphoSer^{15}]p53 ('phospho-p53^{ser15}') (lane 3) is unaffected by Aβ (lane 4). Results are means ± S.E.M. from six independent observations.

where phospho-JNK immunoreactivity was detected in some cells in the absence of Aβ. Basal JNK activity also has been observed in other studies [31] and may reflect an endogenous role for JNK2 in regular cell physiology.

Effect of Aβ on p53 mRNA and protein expression

Since p53 is a target for modulation by JNK [27], the effect of Aβ on p53 expression and phosphorylation was examined in the present study (Figure 2). Figure 2(A) demonstrates that Aβ (2 μM, 1 h) evoked a significant 30% increase in p53 protein expression from 905 ± 78 (means ± S.E.M.; arbitrary units) to 1141 ± 88 ($P < 0.01$, Student's paired *t* test, $n = 6$). This increase in p53 expression was not attributable to a transcription event, since Aβ had no modulatory effect on p53 mRNA expression at any of the time points examined (5 and 30 min, 1 and 18 h; Figure 2B). There was no time-dependent

effect on basal levels of p53 mRNA expression and hence the control data were pooled on the graph for clarity. Since p53 phosphorylation at Ser^{15} can stabilize p53 by preventing ubiquitin-mediated degradation [33], we examined the effect of Aβ on p53 phosphorylation using an antibody that recognizes phospho-Ser^{15} on p53 (Figure 2C). Aβ significantly increased expression of [phosphoSer^{15}]p53 from 587 ± 55 to 1030 ± 116 at 5 min ($P < 0.01$, Student's paired t test, $n = 8$) and from 837 ± 19 to 1265 ± 118 at 1 h ($P < 0.05$, Student's paired t test, $n = 6$). In contrast, Aβ failed to induce phosphorylation of p53 at Ser^{392} at these time points. This result suggests that Aβ increases p53 protein expression by stabilizing the p53 protein via phosphorylation at Ser^{15}.

Depletion of JNK1 and JNK2 by antisense oligonucleotides

To examine the respective roles of JNK1 and JNK2 in the Aβ-mediated modulation of p53 stabilization, antisense technology was employed. We first evaluated the effectiveness of the selected antisense oligonucleotide sequences in down-regulating expression of the JNK1 or JNK2 proteins using immunocytochemistry and Western-immunoblot analysis (Figure 3). Immunocytochemical analysis of JNK1 (Figure 3A, i and ii) and JNK2 (Figure 3A, iii and iv) expression revealed intracellular JNK1 and JNK2 immunoreactivity in control cells that was markedly down-regulated in cells transfected with the respective JNK1 and JNK2 antisense sequences. To quantify the antisense-mediated depletion of the respective JNK isoforms, Western-immunoblot analysis was employed. Figure 3(B) demonstrates that there was no difference in JNK1 expression in untreated cells when compared with cells treated with the scrambled JNK1 control oligonucleotide. However, in cells treated with the antisense JNK1 oligonucleotide for 48 h, JNK1 expression was significantly decreased by 80 % ($P < 0.01$, Student's paired t test; compared with cells treated with JNK1 scrambled oligonucleotide $n = 4$). Figure 3(C) demonstrates an identical result for JNK2. However, in cells treated with the antisense JNK2 oligonucleotide for 48 h, JNK2 expression was also significantly attenuated. Sample immunoblots demonstrating the efficacy of the JNK1 and JNK2 antisense oligonucleotides in down-regulating expression of JNK1 and JNK2 proteins respectively are shown as insets in Figures 3(B) and 3(C). We also verified that the JNK1 antisense had no effect on JNK2 expression (Figure 3D) and that the JNK2 antisense too had no effect on expression of JNK1 (Figure 3E). These results demonstrate that the JNK1 and JNK2 antisense sequences evoke a selective down-regulation in expression of their respective target proteins.

We confirmed that this extent of JNK depletion was sufficient to abrogate Aβ-mediated JNK activation (Figures 3F and 3G). Since the maximal activation of JNK1 and JNK2 occurred after 1 and 24 h treatment with Aβ respectively, the effect of JNK depletion on JNK1 and JNK2 activation was examined at these time points. For JNK1 (Figure 3F) in scrambled oligonucleotide-treated cells, Aβ (2 μM, 1 h) evoked a significant increase in expression of phospho-JNK1 ($P < 0.05$, ANOVA; compared with cells treated with JNK1 scrambled oligonucleotide alone, $n = 6$). However, in JNK1 antisense oligonucleotide-treated cells, the basal expression of activated phospho-JNK1 was 613 ± 39, and 503 ± 57 after incubation with Aβ (2 μM, 1 h, $n = 6$), demonstrating that the JNK1 antisense was effective in reducing the Aβ-mediated stimulation of JNK1 phosphorylation. Figure 3(G) demonstrates that in cells treated with the JNK2 scrambled oligonucleotide, expression of activated phospho-JNK2 was significantly increased by Aβ (2 μM, 24 h; $P < 0.05$, ANOVA; compared with cells

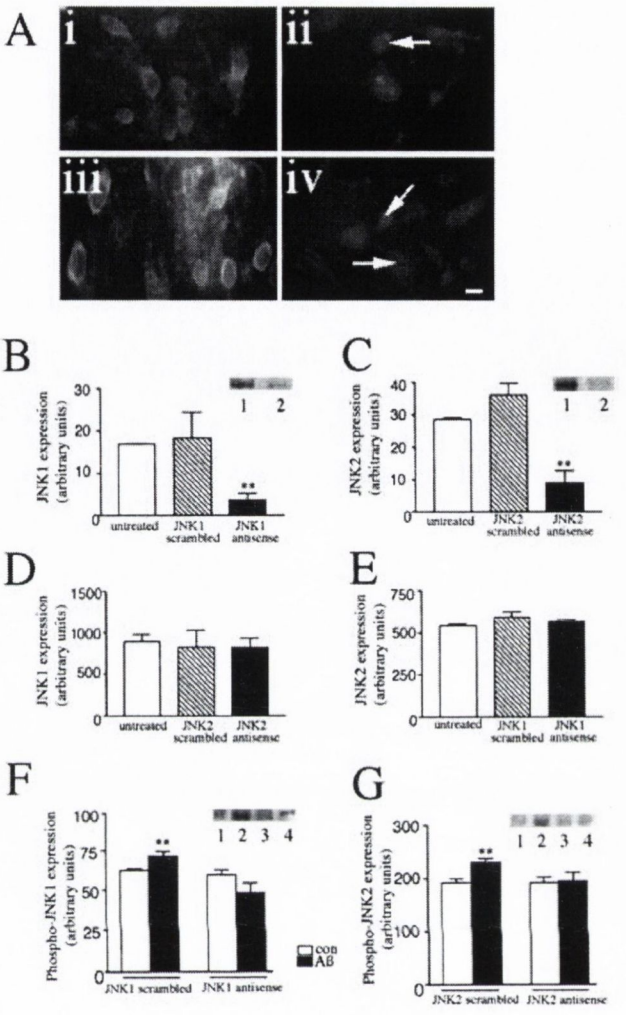

Figure 3 Determination of the efficacy of the JNK antisense sequences in down-regulating JNK1/JNK2 expression

(**A**) Cells were treated with either JNK1 or JNK2 antisense (2 μM) for 48 h and the consequence on JNK1 and JNK2 expression was examined by fluorescence immunocytochemistry using monoclonal JNK1 or JNK2 antibodies. (**i**) In untreated cells, JNK1 expression was localized throughout the cytoplasm with a high level of immunoreactivity at the inner plasma membrane; (**ii**) JNK1 immunostaining was significantly decreased in JNK1 antisense-treated cells; (**iii**) in untreated cells, JNK2 expression was abundant in the cytosol and inner plasma membrane; and (**iv**) JNK2 immunostaining was significantly decreased in JNK2 antisense-treated cells. Cells that have been successfully depleted of JNK are indicated by the arrows. Scale bar = 5 μm. (**B**) Antisense-mediated depletion of JNK1 was quantified by Western-immunoblot analysis. The JNK1 scrambled sequence had no effect on JNK1 expression; however, the JNK1 antisense significantly decreased JNK1 expression by approx. 80 %. A sample immunoblot demonstrating the JNK1 antisense-mediated depletion of JNK1 is shown as an inset. JNK1 is abundant in JNK1 scrambled-treated cells (lane 1) and JNK1 expression is down-regulated in JNK1 antisense-treated cells (lane 2). Results are expressed as means ± S.E.M. from four observations. $^{**}P < 0.01$. Student's paired t test was used for statistical analysis. (**C**) Antisense-mediated depletion of JNK2. The procedure is same as in (**B**). (**D**) Neither JNK2 scrambled nor JNK2 antisense oligonucleotides had any effect on JNK1 expression. Results are expressed as means (arbitrary units) ± S.E.M. from four observations. (**E**) Same as in (**D**), but with JNK2. (**F**) In JNK1 scrambled oligonucleotide-treated cells, Aβ (2 μM, 1 h) retained the ability to stimulate JNK1 activity, as assessed by phospho-JNK1 expression. However, JNK1 antisense abrogated the Aβ-mediated increase in JNK1 activity. Results are expressed as means ± S.E.M. from six observations. $^{**}P < 0.05$. Statistical analysis was performed using ANOVA. (**G**) In JNK2 scrambled oligonucleotide-treated cells, Aβ (2 μM, 24 h) retained the ability to stimulate JNK2 activity, as assessed by phospho-JNK2 expression. However, JNK2 antisense abrogated the Aβ-mediated increase in JNK2 activity. Results are expressed as means ± S.E.M. from six observations, $^{**}P < 0.05$. Statistical analysis was performed using ANOVA.

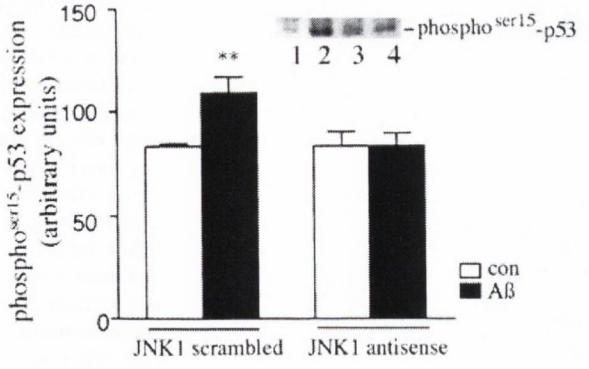

Figure 4 Depletion of JNK1 prevents the Aβ-mediated stimulation of p53 phosphorylation

The consequence of JNK1 depletion on the ability of Aβ to impact on p53 was examined by Western-immunoblot analysis using an antibody that recognizes p53 phosphorylated at Ser[15]. In control scrambled oligonucleotide-treated cells, Aβ (2 μM, 1 h) significantly increased [phosphoSer[392]]p53 expression. In contrast, JNK1 depletion prevented the Aβ-mediated increase in [phosphoSer[15]]p53 expression. Results are the means ± S.E.M. from six independent observations. $^{**}P < 0.05$. Statistical analysis was performed using ANOVA.

treated with JNK2 scrambled oligonucleotide alone, $n = 6$). However, in JNK2 antisense oligonucleotide-treated cells the expression of activated phospho-JNK2 was unaffected by Aβ (2 μM, 24 h, $n = 6$) and this result demonstrates that the JNK2 antisense had the capacity to reduce the Aβ-mediated stimulation of phospho-JNK2.

Having established the efficacy of the JNK1 and JNK2 antisense sequences in depleting expression of their respective target proteins and abrogating the stimulatory effect of Aβ on JNK1 and JNK2 phosphorylation, we used the antisense approach to determine the role of the JNK isoforms in Aβ-mediated activation of p53 and induction of the apoptotic cascade.

JNK1 is involved in Aβ-mediated phosphorylation of p53

Since JNK2 activation by Aβ was only observed at the later time point of 24 h, it seemed unlikely that JNK2 was involved in p53 phosphorylation, since the impact of Aβ on p53 occurred within 60 min. In contrast, Aβ-mediated activation of JNK1 was an earlier event that could potentially be upstream of p53 phosphorylation. Therefore the antisense approach was used to examine the role of JNK1 in the Aβ-mediated phosphorylation of p53 at Ser[15] (Figure 4). After treatment with Aβ (2 μM, 1 h), phospho-p53 expression is significantly increased from 84 ± 1 (means ± S.E.M.; arbitrary units) to 109 ± 8 ($P < 0.05$, ANOVA; compared with control cells, $n = 8$). Although the JNK1 antisense oligonucleotide alone had no effect on p53 phosphorylation, it abolished the stimulatory effect of Aβ on p53 phosphorylation at Ser[15]. A sample immunoblot demonstrating that JNK1 antisense abrogates the Aβ-mediated increase in phospho-p53 expression in shown as an inset in Figure 4.

Thus this result provides evidence of a role for JNK1 in the Aβ-mediated phosphorylation of p53 at Ser[15].

Role of JNK1 and JNK2 in Aβ-mediated activation of apoptotic cascade

A downstream consequence of JNK activation and p53 phosphorylation at Ser[15] is a commitment to the cell death pathway

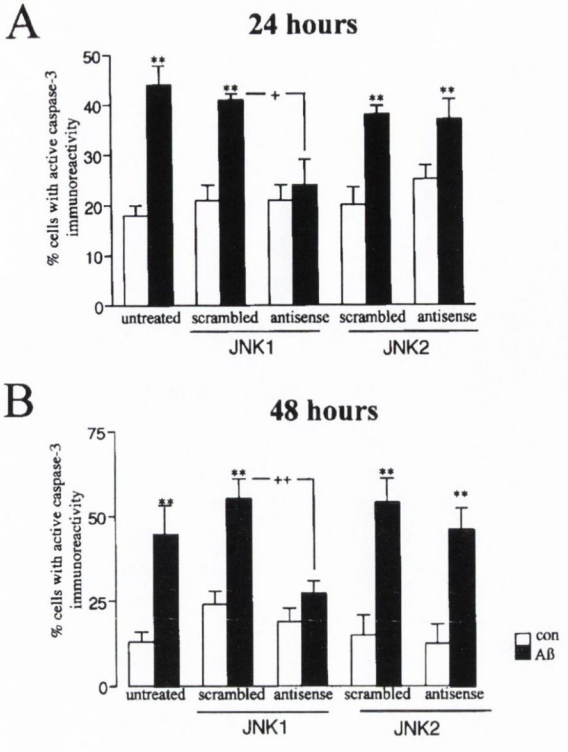

Figure 5 Consequences of JNK1 and JNK2 depletion on Aβ-induced activation on caspase 3 activation

(**A**) The percentage of cells displaying anti-active caspase 3 immunoreactivity was assessed by immunocytochemistry. In cells that had not been treated with oligonucleotide (untreated), Aβ (2 μM, 24 h) significantly increased the percentage of cells displaying active caspase 3 immunostaining by 40 %. In JNK1 scrambled oligonucleotide-treated cells, Aβ also evoked a significant increase in active caspase 3 immunoreactivity. However, this effect was abrogated in JNK1 antisense-treated cells. In contrast, neither the JNK2 scrambled nor the JNK2 antisense oligonucleotide had any effect on the proclivity of Aβ to evoke the increase in active caspase 3 immunoreactivity. Results are the means ± S.E.M. from six independent observations. $^{**}P < 0.05$; $^{+}P < 0.05$. (**B**) The effect of JNK1 and JNK2 depletion on the Aβ-mediated activation of caspase 3 at 48 h was assessed. Other details are the same as in (**A**). $^{**}P < 0.05$; $^{++}P < 0.05$. All statistical analyses were performed using ANOVA.

[17,32]. Since Aβ activates both JNK1 and JNK2 in cortical neurons, the respective roles of JNK1 and JNK2 in coupling Aβ with activation of the apoptotic cascade were examined using the JNK1 and JNK2 antisense oligonucleotides. The components of the apoptotic cascade that were examined in the present study were activation of the caspase 3 and DNA fragmentation.

Caspase 3 activity was examined by immunocytochemistry using an anti-active caspase 3 antibody. Figure 5(A) demonstrates that in untreated cells, the percentage of cells displaying active caspase 3 immunoreactivity was 18 ± 2 % (means ± S.E.M.) and this was significantly increased to 45 ± 4 % after treatment with Aβ for 24 h ($P < 0.05$, ANOVA; compared with untreated cells, $n = 6$ coverslips). After transfection with the JNK1 scrambled oligonucleotide, the Aβ-mediated stimulation of caspase 3 was retained ($P < 0.05$, ANOVA, $n = 6$ coverslips). In contrast, the JNK1 antisense oligonucleotide significantly decreased the Aβ-mediated stimulation of caspase 3 activity ($P < 0.05$, ANOVA; compared with cells treated with Aβ + JNK1 scrambled oligonucleotide, $n = 6$ coverslips). Thus in cells transfected with JNK1 antisense alone, the percentage of cells with active caspase 3 immunostaining was 21 ± 3 % and, in cells treated with Aβ in the presence of JNK1 antisense

oligonucleotide, 24 ± 4 % of cells displayed active caspase 3 immunoreactivity ($n = 6$ coverslips). This result demonstrates that JNK1 is pertinent in the Aβ-mediated activation of caspase 3 in cultured cortical neurons. In contrast, depletion of JNK2 had no effect on Aβ-mediated activation of caspase 3 at 24 h. Thus in cells treated with JNK2 antisense alone, 25 ± 3 % of cells displayed active caspase 3 immunoreactivity and this was significantly increased to 38 ± 4 % in JNK2-depleted cells treated with Aβ for 24 h ($P < 0.05$, ANOVA; compared with cells treated with JNK2 antisense alone, $n = 6$). Since the Aβ-mediated stimulation of JNK2 was retained after depletion of JNK2, we conclude that JNK2 is not involved in the Aβ-mediated activation of caspase 3 that is found to occur at the 24 h time point.

Since cells had to be incubated with Aβ for 24 h before JNK2 activation was detected, our finding that JNK2 was not involved in the Aβ-mediated activation of caspase 3 at 24 h is not surprising. To determine whether JNK2 was involved in caspase 3 activation at later time points, we repeated the experiment by monitoring the effect of JNK1 and JNK2 antisense on Aβ-mediated activation of caspase 3 at 48 h, a time point that would be downstream of JNK2 activation. Figure 5(B) demonstrates that in untreated cells, the percentage of cells displaying active caspase 3 immunoreactivity was 13 ± 3 % (means ± S.E.M.) and this was significantly increased to 45 ± 8 % after treatment with Aβ for 48 h ($P < 0.05$, ANOVA; compared with untreated cells, $n = 6$ coverslips). After transfection with the JNK1 scrambled oligonucleotide, the Aβ-mediated stimulation of caspase 3 was retained ($P < 0.05$, ANOVA; $n = 6$ coverslips). In contrast, the JNK1 antisense oligonucleotide significantly decreased the Aβ-mediated stimulation of caspase 3 activity ($P < 0.05$, ANOVA; compared with cells treated with Aβ + JNK1 scrambled oligonucleotide, $n = 6$ coverslips). Thus in cells transfected with JNK1 antisense alone, the percentage of cells with active caspase 3 immunostaining was 19 ± 4 % and, in cells treated with Aβ in the presence of JNK1 antisense oligonucleotide, 25 ± 4 % of cells displayed active caspase 3 immunoreactivity ($n = 6$ coverslips). This result demonstrates that JNK1 is pertinent in the Aβ-mediated activation of caspase 3 in cultured cortical neurons at 48 h. In contrast, depletion of JNK2 had no effect on Aβ-mediated activation of caspase 3 at 48 h. Thus in cells treated with JNK2 antisense alone, 13 ± 6 % of cells displayed active caspase 3 immunoreactivity and this was significantly increased to 46 ± 6 % in JNK2-depleted cells treated with Aβ for 48 h ($P < 0.05$, ANOVA; compared with cells treated with JNK2 antisense, $n = 6$). These results demonstrate that JNK1, and not JNK2, is involved in the coupling of Aβ with caspase 3 activation.

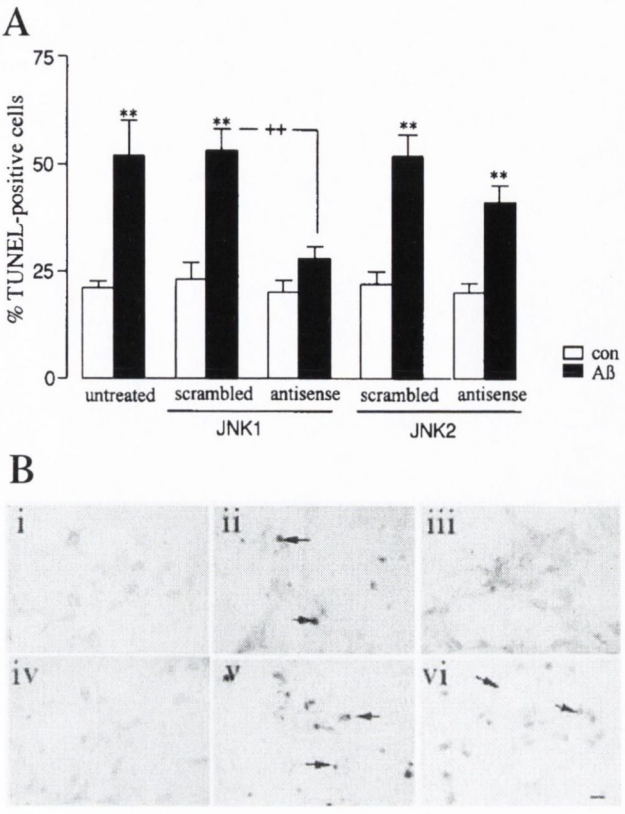

Figure 6 Effect of JNK1 and JNK2 depletion on Aβ-induced DNA fragmentation

(**A**) The effect of JNK1 and JNK2 depletion on the ability of Aβ ('Aß') to induce DNA fragmentation (TUNEL-positive) was assessed. In untreated cells, Aβ significantly increased the percentage of TUNEL-positive cells by 40 %. For JNK1 scrambled oligonucleotide, Aβ also evoked a significant increase in TUNEL-positive cells; however, this effect was significantly decreased in JNK1 antisense-treated cells. Neither the JNK2 scrambled nor the JNK2 antisense oligonucleotides had any effect on the proclivity of Aβ to evoke an increase in active DNA fragmentation. Results are the means ± S.E.M. from six independent observations. $^{**}P < 0.05$; $^{++}P < 0.05$. Statistical analysis was performed using ANOVA. con, control. (**B**) Representative TUNEL staining for cells treated with (i) JNK1 scrambled oligonucleotide, (ii) Aβ + JNK1 scrambled oligonucleotide, (iii) Aβ + JNK1 antisense oligonucleotide, (iv) JNK2 scrambled oligonucleotide, (v) Aβ + JNK2 scrambled oligonucleotide and (vi) Aβ + JNK2 antisense oligonucleotide. Scale bar = 20 μm.

Role of JNK1 and JNK2 in Aβ-mediated DNA fragmentation

One of the later stages in apoptosis is the fragmentation of nuclear DNA. We have previously shown that $A\beta_{1-40}$ has no effect on DNA fragmentation before 48 h, but a maximal 35 % increase in DNA fragmentation is observed after exposure of cortical neurons to $A\beta_{1-40}$ for 72 h [8]; we therefore chose to use that time point in the present study. The effect of Aβ on DNA fragmentation was analysed by TUNEL and the roles of JNK1 and JNK2 in Aβ-mediated DNA fragmentation were assessed after antisense-mediated depletion of the JNK1 and JNK2 isoforms (Figure 6). In untreated cortical neurons, the percentage of cells with fragmented DNA (TUNEL-positive cells) was 21 ± 2 % (means ± S.E.M.) and this was maximally increased to 52 ± 8 % by Aβ (72 h, 2 μM) ($P < 0.05$, ANOVA, $n = 6$ coverslips) as has been previously reported [5]. After transfection with the JNK1 scrambled control oligonucleotide, the Aβ-induced DNA fragmentation was retained ($P < 0.05$, ANOVA, $n = 6$ coverslips). In contrast, the JNK1 antisense oligonucleotide abolished the Aβ-mediated stimulation in DNA fragmentation. Thus in cells transfected with JNK1 antisense oligonucleotide, the percentage of cells with DNA fragmentation was 20 ± 2 % in control cells and 28 ± 3 % in Aβ-treated cells. This result demonstrates that JNK1 is pertinent in the induction of DNA fragmentation by Aβ. Since JNK1 was also found to have a role in the Aβ-mediated activation of caspase 3, a key executioner of apoptosis, the JNK1-dependent DNA fragmentation probably involves caspase 3 as an upstream component of this pathway. To determine the role of JNK2 in Aβ-mediated DNA fragmentation, the cells were transfected with the JNK2 antisense oligonucleotide. Figure 6 demonstrates that after depletion of JNK2, Aβ retained the ability to evoke a significant increase in DNA fragmentation ($P < 0.05$, ANOVA, $n = 6$). Thus JNK1 is the principal isoform involved in

coupling Aβ with activation of caspase 3 and DNA fragmentation in cortical neurons.

DISCUSSION

The aim of the present study was to examine the roles of JNK1 and JNK2 in Aβ-mediated induction of the apoptotic cascade in cultured cortical neurons. In the absence of a suitable pharmacological inhibitor to distinguish between JNK1- and JNK2-mediated effects, antisense technology was employed to cause a selective down-regulation in expression of JNK1 and JNK2 to examine their respective roles in the apoptotic pathway. Aβ increased phospho-JNK expression in isolated cortical neurons with activated JNK immunoreactivity being localized to discrete regions within the nucleus and cytosol. This pattern of distribution is consistent with the distribution of phospho-JNK in response to other stress stimuli, where nuclear staining may reflect the ability of JNK to regulate transcription of stress-induced genes [33]. The punctate distribution of phospho-JNK that we detect in the cytosol after exposure to Aβ may represent mitochondrial targeting of JNK [34] or association of JNK with cytosolic substrates such as p53 [28]. The results obtained from Western-immunoblot analysis of cell lysates demonstrate a differential temporal activation of JNK1 and JNK2 in cultured cortical neurons. JNK1 was activated rapidly (within 5 min) by Aβ and sustained for several hours. By 18 h, the Aβ-mediated activation of JNK1 had returned to basal levels, demonstrating the temporal effectiveness of this signalling cascade. In contrast, Aβ failed to induce an early activation of JNK2 but JNK2 activity was increased by Aβ at the later time points of 24 and 48 h. The finding that Aβ activates JNK1 and JNK2 within dissimilar time frames suggests that JNK1 and JNK2 may have distinct roles in cellular stress responses to Aβ. Expression of p53 and phosphorylation of p53 at Ser^{15} were increased by Aβ. Phosphorylation of p53 at Ser^{15} has been reported as a proximal event in cellular apoptosis [23] and the ability of Aβ to phosphorylate p53 was abolished in JNK1-depleted cells. The effect of Aβ on downstream apoptotic events, namely caspase 3 activation and DNA fragmentation, was also significantly attenuated after JNK1 antisense treatment. In contrast, depletion of JNK2 had no effect on the ability of Aβ to activate caspase 3 or induce DNA fragmentation.

Our finding that $A\beta_{1-40}$ increases phospho-JNK expression in cortical neurons agrees closely with the effects of other Aβ fragments in neuronal systems. $A\beta_{1-42}$ and $A\beta_{25-35}$ have been reported to increase JNK activity in cortical neurons [13] and $A\beta_{1-42}$ increases JNK phosphorylation in sympathetic neurons and PC12 cells [14]. Although there are similarities in the effects of different Aβ peptides on the JNK pathway, it is to be noted that the time frame for JNK activation varies considerably between different Aβ peptide species. In the present study, we have demonstrated that JNK1 is activated within 5 min of exposure to $A\beta_{1-40}$, whereas the Aβ-mediated activation of JNK2 is not apparent until 24 h. In contrast, $A\beta_{25-35}$ increases JNK1 activity at 4 h, but not at earlier time points [13], and $A\beta_{1-42}$ causes peak activation of both JNK1 and JNK2 within 2–6 h in PC12 cells [14]. It is therefore probable that temporal variations in JNK activation may depend on the nature of the Aβ fragment and cell type.

There has been much interest in the signalling events that underlie Aβ-mediated induction of the apoptotic cascade. The present study and the work of other groups [13,15] provide evidence for Aβ impinging on the JNK signalling pathway. Induction of the apoptotic cascade has been attributed to activation of JNK in several systems [32]. In support of a role for JNK in Aβ-mediated cell death, synthetic inhibitors of JNK protect against Aβ-mediated cell [13], although the exact nature of the JNK isoforms that mediate the Aβ neurodegeneration remains to be established. In the present study, we have successfully employed antisense technology to cause a selective down-regulation in expression of JNK1 and JNK2 proteins. After antisense-mediated down-regulation of JNK1 and JNK2, the ability of Aβ to induce phosphorylation of JNK1 and JNK2 was selectively abolished. However, it was surprising that the antisense-mediated down-regulation in JNK1/2 protein expression was not accompanied by a reduction in basal phospho-JNK expression. This may reflect endogenous activity of the residual JNK that remained after antisense treatment or may be due to an enhanced stability of the phosphorylated form of JNK. Since the selected antisense oligonucleotides blocked Aβ-mediated activation of each of the JNK isoforms, this approach was used to elucidate the respective roles of JNK1 and JNK2 in the Aβ-mediated induction of apoptotic events such as phosphorylation of p53, caspase 3 activation and DNA fragmentation.

Our results demonstrate that $A\beta_{1-40}$ increases p53 expression and phosphorylation of p53 at Ser^{15} in cortical neurons. Aβ had no effect on p53 mRNA expression, although other Aβ fragments (i.e. $A\beta_{31-35}$) have been found to increase p53 mRNA expression within 1–3 h of exposure to Aβ in murine neurons [35]. Thus in the rat cortex, the increase in p53 expression occurs in a transcription-independent manner. p53 has a short half-life, which is prolonged in response to cellular stress [22]. Stress-mediated phosphorylation of p53 at residue 15 disrupts its association with the oncoprotein, Mdm-2, preventing ubiquitin-mediated degradation of p53 and thus stabilizing the p53 protein [36]. The finding that Aβ rapidly phosphorylates p53 at Ser^{15} provides a mechanism for the Aβ-mediated increase in p53 expression. In contrast with the ability of Aβ to phosphorylate p53 at Ser^{15} within 5–60 min, no phosphorylation of the Ser^{392} epitope was observed at this time point. Phosphorylation at Ser^{392} occurs in response to DNA damage [37], but since Aβ does not induce DNA damage until 48–96 h [8], phosphorylation at Ser^{392} would be unlikely to occur within the time frame (5–60 min) used here. Thus phosphorylation of p53 at Ser^{15} is an early event in Aβ signalling that may serve to act as an upstream event in the degenerative pathway. The evidence from the present study and by others [16,21], supports an interaction between Aβ and p53. However, the mechanism of Aβ-induced stabilization of p53 remains to be elucidated. Several mechanisms for p53 stabilization have been proposed and these include caesin kinase [38], DNA-activated kinase [39] and JNK [27,40]. Since we have demonstrated that JNK1 is activated rapidly by Aβ in cortical neurons, we used selective antisense oligonucleotides to down-regulate JNK1 expression to elucidate the role of JNK1 in Aβ-mediated activation of p53. Depletion of JNK1 prevented the Aβ-mediated phosphorylation of p53 at Ser^{15} and this result demonstrates that JNK1 is upstream of p53. In non-neuronal cells, JNK1 has also been shown to bind to and phosphorylate p53 [41], although there is also evidence for activation of p53 in response to DNA damage being upstream of JNK activation [42]. Thus the interrelationship between JNK and p53 signalling probably depends on the type of stress stimulus and status of the cell. JNK2 and JNK3 can also serve as p53 N-terminal Ser^{34} kinases in response to cellular stress [40]. However, since the JNK1 antisense completely abrogated the Aβ-mediated phosphorylation of p53 and Aβ-mediated activation of JNK2 was only detected at the later time points of 24–48 h, which was much later than the time required to stabilize p53, we conclude that JNK2 was not pertinent in the Aβ-mediated activation of p53.

After phosphorylation at Ser^{15}, p53 can contribute to apoptosis by inducing transcription of proapoptotic genes such as *bax*,

leading to release of mitochondrial cytochrome *c* and activation of caspase 3, a key executioner of apoptosis [23]. Alternatively, p53 may target directly to the mitochondria to induce a transcription-independent apoptotic signal [43]. Thus potential downstream consequences of JNK1-mediated activation of p53 include induction of caspase 3 and the appearance of apoptotic hallmarks such as DNA fragmentation. After depletion of JNK1, the proclivity of Aβ to activate caspase 3 and induce DNA fragmentation was significantly attenuated. JNK2 depletion had no effect on the Aβ-mediated activation of caspase 3 or increase in DNA fragmentation and this suggests that JNK1 is the principal JNK isoform involved in Aβ-mediated activation of the apoptotic cascade. Although Aβ induced caspase 3 cleavage in this system, it is important to note that the role of caspase 3 in Aβ-mediated neurodegeneration remains a matter of debate. In cortical neurons, a caspase 3 inhibitor has been found to protect neurons against some aspects of Aβ-mediated cell death [44], whereas caspase 3 has been found to have no role in Aβ-mediated hippocampal cell death [5]. The role of caspase 3 in Aβ neurodegeneration has therefore been proposed to be brain-region-specific [45]. Our findings that JNK1 and JNK2 have distinct activation profiles and different roles in the Aβ-mediated induction of the apoptotic cascade highlights the complexity of JNK signalling. In ischaemic death, differential roles of JNK1 and JNK2 have also been reported [29] and there is evidence that the profile of JNK activation is dependent on neuronal cell type and the applied stress paradigm [46]. Furthermore, the use of *jnk3* knockout mice has identified a role for JNK3 in Aβ-mediated neurotoxicity [15], whereas in the present study, we found no evidence of JNK3 activation by $A\beta_{1-40}$ (results not shown) and our result suggests a prominent role for JNK1 in Aβ-mediated DNA fragmentation in this system. This lends further support for the idea that the patterns of JNK signalling utilized by Aβ are diverse and may be subject to developmental factors, cell type and animal species. The present study provides evidence for the 1–40 fragment of Aβ coupling with JNK1 upstream of cell death in the cortex and this is relevant since $A\beta_{1-40}$ is detected in the mature senile plaque [2]. However, the nature of the JNK isoform responsible for evoking cell death by $A\beta_{1-42}$, the principal component of the plaque, remains to be resolved.

In conclusion, Aβ induces phosphorylation of JNK1 and JNK2 in cortical neurons with a distinct temporal pattern. Although JNK1 is pertinent in the Aβ-mediated stabilization of p53, activation of caspase 3 and induction of DNA fragmentation, JNK2 is not involved in coupling Aβ with these apoptotic events. An increase in phospho-JNK expression in the AD brain has been reported [47] and our study indicates that JNK1 may contribute to the pathology of the disease by activating p53 and inducing the apoptotic cascade.

This work was supported by the Health Research Board, Ireland.

REFERENCES

1 Miller, D. L., Papayannopoulos, I. A., Styles, J., Bobin, S. A., Lin, Y. Y., Bieman, K. and Iqbal, K. (1993) Peptide composition of the cerebrovascular and senile plaque core amyloid deposits of Alzheimer's disease. Arch. Biochem. Biophys. **301**, 41–52

2 Iwatsubo, T., Odaka, A., Suzuki, N., Mizusawa, H., Nukina, N. and Ihara, Y. (1994) Visualization of Aβ42 and Aβ40 in senile plaques with end-specific β monoclonals: evidence that an initially deposited species is Aβ42. Neuron **13**, 45–53

3 Adamec, E., Vonsattel, J. F. and Nixon, R. A. (1999) DNA strand breaks in Alzheimer's disease. Brain Res. **849**, 67–77

4 Li, Y. P., Bushnell, A. F., Lee, C. M., Perlmutter, L. S. and Wong, S. K. (1996) β-Amyloid induces apoptosis in human-derived neurotypic SH-SY5Y cells. Brain Res. **738**, 196–204

5 Troy, C. M., Rabacchi, S. A., Friedman, W. J., Frappier, T. F., Brown, K. and Shelanski, M. L. (2000) Caspase-2 mediates neuronal cell death induced by β-amyloid. J. Neurosci. **20**, 1386–1392

6 White, A. R., Guirguis, R., Brazier, M. W., Jobling, M. F., Hill, A. F., Beyreuther, K., Barrow, C. J., Master, C. L., Collins, S. J. and Cappai, R. (2001) Sublethal concentration of prion peptide PrP106–126 or the amyloid peptide protein of Alzheimer's disease activates expression of proapoptotic markers in primary cortical neurons. Neurobiol. Dis. **8**, 299–316

7 Suo, Z., Fang, C., Crawford, F. and Mullan, M. (1997) Superoxide free radical and intracellular calcium mediate Aβ(1–42)-induced endothelial toxicity. Brain Res. **762**, 144–152

8 Boland, B. and Campbell, V. (2003) β-Amyloid$_{(1-40)}$-induced apoptosis of cultured cortical neurons involves calpain-mediated cleavage of poly-ADP ribose polymerase. Neurobiol. Aging **24**, 179–186

9 Jordan, J., Galindo, M. F. and Miller, R. J. (1997) Role of calpain and interleukin-1β converting enzyme-like proteases in the β-amyloid-induced death of rat hippocampal neurons in culture. J. Neurochem. **68**, 1612–1621

10 Eilers, A., Whitfield, J., Shah, B., Spadoni, C., Desmond, H. and Ham, J. (2001) Direct inhibition of c-jun N-terminal kinase in sympathetic neurons prevents c-jun promoter activation and NGK-withdrawal-induced death. J. Neurochem. **76**, 439–1454

11 Yang, D. D., Kuan, C. Y., Whitmarsh, A. J., Rincon, M., Zheng, T. S., Davis, R. J., Rakic, P. and Flavel, R. A. (1997) Absence of excitotoxicity-induced apoptosis in the hippocampus of mice lacking the jnk3 gene. Nature (London) **389**, 865–870

12 Yoshizumi, M., Kogame, T., Suzaki, Y., Fujita, Y., Kyaw, M., Kirima, K., Ishizawa, K., Tsuchiya, K., Kagami, S. and Tamaki, T. (2002) Ebselen attenuates oxidative stress-induced apoptosis via the inhibition of the c-jun N-terminal kinase and activator protein-1 signalling pathway in PC12 cells. Br. J. Pharmacol. **136**, 1023–1032

13 Bozcyzko-Coyne, D., O'Kane, T. M., Wu, Z.-L., Dobrzanski, P., Murthy, S., Vaught, J. L. and Scott, R. W. (2001) CEP-1347/KT-7515, an inhibitor of SAPK/JNK pathway activation, promotes survival and blocks multiple events associated with Aβ-induced cortical neuron apoptosis. J. Neurochem. **77**, 849–863

14 Troy, C. M., Rabacchi, S. A., Xu, Z., Maroney, A. C., Connors, T. J., Shelanski, M. L. and Greene, L. A. (2001) β-Amyloid-induced neuronal apoptosis requires c-jun N-terminal kinase activation. J. Neurochem. **77**, 157–164

15 Morishima, Y., Gotoh, Y., Zieg, J., Barrett, T., Takano, H., Flavell, R., Davis, R. J., Shirasaki, Y. and Greenberg, M. E. (2001) β-Amyloid induces neuronal apoptosis via a mechanism that involves the c-jun N-terminal kinase pathway and the induction of the Fas ligand. J. Neurosci. **21**, 7551–7560

16 Gupta, S., Barrett, T., Whitmarsh, A. J., Cavanagh, J., Sluss, H. K., Derijard, B. and Davis, R. J. (1996) Selective interaction of JNK protein kinase isoforms with transcription factors. EMBO J. **15**, 2760–2770

17 Oren, M. (1994) Relationship of p53 in the control of apoptotic cell death. Semin. Cancer Biol. **5**, 221–227

18 Kitamura, Y., Shimohama, S., Kamoshima, W., Matsuoka, Y., Nomura, Y. and Taniguchi, T. (1997) Changes in p53 in the brains of patients with Alzheimer's disease. Biochem. Biophys. Res. Commun. **232**, 418–421

19 LaFerla, F. M., Hall, C. K., Ngo, L. and Jay, G. (1996) Extracellular deposition of β-amyloid upon p53-dependent cell death in transgenic mice. J. Clin. Invest. **98**, 1626–1632

20 Zhang, Y., McLaughlin, R., Goodyer, C. and LeBlanc, A. (2002) Selective cytotoxicity of intracellular β-amyloid peptide 1–42 through p53 and bax in cultured primary human neurons. J. Cell Biol. **156**, 519–529

21 Culmsee, C., Zhu, X., Yu, Q.-S., Chan, S. L., Camandol, S., Guo, Z., Greig, N. H. and Mattson, M. P. (2001) A synthetic inhibitor of p53 protects neurons against death induced by ischemic and excitotoxic insults, and amyloid β-peptide. J. Neurochem. **77**, 220–228

22 Miller, F. D., Pozniak, C. D. and Walsh, G. S. (2000) Neuronal life and death: an essential role for the p53 family. Cell Death Differ. **7**, 880–888

23 Unger, T., Sionov, R. V., Moallem, E., Yee, C. L., Howley, P. M., Oren, M. and Haupt, Y. (1999) Mutation in serines 15 and 20 of human p53 impair its apoptotic activity. Oncogene **18**, 3205–3212

24 Sakaguchi, K., Sakamoto, H., Lewis, M. S., Anderson, C. W., Erickson, J. W., Appella, E. and Xie, D. (1997) Phosphorylation of serine 392 stabilizes the tetramer formation of tumor-suppressor protein p53. Biochemistry **36**, 10117–10124

25 Zhu, Y., Mao, X. O., Sun, Y., Xia, Z. and Greenberg, D. A. (2002) p38 mitogen-activated protein kinase-mediated hypoxic regulation of Mdm2 and p53 in neurons. J. Biol. Chem. **277**, 22909–22914

26 Kwon, Y. W., Ueda, S., Ueno, M., Yodoi, J. and Masutani, H. (2002) Mechanism of p53-dependent apoptosis induced by 3-methylcholanthrene: involvement of p53 phosphorylation and p38 MAPK. J. Biol. Chem. **277**, 1837–1844

27 Adler, V., Pincus, M. R., Minamoto, T., Fuchs, S. Y., Bluth, M. J., Brandt-Rauf, P. W., Friedman, F. K., Robinson, R. C., Chen, J. M., Wang, X. W. et al. (1997) Conformation-dependent phosphorylation of p53. Proc. Natl. Acad. Sci. U.S.A. **94**, 1686–1691

28 Fuchs, S. Y., Adler, V., Pincus, M. R. and Ronai, Z. (1998) MEKK1/JNK signaling stabilizes and activates p53. Proc. Natl. Acad. Sci. U.S.A. **95**, 10541–10546
29 Hreniuk, D., Garay, M., Gaarde, W., Monia, B. P., McKay, R. A. and Cioffi, C. L. (2001) Inhibition of c-Jun N-terminal kinase 1, but not c-Jun N-terminal kinase 2, suppresses apoptosis induced by ischemia/reoxygenation in rat cardiac myocytes. Mol. Pharmacol. **59**, 867–874
30 Nakajima-Iijima, S., Hamada, H., Reddy, P. and Kakunaga, T. (1985) Molecular structure of the human cytoplasmic β-actin gene: interspecies homology of sequences in the introns. Proc. Natl. Acad. Sci. U.S.A. **82**, 6133–6137
31 Lee, J. K., Park, J., Lee, S. H. and Han, P. L. (1999) Distinct localization of SAPK isoforms in neurons of adult mouse brain implies multiple signaling modes of SAPK pathway. Brain Res. Mol. Brain Res. **70**, 116–124
32 Mielke, K. and Herdegen, T. (2000) JNK and p38 stress kinases – degenerative effectors of signal transduction cascades in the nervous system. Prog. Neurobiol. **61**, 45–60
33 Pena, E., Berciano, M. T., Fernandez, R., Crespo, P. and Lafarga, M. (2000) Stress-induced activation of c-jun N-terminal kinase in sensory ganglion neurons: accumulation in nuclear domains enriched in splicing factors and distribution in perichromatin fibrils. Exp. Cell Res. **256**, 179–191
34 Ito, Y., Mishra, N. C., Yoshida, K., Kharbanda, S., Saxena, S. and Kufe, D. (2001) Mitochondrial targeting of JNK/SAPK in the phorbal ester response of myeloid leukemia cells. Cell Death Differ. **8**, 794–800
35 Yan, X.-Z., Xia, R., Dou, Y., Wang, S.-D., Qiao, Z.-D. and Qiao, J.-T. (2000) Carbachol blocks β-amyloid fragment 31–35-induced apoptosis in cultured cortical neurons. Brain Res. Bull. **51**, 465–470
36 Shieh, S. Y., Ikeda, M., Taya, Y. and Prives, C. (1997) DNA damage-induced phosphorylation of p53 alleviates inhibition by Mdm2. Cell (Cambridge, Mass.) **91**, 325–334
37 Lu, H., Taya, Y., Ikeda, M. and Levine, A. J. (1998) Ultraviolet radiation, but not γ radiation or etoposide-induced DNA damage, results in phosphorylation of the murine p53 protein at serine 389. Proc. Natl. Acad. Sci. U.S.A. **95**, 6399–6402
38 Wang, Y. and Eckhart, W. (1992) Phosphorylation sites in the amino-terminal region of mouse p53. Proc. Natl. Acad. Sci. U.S.A. **89**, 4231–4235
39 Lees-Miller, S. P., Sakaguchi, K., Ullrich, S. J., Appella, E. and Anderson, C. W. (1992) Human DNA-activated protein kinase phosphorylates serines 15 and 37 in the amino-terminal transactivation domain of human p53. Mol. Cell. Biol. **12**, 5041–5049
40 Hu, M. C., Qiu, W. R. and Wang, Y. P. (1997) JNK1, JNK2, and JNK3 are p53 N-terminal serine 34 kinases. Oncogene **15**, 2277–2287
41 Wang, J. and Friedman, E. (2000) Downregulation of p53 by sustained JNK activation during apoptosis. Mol. Carcinog. **29**, 179–188
42 Inamaura, N., Enokido, Y. and Hatanaka, H. (2001) Involvement of c-jun N-terminal kinase and caspase-3-like protease in DNA damage-induced, p53-mediated apoptosis of cultured mouse cerebellar granule neurons. Brain Res. **904**, 270–278
43 Marchenko, N. D., Zaika, A. and Moll, U. M. (2000) Death signal-induced localization of p53 protein to mitochondria. J. Biol. Chem. **275**, 16202–16212
44 Harada, J. and Sugimoto, M. (1999) Activation of caspase-3 in β-amyloid-induced apoptosis of cultured rat cortical neurons. Brain Res. **842**, 311–323
45 Selznick, L. A., Holtzman, D. M., Han, B. H., Gokden, M., Srinivasan, A. N., Johnson, E. M. and Roth, K. A. (1999) *In situ* immunodetection of neuronal caspase-3 activation in Alzheimer's disease. J. Neuropathol. Exp. Neurol. **58**, 1020–1026
46 Mielke, K., Damm, A., Yang, D. D. and Herdegen, T. (2000) Selective expression of JNK isoforms and stress-specific JNK activity in different neuronal cell lines. Mol. Brain Res. **75**, 128–137
47 Zhu, X., Raina, A. K., Rottkamp, C. A., Aliev, G., Perry, G., Boux, H. and Smith, M. A. (2001) Activation and redistribution of c-jun N-terminal kinase/stress-activated protein kinase in degenerating neurons in Alzheimer's disease. J. Neurochem. **76**, 435–441

Received 23 October 2002/16 December 2002; accepted 21 January 2003
Published as BJ Immediate Publication 21 January 2003, DOI 10.1042/BJ20021660

THE JOURNAL OF BIOLOGICAL CHEMISTRY

Vol. 278, No. 30, Issue of July 25, pp. 27971–27980, 2003
Printed in U.S.A.

Activation of the c-Jun N-terminal Kinase Signaling Cascade Mediates the Effect of Amyloid-β on Long Term Potentiation and Cell Death in Hippocampus

A ROLE FOR INTERLEUKIN-1β?*

Received for publication, March 12, 2003, and in revised form, April 30, 2003
Published, JBC Papers in Press, May 7, 2003, DOI 10.1074/jbc.M302530200

Aedín M. Minogue‡§, Adrian W. Schmid¶, Marie P. Fogarty‡, Alison C. Moore‡, Veronica A. Campbell‡, Caroline E. Herron¶, and Marina A. Lynch‡‖

From the ‡Trinity College Institute of Neuroscience, Department of Physiology, Trinity College, Dublin 2, Ireland and the ¶Department of Human Anatomy and Physiology, Conway Institute, University College Dublin, Earlsfort Terrace, Dublin 2, Ireland

Amyloid-β (Aβ) is a major constituent of the neuritic plaque found in the brain of Alzheimer's disease patients, and a great deal of evidence suggests that the neuronal loss that is associated with the disease is a consequence of the actions of Aβ. In the past few years, it has become apparent that activation of c-Jun N-terminal kinase (JNK) mediates some of the effects of Aβ on cultured cells; in particular, the evidence suggests that Aβ-triggered JNK activation leads to cell death. In this study, we investigated the effect of intracerebroventricular injection of $Aβ_{(1-40)}$ on signaling events in the hippocampus and on long term potentiation in Schaffer collateral CA1 pyramidal cell synapses *in vivo*. We report that $Aβ_{(1-40)}$ induced activation of JNK in CA1 and that this was coupled with expression of the proapoptotic protein, Bax, cytosolic cytochrome *c*, poly-(ADP-ribose) polymerase cleavage, and Fas ligand expression in the hippocampus. These data indicate that $Aβ_{(1-40)}$ inhibited expression of long term potentiation, and this effect was abrogated by administration of the JNK inhibitor peptide, D-JNKI1. In parallel with these findings, we observed that Aβ-induced changes in caspase-3 activation and TdT-mediated dUTP nick-end labeling staining in neuronal cultured cells were inhibited by D-JNKI1. We present evidence suggesting that interleukin (IL)-1β plays a significant role in mediating the effects of $Aβ_{(1-40)}$ because $Aβ_{(1-40)}$ increased hippocampal IL-1β and because several effects of $Aβ_{(1-40)}$ were inhibited by the caspase-1 inhibitor Ac-YVAD-CMK. On the basis of our findings, we propose that Aβ-induced changes in hippocampal plasticity are likely to be dependent upon IL-1β-triggered activation of JNK.

One of the pathological hallmarks of Alzheimer's disease (AD)[1] is an accumulation of plaques consisting predominately of amyloid-β (Aβ) peptide, which is processed from amyloid precursor protein by the action of β- and γ-secretase (1). Neuronal cell loss is one feature of AD, and evidence from analysis of changes in cultured cells suggests that Aβ acts as the executioner. Thus, neuronal cultures exposed to Aβ demonstrate signs of apoptosis (2–4), and previous evidence from this laboratory has revealed that cultured cortical neurons exposed to $Aβ_{(1-40)}$ exhibited increased expression of the tumor suppressor p53; increased activation of caspase-3, a marker of apoptotic cell death; and increased TUNEL reactivity (5). The evidence is consistent with the idea that activation of the stress-activated protein kinase, c-Jun N-terminal kinase (JNK) played a significant role, because depletion of JNK1 following exposure to antisense oligonucleotide prevented the effects of Aβ (5). Similarly, Morishima *et al.* (6) reported that Aβ increased phosphorylation of JNK and c-Jun in cultured cortical neurons and that these changes were associated with expression of the death inducer Fas ligand (FasL). Others have reported findings that support a role for JNK activation in mediating at least certain effects of Aβ. For instance, Aβ-induced parallel increases in JNK activation and TUNEL reactivity in PC12 cells (7), whereas activation of JNK was shown to be localized to amyloid deposits in 7- and 12-month-old mice that overexpress amyloid precursor protein (8).

It has emerged in several experimental models that increased JNK phosphorylation is associated with deficits in synaptic function; for instance, increased activation of JNK has been reported in the hippocampi of aged rats (9, 10), rats exposed to whole body irradiation (11), and rats injected with the proinflammatory cytokine, interleukin (IL)-1β (12) or lipopolysaccharide (13), and in all cases glutamate release was decreased. In each of these experimental conditions, long term potentiation (LTP), a model of synaptic plasticity, was markedly impaired, and this impairment was coupled with an increased hippocampal concentration of IL-1β.

A number of groups have reported that Aβ administration exerts an inhibitory effect on LTP. For instance, Aβ peptides (14–16) and naturally secreted Aβ oligomers (17) inhibited LTP in the CA1 region *in vivo*, and Aβ peptides also inhibit LTP in dentate gyrus and the CA1 *in vitro* (18–21). Similarly, a deficit in LTP was reported in aged mice that overexpress amyloid precursor protein and in which deposition of Aβ was observed (22). In this study, we investigated the signaling

* This work was supported by grants from Enterprise Ireland, the Roche Research Foundation, and the Health Research Board, Ireland (to M. P. F.). The costs of publication of this article were defrayed in part by the payment of page charges. This article must therefore be hereby marked "*advertisement*" in accordance with 18 U.S.C. Section 1734 solely to indicate this fact.

§ Recipient of a Trinity College Ussher Fellowship.

‖ To whom correspondence should be addressed. Tel.: 353-1-608-1770; Fax: 353-1-679-3545; E-mail: lynchma@tcd.ie.

[1] The abbreviations used are: AD, Alzheimer's disease; Aβ, amyloid-β; JNK, c-Jun N-terminal kinase; FasL, Fas ligand; IL, interleukin; LTP, long term potentiation; NBM, neurobasal medium; PARP, poly-(ADP-ribose) polymerase; TBS, Tris-buffered saline; BSA, bovine serum albumin; PBS, phosphate-buffered saline; HFS, high frequency stimuli; EPSP, base-line excitatory postsynaptic potential; TUNEL, TdT-mediated dUTP nick-end labeling; ANOVA, analysis of variance.

events induced by $A\beta_{(1-40)}$ that might explain its impact on LTP and report that activation of JNK is a pivotal event in Aβ-induced inhibition of LTP and in Aβ-induced cell death.

EXPERIMENTAL PROCEDURES

Preparation of Aβ—$A\beta_{(1-40)}$ (BioSource International) was made up as a 1 mM stock solution in sterile water and allowed to aggregate for 48 h at 30 °C as described previously (5). For treatment of cortical neurons, aggregated $A\beta_{(1-40)}$ was diluted to a final concentration of 2 μM in prewarmed neurobasal medium (NBM; Invitrogen). For analysis of signaling events stimulated by Aβ, aggregated $A\beta_{(1-40)}$ at 37 °C was injected intracerebroventricularly (5 μl; 1nmol in sterile water). This Aβ preparation (and concentration) was adopted because it was shown to produce consistent, reliable, and reproducible results in a number of markers, suggesting that cell death occurred in cultured cells (5).

Animals—Groups of young male Wistar rats (200–300 g; Bio Resources Unit, Trinity College, Dublin 2, Ireland), maintained at an ambient temperature of 22–23 °C under a 12 h light-dark schedule, were used in this experiment. The rats were anesthetized by intraperitoneal administration of urethane (1.5 mg/kg) and were injected intracerebroventricularly with either sterile water (5 μl) or $A\beta_{(1-40)}$. 6 h post-injection, the rats were killed by decapitation, the brains were rapidly removed on ice, and area CA1 was dissected free. The tissue was cross-chopped (350 × 350 μm) and frozen in Krebs solution containing 10% Me_2SO as previously described (23) until required for analysis.

Analysis of JNK Phosphorylation, c-Jun Phosphorylation, Cytosolic Cytochrome c Expression, Bax Expression, FasL Expression, and PARP Cleavage—JNK phosphorylation, c-Jun phosphorylation, and expression of Bax, cytosolic cytochrome *c*, PARP, and FasL were analyzed in samples prepared from CA1 tissue using a method previously described (13). In the case of JNK, c-Jun, FasL, and PARP, tissue homogenates were diluted to equalize for protein concentration, and aliquots (100 μl, 2 mg/ml) were added to 100 μl of sample buffer (0.5 mM Tris-HCl, pH 6.8, 10% glycerol, 10% SDS, 5% β-mercaptoethanol, 0.05% bromphenol blue (w/v)), boiled for 5 min, and loaded onto 10% SDS-PAGE gels. In the case of cytochrome *c*, cytosolic fraction was prepared by homogenizing slices of hippocampus in lysis buffer (20 mM HEPES, pH 7.4, 10 mM KCl, 1.5 mM $MgCl_2$, 1 mM EDTA, 1 mM EGTA, 1 mM dithiothreitol, 0.1 mM phenylmethylsulfonyl fluoride, 5 μg/ml pepstatin A, 2 μg/ml leupeptin, 2 μg/ml aprotinin), incubating for 20 min on ice, and centrifuging (15,000 × *g* for 10 min at 4 °C). The supernatant (*i.e.* cytosolic fraction) was suspended in sample buffer to a final concentration of 300 μg/ml, boiled for 3 min, and loaded (6 μg/lane) onto 12% SDS-PAGE gels. The pellet (*i.e.* mitochondrial fraction) was resuspended in sample buffer to a final concentration of 300 μg/ml, boiled for 3 min, and loaded (6 μg/lane) onto 12% SDS-PAGE gels. Bax expression was assessed in the mitochondrial fraction. In all experiments the proteins were separated by application of 32 mA constant current for 25–30 min, transferred onto nitrocellulose strips (225 mA for 90 min), and immunoblotted with the appropriate antibody. For JNK phosphorylation, the proteins were immunoblotted with an antibody that specifically targets phosphorylated JNK (1:300 in Tris-buffered saline (TBS)-Tween (0.05% Tween 20) containing 0.1% BSA; Santa Cruz Biotechnology Inc.) for 2 h at room temperature. The blots were stripped and stained for total JNK. Nitrocellulose strips were probed with a mouse monoclonal IgG_1 antibody (1:200; Santa Cruz Biotechnology Inc.) raised against a recombinant protein corresponding to amino acids 1–384 representing full-length JNK1 of human origin. To assess phosphorylation of c-Jun, we immunoblotted with a mouse monoclonal IgG_1 antibody (1:400 in PBS-Tween (0.1% Tween 20) containing 2% nonfat dried milk) raised against the peptide corresponding to a short amino acid sequence of phosphorylated c-Jun of human origin (Santa Cruz Biotechnology Inc.). To assess cytoplasmic cytochrome *c*, a rabbit polyclonal antibody (1:250 in PBS-Tween containing 2% nonfat dried milk; Santa Cruz Biotechnology Inc.) raised against recombinant protein corresponding to amino acids 1–104 of cytochrome *c* was used. In the case of FasL, we immunoblotted with a rabbit polyclonal antibody (1:500 in TBS-Tween containing 1% BSA; Santa Cruz Biotechnology Inc.) raised against a peptide corresponding to a short amino acid sequence at the N terminus of FasL of human origin. Bax expression was assessed in the mitochondrial fraction using a mouse monoclonal IgG_1 antibody (1:200 in TBS-Tween containing 1% BSA; Santa Cruz Biotechnology Inc.). To assess the cleavage of PARP, we immunoblotted with an antibody (1:500 in PBS-Tween (0.1% Tween 20) containing 2% nonfat dried milk) raised against the epitope corresponding to amino acids 764–1014 of PARP of human origin (Santa Cruz Biotechnology Inc.). All of the nitrocellulose strips were reprobed for actin expression to ensure equal loading of protein on all SDS-PAGE gels. Actin expression was assessed using a mouse monoclonal IgG_1 antibody (1:300 in PBS-Tween containing 2% nonfat dried milk) corresponding to an amino acid sequence mapping at the C terminus of actin of human origin (Santa Cruz Biotechnology Inc.). Immunoreactive bands were detected as follows: peroxidase-conjugated anti-mouse IgG (Sigma) and Supersignal chemiluminescence (Pierce) for JNK, c-Jun, Bax, and actin and peroxidase-conjugated anti-rabbit IgG (Sigma) and Supersignal (Pierce) for cytochrome c, FasL, and PARP.

Induction of LTP in CA1 in Vivo—Male Wistar rats (175–200 g; Biomedical Facility, University College, Dublin, Ireland) were anesthetized with urethane (1.5 mg/kg), placed in a stereotaxic frame, and assessed for LTP as described previously (16). Small holes were drilled in the skull to allow insertion of a guide cannula to facilitate intracerebroventricular injection and to allow insertion of the reference, stimulating, and recording electrodes. The recording electrode was positioned in the stratum radiatum of area CA1 (3 mm posterior and 2 mm lateral to bregma), and a bipolar stimulating electrode was placed in the Schaffer collateral/commissural pathway distal to the recording electrode (4 mm posterior and 3 mm lateral to bregma). The cannula was positioned above the lateral ventricle in the opposite hemisphere to that of the electrodes (1 mm posterior and 1.2 mm lateral to bregma). Test shocks (0.033 Hz) were delivered to the Schaffer collateral/commissural pathway, and base-line excitatory postsynaptic potentials (EPSPs), recorded at 35–40% of maximal response, were sampled for at least 30 min to allow the response to stabilize. Rats were then injected intracerebroventricularly with either $A\beta_{(1-40)}$ (1nmol in 5 μl), the membrane soluble JNK inhibitor D-JNKI1 (1 nmol in 5 μl), combined $A\beta_{(1-40)}$ and D-JNKI1 (1nmol of each in 5 μl) or vehicle (5 μl sterile water); and base-line recordings were monitored for a further 60 min before delivery of a series of high frequency stimuli (HFS; 3 × 10 trains of 10 stimuli at 200Hz; intertrain interval, 20 s). Responses to test shock stimulation were recorded for a further 5 h post-HFS, and deep body temperature was maintained at 36.5 ± 0.5 °C using heating pads. Paired pulse facilitation with an interstimulus interval of 50 ms was also examined preinjection, 1 h post-injection of drug/vehicle (prior to HFS), and 5 h following HFS. Deep body temperature was maintained at 36.5 ± 0.5 °C using heating pads. Extracellular field potentials were amplified (×100), filtered at 5 kHz, digitized, and recorded using MacLab software. The EPSP slope was used to measure synaptic efficacy. EPSPs are expressed as percentages of the mean initial slope measured during the first 10 min of the base-line recording period.

Analysis of IL-1β Concentration—IL-1β concentration was analyzed in homogenate prepared from CA1 by enzyme-linked immunosorbent assay (R & D Systems) and in supernatants prepared from cultured cells as described below. Antibody-coated (100 μl; final concentration, 1.0 μg/ml; diluted in PBS, pH 7.3; goat anti-rat IL-1β antibody) 96-well plates were incubated overnight at room temperature, washed several times with PBS containing 0.05% Tween 20, blocked for 1 h at room temperature with 300 μl of blocking buffer (PBS, pH 7.3, containing 5% sucrose, 1% BSA, and 0.05% NaN_3), and washed. IL-1β standards (100 μl; 0–1000 pg/ml in PBS containing 1% BSA) or samples (homogenized in Krebs solution containing 2 mM $CaCl_2$) were added, and incubation proceeded for 2 h at room temperature. Secondary antibody (100 μl; final concentration, 350 ng/ml in PBS containing 1% BSA and 2% normal goat serum; biotinylated goat anti-rat IL-1β antibody) was added and incubated for 2 h at room temperature. The wells were washed, and detection agent (100 μl; horseradish peroxidase-conjugated streptavidin; 1:200 dilution in PBS containing 1% BSA) was added and incubated continued for 20 min at room temperature. Substrate solution (100 μl; 1:1 mixture of H_2O_2 and tetramethylbenzidine) was added and incubated at room temperature in the dark for 1 h, after which time the reaction was stopped using 50 μl of 1 M H_2SO_4. Absorbance was read at 450 nm, and the values were corrected for protein (24) and expressed as pg IL-1β/mg protein.

Preparation of Cultured Cortical Neurons—Primary cortical neurons were isolated and prepared from 1-day-old Wistar rats (BioResources Unit, Trinity College, Dublin 2, Ireland) and maintained in NBM as previously described (5). The rats were decapitated, the cerebral cortices were dissected, and the meninges were removed. The cortices were incubated in PBS with trypsin (0.25 μg/ml) for 25 min at 37 °C. The cortical tissue was then triturated in PBS containing soy bean trypsin inhibitor (0.2 μg/ml) and DNase (0.2 mg/ml) and gently filtered through a sterile mesh filter (40 μm). The suspension was centrifuged at 2000 × *g* for 3 min at 20 °C, and the pellet was resuspended in warm NBM, supplemented with heat inactivated horse serum (10%), penicillin (100 units/ml), streptomycin (100 units/ml), and glutamax (2 mM). The sus-

pended cells were plated at a density of 0.25×10^6 cells on circular 10-mm diameter coverslips, coated with poly-L-lysine (60 μg/ml), and incubated in a humidified atmosphere containing 5% CO_2:95% air at 37 °C for 2 h prior to being flooded with prewarmed NBM. After 48 h, 5 ng/ml cytosine-arabinofuranoside was added to the culture medium to suppress the proliferation of non-neuronal cells. The media were exchanged for fresh media every 3 days, and the cells were grown in culture for up to 7 days prior to treatment. In one set of experiments the neurons were incubated in the absence/presence of $A\beta_{(1-40)}$ (2 μM in NBM) for 72 h with or without caspase-1 inhibitor (100 nM in NBM; Ac-YVAD-CMK; Calbiochem) or D-JNKI1 (1 μM in NBM; Alexis Biochemicals). In the case of Aβ-treated neurones, the supernatant was removed at 20 h, and IL-1β concentration was assessed. At 72 h, the cells were rinsed in TBS and fixed in 4% paraformaldehyde in TBS for immunohistochemical assessment of JNK phosphorylation, caspase-3 activation, and DNA fragmentation. The cells were incubated in $A\beta_{(1-40)}$ (2 μM) for 18 h for analysis of changes in gene expression. In a second series of experiments, the neurons were incubated in the absence/presence of IL-1β (5 ng/ml in NBM) with or without D-JNKI1 (1 μM in NBM) for 18 h and harvested in lysis buffer (20 mM HEPES, pH 7.4, 10 mM KCl, 1.5 mM $MgCl_2$, 1 mM EDTA, 1 mM EGTA, 1 mM dithiothreitol, 0.1 mM phenylmethylsulfonyl fluoride, 5 μg/ml pepstatin A, 2 μg/ml leupeptin, 2 μg/ml aprotinin) for assessment of c-Jun phosphorylation and FasL expression.

Analysis of Bax mRNA and caspase-3 mRNA—Total RNA was extracted from cortical neurones using TRI reagent (Sigma). cDNA synthesis was performed on 1 μg of total RNA using oligo(dT) primer as per the manufacturer's instructions (Superscript reverse transcriptase; Invitrogen). The RNA was treated with RNase-free DNase I (Invitrogen) at 1 unit/μg of RNA for 15 min at 30 °C. Equal amounts of cDNA were used for PCR amplification for a total of 28 cycles. Primers were pretested through an increasing number of amplification cycles to obtain reverse transcriptase-PCR products in the exponential range. In the case of Bax mRNA expression following Aβ treatment primers used were as follows: rat Bax, sense 5′-GCAGAGAGGATGGCTGGGGAGA-3′, and antisense 5′-TCCAGACAAGCAGCCGCTCACG-3′ (25); rat β-actin, sense 5′-GAAATCGTGCGTGACATTAAAGAGAAGCT and antisense 5′-TCAGGAGGAGCAATGATGATCTTGA-3′. The cycling conditions were 95 °C for 5 min followed by cycles of 95 °C for 75 s, 52 °C for 75 s, and 72 °C for 90 s. A final extension step was carried out at 70 °C for 10 min. These primers generated Bax PCR products of 352 base pairs and β-actin PCR product of 360 base pairs. In the case of caspase-3 mRNA expression following treatment with $A\beta_{(1-40)}$ and Bax mRNA expression following treatment with IL-1β, multiplex PCR was performed using the Quantitative PCR Cytopress detection kit (Rat Apoptosis Set 2; BioSource International) generating caspase-3 PCR products of 320 base pairs, Bax PCR products of 352 base pairs and glyceraldehyde-3-phosphate dehydrogenase PCR product of 532 base pairs. The cycling conditions were 94 °C for 1 min and 58 °C for 2 min. A final extension step was carried out at 70 °C for 10 min. The PCR products were analyzed by electrophoresis on 1.5% agarose gels, photographed, and quantified using densitometry. The target genes were normalized to expression of β-actin or glyceraldehyde-3-phosphate dehydrogenase housekeeping genes. No observable change in β-actin or glyceraldehyde-3-phosphate dehydrogenase mRNA was observed in any of the treatment conditions

TUNEL Staining—Apoptotic cell death was assessed using the DeadEnd colorimetric apoptosis detection system (Promega) according to the manufacturer's instructions. Briefly, cultured cortical neurones were prepared from neonatal rats as described above and maintained in NBM for 12 days before incubating in the absence/presence of $A\beta_{(1-40)}$ (1 μM in NBM) for 72 h with or without caspase-1 inhibitor (100 nM in NBM) or D-JNKI1 (1 μM in NBM). Biotinylated nucleotide was incorporated at 3′-OH DNA ends by incubating cells with terminal deoxynucleotidyl transferase for 30 min at 37 °C. The washed cells were incubated in horseradish peroxidase-labeled streptavidin and then incubated in diaminobenzidine chromogen solution, and TUNEL-positive cells were calculated as a proportion of the total cell number.

Immunohistochemical Staining for Phosphorylated JNK and Activated Caspase-3—Cultured cortical neurones were prepared from neonatal rats as described previously (5) and maintained in NBM for 12 days before incubating in the absence/presence of $A\beta_{(1-40)}$ (1 μM in NBM) for 72 h with or without caspase-1 inhibitor (100 nM in NBM) or D-JNKI1 (1 μM in NBM). The cells were fixed in 4% paraformaldehyde in TBS, permeabilized in 0.1% Triton containing 0.2% proteinase K, washed in TBS, and refixed in 4% paraformaldehyde. The cells were incubated with 2.5% (v/v) normal goat serum (Vector Laboratories) in TBS. The blocking serum was removed, and the cells were incubated overnight with either antiactive p-JNK (1:200 in TBS containing 2.5% normal goat serum; Santa Cruz Biotechnology Inc.) or antiactive caspase-3 (1:250 in TBS containing 2.5% (v/v) normal goat serum; Promega) in a humidified chamber. The cells were washed in TBS and incubated in the dark for 2 h at room temperature in either fluorescein isothiocyanate-labeled goat anti-mouse IgG or IgM (1:100; Biosource) to immunolabel p-JNK or L-rhodamine-labeled goat anti-rabbit IgG (1:100; Biosource) to immunolabel active caspase-3. The cells were washed

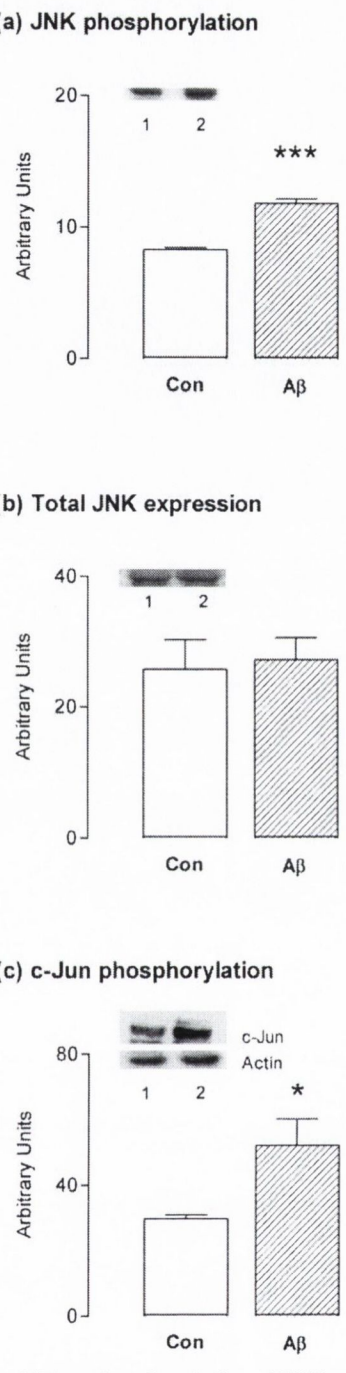

FIG. 1. **Effect of Aβ on phosphorylation of JNK and c-Jun.** JNK (*a*) and c-Jun (*c*) phosphorylation were significantly increased in hippocampal tissue prepared from Aβ-treated rats compared with control rats (***, $p < 0.001$; *, $p < 0.05$; Student's *t* test for independent means; $n = 5$ for JNK and c-Jun, respectively (compare *lanes 2* with *lanes 1*)). Total JNK (*b*) was assessed to ensure equal protein loading, and no significant difference was observed between groups. c-Jun blots were stripped and reprobed for actin to ensure equal protein loading (see second sample immunoblot in *c*).

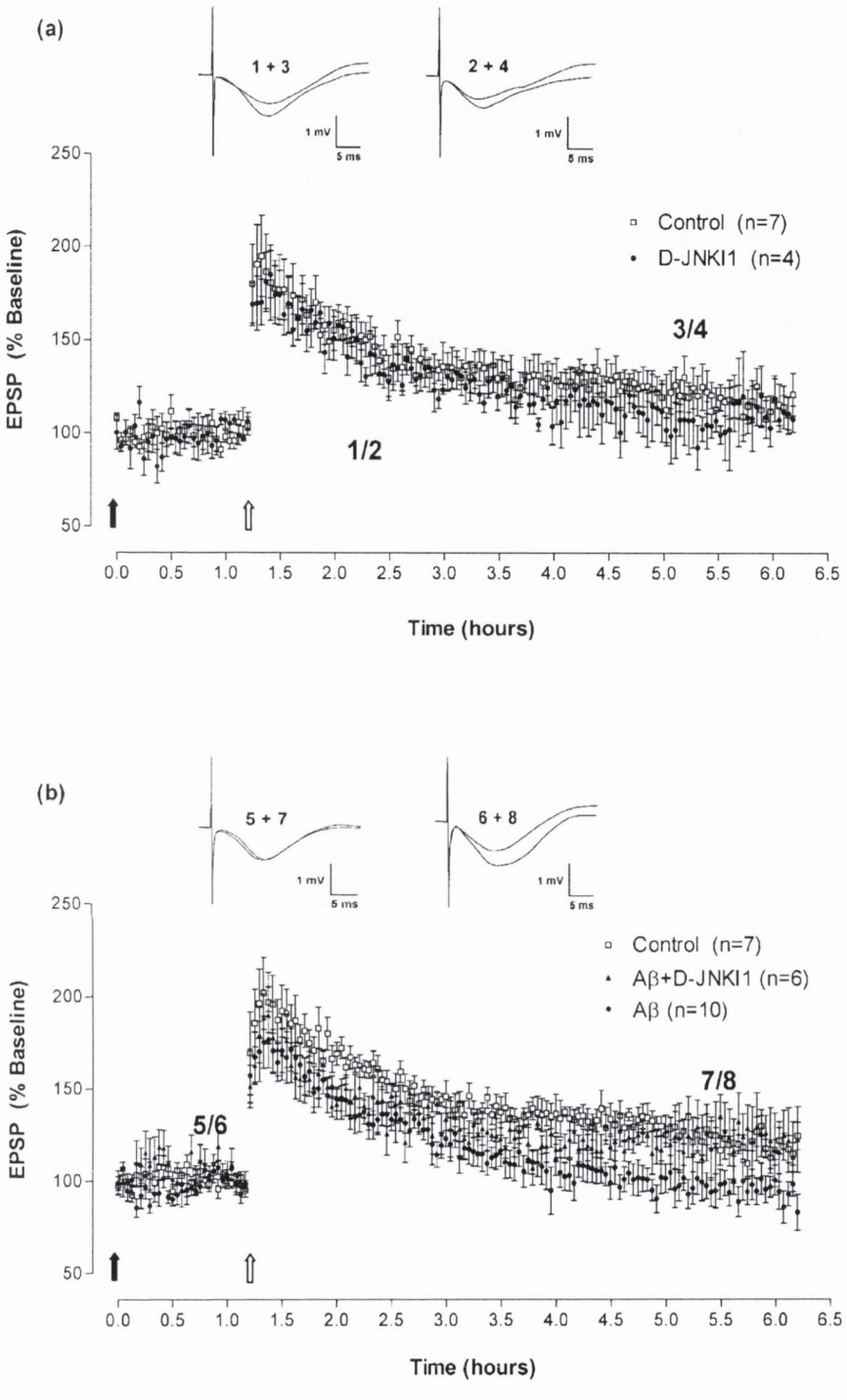

FIG. 2. **Effect of D-JNKI1 on Aβ-induced impairment of LTP.** *a*, LTP recorded up to 5 h post-HFS in two groups of animals either injected intracerebroventricularly with sterile water/vehicle as a control (□) or with D-JNKI1 (●). The *black arrow* indicates the time of intracerebroventricular injection, and the *open arrow* indicates the time of delivery of HFS. The *insets above* show examples of the corresponding EPSPs recorded prior to HFS and 5 h post-HFS in control animals (*1 + 3*) and those receiving D-JNKI1 (*2 + 4*). *b*, LTP recorded 5 h post-HFS in control animals (□) and those injected intracerebroventricularly with either Aβ (●) or Aβ+D-JNKI1 (▲). The *black arrow* indicates the time of intracerebroventricular injection, and the *open arrow* indicates the delivery of HFS. The *insets* show EPSPs recorded prior to HFS and 5 h post-HFS in animals injected with Aβ (*5 + 7*) or Aβ+D-JNKI1 (*6 + 8*).

in TBS, mounted with an aqueous mounting medium (Vectastain; Vector Laboratories), and sealed. The slides were examined under a Zeiss fluorescence microscope with the appropriate filter (fluorescein isothiocyanate: excitation, 495 nm, and emission, 525 nm; L-rhodamine: excitation, 540 and 574 nm, and emission, 602 nm).

Statistical Analysis—The data are expressed as the means ± S.E. A one-way analysis of variance (ANOVA) was performed to determine whether there were significant differences between conditions. When this analysis indicated significance (at the 0.05 level), *post hoc* Student Newmann-Keuls test analysis was used to determine which conditions were significantly different from each other. A repeated measures ANOVA was used to compare mean EPSP slopes at different time points in the electrophysiological experiments. When comparisons were being made between two treatments, an unpaired Student's *t* test for independent means was performed.

RESULTS

Fig. 1*a* shows a sample immunoblot in which a marked increase in p-JNK was observed following intracerebroventricular injection of $A\beta_{(1-40)}$; assessment of the mean data obtained from densitometric analysis revealed a statistically significant increase in JNK phosphorylation induced by Aβ ($p < 0.001$; Student's *t* test for independent means; $n = 5$). In contrast to the change in JNK phosphorylation, total JNK

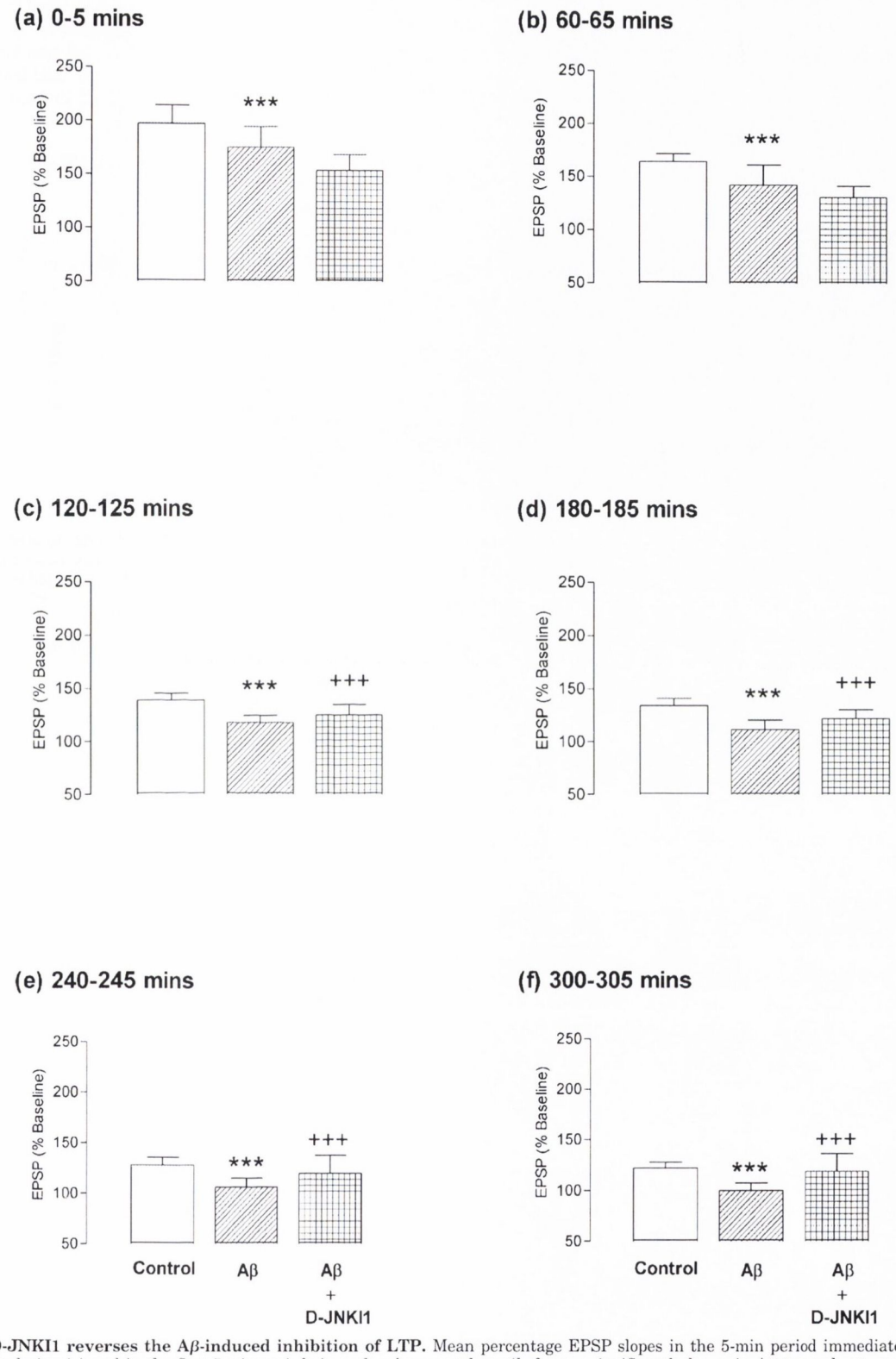

FIG. 3. **D-JNKI1 reverses the Aβ-induced inhibition of LTP.** Mean percentage EPSP slopes in the 5-min period immediately following tetanic stimulation (*a*) and in the first 5-min periods in each subsequent hour (*b–f*) were significantly lower in Aβ-treated rats compared with controls (***, $p < 0.001$; ANOVA). This inhibition was reversed by D-JNKI1 treatment from 2 h so that there was a significant difference between mean EPSP slopes in Aβ-treated and Aβ+D-JNKI1-treated rats (+++, $p < 0.001$; ANOVA).

expression was similar in Aβ-treated and control rats as demonstrated in the sample immunoblot and the mean data (Fig. 1*b*). The Aβ-induced increase in JNK phosphorylation was paralleled by the change in c-Jun phosphorylation; thus, the sample immunoblot shown in Fig. 1*c* and the mean data obtained from densitometric analysis indicated that $A\beta_{(1-40)}$ induced a marked increase in c-Jun phosphorylation ($p < 0.05$; Student's *t* test for independent means; $n = 5$). Protein loading

was checked by reprobing immunoblots for actin, and the data indicate that its expression was similar in samples prepared from control and Aβ-treated rats.

We argued that this Aβ-induced increase in JNK activation may contribute to the previously reported Aβ-induced inhibition of LTP (16), and to assess this, rats were injected intracerebroventricularly with $A\beta_{(1-40)}$ alone or in combination with the peptide inhibitor, D-JNKI1. Fig. 2*a* shows that, in control rats tetanic stimulation led to an immediate and persistent increase in EPSP slope ($p < 0.001$; ANOVA); treatment with D-JNKI1 (1nmol) did not significantly affect this change. In contrast, intracerebroventricular injection of $A\beta_{(1-40)}$ inhibited LTP ($p < 0.001$; ANOVA, Fig. 2*b*); the effect was observed immediately such that the mean percentage change in the EPSP slope in the 5 min immediately following tetanic stimulation was significantly reduced in Aβ-treated compared with control rats ($p < 0.01$; ANOVA; Fig. 3*a*). The Aβ-associated change persisted so that the mean percentage changes in EPSP slopes in the final 5-min period of each hour were also significantly reduced in Aβ-treated rats compared with control animals (***, $p < 0.001$ in all cases; ANOVA; Fig. 3, *b–f*). Co-injection of D-JNKI1 and $A\beta_{(1-40)}$ reversed the inhibitory effect of $A\beta_{(1-40)}$ (Fig. 2*b*), but this effect was not apparent until 2 h after tetanic stimulation (+++, $p < 0.001$; ANOVA; Fig. 3, *b–f*). The mean percentage EPSP slopes at 0–5 min post-tetanus were significantly reduced in rats treated with Aβ and D-JNKI1 compared with control rats ($p < 0.001$; ANOVA; Fig. 2*b*). The results from paired pulse facilitation experiments found that there was no significant change in paired pulse facilitation observed either between groups of animals or preinjection compared with 1 h post-injection or 5 h following HFS. This indicates that at the

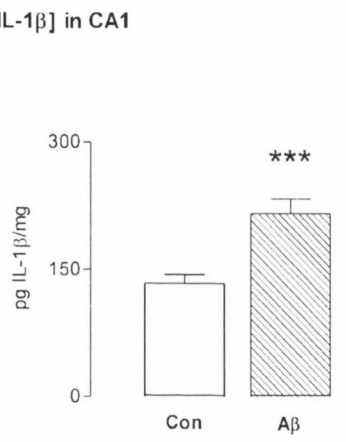

FIG. 4. **Effect of Aβ on IL-1β concentration in hippocampus.** IL-1β concentration was significantly increased in hippocampus of Aβ-treated rats compared with control (*Con*) rats (***, $p < 0.001$; Student's *t* test for independent means; $n = 5$).

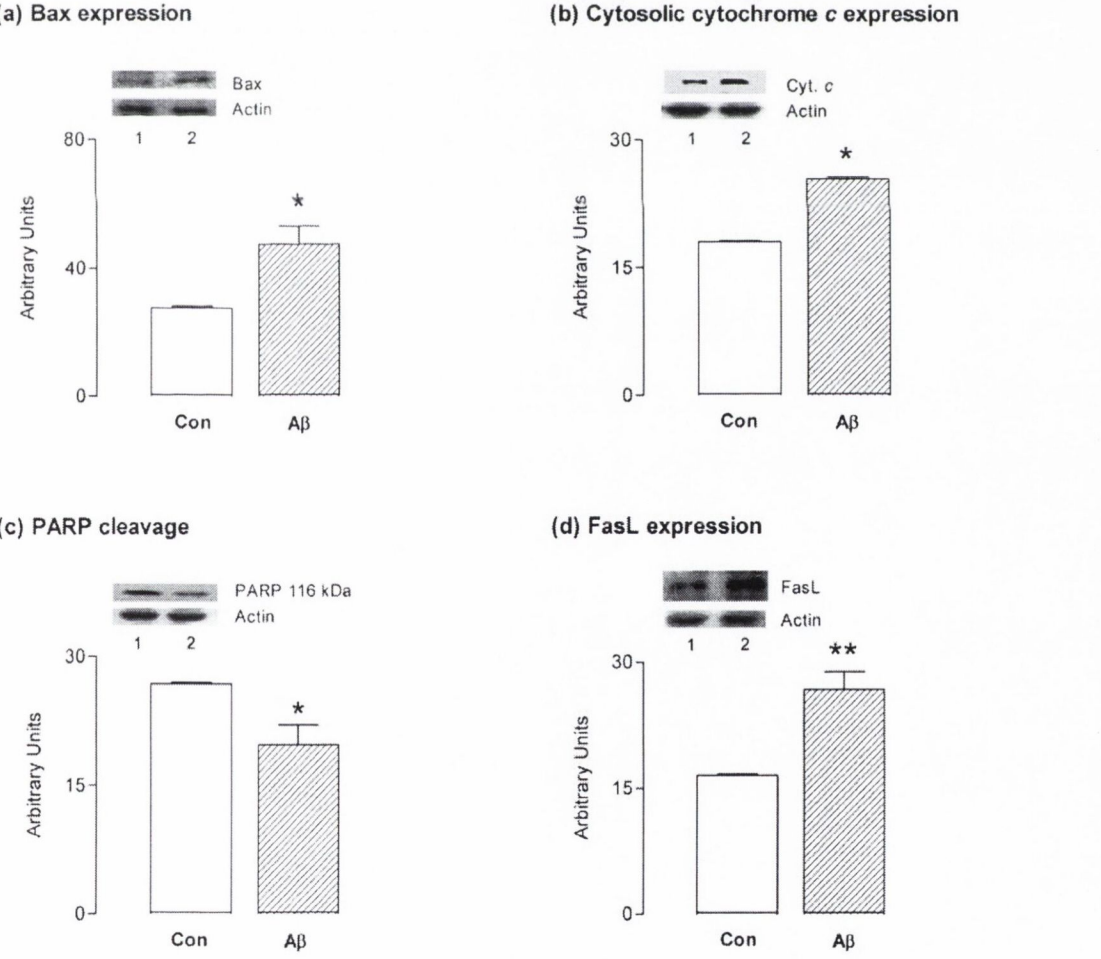

FIG. 5. **Effects of Aβ on Bax, cytochrome *c*, and FasL expression and PARP cleavage.** Aβ induced a significant increase in mitochondrial Bax expression, cytosolic cytochrome *c* expression, cleavage of PARP, and FasL expression (*, $p < 0.05$; **, $p < 0.01$; Student's *t* test for independent means; $n = 5$, compare *lane 2* with *lane 1* in all cases). All of the blots were stripped and reprobed with actin to ensure equal protein loading (see second sample immunoblots in *a–d*). *Con*, control.

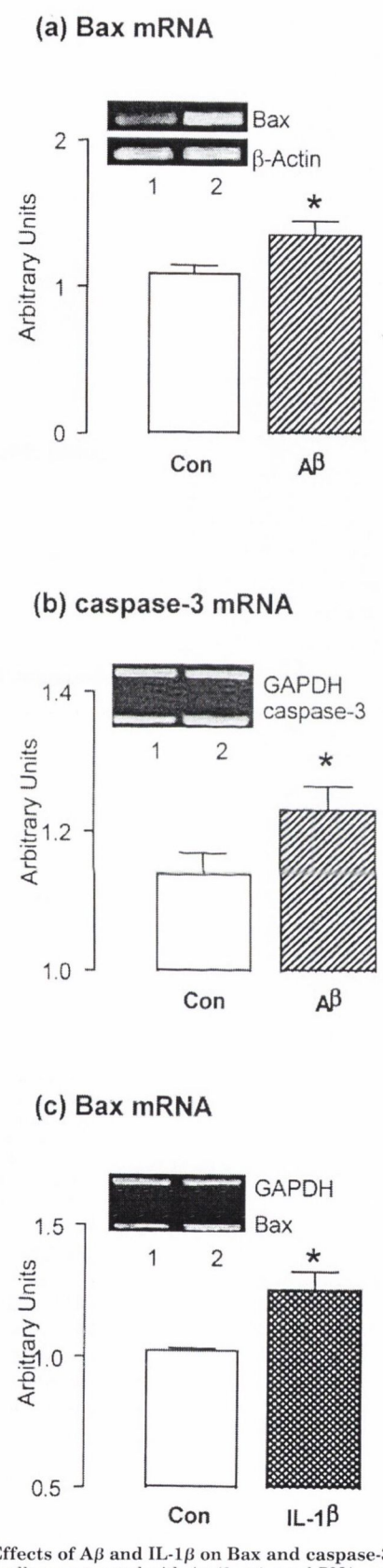

FIG. 6. **Effects of Aβ and IL-1β on Bax and caspase-3 mRNA *in vitro*.** The cells were treated with Aβ (2 μM), total RNA was extracted, and expression of Bax (*a*) and caspase-3 (*b*) mRNA was examined by PCR. Aβ evoked a significant increase in Bax and caspase-3 mRNA expression. Representative images of the ethidium bromide-stained gels are shown in the *insets*. The results are the means ± S.E. for six independent observations. In cells treated with IL-1β (5 ng/ml) (*c*), a significant increase in Bax mRNA expression was observed. A representative image of the ethidium bromide-stained gel is shown as an *inset*. The results are the means ± S.E. for six independent observations (*, $p < 0.05$). *Con*, control.

doses used here, $A\beta_{(1-40)}$ and D-JNKI1 do not alter neurotransmitter release, suggesting a postsynaptic site for the modulation of LTP observed in our experiments.

The findings of several studies have indicated that enhanced JNK phosphorylation in the hippocampus is coupled with enhanced IL-1β concentration and impaired LTP (9, 12, 25); therefore we considered that the effect of $A\beta_{(1-40)}$ might be mediated by IL-1β. Fig. 4 shows that the concentration of IL-1β in hippocampus was significantly increased in hippocampus of Aβ-treated rats compared with control rats ($p < 0.001$; Student's *t* test for independent means; $n = 5$).

Our findings from a previous study (11) linked activation of JNK with translocation of cytochrome *c* from mitochondria, suggesting that the patency of the mitochondrial membrane was affected by JNK activation. In an effort to address this question, we assessed expression of the pro-apoptotic protein Bax in a mitochondrial fraction and cytochrome *c* in a cytosolic preparation obtained from control and Aβ-treated rats. The sample immunoblot shown in Fig. 5*a* indicates that $A\beta_{(1-40)}$ increased expression of Bax, and densitometric analysis revealed that the mean value in samples prepared from Aβ-treated rats was significantly enhanced compared with that in control rats ($p < 0.05$; Student's *t* test for independent means; $n = 5$). The sample immunoblot and mean data in Fig. 5*b* indicate that cytochrome *c* expression in cytosolic samples prepared from Aβ-treated rats was enhanced compared with samples from control rats; comparison of mean values indicated that the difference was statistically significant ($p < 0.05$; Student's *t* test for independent means; $n = 5$). A similar pattern was observed in terms of expression of the intact fragment (116 kDa) of PARP; Fig. 5*c* shows one sample immunoblot and the mean data indicating that $A\beta_{(1-40)}$ significantly decreased expression of 116-kDa PARP in hippocampal tissue prepared from Aβ-treated rats ($p < 0.05$; Student's *t* test for independent means; $n = 5$). It is considered that, in addition to increased Bax expression, cytosolic cytochrome *c* expression, and PARP cleavage, expression of FasL is indicative of apoptotic cell death, and, in parallel with the increases in Bax expression, cytosolic cytochrome *c* expression and PARP cleavage, $A\beta_{(1-40)}$ significantly enhanced expression of FasL ($p < 0.01$; Student's *t* test for independent means; $n = 5$; Fig. 5*d*), and in the case of Bax, cytochrome *c*, PARP, and FasL, equal protein loading was confirmed by reprobing for actin.

The Aβ-associated increase in Bax protein was mirrored by an Aβ-induced increase in Bax mRNA in cultured cortical neurons as shown by the sample gel and by analysis of the mean data indicating that the difference between expression in Aβ-treated and control cultured cells reached statistical significance ($p < 0.05$; Student's *t* test for independent means; $n = 5$; Fig. 6*a*). Fig. 6*c* shows that IL-1β induced a similar increase in Bax mRNA; the increase shown in the sample gel reflected the mean changes, which revealed a significant IL-1β-induced increase ($p < 0.05$; Student's *t* test for independent means; $n = 5$). Consistent with the evidence that $A\beta_{(1-40)}$ induces cell death is the finding that it also increased caspase-3 mRNA in cortical cells (Fig. 6*b*).

We addressed the question of whether IL-1β might mediate some of the actions of Aβ by investigating the effect of $A\beta_{(1-40)}$ on IL-1β concentration and also on JNK phosphorylation, caspase-3 activation, and TUNEL staining in cortical neuronal cells in the presence or absence of the caspase-1 inhibitor,

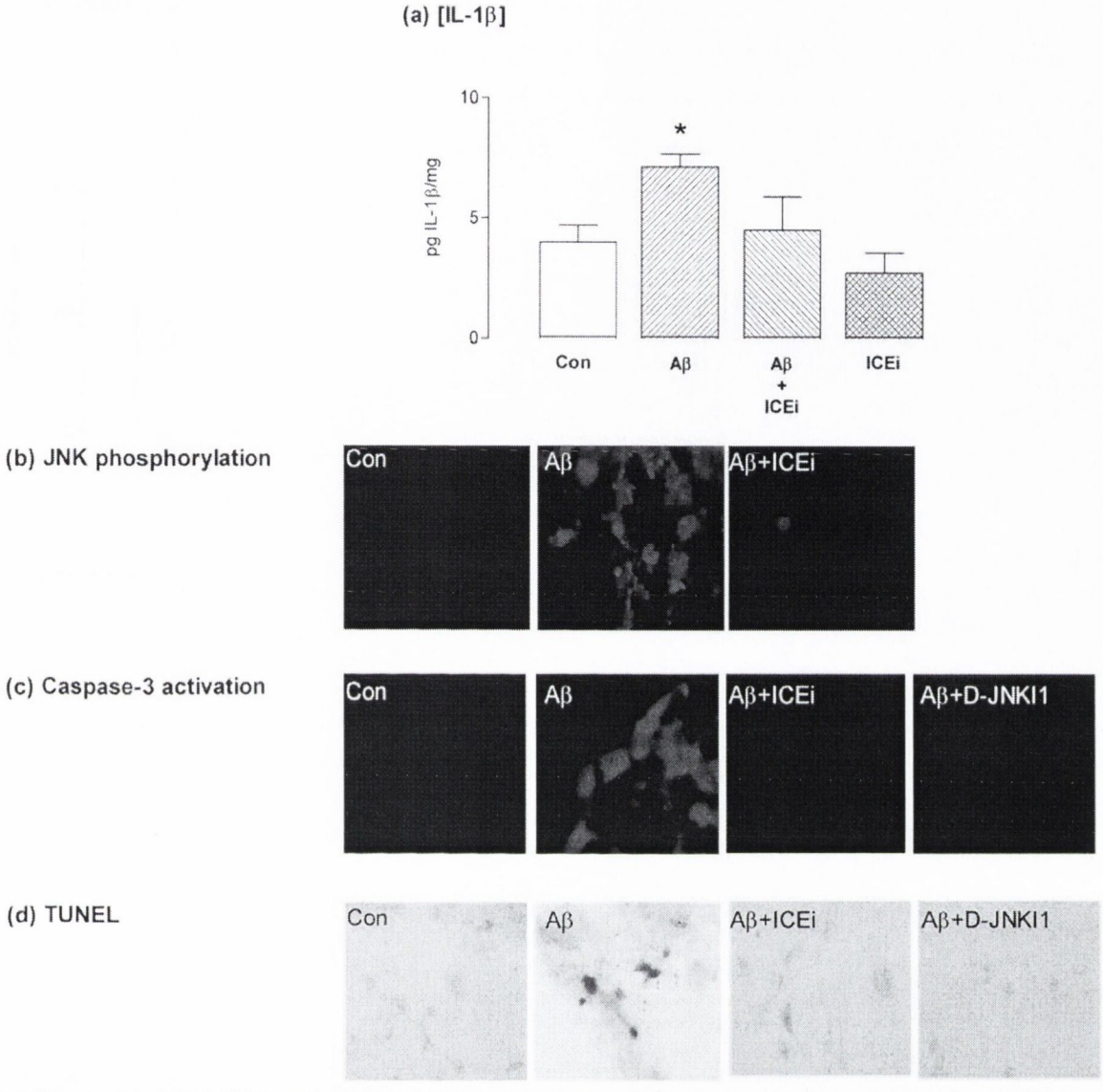

FIG. 7. **Effects of Ac-YVAD-CMK and D-JNKI1 on Aβ-induced increases in IL-1β concentration and activation of JNK, caspase-3, and DNA fragmentation.** IL-1β concentration was assessed in supernatant from cells incubated in the absence/presence of Aβ with or without caspase-1 inhibitor (Ac-YVAD-CMK) 20 h post-treatment. The mean values for IL-1β concentration (*a*) show a significant increase in Aβ-treated cells compared with control (*Con*) cells (*, $p < 0.05$; ANOVA; $n = 4$). Pretreatment with Ac-YVAD-CMK reversed the Aβ-induced increase in IL-1β concentration so that values were similar to those in control groups. JNK phosphorylation (*b*), caspase-3 activation (*c*), and TUNEL reactivity (*d*) were significantly increased in Aβ-treated cells compared with control cells. Ac-YVAD-CMK reversed the Aβ-induced increase in all of these. D-JNKI1 reversed the Aβ-induced increase in caspase-3 activation and TUNEL reactivity.

Ac-YVAD-CMK. Fig. 7*a* indicates that incubation of cells in the presence of $A\beta_{(1-40)}$ significantly increased IL-1β in supernatant ($p < 0.05$; ANOVA; $n = 4$), and this effect was inhibited by co-incubation in the presence of Ac-YVAD-CMK. The cultured cells were stained with an antibody that identified the phosphorylated form of JNK, and Fig. 7*b* shows that $A\beta_{(1-40)}$ induced a marked increase in the number of cells staining positively for phosphorylated JNK; significantly, this effect of $A\beta_{(1-40)}$ was abolished by co-incubation of cultures in the presence of $A\beta_{(1-40)}$ and the caspase-1 inhibitor. Similarly, $A\beta_{(1-40)}$ markedly increased the number of cells that stained positively for activated caspase-3 (Fig. 7*c*) and for TUNEL (Fig. 7*d*), and these changes were abolished by co-incubation of cells in the presence of $A\beta_{(1-40)}$ and the caspase-1 inhibitor, Ac-YVAD-CMK. In an effort to establish whether JNK activation contributed to the effects induced by $A\beta_{(1-40)}$, neuronal cells were treated with $A\beta_{(1-40)}$ alone or in combination with D-JNKI1. Fig. 7 (*c* and *d*) indicates that inhibition of JNK abolished the Aβ-associated increase in the number of cells that stained positively for activated caspase-3 and TUNEL.

To confirm the finding that IL-1β mimics at least some of the effects of $A\beta_{(1-40)}$, cultured cortical neurons were incubated with IL-1β in the presence or absence of D-JNKI1 and the cell lysates assessed for activation of c-Jun and for expression of FasL. Fig. 8*a* indicates that IL-1β enhanced c-Jun phosphorylation, and analysis of the mean data indicated that the IL-1β-induced effect was statistically significant ($p < 0.05$; ANOVA; $n = 2$); the increase in c-Jun phosphorylation was abrogated by co-incubation in the presence of D-JNKI1. Similarly, IL-1β significantly increased expression of FasL (Fig. 8*b*; $p < 0.05$; ANOVA; $n = 4$), and this effect was also abrogated by co-incubation in the presence of D-JNKI1. In both cases, equal protein loading was confirmed by reprobing blots for actin expression.

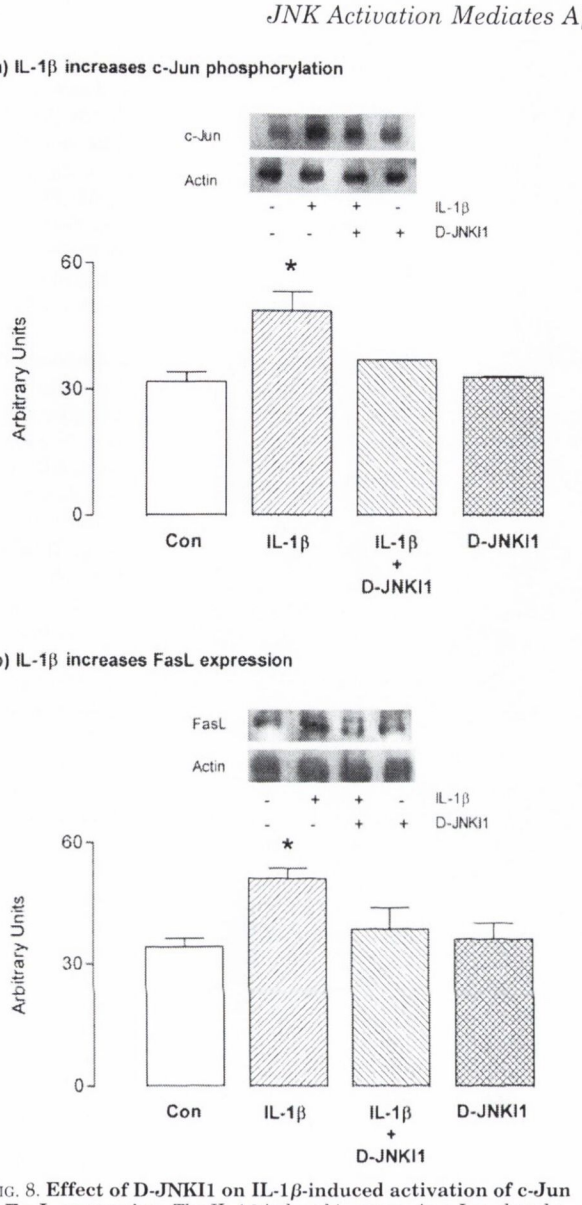

FIG. 8. **Effect of D-JNKI1 on IL-1β-induced activation of c-Jun and FasL expression.** The IL-1β-induced increases in c-Jun phosphorylation (*a*) and FasL expression (*b*) were abrogated by D-JNKI1. IL-1β (5 ng/ml) significantly increased c-Jun phosphorylation (*, $p < 0.05$; ANOVA; $n = 2$) and FasL expression (*, $p < 0.05$; ANOVA; $n = 4$; compare *lanes 2* and *1* in sample immunoblots), and these effects were blocked by D-JNKI1 (compare *lanes 3* and *1*), which alone exerted no effect (compare *lanes 4* and *1*). The blots were stripped and reprobed for actin to ensure equal protein loading, and no significant differences in actin expression among the groups were observed (second sample immunoblot in *a* and *b*). *Con*, control.

DISCUSSION

We report that $A\beta_{(1-40)}$ induces an increase in IL-1β in hippocampal tissue and in neuronal cell cultures and that this increase, in combination with enhanced activation of JNK, mediates the inhibitory effects of $A\beta_{(1-40)}$ on LTP in CA1 and the Aβ-induced activation of cell death events. Intracerebroventricular injection of $A\beta_{(1-40)}$ led to a marked increase in phosphorylation of JNK in the hippocampus, coupled with a parallel increase in c-Jun phosphorylation. These observations, which we believe are the first such findings *in vivo*, bear a marked similarity to those described by Morishima *et al.* (6), who reported that Aβ induced activation of JNK and c-Jun in cortical neurons. A number of previous studies have indicated that an inverse correlation exists between JNK phosphorylation and LTP expression; for example impaired LTP is coupled with JNK phosphorylation in the hippocampus of aged rats (9), rats treated with lipopolysaccharide (13, 26) or IL-1β (12), and rats exposed to γ-irradiation (11). Consistently, LTP is restored when the increase in JNK phosphorylation is blocked, for example by IL-10 (26), by inhibition of caspase-1 (13), or by treatment with eicosapentaenoic acid (11). The present findings demonstrate that LTP in area CA1 of the hippocampus was profoundly inhibited by $A\beta_{(1-40)}$ administration and that this inhibition was abrogated by D-JNKI1, providing another example of the inverse correlation between JNK activation and LTP. The Aβ-induced inhibition of LTP supports previous reports in CA1 *in vivo* (15–17) and in dentate gyrus *in vitro* (20, 21, 27) but provides the first demonstration of an effect of $A\beta_{(1-40)}$ on LTP that is dependent on JNK activation. The evidence presented indicates that the effect of D-JNKI1 is not immediate but rather becomes evident after 2 h. The mechanism by which Aβ inhibits LTP may derive from the ability of Aβ to induce cell death in hippocampus, and this is supported by the finding that DJNKI1 inhibits these changes and, in parallel, suppresses Aβ-induced inhibition of LTP. These findings also indicate a pivotal role for JNK activation in the events triggered by Aβ. Thus, we present several findings indicating that the Aβ-stimulated increase in JNK phosphorylation is paralleled by several changes that are hallmarks of cell death. For example, Aβ treatment enhanced phosphorylation of c-Jun in the hippocampus, which is a downstream consequence of JNK activation and which has been shown to play a significant role in triggering neuronal apoptosis in a variety of cells *in vitro* (28–30). Similarly, increased Bax expression, cytosolic expression of cytochrome *c* and PARP cleavage, as well as caspase-3 activation and Fas ligand expression were observed in tissue treated with Aβ, whereas DJNKI1 prevented all of these actions, suggesting that sequential activation of JNK and c-Jun triggers apoptotic changes in hippocampus. Increased Bax translocation to mitochondria has been identified as an important factor in triggering Aβ-induced changes (31–34), because it reduces the patency of the mitochondrial membrane and leads to the release of proteins normally contained within the intermembrane space, like cytochrome *c* (35, 36); in turn, the presence of cytochrome *c* in cytoplasm initiates caspase-3 activation, which results in apoptosis (37). Interestingly cell death induced by treatment of neuroblastoma cell lines with $A\beta_{(17-42)}$ was associated with activation of JNK and caspase-3, and because the apoptotic changes were attenuated by caspase-3 inhibition or by overexpression of a dominant-negative mutant of SEK1, it was concluded that activation of both caspase-3 and JNK significantly contributed to Aβ-induced apoptosis in these cells (38). The present findings concur with these data because D-JNKI1 prevented all Aβ-induced apoptotic changes investigated, and they are also consistent with several findings indicating that JNK phosphorylation is a pivotal event in the induction of Aβ-stimulated cell death (6, 7, 39).

Several observations have contributed to the development of the idea that FasL expression and consequently Fas activation play a role in neurodegeneration, and we report that increased hippocampal expression of FasL accompanied the Aβ-induced increases in JNK phosphorylation, cytochrome *c* translocation, PARP cleavage, and caspase-3 activation and that these changes were abrogated by D-JNKI1. These data suggest that in the hippocampus a causal relationship between these factors exists that has been shown previously in experimental ischemic injury (28, 40, 41), Parkinson's disease, and Down's syndrome (42–44). Specifically, activation of the JNK cascade has been shown to play a significant role in FasL expression that mediates cell death in cortical neurons (6), PC12 cells (30), and

epithelial and lymphoid cells (45, 46), whereas Fas-Fc, which prevents Fas binding to FasL, protects cells from apoptotic cell death (47, 48). Significantly, increases in JNK and c-Jun phosphorylation and expression of FasL are found in association with apoptotic neurons that are detected in the AD brain (2, 42–44, 49, 50), suggesting that activation of the JNK-c-Jun-FasL signaling cascade may mediate Aβ-induced neuronal cell death. Indeed the finding that JNK activation is detected in degenerating neurons in AD brains has led to the hypothesis that JNK activation plays a key role in neuronal loss in AD (51, 52).

We demonstrate that Aβ treatment increased in IL-1β concentration in hippocampus *in vivo* and cortical neurons *in vitro*. Interestingly the Aβ-induced increase in IL-1β concentration observed in cortical neurons was blocked by co-incubation of cells in the presence of the caspase-1 inhibitor Ac-YVAD-CMK. The Aβ-induced increases in activation of JNK and caspase-3 and in TUNEL staining were also inhibited by Ac-YVAD-CMK, consolidating a role for IL-1β in Aβ-induced changes. A link between Aβ and IL-1β has been described in other studies; for example, Aβ has been shown to stimulate production of proinflammatory cytokines, like IL-1β from differentiated human monocytes and from a microglial cell line (53), whereas IL-1β was induced in reactive astrocytes surrounding Aβ-containing deposits in 14-month-old transgenic mice that overexpress human amyloid precursor protein (54). Interestingly, astrocytic overexpression of S100β, a component of Aβ-containing plaques, has been reported to be triggered by IL-1β (55). Consistently, several reports have provided evidence demonstrating a role for IL-1β in the etiology of AD based largely on the finding that IL-1β expression in different brain areas in AD and also in the cerebrospinal fluid of AD patients (56–58), and it has been shown that a common polymorphism in *IL-1B* (the gene encoding IL-1β) is associated with a 4-fold increase in IL-1β production and an associated increased risk of the disease (55). Of particular significance are our observations that the inhibitory effect of Ac-YVAD-CMK on Aβ-induced changes is closely paralleled by similar effects of D-JNKI1 and that D-JNKI1 also inhibited IL-1β-triggered changes in c-Jun phosphorylation and FasL expression.

Several studies have revealed that increased hippocampal IL-1β concentration, paralleled by increased JNK activation, exerts an inhibitory effect on LTP (9, 12), and these changes, both of which are induced by Aβ, undoubtedly contribute to the deficit in LTP observed here. Coupled with these changes are the downstream consequences of enhanced IL-1β and JNK activation on cell viability, and we therefore conclude that the Aβ-induced deficit in LTP is a consequence of activation of cellular cascades induced by IL-1β and JNK that lead to cell death.

REFERENCES

1. Yankner, B. A. (1996) *Neuron* **16,** 921–932
2. Anderson, A. J., Su, J. H., and Cotman, C. W. (1996) *J. Neurosci.* **16,** 1710–1719
3. Estus, S., Tucker, H. M., van Rooyen, C., Wright, S., Brigham, E. F., Wogulis, M., and Rydel, R. E. (1997) *J. Neurosci.* **17,** 7736–7745
4. Stadelmann, C., Deckwerth, T. L., Srinivasan, A., Bancher, C., Bruck, W., Jellinger, K., and Lassmann, H. (1999) *Am. J. Pathol.* **155,** 1459–1466
5. Fogarty, M. P., Downer, E. J., and Campbell, V. A. (2003) *Biochem. J.* **371,** 789–798
6. Morishima, Y., Gotoh, Y., Zieg, J., Barrett, T., Takano, H., Flavell, R., Davis, R. J., Shirasaki, Y., and Greenberg, M. E. (2001) *J. Neurosci.* **21,** 7551–7560
7. Jang, J.-H., and Surh, Y.-J. (2002) *Ann. N. Y. Acad. Sci.* **973,** 228–236
8. Savage, M. J., Lin, Y.-G., Ciallella, J. R., Flood, D. G., and Scott, R. W. (2002) *J. Neurosci.* **22,** 3376–3385
9. O'Donnell, E., Vereker, E., and Lynch, M. A. (2000) *Eur. J. Neurosci.* **12,** 345–352
10. Lynch, A. M., and Lynch, M. A. (2002) *Eur. J. Neurosci.* **15,** 1779–1788
11. Lonergan, P. E., Martin, D. S. D., Horrobin, D. F., and Lynch, M. A (2002) *J. Biol. Chem.* **277,** 20804–20811
12. Vereker, E., O'Donnell, E., and Lynch, M. A. (2000) *J. Neurosci.* **20,** 6811–6819
13. Vereker, E., Campbell, V., Roche, E., McEntee, E., and Lynch, M. A. (2000) *J. Biol. Chem.* **275,** 26252–26258
14. Cullen, W. K., Suh, Y. H., Anwyl, R., and Rowan, M. J. (1997) *Neuroreport* **8,** 3213–3217
15. Freir, D. B., Holscher, C., and Herron, C. E. (2001) *J. Neurophysiol.* **85,** 708–713
16. Freir, D. B., and Herron, C. E. (2003) *J. Neurophysiol.* **89,** 2917–2922
17. Walsh, D. M., Klyubin, I., Fadeeva, J. V., Cullen, W. K., Anwyl, R., Wolfe, M. S., Rowan, M. J., and Selkoe, D. J. (2002) *Nature* **416,** 535–539
18. Chen, Q. S., Kagan, B. L., Hirakura, Y., and Xie, C. W. (2000) *J. Neurosci. Res.* **60,** 65–72
19. Freir, D. B., Costello, D. A., and Herron, C. E. (2003) *J. Neurophysiol.* **89,** 3061–3069
20. Wang, H.-W., Pasternak, J. F., Kuo, H., Ristic, H., Lambert, M. P., Chromy, B., Viola, K. L., Klein, W. L., Stine, W. B., Krafft, G. A., and Trommer, B. L. (2002) *Brain Res.* **924,** 133–140
21. Saleshando, G., and O'Connor, J. J. (2000) *Neurosci. Lett.* **288,** 119–122
22. Chapman, P. F., White, G. L., Jones, M. W., Cooper-Blacketer, D., Marshall, V. J., Irizarry, M., Younkin, L., Good, M. A., Bliss, T. V. P., Hyman, B., Younkin, S. G., and Hsiao, K. K. (1999) *Nat. Neurosci.* **2,** 271–276
23. McGahon, B., and Lynch, M. A. (1996) *Neuroscience* **72,** 847–855
24. Bradford, M. M. (1976) *Anal. Biochem.* **72,** 248–254
25. Ray, S. K., Fidan, M., Nowak, M. W., Wilford, G. G., Hogan, E. L., and Banik, N. L. (2000) *Brain Res.* **852,** 326–334
26. Kelly, A., Lynch, A., Vereker, E., Nolan, Y., Queenan, P., Whittaker, E., O'Neill, L. A. J., and Lynch, M. A. (2001) *J. Biol. Chem.* **276,** 45564–45572
27. Chen, Q.-S., Wei, W.-Z., Shimahara, T., and Xie, C.-W. (2002) *Neurobiol. Learn. Mem.* **77,** 354–371
28. Herdegen, T., Claret, F. X., Kallunki, T., Martin-Villalba, A., Winter, C., Hunter, T., and Karin, M. (1998) *J. Neurosci.* **18,** 5124–5135
29. Behrens, A., Sibilia, M., and Wagner, E. F. (1999) *Nat. Genet.* **21,** 326–329
30. Le-Niculescu, H., Bonfoco, E., Kasuya, Y., Claret, F. X., Green, D. R., and Karin, M. (1999) *Mol. Cell. Biol.* **19,** 751–763
31. Gross, A., Jockel, J., Wei, M. C., and Korsmeyer, S. J. (1998) *EMBO J.* **17,** 3878–3885
32. Green, D. R., and Reed, J. C. (1998) *Science* **281,** 1309–1312
33. Wei, W., Norton, D. D., Wang, X., and Kusiak, J. W. (2002) *Brain* **125,** 2036–2043
34. Kihiko, M. E., Tucker, H. M., Rydel, R. E., and Estus, S. (1999) *J. Neurochem.* **73,** 2609–2612
35. Paradis, E., Douillard, H., Koutroumanis, M., Goodyer, C., and LeBlanc, A. (1996) *J. Neurosci.* **16,** 7533–7539
36. Zhang, Y., McLaughlin, R., Goodyer, C., and LeBlanc, A. (2002) *J. Cell Biol.* **156,** 519–529
37. Giovanni, A., Keramaris, E., Morris, E. J., Hou, S. T., O'Hare, M., Dyson, N., Robertson, G. S., Slack, R. S., and Park, D. S. (2000) *J. Biol. Chem.* **275,** 11553–11560
38. Selznick, L. A., Zheng, T. S., Flavell, R. A., Rakic, P., and Roth, K. A. (2000) *J. Neuropathol. Exp. Neurol.* **59,** 271–279
39. Desagher, S., Osen-Sand, A., Nichols, A., Eskes, R., Montessuit, S., Lauper, S., Maundrell, K., Antonsson, B., and Martinou, J. C. (1999) *J. Cell Biol.* **144,** 891–901
40. Matsuyama, T., Hata, R., Yamamoto, Y., Tagaya, M., Akita, H., Uno, H., Wanaka, A., Furuyama, J., and Sugita, M. (1995) *Brain Res. Mol. Brain Res.* **34,** 166–172
41. Martin-Villalba, A., Herr, I., Jeremias, I., Hahne, M., Brandt, R., Vogel, J., Schenkel, J., Herdegen, T., and Debatin, K. M. (1999) *J. Neurosci.* **19,** 3809–3817
42. de la Monte, S. M., Sohn, Y. K., and Wands, J. R. (1997) *J. Neurol. Sci.* **152,** 73–83
43. de la Monte, S. M., Sohn, Y. K., Ganju, N., and Wands, J. R. (1998) *Lab. Invest.* **78,** 401–411
44. Seidl, R., Fang-Kircher, S., Bidmon, B., Cairns, N., and Lubec, G. (1999) *Neurosci. Lett.* **260,** 9–12
45. Chen, Y. R., Wang, X., Templeton, D., Davis, R. J., and Tan, T. H. (1996) *J. Biol. Chem.* **271,** 31929–31936
46. Verheij, M., Bose, R., Lin, X. H., Yao, B., Jarvis, W. D., Grant, S., Birrer, M. J., Szabo, E., Zon, L. I., Kyriakis, J. M., Haimovitz-Friedman, A., Fuks, Z., and Kolesnick, R. N. (1996) *Nature* **380,** 75–79
47. Suda, T., and Nagata, S. (1994) *J. Exp. Med.* **179,** 873–879
48. Brunner, T., Mogil, R. J., LaFace, D., Yoo, N. J., Mahboubi, A., Echeverri, F., Martin, S. J., Force, W. R., Lynch, D. H., Ware, C. F., and Green, D. R. (1995) *Nature* **373,** 441–444
49. Anderson, A. J., Cummings, B. J., and Cotman, C. W. (1994) *Exp. Neurol.* **125,** 286–295
50. Marcus, D. L., Strafaci, J. A., Miller, D. C., Masia, S., Thomas, C. G., Rosman, J., Hussain, S., and Freedman, M. L. (1998) *Neurobiol. Aging* **19,** 393–400
51. Shoji, M., Iwakami, N., Takeuchi, S., Waragai, M., Suzuki, M., Kanazawa, I., Lippa, C. F., Ono, S., and Okazawa, H. (2000) *Brain Res. Mol. Brain Res.* **85,** 221–233
52. Zhu, X., Raina, A. K., Rottkamp, C. A., Aliev, G., Perry, G., Boux, H., and Smith, M. A. (2001) *J. Neurochem.* **76,** 435–441
53. Szczepanik, A. M., Funes, S., Petko, W., and Ringheim, G. E. (2001) *J. Neuroimmunol.* **113,** 49–62
54. Mehlhorn, G., Hollborn, M., and Schliebs, R. (2000) *Int. J. Dev. Neurosci.* **18,** 423–431
55. Mrak, R. E., and Griffin, W. S. (2001) *Neurobiol. Aging* **22,** 903–908
56. Griffin, W. S. T., Stanley, L. C., Ling, C., White, L., MacLeod, V., Perrot, L. J., White, C. L., and Araoz, C. (1989) *Proc. Natl. Acad. Sci. U. S. A.* **86,** 7611–7615
57. Blum-Degen, D., Muller, T., Kuhn, W., Gerlach, M., Przuntek, H., and Riederer, P. (1995) *Neurosci. Lett.* **202,** 17–20
58. Sheng, J. G., Zhu, S. G., Jones, R. A., Griffin, W. S., and Mrak, R. E. (2000) *Exp. Neurol.* **163,** 388–391

British Journal of Pharmacology (2003) 140, 547–557
www.nature.com/bjp

Tetrahydrocannabinol-induced neurotoxicity depends on CB_1 receptor-mediated c-Jun N-terminal kinase activation in cultured cortical neurons

[1]Eric J. Downer, [1]Marie P. Fogarty & *,[1]Veronica A. Campbell

[1]Department of Physiology, Trinity College, Trinity College Institute of Neuroscience, Dublin 2, Ireland

1 Δ^9-Tetrahydrocannabinol (THC), the main psychoactive ingredient of marijuana, induces apoptosis in cultured cortical neurons. THC exerts its apoptotic effects in cortical neurons by binding to the CB_1 cannabinoid receptor. The CB_1 receptor has been shown to couple to the stress-activated protein kinase, c-Jun N-terminal kinase (JNK). However, the involvement of specific JNK isoforms in the neurotoxic properties of THC remains to be established.

2 The present study involved treatment of rat cultured cortical neurons with THC (0.005–50 μM), and combinations of THC with the CB_1 receptor antagonist, AM 251 (10 μM) and pertussis toxin (PTX; 200 ng ml^{-1}). Antisense oligonucleotides (AS) were used to deplete neurons of JNK1 and JNK2 in order to elucidate their respective roles in THC signalling.

3 Here we report that THC induces the activation of JNK *via* the CB_1 receptor and its associated G-protein, $G_{i/o}$. Treatment of cultured cortical neurons with THC resulted in a differential timeframe of activation of the JNK1 and JNK2 isoforms.

4 Use of specific JNK1 and JNK2 AS identified activation of caspase-3 and DNA fragmentation as downstream consequences of JNK1 and JNK2 activation.

5 The results from this study demonstrate that activation of the CB_1 receptor induces JNK and caspase-3 activation, an increase in Bax expression and DNA fragmentation. The data demonstrate that the activation of both JNK1 and JNK2 isoforms is central to the THC-induced activation of the apoptotic pathway in cortical neurons.
British Journal of Pharmacology (2003) **140,** 547–557. doi:10.1038/sj.bjp.0705464

Keywords: Δ^9-Tetrahydrocannabinol; antisense; c-Jun N-terminal kinase; apoptosis; caspase-3; bax

Abbreviations: AS, antisense oligonucleotides; JNK, c-Jun N-terminal kinase; MAPK, mitogen-activated protein kinase; SC, scrambled control oligonucleotides; THC, Δ^9-tetrahydrocannabinol; TUNEL, terminal deoxynucleotidyltransferase-mediated biotinylated UTP nick end labelling

Introduction

Δ^9-Tetrahydrocannabinol (THC), the predominant psychoactive ingredient in preparations of marijuana (*Cannabis saliva*), exerts a broad spectrum of central effects, such as alterations in cognition (Howlett, 1990) and impairment of short-term memory consolidation (Abood & Martin, 1992). THC exerts these effects by binding to G-protein-coupled receptors (Howlett, 1995). While two different subtypes of cannabinoid receptor have been characterised from mammalian tissues, CB_1 (Matsuda *et al.*, 1990) and CB_2 (Munro *et al.*, 1993), the CB_1 receptor is associated with brain regions responsible for mediating the psychoactive effects of THC, such as the cortex and hippocampus (Twitchell *et al.*, 1997; Tsou *et al.*, 1998).

At a cellular level, THC has been shown to modulate a number of neuronal functions, including ion channel activity (Turkanis *et al.*, 1991; Mackie *et al.*, 1995; Twitchell *et al.*, 1997) and neurotransmitter release (Shen *et al.*, 1996; Gessa *et al.*, 1998; Jentsch *et al.*, 1998), and there is increasing evidence suggesting a role for THC in the regulation of neuronal viability. THC has a toxic effect on cultured hippocampal neurons (Chan *et al.*, 1998), glioma cells (Sanchez *et al.*, 1998) and cortical neurons (Campbell, 2001), and inhibits glioma cell growth *in vivo* (Galve-Roperh *et al.*, 2000). In contrast, there is also evidence that THC and other cannabinoids act as neuroprotectants in certain systems. Cannabinoid receptor agonists are neuroprotective in excitotoxic cell death *in vivo* (Panikashvili *et al.*, 2001; van der Stelt *et al.*, 2001) and *in vitro* (Shen & Thayer, 1998; Abood *et al.*, 2001), which is dependent on CB_1 receptor activation. Furthermore, cannabinoids have been shown to protect cultured neurons against glutamate-induced toxicity (Hampson *et al.*, 1998) and *in vitro* hypoxia and glucose deprivation (Nagayama *et al.*, 1999). However, the precise role of the cannabinoid receptors in regulating neuronal viability is poorly understood, although some of the *in vitro* protective effects of cannabinoids (Hampson *et al.*, 1998; Nagayama *et al.*, 1999) are receptor-independent while the neurotoxic effects of THC on cortical (Campbell, 2001) and hippocampal (Chan *et al.*, 1998) cultures are blocked by CB_1 receptor antagonists.

We have recently reported that THC activates the caspase-3 cell death pathway in cultured cortical neurons, resulting in

*Author for correspondence; E-mail: vacmpbll@tcd.ie

DNA fragmentation and programmed cell death (Campbell, 2001). Furthermore, we have shown that the activation of the central CB_1 cannabinoid receptor is vital in the execution of this cell death cascade (Downer *et al.*, 2001). It has been established that the CB_1 receptor couples to several signal transduction pathways (Dill & Howlett, 1988; Bouaboula *et al.*, 1995; Bouaboula *et al.*, 1996; Sanchez *et al.*, 1998; Gomez del Pulgar *et al.*, 2000; Derkinderen *et al.*, 2001) including the stress-activated protein kinase pathway (Rueda *et al.*, 2000). While there is growing evidence that the c-Jun N-terminal kinase (JNK) pathway is central to cell death in the nervous system (Mielke & Herdegen, 2000), the role of JNK in the CB_1 receptor-dependent induction of neuronal apoptosis remains to be established. The present work was therefore undertaken to examine the nature of the link between the CB_1 receptor, activation of JNK and downstream apoptotic consequences in cultured cortical neurons. Furthermore, three JNK isoforms, JNK1, JNK2 and JNK3, have been identified in the mammalian brain (Gupta *et al.*, 1996), and current commercially available JNK inhibitors are unable to distinguish between JNK1-, JNK2- and JNK3-mediated effects. We therefore treated neurons with specific antisense oligonucleotides (AS) that target rat JNK1 or JNK2 mRNA in order to investigate the upstream roles of these JNK isoforms in the THC-induced activation of caspase-3 and subsequent DNA fragmentation.

Methods

Culture of cortical neurons

Primary cortical neurons were prepared from 1-day-old Wistar rats and maintained in neurobasal medium (Gibco BRL, Paisley, U.K.). Rats were decapitated, the cerebral cortices dissected and the meninges removed. The cortices were incubated in phosphate-buffered saline (PBS) with trypsin ($0.25\,\mu g\,ml^{-1}$) for 25 min at 37°C. The cortical tissue was then triturated ($\times 5$) in PBS containing soyabean trypsin inhibitor ($0.2\,\mu g\,ml^{-1}$) and DNAse ($0.2\,mg\,ml^{-1}$) and gently filtered through a sterile mesh filter ($40\,\mu m$). The suspension was centrifuged at $2000 \times g$ for 3 min at 20°C and the pellet resuspended in warm neurobasal medium, supplemented with heat-inactivated horse serum (10%), penicillin ($100\,U\,ml^{-1}$), streptomycin ($100\,U\,ml^{-1}$) and glutamax (2 mM). Suspended cells were plated at a density of 0.25×10^6 cells on circular 10 mm diameter coverslips, coated with poly-L-lysine ($60\,\mu g\,ml^{-1}$), and incubated in a humidified atmosphere containing 5% CO_2:95% air at 37°C for 2 h prior to being flooded with prewarmed neurobasal medium. After 48 h, $5\,ng\,ml^{-1}$ cytosine-arabino-furanoside was added to the culture medium to suppress the proliferation of non-neuronal cells and maintain the purity of the cortical neuronal culture. This ensures that microglia and astrocyte contamination is less than 5% in culture preparations. Medium was exchanged for fresh medium every 3 days and cells were grown in culture for up to 14 days.

Oligonucleotide treatment

JNK antisense (AS) and scrambled control (SC) phosphorothioated oligonucleotides were synthesized by Biognostik (Gottingen, Germany). The sequences used were according to previously published work (Hreniuk *et al.*, 2001) and are complementary to the mRNA encoding rat JNK1 and JNK2 protein: JNK1 AS, 5′-CTCATGATGGCAAGCAATTA-3′; JNK1 SC, 5′-ACTACTACACTAGACTAC-3′; JNK2 AS, 5′-GCTCAGTGGACATGGATGAG-3′ and JNK2 SC, 5′-GGACTACTACACTAGACTAC-3′. Neurons were maintained in supplemented media in the presence of the oligonucleotides for 48 h prior to treatment with THC. *N*-[1-(2,3-dioleoyloxy)propyl]-*N*,*N*,*N*-trimethylammonium/dioleoylphosphatidylethanolamine (DOTMA/DOPE $5\,\mu g\,ml^{-1}$; Life Technologies, Paisley, U.K.) was incorporated into serum-free media for the first 4 h of oligonucleotide treatment to ensure sufficient oligonucleotide uptake. Downregulation of JNK1 and JNK2 protein expression was achieved by using JNK1 AS and JNK2 AS at a final concentration of $2\,\mu M$.

Terminal deoxynucleotidyltransferase-mediated biotinylated UTP nick end labelling (TUNEL)

Apoptotic cell death was determined in cultures using TUNEL staining according to the manufacturer's instructions (Dead-End Colorimetric Apoptosis Detection System; Promega Corporation, Madison, MD, U.S.A.). Following treatment with THC ($5\,\mu M$) for 3 h, cells were fixed with paraformaldehyde (4%) for 30 min at room temperature. Neurons were permeabilised with Triton X-100 (0.2%) and Proteinase K (0.2%) and biotinylated nucleotide was incorporated at the 3′-OH DNA ends using the enzyme terminal deoxynucleotidyl transferase (TdT). Endogenous peroxidases were blocked using 0.3% H_2O_2, and horseradish-peroxidase-labelled streptavidin was bound to the biotinylated nucleotides. Apoptotic cells (TUNEL-positive) were detected using diaminobenzidine, a stable chromagen that stains the apoptotic nuclei of TUNEL-positive cells dark brown. After mounting coverslips on slides, the neurons were viewed under light microscopy at $\times 100$ magnification. Cells displaying apoptotic nuclei were counted and expressed as a percentage of the total number of cells examined (400–500 cells coverslip^{-1}).

Western blot analysis

Cortical neurons were harvested in lysis buffer (25 mM HEPES, 5 mM $MgCl_2$, 5 mM dithiothreitol, 5 mM EDTA, 2 mM PMSF, $5\,\mu g\,ml^{-1}$ leupeptin, $5\,\mu g\,ml^{-1}$ pepstatin, $5\,\mu g\,ml^{-1}$ aprotinin, pH 7.4) and homogenised on ice. Lysates were then centrifuged ($13{,}000 \times g$ for 15 min at 4°C) and the supernatant containing the cytosolic fraction was prepared for SDS–polyacrylamide gel electrophoresis. The cytosolic fraction was diluted to $50\,\mu g\,ml^{-1}$ protein concentration with sodium dodecyl sulphate (SDS) sample buffer (150 mM Tris-HCl pH 7.4, 10% w v^{-1} glycerol, 4% w v^{-1} SDS, 5% v v^{-1} β-mercaptoethanol, 0.002% w v^{-1} bromophenol blue) and samples heated to 100°C for 5 min. Samples were separated by electrophoresis on 10 and 12% polyacrylamide minigels and cytosolic proteins were transferred from the gel onto nitrocellulose membrane (Sigma, U.K.). The blots were blocked with 2% BSA for 1 h at 37°C and then incubated with the primary antibody overnight at 4°C. The blots were washed thoroughly with Tris-buffered saline (TBS) containing 0.05% Tween and immunoreactive bands detected using horseradish-peroxidase-conjugated anti-mouse IgG (Sigma, U.K.) or

anti-rabbit IgG (Sigma, U.K.) and an enhanced chemiluminescence (ECL) system (Amersham, U.K.). Primary antibodies used were: monoclonal JNK1 and JNK2 antibodies (Santa Cruz Biotechnology Inc., Santa Cruz, CA, U.S.A.) purified from mouse serum that recognise JNK1 (46 kDa) and JNK2 (54 kDa) protein expression; monoclonal anti-phospho-specific JNK antibody (Santa Cruz Biotechnology Inc., Santa Cruz, CA, U.S.A.) purified from mouse serum that recognises phosphorylated JNK1, JNK2 and JNK3 isoforms; polyclonal Bax antibody (DAKO Corporation, Carpinteria, CA, U.S.A.) purified from rabbit serum that recognises amino acids 43–61 of human Bax. Molecular weight markers were used to confirm the molecular weight of protein bands. Bandwidths were quantified using densitometric analysis (D-Scan PC software).

Measurement of caspase-3 activity

Cleavage of the fluorogenic caspase-3 substrate (Ac-DEVD-7-amino-4-trifluoromethylcoumarin peptide (AFC); Alexis Corporation, U.S.A.) to its fluorescent product was used as a measure of caspase-3 activity. Following treatment with THC (5 μM) for 2 h, cells were harvested in lysis buffer (25 mM HEPES, 5 mM $MgCl_2$, 5 mM dithiothreitol, 5 mM EDTA, 2 mM PMSF, 10 $\mu g\,ml^{-1}$ leupeptin, 10 $\mu g\,ml^{-1}$ pepstatin, 10 $\mu g\,ml^{-1}$ aprotinin, pH 7.4) and homogenised on ice. Samples of supernatant (50 μl) were incubated with the DEVD peptide (10 μM; 4 μl) or incubation buffer (50 μl; 50 mM HEPES, 10 mM dithiothreitol, 20% w v^{-1} glycerol, pH 7.4) for 1 h at 37°C and the fluorescence assessed (excitation, 400 nm; emission, 505 nm) using a Fluoroscan Ascent FL plate reader (MSC Medical Supply Co. Ltd, U.K.).

Drug treatment

THC was obtained from Sigma-Aldrich Company Ltd (Dorset, U.K.). The drug was initially dissolved in methanol and stored at −20°C as an 80 mM stock solution. For use, the stock drug was diluted to a final concentration of 5 μM in prewarmed culture media and 0.007% methanol was used as vehicle control. The selective CB_1 receptor antagonist AM 251 (Tocris Cookson Ltd, Bristol, U.K.) was stored as a 10 mM stock solution in dimethylsulphoxide (DMSO) and diluted to a final concentration of 10 μM in warm culture media for addition to cultures; 0.0001% DMSO was used as a vehicle control for AM 251. Neurons were preincubated with AM 251 for 30 min before treating with THC. Pertussis toxin (PTX; Sigma, Dorset, U.K.) was reconstituted in PBS and neurons were incubated with 200 $ng\,ml^{-1}$ PTX for 24 h prior to THC treatment.

Statistical analysis

Data are reported as the mean ± s.e.m. of the number of experiments indicated in every case. Statistical analysis was performed by Student's *t*-tests and a one-way ANOVA. A *post hoc* analysis was made by the Student–Neumann–Keuls test. Our criterion for significance was $P<0.05$. Extreme significance differences were expressed by probability values of $P<0.01$ and $P<0.001$.

Results

THC activates JNK1 and JNK2 isoforms within a differential timeframe

Exposure of cultured cortical neurons to THC (5 μM) resulted in the activation of the JNK protein within the cytosol in a time-dependent manner (Figure 1). Cytosolic expression levels of the phosphorylated (active) forms of JNK1 and JNK2 were measured by Western immunoblot and bandwidths were quantified using densitometry. Interestingly, there was a differential timeframe of activation for JNK1 and JNK2. In terms of the JNK1 time course of activation (Figure 1a), in control cells phospho-JNK1 expression was 7.28 ± 0.80 (arbitrary units; mean bandwidth ± s.e.m.) and this was significantly increased to 13.41 ± 1.63 following treatment with THC for 5 min ($P<0.001$, ANOVA; $n=7$). However, no change in phospho-JNK1 expression was observed at subsequent time points, and phospho-JNK1 expression was in fact significantly reduced to 4.21 ± 0.40 following treatment with THC for 2 h ($P<0.05$, ANOVA, $n=7$; Figure 1a).

In contrast, Figure 1b demonstrates that expression of phospho-JNK2 in control neurons was 21.44 ± 3.89 (arbitrary units; mean bandwidth ± s.e.m.) and this was significantly increased to 38.79 ± 6.25 when neurons were cultured in media containing THC (5 μM) for 2 h ($P<0.001$, ANOVA; $n=7$). At earlier time points, treatment with THC had no effect on phospho-JNK2 expression. A sample immunoblot demonstrating the THC-induced activation of JNK1 at 5 min and JNK2 at 2 h is shown in Figure 1c.

Total JNK1 and JNK2 expression was unaffected by THC (5 μM; sample immunoblots shown). In vehicle-treated cells, JNK1 total protein expression was 46.53 ± 1.15 (arbitrary units; mean bandwidth ± s.e.m.) and exposure of neurons to THC for 5 min had no effect on total JNK1 expression (46.92 ± 2.66, $n=5$; Figure 1d). In neurons treated with vehicle alone for 2 h, mean total JNK2 expression was 56.32 ± 7.31 and this was unaffected by exposure to THC for 2 h (56.26 ± 9.09; $n=5$; Figure 1e). Thus, the increase in expression of phosphorylated JNK1 (Figure 1a) and phosphorylated JNK2 (Figure 1b) is not attributable to a THC-induced increase in total JNK protein expression. Furthermore, in our cell culture model, JNK3 expression was very moderate (Figure 1f), hence the relative contribution of JNK1 and JNK2 to the apoptotic cascade was assessed.

Since we have previously shown that 5 μM is the concentration of THC required to induce maximal neuronal degeneration in a CB_1 receptor-dependent manner (Downer *et al.*, 2001), we performed a dose–response analysis of THC-induced JNK activation. Figure 1(g and h) represents sample immunoblots which demonstrate that treatment of cells with THC (0.005–50 μM) evoked a dose-dependent increase in phospho-JNK1 (Figure 1g) and phospho-JNK2 (Figure 1h) expression at 5 and 120 min, respectively.

AM 251 pretreatment prevents THC-induced JNK activation

To determine whether THC-induced JNK activation was dependent on the CB_1 receptor, we employed the use of the selective CB_1 receptor antagonist AM 251 (10 μM). Figure 2 demonstrates that AM 251 prevented the THC-induced

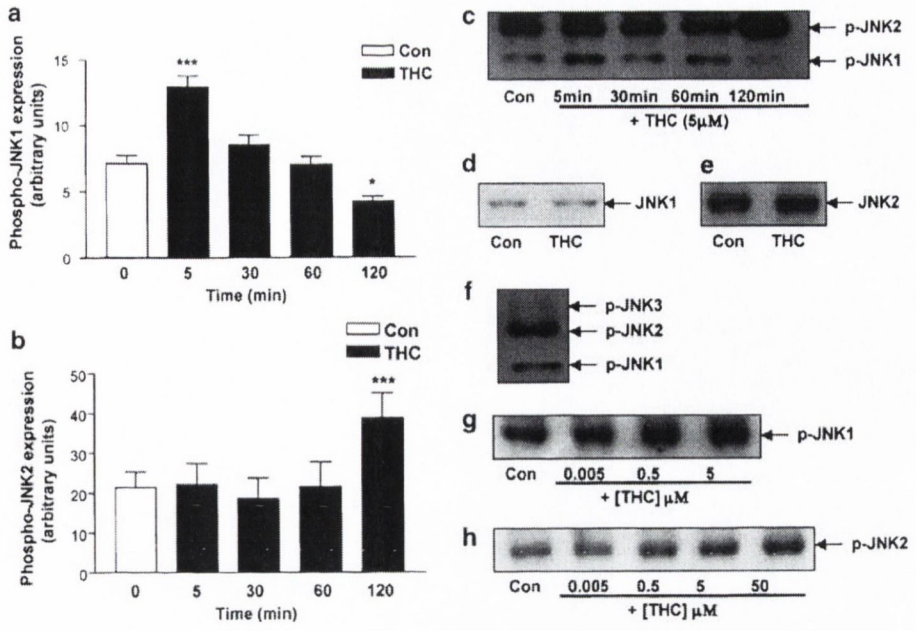

Figure 1 Time course of THC-induced activation of JNK. Cortical neurons were exposed to THC for 5–120 min, then cells were harvested and the cytosolic fractions analysed for the expression levels of the phosphorylated active forms of JNK 1 and JNK2 using Western immunoblot. (a) A significant increase in phospho-JNK1 expression was found following treatment with THC (5 μM) for 5 min. Exposure to THC for 30 and 60 min had no effect on phospho-JNK1 expression. However, treatment with THC for 120 min significantly decreased phospho-JNK1 expression. Results are expressed as mean $\pm$ s.e.m. for seven observations, $^{***}P<0.001$, $^{*}P<0.05$. (b) Phospho-JNK2 expression was significantly increased when neurons were treated with THC (5 μM) for 120 min. Exposure to THC for 5, 30 and 60 min had no effect on phospho-JNK2 expression. Results are expressed as mean $\pm$ s.e.m. for seven observations, $^{***}P<0.001$. (c) A sample Western immunoblot demonstrating the increase in phospho-JNK1 expression at 5 min of THC treatment and the corresponding increase in phospho-JNK2 expression following treatment with THC for 120 min. (d) Neurons were treated with THC (5 μM) for 5 min, then cells were harvested in lysis buffer and the cytosolic fractions analysed for total JNK1 protein expression using Western immunoblot. THC had no effect on JNK1 protein expression at 5 min. Inset: A sample Western immunoblot showing that THC treatment for 5 min had no effect on JNK1 protein expression as compared to vehicle-treated neurons. (e) Cortical neurons were treated with THC (5 μM) for 2 h, then cells were harvested and analysed for total JNK2 protein expression by Western blot analysis. Incubation of cells with THC for 2 h did not affect JNK2 protein expression. Inset: A sample Western immunoblot demonstrating total JNK2 protein expression in vehicle-treated neurons and neurons treated with THC for 2 h. (f) Untreated cortical neurons were harvested and analysed for phosphorylated JNK1, JNK2 and JNK3 expression. JNK3 expression was moderate compared to JNK1/2 expression. (g) A sample Western immunoblot showing that a 5 min treatment with THC increases phospho-JNK1 expression in a dose-dependent manner. Similar results were observed in five separate experiments. (h) A sample Western immunoblot showing that a 120 min treatment with THC increases phospho-JNK2 expression in a dose-dependent manner. Similar results were observed in five separate experiments.

activation of JNK1 and JNK2. Thus, in neurons treated with vehicle for 5 min, phosphorylated JNK1 expression was 44.95 $\pm$ 4.86 (arbitrary units; mean bandwidth $\pm$ s.e.m.) and this was significantly increased following THC treatment (5 μM; 5 min) to 58.67 $\pm$ 3.59 ($P<0.05$, ANOVA, $n=6$; Figure 2a). While pretreatment with AM 251 alone had no effect on phosphorylated JNK1 expression (37.35 $\pm$ 3.43), it prevented the THC-induced increase in phospho-JNK1 expression (38.14 $\pm$ 5.99). Although it has been shown that AM 251 behaves as an inverse agonist (New & Wong, 2003), we were unable to detect any effect of AM 251 on basal JNK activity (Figure 2).

Figure 2b demonstrates that phosphorylated JNK2 expression was significantly increased from 12.83 $\pm$ 0.54 (arbitrary units; mean bandwidth $\pm$ s.e.m.) to 15.72 $\pm$ 0.34 following treatment with THC (5 μM) for 2 h ($P<0.01$, Student's t-test, $n=6$). Exposure to AM 251 (10 μM) alone had no effect on basal phosphorylated JNK2 expression (11.55 $\pm$ 1.75) and it prevented the THC-induced increase in phosphorylated JNK2 expression (12.55 $\pm$ 0.52; Figure 2b). Sample immunoblots demonstrating the activation of JNK1 and JNK2 following THC treatment, and the abolition of these effects in AM 251-treated cells are shown as insets in Figure 2a and b. This result provides evidence of a role for the CB_1 cannabinoid receptor in the THC-induced activation of both JNK1 and JNK2.

PTX abrogates THC-induced JNK1/2 activation

The central CB_1 cannabinoid receptor is coupled to $G_{i/o}$-proteins (Howlett, 1995). The involvement of $G_{i/o}$ in coupling the CB_1 receptor to JNK activation in this system was assessed using PTX (200 ng ml^{-1}). As shown in Figure 3a, PTX pretreatment prior to THC (5 μM) treatment for 5 min (31.92 $\pm$ 5.59 arbitrary units; mean bandwidth $\pm$ s.e.m.) prevented THC-induced JNK1 activation at 5 min (55.98 $\pm$ 4.74; $P<0.05$, ANOVA, $n=5$). Incubation of neurons with methanol vehicle for 5 min (41.44 $\pm$ 2.72) or PTX alone for 24 h (35.06 $\pm$ 3.71) had no effect on JNK1 activity (Figure 3a).

Similarly, Figure 3b demonstrates that phospho-JNK2 expression was significantly increased from 13.90 $\pm$ 0.54 to 22.34 $\pm$ 2.75 (arbitrary units; mean bandwidth $\pm$ s.e.m.) following treatment with THC (5 μM) for 2 h ($P<0.05$, ANOVA, $n=5$). Treatment with PTX (200 ng ml^{-1}) alone had no effect on phosphorylated JNK2 expression (16.05 $\pm$ 1.99), but it

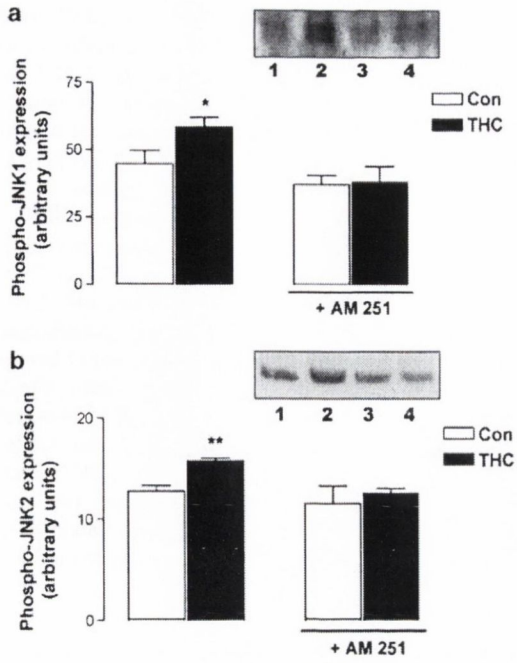

Figure 2 THC-induced activation of JNK is mediated by the CB_1 receptor. (a) Treatment of neurons with THC (5 μM) for 5 min evoked a significant increase in phospho-JNK1 expression. Pre-incubation of cortical neurons with the CB_1 receptor antagonist AM 251 (10 μM) for 30 min abolished the THC-induced increase in phospho-JNK1 expression. Results are expressed as mean $\pm$ s.e.m. for six observations, $^*P<0.05$. Inset: A sample Western immunoblot demonstrating the increase in phospho-JNK1 expression after 5 min of THC treatment (lane 2) compared to control cells (lane 1). While AM 251 had no effect on phospho-JNK1 expression (lane 3), it abolished the ability of THC to increase phospho-JNK1 expression (lane 4). (b) Treatment of neurons with THC (5 μM) for 120 min evoked a significant increase in phospho-JNK2 expression. Pre-incubation of cortical neurons with the CB_1 receptor antagonist AM 251 (10 μM) for 30 min abolished the THC-induced increase in phospho-JNK2 expression. Results are expressed as mean $\pm$ s.e.m. for six observations, $^{**}P<0.01$. Inset: A sample Western immunoblot demonstrating the increase in phospho-JNK2 expression after 5 min of THC treatment (lane 2) compared to control cells (lane 1). While AM 251 had no effect on phospho-JNK2 expression (lane 3), it abolished the ability of THC to increase phospho-JNK2 expression (lane 4).

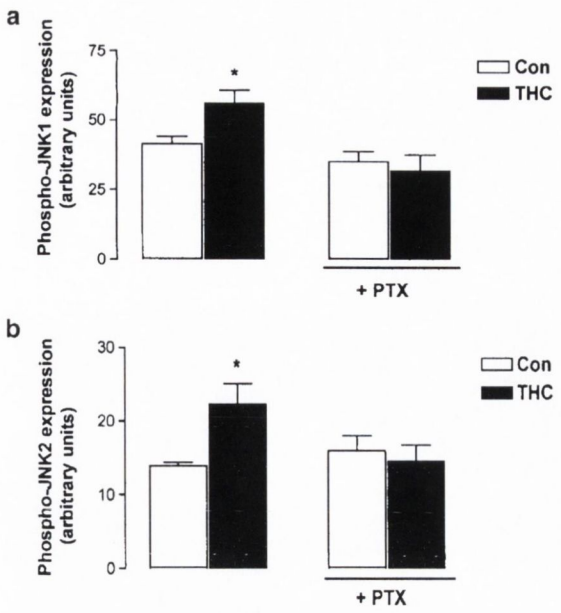

Figure 3 THC-induced JNK activation is mediated by G-protein subtypes $G_{i/o}$. (a) THC (5 μM; 5 min) significantly increased phospho-JNK1 expression and this was prevented by pretreatment with PTX (200 ng ml^{-1}; 24 h). Results are expressed as mean $\pm$ s.e.m. for five observations, $^*P<0.05$. (b) THC (5 μM; 120 min) significantly increased phospho-JNK2 expression and this was prevented by pretreatment with PTX (200 ng ml^{-1}; 24 h). Results are expressed as mean $\pm$ s.e.m. for five observations, $^*P<0.05$.

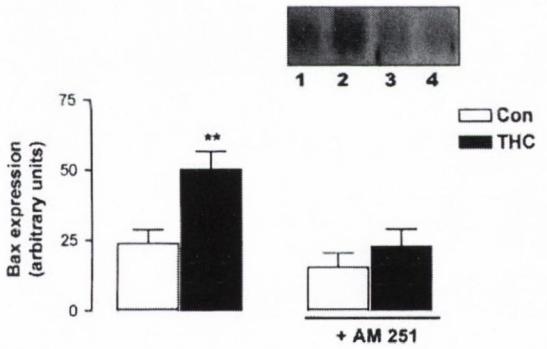

Figure 4 THC increases Bax expression *via* the CB_1 receptor. Neurons were preincubated with AM 251 (10 μM) for 30 min, treated with THC (5 μM) for 2 h and analysed for the expression levels of Bax using Western immunoblotting. THC significantly increased Bax expression and this was abolished by AM 251. Results are expressed as mean $\pm$ s.e.m. for five observations, $^{**}P<0.01$. Inset: A sample Western immunoblot showing that THC increases Bax expression (lane 2) compared to vehicle-treated neurons (lane 1). The stimulatory effect of THC on Bax expression was prevented by AM 251 (lane 4). Exposure of cells to AM 251 alone had no effect on Bax expression (lane 3).

prevented the THC-induced increase in JNK2 activity at 2 h (14.65 $\pm$ 2.12; Figure 3b). These data suggest that the coupling of the CB_1 receptor to G-protein subtypes $G_{i/o}$ facilitates THC-induced JNK1 and JNK2 activation.

AM 251 prevents THC-induced Bax expression

JNK kinases have been linked to neuronal apoptosis by altering the expression of the Bcl family of mitochondrial-associated proteins (Mielke & Herdegen, 2000). In this study, expression levels of the proapoptotic protein Bax were measured by Western immunoblot in cells treated with THC (5 μM) for 2 h and the effect of the CB_1 antagonist AM 251 (10 μM) was assessed. Figure 4 demonstrates that Bax expression in control cells was 23.82 $\pm$ 4.89 (arbitrary units; mean $\pm$ s.e.m.) and this was significantly increased following THC treatment for 2 h to 50.18 $\pm$ 6.43 ($P<0.01$, ANOVA, $n=5$). AM 251 alone had no effect on Bax expression (15.39 $\pm$ 4.96); however, it prevented the THC-induced increase in Bax expression (22.67 $\pm$ 6.01). A sample Western immunoblot demonstrating the CB_1-dependent increase in Bax expression is shown as an inset in Figure 4.

JNK AS downregulates JNK protein expression

Since JNK activation was observed following THC treatment, we employed the use of antisense technology to analyse

whether JNK has an upstream role in the regulation of apoptotic effectors. Cells were exposed to 2 μM of either JNK1 AS or JNK2 AS to downregulate JNK1 and JNK2 protein expression in order to delineate the specific role of each isoform in the cell death pathway. Upon treatment with JNK1 and JNK2 AS, cellular levels of JNK1 and JNK2 protein were markedly reduced (Figure 5a, b). In cells treated with JNK1 SC, JNK1 expression was 19.20$\pm$2.89 (arbitrary units; mean$\pm$s.e.m.) and this was significantly decreased by 79% when JNK1 AS was incorporated into the media for 48 h ($P<0.05$, Student's t-test, $n=4$; Figure 5a). Similarly, JNK2 AS significantly decreased JNK2 protein expression by 70%, compared to the cells treated with JNK2 SC for 48 h ($P<0.05$, Student's t-test, $n=5$; Figure 5b). The antisense-mediated depletion of JNK1 and JNK2 was specific since JNK2 AS had no effect on JNK1 protein expression (Figure 5a) and, similarly, JNK1 AS had no effect on JNK2 protein expression (Figure 5b). Sample immunoblots demonstrating the antisense-mediated downregulation of JNK1 and JNK2 protein expression are shown as insets in Figure 5a and b.

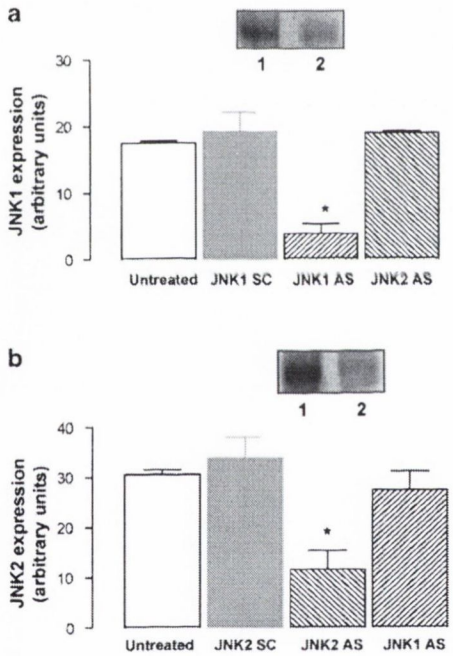

Figure 5 JNK AS effectively reduces JNK protein expression. Neurons were incubated with 2 μM JNK1/JNK2 antisense (AS) or JNK1/JNK2 scrambled control (SC) for 48 h. Cells were harvested in lysis buffer and the total expression of JNK1 and JNK2 protein was examined by Western blot analysis. (a) Treatment with JNK1 AS significantly decreased JNK1 protein expression in comparison to untreated cells and cells treated with JNK1 SC. JNK2 AS had no effect on JNK1 protein expression. Results are expressed as mean$\pm$s.e.m. for four experiments, $^*P<0.05$. Inset: A sample immunoblot demonstrating that JNK1 AS significantly reduces JNK1 protein expression (lane 2) compared to JNK1 SC-treated neurons (lane 1). (b) JNK2 AS significantly reduced JNK2 protein expression. JNK1 AS had no effect on JNK2 protein expression. Results are expressed as mean$\pm$s.e.m. for four experiments, $^*P<0.05$. Inset: A sample immunoblot demonstrating the significant reduction in JNK2 protein expression in JNK2 AS-treated neurons (lane 2) compared to JNK2 SC-treated cells (lane 1).

JNK AS prevents THC-induced caspase-3 activation

Apoptotic cell death is typically accompanied by the activation of the cysteine protease caspase-3 (Janicke *et al.*, 1998). Our lab has previously shown the pivotal role of this enzyme in the cell death pathway triggered by THC within the rat cortex (Campbell, 2001; Downer *et al.*, 2001). Here we analysed whether JNK1 or JNK2 is involved in the THC-induced activation of caspase-3. Following downregulation of each of the JNK isoforms using appropriate AS, the role of JNK1 and JNK2 in THC-induced caspase-3 activation was assessed (Figure 6a, b).

The data presented in Figure 6a indicate that treatment with THC (5 μM) for 2 h significantly increased caspase-3 activity from 22.50$\pm$1.67 (mean$\pm$s.e.m.) to 50.66$\pm$6.86 pmol AFC produced (mg protein)$^{-1}$ min^{-1} ($P<0.05$, ANOVA; $n=8$). In cells treated with JNK1 SC (2 μM) alone for 48 h, caspase-3 activity was comparable to control values (25.09 $\pm$5.80 pmol AFC produced (mg protein)$^{-1}$ min^{-1}). Pretreatment with JNK1 AS (2 μM) for 48 h prior to THC treatment prevented the THC-induced increase in caspase-3 activity (31.79$\pm$6.53 pmol AFC produced (mg protein)$^{-1}$ min^{-1}; Figure 6a).

Similarly, Figure 6b demonstrates that a 2 h exposure of cortical neurons to THC (5 μM) significantly increased caspase-3 activity from 22.05$\pm$1.48 (mean$\pm$s.e.m.) to 63.05$\pm$11.10 pmol AFC produced (mg protein)$^{-1}$ min^{-1} ($P<0.05$, ANOVA, $n=7$). Neurons incubated with JNK2 SC (2 μM) for 48 h showed a level of caspase-3 activity similar

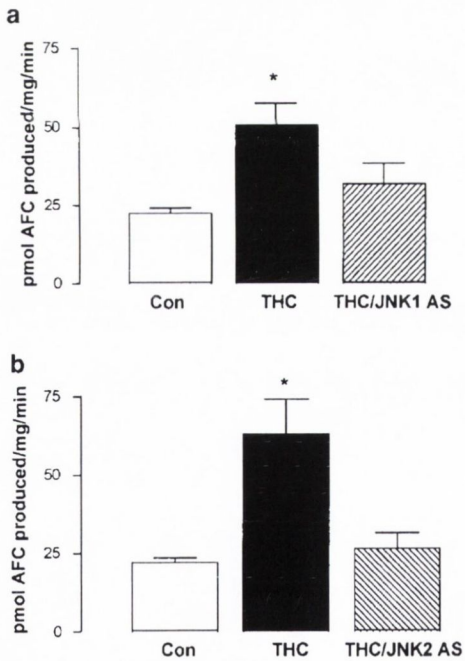

Figure 6 JNK is required for caspase-3 activity in THC-induced apoptosis. (a) Treatment of cortical neurons with THC (5 μM) for 2 h significantly increased caspase-3 activity, as assessed by the cleavage of the fluorogenic DEVD substrate. The stimulatory effect of THC on caspase-3 activity was prevented by pretreatment with JNK1 AS (2 μM; 48 h). Results are expressed as mean$\pm$s.e.m. for eight observations, $^*P<0.05$. (b) Similarly, pretreatment of cells with JNK2 AS (2 μM; 48 h) prior to THC treatment abolished the stimulatory effect of THC on caspase-3 activity. Results are expressed as mean$\pm$s.e.m. for seven observations, $^*P<0.05$.

to that measured in vehicle-treated neurons (32.73±8.74 pmol AFC produced (mg protein)$^{-1}$ min^{-1}). Pretreatment with JNK2 AS (2 μM) for 48 h prior to THC treatment prevented the THC-induced increase in caspase-3 activity (26.06±5.20 pmol AFC produced (mg protein)$^{-1}$ (min)$^{-1}$; Figure 6b). These results demonstrate a role for both JNK1 and JNK2 in the THC-induced activation of caspase-3.

JNK AS prevents THC-induced DNA fragmentation

The TUNEL technique was used to demonstrate that the THC-induced DNA fragmentation that we have previously reported (Campbell, 2001) involves JNK1 and JNK2 (Figure 7). In control cells, 19±2% (mean±s.e.m.) of cells displayed fragmented DNA (TUNEL-positive), and this was significantly increased to 50±6% in cells treated with THC (5 μM) for 3 h ($P<0.001$, ANOVA, $n=5$ coverslips; Figure 7a). AS-mediated depletion of JNK1 or JNK2 prevented the THC-induced increase in DNA fragmentation. Thus, exposure of cells to JNK1 AS (2 μM) for 48 h prior to THC treatment prevented the THC-induced increase in TUNEL staining (26±7% TUNEL-positive cells; Figure 7a, b). In contrast, in cells pretreated with JNK1 SC (2 μM), the THC-induced increase in DNA fragmentation was retained (46±6% TUNEL-positive cells, $P<0.001$, ANOVA, $n=5$ coverslips; Figure 7a). Treatment with JNK1 AS (2 μM) alone for 48 h had no effect of the percentage of neurons displaying fragmented DNA (26±6% TUNEL-positive cells.

Similarly, in cells pretreated with JNK2 AS (2 μM) for 48 h before THC (5 μM) treatment, 20±3% of cells were TUNEL-positive (Figure 7a, c). In contrast, cells preincubated with JNK2 SC oligonucleotides (2 μM) for 48 h prior to treatment with THC showed a significant increase in DNA fragmentation (56±3% TUNEL-positive cells, $P<0.001$, ANOVA, $n=5$ coverslips; Figure 7a). Treatment of neurons with JNK2 AS (2 μM) alone for 48 h did not have a neurotoxic effect (20±3% TUNEL-positive cells.

These results demonstrate that depletion of either JNK1 or JNK2 prevents the THC-induced DNA fragmentation. These data are consistent with the caspase-3 result and suggest that both JNK1 and JNK2 are intricately involved in regulating the THC-induced activation of caspase-3 and resultant DNA fragmentation in the apoptotic pathway.

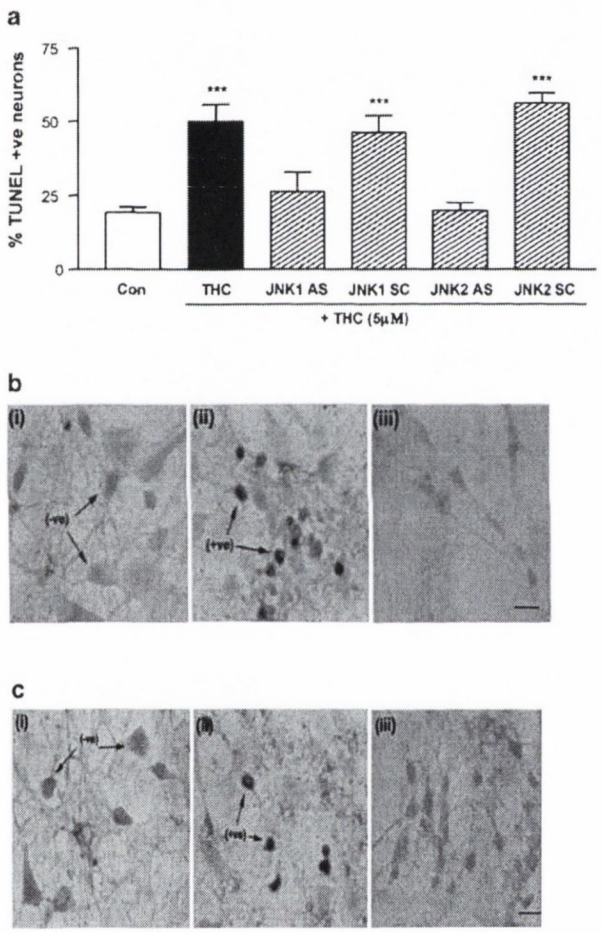

Figure 7 JNK activity is required for THC-induced DNA fragmentation. (a) Exposure of neurons to THC (5 μM) for 3 h significantly increased the percentage of cells with DNA fragmentation. Treatment with JNK1 AS or JNK2 AS (2 μM; 48 h) prior to THC treatment prevented the THC-induced increase in DNA fragmentation. In contrast, in neurons treated with JNK1 SC or JNK2 SC (2 μM; 48 h), THC still evoked a significant increase in DNA fragmentation. Results are expressed as mean±s.e.m. for five observations, ***$P<0.001$. (b) Representative images of (i) control, (ii) THC-treated and (iii) THC/JNK1 AS-treated cortical neurons following TUNEL staining for DNA fragmentation. Arrows indicate TUNEL-negative (−ve) and TUNEL-positive (+ve) cells. Scale bar is 50 μM. (c) Representative images of TUNEL staining of (i) control, (ii) THC-treated and (iii) THC/JNK2 AS-treated cortical neurons. Scale bar is 50 μM.

JNK1 AS pretreatment has no effect on THC-induced JNK2 activity

Since THC was found to increase JNK1 activity (at 5 min) prior to JNK2 activity (at 2 h), we employed the use of antisense technology to analyse whether JNK1 is involved upstream in the regulation of JNK2 activity (Figure 8). Neurons were treated with JNK1 AS (2 μM; 48 h) to down-regulate JNK1 protein expression prior to exposure to THC (5 μM) for 2 h. Treatment of cells with THC for 2 h significantly increased phospho-JNK2 expression from 21.87±2.38 (arbitrary units; mean bandwidth±s.e.m.) to 31.14±2.85 ($P<0.05$, ANOVA, $n=4$). Neurons treated with JNK1 AS alone for 48 h showed a level of JNK2 activity comparable to that found in vehicle-treated neurons (23.99±2.31, $n=4$) and JNK1 AS

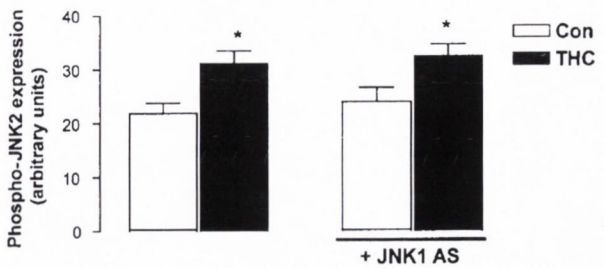

Figure 8 JNK1 is not upstream of JNK2 in THC-induced apoptosis. Neurons were preincubated with JNK1 AS (2 μM) for 48 h, treated with THC (5 μM) for 2 h and analysed for phosphorylated JNK2 expression using Western immunoblot. THC evoked a significant increase in phospho-JNK2 expression. In cells exposed to JNK1 AS, THC was still capable of inducing a significant increase in phospho-JNK2. Results are expressed as mean±s.e.m. for four observations, *$P<0.05$.

failed to prevent the THC-induced increase in phospho-JNK2 expression (32.49 ± 1.90, $P<0.05$, ANOVA, $n=4$). These data suggest that JNK1 does not occupy an upstream role in the regulation of JNK2 activity, despite the differential time course of activation of these JNK isoforms.

Discussion

The aim of this study was to examine the ability of the CB_1 cannabinoid receptor to couple to the JNK signalling pathway, and to assess the role of JNK in THC-induced neurotoxicity in cultured cortical neurons. THC was found to induce the activation of JNK1 and JNK2 within 5 min and 2 h, respectively. The ability of THC to induce activation of both JNK isoforms was blocked by AM 251 and PTX. THC significantly increased Bax expression in an AM 251-sensitive manner. Treatment of cortical neurons with specific AS targeted to rat JNK1 or JNK2 mRNA effectively reduced the protein expression of the respective JNK isoform. AS-mediated reduction of JNK1 and JNK2 protein expression prevented the THC-induced activation of caspase-3 and downstream DNA fragmentation. Data herein suggest that the CB_1 cannabinoid receptor is coupled to JNK in cortical neurons, and that both JNK1 and JNK2 are involved in the regulation of the downstream effectors that are pertinent in the THC-induced apoptotic pathway.

Recently, there has been a growing interest in the proclivity of cannabinoids to control the cell survival/death decision, particularly in neurons. Several studies have revealed that THC can induce neurotoxic effects in a number of cultured cell systems. Specifically, THC has a toxic effect on cultured hippocampal neurons (Chan *et al.*, 1998), cultured cortical neurons (Campbell, 2001) and glioma cells (Sanchez *et al.*, 1998). THC has also been shown to inhibit neuronal cell growth *in vivo* (Galve-Roperh *et al.*, 2000), in addition to its antiproliferative action in neuronal cultures. Furthermore, anandamide, an endogenous ligand of cannabinoid receptors (Devane *et al.*, 1992), induces apoptosis in PC12 cells (Sarker *et al.*, 2003) and lymphocytes (Schwarz *et al.*, 1994). THC-induced apoptosis in hippocampal (Chan *et al.*, 1998) and cortical (Downer *et al.*, 2001) cultures is CB_1 receptor-dependent. Proposed mechanisms of cannabinoid-induced neurotoxicity have included the generation of reactive oxygen species (Chan *et al.*, 1998), activation of the caspase-3 cell death pathway (Campbell, 2001; Downer *et al.*, 2001), sphingomyelin hydrolysis (Sanchez *et al.*, 1998), sustained ceramide accumulation (Galve-Roperh *et al.*, 2000) and activation of the JNK cascade (Sarker *et al.*, 2003).

It should be considered that in contrast to the data supporting cannabinoid-induced neurodegeneration, the bulk of the experimental evidence indicates that cannabinoids may protect neurons from toxic insults. However, it is not clear if this is a CB_1 receptor-dependent process. Nagayama *et al.* (1999) have shown that synthetic cannabinoid receptor agonists decrease hippocampal loss following transient global cerebral ischaemia *via* the CB_1 receptor, and increase cell viability in cerebral cortical cultures subjected to 8 h of hypoxia and glucose deprivation in a CB_1 receptor-independent manner. Cannabinoid receptor agonists are neuroprotective against excitotoxicity *in vivo* (Panikashvili *et al.*, 2001; van der Stelt *et al.*, 2001) and *in vitro* (Shen & Thayer, 1998; Abood *et al.*, 2001), which is prevented by CB_1 antagonists. Furthermore, THC and nonpsychotropic cannabinoids decrease glutamate toxicity in rat cortical neuronal cultures in a receptor-independent process that is not blocked by CB_1 receptor antagonists (Hampson *et al.*, 1998). Overall, it appears that neurotoxic and neuroprotective effects of cannabinoids can be observed, and these differences are likely to depend on a variety of influences, including the nature of the toxic insult, the cell type under study and the particular cannabinoid used.

The cannabinoid CB_1 receptor is distributed mainly in the central nervous system and is localised in brain regions most likely involved in contributing to the psychoactive effects of THC (Twitchell *et al.*, 1997). The rat cortex shows an intense pattern of CB_1 receptor expression, in particular in frontal regions where the CB_1 receptor subtype is found in cortical axons, cell bodies and dendrites (Tsou *et al.*, 1998).

The JNK protein kinases belong to the family of mitogen-activated protein kinases (MAPK) and represent a group of enzymes that are activated by cytokines and environmental stresses (Ip & Davis, 1998). The function of these kinases is to convert extracellular stimuli to intracellular signals that, in turn, control the expression of genes that are essential for many cellular responses, including cell growth and death (Marshall, 1995). These widely distributed kinases are activated by dual phosphorylation on threonine and tyrosine residues by upstream kinases as part of the cellular response to stress (Derkinderen *et al.*, 1999). JNKs are encoded by three different genes *jnk1*, *jnk2* and *jnk3*, and the products of each gene reveal isoforms with approximate molecular weights of 46 (JNK1), 54 (JNK2) and 57 kDa (JNK3), all of which are found in the mammalian brain (Gupta *et al.*, 1996). Although it is recognised that the JNK3 isoform is distributed throughout the rat cerebral cortex (Carboni *et al.*, 1998), JNK3 protein expression was moderate in our cell culture model, hence the relative contribution of the JNK1 and JNK2 isoforms to the apoptotic process was investigated.

In this study, the time course of THC-induced activation of JNK1 and JNK2 in cultured cortical neurons was assessed. JNK activity was assessed up to the 2 h time point as this is within the timeframe at which we have found significant levels of THC toxicity in cortical neuronal cultures (Campbell, 2001). It was found that THC increases JNK1 and JNK2 activity after 5 min and 2 h of treatment, respectively. Half-maximal stimulation of JNK1 occurred at a lower dose of THC than JNK2, indicating that THC-induced JNK2 activation was more reluctant than JNK1 activation in our cell culture model. It has been established that JNK activation may occur early (Xia *et al.*, 1995) or late (Virdie *et al.*, 1997) in apoptosis, and the finding that THC activates JNK1 and JNK2 within dissimilar timeframes suggests that the JNK isoforms may mediate different signals in cultured cortical neurons. A potential function of JNK may be to initiate programmed cell death (Johnson *et al.*, 1996), and our data demonstrating the early activation of JNK1 (within 5 min), may reflect a role for JNK1 in regulating downstream apoptotic effectors. However, our finding that THC activates JNK2 at 2 h of treatment is consistent with the time point at which maximal neuronal cell death has been previously shown in cortical neurons (Campbell, 2001). It is therefore possible that JNK2 activation may have occurred in response to DNA fragmentation, which is consistent with other studies (Ghahremani *et al.*, 2002).

Furthermore, considering that JNK activity may be regulated by caspase-3 (Ozaki *et al.*, 1999; Hatai *et al.*, 2000), it is possible that JNK2 activity is modulated by caspase-3 in this system. In refute of these hypotheses, antisense-mediated downregulation of JNK2 prevented the THC-induced increase in caspase-3 activation and DNA fragmentation, suggesting that JNK2 is upstream of these components of the apoptotic cascade. It is possible that an early cellular redistribution of JNK2, as opposed to an increase in overall JNK2 activity, may be involved in the apoptotic process. It is of note that although JNK2 activity was increased at 2 h, a concomitant decline in JNK1 activity was observed at this time point. This suggests a functional interaction between JNK1 and JNK2 isoforms and this is supported by evidence that JNK2 negatively regulates JNK1 phosphorylation (Hochedlinger *et al.*, 2002). However, our finding that AS-induced depletion of JNK1 failed to prevent the THC-induced increase in JNK2 activity suggests that JNK1 does not occupy an upstream role in regulating JNK2.

The involvement of JNK cascades in the regulation of cell proliferation *via* G-protein-coupled receptors has been demonstrated (Coso *et al.*, 1996). Our previous studies have demonstrated that the toxic effects of THC involve a PTX-sensitive G-protein (Campbell, 2001). This is consistent with evidence that links the central CB_1 receptor to activation of G-protein subtypes $G_{i/o}$ (Howlett, 1995). To date, the role of G-proteins in neuronal cell death has not been completely clarified since PTX-sensitive G-proteins have been found to exert both proapoptotic (Farkas *et al.*, 1998) and antiapoptotic effects (Jakob & Kreiglsten, 1997). However, data presented here demonstrate that coupling of the CB_1 receptor to PTX-sensitive G-proteins facilitates JNK activation.

JNK has the proclivity to phosphorylate a variety of nuclear and cytoplasmic substrates, some of which are vital for the apoptotic actions of JNK. It has been reported that JNK promotes cell death by promoting cytochrome *c* release from the mitochondria (Tournier *et al.*, 2000). In the nervous system, the proapoptotic mitochondrial-associated protein Bax acts downstream of JNK in regulating the translocation of mitochondrial cytochrome *c* into the cytosol (Kang *et al.*, 1998), and several studies have demonstrated an interaction between JNK and Bax in the cell death cascade (Lei *et al.*, 2002). The apoptotic events that are evoked by THC in cortical neurons include the release of mitochondrial cytochrome *c* into the cytosol following CB_1 receptor activation (Downer *et al.*, 2001), and our finding that THC induces Bax expression following CB_1 activation is a likely mechanism for this event.

Once in the cytosol, cytochrome *c* complexes with a cytosolic factor designated as apoptotic protease activating factor-1 (APAF-1), which in turn triggers the activation of the cysteine protease caspase-3, which contributes to the drastic morphological changes associated with apoptosis by disabling a number of key substrates (Zou *et al.*, 1997). We have previously shown that caspase-3 is central to the apoptotic cascade triggered by THC in cortical neurons (Campbell, 2001; Downer *et al.*, 2001). To elucidate the respective roles of JNK1 and JNK2 in THC-induced caspase-3 activation, we employed antisense technology to downregulate temporarily JNK1 and JNK2 expression. In neurons treated with JNK1 and JNK2 AS, JNK1 and JNK2 protein expression was selectively downregulated. Depletion of JNK1 and JNK2 prevented the THC-induced activation of caspase-3, indicating that both JNK1 and JNK2 isoforms are upstream of caspase-3 in the THC-induced apoptotic cascade.

We have recently shown that THC promotes degeneration of cultured cortical neurons in a time-dependent manner, with a maximal effect occurring 3 h post-treatment (Campbell, 2001). The evidence presented here and by others (Rueda *et al.*, 2000) supports an early interaction between THC and JNK, indicating that JNK activation is an upstream event in the degenerative pathway. The finding that the downregulation of JNK1 and JNK2 using antisense technology effectively blocked THC-induced activation of caspase-3 and downstream DNA fragmentation indicates that both JNK1 and JNK2 are intricately involved in the transduction of THC-induced apoptotic signals. It is of particular note that depletion of either JNK1 or JNK2 isoforms completely abrogated the THC-induced caspase-3 activation and DNA fragmentation. It may be expected that, since THC has the proclivity to couple to both JNK1 and JNK2, depletion of one isoform may result in THC coupling to the remaining isoform to evoke caspase-3 activation and resultant DNA fragmentation. This clearly was not the case and our result may reflect an interaction between JNK1 and JNK2 with respect to the regulation of upstream effectors involved in caspase-3 activation. Indeed, a requirement for both JNK1 and JNK2 has been implicated in the phosphorylation of the p53 tumour suppressor protein (Buschmann *et al.*, 2001), a potential upstream event in the regulation of caspase-3 activity. Furthermore, it has been shown that inhibition of the active forms of both JNK1 and JNK2 prevents cytochrome *c* release from the mitochondria and activation of enzymes upstream of caspase-3 (Bozyczko-Coyne *et al.*, 2001). This study provides evidence of a requirement for both JNK1 and JNK2 in the THC-induced activation of caspase-3 and DNA fragmentation, and may reflect cooperativity between JNK1 and JNK2 in relation to these aspects of the cell death cascade.

To date, little is known about the role of JNK in THC signalling. Rueda *et al.* (2000) have found that JNK1/2 are activated within 5 min of THC treatment and that sustained JNK activation over 3 days of THC insult is required to induce cell death in glioma cells. This suggests that the duration of JNK induction may be the determining factor in the cell death/survival decision. These differences may reflect differential cellular responses of neuronal populations to THC, with cortical neurons being susceptible to early insult of cannabinoid exposure due to the differential activation of the JNK1/2 signalling cascades. We are aware that in the same study of Rueda *et al.* (2000), rat cortical primary neurons were not susceptible to a 3-day exposure to THC, which may reflect the lower dose of THC used in that study. It has recently been found that the endogenous cannabinoid, anandamide, induces apoptosis in PC12, and this is accompanied by the activation of the JNK pathway (Sarker *et al.*, 2003). Furthermore, JNK activity is not affected by THC in hippocampal slices prepared from the adult rat brain (Derkinderen *et al.*, 2001). Thus, the effects of cannabinoids may be dependent on neuronal maturity, with neonatal cultures being susceptible to JNK activation following cannabinoid challenge.

The dose of THC used in the present study to induce the activation of JNK1 and JNK2 was within the concentration range we have previously shown to be neurotoxic to cultured cortical neurons (Campbell, 2001) and is also consistent with the human plasma concentrations of THC (low μM; Chiang & Barnett, 1984). Furthermore, the data demonstrate that THC is toxic for cortical cultures obtained from neonatal rats. Interestingly to date, there is no evidence to suggest that THC is neurotoxic in the adult rat central nervous system (Galve-Roperh *et al.*, 2000). Our findings support the proposal that the apoptotic effects of THC may be operative early during development and may play a modulatory role in neural development (Fernandez-Ruiz *et al.*, 1999). Indeed the consumption of marijuana by women during pregnancy and/or lactation has been shown to affect the neurobehavioural development of their children (Fried, 1995).

In summary, treatment of cortical cultures with THC activates the JNK pathway *via* the CB_1 cannabinoid receptor. An antisense approach revealed that JNK1 and JNK2 are required for the THC-induced activation of caspase-3 and DNA fragmentation in cortical neurons. These findings identify a cannabinoid receptor-dependent transduction pathway associated with THC-induced neurotoxicity.

This study was supported by the Health Research Board Ireland and Enterprise Ireland.

References

ABOOD, M.E. & MARTIN, B.R. (1992). Neurobiology of marijuana abuse. *Trends Pharmacol. Sci.*, **13**, 201–206.

ABOOD, M.E., RIZVI, G., SALLAPUDI, N. & MCALLISTER, S. (2001). Activation of the CB_1 cannabinoid receptor protects cultured mouse spinal neurons against excitotoxicity. *Neurosci. Lett.*, **309**, 197–201.

BOUABOULA, M., POINOT-CHAZEL, C., BOURRIE, B., CANAT, X., CALANDRA, B., RINALDI-CARMONA, M., LE FUR, G. & CASELLAS, P. (1995). Activation of mitogen-activated protein kinases by stimulation of the central cannabinoid receptor CB_1. *Biochem. J.*, **312**, 637–641.

BOUABOULA, M., POINOT-CHAZEL, C., MARCHAND, J., CANAT, X., BOURRIE, B., RINALDI-CARMONA, M., CALANDRA, B., LE FUR, G. & CASELLAS, P. (1996). Signaling pathway associated with stimulation of CB_2 peripheral cannabinoid receptor: involvement of both mitogen-activated protein kinase and induction of Krox-24 expression. *Eur. J. Biochem.*, **237**, 704–711.

BOZYCZKO-COYNE, D., O'KANE, T.M., WU, Z.L., DOBRZANSKI, P., MURTHY, S., VAUGHT, J.L. & SCOTT, R.W. (2001). CEP-1347/KT-7515, an inhibitor of SAPK/JNK pathway activation, promotes survival and blocks multiple events associated with Aβ-induced cortical neuron apoptosis. *J. Neurochem.*, **77**, 849–863.

BUSCHMANN, T., POTAPOVA, O., BAR-SHIRA, A., IVANOV, V.L., FUCHS, S.Y., HENDERSEN, S., FRIED, V.A., MINAMOTO, T., ALARCON-VARGAS, D., PINCUS, M.R., GAARDE, W.A., HOLBROOKE, N.J., SHILOH, Y. & RONAI, Z. (2001). Jun NH_2-terminal kinase phophorylation of p53 on thr-81 is important for p53 stabilization and transcriptional activities in response to stress. *Mol. Cell. Biol.*, **21**, 2743–2754.

CAMPBELL, V.A. (2001). Tetrahydrocannabinol-induced apoptosis in cultured cortical neurones is associated with cytochrome *c* release and caspase-3 activation. *Neuropharmacology*, **40**, 702–709.

CARBONI, L., CARLETTI, R., TACCONI, S., CORTI, C. & FERRAGUTI, F. (1998). Differential expression of SAPK isoforms in the rat brain. An *in situ* hybridisation study in the adult rat brain and during post-natal development. *Mol. Brain Res.*, **60**, 57–68.

CHAN, G.C., HINDS, T.R., IMPEY, S. & STORM, D.R. (1998). Hippocampal neurotoxicity of Δ^9-tetrahydrocannabinol. *J. Neurosci.*, **18**, 5322–5332.

CHIANG, C.W. & BARNETT, G. (1984). Marijuana effect and delta-9-tetrahydrocannabinol plasma level. *Clin. Pharmacol. Ther.*, **36**, 234–238.

COSO, O.A., TERAMOTO, H., SIMONDS, W.F. & GUTKIND, J.S. (1996). Signaling from G protein-coupled receptors to c-Jun kinase involves $\beta\gamma$ subunits of heterotrimeric G proteins acting on a Ras and Racl-dependent pathway. *J. Biol. Chem.*, **271**, 3963–3966.

DERKINDEREN, P., ENSLEN, H. & GIRAULT, J.-A. (1999). The ERK/MAP-kinases cascade in the nervous system. *Neuroreport*, **10**, R24–R34.

DERKINDEREN, P., LEDENT, C., PARMENTIER, M. & GIRAULT, J.-A. (2001). Cannabinoids activate p38 mitogen-activated protein kinases through CB_1 receptors in hippocampus. *J. Neurochem.*, **77**, 957–960.

DEVANE, W.A., HANUS, L., BREUER, A., PERTWEE, R.G., STEVENSON, L.A., GRIFF, C., GIBSON, D., MANDELBAUM, A., ETINGER, A. & MECHOULAM, R. (1992). Isolation and structure of a brain constituent that binds to the cannabinoid receptor. *Science*, **258**, 1946–1949.

DILL, J.A. & HOWLETT, A.C. (1988). Regulation of adenylate cyclase by chronic exposure to cannabimimetic drugs. *J. Pharmacol. Exp. Ther.*, **244**, 1157–1163.

DOWNER, E., BOLAND, B., FOGARTY, M. & CAMPBELL, V. (2001). Δ^9-Tetrahydrocannabinol induces the apoptotic pathway in cultured cortical neurones via activation of the CB1 receptor. *Neuroreport*, **12**, 3973–3978.

FARKAS, I., BARANYI, L., TAKAHASHI, M., FUKUDA, A., LIPOSITS, Zs., YAMAMOTO, T. & OKADA, H. (1998). A neuronal C5a receptor and an associated apoptotic signal transduction pathway. *J. Physiol.*, **507**, 679–687.

FERNANDEZ-RUIZ, J.J., BERRENDERO, F., HERNANDEZ, M.L., ROMERO, J. & RAMOS, J.A. (1999). Role of endocannabinoids in brain development. *Life Sci.*, **65**, 725–736.

FRIED, P.A. (1995). The Ottawa Prenatal Prospective Study (OPPS): methodological issues and findings – Its easy to throw the baby out with the bath water. *Life Sci.*, **56**, 2159–2168.

GALVE-ROPERH, I., SANCHEZ, C., LUISA CORTES, M., GOMEZ DEL PULGAR, T., IZQUIERDO, M. & GUZMAN, M. (2000). Anti-tumoral action of cannabinoids: involvement of sustained ceramide accumulation and extracellular signal-regulated kinase activation. *Nat. Med.*, **6**, 313–319.

GESSA, G.L., CASU, M.A., CARTA, G. & MASCIA, M.S. (1998). Cannabinoids decrease acetylcholine release in the medial-prefrontal cortex and hippocampus, reversal by SR 141716A. *Eur. J. Pharmacol.*, **355**, 119–124.

GHAHREMANI, M.H., KERAMARIS, E., SHREE, T., XIA, Z., DAVIS, R.J., FLAVELL, R., SLACK, R.S. & PARK, D.S. (2002). Interaction of the c-Jun/JNK pathway and cyclin-dependent kinase in death of embryonic cortical neurones evoked by DNA damage. *J. Biol. Chem.*, **277**, 35586–35596.

GOMEZ DEL PULGAR, T., VELASCO, G. & GUZMAN, M. (2000). The CB_1 cannabinoid receptor is coupled to the activation of protein kinase B/Akt. *Biochem. J.*, **347**, 369–373.

GUPTA, S., BARRETT, T., WHITMARSH, A.J., CAVANAGH, J., SLUSS, H.K., DERIJARD, B. & DAVIS, R.J. (1996). Selective interaction of JNK protein kinase isoforms with transcription factors. *EMBO J.*, **15**, 2760–2770.

HAMPSON, A.J., GRIMALDI, M., AXELROD, J. & WINK, D. (1998). Cannabidiol and (−)Δ^9-tetrahydrocannabinol are neuroprotective antioxidants. *Proc. Natl. Acad. Sci. U.S.A.*, **95**, 8268–8273.

HATAI, T., MATSUZAWAI, A., INOSHITA, S., MOCHHIDA, Y., KURODA, T., SAKAMAKI, K., KUIDA, K., YONEHARA, S., ICHIJO, H. & TAKEDA, K. (2000). Execution of Apoptosis Signal-regulating Kinase 1 (ASK1)-induced apoptosis by mitochondria-dependent caspase activation. *J. Biol. Chem.*, **275**, 26576–26581.

HOCHEDLINGER, K., WAGNER, E.F. & SABAPATHY, K. (2002). Differential effects of JNK1 and JNK2 on signal specific induction of apoptosis. *Oncogene*, **21**, 2441–2445.

HOWLETT, A.C. (1990). Reverse pharmacology of the cannabinoid receptor. *Trends Pharmacol. Sci.*, **11**, 395–397.

HOWLETT, A.C. (1995). Pharmacology of cannabinoid receptors. *Annu. Rev. Pharmacol. Toxicol.*, **35**, 607–634.

HRENIUK, D., GARAY, M., GAARDE, W., MONIA, B.P., MCKAY, R.A. & CIOFFI, C.L. (2001). Inhibition of c-Jun N-terminal kinase 1, but not c-Jun N-terminal kinase 2, suppresses apoptosis induced by ischemia/reoxygenation in rat cardiac myocytes. *Mol. Pharmacol.*, **59**, 867–874.

IP, Y.T. & DAVIS, R.J. (1998). Signal transduction by the c-Jun N-terminal kinase (JNK) – from inflammation to development. *Curr. Opin. Cell Biol.*, **10**, 205–219.

JAKOB, R. & KREIGLSTEN, J. (1997). Influence of flupirtine on a G-protein coupled inwardly rectifying potassium current in hippocampal neurones. *Br. J. Pharmacol.*, **122**, 1333–1338.

JANICKE, R.U., SPRENGART, M.L., WATU, M.R. & PORTER, A.G. (1998). Caspase-3 is required for DNA fragmentation and morphological changes associated with apoptosis. *J. Biol. Chem.*, **273**, 9357–9360.

JENTSCH, J.D., VERRICO, C.D., LE, D. & ROTH, R.H. (1998). Repeated exposure to Δ^9-tetrahydrocannabinol reduces prefrontal cortical dopamine metabolism in the rat. *Neurosci. Lett.*, **246**, 169–172.

JOHNSON, N.L., GARDNER, A.M., DIENER, K.M., LANGE-CARTER, C.A., GLEAVY, J., JARPE, M.B., MINDEN, A., KARIN, M., ZON, L.I. & JOHNSON, G.L. (1996). Signal transduction pathways regulated by mitogen-activated/extracellular response kinase kinase kinase induce cell death. *J. Biol. Chem.*, **271**, 3229–3237.

KANG, C.-D., JANG, J.-H., KIM, K.-W., LEE, H.-J., JEONG, C.-S., KIM, C.-M., KIM, S.-H. & CHUNG, B.-S. (1998). Activation of c-Jun N-terminal kinase/stress-activated protein kinase and the decreased ratio of Bcl-2 to Bax are associated with the auto-oxidized dopamine-induced apoptosis in PC12 cells. *Neurosci. Lett.*, **256**, 37–40.

LEI, K., NIMUAL, A., ZONG, W.X., KENNEDY, N.J., FLAVELL, R.A., THOMPSON, C.B., BAR-SAGI, D. & DAVIS, R.J. (2002). The Bax subfamily of Bcl2-related proteins is essential for apoptotic signal transduction by c-Jun NH(2)-terminal kinase. *Mol. Cell. Biol.*, **22**, 4929–4942.

MACKIE, K., LAI, Y., WESTENBROEK, R. & MITCHELL, R. (1995). Cannabinoids activate an inwardly rectifying potassium conductance and inhibit Q-type currents in AtT20 cells transfected with rat brain cannabinoid receptor. *J. Neurosci.*, **15**, 6552–6561.

MARSHALL, C.J. (1995). Specificity of receptor protein kinase signaling: transient versus sustained extracellular signal-regulated kinase activation. *Cell*, **80**, 179–185.

MATSUDA, L.A., LOIAIT, S.J., BROWNSTEIN, M.J., YOUNG, A.C. & BONNER, T.I. (1990). Structure of a cannabinoid receptor and functional expression of the cloned cDNA. *Nature*, **346**, 561–564.

MIELKE, K. & HERDEGEN, T. (2000). JNK and p38 stress kinases – degenerative effectors of signal-transduction-cascades in the nervous system. *Prog. Neurobiol.*, **61**, 46–60.

MUNRO, S., THOMAS, K.L. & ABU-SHAAR, M. (1993). Molecular characterization of a peripheral receptor for cannabinoids. *Nature*, **365**, 61–65.

NAGAYAMA, T., SINOR, A.D., SIMON, R.P., CHEN, J., GRAHAM, S.H., JIN, K. & GREENBER, D.A. (1999). Cannabinoids and neuroprotection in global and focal cerebral ischemia and in neuronal cultures. *J. Neurosci.*, **19**, 2987–2995.

NEW, D.C. & WONG, Y.H. (2003). BML-190 and AM251 act as inverse agonists at the human cannabinoid CB2 receptor: signalling *via* camp and inositol phosphate. *FEBS Lett.*, **536**, 157–160.

OZAKI, I., TANI, E., IKEMOTO, H., KITAGAWA, H. & FUJIKAWA, H. (1999). Activation of stress-activated protein kinase/c-Jun NH_2-terminal kinase and p38 kinase in calphostin c-induced apoptosis requires caspase-3-like proteases but is dispensable for cell death. *J. Biol. Chem.*, **274**, 5310–5317.

PANIKASHVILI, D., SIMEONIDOU, C., BEN-SHABAT, S., HANUS, L., BREUER, A., MECHOULAM, R. & SHOHAMI, E. (2001). An endogenous cannabinoid (2-AG) is neuroprotective after brain injury. *Nature*, **413**, 527–531.

RUEDA, D., GALVE-ROPERH, I., HARO, A. & GUZMAN, M. (2000). The CB_1 cannabinoid receptor is coupled to the activation of c-Jun N-terminal kinase. *Mol. Pharmacol.*, **58**, 814–820.

SANCHEZ, C., GALVE-ROPERH, I., CANOVA, C., BRACHET, P. & GUZMAN, M. (1998). Δ^9-Tetrahydrocannabinol induces apoptosis in C6 glioma cells. *FEBS Lett.*, **436**, 6–10.

SARKER, K.P., BISWAS, K.K., YAMAKUCHI, M., LEE, K.-Y., HAHIGUCHI, T., KRACHT, M., KITAJIMA, I. & MARUYAMA, I. (2003). ASK1-p38 MAPK/JNK signaling cascade mediates anandamide-induced PC 12 cell death. *J. Neurochem.*, **85**, 50–61.

SCHWARZ, H., BLANCO, F.J. & LOTZ, M. (1994). Anandamide, an endogenous cannabinoid receptor agonist inhibits lymphocytes proliferation and induces apoptosis. *J. Neuroimmunol.*, **55**, 107–115.

SHEN, M., PISER, T.M., SEYBOLD, V.S. & THAYER, S.A. (1996). Cannabinoid receptor agonists inhibit glutamatergic synaptic transmission in rat hippocampal cultures. *J. Neurosci.*, **16**, 4322–4334.

SHEN, M. & THAYER, S.A. (1998). Cannabinoid receptor agonists protect cultured rat hippocampal neurons from excitotoxicity. *Mol. Pharmacol.*, **54**, 459–462.

TOURNIER, C., HESS, P., YANG, D.D., XU, J., TURNER, T.K., NIMUAL, A., BAR-SAGI, D., JONES, S.N., FLAVELL, R.A. & DAVIS, R.J. (2000). Requirement of JNK for stress-induced activation of the cytochrome *c*-mediated death pathway. *Science*, **288**, 870–873.

TSOU, K., BROWN, S., SANUDO-PENA, M.C., MACKIE, K. & WALKER, J.M. (1998). Immunohistochemical distribution of cannabinoid CB_1 receptors in the rat central nervous system. *Neuroscience*, **83**, 393–411.

TURKANIS, S.A., PARTLOW, L.M. & KARLER, R. (1991). Delta-9-tetrahydrocannabinol depresses inward sodium current in mouse neuroblastoma cells. *Neuropharmacology*, **30**, 73–77.

TWITCHELL, W., BROWN, S. & MACKIE, K. (1997). Cannabinoids inhibit N- and P/Q-type calcium channels in cultured rat hippocampal neurons. *J. Neurophysiol.*, **78**, 43–50.

VAN DER STELT, M., VELDHEIS, W.B., BAR, P.R., VELDINK, G.A., VLIEGENTHART, J.F.G. & NICOLAY, K. (2001). Neuroprotection by Δ^9-tetrahydrocannabinol, the main active compound in marijuana, against ouabain-induced *in vivo* excitotoxicity. *J. Neurosci.*, **21**, 6475–6479.

VIRDIE, K., BANNISTER, A.J., HUNT, S.P. & TOLKOVSKL, A.M. (1997). Comparison between the timing of JNK activation, c-Jun phosphorylation, and the onset of death commitment in sympathetic neurones. *J. Neurochem.*, **66**, 550–561.

XIA, Z., DICKENS, M., RAINGEAUD, J., DAVIS, R.J. & GREENBERG, M.E. (1995). Opposing effects of ERK and JNK-p38 MAP kinases on apoptosis. *Science*, **270**, 1326–1331.

ZOU, H., HENZEL, W.J., LIU, X., LUTSCHG, A. & WANG, X. (1997). Apaf-1, a human protein homologous *C. elegans* CED-4, participates in cytochrome *c*-dependent activation of caspase-3. *Cell*, **90**, 405–413.

(Received May 8, 2003
Revised July 10, 2003
Accepted July 21, 2003)

THE JOURNAL OF BIOLOGICAL CHEMISTRY
Vol. 277, No. 37, Issue of September 13, pp. 34239–34246, 2002
Printed in U.S.A.

Apoptotic Changes in the Aged Brain Are Triggered by Interleukin-1β-induced Activation of p38 and Reversed by Treatment with Eicosapentaenoic Acid*

Received for publication, May 29, 2002, and in revised form, June 27, 2002
Published, JBC Papers in Press, June 28, 2002, DOI 10.1074/jbc.M205289200

Darren S. D. Martin, Peter E. Lonergan, Barry Boland, Marie P. Fogarty, Marcella Brady, David F. Horrobin‡, Veronica A. Campbell, and Marina A. Lynch§

From the Department of Physiology, Trinity College Institute of Neuroscience, Trinity College, Dublin 2, Ireland and ‡Laxdale Research Ltd., Stirling FK7 9JQ, Scotland, United Kingdom

Among the several changes that occur in the aged brain is an increase in the concentration of the proinflammatory cytokine interleukin-1β that is coupled with a deterioration in cell function. This study investigated the possibility that treatment with the polyunsaturated fatty acid eicosapentaenoic acid might prevent interleukin-1β-induced deterioration in neuronal function. Assessment of four markers of apoptotic cell death, cytochrome *c* translocation, caspase-3 activation, poly(ADP-ribose) polymerase cleavage, and terminal dUTP nick-end staining, revealed an age-related increase in each of these measures, and the evidence presented indicates that treatment of aged rats with eicosapentaenoate reversed these changes as well as the accompanying increases in interleukin-1β concentration and p38 activation. The data are consistent with the idea that activation of p38 plays a significant role in inducing the changes described since interleukin-1β-induced activation of cytochrome *c* translocation and caspase-3 activation in cortical tissue *in vitro* were reversed by the p38 inhibitor SB203580. The age-related increases in interleukin-1β concentration and p38 activation in cortex were mirrored by similar changes in hippocampus. These changes were coupled with an age-related deficit in long term potentiation in perforant path-granule cell synapses, while eicosapentaenoate treatment was associated with reversal of age-related changes in interleukin-1β and p38 and with restoration of long term potentiation.

Increased expression of the proinflammatory cytokine interleukin-1β (IL-1β)[1] has been linked with neurodegenerative disorders like Down's syndrome, Alzheimer's disease, and Parkinson's disease (1, 2). Consistent with the view that IL-1β plays a role in deterioration of cell function are the findings that IL-1β expression is increased, in parallel with cell damage, in experimental models of ischemia (3), excitotoxicity (4), and traumatic lesions (5). Indeed, IL-1β has been shown to trigger cell death in primary cultures of human fetal neurons (6) and inhibition of caspase-1, which leads to formation of active IL-1β, and blocks lipopolysaccharide-induced changes in cell morphology, which are consistent with cell death (7).

IL-1β has been shown to stimulate the mitogen-activated protein kinases p38 and c-Jun NH_2-terminal kinase (8, 9), and activation of both c-Jun NH_2-terminal kinase (10, 11) and p38 (10, 12–16) has been closely linked with apoptotic cell death. Significantly, an increase in p38 activity has been coupled with apoptotic changes in Alzheimer's disease (17, 18). Concomitant increases in IL-1β concentration and p38 activity have been reported in the aged rat brain (19–21); in hippocampus these changes are correlated with compromised synaptic function and with an age-related impairment in long term potentiation (LTP) (19–22), while consistent with the high expression of IL-1β and IL-1RI in hippocampus is the finding that the cytokine depresses LTP in dentate gyrus (8, 19, 20, 23, 24). Significantly, we have recently reported that the age-related increases in IL-1β concentration and c-Jun NH_2-terminal kinase activity, as well as the decrease in LTP, are reversed by treatment with the *n*-3 polyunsaturated fatty acid docosahexaenoic acid (22).

In this study we have attempted to identify the downstream consequences of the coupled age-related increases in IL-1β concentration and p38 activation in neuronal tissue. In particular, we have focused on assessing whether these changes might trigger apoptotic changes in neuronal tissue as it does in other tissues and have analyzed the effect of the ethyl ester of the ω-3 fatty acid eicosapentaenoic acid (EPA) on age-related changes in cortex and hippocampus. The data indicate that dietary manipulation reversed several changes in the aged cortex that are indicative of apoptotic cell death as well as age-related changes in IL-1β concentration, p38 activation, and LTP in hippocampus.

EXPERIMENTAL PROCEDURES

Animals—Groups of young and aged male Wistar rats (300–350 g), maintained at an ambient temperature of 22–23 °C under a 12-h light-dark schedule, were subdivided into those that were fed on a diet enriched in eicosapentaenoic acid (ethyl eicosapentaenoate, 10 mg/rat/day for 3 weeks and 20 mg/rat/day for 5 weeks; Laxdale Research Ltd.) or standard laboratory chow for 8 weeks. Daily food intake was assessed for 2 weeks prior to commencement of the treatment: mean values (±S.E.) were 21.25 ± 1.4 and 18.55 ± 0.6 g/day for 4- and 22-month-old rats, respectively. At this time the mean body weights of young rats assigned to control and experimental groups were 265.6 ± 9.1 and 250.2 ± 11.7 g, respectively; corresponding values in aged rats were 483.6 ± 9.8 and 481.2 ± 7.9 g, respectively. Diet was prepared fresh each day, and rats were offered 100% of their daily intake. Mean daily food intake in all groups remained unchanged throughout the 8-week treatment period, and at the end of this time mean body weights of

* This work was supported by the Health Research Board (to M. F.) and Enterprise Ireland (to B. B.). The costs of publication of this article were defrayed in part by the payment of page charges. This article must therefore be hereby marked "*advertisement*" in accordance with 18 U.S.C. Section 1734 solely to indicate this fact.

§ To whom correspondence should be addressed. Tel.: 353-1-608-1770; Fax: 353-1-679-3545; E-mail: lynchma@tcd.ie.

[1] The abbreviations used are: IL-1β, interleukin-1β; PARP, poly(ADP-ribose) polymerase; TUNEL, terminal dUTP nick-end labeling; LTP, long term potentiation; IL-1RI, type I IL-1 receptor; IL-1ra, IL-1R antagonist; EPA, eicosapentaenoic acid; PBS, phosphate-buffered saline; AFC, 7-amino-4-trifluoromethyl coumarin; ANOVA, analysis of variance.

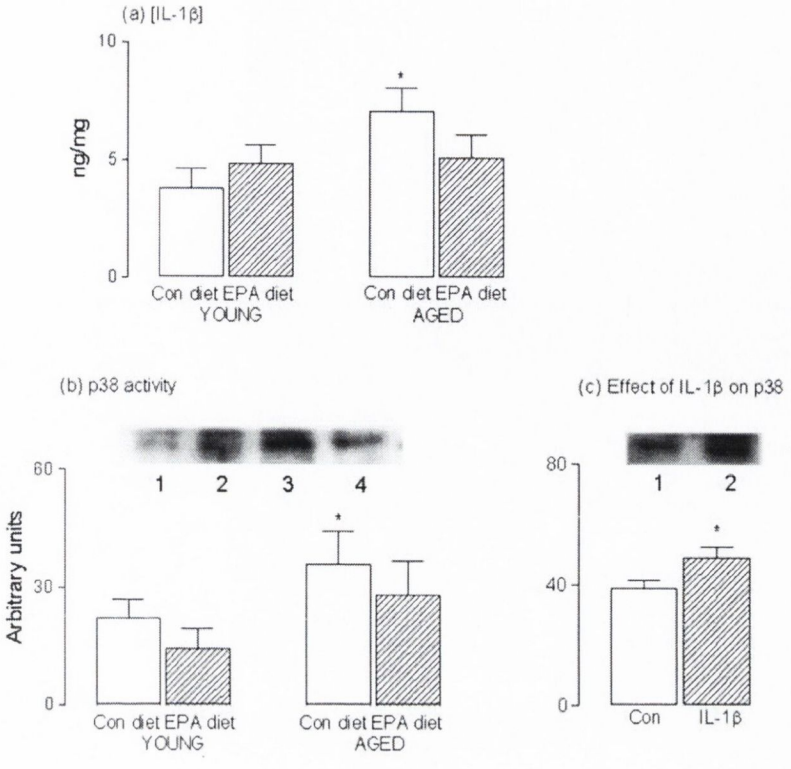

FIG. 1. **The age-related increases in IL-1β concentration and p38 activity in cortex are abolished by EPA.** *a*, IL-1β concentration was significantly enhanced in cortical tissue prepared from aged rats fed on the control diet ($n = 10$) compared with young rats fed on either diet (*, $p < 0.05$, ANOVA; $n = 6$), but this change was not evident in tissue prepared from aged rats fed on the EPA-enriched diet ($n = 10$). *b*, p38 activity was significantly enhanced in cortical tissue prepared from aged rats fed on the control diet (*lane 3*) compared with young rats fed on either control (*lane 1*) or EPA (*lane 2*) diet (*, $p < 0.05$, ANOVA), but this change was not evident in tissue prepared from aged rats fed on the EPA-enriched diet (*lane 4*). *c*, IL-1β (*lane 2*) significantly enhanced p38 activity in cortical tissue *in vitro* (*, $p < 0.05$, Student's *t* test for paired values; $n = 6$). *Con*, control.

young rats assigned to control and experimental groups were 366.4 ± 13.4 and 354.5 ± 19.4 g, respectively; corresponding values in aged rats were 473.7 ± 11.4 and 462.9 ± 6.3 g, respectively. At this time rats were 4 and 22 months old. Rats were maintained under veterinary supervision for the duration of this experiment.

Induction of LTP in Perforant Path-Granule Cell Synapses in Vivo—At the end of the 8-week treatment, LTP was induced as described previously (19). Rats were anesthetized by intraperitoneal injection of urethane (1.5g/kg), recording and stimulating electrodes were placed in the molecular layer of the dentate gyrus (2.5 mm lateral and 3.9 mm posterior to bregma) and perforant path, respectively (angular bundle, 4.4 mm lateral to lambda), and stable baseline recordings were made before electrophysiological recording at test shock frequency (1/30 s) commenced for 10 min before and 40 min after tetanic stimulation (three trains of stimuli; 250 Hz for 200 ms; intertrain interval, 30 s). Rats were then killed by decapitation, and the hippocampus and cortex were removed, cross-chopped into slices (350 × 350 μm), and frozen separately in 1 ml of Krebs' solution (136 mM NaCl, 2.54 mM KCl, 1.18 mM KH_2PO_4, 1.18 mM $MgSO_4{\cdot}7H_2O$, 16 mM $NaHCO_3$, 10 mM glucose, 1.13 mM $CaCl_2$) containing 10% dimethyl sulfoxide (22). For analysis, thawed slices were rinsed three times in fresh buffer and used as described below.

Analysis of IL-1β Concentration—IL-1β concentration was analyzed in homogenate prepared from cortex and hippocampus by enzyme-linked immunosorbent assay (R&D Systems). Antibody-coated (100 μl; 1.0 μg/ml final concentration diluted in phosphate-buffered saline (PBS), pH 7.3; goat anti-rat IL-1β antibody) 96-well plates were incubated overnight at room temperature, washed several times with PBS containing 0.05% Tween 20, blocked for 1 h at room temperature with 300 μl of blocking buffer (PBS, pH 7.3 containing 5% sucrose, 1% bovine serum albumin, and 0.05% NaN_3), and washed. IL-1β standards (100 μl; 0–1,000 pg/ml in PBS containing 1% bovine serum albumin) or samples (homogenized in Krebs' solution containing 2 mM $CaCl_2$) were added, and incubation proceeded for 2 h at room temperature. Secondary antibody (100 μl; final concentration, 350 ng/ml in PBS containing 1% bovine serum albumin and 2% normal goat serum; biotinylated goat anti-rat IL-1β antibody) was added and incubated for 2 h at room temperature. Wells were washed, detection agent (100 μl; horseradish peroxidase-conjugated streptavidin; 1:200 dilution in PBS containing 1% bovine serum albumin) was added, and incubation continued for 20 min at room temperature. Substrate solution (100 μl; 1:1 mixture of H_2O_2 and tetramethylbenzidine) was added and incubated at room temperature in the dark for 1 h after which time the reaction was stopped using 50 μl of 1 M H_2SO_4. Absorbance was read at 450 nm, and values were corrected for protein (25) and expressed as pg of IL-1β/mg of protein.

Analysis of p38 Phosphorylation, Cytochrome c Translocation, and PARP Cleavage—p38 phosphorylation was analyzed in samples of homogenate prepared from hippocampus and cortex; cytosolic cytochrome *c* and expression of 116-kDa PARP were analyzed in cortical tissue. p38 activity was also assessed in freshly prepared hippocampal and cortical tissue that was incubated for 20 min in the absence or presence of IL-1β (3.5 ng/ml), while cytochrome *c* translocation was assessed *in vitro* following incubation of slices of cortex with IL-1β (3.5 ng/ml) in the presence or absence of IL-1ra (350 ng/ml) or SB203580 (50 μM). For analysis of p38 in all experiments and also for PARP, homogenate was diluted to equalize for protein concentration, and aliquots (10 μl, 1 mg/ml) were added to 10 μl of sample buffer (0.5 mM Tris-HCl, pH 6.8, 10% glycerol, 10% SDS, 5% β-mercaptoethanol, 0.05% (w/v) bromphenol blue), boiled for 5 min, and loaded onto 10% SDS gels. In the case of cytochrome *c*, cytosolic fractions were prepared by homogenizing slices of cortex in lysis buffer (20 mM HEPES, pH 7.4, 10 mM KCl, 1.5 mM $MgCl_2$, 1 mM EGTA, 1 mM EDTA, 1 mM dithiothreitol, 0.1 mM phenylmethylsulfonyl fluoride, 5 μg/ml pepstatin A, 2 μg/ml leupeptin, 2 μg/ml aprotinin), incubating for 20 min on ice, and centrifuging (15,000 × *g* for 10 min at 4 °C). The supernatant (*i.e.* cytosolic fraction) was suspended in sample buffer (150 mM Tris-HCl, pH 6.8, 10% (v/v) glycerol, 4% (w/v) SDS, 5% (v/v) β-mercaptoethanol, 0.002% (w/v) bromphenol blue) to a final concentration of 300 μg/ml, boiled for 3 min, and loaded (6 μg/lane) onto 12% gels. In all cases proteins were separated by application of 30 mA constant current for 25–30 min, transferred onto nitrocellulose strips (225 mA for 75 min), and immunoblotted with the appropriate primary and secondary antibodies. In the case of p38, anti-phospho-p38 (Santa Cruz Biotechnology; 1:500 in phosphate-buffered saline-Tween (0.1% Tween 20) containing 2% nonfat dried milk) and peroxidase-linked anti-mouse IgM (1:1,000; Amersham Biosciences) were used. In the case of PARP, we immunoblotted with an antibody (1:2,000) raised against the epitope corresponding to amino acids 764–1014 of poly-(ADP-ribose) polymerase of human origin (Santa Cruz Biotechnology), and immunoreactive bands were detected using peroxidase-conjugated anti-rabbit IgG (Sigma) and ECL (Amersham Biosciences). To assess cytochrome *c*, a rabbit polyclonal antibody raised against recombinant protein corresponding to amino acids 1–104 of cytochrome *c* (Santa Cruz Biotechnology) was used. In addition to loading equal amounts of protein, some blots were reprobed for analysis of total (rather than phosphorylated) p38, and in other cases blots were probed with an anti-actin

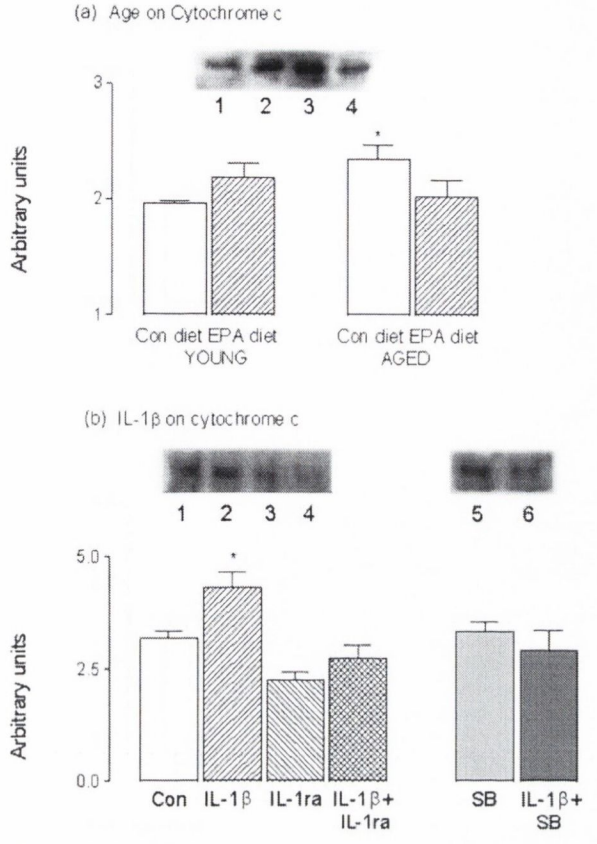

FIG. 2. **The age-related increase in cytochrome *c* translocation is abolished by EPA and mimicked by IL-1β.** *a*, cytochrome *c* translocation was significantly enhanced in cortical tissue prepared from aged rats fed on the control diet compared with young rats fed on control diet (*, $p < 0.05$, ANOVA; compare *lane 3* with *lane 1*), but this change was not evident in tissue prepared from aged rats fed on the EPA-enriched diet (*lane 4*). *b*, incubation of cortical tissue in the presence of IL-1β (*lane 2*) significantly increased cytochrome *c* translocation (*, $p < 0.05$, ANOVA), but this effect was inhibited by IL-1ra (*lane 4*) and by SB203580 (*lane 6*); neither IL-1ra (*lane 3*) nor SB203580 (*lane 5*) affected cytochrome *c* translocation ($n = 6$ in each group). *Con*, control; *SB*, SB203580.

antibody to confirm equal loading. Data from these experiments showed no differences between treatment groups. In all experiments, immunoreactive bands were detected using peroxidase-conjugated anti-rabbit antibody (Sigma) and ECL (Amersham Biosciences). Quantification of protein bands was achieved by densitometric analysis using two software packages, Grab It (Grab It Annotating Grabber, Version 2.04.7, Synotics, UVP Ltd.) and Gelworks (Gelworks ID, Version 2.51, UVP Ltd.) for photography and densitometry, respectively.

Analysis of Caspase-3 Activity—Slices of cortical tissue prepared from young and aged rats were washed, homogenized in lysis buffer (400 μl; 25 mM HEPES, 5 mM $MgCl_2$, 5 mM dithiothreitol, 5 mM EDTA, 2 mM phenylmethylsulfonyl fluoride, 10 μg/ml leupeptin, 10 μg/ml pepstatin, pH 7.4), incubated on ice for 20 min, analyzed for protein concentration, and diluted to equalize for protein concentration. In some experiments, slices prepared from control young rats were incubated for 60 min at 37 °C in the presence or absence of IL-1β (3.5 ng/ml) to which IL-1ra (350 ng/ml) or SB203580 (50 μM) was added; these samples were treated as described above. All samples (98 μl) were added to 2 μl of caspase-3 substrate (Ac-DEVD-AFC peptide, Alexis Corp.; 5 μM), transferred to a 96-well plate, and incubated for 1 h at 37 °C. Fluorescence was assessed (excitation, 390 nm; emission, 510 nm), and enzyme activity was calculated with reference to a standard curve of AFC (0–10 μM) concentration *versus* absorbance.

Analysis of Caspase-3 mRNA—Total RNA was extracted from cortical neurons (26) using TRI reagent (Sigma). cDNA synthesis was performed on 1 μg of total RNA using oligo(dT) primer (Superscript reverse transcriptase, Invitrogen). Equal amounts of cDNA were used for PCR amplification for a total of 30 cycles at 94 °C for 1 min and 58 °C for 2 min. A final extension step was carried out at 70 °C for 10 min. Multiplex PCR was performed using the Quantitative PCR Cytopress Detection kit (Rat Apoptosis Set 2; BioSource International, Camarillo, CA) generating caspase-3 PCR products of 320 bp and glyceraldehyde-3-phosphate dehydrogenase PCR products of 532 bp. The PCR products were analyzed by electrophoresis on 2% agarose gels, photographed, and quantified using densitometry. Expression of glyceraldehyde-3-phosphate dehydrogenase mRNA was used as a standard to quantify the relative expression of caspase-3 mRNA.

Preparation of Dissociated Cells and Colocalization of p38 and Caspase-3—Cortical slices (350 × 350 μm) were incubated at 37 °C for 30 min in HEPES-buffered Krebs' solution (145 mM NaCl, 5 mM KCl, 1 mM $MgCl_2$, 2 mM $CaCl_2$, 1 mM Mg_2SO_4, 1 mM KH_2PO_4, 10 mM glucose, 30 mM HEPES at pH 7.4) containing trypsin (1 mg/ml), DNase (1,600 kilounits/liter), protease X (1 mg/ml), and protease XIV (1 mg/ml). Slices were washed, triturated, and passed through a nylon mesh filter. Cells were centrifuged (1,000 rpm for 1 min), resuspended in HEPES-buffered Krebs' solution, plated onto coverslips, fixed in 4% paraformaldehyde in PBS (w/v) for 30 min, and permeabilized in 0.1% Triton in PBS (v/v) for 15 min. Cells were incubated in normal goat serum in PBS (v/v) to block nonspecific binding, treated with anti-phosphospecific p38 antibody (1:100; Santa Cruz Biotechnology) or anti-caspase-3 (1:500; BioSource), and incubated overnight at 4 °C. Cells were washed and incubated in the dark for 2 h in either fluorescein isothiocyanate-labeled goat anti-mouse IgG and IgM (1:100; BioSource) or R-phycoerythrin-labeled goat anti-rabbit IgG (1:100; BioSource) to visualize labeling with p38 and caspase-3, respectively. Following a further wash, slides were mounted using 2 mg/ml *p*-phenylenediamine in 50% glycerol in PBS (v/v) and sealed. Fluorescence was analyzed using the Bio-Rad MRC-1024 laser scanning confocal imaging system in which the fluorochromes were excited by laser light emitted at 565 and 494 nm and detected at 578 and 520 nm, which measured bound R-phycoerythrin and fluorescein isothiocyanate, respectively. Cells were analyzed at ×63 magnification under oil immersion with the laser at 100% power. The images were analyzed using the Bio-Rad software, and the Kalman filter was used to decrease background. In this system R-phycoerythrin-labeled cells are stained red, and fluorescein isothiocyanate-labeled cells are stained green. In a separate series of experiments, groups of aged and young rats were killed and brains were rapidly removed, coated in OCT compound, immersed in an isopentane bath over liquid nitrogen, and used to prepare sections for analysis of phosphorylated p38 as described above.

TUNEL Staining—Apoptotic cell death was assessed using the DeadEnd colorimetric apoptosis detection system (Promega). Cells were permeabilized and fixed in paraformaldehyde as described above. In separate experiments cultured cortical neurons were prepared from neonatal rats as described previously (26) and maintained in neurobasal medium for 12 days before incubating in the absence or presence of IL-1β (5 ng/ml) for 72 h. Biotinylated nucleotide was incorporated at 3′-OH DNA ends by incubating cells with terminal deoxynucleotidyltransferase for 30 min at 37 °C. Washed cells were incubated in horseradish peroxidase-labeled streptavidin and then incubated in 3,3′-diaminobenzidine chromogen solution, and TUNEL-positive cells were calculated as a proportion of the total cell number.

RESULTS

IL-1β concentration and p38 activity were both significantly increased in cortical tissue prepared from aged rats fed on the control diet compared with young rats ($p < 0.05$, ANOVA; Fig. 1, *a* and *b*), but EPA suppressed these age-related changes so that the values in tissue prepared from EPA-treated rats were not significantly different from control values. *In vitro* analysis revealed that IL-1β significantly enhanced p38 activity in cortical tissue (Fig. 1*c*). In parallel with this observation, we found that cytochrome *c* translocation was significantly increased in cortical tissue prepared from aged rats fed on the control diet compared with tissue prepared from either group of young rats ($p < 0.05$, ANOVA; Fig. 2*a*). A causal relationship between the age-related changes in cytochrome *c* translocation and IL-1β is suggested by the finding that cytochrome *c* translocation was significantly enhanced by IL-1β ($p < 0.05$, ANOVA; Fig. 2*b*) and that this action relied on IL-1RI activation since the IL-1β-induced change was inhibited by IL-1ra. Fig. 2*b* also demonstrates that the IL-1β-induced change was inhibited by SB203580 suggesting that the effect was mediated by activation of p38.

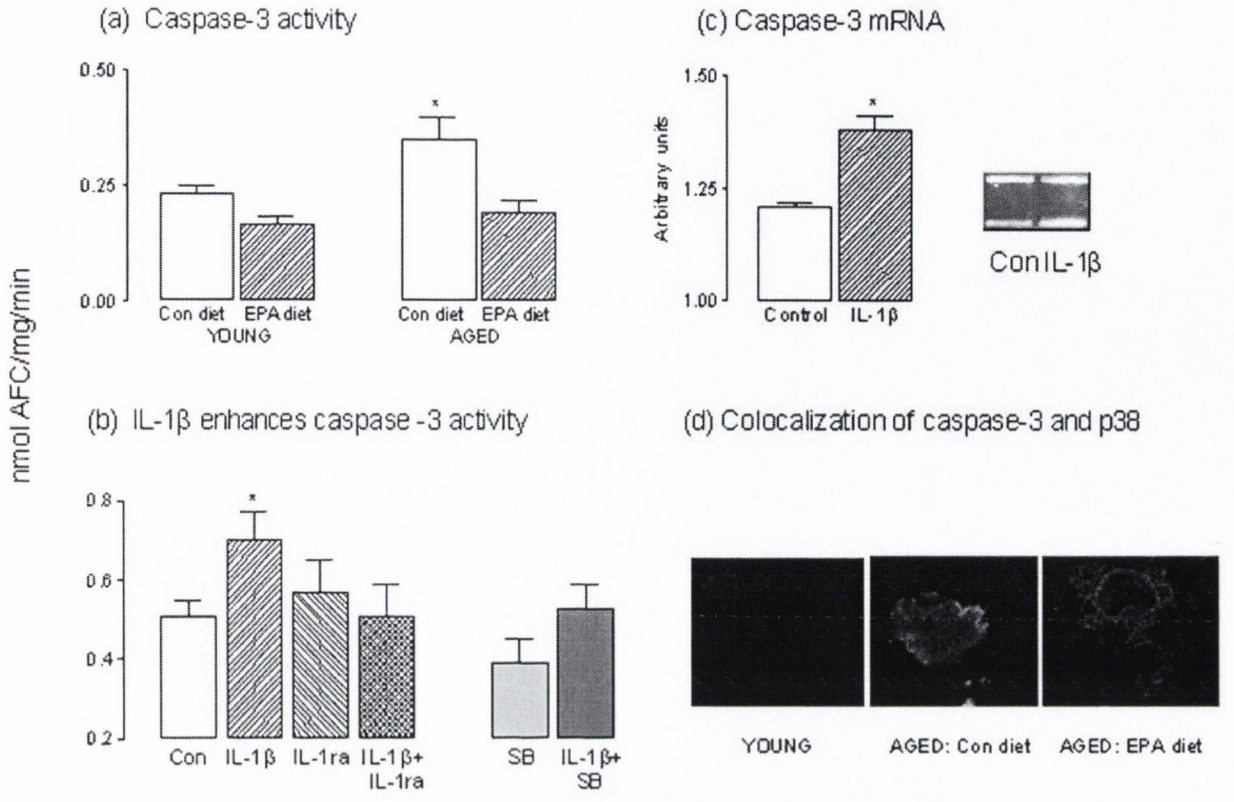

FIG. 3. **The age-related increase in caspase-3 activity is mimicked by IL-1β: evidence for a role for p38 activation.** *a*, caspase-3 activity was significantly enhanced in cortical tissue prepared from aged rats fed on the control diet compared with young rats fed on either diet (*, $p < 0.05$, ANOVA), but this change was not evident in tissue prepared from aged rats fed on the EPA-enriched diet. *b*, *in vitro* analysis indicated that IL-1β significantly increased enzyme activity (*, $p < 0.05$, ANOVA; $n = 6$) but that the IL-1β-induced effect was inhibited by IL-1ra and also by SB203580. *c*, incubation of cultured cortical neurons in IL-1β (*lane 2*) for 72 h significantly increased caspase-3 mRNA (*, $p < 0.05$, Student's *t* test for paired means); values were normalized with reference to expression of glyceraldehyde-3-phosphate dehydrogenase (*lower bands*). *d*, colocalization of activated p38 and caspase-3 was observed in several cells obtained from aged rats that were fed on the control diet but in none of the cells obtained from young rats fed on either diet. There was some evidence of p38 staining in aged rats fed on the experimental diet but no evidence of colocalization with caspase-3. *Con*, control; *SB*, SB203580.

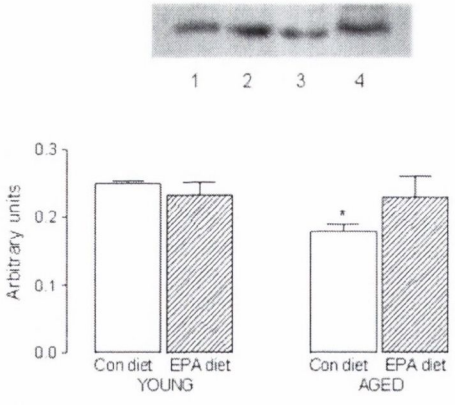

FIG. 4. **Attenuation of the age-related increase in PARP cleavage by EPA.** PARP (116 kDa) expression was significantly reduced in cortical tissue prepared from aged rats fed on the control diet (*lane 3*) compared with tissue prepared from young rats fed on the control (*lane 1*) or EPA-enriched (*lane 2*) diet (*, $p < 0.05$, ANOVA). EPA reversed this effect (*lane 4*). *Con*, control.

One downstream consequence of cytochrome *c* translocation is activation of caspase-3, therefore we analyzed enzyme activity in tissue prepared from aged and young rats fed on either the control or experimental diet. Fig. 3*a* demonstrates that there was a significant age-related increase in caspase-3 activity; thus the mean value in cortical tissue prepared from aged rats fed on the control diet was significantly increased compared with the value in tissue prepared from young rats ($p < 0.05$, ANOVA), but EPA suppressed this change. In an effort to establish whether the change in caspase-3 activation was coupled with the increases in IL-1β concentration and p38 activation, a series of *in vitro* experiments were undertaken that revealed that IL-1β significantly enhanced caspase-3 activity in cortical tissue ($p < 0.05$, ANOVA; Fig. 3*b*); this effect was blocked by IL-1ra, suggesting that the action of IL-1β was dependent on receptor interaction, and by SB203580, indicating that the action of IL-1β also required activation of p38. Cells prepared from cortex of young and aged rats fed on both diets were stained for phosphorylated p38 and caspase-3, and staining was assessed using confocal microscopy. We found no cell in preparations obtained from young rats in which there was evidence of colocalization of activated p38 and caspase-3. In contrast, several cells prepared from aged rats fed on the control diet stained positively for both; an example is shown in Fig. 3*d*. However, while some cells prepared from aged EPA-treated rats stained positively for p38, there was little staining for caspase-3, and we found no evidence of colocalization. These findings support the idea that caspase-3 activation is closely coupled with p38 activation. In addition to the stimulatory effect of IL-1β on caspase-3 activity, we observed that IL-1β significantly increased caspase-3 mRNA in cultured cortical cells (Fig. 3*c*).

In an effort to consolidate these findings, which suggested

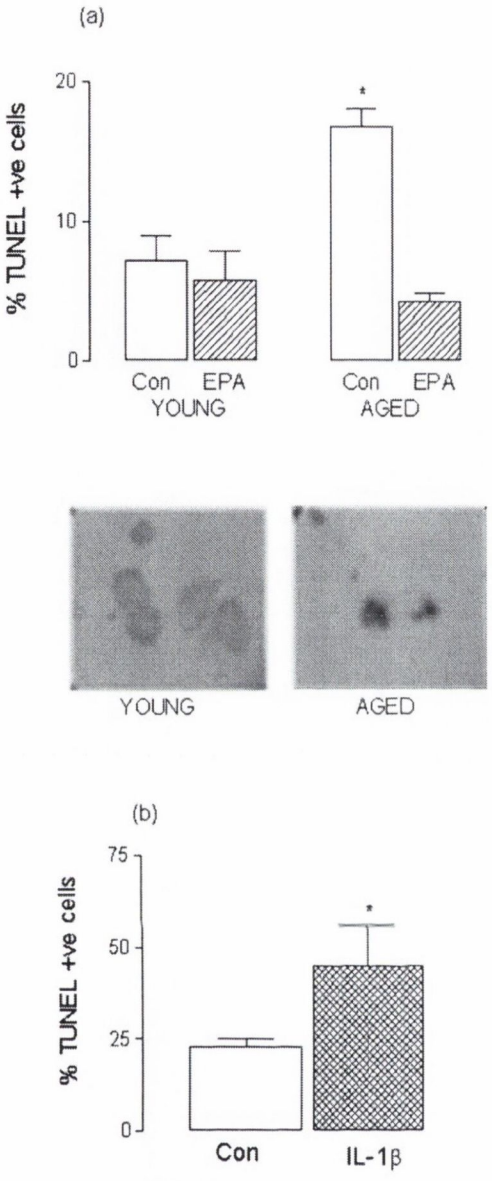

FIG. 5. **The increase in TUNEL staining with age is blocked by EPA and mimicked by IL-1β.** *a*, the number of cells that stained positively for TUNEL was significantly enhanced in cortex of aged rats fed on the control diet (*e.g. left-hand picture*) compared with that in young rats fed on either diet (*, $p < 0.05$, ANOVA); dietary manipulation with EPA reversed this effect. *b*, incubation of cultured cortical neurons in the presence of IL-1β significantly increased the number of TUNEL-positive cells (*, $p < 0.05$, Student's *t* test for independent means; $n = 5$). *Con*, control; *+ve*, positive.

that there was significant evidence of cell death in the aged cortex, we investigated cleavage of PARP by assessing expression of the 116-kDa form of the enzyme. Fig. 4 indicates, in a sample immunoblot and by analysis of the mean data obtained from densitometric analysis, that there was a significant decrease in expression of 116-kDa PARP in cortical tissue prepared from aged rats fed on the control diet compared with young rats ($p < 0.05$, ANOVA) but that this effect was reversed in tissue prepared from aged rats treated with EPA. These data were paralleled by changes in TUNEL staining; thus a significantly greater number of cells stained positively for TUNEL in preparations obtained from aged rats fed on the control diet compared with young rats fed on either diet ($p < 0.05$, ANOVA; Fig. 5*a*). The number of TUNEL-positive cells in preparations obtained from aged rats fed on the EPA-enriched diet was similar to that in tissue prepared from young rats. Fig. 5*b* shows that exposure of cultured cortical neurons to IL-1β for 72 h also significantly increased the number of TUNEL-positive cells ($p < 0.05$, Student's *t* test for independent means).

In an effort to explore the synaptic changes that might occur as a consequence of IL-1β-induced cell death, we turned to analysis of changes in hippocampus and first assessed age- and diet-related changes in IL-1β concentration and p38 activation. Fig. 6*a* shows that, in parallel with the age-related findings in cortical tissue, IL-1β concentration was significantly increased in hippocampal tissue prepared from aged rats fed on the control diet compared with young rats fed on either diet ($p < 0.05$, ANOVA). There was no evidence of a similar age-related increase in aged rats fed on the EPA-enriched diet. Analysis of p38 activation revealed a similar pattern; thus there was a significant age-related increase in p38 activity ($p < 0.05$, ANOVA, aged rats fed on the control diet *versus* young rats; Fig. 6*b*), which was not observed in tissue prepared from aged rats fed on the EPA-enriched diet. A likely causal relationship between IL-1β concentration and p38 activation is suggested by the finding that IL-1β significantly increased p38 activity in hippocampus *in vitro* (Fig. 6*c*). In a separate series of experiments, in which no dietary manipulation was made, cryostat sections of tissue were prepared from young and aged rats. We observed that there was a marked increase in p38 staining in hippocampus of aged compared with young rats; sample sections are demonstrated in Fig. 6*d*.

Analysis of LTP in dentate gyrus was undertaken in the same rats in which biochemical analyses were performed. Fig. 7 demonstrates that LTP was successfully induced in both groups of young rats (Fig. 7*a*) but was impaired in aged rats fed on the control diet (Fig. 7*b*); in the latter group of rats the mean percent changes in population excitatory postsynaptic potential slope in the 2 min immediately following tetanic stimulation (Fig. 7*c*) and in the last 5 min of the experiment (Fig. 7*d*; compared with the mean value in the 5 min prior to the tetani) were 136.5 ± 3.92 and 111.8 ± 0.86, respectively. In contrast, the corresponding values in aged rats fed on the EPA-enriched diet were 181.3 ± 3.12 and 149.1 ± 0.82, respectively. These latter values were similar to those observed in young rats fed on the control (190.5 ± 4.83 and 147.48 ± 1.31, respectively) and EPA-enriched (184.0 ± 3.24 and 154.8 ± 0.92, respectively) diets, indicating that EPA treatment restored the ability of aged rats to respond to tetanic stimulation.

DISCUSSION

We present evidence demonstrating that treatment with EPA prevents neuronal cell death in aged rats and show that suppression of the age-related coupled increases in IL-1β concentration and p38 activity is the key to inhibiting the cascade of cellular events that leads to apoptosis. The age-related increase in IL-1β concentration in cortical and hippocampal tissue, which confirms previous findings (19–21), is coupled with increased TUNEL staining *in vivo*. The implicit suggestion that endogenous IL-1β induces cell death is supported by the finding that IL-1β also enhances TUNEL staining in cultured cortical cells, although a comparison of data from two such different experimental conditions must be made with caution. Significantly, treatment with EPA, which has been shown to have anti-inflammatory properties (27, 28), prevented the age-related increases in IL-1β concentration and TUNEL staining in cortex. These data support the previous finding that fish oils, which contain EPA, reduce production of proinflammatory cytokines in circulating cells (29–32) and chondrocytes (33) and suppress the lipopolysaccharide-induced increase in circulating IL-1β (34).

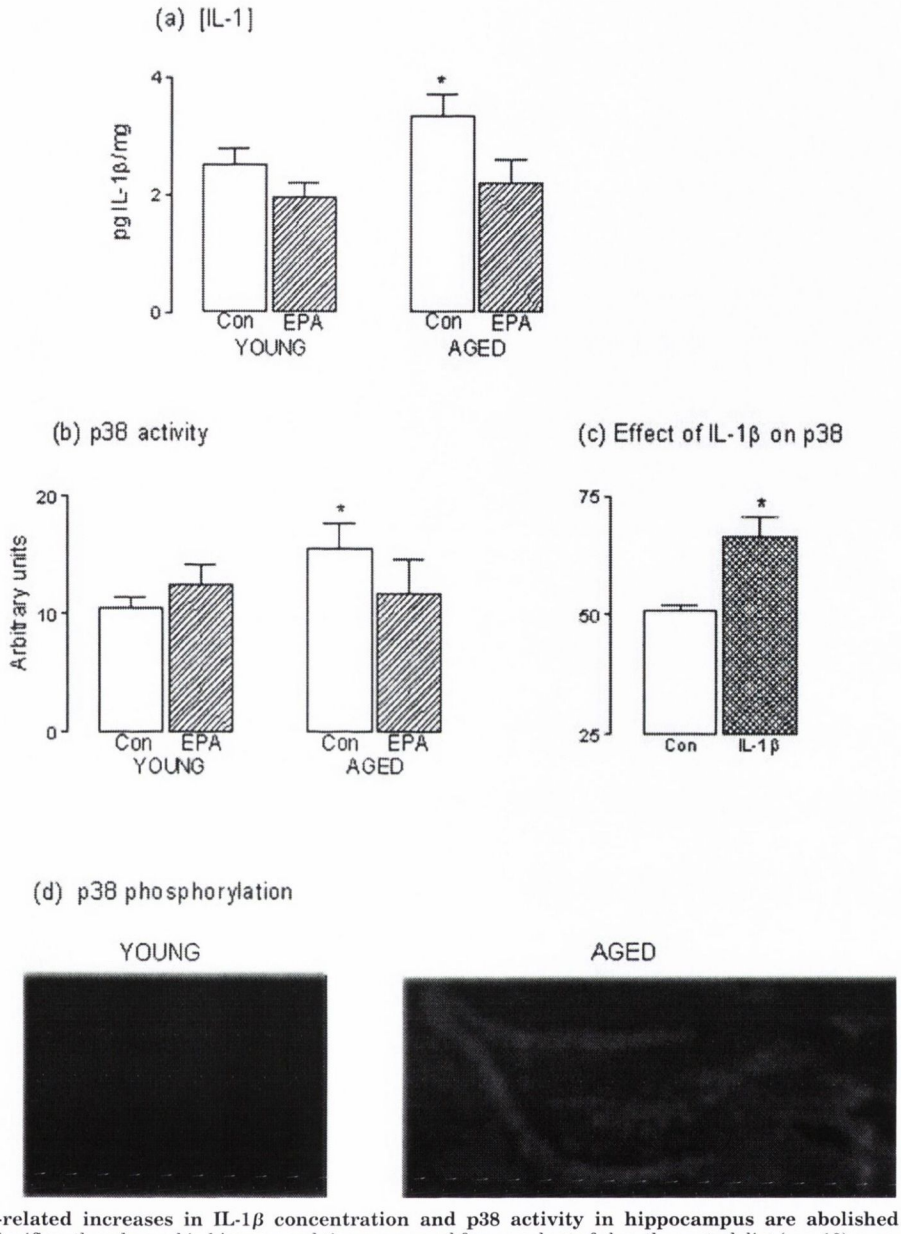

FIG. 6. **The age-related increases in IL-1β concentration and p38 activity in hippocampus are abolished by EPA.** *a*, IL-1β concentration was significantly enhanced in hippocampal tissue prepared from aged rats fed on the control diet ($n = 10$) compared with young rats fed on either diet (*, $p < 0.05$, ANOVA; $n = 6$), but this change was not evident in tissue prepared from aged rats fed on the EPA-enriched diet ($n = 10$). *b*, p38 activity was significantly enhanced in hippocampal tissue prepared from aged rats fed on the control diet compared with young rats fed on either control or EPA diet (*, $p < 0.05$, ANOVA), but this change was not evident in tissue prepared from aged rats fed on the EPA-enriched diet (*lane 4*). *c*, IL-1β significantly enhanced p38 activity in hippocampal tissue *in vitro* (*, $p < 0.05$, Student's *t* test for paired values; $n = 6$). *d*, expression of phosphorylated p38 is markedly increased in cryostat sections prepared from aged compared with young rats. *Con*, control.

Increased activation of p38 accompanied the age-related increase in IL-1β concentration consistent with previous observations in hippocampal cells (8, 19–21) and in other cell types (35–39). The evidence presented here pinpoints IL-1β-induced increased activation of p38 as a pivotal event in triggering changes that are characteristic of apoptotic cell death, for example cytochrome *c* translocation and caspase-3 activation. This suggestion concurs with previous findings. Thus inhibition of p38 by SB203580 has been shown to prevent singlet oxygen-induced apoptosis in HL-60 cells (40), while another p38 inhibitor, SB2390663, prevents caspase cleavage in thiol-oxidant-induced apoptosis in forebrain neuronal-enriched cell cultures (41). That inhibition of p38 proffers protection is further supported by the finding that its activation spared dopaminergic neurons deprived of serum (42) and markedly reduced infarct size induced by ischemia (16). In parallel with the effect of dietary manipulation on IL-1β concentration, the data indicate that EPA treatment blocked the age-related increase in p38 activation in hippocampus and cortex.

The data from *in vitro* analysis suggested that IL-1β, through an action on IL-1RI and mediated through activation of p38, stimulates cytochrome *c* translocation in cortical tissue. Since IL-1β concentration and p38 activation were enhanced in cortical tissue prepared from aged rats, it was predicted that translocation of cytochrome *c* might also be a feature of the aged brain; the present data indicate that there was an age-related increase in cytochrome *c* translocation that paralleled the increases in IL-1β concentration and p38 activation. Sig-

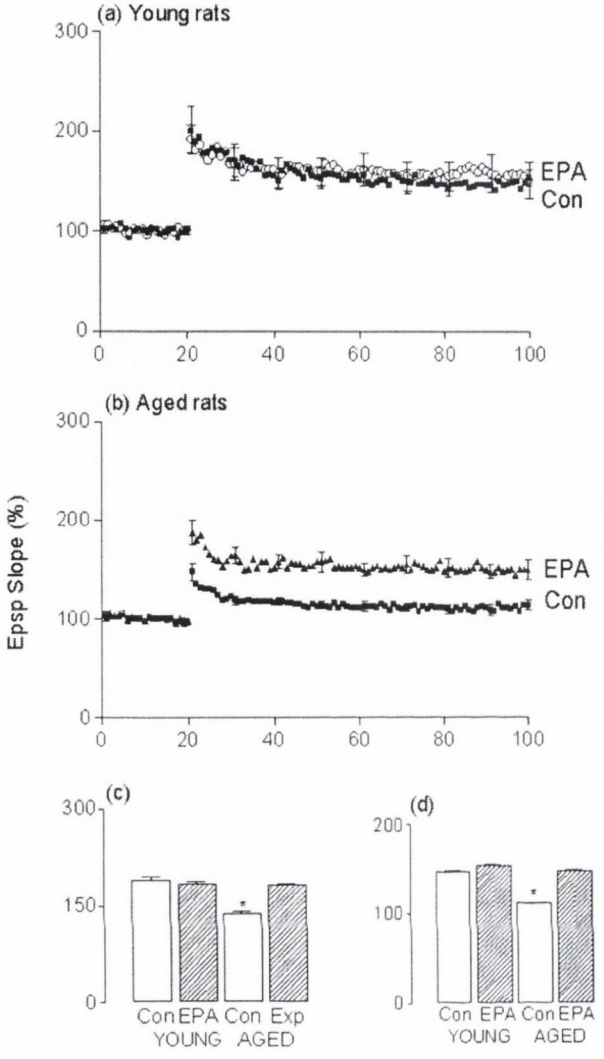

FIG. 7. **The age-related impairment in LTP in dentate gyrus is suppressed by EPA.** *a* and *b*, tetanic stimulation (time 0) resulted in an immediate and sustained increase in the mean population excitatory postsynaptic potential (*Epsp*) slope in young rats (*a*) fed on either diet. A similar change was observed in aged rats (*b*) fed on the EPA-enriched diet, but aged rats that were fed on the control diet exhibited a marked attenuation in response to tetanic stimulation. *c* and *d*, analysis of the mean changes in the 2 min immediately following tetanic stimulation and in the last 5 min of the experiment (compared with the mean excitatory postsynaptic potential slope in the 5 min preceding the tetanus) revealed a significant decrease in excitatory postsynaptic potential slope in aged rats fed on the control diet compared with the other three groups (*, $p < 0.01$, ANOVA; $n = 8$ in the case of young and $n = 12$ in the case of aged rats). *Con*, control.

nificantly, this increase was absent in cortical tissue prepared from EPA-treated aged rats. Disruption of the mitochondrial transmembrane potential, which is accompanied by cytochrome *c* translocation from the mitochondria to the cytosol (43), is a relatively early event in apoptotic cell death. It has been shown that among the stimuli that lead to these events is oxidative stress (43); indeed it is possible that enhanced reactive oxygen species accumulation, which we have shown to accompany increased IL-1β concentration in other studies (19–21) and in the present one (data not shown), is responsible for the observed age-related increase in cytochrome *c* translocation.

Cytochrome *c* translocation triggers a cascade of reactions initiated by interaction with apoptosis protease-activating factor-1 and propagated by activation of caspase-9 and subsequently other caspases that eventually culminates in cell death (44). The importance of the role of cytochrome *c* translocation in this cascade was underscored by the demonstration that injection of active cytochrome *c* into cells led to apoptosis (45). The present findings, which show parallel changes in cytochrome *c* translocation and caspase-3, are consistent with the view that caspase-3 activation is triggered by cytosolic cytochrome *c* (46, 47). Our data also indicate that caspase-3 mRNA, as well as enzyme activity, was increased by IL-1β *in vitro* and, furthermore, that caspase-3 activation was dependent on interaction of IL-1β with IL-1RI and mediated through the subsequent activation of p38. The observation that caspase-3 colocalized with activated p38 was a further indication of a coupling between these parameters. This finding is strikingly similar to data reported in a recent study that showed that SB203580 diminishes caspase activity and protects SH-Sy5Y neuroblastoma cells and cultured cortical neurons from NO-induced cell death (48). EPA reversed the age-related increases in p38 activation, cytochrome *c* translocation, and caspase-3 activity, and we view this concurrence as strong evidence of a causal relationship between the parameters.

One downstream substrate for caspase-3 is the DNA repair enzyme PARP, and the present findings indicate that, in parallel with the effects of age and diet on caspase-3 activation, PARP cleavage was increased in aged rats fed on the control, but not the EPA-enriched, diet. We have previously reported that cleavage of PARP was increased in entorhinal cortex of lipopolysaccharide-treated rats, and this change was accompanied by changes in morphology of cells that were indicative of cell death (20). Indeed cleavage of PARP has been considered to be a reliable marked of apoptosis (49, 50). Significantly, we observed that these lipopolysaccharide-induced changes were blocked by caspase-1 inhibition pinpointing a role for IL-1β in the cascade of events leading to cell death (8). In the present study the age-related enhancement in PARP cleavage was coupled with evidence of reduced cell viability, but evidence of both changes was absent in tissue prepared from EPA-treated aged rats.

Our data indicate that the age-related increases in IL-1β concentration and p38 activation observed in cortical tissue were also observed in the hippocampus; these findings support our previous observations (19, 20). However, we report that no such changes were observed in hippocampus of aged rats that were fed on the EPA-enriched diet. LTP in perforant path-granule cell synapses was markedly depressed with age, confirming data from several previous studies (19–22, 51); significantly, this age-related impairment in LTP was completely absent in aged rats fed on the EPA-enriched diet. The negative correlation between the IL-1β concentration and p38 activation and the expression of LTP together with the observation that the IL-1β-induced inhibition of LTP was suppressed by p38 inhibition provides strong evidence of a causal relationship between these measures. The question of how polyunsaturated fatty acid, specifically EPA, uptake into neuronal tissue is achieved should be considered. It has been shown that circulating fatty acids cross the blood-brain barrier, and the rate of incorporation is proportional to plasma concentration; evidence indicates that transport is mainly by diffusion, although a facilitated process may also contribute (52). The question of the underlying cause of the decrease in polyunsaturated fatty acids in aged rats remains to be fully resolved, but it appear that fatty acid uptake into brain tissue is not altered with age (53).

Our working hypothesis is that aging is coupled with a significant increase in IL-1β concentration in neuronal tissue that is likely to exert multiple effects including activation of p38. We propose that increased p38 causes mitochondrial mem-

brane perturbation leading to translocation of cytochrome *c*. One consequence of these changes is an increase in caspase-3 activation; caspase-3 acts on its substrate, PARP, resulting in its cleavage. Apoptotic changes in cells occur since DNA repair is compromised as a result of this action. The evidence presented points to a pivotal role for IL-1β in triggering the cellular events that lead to an increase in cell death in the aged brain and identify activation of p38 as a key mediator. It is proposed that, although EPA abolished several age-related changes, the primary action of EPA may be to block the age-related increase in IL-1β concentration.

REFERENCES

1. Griffin, W. S. T., Stanley, L. C., Ling, C., White, L., MacLeod, V., Perrot, L. J., White, C. L., III, and Araoz, C. (1989) *Proc. Natl. Acad. Sci. U. S. A.* **86,** 7611–7615
2. Mogi, M., Harada, M., Kondo, T., Riederer, P., Inagaki, J., Minami, and M., Nagatsu, T. (1994) *Neurosci. Lett.* **180**, 147–150
3. Boutin, H., LeFeuvre, R. A., Horai, R., Asano, M., Iwakura, Y., and Rothwell, N. J. (2001) *J. Neurosci.* **21,** 5528–5534
4. Panegyres, P. K., and Hughes, J. (1998) *J. Neurol. Sci.* **154,** 123–132
5. Taupin, V., Toulmond, S., Serrano, A., Benavides, J., and Zavala, F. (1993) *J. Neuroimmunol.* **42,** 177–185
6. Hu, S., Peterson, P. K., and Chao, C. C. (1997) *Neurochem. Int.* **30,** 427–431
7. Vereker, E., Campbell, V., Roche, E., McEntee, E., and Lynch, M. A. (2000) *J. Biol. Chem.* **275,** 26252–26528
8. Vereker, E., O'Donnell, E., and Lynch, M. A. (2000) *J. Neurosci.* **20,** 6811–6819
9. O'Neill, L. A. J., and Greene, C. (1998) *J. Leukoc. Biol.* **63,** 650–657
10. Xia, Z., Dickens, M., Raingeaud, J., Davis, R. J., and Greenberg, M. E. (1995) *Science* **270,** 1326–1331
11. Mielke, K., and Herdegen, T. (2000) *Prog. Neurobiol.* **61,** 45–60
12. Kummer, J. L., Rao, P. K., and Heidenreich, K. A. (1997) *J. Biol. Chem.* **272,** 20490–20494
13. Harada, J., and Sugimoto, M. (1999) *Brain. Res.* **842,** 311–323
14. Castagne, V., and Clarke, P. G. (1999) *Brain. Res.* **842,** 215–219
15. Barancik, M., Htun, P., Strohm, C., Kilian, S., and Schaper, W. (2000) *J. Cardiovasc. Pharmacol.* **35,** 474–483
16. Barone, F. C., Irving, E. A., Ray, A. M., Lee, J. C., Kassis, S., Kumar, S., Badger, A. M., Legos, J. J., Erhardt, J. A., Ohlstein, E. H., Hunter, A. J., Harrison, D. C., Philpott, K., Smith, B. R., Adams, J. L., and Parsons, A. A. (2001) *Med. Res. Rev.* **21,** 129–145
17. Zhu, X., Rottkamp, C. A., Boux, H., Takeda, A., Perry, G., and Smith, M. A. (2000) *J. Neuropathol. Exp. Neurol.* **59,** 880–888
18. Hensley, K., Floyd, R. A., Zheng, N. Y., Nael, R., Robinson, K. A., Nguyen, X., Pye, Q. N., Stewart, C. A., Geddes, J., Markesbery, W. R., Patel, E., Johnson, G. V., and Bing, G. (1999) *J. Neurochem.* **72,** 2053–2058
19. Murray, C. A., and Lynch, M. A. (1998) *J. Neurosci.* **18,** 2974–2981
20. Murray, C. A., and Lynch, M. A. (1998) *J. Biol. Chem.* **273,** 12161–12168
21. O'Donnell, E., Vereker, E., and Lynch, M. A. (2000) *Eur. J. Neurosci.* **12,** 345–352
22. McGahon, B. M., Martin, D. S. D., Horrobin, D. F., and Lynch, M. A. (1999) *Neuroscience* **94,** 305–314
23. Cunningham, A. J., Murray, C. A., O'Neill, L. A. J., Lynch, M. A., and O'Connor, J. J. (1996) *Neurosci. Lett.* **203**, 1–4
24. Lynch, M. A. (1998) *Prog. Neurobiol.* **56,** 1–19
25. Bradford, M. M. (1976) *Anal. Biochem.* **72,** 248–254
26. MacManus, A., Ramsden, M., Murray, M., Pearson, H. A., and Campbell, V. (2000) *J. Biol. Chem.* **275,** 4713–4718
27. Hayashi, H., Tanaka, Y., Hibino, H., Umeda, Y., Kawamitsu, H., Fujimoto, H., and Amakawa, T. (1999) *Curr. Med. Res. Opin.* **15,** 177–184
28. Babcock, T., Helton, W. S., and Espat, N. J. (2000) *Nutrition* **16,** 1116–1118
29. Endres, S., Ghorbani, R., Kelley, V. E., Georgilis, K., Lonnemann, G., van der Meer, J. W., Cannon, J. G., Rogers, T. S., Klempner, M. S., and Weber, P. C. (1989) *New Engl. J. Med.* **320,** 265–271
30. McCarthy, M. F. (1999) *Med. Hypotheses* **53,** 369–374
31. Wallace, F. A., Miles, E. A., and Calder, P. C. (2000) *Cytokine* **12,** 1374–1379
32. Calder, P. C., and Zurier, R. B. (2001) *Curr. Opin. Clin. Nutr. Metab. Care* **4,** 115–121
33. Curtis, C. L., Hughes, C. E., Flannery, C. R., Little, C. B., Harwood, J. L., and Caterson, B. (2000) *J. Biol. Chem.* **275,** 721–724
34. Sadeghi, S., Wallace, F. A., and Calder, P. C. (1999) *Immunology* **96,** 404–410
35. Raingeaud, J., Gutpa, S., Rogers, J. S., Dickens, M., Han, J., Ulevitch, R. J., and Davis, R. J. (1995) *J. Biol. Chem.* **270,** 7420–7426
36. Guay, J., Lambert, H., Gingras-Breton, G., Lavoie, J. N., Huot, J., and Landry, J. (1997) *J. Cell. Sci.* **110,** 357–368
37. Palsson, E. M., Popoff, M., Thelestam, M., and O'Neill, L. A. (2000) *J. Biol. Chem.* **275,** 7818–7825
38. Ng, D. C., Long, C. S., and Bogoyevitch, M. A. (2001) *J. Biol. Chem.* **276,** 29490–29498
39. Kumar, S., Votta, B. J., Rieman, D. J., Badger, A. M., Gowen, M., and Lee, J. C. (2001) *J. Cell. Physiol.* **187,** 294–303
40. Kochevar, I. E., Lynch, M. C., Zhuang, S., and Lambert, C. R. (2000) *Photochem. Photobiol.* **72,** 548–553
41. McLaughlin, B., Pal, S., Tran, M. P., Parsons, A. A., Barone, F. C., Erhardt, J. A., and Aizenman, E. (2001) *J. Neurosci.* **21,** 3303–3311
42. Zawada, W. M., Meintzer, M. K., Rao, P., Marotti, J., Wang, X., Esplen, J. E., Clarkson, E. D., Freed, C. R., and Heidenreich, K. A. (2001) *Brain Res.* **891,** 185–196
43. Cortopassi, G. A., and Wong, A. (1999) *Biochim. Biophys. Acta* **1410,** 183–193
44. Green, D. R., and Reed, J. C. (1998) *Science* **281,** 1309–1312
45. Zhivotovsky, B., Hanson, K. P., and Orrenius, S. (1998) *Cell Death Differ.* **5,** 459–460
46. Kluck, R. M., Bossy-Wetzel, E., Green, D. R., and Newmeyer, D. D. (1997) *Science* **275,** 1132–1136
47. Yang, J., Liu, X. S., Bhalla, C. N., Kim, C. N., Ibrado, A. M., Cai, J. Y., Pend, T. I., Jones, D. P., and Wang, X. (1997) *Science* **275,** 1129–1132
48. Ghatan, S., Larner, S., Kinoshita, Y., Hetman, M., Patel, L. M., Xia, Z., Youle, R. J., and Morrison, R. S. (2000) *J. Cell Biol.* **150,** 335–347
49. Martinou, J. C., and Sadoul, R. (1996) *Curr. Opin. Neurobiol.* **6,** 609–614
50. O'Brien, M. A., Moravec, R. A., and Riss, T. L. (2001) *BioTechniques* **30,** 886–891
51. Barnes, C. A. (1979) *J. Comp. Physiol. Psychol.* **93,** 74–104
52. Rapoport, S. I. (2001) *J. Mol. Neurosci.* **16,** 243–261
53. Terracina, L., Brunetti, M., Avellini, L., De Medio, G. E., Trovarelli, G., and Gaiti, A. (1992) *Mol. Cell. Biochem.* **115,** 35–42

Δ^9-Tetrahydrocannabinol induces the apoptotic pathway in cultured cortical neurones via activation of the CB_1 receptor

Eric Downer, Barry Boland, Marie Fogarty and Veronica Campbell[CA]

Department of Physiology, Trinity College, Dublin 2, Ireland

[CA]Corresponding Author

Received 6 September 2001; accepted 15 October 2001

Δ^9-Tetrahydrocannabinol, the principal psychoactive component of marijuana, exerts a variety of effects on the CNS, including impaired cognitive function and neurobehavioural deficits. The mechanisms underlying these neuronal responses to tetrahydrocannabinol are unclear but may involve alterations in neuronal viability. Tetrahydrocannabinol has been shown to influence neuronal survival but the role of the cannabinoid receptors in the regulation of neuronal viability has not been fully clarified. In this study we demonstrate that tetrahydrocannabinol promotes the release of cytochrome c, activates caspase-3, promotes cleavage of the DNA repair enzyme poly-ADP ribose polymerase and induces DNA fragmentation in cultured cortical neurones. These effects of tetrahydrocannabinol were completely abrogated by the CB_1 receptor antagonist AM-251. The findings of this study demonstrate that tetrahydrocannabinol induces apoptosis in cortical neurones in a manner involving the CB_1 subtype of cannabinoid receptor. *NeuroReport* 12:3973–3978 © 2001 Lippincott Williams & Wilkins.

Key words: Apoptosis; Cannabinoid receptor; Caspase-3; Poly-ADP-ribose polymerase; Tetrahydrocannabinol

INTRODUCTION

Δ^9-Tetrahydrocannabinol (THC), the principal psychoactive component of marijuana, exerts a variety of effects on the CNS including alterations in cognitive function [1] and impairments in memory formation and retrieval [2]. At a cellular level THC has been found to play a role in the regulation of cell viability. THC induces apoptosis in glioma cells [3], macrophages [4], hippocampal cells [5] and cortical neurones [6]. In contrast, THC also has cytoprotective properties and has been shown to enhance cell survival in the face of oxidative stress [7] and excitotoxicity [8]. The exact mechanisms underlying these contradictory effects of THC on cellular viability are unclear but since THC is a highly lipophilic molecule [9] it has been proposed that THC may utilise receptor-independent mechanisms, such as acting as a reactive oxygen species scavengers [10], to enhance cell survival. In contrast, linkage to the cannabinoid (CB) receptor has been shown to mediate the toxic effects of THC on glioma [3] and hippocampal neurones [5]. While two subytpes of cannabinoid receptor, CB_1 and CB_2, have been identified [11] the CB_1 receptor is pertinent in the central effects of THC [12] and has been localised in several brain regions including the cortex, hippocampus and cerebellum [13]. The CB_1 receptor is coupled to a G-protein [12] and we have recently reported that the detrimental effects of THC on cortical neurones are sensitive to pertussis toxin [6], indicating that G-protein subtypes G_o or G_i have a role in THC-induced neurotoxicity. To investigate whether the induction of cell death by THC proceeded via activation of the CB_1 receptor we examined the effect of the selective CB_1 antagonist AM-251 [14] on THC-induced neurodegeneration of cultured cortical neurones and characterised the role of the CB_1 receptor in the THC-induced activation of several key component of the apoptotic cascade, namely cytochrome c release, caspase-3 activation, poly-ADP-ribose polymerase cleavage and DNA fragmentation.

MATERIALS AND METHODS

Culture of cortical neurones: Primary cortical neurones were established from postnatal 1-day old Wistar rats and maintained in neurobasal medium. Rats were decapitated and cerebral cortices removed. The dissected cortices were incubated in phosphate-buffered saline (PBS) containing trypsin (0.25%) for 20 min at 37°C. The tissue was then triturated (×5) in PBS containing soyabean trypsin inhibitor (0.1%) and DNAse (0.2 mg/ml) and gently filtered through a sterile mesh filter. Following centrifugation at $2000 \times g$ for 3 min at 20°C, the pellet was resuspended in neurobasal medium, supplemented with heat inactivated horse serum (10%), penicillin (100 U/ml), streptomycin (100 U/ml) and glutamax (2 mM). Suspended cells were plated at a density of 0.25×10^6 cells on circular 10 mm diameter coverslips, coated with poly-L-lysine (60 µg/ml), and incubated in a humidified atmosphere containing 5% CO_2:95% air at 37°C. After 48 h 5 ng/ml cytosine-arabino-

furanoside was included in the culture medium to prevent proliferation of nonneuronal cells. Culture media were exchanged every 3 days and cells were grown in culture for up to 14 days.

Drug treatment: THC (Sigma-Aldrich Co. Ltd, Dorset, UK) was stored at −20°C as a 1 mM stock solution in methanol. For treatment of cortical neurones THC was diluted to a final concentration of 5 μM in prewarmed neurobasal medium and 0.01% methanol was used as vehicle. The selective CB_1 receptor antagonist AM 251 (Tocris Cookson Ltd., Bristol, UK) was stored as a 10 mM stock solution in dimethylsuphoxide and diluted to a final concentration of 10 μM in warm culture media; 0.0001% dimethylsulphoxide was used as vehicle control, AM 251 was added to the cultured neurones 30 min prior to incubation with THC. Cells were incubated with THC for 2 h since this was the time-point at which apoptotic changes had previously been observed [6].

TdT-mediated-UTP-end nick labelling (TUNEL): Apoptotic cell death was assessed using the DeadEnd calorimetric apoptosis detection system (Promega Corporation, Madison, USA). Briefly, cells were fixed with paraformaldehyde (4%), permeabilised with Triton-X100 (0.1%), and biotinylated nucleotide was incorporated at 3′-OH DNA ends using the enzyme terminal deoxynucleotidyl transferase (TdT). Horseradish peroxidase-labelled streptavidin then bound to the biotinylated nucleotide and this was detected using the peroxidase substrate H_2O_2 and the chromogen diaminobenzidine. Cells were then viewed under light microscopy at ×100 magnification, where the nuclei of TUNEL positive cells stained brown. Apoptotic cells (TUNEL positive), were counted and expressed as a percentage of the total number of cells examined (400–500 cells/coverslip).

Cytochrome c Western immunoblot: Following incubation with THC (5 μM) ± AM-251 (10 μM), cortical neurones were harvested in lysis buffer (20 mM HEPES, 10 mM KCl, 1.5 mM $MgCl_2$, 1 mM EGTA, 1 mM EDTA, 1 mM dithiothreitol, 0.1 mM PMSF, 5 μg/ml pepstatin A, 2 μg/ml leupeptin, 2 μg/ml aprotinin, pH 7.4) and left on ice for 20 min. Cells were then centrifuged (10 000 × *g* for 10 min at 4°C) and the supernatant containing the cytosolic fraction was prepared for SDS-polyacrylamide gel electrophoresis. The cytosolic fraction was diluted to 50 μg protein/ml with sodium dodecyl sulphate (SDS) sample buffer (150 mM Tris–HCl pH 6.8, 10% v/v glycerol, 4% w/v SDS, 5% v/v β-mercaptoethanol, 0.002% w/v bromophenol blue). Samples were then heated to 100°C for 3 min. Cytosolic proteins (1 μg/lane) were separated by electrophoresis on a 12% polyacrylamide minigel, transferred to nitrocellulose membrane (Satorius, Germany) and immunoblotted with a polyclonal anti-cytochrome c antibody (Santa Cruz Biotechnology Inc, California) purified from rabbit serum. Immunoreactive bands were detected using horseradish peroxidase conjugated anti-rabbit IgG (Sigma, UK) and an enhanced chemiluminescence (ECL) system (Amersham, UK). Mol. wt markers were used to verify the mol. wt of protein bands and purified cytochrome c protein was used for positive identification of protein bands corresponding to cytochrome c. Band widths were quantified using densitometric analysis (D-Scan PC software).

Poly ADP ribose polymerase (PARP) immunocytochemistry: Following treatment of cultured cortical neurones with THC (5 μM) ± AM-251 (10 μM) the cells were fixed in 4% paraformaldehyde, blocked with 5% bovine serum albumin and incubated with an anti-cleavage site specific PARP polyclonal antibody purified from goat serum (BioSource International Inc, UK; 1:50 dilution, 1 h) which specifically recognises the cleaved form of PARP. Immunoreactivity was detected with a biotinylated anti-goat IgG secondary antibody (BioSource International Inc, UK; 1:50 dilution, 1 h incubation) and streptavidin conjugated to horseradish peroxidase (Amersham, UK). Immunoreactive cells were visualised with the chromogen diaminobenzidine. The number of immunoreactive cells were counted and expressed as a percentage of the total number of cells examined (400–500 cells/coverslip).

Measurement of caspase-3 activity: Cleavage of the fluorogenic caspase-3 substrate (DEVD-aminofluorocoumarin (AFC); Alexis Corporation, USA) to its fluorescent product was used as a measure of caspase-3 activity. Cortical neurones were harvested in lysis buffer (25 mM HEPES, 5 mM $MgCl_2$, 5 mM DTT, 5 mM EDTA, 2 mM PMSF, 10 μg/ml leupeptin, 10 μg/ml pepstatin; pH 7.4), subjected to three freeze–thaw cycles and centrifuged at 10 000 r.p.m. for 10 min at 4°C. Samples of supernatant (90 μl) were incubated with the DEVD peptide (500 μM; 10 μl) for 1 h at 30°C. Incubation buffer (900 μl; 100 mM HEPES containing 10 mM DTT; pH 7.4) was added and fluorescence was assessed (excitation, 400 nm; emission, 505 nm).

Caspase-3 activity was also assessed by immunocytochemistry using an anti-active caspase-3 antibody (Promega Corporation, Madison, USA). Briefly, cells were fixed with 4% paraformaldehye, blocked with 5% goat serum in phosphate buffered saline, incubated with anti-active caspase-3 antibody (1:200 dilution, overnight incubation at 4°C). Immunoreactivity was detected using a biotinylated anti-rabbit IgG antibody and streptavidin conjugated to horseradish peroxidase. Immunoreactive cells were visualised with the chromogen diaminobenzidine, the number of immunoreactive cells were counted and expressed as a percentage of the total number of cells examined (400–500 cells/coverslip).

RESULTS

THC-induced DNA-fragmentation is abolished by the CB_1 receptor antagonist AM-251 THC induced a dose-dependent induction of apoptosis in cortical neurones (Fig. 1a). In control cells the percentage of cells displaying DNA fragmentation, as assessed by TUNEL staining was 22 ± 2% (mean ± s.e.m.). The percentage of cells staining TUNEL positive was unaffected by THC at 10 nM (19 ± 4%, $n = 5$). However, treatment of cells with THC at 100 nM, 1 μM, 5 μM and 10 μM for 2 h significantly increased the percentage of cells displaying DNA to 28 ± 2% ($p < 0.05$, Student's *t*-test, $n = 5$), 35 ± 4% ($p < 0.05$, Student's *t*-test, $n = 5$), 49 ± 1% ($p < 0.01$, Student's *t*-test,

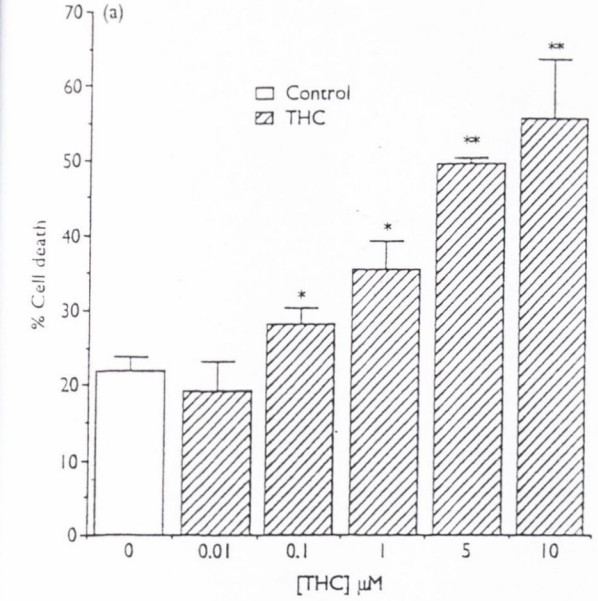

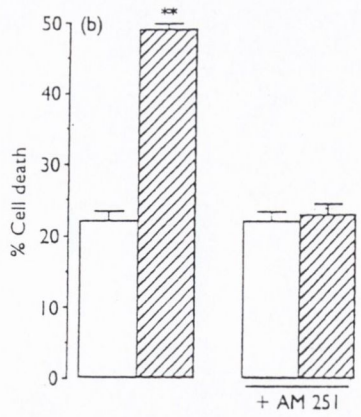

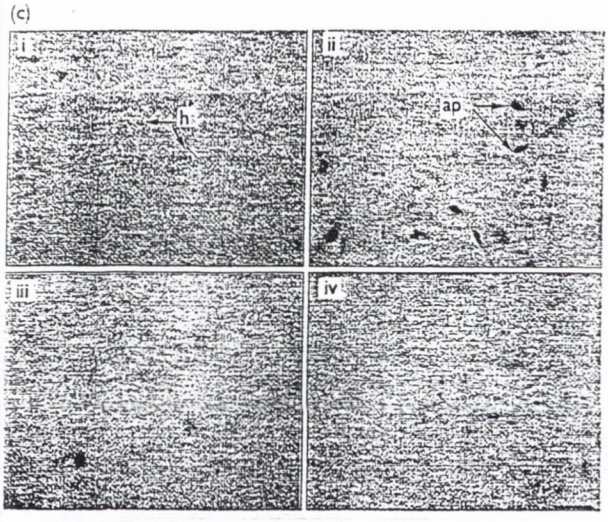

Fig. 1. THC promotes degeneration of cortical neurones via the CB_1 receptor. (**a** Incubation with THC for 2 h induced a dose-dependent increase in DNA fragmentation. Results are expressed as mean ± s.e.m. for 5 observations, * $p < 0.05$; ** $p < 0.01$. (**b**) A significant increase in neuronal degeneration was observed following exposure of cortical neurones to THC (5 μM) for 2 h. Preincubation of the cortical neurones with the CB_1 receptor antagonist AM-251 (10 μM) for 30 min abolished the THC-induced increase in TUNEL-positive cells. Results are expressed as mean ± s.e.m. for 5 observations, ** $p < 0.01$. (**c**) Representative image of cortical neurones stained with TUNEL. (i) Under control conditions few cells stained positive for DNA fragmentation using TUNEL. (ii) 5 μM THC-treated neurones exhibited a significant increase in TUNEL-positive cells. (iii) Treatment with AM-251 alone had no effect on the number of TUNEL-positive neurones. (iv) Treatment with AM-251 in the presence of THC significantly reduced the number of TUNEL-positive cells. (h, healthy neurones; ap, apoptotic TUNEL-positive neurones). Bar = 25 μm.

$n = 5$) and 55 ± 8% ($p < 0.01$, Student's t-test, $n = 5$), respectively.

Figure 1b demonstrates that the CB_1 receptor antagonist AM-251 blocks THC-induced apoptosis. Treatment of cortical neurones with THC (5 μM) for 2 h significantly increased the percentage of cells displaying DNA fragmentation, as assessed by TUNEL staining, from 22 ± 2% to 49 ± 1% ($p < 0.01$, Student's t-test, $n = 5$). While AM-251 (10 μM) alone had no effect on DNA fragmentation (22 ± 3% TUNEL-positive cells) it prevented the THC-induced increase in DNA fragmentation (24 ± 3% TUNEL-positive cells following treatment with THC in the presence of AM-251).

THC-induced translocation of cytochrome c is abolished by AM-251: An upstream event associated with apoptosis is the translocation of mitochondrial cytochrome c into the cytosol. Cytosolic expression levels of cytochrome c were measured by Western immunoblot and band widths were quantified by densitometry (Fig. 2a). In control cells cytosolic levels of cytochrome c were 22.0 ± 2.06 (arbitrary units) and this was significantly increased to 28.67 ± 2.28 ($p < 0.05$, Student's t-test, $n = 9$) by THC (5 μM). AM-251 (10 μM) alone had no effect on cytosolic cytochrome c expression (mean band width 21.40 ± 1.82) but it prevented the THC-induced increase in cytochrome c expression (mean bind width 21.23 ± 1.75 in cortical neurones treated with THC in the presence of AM-251). A sample immunoblot showing that the THC-induced release of cytochrome c into the cytosol is prevented by AM 251 is shown in Fig. 2a.

AM-251 blocks the THC-induced activation of caspase-3: A consequence of mitochoridrial cytochrome c release is the activation of caspase-3. Figure 2b demonstrates that treatment of cortical neurones with THC (5 μM) for 2 h significantly increased caspase-3 activity, as assessed by the fluorogenic assay, from 13.6 ± 6.0 pmol AFC pro-

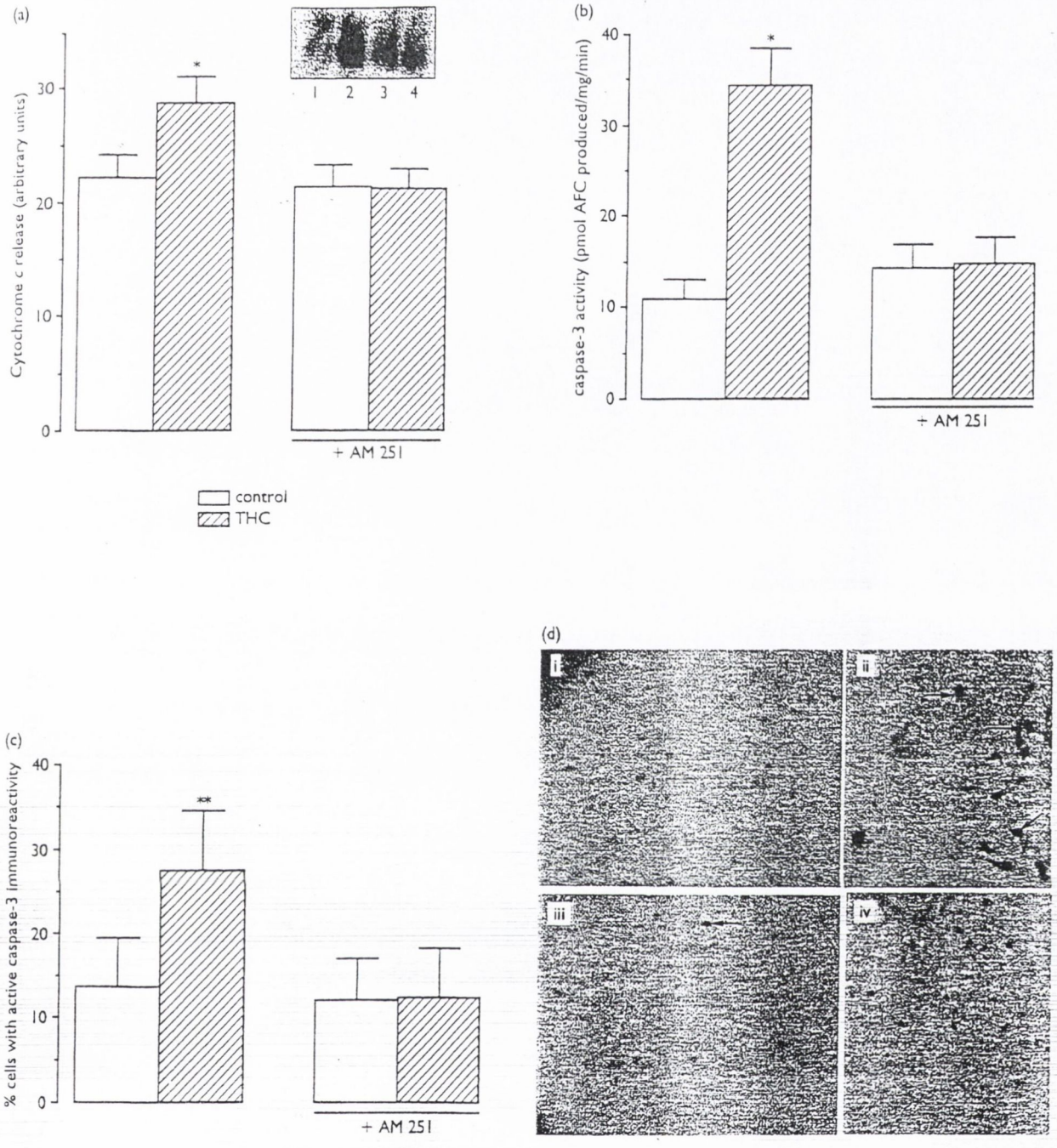

Fig. 2. THC promotes translocation of cytochrome c and activates caspase-3 in a CB_1-receptor-dependent manner A: Cortical neurones were incubated with THC (5 μM), cells were harvested and cytosolic fractions were analysed for cytochrome c expression using western immunoblot. THC significantly increased cytochrome c concentration in the cytosol. While AM-251 treatment had no effect on cytosolic cytochrome c expression, AM-251 inhibited the THC-induced release of mitochondrial cytochrome c. Results are expressed as mean ± s.e.m. of 5 observations, $^*p < 0.05$. Inset, a sample Western immunoblot which demonstrates the increase in cytosolic cytochrome c expression in THC-treated cortical neurones (lane 2) compared to control cells (lane 1). While AM-251 had no effect on cytosolic cytochrome c expression (lane 3) it abolished the ability of THC to promote translocation of mitochondrial cytochromic c to the cytoplasm (lane 4). (**b**) caspase-3 activity was assessed by cleavage of the fluorogenic peptide DEVD. Exposure of cells to THC (5 μM) for 2 h significantly increased caspase-3 activity. Pretreatment of the cells with AM-251 abolished the THC-induced increase in caspase-3 activity. Results are expressed as mean ± s.e.m. for 5 observations, $^*p < 0.05$. (**c**) The percentage of cells with caspase-3 activity was detected using the anti-active caspase-3 antibody. THC significantly increased the percentage of cortical neurones displaying active caspase-3 immunoreactivity and this was abolished by the CB_1 antagonist AM-251. Results are expressed as mean ± s.e.m. for 7 observations. $^*p < 0.05$. (**d**) Representative image of cortical neurones stained with the anti-active caspase-3 antibody. (i) Under control conditions few cells stained positive for active caspase-3 immunoreactivity. (ii) THC-treated neurones exhibited a significant increase in the number of cells displaying active caspase-3 immunoreactivity. (iii) Treatment with AM-251 alone had no effect on the number of cells with active caspase-3. (iv) Treatment with AM-251 in the presence of THC significantly reduced the number of cells displaying cells displaying active caspase-3 immunoreactivity (cells with activated caspase-3 immunoreactivity are indicated by arrows). Bar = 25 μm.

duced/mg protein/min to 27.4 ± 6.30 pmol AFC produced/mg protein/min ($p < 0.05$, Student's t-test, $n = 5$). While AM-251 (10 μM) alone had no effect caspase-3 activity (12.1 ± 4.9 pmol AFC produced/mg protein/min) it prevented the THC-induced increase caspase-3 activity (caspase-3 activity 12.3 ± 6.0 pmol AFC produced/mg protein/min in cortical neurones treated with THC in the presence of AM-251).

An additional method with which to evaluate caspase-3 activity is immunocytochemistry using an anti-active caspase-3 antibody (Fig. 2c). In control cells the percentage of neurones displaying active-caspase-3 immunoreactivity was 11.0 ± 2.2% and this was significantly increased to 34 ± 3.9% ($p < 0.05$, Student's t-test, $n = 7$) by THC (5 μM). AM-251 (10 μM) alone had no effect on active caspase-3 immunoreactivity (14.5 ± 2.7% of neurones displayed active caspase-3 immunoreactivity following AM-251 treatment) but it prevented the THC-induced increase in active caspase-3 immunostaining (14.9 ± 2.8% of cells displayed active caspase-3 immunoreactivity following treatment with THC in combination with AM-251). A photograph of representative anti-active caspase-3 immunostaining for control, THC, AM 251 and THC + AM 251-treated cells is shown in Fig. 2d.

THC-induced PARP cleavage involves the CB_1 receptor: The DNA repair enzyme PARP is a substrate for caspase-3. To determine whether the THC-induced activation of caspase-3 resulted in cleavage of PARP we monitored expression of the 85kDa cleaved form of PARP by immunocytochemistry using a cleavage-site specific anti-PARP antibody (Fig. 3). In vehicle-treated cultures the percentage of neurones displaying immunoreactivity for the 85 kDa form of PARP was 8.4 ± 0.5% and this was significantly increased to 40 ± 3.9% ($p < 0.01$, Student's t-test, $n = 7$) by THC (5 μM). AM-251 (10 μM) alone had no effect on PARP cleavage (8.3 ± 0.8% of neurones displayed immunoreactivity for the 85 kDa form of PARP following AM-251 treatment). However, AM-251 prevented the THC-induced increase in cleaved PARP immunoreactivity (8.1 ± 0.9% of cells displayed immunostaining for the 85 kDa form of PARP following treatment with THC in combination with AM-251). A photograph of representative anti-cleaved PARP immunostaining is shown in Fig. 3b.

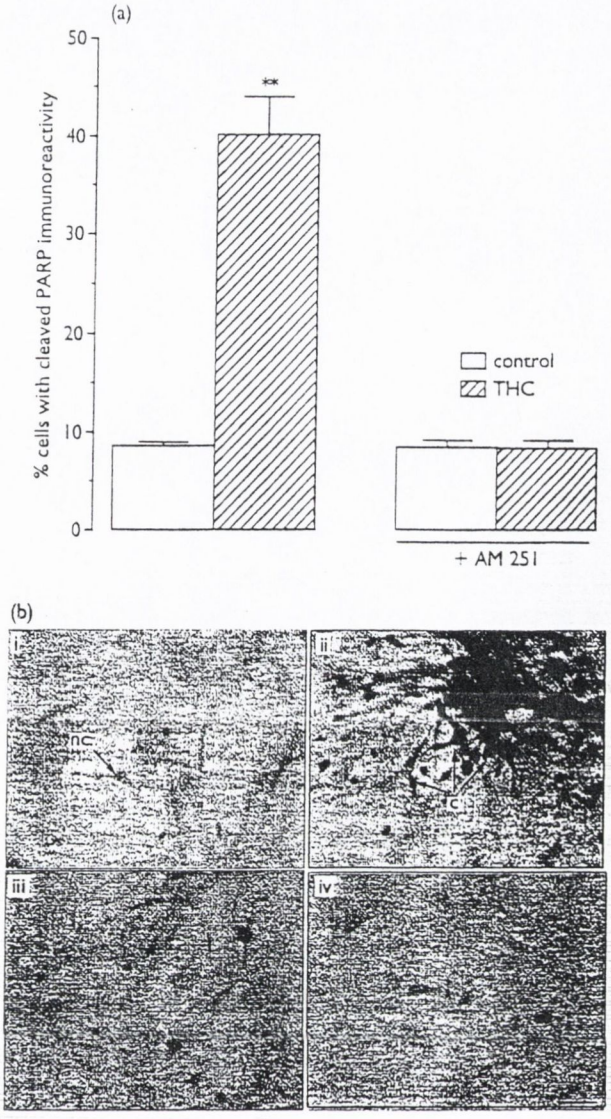

Fig. 3. The THC-induced cleavage of PARP is abolished by AM-251. (a) The percentage of cells with PARP cleavage was detected using the anti-cleavage site specific PARP antibody. THC significantly increased the percentage of cortical neurones displaying cleaved PARP immunoreactivity and this was abolished by the CB_1 antagonist AM-251. Results are expressed as mean ± s.e.m. for 7 observations, ** $p < 0.01$. (b) Representative image of cortical neurones stained with the anti-cleavage site specific PARP antibody. (i) Under control conditions few cells stained positive for cleaved PARP. (ii) THC-treated neurones exhibited a significant increase in the number of cells displaying cleaved PARP immunoreactivity. (iii) Treatment with AM-251 alone had no effect on the number of cells with cleaved PARP. (iv) Treatment with AM-251 in the presence of THC significantly, reduced the number of cells displaying cells displaying cleaved PARP immunoreactivity (cells with non-cleaved (nc) and cleaved (c) PARP are indicated by arrows). Bar = 25 μm.

DISCUSSION

The aim of this study was to examine whether induction of the apoptotic cascade by THC involved the CB_1 subtype of cannabinoid receptor. The results demonstrate that THC promotes release of mitochondrial cytochrome c into the cytosol, activates the cysteine protease caspase-3, cleaves the DNA-repair enzyme PARP and induces DNA fragmentation in cultured cortical neurones. Each of these events are components of the apoptotic cascade and were Completely blocked by the selective CB_1 receptor antagonist AM 251, demonstrating that THC-induced activation of the cell death pathway is CB_1 receptor-dependent.

Plasma concentrations of THC are in the low micromolar range following consumption of a single marijuana cigarette [16] and THC concentrations in the brain are likely to be comparable given that THC is a lipophilic molecule and will readily cross the blood–brain barrier. The minimal dose of THC which was found to be neurotoxic to cultured cortical neurones was within this concentration range.

Our previous study demonstrated that THC induces neuronal cell death in a manner involving activation of the G-protein subtypes $G_{o/i}$, since the detrimental effects of THC on neuronal viability were blocked by pertussis toxin

[6]. Those results suggested that THC may induce apoptosis in a receptor-dependent manner. However, THC is a lipophilic molecule and it remained a possibility that THC could exert a direct influence on G-proteins in the absence of receptor activation. It has been reported that THC has the proclivity to impact on other signalling mechanisms such as sphingomyelin breakdown [3] and scavenging of reactive oxygen species [7] in a receptor-independent manner.

The role of THC and its associated receptors in the induction of apoptosis is also controversial; THC having been found to possess both pro- and anti-apoptotic properties. THC is neurotoxic to hippocampal neurones [5] and C6 gliomna cells [3] *in vitro* yet it protects neurones from glutamate neurotoxicity [8] and ischemia [15]. The THC-induced degeneration of cultured hippocampal neurones [5] and transformed neural cells *in vivo* [17] was found to involve the CB_1 receptor while induction of apoptosis in C6 glioma cells *in vitro* [3] was receptor-independent. The cyoprotective properties of THC have been attributed to the ability of THC to act as an antioxidant in a receptor-independent manner [7,10]. However, the neuroprotective properties of cannabimimetic drugs have also been demonstrated to involve CB_1 receptor activation. The results from this study demonstrate that THC induces apoptosis in cultured cortical neurones via a CB_1 receptor-dependent mechanism.

The apoptotic events that are evoked by THC in cortical neurones include the release of mitochondrial cytochrome c into the cytosol. This serves as an initiator of downstream apoptotic events since cytosolic cytochrome c can form a complex with APAF-1 which results in the activation of the cysteine protease caspase-3, a key executor of the cell death pathway [18]. THC was found to increase caspase-3 activity in cortical neurones and induce cleavage of the caspase-3 substrate PARP, demonstrating that the THC-induced cell death proceeds via activation of the caspase-3 branch of the apoptotic cascade. The ability of THC to impact on each of those apoptotic phenomenon was completely abrogated by AM 251 thereby demonstrating that the CB_1 receptor couples THC to these apoptotic signalling events.

The release of cytochrome c is an early event in apoptosis, however, the nature of the link between the CB_1 receptor and cytochrome c release is not fully understood. It is likely that the CB_1 receptor-induced activation of the heterotrimeric G proteins $G_{i/o}$ is involved since we have previously demonstrated that the THC-induced release of cytochrome c is blocked by pertussis toxin [6]. CB_1 receptors can couple to activation of stress-activated protein kinases in a G-protein-dependent manner [19] and these protein kinases regulate the mitochondrial expression of members of the Bcl family of proteins [20]. Given that cytochrome c release is regulated by the mitochondria-associated proteins Bcl and Bax [21] a potential effector for G-protein-mediated modulation includes activation of stress-activated protein kinases and downstream regulation of Bcl and Bax expression at the mitochondrial membrane.

CONCLUSION

THC exerts neurotoxic properties on cultured cortical neurones by promoting the release of cytochrome c, activation of caspase-3 and cleavage of DNA repair enzymes in a CB_1 receptor-dependent manner. The proclivity of cannabinoid receptors to induce apoptosis in neonatal neurones may reflect the role of endogenous cannabinoids in development of the CNS [22] and may also underlie the central nervous system abnormalities that occur in infants exposed to marijuana *in utero* [23].

REFERENCES

1. Reisine T and Brownstein MJ. *Curr Opin Neurobiol* 4 (3), 406–412 (1994).
2. Block RI and Ghoneim MM. *Psychopharmacology* 110, 219–228 (1993).
3. Sanchez C, Galve-Roperh I, Canova C *et al. FEBS Lett* 25, 6–10 (1998).
4. Zhu W, Freidman H and Klein TW. *J Pharmacol Exp Ther* 286, 1103–1109 (1998).
5. Chan GC, Hinds TR, Impey S and Storm DR. *J Neurosci* 18, 5322–5332 (1998).
6. Campbell VA. *Neuropharmacology* 40, 702–709 (2001).
7. Chen Y and Buck J. *J Pharmacol Exp Ther* 293, 807–812 (2000).
8. Shen M and Thayer SA. *Mol Pharmacol* 54, 459–462 (1998).
9. Di Marzo V, Melck D, Bisogno T and De Petrocellis L. *Trends Neurosci* 21, 521–528 (1998).
10. Hampson AJ, Grimaldi M, Lolic M *et al. Ann NY Acad Sci* 899, 274–282 (2000).
12. Matsuda LA, Lolait SJ, Brownstein MJ *et al. Nature* 346, 561–564 (1990).
13. Berrendero F, Garcia L, Hernandez ML *et al. Development* 125, 3179–3188 (1998).
15. Nagayama T, Sinor AD, Simon RP *et al. J Neurosci* 19, 2987–2995 (1999).
16. Chiang CW and Barnett G. *Clin Pharmacol Ther* 36, 234–238 (1984).
17. Galve-Roperh I, Sanchez C, Cortes ML *et al. Nature Med* 6, 313–319 (2000)
19. Rueda D, Galve-Roperh I, Haro A and Guzman M. *Mol Pharmacol* 58, 814–820 (2000)
20. Ghatan S, Larner S, Kinoshita Y *et al. J Cell Biol* 150, 335–347 (2000).
21. Rosse T, Olivier R, Monney L *et al. Nature* 391, 496–499 (1998).
22. Fernandez-Ruiz JJ, Berrendero F, Hernandez ML *et al. Life Sci* 65, 725–736 (1999).
23. Fried PA and Watkinson B. *J Dev Behav Pediatr* 11, 49–58 (1990).